ISSN 0390-6078
Volume 104
OCTOBER
2019 - 10

haematologica

Journal of The Ferrata Storti Foundation

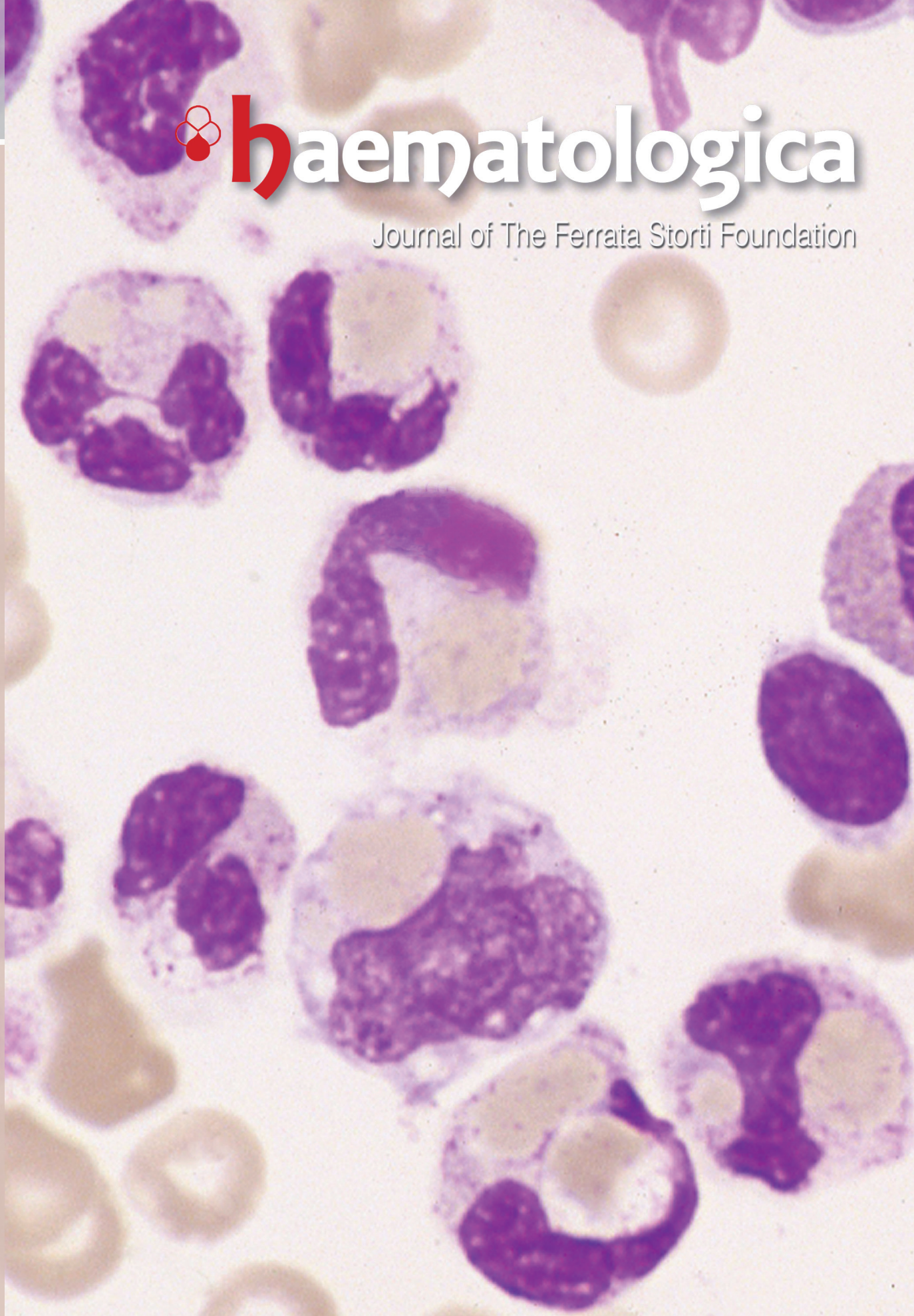

www.haematologica.org

haematologica
Journal of the Ferrata Storti Foundation

Affiliated Scientific Societies
SIE (Italian Society of Hematology, *www.siematologia.it*)
SIES (Italian Society of Experimental Hematology, *www.siesonline.it*)

haematologica
Journal of the Ferrata Storti Foundation

Information for readers, authors and subscribers

Haematologica (print edition, pISSN 0390-6078, eISSN 1592-8721) publishes peer-reviewed papers on all areas of experimental and clinical hematology. The journal is owned by a non-profit organization, the Ferrata Storti Foundation, and serves the scientific community following the recommendations of the World Association of Medical Editors (www.wame.org) and the International Committee of Medical Journal Editors (www.icmje.org).

Haematologica publishes editorials, research articles, review articles, guideline articles and letters. Manuscripts should be prepared according to our guidelines (www.haematologica.org/information-for-authors), and the Uniform Requirements for Manuscripts Submitted to Biomedical Journals, prepared by the International Committee of Medical Journal Editors (www.icmje.org).

Manuscripts should be submitted online at http://www.haematologica.org/.

Conflict of interests. According to the International Committee of Medical Journal Editors (http://www.icmje.org/#conflicts), "Public trust in the peer review process and the credibility of published articles depend in part on how well conflict of interest is handled during writing, peer review, and editorial decision making". The ad hoc journal's policy is reported in detail online (www.haematologica.org/content/policies).

Transfer of Copyright and Permission to Reproduce Parts of Published Papers. Authors will grant copyright of their articles to the Ferrata Storti Foundation. No formal permission will be required to reproduce parts (tables or illustrations) of published papers, provided the source is quoted appropriately and reproduction has no commercial intent. Reproductions with commercial intent will require written permission and payment of royalties.

Detailed information about subscriptions is available online at www.haematologica.org. Haematologica is an open access journal. Access to the online journal is free. Use of the Haematologica App (available on the App Store and on Google Play) is free.
For subscriptions to the printed issue of the journal, please contact: Haematologica Office, via Giuseppe Belli 4, 27100 Pavia, Italy (phone +39.0382.27129, fax +39.0382.394705, E-mail: info@haematologica.org).

Rates of the International edition for the year 2019 are as following:

	Institutional	*Personal*
Print edition	*Euro 700*	*Euro 170*

Advertisements. Contact the Advertising Manager, Haematologica Office, via Giuseppe Belli 4, 27100 Pavia, Italy (phone +39.0382.27129, fax +39.0382.394705, e-mail: marketing@haematologica.org).

Direttore responsabile: Prof. Edoardo Ascari; Autorizzazione del Tribunale di Pavia n. 63 del 5 marzo 1955.
Printing: Press Up, zona Via Cassia Km 36, 300 Zona Ind.le Settevene - 01036 Nepi (VT)

haematologica
Journal of the Ferrata Storti Foundation

Table of Contents
Volume 104, Issue 10: October 2019

Cover Figure

Editorials

Review Articles

Guideline Article

Articles

Hematopoiesis

Bone Marrow Failure

Red Cell Biology and its Disorders

Phagocyte Biology and its Disorders

Jivi: a new rFVIII with the proven power to protect for up to 7 days

▼**THIS MEDICINAL PRODUCT IS SUBJECT TO ADDITIONAL MONITORING.** Adverse events should be reported. Please report any suspected adverse reaction to the applicable national authority.

JIVI 250 / 500 / 1000 / 2000 / 3000 IU POWDER AND SOLVENT FOR SOLUTION FOR INJECTION
(Refer to full SmPC before prescription.)

COMPOSITION: site specifically PEGylated recombinant human coagulation factor VIII, 250/500/1000/2000/3000 IU/vial (100/200/400/800/1200 IU/ml after reconstitution). *Excipients:* Powder: Sucrose, Histidine, Glycine, Sodium chloride, Calcium chloride dihydrate, Polysorbate 80, glacial acetic acid (for pH adjustment). Solvent: Water for injections. **INDICATION:** Treatment and prophylaxis of bleeding in previously treated patients ≥ 12 years of age with haemophilia A (congenital factor VIII deficiency). **CONTRAINDICATIONS:** Hypersensitivity to the active substance or to any of the excipients. Known allergic reactions to mouse or hamster proteins. **WARNINGS AND PRECAUTIONS:** Allergic type hypersensitivity reactions are possible. Hypersensitivity reactions could also be related to antibodies against polyethylene glycol (PEG). If symptoms of hypersensitivity occur, patients should be advised to discontinue the use of the medicinal product immediately and contact their physician. The formation of neutralising antibodies (inhibitors) to FVIII is a known complication in the management of individuals with haemophilia A. A clinical immune response associated with anti-PEG antibodies, manifested as symptoms of acute hypersensitivity and/or loss of drug effect has been observed primarily within the first 4 exposure days. In patients with existing cardiovascular risk factors, substitution therapy with factor VIII may increase the cardiovascular risk. If a central venous access device (CVAD) is required, risk of CVAD-related complications including local infections, bacteraemia and catheter site thrombosis should be considered. **UNDESIRABLE EFFECTS:** *very common:* headache; *common:* hypersensitivity, insomnia, dizziness, cough, abdominal pain, nausea, vomiting, erythema (incl. erythema and erythema multiforme), rash (incl. rash and rash popular), injection site reactions (incl. injection site pruritus/rash and vessel puncture site pruritus), pyrexia; *uncommon:* FVIII inhibition (previously treated patients), dysgeusia, flushing, pruritus.

ON PRESCRIPTION ONLY.

MARKETING AUTHORISATION HOLDER:
Bayer AG, 51368 Leverkusen, Germany.

DATE OF REVISION OF THE UNDERLYING PRESCRIBING INFORMATION:
November 2018

PP-JIV-ALL-0215-1
February 2019

Jivi®
Recombinant Factor VIII (damoctocog alfa pegol)

LET'S GO

haematologica
Journal of the Ferrata Storti Foundation

Errata Corrige

Letters to the Editor

Letters are available online only at www.haematologica.org/content/104/10.toc

ESH EUROPEAN SCHOOL OF HAEMATOLOGY

UPCOMING CONFERENCES 2019

- **24-26 FEBRUARY**, 2019 – London, UK
  3rd Scientific Workshop on
  HAEMATOLOGICAL TUMOUR MICROENVIRONMENT AND ITS THERAPEUTIC TARGETING
  CHAIRS: **M. Andreeff, D. Bonnet, D.S. Krause, S. Mendez-Ferrer**

- **8-10 MARCH**, 2019 – Saggart (Dublin), Ireland
  How to Diagnose and Treat
  CML/MPN
  CHAIRS: **C. Harrison, A. Hochhaus, R. Mesa**

- **15-17 MARCH,** 2019 – Budapest, Hungary
  International Conference on
  ERYTHROPOIESIS CONTROL AND INEFFECTIVE ERYTHROPOIESIS: From Bench to Bedside
  CHAIRS: **M.D. Cappellini, S. Orkin, V. Santini**

- **5-7 APRIL,** 2019 – Berlin, Germany
  2nd How to Diagnose and Treat
  MULTIPLE MYELOMA
  CHAIRS: **H. Einsele, I. Ghobrial, S. Zweegman**

- **17-19 MAY,** 2019 – Berlin, Germany
  International Conference on
  ACUTE LYMPHOBLASTIC LEUKEMIA
  CHAIRS: **J. Cools, H. Dombret, A. Fielding, M. Litzow**

- **12-15 SEPTEMBER,** 2019 – Bordeaux, France
  21st Annual Goldman Conference on
  CHRONIC MYELOID LEUKEMIA: BIOLOGY AND THERAPY
  CHAIRS: **J. Cortes, T.P. Hughes, D.S. Krause**

- **20-22 SEPTEMBER**, 2019 – Mandelieu, France
  Annual International Conference on
  IMMUNE AND CELLULAR THERAPIES: FOCUS ON IMMUNE BASED THERAPEUTIC CONCEPTS
  CHAIRS: **C. Bonini, C. June, M. Topp**

- **3-5 OCTOBER**, 2019 – Estoril, Portugal
  5th International Conference on
  NEW CONCEPTS IN LYMPHOID MALIGNANCIES
  CHAIRS: **M. Hallek, G. Lenz, F. Morschhauser, L. Sehn, L. Staudt, S. Stilgenbauer, A. Thomas-Tikhonenko**

- **24-26 OCTOBER**, 2018 – Estoril, Portugal
  5th International Conference on
  ACUTE MYELOID LEUKEMIA "MOLECULAR AND TRANSLATIONAL":
  ADVANCES IN BIOLOGY AND TREATMENT
  CHAIRS: **B. Löwenberg, H. Döhner, M. Tallman**

PLEASE VISIT OUR WEBSITE: www.esh.org

haematologica
Journal of the Ferrata Storti Foundation

Case Reports

Case Reports are available online only at www.haematologica.org/content/104/10.toc

Comment

Comments are available online only at www.haematologica.org/content/104/10.toc

ANNOUNCING THE AWARDEE 2019

Dr. Ilaria Pagani

Leukaemia Research Group, Cancer Program, SAHMRI, Adelaide, Australia

for her two year project on

'Use of machine learning to integrate clinical data and biomarkers to optimise prediction of TFR'

"It is an honour and a pleasure to be the first John Goldman Research Prize Awardee. Receiving funding support from the European School of Haematology (ESH) is a privilege. It represents a critical step in my career towards becoming an independent investigator and provides the opportunity to build new collaborations.

My project aims to identify bioassays that can be integrated with clinical data in a machine learning system to develop a personalized predictive model for treatment free remission (TFR). I expect it will bring novel insights into the biology of TFR, opening new horizons toward the discovery of targeted therapies and improving TFR patient outcome."

APPLY FOR THE JOHN GOLDMAN AWARD 2020

Submitted projects must:

- aim to develop a method, algorithm or test to reliably identify patients able to benefit from treatment discontinuation, thereby significantly improving the probability of TFR success,
- demonstrate potential to improve healthcare standards for Chronic Myeloid Leukaemia (CML) patients or for patients suffering from other haematological malignancies.

The recipient of this annual award will receive a total of 80 000€ to finance or co-finance a research project on **Treatment Free Remission (TFR).**

DEADLINE FOR SUBMISSION: MARCH 1, 2020

For further information: Didi.jasmin@univ-paris-diderot.fr
European School of Haematology (ESH)
Saint-Louis Research Institute, Saint-Louis Hospital, Paris 75010,France
www.esh.org

The stromal microenvironment provides an escape route from FLT3 inhibitors through the GAS6-AXL-STAT5 axis

Anna Orlova[1], Heidi A. Neubauer[1] and Richard Moriggl[1,2]

[1]Institute of Animal Breeding and Genetics, University of Veterinary Medicine and [2]Medical University Vienna, Vienna, Austria

E-mail: RICHARD MORIGGL - richard.moriggl@vetmeduni.ac.at

doi:10.3324/haematol.2019.225862

The *FLT3-ITD* mutation is one of the most common rearrangements in acute myeloid leukemia (AML), and is particularly associated with poor prognosis and recurrent development of resistance. In 2017, the FLT3 tyrosine kinase inhibitor (TKI) midostaurin was approved for use in combination with standard cytarabine-based chemotherapy. Several other small molecule inhibitors against FLT3 tyrosine kinase are currently being tested in phase III clinical trials (e.g. gilteritinib and quizartinib). Despite successful application of the targeted therapy in patients, emergence of resistance is still a major drawback in clinical practice.[1] A better understanding of resistance mechanisms in cancer is key to defining better treatment strategies for patients. The new study by Dumas *et al.* in this issue of the Journal unravels mechanisms involving the tyrosine kinase receptor AXL contributing to the development of resistance to quizartinib in FLT3-ITD$^+$ AML.[2]

AXL belongs to the family of TAM receptors, and together with two other members, TYRO3 and MER, it was first shown to have malignant roles in solid cancers.[3,4] AXL was identified as one of the most prominently activated tyrosine kinase receptors in colorectal, esophageal, thyroid, breast, prostate and lung carcinomas, and its activation was associated with transforming growth factor beta (TGFβ) signaling.[4,5] AXL is selectively activated by GAS6 ligand, which has a significantly higher affinity to AXL compared to the other family members. Further ligands for TAM receptors include Protein S, Tubby, Tubby-like protein 1, and Galectin-3.[4] Soluble forms of AXL (sAXL) are also reported, and result from cleavage by ADAM10/17 proteases in the plasma of patients with advanced liver cancer; they are, therefore, of extremely important diagnostic value for liver cancer progression.[6] TAM receptors are involved in processes promoting cell growth and survival, cell adhesion, migration, blood coagulation, and cytokine release.[7] However, TAM receptors were also reported to impede cancer cells through stimulation of tumor cell-targeting immune cells.[8]

The new findings reported by Dumas *et al.*[2] confirm an important cancer-protective role for the stromal microenvironment, mechanistically identifying that it induces cytokine production and hypoxic conditions to trigger the activation of AXL and the transcription factor STAT5 in FLT3-ITD$^+$ AML (Figure 1A). The authors further show that stroma-induced expression of *AXL*, mediated by STAT5, drives progression of the disease. The paper provides evidence that growth arrest specific protein 6 (GAS6) ligand secreted from stromal cells activates AXL and, together with hypoxia, contributes to AML progression and resistance to quizartinib. Notably, a bypass mechanism was described involving activation of the AXL receptor kinase to compensate for FLT3 inhibition to promote AML progression.

Interestingly, similar findings also implicated AXL activation, together with another receptor tyrosine kinase MET, in driving resistance mechanisms in *HER2*-positive gastric cancer with TKI treatment.[9] Here, the authors generated and exploited afatinib-resistant gastric cancer cell lines to identify AXL and MET as key players in the development of drug resistance. Yoshioka *et al.* proposed combinatorial treatment using afatinib with pan-kinase inhibitor cabozantinib, which also targets AXL/MET, to prevent development of therapy resistance or to potentially sensitize patients who have already developed resistance.[9]

STAT5A/B proteins are key downstream transcription factors in FLT3-ITD$^+$ AML, and they mediate signals from hyperactive FLT3. STAT5 inhibition was reported to be a promising strategy for FLT3-ITD$^+$ AML treatment.[10-13] The oncogenic roles of highly tyrosine-phosphorylated STAT5 (pYSTAT5) in hematopoietic diseases were best exemplified using graded expression and activity levels of STAT5A/B in gain-of-function transgenic mouse models.[14,15] Important downstream transcriptional changes triggered by STAT5 in neoplastic myeloid cells can involve enhanced expression of *DNMT3A*, *BCL2* or *D-type cyclin* family members, as well as *MYC* induction. This panel of downstream STAT5 target genes has now been expanded to include AXL in quizartinib-resistant FLT3-ITD$^+$ AML, and it will be of particular interest to explore whether this finding is also applicable in other cancers.[2] Interestingly, *TET* or *DNMT3* genes are often mutated in AML, and both have been reported to either form protein interactions with STAT5 or undergo direct gene regulation by STAT5. In particular, mutations in chromatin modifiers *TET2*, *DNMT3A*, *ASXL1*, *IDH1/2*, as well as *STAT5*, were found to be of important prognostic value in FLT3-ITD$^+$ mutated AML cases. It will be important to explore further the impact of these proteins and the chromatin landscape on the GAS6-AXL-STAT5 AML progression axis.[16,17]

A previous study also examined the effects of PI3K/AKT/mTOR inhibitors on a FLT3-ITD$^+$ AML cell line compared with a cell line harboring point mutations within the TKD2 domain of FLT3 (*FLT3-TKD*). The authors reported that FLT3-ITD$^+$ cells are more resistant to the aforementioned FLT3 inhibitors compared with FLT3-TKD$^+$ cells. The authors proposed hyperactivation of STAT5 in FLT3-ITD$^+$ AML cells as a protective mechanism against PI3K/AKT/mTOR inhibition.[18] Interestingly, Dumas *et al.* showed in their model that inhibition of PI3K/AKT signaling had no effect on AXL or STAT5 phosphorylation, and, therefore, this did not directly mediate the development of resistance to therapy.[2]

Based on these recent findings, we used public gene expression datasets available from the Oncomine database to independently evaluate *AXL* gene expression data from patients with AML as well as from patients with other hematopoietic cancers.[19] As also discussed by Dumas *et al.*, we found *AXL* to be significantly up-regulated in AML patient samples (Figure 1B). Interestingly, upregulation of *AXL* was also clearly evident in various subtypes of B-cell and T-cell leukemias/lymphomas (Figure 1B), suggesting a potentially broader relevance for the oncogenic action of *AXL* upregulation in hematopoietic can-

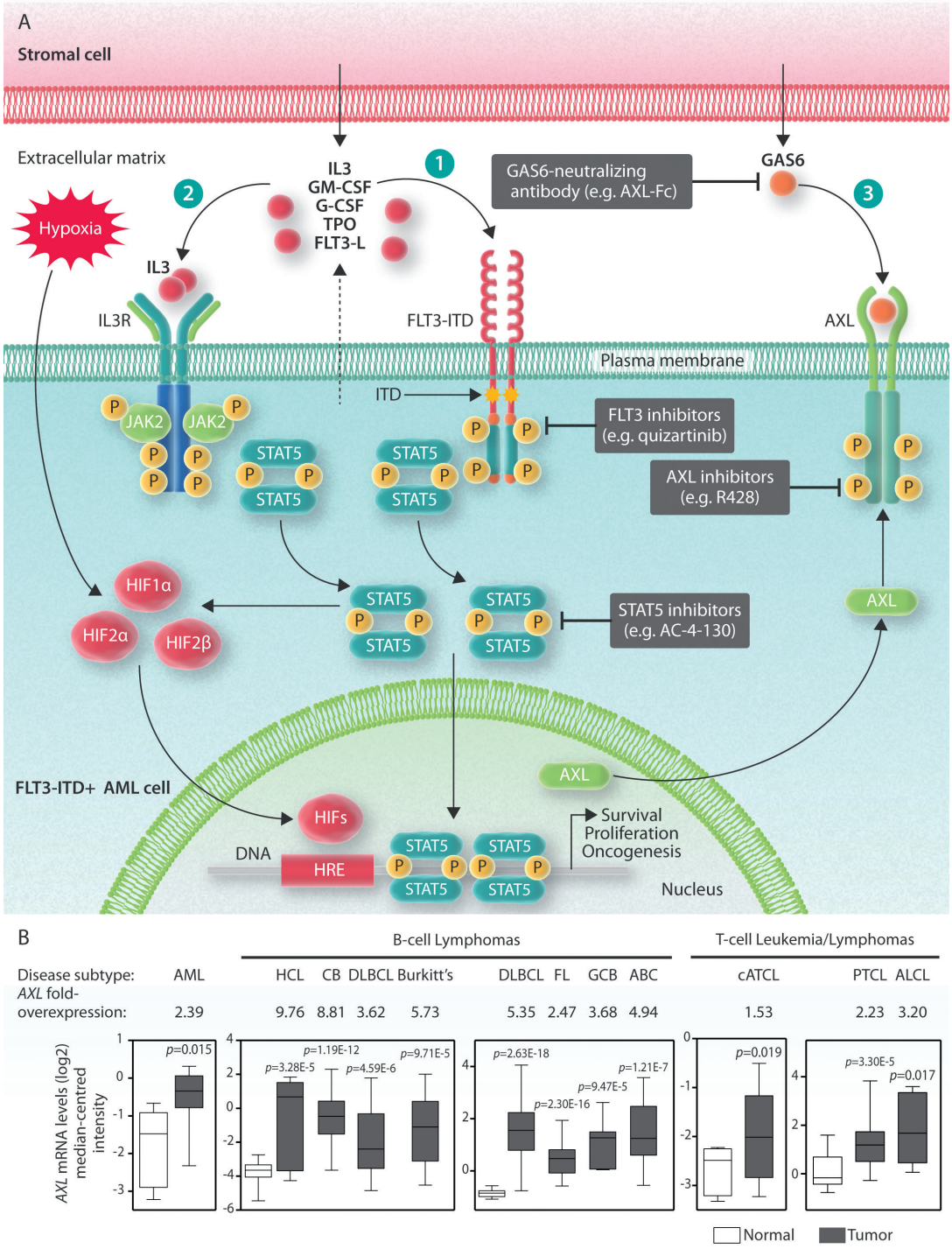

Figure 1. AXL promotes acute myeloid leukemia (AML) progression upon development of resistance. (A) Stromal cells were shown to express cytokines and ligands (see 1 and 2) (such as IL3 or FLT3-L, solid arrow) to a greater extent than AML cells (dashed arrow). Additionally, stromal cells were shown to produce GAS6 (see 3), which activates AXL receptor signaling. JAK2 binds to the cytosolic juxta-membrane region of dimeric cytokine receptors such as IL3R *via* the BOX1 and BOX2 receptor motifs upon stimulation by respective cytokines (see 2). JAK2 activation triggers STAT5 signaling, which promotes oncogenic gene transcription to propagate cancer cell survival, proliferation, and metabolic reprogramming. Additionally, STAT5 was shown to bind to the *AXL* promoter to induce expression. Mutated FLT3 (FLT3-ITD, yellow stars), frequently found in AML patients, can induce phosphorylation of STAT5 directly. Therapeutic agents used by Dumas *et al.*[2] to target these key proteins/pathways in AML are summarized in gray boxes. Hypoxia induced by the stromal microenvironment induces expression of HIF transcription factors, and STAT5 can induce expression of HIF2α. Subsequently, HIF can bind to HRE elements in the *AXL* promoter. AML: acute myeloid leukemia; IL3: Interleukin 3; IL3R: Interleukin 3 receptor; GM-CSF: granulocyte-macrophage colony-stimulating factor; TPO: thrombopoietin; FLT3: Fms-like tyrosine kinase 3; ITD: internal tandem duplication; FLT3-L: Fms-like tyrosine kinase 3 ligand; GAS6: growth arrest-specific 6; HIF: hypoxia-inducible factor; HRE: hypoxia-response element; JAK: Janus kinase; STAT: signal transducer and activator of transcription. (B) *AXL* mRNA expression levels in patients with hematopoietic cancers using data from the Oncomine database. Box plots showing human hematopoietic cancers with significant upregulation of *AXL* mRNA levels in tumor cells, compared with tissue-matched normal control cells. Data were extracted from the Oncomine database from the following studies (graphs from left to right): Stegmaier Leukemia, Basso Lymphoma, Compagno Lymphoma, Choi Leukemia, and Piccaluga Lymphoma. Data from multiple normal-tissue subtypes included in some datasets were pooled for clarity. For all analyses, the *P*-value threshold was set to 0.05, the fold-change threshold was set to 1.5, and the gene rank threshold was set to 'all'. HCL: hairy cell leukemia; CB: centroblastic lymphoma; DLBCL: diffuse large B-cell lymphoma; FL: follicular lymphoma; GCB: germinal center B-cell-like DLBCL; ABC: activated B-cell-like DLBCL; cATCL: chronic adult T-cell leukemia/lymphoma; PTCL: unspecified peripheral T-cell lymphoma; ALCL: anaplastic large cell lymphoma.

cers. Notably, mining the Oncomine database additionally revealed significant overexpression of both TYRO3 and MER in various B- and T-cell leukemia/lymphoma datasets, but not in AML (*data not shown*). This might suggest a potentially different mechanism of oncogenic signaling in lymphoid neoplasms involving all three receptor family members, as opposed to the clear role of AXL in FLT3-ITD$^+$ AML; this could be a focus point for further investigations.

The new study by Dumas *et al.* described a resistance mechanism against the FLT3 inhibitor quizartinib, where both the *FLT3-ITD* mutation and the GAS6-AXL axis trigger important kinase signaling cascades. Their results suggest that a combination of FLT3- and AXL-specific inhibitors, or the exploitation of dual FLT3-AXL inhibitors (e.g. cabozantinib), might be beneficial in FLT3-ITD$^+$ AML patients at risk of relapse. Furthermore, selective STAT5 inhibitors have the potential to become an effective tool for targeted and combinatorial therapy in AML.

In summary, FLT3 inhibitors display efficacy in the treatment of FLT3-ITD-driven AML, but more efficient targeting of AML blasts remains an unresolved medical need to fight therapeutic resistance, and to improve the poor overall survival and quality of life of patients.

Funding

HAN and RM are supported by the Austrian Science Fund (FWF) [SFB-F04707, SFB-F06105, and under the frame of ERA PerMed (I 4218-B) and ERA-NET (I 4157-B)]. RM, HAN and AO were also generously supported by a private donation from Liechtenstein.

References

1. Daver N, Schlenk RF, Russell NH, et al. Targeting FLT3 mutations in AML: review of current knowledge and evidence. Leukemia. 2019;33(2):299-312.
2. Dumas PY, Naudin C, Maetin-Lannerée S, et al. Hematopoietic niche drives FLT3-ITD acute myeloid leukemia resistance to quizartinib via STAT5- and hypoxia- dependent up-regulation of AXL. Haematologica. 2019;104(10):2017-2027.
3. Kirane A, Ludwig KF, Sorrelle N, et al. Warfarin Blocks Gas6-Mediated Axl Activation Required for Pancreatic Cancer Epithelial Plasticity and Metastasis. Cancer Res. 2015;75(18):3699-3705.
4. Wu X, Liu X, Koul S, et al. AXL kinase as a novel target for cancer therapy. Oncotarget. 2014;5(20):9546-9563.
5. Lee HJ, Jeng YM, Chen YL, et al. Gas6/Axl pathway promotes tumor invasion through the transcriptional activation of Slug in hepatocellular carcinoma. Carcinogenesis. 2014;35(4):769-775.
6. Holstein E, Binder M, Mikulits W, et al. Dynamics of Axl Receptor Shedding in Hepatocellular Carcinoma and Its Implication for Theranostics. Int J Mol Sci. 2018;19(12).
7. Linger RMA, Keating AK, Earp HS, et al. TAM Receptor Tyrosine Kinases: Biologic Functions, Signaling, and Potential Therapeutic Targeting in Human Cancer. Adv Cancer Res. 2008;100:35-83
8. Paolino M, Penninger JM. The Role of TAM Family Receptors in Immune Cell Function: Implications for Cancer Therapy. Cancers (Basel). 2016;8(10).
9. Yoshioka T, Shien K, Takeda T, et al. Acquired resistance mechanisms to afatinib in HER2-amplified gastric cancer cells. Cancer Sci. 2019 Jun 4. [Epub ahead of print]
10. Mizuki M, Schwable J, Steur C, et al. Suppression of myeloid transcription factors and induction of STAT response genes by AML-specific Flt3 mutations. Blood. 2003;101(8)3164-3173.
11. Nelson EA, Walker SR, Xiang M, et al. The STAT5 Inhibitor Pimozide Displays Efficacy in Models of Acute Myelogenous Leukemia Driven by FLT3 Mutations. Genes Cancer. 2012;3(7-8):503-511.
12. Wingelhofer B, Maurer B, Heyes EC, et al. Pharmacologic inhibition of STAT5 in acute myeloid leukemia. Leukemia. 2018;32(5):1135-1146.
13. Yoshimoto G, Miyamoto T, Jabbarzadeh-Tabrizi S, et al. FLT3-ITD up-regulates MCL-1 to promote survival of stem cells in acute myeloid leukemia via FLT3-ITD–specific STAT5 activation. Blood. 2009;114(24):5034-5043.
14. Maurer B, Nivarthi H, Wingelhofer B, et al. High activation of STAT5A drives peripheral T-cell lymphoma and leukemia. Haematologica. 2019 May 23. [Epub ahead of print]
15. Pham HTT, Maurer B, Prchal-Murphy M, et al. STAT5BN642H is a driver mutation for T cell neoplasia. J Clin Invest. 2018;128(1):387-401.
16. Bowman RL, Busque L, Levine RL, et al. Clonal Hematopoiesis and Evolution to Hematopoietic Malignancies. Cell Stem Cell. 2018;22(2):157-170.
17. Fuster JJ and Walsh K. Somatic Mutations and Clonal Hematopoiesis. Circ Res. 2018;122(3):523-532.
18. Nogami A, Oshikawa G, Okada K, et al. FLT3-ITD confers resistance to the PI3K/Akt pathway inhibitors by protecting the mTOR/4EBP1/Mcl-1 pathway through STAT5 activation in acute myeloid leukemia. Oncotarget. 2016;6(11):9189-9205.
19. Rhodes DR, Yu J, Shanker K, et al. ONCOMINE: a cancer microarray database and integrated data-mining platform. Neoplasia. 2004;6(1):1-6.

Pediatric aplastic anemia treatment patterns and responses; power in the numbers

Lucy C. Fox[1,2] and David S. Ritchie[2,3]

[1]Diagnostic Haematology, Peter MacCallum Cancer Centre; [2]University of Melbourne and [3]Clinical Haematology, Peter MacCallum Cancer Centre and Royal Melbourne Hospital, Melbourne, Australia

E-mail: DAVID S. RITCHIE - david.ritchie@mh.org.au

doi:10.3324/haematol.2019.225870

In this edition of *Haematologica*, Rogers *et al.*, representing 25 individual institutions, collectively report on their findings of the diagnostic approaches, applied therapies and responses in a cohort of 314 pediatric patients (aged 1-20 years) with a diagnosis of aplastic anemia (AA) collected through the North American Pediatric Aplastic Anemia Consortium (NAPAAC).[1] This study highlights a number of important messages; specifically the power of collated registry data in a rare disease, the need to retest and continually refine diagnostic criteria to be fit for real-world purposes, the patterns of response and relapse to immunosuppressive therapy (IST) in a pediatric setting including the substantial differences in outcomes from IST in children compared with that in adults, and the importance of allogeneic stem cell transplant (HCT) in the therapy of refractory or relapsed disease.

Although AA can affect people at any stage of life, with a well reported bimodal peak of age incidence observed in older children/young adults and those over sixty years,

it is a rare condition that often poses a diagnostic dilemma with acquired AA potentially confounded by a differential of inherited bone marrow failure syndromes in younger patients and hypoplastic myelodysplasia in older patients. These variations in clinical presentation and potential differences in pathophysiology between pediatric and adult patients with AA emphasize the importance of having data sets dedicated to pediatric cases on which to analysis patterns of presentation, diagnosis and treatment outcome and thereby recommend consensus-driven therapeutic algorithms, particularly in an environment in which there has been substantial historical variations in practice.[2]

The insights provided in the Rogers *et al.* analysis provides substantial clarity around several management issues in pediatric AA, but also pose several other ques-

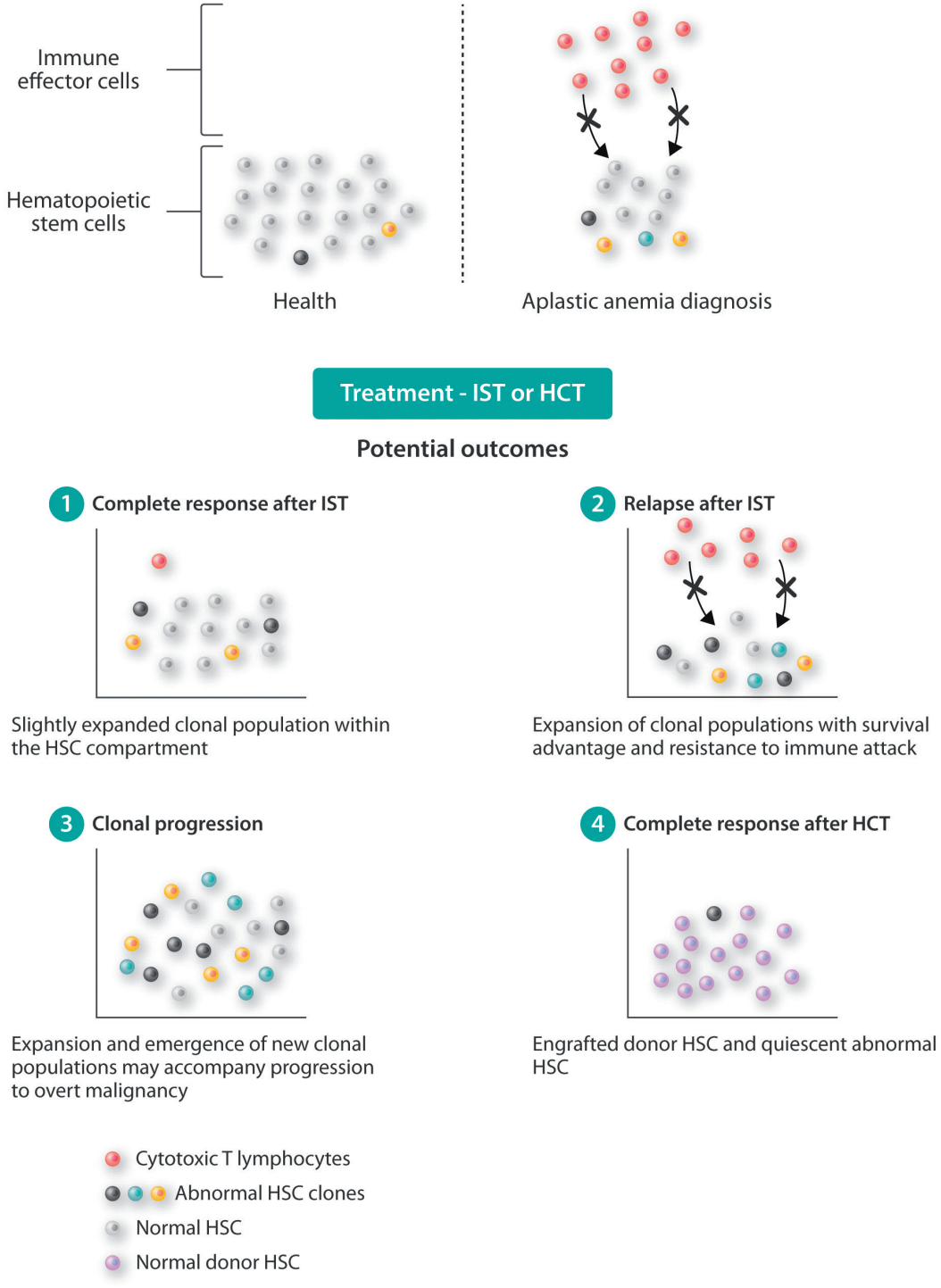

Figure 1. Immune mediated attack on hematopoietic stem cells (HSC) and potential responses to therapy. IST: immunosuppressive therapy; HCT: hematopoietic stem cell transplant.

tions either for ongoing analysis as their data set continues to expand and mature or as hypotheses to be tested in prospective studies.

A practical outcome of this consortium analysis is a real-world assessment of the applicability of the modified Camitta criteria for AA diagnosis first described in 1976.[3] These diagnostic criteria are still recommended by international guidelines for assessment of AA severity.[4] In these criteria, in addition to the depth of marrow hypocellularity and peripheral blood cytopenias, a reticulocyte count is required both as a diagnostic criterion for AA and also to assist with severity classification. However, in a prior analysis by the NAPAAC, it was established that reticulocyte values substantially vary between institutions, making their inclusion in diagnostic criteria uncertain.[2] To address this conundrum, Rogers *et al.* offer the interesting observation from their data set of a lack of correlation between hemoglobin and reticulocyte count in their pediatric cohort at the time of diagnosis, and suggest that hemoglobin may be a more accurate and clinically relevant parameter on which to base management decisions. Whilst the Camitta criteria have stood the test of time, and their use is a strong recommendation, some of their elements are based on relatively low quality C level source data.[4] The findings outlined in the Rogers *et al.* paper re-iterate the importance of ongoing review and modification of diagnostic criteria as new data sets, such as that collated by the NAPAAC, come to hand.

Similarly, collation and description by co-operative groups of current patterns of clinical practice and the degree of its adherence to consensus guideline is an important element of continued improvement in practice, particularly for rare conditions where individual institutional experience may be limited. Currently, one of the most widely accepted management decisions in the treatment of young patients with AA is to offer HCT in patients aged under 40 years with an HLA matched sibling donor (MSD).[4-7] For those without a MSD, IST with anti-thymocyte globulin (ATG), most commonly horse-derived, in combination with cyclosporine is used as initial therapy with HCT from unrelated donors (UD) reserved for those who do not respond or who relapse after IST. Of the cohort outlined in the Rogers *et al.* analysis, the majority of HCT undertaken as second-line therapy utilized UD, indicating the lack of a MSD for upfront use, and in those who eventually received second-line HSCT from a MSD, it is unclear why this donor was not used in the upfront setting. This particular question may be answerable in future analyses by the NAPAAC.

The Rogers *et al.* analysis demonstrated a striking difference in outcome following IST in pediatric patients compared to that in a historical cohort of adult patients. While complete response (CR) was only seen in 10% of adults treated with IST,[8] the pediatric cohort showed CR rates of nearly 60%. Despite this excellent response rate, a pattern of continual events, including death, relapse or transformation to hematologic malignancy following IST, resulted in a disappointing 5-year event-free survival (EFS) of 62%, similar to the findings showing by Yoshida *et al*.[6] The finding of a continued pattern of events even after apparent successful therapy with IST further reinforces the view that normalization of peripheral blood parameters and marrow cellularity after immunosuppression does not imply normalization of hematopoietic clonality and/or immunological repertoire, and, as a consequence, the once-aplastic marrow remains at ongoing risk of recurrent aplasia, clonal evolution, and/or malignant transformation (Figure 1).

This description of the patterns of response and subsequent relapse (or other event) in pediatric AA raises at least three important questions. Firstly, what is the most appropriate salvage therapy for those patients relapsing after initial IST? Secondly, given the high rate of relapse/events, should HCT from any matched donor be considered as front-line therapy in children? Thirdly, are there better biomarkers under development that might provide greater guidance in the choice between these treatment options? With regards to the first question, the Rogers *et al.* paper provides clear guidance. Re-treatment was required in 35%, and second-line therapy with an allogeneic HCT offered superior EFS to pursuing a second course of IST. These combined findings of unstable responses to IST, and the high rate of durable responses to HCT, contribute to the evolving debate as to whether HCT from any matched donor (related or unrelated) is preferable over IST as initial therapy for pediatric patients with proven AA. This question is clearly best answered in a randomized clinical trial, although such an undertaking would require a long-term commitment for feasible accrual and is only likely to succeed through consortia such as the NAPAAC. Lastly, biomarker development is critically required to more accurately determine the degree of clonal restriction (and therefore risk of clonal progression) and/or ongoing potential for immunological attack (and therefore post-IST relapse) to help determine whether IST or HCT should be offered as initial therapy. Clearly, in studies where restricted clonality is evident through genomic or cytogenetic analysis, poorer outcomes to IST are seen, indicating that with more sensitive techniques directed at assessment of the stem cell pool, more informed therapeutic decisions should follow.[9] Again, it is likely that only through the co-ordinated efforts of consortia will sufficient biomarker samples be accumulated to begin to address this unmet need.

One clear determinant of clinical outcome from whatever therapy is chosen is the certainty with which the diagnosis is made. Increasingly, there is an appreciation that occult constitutional bone marrow failure syndromes may underlie what is thought to be a presentation of idiopathic AA, with significant implications for patient management. Through the increasingly readily available techniques for telomere length assessment[10] and next generation sequencing for assessment of underlying germline lesions[11] reclassification of many cases of AA is likely both during the prospective work up of new cases and retrospectively from archival diagnostic samples, which will further inform future treatment algorithms. As a greater clinical appreciation of the importance of diagnostic certainly has been met with greater diagnostic technical capacity, consensus recommendations increasingly incorporate evaluation of constitutional syndromes by chromosomal fragility testing in all AA patients presenting at younger than 50 years of age. Telomere length

assessment is likely to be added to the routine work up panel in the near future.[4] Reflecting these guidelines, Rogers *et al.* describe that while chromosomal fragility assessment was performed in most children, telomere length assessment was only performed at diagnosis in one-third of them.

Registries are crucial tools in efforts to improve outcomes for patients with rare diseases and their families. They serve as a means of pooling rare data in a standardized format in order to achieve meaningful sample sizes for subsequent analysis and allow comparison to historical or international cohorts, facilitate collaboration, generate hypotheses for future testing, and provide a framework for annotated sample collection and translational research. Further, participation in registry reporting contributes to achieving consistent and complete work up of new cases and provides a means of formulation and distribution of educational opportunities including multidisciplinary discussions which are so often needed in the management of rare conditions. Registries allow for the identification of patients, informing epidemiology assessments and areas of need, and may assist with allocation of scarce resources. Registries may facilitate feasibility assessments of and planning for clinical trials. The importance of registries focused on AA in particular is reflected in the increasing number of publications describing national outcome data in AA.[2,12-14] In this edition of *Haematologica*, Rogers *et al*. have made an important contribution to this data pool, informing optimal diagnostic and therapeutic approaches and, equally importantly, highlighting opportunities for further research and discussion in pediatric AA.

Funding

LF is supported by a Higher Degree Fellowship in Bone Marrow Failure from Maddie Riewoldt's Vision.

References

1. Rogers ZR, Nakano TA, Olson TS, et al. Immunosuppressive therapy for pediatric aplastic anemia: a North American Pediatric Aplastic Anemia Consortium study. Haematologica. 2019;104(10):1974-1983.
2. Williams DA, Bennett C, Bertuch A, et al. Diagnosis and treatment of pediatric acquired aplastic anemia (AAA): an initial survey of the North American Pediatric Aplastic Anemia Consortium (NAPAAC). Pediatr Blood Cancer. 2014;61(5):869-874.
3. Camitta BM, Thomas ED, Nathan DG, et al. Severe aplastic anemia: a prospective study of the effect of early marrow transplantation on acute mortality. Blood. 1976;48(1):63-70.
4. Killick SB, Bown N, Cavenagh J, et al. Guidelines for the diagnosis and management of adult aplastic anaemia. Br J Haematol. 2016;172(2):187-207.
5. Dufour C, Pillon M, Passweg J, et al. Outcome of aplastic anemia in adolescence: a survey of the Severe Aplastic Anemia Working Party of the European Group for Blood and Marrow Transplantation. Haematologica. 2014;99(10):1574-1581.
6. Yoshida N, Kobayashi R, Yabe H, et al. First-line treatment for severe aplastic anemia in children: bone marrow transplantation from a matched family donor versus immunosuppressive therapy. Haematologica. 2014;99(12):1784-1791.
7. Bacigalupo A. How I treat acquired aplastic anemia. Blood. 2017;129(11):1428-1436.
8. Townsley DM, Scheinberg P, Winkler T, et al. Eltrombopag Added to Standard Immunosuppression for Aplastic Anemia. N Engl J Med. 2017;376(16):1540-1550.
9. Yoshizato T, Dumitriu B, Hosokawa K, et al. Somatic Mutations and Clonal Hematopoiesis in Aplastic Anemia. N Engl J Med. 2015;373(1):35-47.
10. Lai TP, Wright WE, Shay JW. Comparison of telomere length measurement methods. Philos Trans R Soc Lond B Biol Sci. 2018;373(1741).
11. Ghemlas I, Li H, Zlateska B, et al. Improving diagnostic precision, care and syndrome definitions using comprehensive next-generation sequencing for the inherited bone marrow failure syndromes. J Med Genet. 2015;52(9):575-584.
12. Contejean A, Resche-Rigon M, Tamburini J, et al. Aplastic anemia in the elderly: a nationwide survey on behalf of the French Reference Center for Aplastic Anemia. Haematologica. 2019;104(2):256-262.
13. Vaht K, Goransson M, Carlson K, et al. Incidence and outcome of acquired aplastic anemia: real-world data from patients diagnosed in Sweden from 2000-2011. Haematologica. 2017;102(10):1683-1690.
14. Zhu XF, He HL, Wang SQ, et al. Current Treatment Patterns of Aplastic Anemia in China: A Prospective Cohort Registry Study. Acta Haematol. 2019:1-9.

Mastering the multitude of monocytoses

Ulrich Germing and Norbert Gattermann

Department of Hematology, Oncology and Clinical Immunology, Heinrich Heine University Düsseldorf, Düsseldorf, Germany

E-mail: ULRICH GERMING - germing@med.uni-duesseldorf.de

doi:10.3324/haematol.2019.227546

In this issue of the journal, Valent and coworkers report on diagnostic criteria for chronic myelomonocytic leukemia (CMML), CMML variants, and pre-CMML conditions.[1] These CMML disorders have always been like orphans, trying to find their place in a suitable environment. They are rare entities but share chromosomal, molecular, morphological, hematologic, clinical, and prognostic features with other diseases in the large family of myeloid malignancies. The French-American-British group classified CMML as a myelodysplastic syndrome (MDS), based on its similarity to refractory anemia with excess blasts, although CMML "may have little in common with MDS showing trilineage dyspoiesis"[2] and despite the fact that CMML features only minimal dysplasia in the erythroid lineage. Pathologists and hematologists felt uncomfortable since there are more differences than similarities between CMML and MDS. World Health Organization classifications placed CMML in a "hermaphrodite" position between myeloproliferative neoplasms (MPN) and MDS,[3-5] taking into consideration that there are proliferative characteristics as well as hematopoietic insufficiency associated with some degree of myelodysplasia. Despite all these efforts, CMML was once described as "lost in classification", as none of the classifications adequately reflects the marked heterogeneity of this group of myeloid neoplasms.[6]

A major problem with all myeloid neoplasias presenting without significant excess of blasts, in particular the cases presenting with monocytosis, is demarcation from reactive

changes. The assumption that this problem might easily be solved by detecting somatic mutations turned out to be a false hope. Matters were complicated by the discovery of "age-related clonal hematopoiesis",[7] also known as "clonal hematopoiesis with indeterminate potential",[8] and "clonal hematopoiesis with oncogenic potential".[9] These conditions are associated with well-known hemato-oncological driver mutations but do not necessarily lead to overt hematologic malignancy. The older the patient, the less certain we can be that detection of a somatic mutation is positive proof of malignant disease.

Against this background, an international working group of hematologists and hemotopathologists met in Vienna and developed proposals on how to tackle the diagnostic problems in the gray area between reactive monocytoses and acute leukemias with monocytosis.[1]

According to their suggestions, the heterogeneous group of reactive monocytoses is now complemented by "idiopathic monocytosis of undetermined significance", which is conceptually equivalent to idiopathic cytopenia of undetermined significance. The category of "idiopathic monocytosis of undetermined significance" includes patients with monocytosis that is neither attributable to a plausible medical cause nor identifiable as a clonal proliferation.

These reactive or unclear monocytoses should be differentiated from clonal disorders that carry a risk of progression to overt CMML or acute myeloid leukemia. Therefore, "clonal monocytosis of undetermined significance" was proposed, in order to classify a disorder that does not yet fulfill the formal criteria of CMML. Very recently, another group showed that patients with clonal monocytosis identified by targeted gene sequencing have a clinical outcome similar to that of those with overt World Health Organization-defined CMML.[10] Accordingly, these "not-yet-CMML" cases might also be called "clonal monocytosis of clinical significance". The relationship between these conditions and CMML resembles that between "clonal cytopenia of undetermined significance" and MDS.[11] Other clonal entities between reactive monocytosis and CMML are "RASopathies", which can develop into juvenile myelomonocytic leukemia, as well as certain histiocytoses.

However, a clinical hematologist is more likely to encounter the three types of CMML, characterized by either a more dysplastic or a more proliferative appearance,

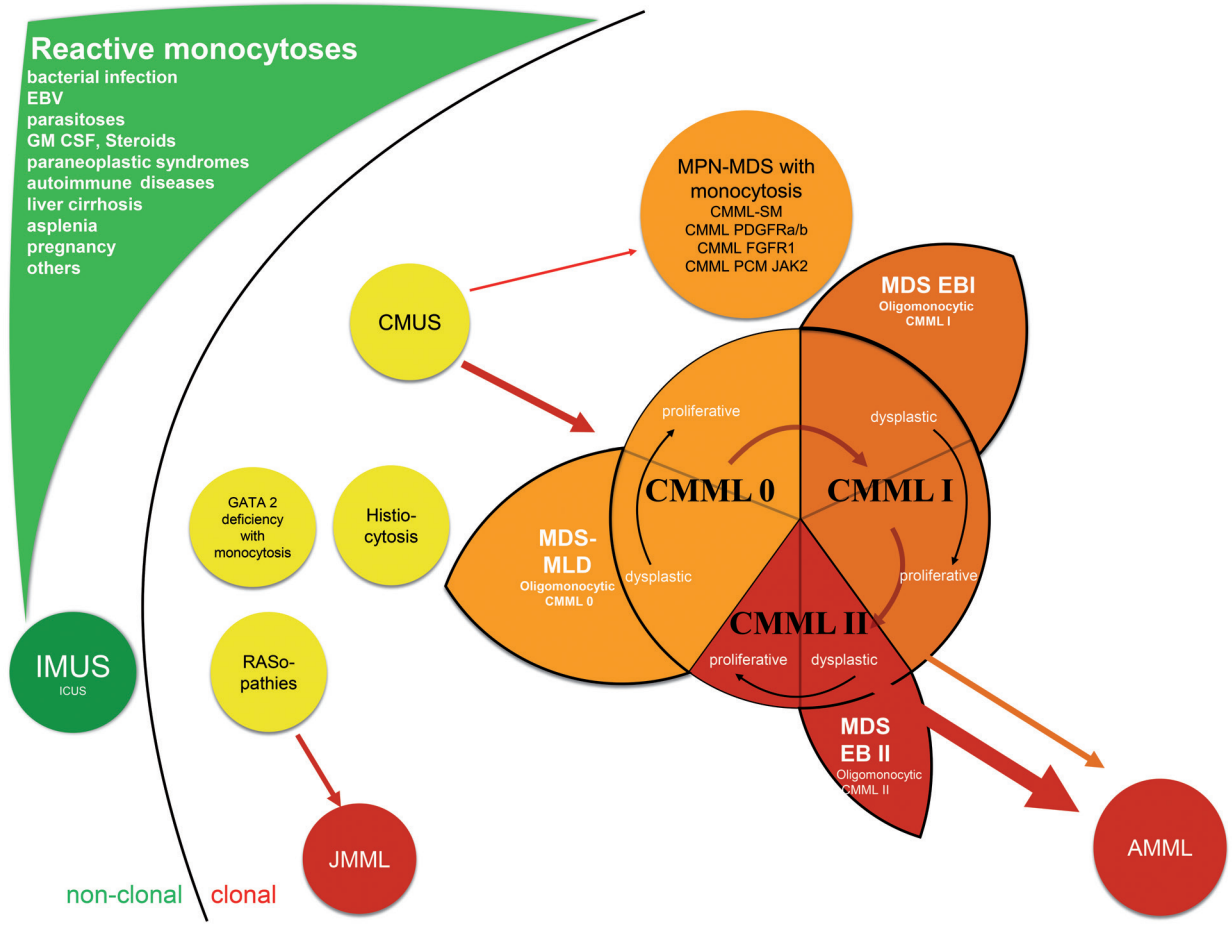

Figure 1. Relationship between different types of clonal monocytosis and demarcation from non-clonal, reactive monocytoses. EBV: Epstein-Barr virus; GM-CSF: granulocyte-macrophage colony-stimulating factor; IMUS: idiopathic monocytosis of undetermined significance; ICUS: idiopathic cytopenia of undetermined significance; CMUS: clonal monocytosis of undetermined significance; MDS-MLD: myelodysplastic syndrome with multilineage dysplasia; MPN-MDS: myeloproliferative neoplasm-myelodyplastic syndrome; CMML-SM: chronic myelomonocytic leukemia with systemic mastocytosis; MDS-EB: myelodysplastic syndrome with excess blasts; JMML: juvenile myelomonocytic leukemia; AMML: acute myelomonocytic leukemia.

based on: (i) the percentage of bone marrow blasts, including promonocytes, and (ii) the white blood cell count in the circulation. The latter criterion, though, is artificial, since most CMML cases present with a white blood cell count of 8-14x10^9/L, often oscillating around the cut-off value of 13x10^9/L.

All types of CMML show similarities with certain types of MDS. The paper by Valent *et al.* refers to a close relationship between MDS with multilineage dysplasia and dysplastic CMML-0, MDS with excess blasts-1 and dysplastic CMML-1, as well as MDS with excess blasts-2 and dysplastic CMML-2. In Figure 1, we try to illustrate the relationships within the large family of monocytoses.

Valent *et al.* propose the term "oligomonocytic CMML" in order to emphasize, as also pointed out by others, that it may be appropriate to diagnose CMML based on bone marrow monocytosis and CMML-typical somatic mutations, even if marked monocytosis is missing in the peripheral blood.[12,13]

The group also points out that CMML can display two different types of acceleration and progression. On the one hand, dysplastic CMML can adopt typical features of MPN by showing accelerated proliferation with organomegaly and constitutional symptoms, without necessarily producing an excess of blasts. This evolution from a dysplastic to a proliferative type may be heralded by increasing white cell counts, often accompanied by splenic enlargement. On the other hand, progression of CMML in terms of increasing blast percentage, i.e. from CMML-0 to CMML-1 or CMML-2, often occurs without a marked increase in white cell count or development of organomegaly. To complicate matters, both types of evolution can occur simultaneously or sequentially, and can be caused (or at least accompanied) by clonal evolution in terms of new somatic mutations, increased variant allele frequencies, or acquisition of chromosomal aberrations. As disease evolution may be more prominent in the bone marrow or peripheral blood, the authors recommend classifying the disease according to the highest blast count detectable.

Finally, the authors recommend complementing the group of CMML entities by including rare MPN-MDS variants, namely CMML with *KIT*D816V$^+$ systemic mastocytosis, and MDS-MPN with *PDGFRA/B*, *FGFR1*, or *PCM-JAK2* rearrangements, because these rare entities are often associated with pronounced monocytosis.

The paper by Valent *et al.* provides a comprehensive description of all the diagnostic tools needed to assign patients to the appropriate category within the heterogeneous group of non-clonal and clonal monocytoses. It summarizes our current knowledge and represents a starting point for future refinements of the classification of bone marrow disorders characterized by monocytosis.

References

1. Valent P, Orazi A, Savona MR, et al. PProposed diagnostic criteria for classical chronic myelomonocytic leukemia (CMML), CMML variants and pre-CMML conditions. Haematologica. 2019;10410):1935-1949.
2. Bennett JM, Catovsky D, Daniel MT, et al. Proposals for the classification of the myelodysplastic syndromes. Br J Haematol. 1982;51(2):189-199.
3. Brunning RD, Bennett JM, Flandrin G, et al. Myelodysplastic syndromes: introduction. In: Jaffe ES, Harris NL, Stein H, Vardiman JW, editors. WHO Classification of Tumours of Haematopoietic and Lymphoid Tissues. 3rd ed. Lyon: IARC; 2001.
4. Orazi A, Bennett JM, Germing U, Brunning RD, Bain BJ, Thiele J. Chronic myelomonocytic leukemia. In: Swerdlow SH, Campo E, Harris NL, Jaffe ES, Pileri SA, Stein H, et al., editors. WHO Classification of Tumours of Haematopoietic and Lymphoid Tissues. Lyon: IARC; 2008.
5. Orazi A, Bennett JM, Germing U, et al. Chronic myelomonocytic leukemia. In: Swerdlow SH, Campo E, Harris NL, Jaffe ES, Pileri SA, Stein H, et al., editors. WHO Classification of Tumours of Haematopoietic and Lymphoid Tissues. Lyon: IARC; 2017.
6. Bowen DT. Chronic myelomonocytic leukemia: lost in classification? Hematol Oncol. 2005;23(1):26-33.
7. Jaiswal S, Fontanillas P, Flannick J, et al. Age-related clonal hematopoiesis associated with adverse outcomes. N Engl J Med. 2014;371(26):2488-2498.
8. Steensma DP, Bejar R, Jaiswal S, et al. Clonal hematopoiesis of indeterminate potential and its distinction from myelodysplastic syndromes. Blood. 2015;126(1):9-16.
9. Valent P, Kern W, Hoermann G, et al. Clonal hematopoiesis with oncogenic potential (CHOP): separation from CHIP and roads to AML. Int J Mol Sci. 2019;20(3).
10. Cargo C, Cullen M, Taylor J, et al. The use of targeted sequencing and flow cytometry to identify patients with a clinically significant monocytosis. Blood. 2019;133(12):1325-1334.
11. Cazzola M. Clonal monocytosis of clinical significance. Blood. 2019;133(12):1271-1272.
12. Geyer JT, Tam W, Liu YC, et al. Oligomonocytic chronic myelomonocytic leukemia (chronic myelomonocytic leukemia without absolute monocytosis) displays a similar clinicopathologic and mutational profile to classical chronic myelomonocytic leukemia. Mod Pathol. 2017;30(9):1213-1222.
13. Schuler E, Frank F, Hildebrandt B, et al. Myelodysplastic syndromes without peripheral monocytosis but with evidence of marrow monocytosis share clinical and molecular characteristics with CMML. Leuk Res. 2018;65:1-4.

p66Shc deficiency sets the scene for clinically aggressive chronic lymphocytic leukemia

Richard Rosenquist

Dept. of Molecular Medicine and Surgery, Karolinska Institutet, Stockholm, Sweden

E-mail: RICHARD ROSENQUIST - richard.rosenquist@ki.se

doi:10.3324/haematol.2019.225904

Chronic lymphocytic leukemia (CLL) is a paradigmatic malignancy in which both cell-extrinsic (microenvironmental) and cell-intrinsic (genetic) factors contribute not only to the pathogenesis of the disease but also to disease evolution and outcome.[1,2] In more recent years, the genomic landscape of CLL has been unraveled with the identification of "driver" gene mutations associated with clinical aggressiveness and chemorefractory disease, such as *ATM*, *BIRC3*, *NOTCH1*, *NFKBIE*, *SF3B1* and *TP53*.[3-5] In addition to genetic aberrations, we also know that the B-cell receptor (BCR) immunoglobulin plays a pivotal role in driving the disease onset and evolution. The somatic hypermutation status of IGHV genes divides patients into two major

clinical subgroups of CLL, with IGHV-unmutated patients displaying a more rapidly progressing disease and an overall poor survival compared with IGHV-mutated patients.[6,7] The importance of BCR signaling was reinforced with the successful introduction of BCR inhibitors (e.g. ibrutinib) in the treatment of CLL, which abrogate downstream BCR signaling and are effective in patients with a poor prognosis, i.e. patients with *TP53* aberrations and/or unmutated IGHV genes.[8] Finally, the micromilieau strongly contributes to CLL cell survival through direct/indirect interactions with different cell types (e.g., T cells, stromal cells) and receptors (e.g. CRCX4 and CCR7), in particular within the proliferation centers in secondary lymphoid organs.[9]

One of the few existing *in vivo* CLL models is the transgenic Eμ-TCL1 mouse, which recapitulates clinically aggressive human CLL.[10] Thanks to this model, it is possible to study the different phases of disease development. In the current issue of Haematologica, Petrussi *et al.* have taken advantage of the Eμ-TCL1 mouse model to investigate the potential role of p66Shc deficiency in CLL pathobiology.[11] The authors previously reported a significant association between p66Shc deficiency and dismal outcome, potentially linking this event to clinical aggressiveness.[12] p66Shc is a Shc family adaptor that promotes production of reactive oxygen species (ROS), which in turn activate cell apoptosis. p66Shc is also known to act as a negative regulator of BCR signaling and to regulate lymphocyte homing by controlling the expression of different chemokine receptors (e.g., CXCR4 and CCR7).[13]

In their present study, Patrussi and colleagues first showed that leukemic B cells from Eμ-TCL1 mice with more advanced disease displayed lower levels of p66Shc expression compared with the levels in normal B cells.[11] STAT4, an essential transcription factor for p66Shc,[14] was also downregulated in Eμ-TCL1 mice. Notably, by treating leukemic Eμ-TCL1 splenic cells with ibrutinib they could restore p66Shc expression along with STAT4 expression, similar to what they had reported earlier in primary CLL.[13]

Next, by crossing the Eμ-TCL1 mice with p66Shc deficient mice, to produce Eμ-TCL1/p66Shc$^{-/-}$ mice, the latter demonstrated a markedly more rapid increase of CD5^{+}/CD19^{+} cells in peripheral blood, a 2-month earlier disease onset and shorter overall survival compared to Eμ-TCL1 mice.[11] When leukemic cells from Eμ-TCL1/p66Shc$^{-/-}$ mice, which expressed higher *Bcl2* levels, were treated with fludarabine, they were more resistant than Eμ-TCL1 cells, indicating that p66Shc loss also contributes to decreased chemo-sensitivity.

The Eμ-TCL1 model also offers the unique possibility to study the pattern of disease infiltration. In Eμ-TCL1/p66Shc$^{-/-}$ mice, an increased accumulation of leukemic cells was observed in both nodal and extranodal sites; higher percentages and proliferation rates of leukemic cells were preferentially seen in lymph nodes, liver and lung, but not in spleen and bone marrow. While expression of CXCR4 was unchanged in leukemic cells, the expression of CCR7, a key lymph node B-cell homing receptor, CCR2 (associated with both lung and liver homing) and CXCR3 (linked to lung homing) was higher in Eμ-TCL1/p66Shc$^{-/-}$ leukemic cells than in cells from Eμ-TCL1 mice.[11] Hence, a more efficient accumulation in nodal and extranodal sites appears to depend on distorted chemokine receptor expression due to p66Shc deficiency.

p66Shc deficiency was also confirmed in primary CLL cells, in particular in IGHV-unmutated CLL; however, the authors could not find any correlation with 13q deletion or *TP53* aberrations. Similar to Eμ-TCL1/p66Shc$^{-/-}$ mice, both CCR2 and CXCR3 were overexpressed in IGHV-unmutated CLL, and p66Shc re-expression in CLL cells resulted in decreases in CCR2 and CXCR3 mRNA expression. The number and size of infiltrated lymph nodes and presence of spleen and/or liver enlargement were also higher in patients with low p66Shc mRNA levels. Interestingly, the authors observed that p66Shc expression was higher in CLL patients with a known response to second-line ibrutinib treatment than in patients who did not respond.

Finally, Patrussi *et al.* demonstrated a correlation between decreased ROS production and p66Shc deficiency both in CLL cells and Eμ-TCL1/p66Shc$^{-/-}$ cells.[11] Using transfection experiments, wildtype p66Shc-expressing transfectants, but not the ROS-defective mutant, showed lower CCR2 and CXCR3 expression compared to control cells, implying that p66Shc directly modulates CCR2 and CXCR3 expression through elevation of ROS.

Based on the novel results from this study, p66Shc deficiency in Eμ-TCL1 mice was shown to accelerate disease onset and progression to an aggressive phenotype. The authors also followed organ selectivity which correlated with deregulation of specific chemokine receptors. Importantly, p66Shc expression could be restored by ibrutinib treatment, along with enhanced chemo-sensitivity. Considering the potential role of p66Shc deficiency preceding a more aggressive phase of the disease, it will now be important to follow CLL patients longitudinally and in relation to therapy in order to determine if p66Shc could be used as a potential biomarker. Could p66Shc expression predict a shift from a more indolent to a more aggressive disease in need of therapy? Could p66Shc be monitored after treatment with chemo-immunotherapy or targeted therapy as an early indicator of disease progression/chemo-refractoriness? From a biological point of view, it will also be important to identify what cellular/molecular factors are involved in and lead to p66Shc downregulation. Do other cell types in the CLL microenvironment influence p66Shc levels? Is there any correlation with gene mutations affecting key cellular pathways and processes linked to an aggressive phenotype or chemo-resistance? While the study by Petrussi *et al.* using Eμ-TCL1/p66Shc$^{-/-}$ mice has provided us with important insights, further studies are now necessary to investigate the potential clinical role of p66Shc deficiency, preferably in uniformly treated cohorts and involving novel therapies.

References

1. Sutton LA, Rosenquist R. Deciphering the molecular landscape in chronic lymphocytic leukemia: time frame of disease evolution. Haematologica. 2015;100(1):7-16.
2. Sutton LA, Rosenquist R. The complex interplay between cell-intrinsic and cell-extrinsic factors driving the evolution of chronic lymphocytic leukemia. Semin Cancer Biol. 2015;34:22-35.

3. Landau DA, Tausch E, Taylor-Weiner AN, et al. Mutations driving CLL and their evolution in progression and relapse. Nature. 2015;526(7574):525-530.
4. Mansouri L, Sutton LA, Ljungstrom V, et al. Functional loss of IkappaBepsilon leads to NF-kappaB deregulation in aggressive chronic lymphocytic leukemia. J Exp Med. 2015;212(6):833-843.
5. Puente XS, Bea S, Valdes-Mas R, et al. Non-coding recurrent mutations in chronic lymphocytic leukaemia. Nature. 2015;526(7574):519-524.
6. Rosenquist R, Ghia P, Hadzidimitriou A, et al. Immunoglobulin gene sequence analysis in chronic lymphocytic leukemia: updated ERIC recommendations. Leukemia. 2017;31(7):1477-1481.
7. Sutton LA, Hadzidimitriou A, Baliakas P, et al. Immunoglobulin genes in chronic lymphocytic leukemia: key to understanding the disease and improving risk stratification. Haematologica. 2017;102(6):968-971.
8. Byrd JC, O'Brien S, James DF. Ibrutinib in relapsed chronic lymphocytic leukemia. N Engl J Med. 2013;369(13):1278-1279.
9. Caligaris-Cappio F, Bertilaccio MT, Scielzo C. How the microenvironment wires the natural history of chronic lymphocytic leukemia. Semin Cancer Biol. 2014;24:43-48.
10. Johnson AJ, Lucas DM, Muthusamy N, et al. Characterization of the TCL-1 transgenic mouse as a preclinical drug development tool for human chronic lymphocytic leukemia. Blood. 2006;108(4):1334-1338.
11. Patrussi L, Capitani N, Ulivieri C, et al. p66Shc deficiency in the Emu-TCL1 mouse model of chronic lymphocytic leukemia enhances leukemogenesis by altering the chemokine receptor landscape. Haematologica. 2019;104(10):2040-2052.
12. Capitani N, Lucherini OM, Sozzi E, et al. Impaired expression of p66Shc, a novel regulator of B-cell survival, in chronic lymphocytic leukemia. Blood. 2010;115(18):3726-3736.
13. Patrussi L, Capitani N, Cattaneo F, et al. p66Shc deficiency enhances CXCR4 and CCR7 recycling in CLL B cells by facilitating their dephosphorylation-dependent release from beta-arrestin at early endosomes. Oncogene. 2018;37(11):1534-1550.
14. Cattaneo F, Patrussi L, Capitani N, et al. Expression of the p66Shc protein adaptor is regulated by the activator of transcription STAT4 in normal and chronic lymphocytic leukemia B cells. Oncotarget. 2016;7(35):57086-57098.

Hereditary thrombotic thrombocytopenic purpura

Marie Scully

Department of Haematology, UCLH and Cardiometabolic Programme-NIHR UCLH/UC BRC London, UK

E-mail: MARIE SCULLY - m.scully@nhs.net

doi:10.3324/haematol.2019.225896

The first description of thrombotic thrombocytopenic purpura (TTP) by Moschowitz was published nearly 100 years ago.[1] This was likely to have been an immune-mediated TTP episode and the author described multi organs affected with worsening, untreated disease. Accounts of hereditary TTP were otherwise acknowledged to be Upshaw Shulman syndrome. In 1960, Schulman reported an 8-year old girl who had repeated episodes of thrombocytopenia and hemolytic anemia from infancy. Treatment with plasma was associated with normalization of the platelet count and resolution of hemolysis, and remission was maintained with prophylactic plasma every 1-2 weeks.[2] Upshaw presented a 16-year old girl with relapsing hemolytic anemia and thrombocytopenia since infancy. The patient responded to blood transfusions. During the next 11 years, Upshaw treated 32 episodes of thrombocytopenia and microangiopathic hemolysis with plasma infusions. The acute episodes invariably had a trigger, such as a minor infection, surgical procedure, pregnancy, or pancreatitis. Acute intervals lasted from three weeks to 20 months, at which time the platelet count was normal and there was a compensated hemolysis. Between these acute episodes, it was observed that intravascular platelet and red cell survival was shortened; these abnormalities normalized after the infusion of two units of plasma.[3]

In this edition of *Haematologica*, Van Dorland *et al.*[4] present an international collaborative study on hereditary TTP. As an ultra-rare disorder, collection of meaningful data is critical to understand the clinical features of this condition, the therapy, and the long-term impact. The international registry presents data from over an 11-year period, incorporating 123 patients from four continents who presented the disease from the neonatal period, up to the seventh decade of life. We know, from numerous publications relating to the mutations identified in hereditary TTP, that there is a heterogenous distribution throughout the *ADAMTS 13* gene.[5-8] There are, however, two specific variants that have been identified at increased frequency in hereditary TTP. R1060W, exon 24, is prominent in Caucasians presenting with late onset congenital TTP specifically associated with pregnancy.[9,10] Within the international hereditary TTP registry, c.4143_4144dupA (exon 29; p.Glu1382Argfs*6) was prevalent, specifically within northern Europe, and was initially described at increased prevalence from central Norway.[11] Further cases were documented in the international registry, confirming that those patients with compound heterozygous mutations were more likely to have an earlier presentation, specifically in the neonatal period. There were other mutations which have been identified in more than one individual in the international registry. This allows us to predict the impact of such variations within the *ADAMTS 13* gene with respect to clinical features. Such observations are only possible within the breadth of a registry.[4]

The international registry has identified the significant delay in diagnosis of hereditary TTP; overall median age of overt presentation was 4.5 years but the clinical diagnosis was not made until a median of 16.7 years. Acute TTP episodes occurred at a median rate of 0.1 per year, ranging up to nine per year, and triggers included infections, childbirth, trauma, and in males, excess alcohol intake. The median time to resolution following an acute presentation was seven days.

There was an equal male to female ratio; this is in contrast to immune-mediated disease, which has a female preponderance. Residual ADAMTS 13 activity could not reliably predict age of onset or, indeed, disease severity, despite a cut-off of 1%. This may also help to explain why patients with identical genetic variants have significant differences in the clinical phenotype. What is particularly striking and important is the clinical impact of hereditary TTP: 1) the degree of end-organ damage symptoms, either at presentation or as complications of the disease; and 2) the proportion of patients with arterial thromboembolic events, present in 28% and covering all age groups. This was especially striking in 40-50 years old; >50% of these patients had at least one arterial thromboembolic event.

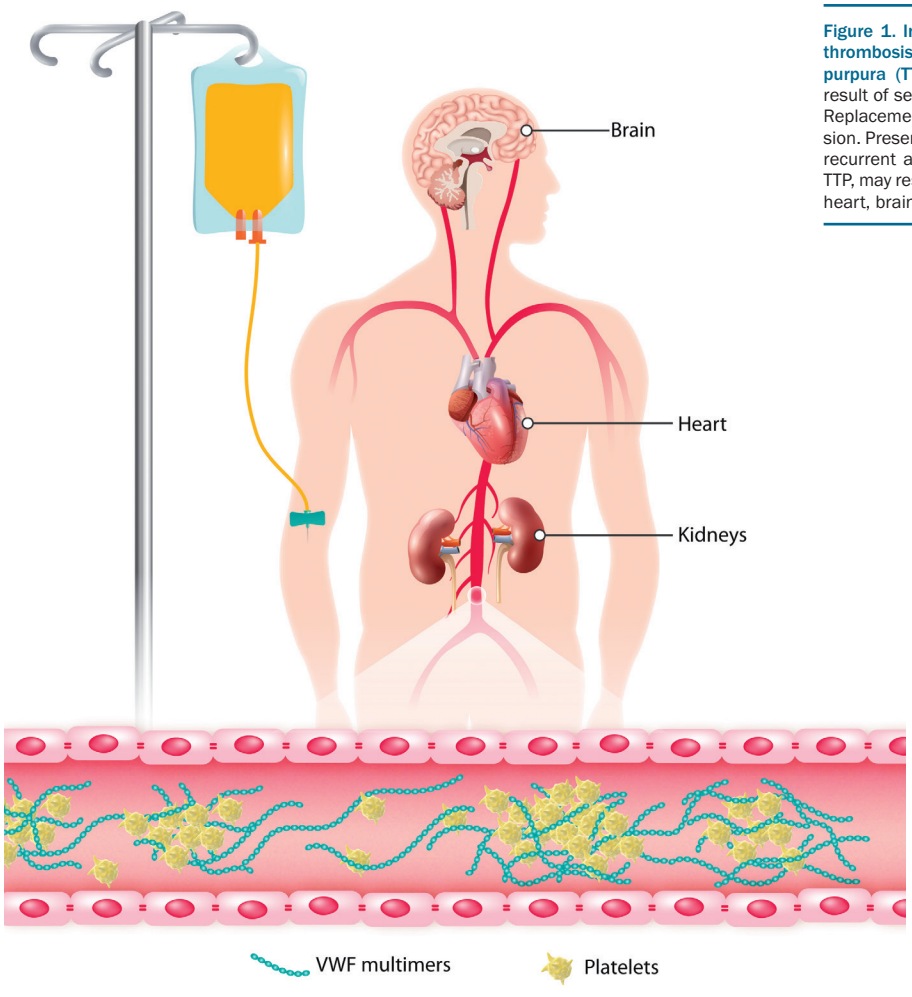

Figure 1. Impact of acute and long-term microvascular thrombosis in congenital thrombotic thrombocytopenic purpura (TTP). Microvascular thrombi formation is the result of severe ADAMTS 13 deficiency in congenital TTP. Replacement of ADAMTS 13 is currently *via* plasma infusion. Presentation of acute TTP episodes, or the impact of recurrent acute or subacute TTP episodes in hereditary TTP, may result in organ damage, specifically affecting the heart, brain and kidneys.

Other neurological complications include epilepsy, headaches, and a significant history of psychiatric symptoms. Renal impairment occurred in 26%, some patients requiring renal replacement therapy or renal transplant and nearly 50% experiencing jaundice/liver disease.

Complimentary findings relating to the longer-term impact of hereditary TTP on end-organ damage were captured within the UK TTP registry. Furthermore, the latter cohort identified non-overt symptoms, including headaches, lethargy, and abdominal pain that, despite a normal platelet count, responded to regular plasma infusion. Indeed, ADAMTS 13 replacement therapy, primarily using plasma infusion, was associated with resolution of proteinuria and a significant reduction in stroke in those receiving treatment compared to patients not on a regular regime.[12] The proportion of patients on replacement therapy within the international registry was surprising. However, nearly one-third of the cohort only received treatment on demand.[4] Both recent papers, therefore, raise the question of treatment in hereditary TTP. Firstly, the frequency of therapy. Despite a half-life of ADAMTS 13 of 2-4 days,[13] in the international registry, trough levels were reached within 7-10 days. This has also been shown in a recent pharmacokinetic study in hereditary TTP.[14] We need to reconsider how we treat patients, with particular attention to the dose of plasma and the frequency. The completion of the phase I trial of recombinant ADAMTS 13, which was the first-in-human trial, using increasing doses, offers a significant advancement in the future treatment of patients with hereditary TTP, delivering a pure form of the deficient enzyme, ADAMTS 13.[15]

In summary, the international registry presents the impact of hereditary TTP on end-organ damage, which is evident much earlier than expected within the general population; the most prevalent is arterial disease affecting the brain, heart and kidneys. Based on this important international collaborative study, in conjunction with other large cohorts, we must question how we should treat patients in the form of prophylactic ADAMTS 13 replacement (Figure 1). Should all patients with hereditary TTP be on prophylaxis? Do we wait for the patient to experience frequent acute episodes before initiating therapy? Given the increased risk, particularly of arterial events after the age of 40, at what age should prophylaxis be initiated? What is the correct frequency of prophylaxis and what ADAMTS 13 activity level should we be aiming to achieve? Specific genetic variants may be the catalyst to personalized ADAMTS 13 replacement protocols. While there are many questions to be answered, without the information from important registries incorporating larger patient numbers the clinical impact of this ultra-rare disease cannot be addressed.

References

1. Moschowitz E. An acute febrile pleiochromic anemia with hyaline thrombosis of terminal arterioles and capillaries: An undescribed disease. Arch Intern Med.1925;36:89.
2. Schulman I, Pierce M, Lukens A, Currimbhoy Z. Studies on thrombopoiesis. I. A factor in normal human plasma required for platelet production; chronic thrombocytopenia due to its deficiency. Blood. 1960;16:943-957.
3. Upshaw JD Jr. Congenital deficiency of a factor in normal plasma that reverses microangiopathic hemolysis and thrombocytopenia. N Engl J Med. 1978;298(24):1350-1352.
4. van Dorland HA, Mansouri Taleghani M, et al. The International Hereditary Thrombotic Thrombocytopenic Purpura Registry: Key findings at enrolment until 2017. Haematologica. 2019;104(10):2107-2116.
5. Kinoshita S, Yoshioka A, Park YD, et al. Upshaw-Schulman syndrome revisited: a concept of congenital thrombotic thrombocytopenic purpura. Int J Hematol. 2001;74(1):101-108.
6. Kokame K, Matsumoto M, Soejima K, et al. Mutations and common polymorphisms in ADAMTS13 gene responsible for von Willebrand factor-cleaving protease activity. Proc Natl Acad Sci U S A. 2002;99(18):11902-11907.
7. Lotta LA, Garagiola I, Palla R, Cairo A, Peyvandi F. ADAMTS13 mutations and polymorphisms in congenital thrombotic thrombocytopenic purpura. Hum Mutat. 2010;31(1):11-19.
8. Levy GG, Nichols WC, Lian EC, et al. Mutations in a member of the ADAMTS gene family cause thrombotic thrombocytopenic purpura. Nature. 2001;413(6855):488-494.
9. Scully M, Thomas M, Underwood M, et al. Thrombotic thrombocytopenic purpura and pregnancy: presentation, management, and subsequent pregnancy outcomes. Blood. 2014;124(2):211-219.
10. Camilleri RS, Cohen H, Mackie IJ, et al. Prevalence of the ADAMTS-13 missense mutation R1060W in late onset adult thrombotic thrombocytopenic purpura. J Thromb Haemost. 2008;6(2):331-338.
11. von Krogh AS, Quist-Paulsen P, Waage A, et al. High prevalence of hereditary thrombotic thrombocytopenic purpura in central Norway: from clinical observation to evidence. J Thromb Haemost. 2016;14(1):73-82.
12. Alwan F, Vendramin C, Liesner R, et al. Characterization and treatment of congenital thrombotic thrombocytopenic purpura. Blood. 2019;133(15):1644-1651.
13. Furlan M, Robles R, Morselli B, Sandoz P, Lammle B. Recovery and half-life of von Willebrand factor-cleaving protease after plasma therapy in patients with thrombotic thrombocytopenic purpura. Thromb Haemost. 1999;81(1):8-13.
14. Taylor A, Vendramin C, Oosterholt S, Della Pasqua O, Scully M. Pharmacokinetics of plasma infusion in congenital thrombotic thrombocytopenic purpura. J Thromb Haemost. 2019;17(1):88-98.
15. Scully M, Hibbard C, Ewenstein B. Recombinant ADAMTS 13 in thrombotic thrombocytopenic purpura. Oncoscience. 2017;4(11-12):160-161.

REVIEW ARTICLE

To be red or white: lineage commitment and maintenance of the hematopoietic system by the "inner myeloid"

Hiroki Kato[1,2,3] and Kazuhiko Igarashi[1]

[1]Department of Biochemistry, Tohoku University Graduate School of Medicine, Sendai, Japan; [2]Department of Hematology and Rheumatology, Tohoku University Graduate School of Medicine, Sendai, Japan and [3]Present address, Center for Regenerative Medicine, Massachusetts General Hospital, Boston, MA, USA

Ferrata Storti Foundation

Haematologica 2019
Volume 104(10):1919-1927

ABSTRACT

Differentiation of hematopoietic stem and progenitor cells is tightly regulated depending on environmental changes in order to maintain homeostasis. Transcription factors direct the development of hematopoietic cells, such as GATA-1 for erythropoiesis and PU.1 for myelopoiesis. However, recent findings obtained from single-cell analyses raise the question of whether these transcription factors are "initiators" or just "executors" of differentiation, leaving the initiation of hematopoietic stem and progenitor cell differentiation (i.e. lineage commitment) unclear. While a stochastic process is likely involved in commitment, it cannot fully explain the homeostasis of hematopoiesis nor "on-demand" hematopoiesis in response to environmental changes. Transcription factors BACH1 and BACH2 may regulate both commitment and on-demand hematopoiesis because they control erythroid-myeloid and lymphoid-myeloid differentiation by repressing the myeloid program, and their activities are repressed in response to infectious and inflammatory conditions. We summarize possible mechanisms of lineage commitment of hematopoietic stem and progenitor cells suggested by recent findings and discuss the erythroid and lymphoid commitment of hematopoietic stem and progenitor cells, focusing on the gene regulatory network composed of genes encoding key transcription factors. Surprising similarity exists between commitment to erythroid and lymphoid lineages, including repression of the myeloid program by BACH factors. The suggested gene regulatory network of BACH factors sheds light on the myeloid-based model of hematopoiesis. This model will help to understand the tuning of hematopoiesis in higher eukaryotes in the steady-state condition as well as in emergency conditions, the evolutional history of the system, aging and hematopoietic disorders.

Introduction

Hematopoietic stem cells (HSC) possess the abilities of self-renewal and multilineage differentiation, including that to red and white blood cells and platelets (i.e., erythrocytes, megakaryocytes, innate immune cells and acquired immune cells).[1] Salient aspects of the hematopoietic system include its potential to produce huge numbers of cells with distinct functions throughout the life span of a human and its tunability, by which the output is balanced in response to environmental changes, such as from the steady state to an infectious state.

Erythrocytes are the most abundant cells in the human body, accounting for around 70% of the total cell number[2] and 200x10^9 erythrocytes are produced daily.[3] Although the estimated number of white blood cells is much lower than that of erythrocytes,[2] the short life span of myeloid cells necessitates the production of a huge number of these cells as well. For instance, the circulating half-life of neutrophils is 6-8 h, and their estimated production rate is 50-100x10^9 cells per day.[4] In line with this, label tracing analyses of HSC have revealed that the production rate of erythroid-myeloid progenitors is about 180 times higher than that of lymphoid progenitors in unperturbed hematopoiesis.[5] Thus, hematopoietic

Correspondence:

KAZUHIKO IGARASHI
igarashi@med.tohoku.ac.jp

Received: February 14, 2019.

Accepted: May 10, 2019.

Pre-published: September 12, 2019.

doi:10.3324/haematol.2019.216861

Check the online version for the most updated information on this article, online supplements, and information on authorship & disclosures: www.haematologica.org/content/104/10/1919

stem and progenitor cells (HSPC) have an exceptionally vigorous ability to produce huge numbers of cells constitutively. To maintain its homeostasis, the production pace of each mature cell lineage must be tightly regulated according to environmental changes ("on-demand" hematopoiesis).

Infection is one of the most common challenges facing hematopoiesis and evokes the induction of myelopoiesis as well as the suppression of erythropoiesis.[6] Induced myelopoiesis during an infection is an effective way of eliminating pathogens, whereas the repression of erythropoiesis may help by limiting the availability of nutritional iron supply to pathogens and/or red blood cells as a target of infection, such as in malaria infection.[7] However, infection and prolonged inflammation can cause anemia of inflammation, which is the second-most prevalent type of anemia after iron-deficiency anemia.[8]

As with infection, the activity of HSPC is also altered with aging and in various disease conditions. The production of erythrocytes is often reduced in elderly people, leading to anemia,[9] and acquired immunity becomes less effective with aging, which can result in increased susceptibility to infectious diseases and malignancy in the elderly.[10,11] In contrast, the production of myeloid cells often increases with aging.[11,12] This skewed trajectory selection of HSPC induced by aging might be related to the development of aging-related hematopoietic disorders, such as myelodysplastic syndrome (MDS). Although the molecular mechanisms by which the function and differentiation of HSPC are altered by aging are still largely unknown, emerging evidence suggests contributions of inflammation and/or inflammatory signaling to aging of HSPC.[13]

In order to facilitate the treatment of infection-associated and aging-associated diseases, it is important to understand the mechanisms by which the differentiation trajectory of HSPC and their commitment are defined at steady state and how these mechanisms are altered in inflammatory conditions. Although accumulating knowledge has shown that transcription factors (TF) play central roles in the differentiation of HSPC, the precise mechanisms underlying the initial lineage commitment and "on-demand" hematopoiesis are still unclear and cannot be wholly attributed to TF. Complicating matters further is the fact that HSPC are substantially heterogeneous and many appear to be already committed to certain differentiation fates.[14-16] It is, therefore, important to distinguish the roles of TF in initiating the commitment of uncommitted progenitors from that of their executive roles in the progression of differentiation toward a particular fate. Thus, the actual point of differentiation commitment may need to be reconsidered.

We recently demonstrated the roles of BTB and CNC homology (BACH) TF, BACH1 and BACH2 (BACH factors), in instructing erythroid-myeloid progenitors and lymphoid-myeloid progenitors to respond to environmental changes.[17-19] BACH factors form heterodimers with small Maf proteins to bind to the Maf recognition element (MARE), which contains an AP-1 site.[20] Importantly, AP-1 sites play central roles in hematopoietic cell immune reactions.[20,21] BACH1 plays important roles in the maturation of erythrocytes by balancing heme and globin proportions, especially in the condition of iron deficiency,[22] whereas BACH2 plays important roles in the development of plasma cells, memory B cells, regulatory T cells and memory T cells.[23-30] These findings suggest ubiquitous roles for BACH factors in the maintenance of homeostasis in both steady-state and inflammatory-state hematopoiesis, as described below.

In this review, we summarize the latest findings concerning the mechanisms underlying lineage commitment of HSPC and potential questions to be addressed. We also discuss gene regulatory networks composed of genes encoding key TF which compete for lineage identities and downstream genes encoding effector molecules, focusing particularly on erythroid-myeloid and lymphoid-myeloid differentiation, two major points of commitment in HSPC differentiation. In addition, we review the roles of BACH factors in the myeloid-based model of hematopoiesis, which may provide a new concept of the fundamental mechanism in HSPC differentiation, and its meaning in an evolutionary perspective. We also discuss the diverse functions of BACH factors in mature hematopoietic cells as a strategy to cope with environmental changes through the maintenance of hematopoiesis. Finally, we describe how changes in lineage commitment can lead to diseases, such as anemia of inflammation and MDS.

Lineage commitment of hematopoietic stem and progenitor cells

The multipotency of HSC has been demonstrated by single-cell transplantation into irradiated mice.[31] This led to vigorous investigations into how HSC differentiate into diverse lineages of cells with distinct functions. The isolation and characterization of progenitor cells led to the idea that HSC gradually and systematically lose multipotency, generating progenitor cells with limited differentiation trajectories, such as common myeloid progenitors (CMP),[32] which can generate myeloid cells and erythroid cells but not lymphoid cells. On the other hand, although all blood cells derive from a $FLT3^+$ multipotent progenitor stage,[33] lymphoid-primed multipotent progenitors (LMPP) preferentially differentiate into lymphoid cells and myeloid cells with a low differentiation potential to erythroid cells.[34-36] This led to the recognition that HSC eventually lose their ability to differentiate to erythroid or lymphoid cells, leaving erythroid-myeloid bifurcation and lymphoid-myeloid bifurcation as the two major subsequent points of branching.

Such subpopulations of progenitors have been defined based on the presence or absence of a limited number of cell surface markers, leaving the potential impurity of these subpopulations as a limitation. Indeed, recent comprehensive, single-cell transcriptomic analyses have shown that the known subpopulations of HSPC are composed of heterogeneous cells in terms of gene expression.[14,16] In addition, *in vitro* and *in vivo* single-cell differentiation analyses have shown that only a limited number of cells in progenitor cell populations can produce multilineage mature cells and that a majority of the cells in these populations are already committed to become unilineage mature cells.[14,15] Furthermore, an *in vivo* HSC chasing system using endogenous fluorescent tagging revealed that the differentiation trajectory of HSC is already oriented to specific lineage outputs by epigenetic memory.[37] These observations raise two possibilities: (i) HSPC can be further divided into subpopula-

tions representing pure differentiation bifurcation points; or (ii) lineage commitments occur only in HSC, whereas each progenitor population is a mixture of committed cells sharing the same cell surface markers at the time of isolation. Since single-cell differentiation analysis from CMP and LMPP showed that a minor part of these populations can produce multilineage mature cells,[14,15] there might be further subpopulations that represent actual bifurcation points of erythroid-myeloid or lymphoid-myeloid differentiation. However, whether or not these hypothetical subpopulations can be defined using additional cell surface markers remains unclear. Before addressing these two possibilities, we need to stop and consider the potential limitations of recent studies using single-cell analyses. A single-cell transcriptomic analysis is a 'snapshot' observation. Therefore, if a set of genes shows dynamic fluctuations in expression with coherent patterns in cells of a specific subpopulation, these cells might be considered heterogeneous. However, these subpopulations can be homogenous when time-dependent fluctuations are considered, like those observed in neural progenitors.[38] In addition, despite the importance of the microenvironment for HSPC biology,[39] an *ex vivo* single-cell transcriptomic analysis is devoid of anatomical information. Furthermore, single-cell *in vivo* or *in vitro* differentiation analyses can only examine the differentiation potential under stress and/or artificial conditions (i.e., cell sorting, culture and transplantation into irradiated mice), which can skew the original differentiation trajectory of progenitor cells,[40] possibly by altering activities of critical TF whose expression is thought to be maintained to some extent for multilineage priming,[41] a state in which multiple, conflicting lineage-affiliated genes can be induced or co-expressed. In other words, there is a chance that progenitor cells with unilineage output potential in perturbed conditions still possess multilineage output potential in an unperturbed condition. Recent studies using single-cell analyses may, therefore, lack information about the dynamics (time and three-dimensional information) of lineage commitment,[42] especially regarding unperturbed hematopoiesis. Potential effects of circadian rhythm in HSC differentiation might also have to be considered.[43] The analysis of entropy in gene expression within single cells[44] and the three-dimensional detection of transcriptomics[45] might be helpful. Remarkably, recent *in vivo* barcoding analyses give new support to the existence of a hierarchical development model in hematopoiesis.[46,47]

We must therefore reconsider the actual point at which lineage commitment occurs. An alternative approach to define such a point involves using the regulatory mechanisms of the differentiation of HSPC. To this end, the precise understanding of gene regulatory networks governed by TF may provide a dynamic view of lineage commitment.

This leads us to the second point that should be considered: how are the differentiation trajectories shaped and restricted along the path of differentiation? Several models of lineage commitment have been proposed, showing that TF are critical to shaping and resolving the patterns of lineage-affiliated gene expression.[48-50] One model features a network of two TF, each promoting differentiation into a specific lineage. If the expression of these two TF is inhibited in a mutual manner and thus they induce their own expression, they can define two cell types with distinct expression patterns of the two TF and thus their downstream target genes (Figure 1).[48] Machine-learning methods using single-cell transcriptomic data support the notion that gradual, stochastic changes in a few TF have a strong influence on the lineage commitment of progenitor cells.[50] Such a gene regulatory network may therefore dictate lineage commitment.

However, it has been unclear how one or the other of these TF are initially upregulated or downregulated upon lineage commitment. Stochastic fluctuation in these TF may be involved,[48] but the output of hematopoiesis should be dynamically tuned in response to diverse stressors, as HSPC produce huge numbers of mature cells daily in a fine balance, as noted above. This property of the hematopoietic system may not therefore be fully explained merely by the stochastic fluctuation of TF. The differentiation trajectory of HSPC must be tightly controlled by responding to environmental changes in order to maintain homeostasis. This means that environmental factors, including pathogen-associated molecular patterns (PAMP) and damage-associated molecular patterns (DAMP),[51] may affect the cell-intrinsic TF of gene regulatory networks that control the differentiation trajectory. It is therefore important to understand how cell-intrinsic systems of TF are connected to extrinsic signals.

The gene regulatory network for erythroid lineage commitment

Erythroid cells are derived from progenitor cells that possess the ability to differentiate into erythroid or myeloid cells.[1,52] CMP have long been considered to represent a bifurcation point of erythroid-myeloid differentiation.[32] However, single-cell analyses have challenged this notion. A single-cell RNA sequencing analysis of c-kit$^+$Sca1$^-$lineage$^-$ bone marrow cells revealed at least seven different subpopulations with lineage priming at the transcriptomic level.[16] Importantly, no subpopulations with multilineage priming were observed in that

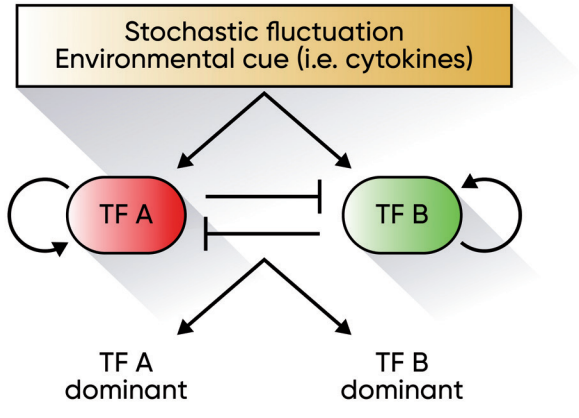

Figure 1. Stochastic model of lineage commitment. Transcription factors (TF) A and TF B play important roles in determining cell differentiation. If these two TF activate themselves and work in a mutually exclusive manner, slight stochastic fluctuations that alter the ratio of TF A to B can affect cell fate.

study. In addition, a barcoded progenitor cell transplantation analysis revealed that the majority of CMP can differentiate into only erythroid or myeloid cells after transplantation.[15] Therefore, CMP are a highly heterogeneous population of progenitor cells, and the dominant populations in CMP are already committed to erythroid or myeloid differentiation. However, it should be noted that these findings were obtained from a "snapshot" analysis, which may have overlooked the plasticity of differentiation potential or gene expression patterns in CMP. Indeed, the introduction of specific TF (such as GATA-1 and DDIT3) into myeloid lineage progenitors can switch the lineage output to the erythroid lineage, suggesting the existence of plasticity under the control of TF in erythroid-myeloid progenitors.[53,54] This idea is not surprising when we consider the fact that TF often alter the epigenetic modifications for lineage commitment (e.g., via pioneer TF[55]) and that epigenetic changes *per se* are reversible.[56,57] Therefore, the observed subpopulations of CMP may show plasticity under physiological conditions, which can be masked during transplantation. In this context, it is still too early to conclude that CMP are heterogeneous populations of already committed progenitors. Further investigations combining single-cell chasing with the comprehensive measurement of epigenomes and transcriptomes in unperturbed conditions will be needed.

In the view of the gene regulatory networks at the erythroid-myeloid bifurcation, key TF, including the CCAAT-enhancer-binding protein (C/EBP) family,[58,59] PU.1[60] and GATA-1,[61] play essential roles in erythroid or myeloid differentiation, which might operate the erythroid-myeloid bifurcation at the level of CMP or multipotent progenitors. Given that GATA-1 and PU.1 show mutually exclusive expression patterns during erythroid and myeloid differentiation and repress each other and activate themselves, the gene regulatory network of *GATA1* and *SPI1* (encoding PU.1) may determine the bifurcation of myeloid and erythroid cells.[48] In this model, stochastic alterations in the ratio of GATA1 to PU.1 activity might initiate the differentiation. However, a recent study found that *GATA1* and *SPI1* are not co-expressed in CMP.[62] Upon erythroid differentiation, the expression of *GATA1* commences with a substantial lag after the cessation of *SPI1* expression. In contrast, upon myeloid differentiation, no progenitor cells showed a period with *GATA1* expression.[62] Thus, GATA-1 may not be the initiator of erythroid differentiation but just the executor of the erythroid development from progenitor cells whose erythroid commitment has already been defined by unknown factors. Recent single-cell proteomic analyses additionally revealed that the TF KLF1 and FLI1 play important roles in the bifurcation of erythroid and megakaryocytes.[63]

Since erythroid cells and myeloid cells are rigorously produced from progenitor cells every day, as described above, there should exist a mechanism to fine tune the differentiation trajectory shift of erythroid-myeloid common progenitor cells depending on the demand, which can vary with environmental changes. For instance, infections and inflammation induce myeloid differentiation and reduce erythroid differentiation, which can lead to anemia of inflammation. It has long been accepted that the major cause of this form of anemia is a disorder of iron utility for erythroid maturation caused by the induction of hepcidin, which inhibits iron uptake and recycling.[8] However, since iron supplementation for the treatment of anemia of inflammation is still controversial[8,64] and infections as well as inflammation can induce a shift in the differentiation trajectory at the level of erythroid-myeloid progenitors,[65] there may be other factors that modulate the differentiation trajectory of progenitors, depending on environmental changes.

We recently reported that BACH factors are required for the efficient commitment of HSPC to an erythroid fate.[19] BACH factors inhibit the expression of *Cebpb*, the gene encoding the TF C/EBPβ, which plays an indispensable role in emergency myelopoiesis.[59] Importantly, BACH factors and C/EBPβ exert opposite effects on their downstream target genes: BACH factors repress a set of myeloid-affiliated genes, whereas C/EBPβ activates these genes at the same genomic loci. Since both BACH factors and the C/EBP family can bind to AP-1 motifs, the balance between repression and activation via the AP-1 motif appears to be critical for determining myeloid fate[21,66] (Figure 2). Since infectious stimuli repress the expression of BACH factors and induce C/EBPβ expression,[18,19] the gene regulatory network of these TF genes can fluctuate in response to environmental input between two states, which correspond to erythroid and myeloid fates.

The gene regulatory network for lymphoid lineage commitment

Lymphoid cells are also derived from common progenitor cells that possess the ability to differentiate into lymphoid or myeloid cells. LMPP are now considered such common progenitors.[1,34,52] Similar to the single-cell transcriptomic observations in CMP, a single-cell analysis of LMPP also showed that LMPP are a heterogeneous population.[14] For instance, a single-cell *in vitro* differentiation assay showed that most LMPP were only able to differentiate into either myeloid or lymphoid cells.[14] Therefore, most LMPP may be cells whose differentia-

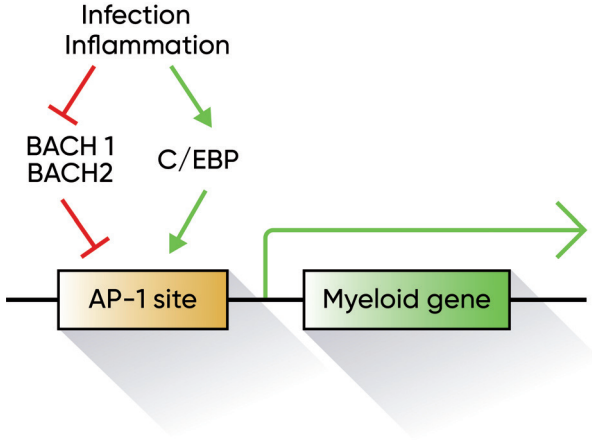

Figure 2. Control of myeloid gene expression by BACH and C/EBP transcription factors in a state of infection. The BACH and C/EBP transcription factors (TF) repress and activate, respectively, myeloid gene expression by binding the same genomic loci. Infection/inflammation-induced alteration of these TF can affect myeloid gene expression, depending on the environment.

tion commitment has already been decided. However, there may be pitfalls associated with these observations, similar to those regarding erythroid-myeloid bifurcation. The presence of myeloid-lymphoid progenitors is also supported by the findings of an analysis of lymphopoiesis in human embryos. This progenitor population first emerges as a myeloid progenitor and later acquires myeloid-lymphoid bipotential, co-expressing genes affiliated with the two lineages in single cells.[67]

A number of key TF have been identified as important factors for the development of lymphoid cells, including the C/EBP family, PU.1, E2A, IKAROS and FOXO1. An analysis combining RNA sequencing and chromatin immunoprecipitation sequencing has suggested the existence of gene regulatory networks that are important for lymphoid-myeloid bifurcation[49] (Figure 3). However, which component in the gene regulatory networks of these TF define lineage commitments and how the expression of the TF is altered in response to environmental changes remain unclear. The initiators of the lymphoid or myeloid lineage commitment also have yet to be clarified, and there may in fact be multiple entry points for commitment.

We previously reported that BACH factors are required for efficient commitment of multipotent progenitors and common lymphoid progenitors to the lymphoid fate.[17,18] BACH factors repress the expression of C/EBP, and C/EBP repress the expression of BACH factors. The gene regulatory networks of these TF therefore define lymphoid or myeloid lineage commitment depending on fluctuations of the expression of C/EBP and BACH TF (Figure 4). Since the expression of these TF is affected by environmental changes,[18,19,59] these TF may be initiators of lymphoid or myeloid lineage commitment responding to environmental changes. The development of fetal myeloid-lymphoid progenitors mentioned above[67] may reflect changes in the interplay between BACH factors and C/EBP. Since steady-state hematopoiesis and emergency hematopoiesis are contrasting, it is still unclear to what extent the altered expression in response to extracellular signals would affect lineage commitment. Further understanding of these issues will help to clarify the mechanisms of lineage commitment in steady-state and emergency conditions. To this end, taking advantage of using TF reporter mice exposed or not to stress might be helpful to expand the TF-based analysis further. Identification of surrogate marker genes whose expression reports activity of particular TF will also be important.

Myeloid cells as the default and evolutionary prototype pathway of hematopoietic stem and progenitor cells

The lineage commitment of HSPC is the process in which these cells lose their multipotency. For erythroid cell differentiation, the progenitor cells first lose their capacity for lymphoid differentiation, resulting in erythroid-myeloid common progenitors,[32,35] at which point the decision of erythroid or myeloid lineage commitment is made. In contrast, for lymphoid cell differentiation, the progenitor cells first lose their capacity for erythroid differentiation, resulting in lymphoid-myeloid common progenitors,[34,35] at which point the decision of lymphoid or myeloid lineage commitment is made.

Interestingly, it has been reported that, even after lymphoid commitment, T-cell or B-cell progenitors retain the capacity to differentiate into myeloid cells.[68-70] Indeed, myeloid differentiation potential might remain until just before terminal differentiation. Results from studies using five blood-lineage marking, which is a precise method of detecting erythroid cells and platelets in addition to myeloid, B and T cells after transplantation, also support the notion that myeloid differentiation potential is retained after losing either erythroid or lymphoid differentiation potential.[71] In addition, at least some platelets are derived from HSC possessing myeloid lineage potential.[72,73] Myeloid cell differentiation might, therefore, be a default and/or prototypical pathway of

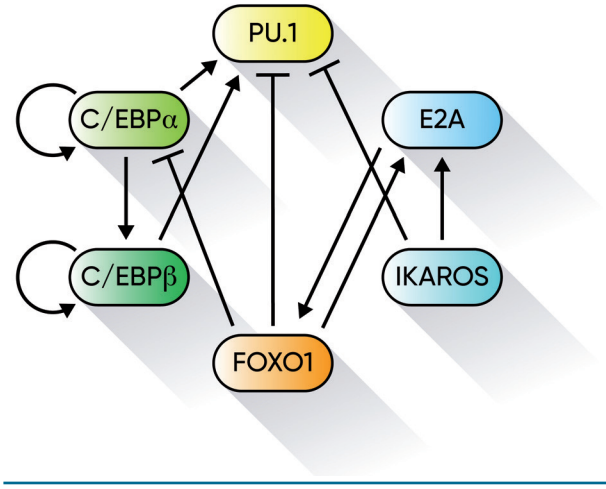

Figure 3. Gene regulatory networks controlling lymphoid cell differentiation. Several factors have been identified as important regulators of lymphoid cell differentiation commitment.[49] Each factor works as an activator and/or repressor of other factors forming complex gene regulatory networks, suggesting the existence of a precise mechanism underlying lymphoid cell differentiation. However, how the activities of these factors are controlled at the initial point of lineage commitment remains unclear.

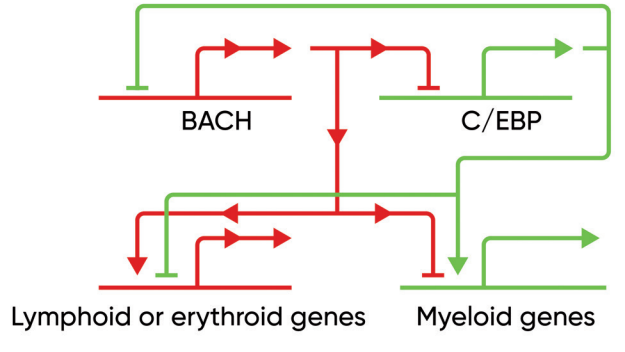

Figure 4. Gene regulatory networks of BACH and C/EBP transcription factors for myeloid and non-myeloid gene expression. The transcription factor (TF) BACH represses C/EBP and myeloid genes and induces lymphoid/erythroid genes. In contrast, the TF C/EBP represses BACH and lymphoid/erythroid genes and induces myeloid genes. Therefore, both stochastic fluctuation and environment-derived changes in the expression of BACH and C/EBP can induce differentiation commitment in progenitor cells.

HSPC, originally described as the "myeloid-based model",[74] and repression of the myeloid differentiation program appears important for lineage commitment in HSPC. In line with this, recent reports suggest the importance of myeloid-biased HSC in emergency myelopoiesis.[75-77] Further analysis is still needed to clarify how the gene regulatory networks are altered in myeloid-biased HSC.

In addition to the repression of the myeloid program during progenitor cell differentiation, re-activation of the myeloid program is observed in some mature hematopoietic cells. During maturation of erythroid and lymphoid cells, the function and expression of BACH factors are repressed, which can induce part of the myeloid program. For instance, *Prdm1* (encoding TF BLIMP-1) is a repressed target of BACH2, and its repression is necessary for the proper development of B cells.[26] BLIMP-1 *per se* is necessary for the proper development of plasma cells and T cells.[78] Since BLIMP-1 is important for myeloid cell development as well,[79] BLIMP-1 can be considered as a part of the myeloid program deployed during plasma-cell and T-cell development. To support this notion, some of the myeloid genes are expressed in plasma cells.[17] From the perspective of erythropoiesis, the expression of *Hmox1* (encoding heme oxygenase-1) is induced to avoid the toxic activity of free heme during erythroblast maturation,[80] On the other hand, heme oxygenase-1 is also important for the proper function of myeloid cells.[81] Therefore, heme oxygenase-1 can be considered as a part of the myeloid program deployed during the development of erythroid cells. Both mature myeloid cells and non-myeloid cells (erythroid and lymphoid cells) must cope with conditions of stress (such as oxidative stress during oxygen transportation or at the site of inflammation). We therefore assume that mature hematopoietic cells may reactivate a part of the myeloid program, such as heme oxygenase-1, to protect themselves from stresses, irrespective of their lineages. The myeloid program, which is temporarily repressed upon lineage commitment, is thus referred to as the "inner myeloid",[82] because part of it can be re-activated in mature cells. Given these findings, we propose "an extended myeloid-based model" of hematopoiesis, which posits that the myeloid program possesses important roles not only in hematopoietic cell differentiation but also in mature cell function.

The extended myeloid-based model with the "inner myeloid" is well understandable when the history of biological evolution is considered. Lower organisms, such as insects, possess phagocytic cells but lack erythroid and lymphoid cells.[83] A human-like HSC system was recently found in the chordate *Botryllus schlosseri*, with stem cells generating solely cells of myeloid lineage, such as phagocytic cells and granulocytes.[84] It should be noted that a BACH-like TF is present in chordates and vertebrates[85] but not in lower organisms. The prototype BACH TF may restrict myeloid differentiation of HSC. Since erythroid cells and lymphoid cells arose in the hematopoietic system during the evolution of higher organisms, repressing the myeloid program in progenitor cells ("inner myeloid") might be necessary to make non-myeloid cells (erythroid and lymphoid cells). The findings regarding the function of BACH factors as repressors of the "inner myeloid" may constitute the molecular foundation of the myeloid-based model of hematopoiesis and lineage commitment. The hematopoietic system in higher eukaryotes is therefore evidence of our ancient history, just like our other body systems.[86]

Fortifying roles of BACH factors in blood homeostasis

BACH factors play not only repressive roles in the myeloid program in progenitor cells but also several indispensable roles in the operation of the hematopoietic system. For instance, BACH1 works as a balancer of globins and heme during erythroid cell maturation.[22] BACH2 is required for the development of non-IgM type plasma cells, memory B cells, regulatory T cells and memory T cells.[23-30,87,88] and therefore works as a regulator of lymphocyte effector *versus* non-effector differentiation. Remarkably, these functions of BACH2 in lymphoid cells might be explained by its binding to the AP-1 site as a transcription repressor, which is in contrast to the other TF (Fos, Jun, etc.) targeting the AP-1 site, many of which work as transcription activators.[89]

These functions of BACH factors in erythroid and lymphoid cells can be interpreted as indicative of their role as 'fortifying factors', since they shape steady-state hematopoiesis to prepare for infection at multiple points, as described below. With regard to erythropoiesis, the hemoglobin concentration in human blood is kept around 14 g/dL in the steady state whereas, in general, a hemoglobin concentration <7 g/dl is life-threatening. There is therefore sufficient capacity for erythropoiesis to endure emergency conditions. For instance, progenitor cell differentiation can be shifted toward myelopoiesis, thus promoting the innate immune defense at the expense of erythropoiesis during a state of infection. This means that BACH factors support erythropoiesis by suppressing myelopoiesis in the steady state, fortifying the system for infection. With regard to the B-cell response, IgM-secreting plasma cells work as the first line of defense against pathogens, whereas non-IgM-type plasma cells and memory B cells are produced at a later phase or after the infection as a more effective second-line defense.[90] With regard to the T-cell response, effector T cells provide the first line of defense against pathogens whereas regulatory T cells and memory T cells work to repress an excess immune response and/or to return the state to the steady condition in preparation for the next infection.[91] These responses may be coordinated by the expression of BACH factors. When their expression is reduced in response to infection, IgM-secreting plasma cells and effector T cells are preferentially generated. Conversely, resumption of the expression of BACH factors leads to the generation of non-IgM plasma cells, memory B cells, regulatory T cells and memory T cells. Therefore, BACH factors are required to fortify the hematopoietic system as a whole, in preparation for future infections (Figure 5).

Hematologic disorders as failures of BACH gene regulatory networks

The gene regulatory networks of HSPC may explain why pathological alterations in one lineage often accom-

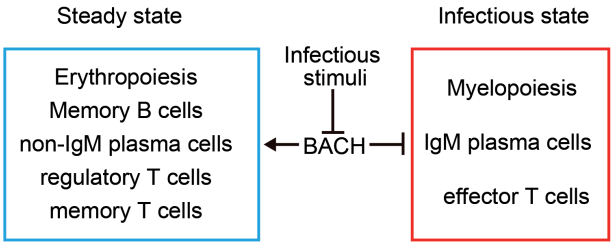

Figure 5. The fortifying role of BACH for the next emergency. BACH factors support erythropoiesis and repress myelopoiesis in steady-state conditions. BACH2 in particular supports the development of memory B cells, non-IgM plasma cells, regulatory T cells and memory T cells in the steady state while repressing the development of IgM plasma cells and effector T cells. Since BACH factors support the development of the cells needed for the suppression of a previous emergency reaction and the preparation for the next emergency, BACH factors can be considered "fortifying factors".

pany changes in other lineages in the opposite direction. Infection and inflammation cause anemia of inflammation, which is frequently observed in chronic infections and autoimmune diseases.[8] Inflammatory cytokines, such as interleukin-6, induce the expression of hepcidin, resulting in the inhibition of ferroportin.[92] This regulatory axis is the mechanism by which the iron supply for erythroblast maturation is limited, resulting in anemia.[8] However, this mechanism may not explain how the differentiation trajectory is modulated at the erythroid-myeloid bifurcation point during an infection and in inflammatory conditions.[6] In those circumstances, the expression of BACH factors is repressed in HSPC,[19,93] leading to increased myelopoiesis at the expense of erythropoiesis. Therefore, the reduced activity of BACH factors might be a novel mechanism underlying anemia of inflammation.

MDS is a major hematopoietic malignancy and is caused by a clonal disorder in HSC.[94] The phenotypic features of MDS, such as anemia, autoimmune reactions and transformation into acute myeloid leukemia, may also be attributed to alterations in the state of gene regulatory networks. The expression of *BACH2* is repressed in MDS.[19] Since the loss of BACH2 is expected to induce anemia, an inflammatory reaction and myeloid skewing of progenitors, the repression of *BACH2* that has been observed in MDS patients might be one of the causes of the characteristic symptoms of MDS. A recent genome-wide analysis showed that MDS clones frequently have mutations in epigenetic modifiers and splicing factors,[95] suggesting that such genetic alterations may lead to a reduction in *BACH2* expression. *BACH2* repression is also observed in lymphocytes on aging, with *PRDM1* induction in humans.[96] Since the loss of BACH2 causes autoimmune-like disorders,[28] BACH2 repression (and the induction of the "inner myeloid") during aging may be one of the causes of aging-related inflammation. Interestingly, HSC in mice become restricted to a myeloid fate upon aging.[97] This may be due to a reduction in BACH2 expression. Moreover, mutations of epigenetic modifiers, such as those observed in clonal hematopoiesis with aging,[98] may cause dysregulation of the repression of the "inner myeloid", resulting in myeloid skewing and inflammation. If this is the case, aging-related dysregulation of the "inner myeloid" is part of a vicious circle since inflammation *per se* can cause DNA mutations.[99] *BACH2* haploinsufficiency in humans has been reported to cause BACH2-related immunodeficiency and autoimmunity (BRIDA),[100] a finding that may further support these possibilities. In contrast, BACH2 overexpression in progenitor cells induces erythropoiesis by repressing myelopoiesis.[19] Therefore, BACH factors might be new therapeutic targets of refractory anemia induced by inflammation and MDS. Further investigations will be needed in order to determine whether or not BACH2 re-activation (or "inner myeloid" repression) in aged HSC can rescue the phenotype related to aging.

Conclusions

In this review, we have highlighted recent findings concerning the differentiation of HSPC and their limitations. Novel findings from single-cell analyses suggest the need to reconsider the canonical hierarchical differentiation model of the hematopoietic system. However, we should also consider the limitations associated with these single-cell analyses, as discussed above. The myeloid-based model involving the gene regulatory networks of BACH factors may provide a further molecular basis for understanding lineage commitment, evolutionary perspectives and pathological processes of the hematopoietic system. Understanding the roles of BACH factors as repressors of the "inner myeloid"' and "fortifying factors" in preparation for future emergency situations will help us to develop a more comprehensive model of the hematopoietic system.

Acknowledgments

We thank Prof. Hideo Harigae, Dr. Akihiko Muto, Dr. Kyoko Ochiai and Dr. Yusho Ishii for discussion and comments on the manuscript. Studies at Tohoku University are supported by Grants-in-Aid from the Japan Society for the Promotion of Science (18H04021, 18H05374, and 15H02506 to KI and 17H06527 to HK).

References

1. Haas S, Trumpp A, Milsom MD. Causes and consequences of hematopoietic stem cell heterogeneity. Cell Stem Cell. 2018;22(5):627-638.
2. Bianconi E, Piovesan A, Facchin F, et al. An estimation of the number of cells in the human body. Ann Hum Biol. 2013;40(6):463-471.
3. Muckenthaler MU, Rivella S, Hentze MW, Galy B. A red carpet for iron metabolism. Cell. 2017;168(3):344-361.
4. Summers C, Rankin SM, Condliffe AM, Singh N, Peters AM, Chilvers ER. Neutrophil kinetics in health and disease. Trends Immunol. 2010;31(8):318-324.
5. Busch K, Klapproth K, Barile M, et al. Fundamental properties of unperturbed haematopoiesis from stem cells in vivo. Nature. 2015;518(7540):542-546.
6. Glatman Zaretsky A, Engiles JB, Hunter CA. Infection-induced changes in hematopoiesis. J Immunol. 2014;192(1):27-33.
7. Doherty CP. Host-pathogen interactions: the role of iron. J Nutr. 2007;137(5):1341-1344.
8. Weiss G, Goodnough LT. Anemia of chronic disease. N Engl J Med. 2005;352(10):1011-1023.

9. Berliner N. Anemia in the elderly. Trans Am Clin Climatol Assoc. 2013;124:230-237.
10. Nikolich-Zugich J. The twilight of immunity: emerging concepts in aging of the immune system. Nat Immunol. 2018;19 (1):10-19.
11. Wang J, Geiger H, Rudolph KL. Immunoaging induced by hematopoietic stem cell aging. Curr Opin Immunol. 2011;23(4):532-536.
12. Chung SS, Park CY. Aging, hematopoiesis, and the myelodysplastic syndromes. Blood Adv. 2017;1(26):2572-2578.
13. Jose SS, Bendickova K, Kepak T, Krenova Z, Fric J. Chronic inflammation in immune aging: role of pattern recognition receptor crosstalk with the telomere complex? Front Immunol. 2017;8:1078.
14. Karamitros D, Stoilova B, Aboukhalil Z, et al. Single-cell analysis reveals the continuum of human lympho-myeloid progenitor cells. Nat Immunol. 2018;19(1):85-97.
15. Perie L, Duffy KR, Kok L, de Boer RJ, Schumacher TN. The branching point in erythro-myeloid differentiation. Cell. 2015; 163(7):1655-1662.
16. Paul F, Arkin Y, Giladi A, et al. Transcriptional heterogeneity and lineage commitment in myeloid progenitors. Cell. 2015;163(7):1663-1677.
17. Itoh-Nakadai A, Hikota R, Muto A, et al. The transcription repressors Bach2 and Bach1 promote B cell development by repressing the myeloid program. Nat Immunol 2014;15(12):1171-1180.
18. Itoh-Nakadai A, Matsumoto M, Kato H, et al. A Bach2-Cebp gene regulatory network for the commitment of multipotent hematopoietic progenitors. Cell Rep. 2017; 18(10):2401-2414.
19. Kato H, Itoh-Nakadai A, Matsumoto M, et al. Infection perturbs Bach2- and Bach1-dependent erythroid lineage 'choice' to cause anemia. Nat Immunol. 2018;19(10): 1059-1070.
20. Igarashi K, Watanabe-Matsui M. Wearing red for signaling: the heme-bach axis in heme metabolism, oxidative stress response and iron immunology. Tohoku J Exp Med. 2014;232(4):229-253.
21. Foletta VC, Segal DH, Cohen DR. Transcriptional regulation in the immune system: all roads lead to AP-1. J Leukoc Biol. 1998;63(2):139-152.
22. Kobayashi M, Kato H, Hada H, et al. Iron-heme-Bach1 axis is involved in erythroblast adaptation to iron deficiency. Haematologica. 2017;102(3):454-465.
23. Igarashi K, Kurosaki T, Roychoudhuri R. BACH transcription factors in innate and adaptive immunity. Nat Rev Immunol. 2017;17(7):437-450.
24. Kim EH, Gasper DJ, Lee SH, Plisch EH, Svaren J, Suresh M. Bach2 regulates homeostasis of Foxp3+ regulatory T cells and protects against fatal lung disease in mice. J Immunol. 2014;192(3):985-995.
25. Kometani K, Nakagawa R, Shinnakasu R, et al. Repression of the transcription factor Bach2 contributes to predisposition of IgG1 memory B cells toward plasma cell differentiation. Immunity. 2013;39(1):136-147.
26. Muto A, Ochiai K, Kimura Y, et al. Bach2 represses plasma cell gene regulatory network in B cells to promote antibody class switch. EMBO J. 2010;29(23):4048-4061.
27. Muto A, Tashiro S, Nakajima O, et al. The transcriptional programme of antibody class switching involves the repressor Bach2. Nature. 2004;429(6991):566-571.
28. Roychoudhuri R, Hirahara K, Mousavi K, et al. BACH2 represses effector programs to stabilize T(reg)-mediated immune homeostasis. Nature. 2013;498(7455):506-510.
29. Tsukumo S, Unno M, Muto A, et al. Bach2 maintains T cells in a naive state by suppressing effector memory-related genes. Proc Natl Acad Sci U S A. 2013;110(26): 10735-10740.
30. Yu X, Lao Y, Teng XL, et al. SENP3 maintains the stability and function of regulatory T cells via BACH2 deSUMOylation. Nature Commun. 2018;9(1):3157.
31. Yamamoto R, Morita Y, Ooehara J, et al. Clonal analysis unveils self-renewing lineage-restricted progenitors generated directly from hematopoietic stem cells. Cell. 2013;154(5):1112-1126.
32. Akashi K, Traver D, Miyamoto T, Weissman IL. A clonogenic common myeloid progenitor that gives rise to all myeloid lineages. Nature. 2000;404(6774):193-197.
33. Boyer SW, Schroeder AV, Smith-Berdan S, Forsberg EC. All hematopoietic cells develop from hematopoietic stem cells through Flk2/Flt3-positive progenitor cells. Cell Stem Cell. 2011;9(1):64-73.
34. Adolfsson J, Mansson R, Buza-Vidas N, et al. Identification of Flt3+ lympho-myeloid stem cells lacking erythro-megakaryocytic potential a revised road map for adult blood lineage commitment. Cell. 2005;121(2):295-306.
35. Pietras EM, Reynaud D, Kang YA, et al. Functionally distinct subsets of lineage-biased multipotent progenitors control blood production in normal and regenerative conditions. Cell Stem Cell. 2015;17 (1):35-46.
36. Naik SH, Perie L, Swart E, et al. Diverse and heritable lineage imprinting of early haematopoietic progenitors. Nature. 2013;496(7444):229-232.
37. Yu VWC, Yusuf RZ, Oki T, et al. Epigenetic memory underlies cell-autonomous heterogeneous behavior of hematopoietic stem cells. Cell. 2016;167(5):1310-1322.e1317.
38. Imayoshi I, Isomura A, Harima Y, et al. Oscillatory control of factors determining multipotency and fate in mouse neural progenitors. Science. 2013;342(6163):1203-1208.
39. Morrison SJ, Scadden DT. The bone marrow niche for haematopoietic stem cells. Nature. 2014;505(7483):327-334.
40. Busch K, Rodewald HR. Unperturbed vs. post-transplantation hematopoiesis: both in vivo but different. Curr Opin Hematol. 2016;23(4):295-303.
41. Nimmo RA, May GE, Enver T. Primed and ready: understanding lineage commitment through single cell analysis. Trends Cell Biol. 2015;25(8):459-467.
42. Skylaki S, Hilsenbeck O, Schroeder T. Challenges in long-term imaging and quantification of single-cell dynamics. Nat Biotechnol. 2016;34(11):1137-1144.
43. Golan K, Kumari A, Kollet O, et al. Daily onset of light and darkness differentially controls hematopoietic stem cell differentiation and maintenance. Cell Stem Cell. 2018;23(4):572-585.e577.
44. Teschendorff AE, Enver T. Single-cell entropy for accurate estimation of differentiation potency from a cell's transcriptome. Nat Commun. 2017;8:15599.
45. Wang X, Allen WE, Wright MA, et al. Three-dimensional intact-tissue sequencing of single-cell transcriptional states. Science. 2018;361(6400).
46. Rodriguez-Fraticelli AE, Wolock SL, Weinreb CS, et al. Clonal analysis of lineage fate in native haematopoiesis. Nature. 2018;553(7687):212-216.
47. Pei W, Feyerabend TB, Rossler J, et al. Polylox barcoding reveals haematopoietic stem cell fates realized in vivo. Nature. 2017;548(7668):456-460.
48. Wolff L, Humeniuk R. Concise review: erythroid versus myeloid lineage commitment: regulating the master regulators. Stem Cells. 2013;31(7):1237-1244.
49. Collombet S, van Oevelen C, Sardina Ortega JL, et al. Logical modeling of lymphoid and myeloid cell specification and transdifferentiation. Proc Natl Acad Sci U S A. 2017;114(23):5792-5799.
50. Teles J, Pina C, Eden P, Ohlsson M, Enver T, Peterson C. Transcriptional regulation of lineage commitment--a stochastic model of cell fate decisions. PLoS Comput Biol. 2013;9(8):e1003197.
51. Liston A, Masters SL. Homeostasis-altering molecular processes as mechanisms of inflammasome activation. Nat Rev Immunol. 2017;17(3):208-214.
52. Laurenti E, Gottgens B. From haematopoietic stem cells to complex differentiation landscapes. Nature. 2018;553(7689):418-426.
53. Heyworth C, Pearson S, May G, Enver T. Transcription factor-mediated lineage switching reveals plasticity in primary committed progenitor cells. EMBO J. 2002;21 (14):3770-3781.
54. Pina C, Teles J, Fugazza C, et al. Single-cell network analysis identifies DDIT3 as a nodal lineage regulator in hematopoiesis. Cell Rep. 2015;11(10):1503-1510.
55. Mayran A, Drouin J. Pioneer transcription factors shape the epigenetic landscape. J Biol Chem. 2018;293(36):13795-13804.
56. Bonifer C. Epigenetic plasticity of hematopoietic cells. Cell Cycle. 2005;4(2): 211-214.
57. Herb BR, Wolschin F, Hansen KD, et al. Reversible switching between epigenetic states in honeybee behavioral subcastes. Nat Neurosci. 2012;15(10):1371-1373.
58. Avellino R, Delwel R. Expression and regulation of C/EBPalpha in normal myelopoiesis and in malignant transformation. Blood. 2017;129(15):2083-2091.
59. Hirai H, Zhang P, Dayaram T, et al. C/EBPbeta is required for 'emergency' granulopoiesis. Nat Immunol. 2006;7(7):732-739.
60. Iwasaki H, Somoza C, Shigematsu H, et al. Distinctive and indispensable roles of PU.1 in maintenance of hematopoietic stem cells and their differentiation. Blood. 2005;106 (5):1590-1600.
61. Fujiwara Y, Browne CP, Cunniff K, Goff SC, Orkin SH. Arrested development of embryonic red cell precursors in mouse embryos lacking transcription factor GATA-1. Proc Natl Acad Sci U S A. 1996;93(22):12355-12358.
62. Hoppe PS, Schwarzfischer M, Loeffler D, et al. Early myeloid lineage choice is not initiated by random PU.1 to GATA1 protein ratios. Nature. 2016;535(7611):299-302.
63. Palii CG, Cheng Q, Gillespie MA, et al. Single-cell proteomics reveal that quantitative changes in co-expressed lineage-specific transcription factors determine cell fate. Cell Stem Cell. 2019;24(5):812-820.e815.
64. Weinberg ED. Iron loading and disease surveillance. Emerg Infect Dis. 1999;5(3):346-352.
65. Yanez A, Goodridge HS, Gozalbo D, Gil ML. TLRs control hematopoiesis during infection. Eur J Immunol. 2013;43(10):2526-2533.
66. Hsu W, Kerppola TK, Chen PL, Curran T, Chen-Kiang S. Fos and Jun repress transcription activation by NF-IL6 through association at the basic zipper region. Mol Cell Biol. 1994;14(1):268-276.

67. Boiers C, Richardson SE, Laycock E, et al. A human IPS model implicates embryonic B-myeloid fate restriction as developmental susceptibility to B acute lymphoblastic leukemia-associated ETV6-RUNX1. Dev Cell. 2018;44(3):362-377.e367.
68. Kawamoto H, Ohmura K, Katsura Y. Presence of progenitors restricted to T, B, or myeloid lineage, but absence of multipotent stem cells, in the murine fetal thymus. J Immunol. 1998;161(8):3799-3802.
69. Wada H, Masuda K, Satoh R, et al. Adult T-cell progenitors retain myeloid potential. Nature. 2008;452(7188):768-772.
70. Kawamoto H, Ohmura K, Katsura Y. Direct evidence for the commitment of hematopoietic stem cells to T, B and myeloid lineages in murine fetal liver. Int Immunol. 1997;9(7):1011-1019.
71. Yamamoto R, Wilkinson AC, Nakauchi H. Changing concepts in hematopoietic stem cells. Science. 2018;362(6417):895-896.
72. Sanjuan-Pla A, Macaulay IC, Jensen CT, et al. Platelet-biased stem cells reside at the apex of the haematopoietic stem-cell hierarchy. Nature. 2013;502(7470):232-236.
73. Carrelha J, Meng Y, Kettyle LM, et al. Hierarchically related lineage-restricted fates of multipotent haematopoietic stem cells. Nature. 2018;554(7690):106-111.
74. Kawamoto H. A close developmental relationship between the lymphoid and myeloid lineages. Trends Immunol. 2006;27(4):169-175.
75. Pietras EM. Inflammation: a key regulator of hematopoietic stem cell fate in health and disease. Blood. 2017;130(15):1693-1698.
76. Mann M, Mehta A, de Boer CG, et al. Heterogeneous responses of hematopoietic stem cells to inflammatory stimuli are altered with age. Cell Rep. 2018;25(11):2992-3005.e2995.
77. Dutta P, Sager HB, Stengel KR, et al. Myocardial infarction activates CCR2(+) hematopoietic stem and progenitor cells. Cell Stem Cell. 2015;16(5):477-487.
78. Fu SH, Yeh LT, Chu CC, Yen BL, Sytwu HK. New insights into Blimp-1 in T lymphocytes: a divergent regulator of cell destiny and effector function. J Biomed Sci. 2017;24(1):49.
79. Chang DH, Angelin-Duclos C, Calame K. BLIMP-1: trigger for differentiation of myeloid lineage. Nat Immunol. 2000;1(2):169-176.
80. Garcia-Santos D, Schranzhofer M, Horvathova M, et al. Heme oxygenase 1 is expressed in murine erythroid cells where it controls the level of regulatory heme. Blood. 2014;123(14):2269-2277.
81. Tzima S, Victoratos P, Kranidioti K, Alexiou M, Kollias G. Myeloid heme oxygenase-1 regulates innate immunity and autoimmunity by modulating IFN-beta production. J Exp Med. 2009;206(5):1167-1179.
82. Igarashi K, Itoh-Nakadai A. Orchestration of B lymphoid cells and their inner myeloid by Bach. Curr Opin Immunol. 2016;39(136-142.
83. Krzemien J, Crozatier M, Vincent A. Ontogeny of the Drosophila larval hematopoietic organ, hemocyte homeostasis and the dedicated cellular immune response to parasitism. Int J Dev Biol. 2010;54(6-7):1117-1125.
84. Rosental B, Kowarsky M, Seita J, et al. Complex mammalian-like haematopoietic system found in a colonial chordate. Nature. 2018;564(7736):425-429.
85. Amoutzias GD, Veron AS, Weiner J, 3rd, et al. One billion years of bZIP transcription factor evolution: conservation and change in dimerization and DNA-binding site specificity. Mol Biol Evol. 2007;24(3):827-835.
86. Shubin N. Your Inner Fish: A Journey into the 3.5-Billion-Year History of the Human Body. Knopf Doubleday Publishing Group. 2008.
87. Shinnakasu R, Inoue T, Kometani K, et al. Regulated selection of germinal-center cells into the memory B cell compartment. Nat Immunol. 2016;17(7):861-869.
88. Roychoudhuri R, Clever D, Li P, et al. BACH2 regulates CD8(+) T cell differentiation by controlling access of AP-1 factors to enhancers. Nat Immunol. 2016;17(7):851-860.
89. Sidwell T, Kallies A. Bach2 is required for B cell and T cell memory differentiation. Nat Immunol. 2016;17(7):744-745.
90. Baumgarth N. B-1 cell heterogeneity and the regulation of natural and antigen-induced IgM production. Front Immunol. 2016;7(324.
91. Hall BM. T Cells: soldiers and spies--the surveillance and control of effector T cells by regulatory T cells. Clin J Am Soc Nephrol. 2015;10(11):2050-2064.
92. Abreu R, Quinn F, Giri PK. Role of the hepcidin-ferroportin axis in pathogen-mediated intracellular iron sequestration in human phagocytic cells. Blood Adv. 2018;2(10):1089-1100.
93. Mitroulis I, Ruppova K, Wang B, et al. Modulation of myelopoiesis progenitors is an integral component of trained immunity. Cell. 2018;172(1-2):147-161.e112.
94. Tefferi A, Vardiman JW. Myelodysplastic syndromes. N Engl J Med. 2009;361(19):1872-1885.
95. Yoshida K, Sanada M, Shiraishi Y, et al. Frequent pathway mutations of splicing machinery in myelodysplasia. Nature. 2011;478(7367):64-69.
96. Chi VLD, Garaud S, De Silva P, et al. Age-related changes in the BACH2 and PRDM1 genes in lymphocytes from healthy donors and chronic lymphocytic leukemia patients. BMC Cancer. 2019;19(1):81.
97. Yamamoto R, Wilkinson AC, Ooehara J, et al. Large-scale clonal analysis resolves aging of the mouse hematopoietic stem cell compartment. Cell Stem Cell. 2018;22(4):600-607.e604.
98. Loh PR, Genovese G, Handsaker RE, et al. Insights into clonal haematopoiesis from 8,342 mosaic chromosomal alterations. Nature. 2018;559(7714):350-355.
99. Kawanishi S, Ohnishi S, Ma N, Hiraku Y, Murata M. Crosstalk between DNA damage and inflammation in the multiple steps of carcinogenesis. Int J Mol Sci. 2017;18(8).
100. Afzali B, Gronholm J, Vandrovcova J, et al. BACH2 immunodeficiency illustrates an association between super-enhancers and haploinsufficiency. Nat Immunol. 2017;18(7):813-823.

REVIEW ARTICLE

Ferrata Storti Foundation

Updates on the hematologic tumor microenvironment and its therapeutic targeting

Dorian Forte,[1,2] Daniela S. Krause,[3] Michael Andreeff,[4] Dominique Bonnet[5] and Simón Méndez-Ferrer[1-2]

[1]Wellcome Trust-Medical Research Council Cambridge Stem Cell Institute and Department of Haematology, University of Cambridge, Cambridge, UK; [2]National Health Service Blood and Transplant, Cambridge Biomedical Campus, Cambridge, UK; [3]Goethe University Frankfurt, Georg-Speyer-Haus, Frankfurt, Germany; [4]Section of Molecular Hematology and Therapy, Department of Leukemia, The University of Texas MD Anderson Cancer Center, Houston, TX, USA and [5]Haematopoietic Stem Cell Laboratory, The Francis Crick Institute, London, UK

Haematologica 2019
Volume 104(10):1928-1934

ABSTRACT

In this review article, we present recent updates on the hematologic tumor microenvironment following the 3rd Scientific Workshop on the Haematological Tumour Microenvironment and its Therapeutic Targeting organized by the European School of Hematology, which took place at the Francis Crick Institute in London in February 2019. This review article is focused on recent scientific advances highlighted in the invited presentations at the meeting, which encompassed the normal and malignant niches supporting hematopoietic stem cells and their progeny. Given the precise focus, it does not discuss other relevant contributions in this field, which have been the scope of other recent reviews. The content covers basic research and possible clinical applications with the major therapeutic angle of utilizing basic knowledge to devise new strategies to target the tumor microenvironment in hematologic cancers. The review is structured in the following sections: (i) regulation of normal hematopoietic stem cell niches during development, adulthood and aging; (ii) metabolic adaptation and reprogramming in the tumor microenvironment; (iii) the key role of inflammation in reshaping the normal microenvironment and driving hematopoietic stem cell proliferation; (iv) current understanding of the tumor microenvironment in different malignancies, such as chronic lymphocytic leukemia, multiple myeloma, acute myeloid leukemia and myelodysplastic syndromes; and (v) the effects of therapies on the microenvironment and some opportunities to target the niche directly in order to improve current treatments.

Correspondence:

DORIAN FORTE
dorian.forte2@unibo.it

SIMÓN MÉNDEZ-FERRER
sm2116@medschl.cam.ac.uk

Received: June 5, 2019.

Accepted: August 7, 2019.

Pre-published: September 12, 2019.

doi:10.3324/haematol.2018.195396

Check the online version for the most updated information on this article, online supplements, and information on authorship & disclosures: www.haematologica.org/content/104/10/1928

The normal niches in development, adulthood and aging

A maladapted vascular niche induces the generation and expansion of tumor-initiating cells

Work from Dr. Rafii's laboratory, among others, has revealed the heterogeneity of endothelial cells, which comprise over 140 different types of endothelium in the human body. Each organ or tumor is vascularized by a specialized endothelium. It is believed that transcription factors belonging to the Ets family, such as Ets variant 2 (ETV2), Fli1 and the Ets-related gene (Erg), make endothelial cells organ-specific. Endothelial cells are important niche cells for hematopoietic stem cells (HSC) and their use as feeder cells in culture allows the expansion of HSC by ~150-fold.[1] As a refinement, a combination of reprogramming factors, including FBJ murine osteosarcoma viral oncogene homolog B (FOSB), growth factor independent 1 transcriptional repressor (GFI1), runt-related transcription factor 1 (RUNX1) and SPI1 (which encodes PU.1), can be combined with sustained vascular niche induction to generate HSC that are endowed with secondary repopulating activity.

However, a maladapted vascular niche can facilitate the expansion of tumor-initi-

ating cells in different organs. A paradigm-shifting concept over the past few years is that blood vessels not only deliver nutrients and oxygen to organs and tissues, but that they also sustain stem cells and cancer cells through an 'angiocrine' mechanism. Consequently, maladapted tumor-associated vascular endothelial cells may confer stem cell-like activity to indolent tumor cells. One example of this is the conversion of dormant lymphoma cells into aggressive lymphoma through the interaction with endothelial cells. This effect is dependent on Notch signaling, since Jagged1 abrogation in endothelial cells can slow down lymphoma progression.[2] Another example is the abnormal activation of the fibroblast growth factor receptor 1 (FGFR1)-ETS2 pathway in tumor-associated-vascular endothelial cells during chemotherapy. Specifically, tumor-derived FGF4 activates FGFR1 in endothelial cells and induces the expression of the transcription factor ETS2. Chemotherapy inhibits the tumor-suppressive checkpoint function of insulin growth factor binding protein 7 (IGFBP7)/angiomodulin and increases the expression of insulin growth factor 1 (IGF1) in endothelial cells, causing an FGFR1-ETS2 feedforward loop which renders naïve IGFR1$^+$ cancer cells resistant to chemotherapy.[3] This research helped to show that the FGF4-FGFR1-ETS2 pathway plays a crucial role in tumor-associated endothelium.

Angiocrine signals regulate quiescence and therapy resistance in bone

Kusumbe and colleagues characterized different vessel subtypes comprising endothelial and sub-endothelial/perivascular cells in murine bone marrow. Type H endothelium (named so because of its high expression of endomucin) nurtures bone-forming cells during development.[4] However, alterations of the vascular microenvironment can affect the fate of disseminated tumor cells.[5] Dormant tumor cells can be awakened through the production of factors such as periostin (POSTN) and transforming growth factor β-1 (TGFβ-1). Importantly, proximity to the sprouting vasculature supports cancer cell proliferation, whereas a stable vasculature keeps cancer cells dormant. In relation to this, vascular remodeling during aging might alter hematopoiesis. For instance, type H endothelium and its associated osteoprogenitor cells are reduced during aging, possibly affecting hematopoiesis. Consistent with these results, reactivation of endothelial Notch signaling can activate HSC in aged mice, although it cannot fully restore HSC self-renewal.[6] Age-associated vascular remodeling might facilitate the development of myeloid malignancies since it promotes myeloid cell expansion.[7]

The hematopoietic stem cell niche in aging

In this regard, Geiger *et al.* uncovered several microenvironmental contributions to HSC aging. It had been previously reported that aged stromal cells secrete more pro-inflammatory CC-chemokine ligand 5 (CCL5 or RANTES) but less osteopontin (OPN); these stromal changes imprint some aging-associated phenotypes in HSC.[8] Specifically, a decreased frequency of endosteal stromal cells and osteoblasts reduces OPN expression, which is associated with HSC aging (manifested as myeloid skewing). The bone marrow microenvironment of adult OPN knockout mice partly resembles an aged wildtype microenvironment in its increased number of HSC which exhibit reduced engraftment and polarity. However, treatment with OPN fraction D can attenuate the dysfunction of aged long-term HSC (LT-HSC) and ameliorates HSC by activating integrin $\alpha_9\beta_1$ in HSC.[9] Additionally, aged endothelial cells drive hematopoietic aging phenotypes in young HSC, whereas infusion of young endothelial cells enhances endogenous HSC activity in aged mice.[10]

Metabolism in the tumor microenvironment

Intense efforts are currently being expended to elucidate how cancer cells reshape their malignant microenvironment to increase their metabolic fitness and chemoresistance.

Subversion of systemic glucose metabolism as a mechanism to support the growth of leukemic cells

Work by Dr. Ye and colleagues in Dr. Jordan's laboratory has revealed how leukemic cells subvert the metabolism of systemic glucose for their proliferation. Insulin resistance, besides playing a key role in obesity and diabetes, may facilitate leukemogenesis: leukemic cells can actively reduce glucose utilization by normal tissues to increase their glucose bioavailability.[11] Collectively, the findings suggest that leukemic cells increase IGFBP1 production from adipose tissue, which can cause insulin resistance. An intricate communication with the gut causes loss of active glucagon-like peptide-1 (GLP1) and serotonin, which suppresses insulin secretion. Overall, these systemic perturbations are believed to cause desensitization of normal tissues to glucose, suggesting a novel therapeutic window based on the restoration of normal glucose regulation.

Mitochondrial trafficking in the tumor microenvironment

Mitochondria are emerging components in the molecular exchange between leukemic cells and their microenvironment. The ability of bone marrow mesenchymal stromal cells (BMSC) to donate mitochondria to different cell types[12] has emerged as a potentially important process in hematologic diseases. Mitochondrial transfer has recently been appreciated to be a previously unrecognized mechanism of intercellular communication associated with chemoresistance.[13,14] Tunneling nanotubules appear to be the primary mitochondrial exchange route used in acute myeloid leukemia (AML).[14] Work from Dr. Rushworth's laboratory indicates that NADPH oxidase 2 (NOX2)-derived reactive oxygen species, induced by H_2O_2 or daunorubicin, may enhance mitochondrial transfer from BMSC to AML blasts. The transferred mitochondria appear functionally active and capable of boosting metabolic activity in AML cells.[13] A similar process has been reported in multiple myeloma. Increased oxidative phosphorylation (OXPHOS) in multiple myeloma cells is associated with CD38-driven mitochondrial transfer.[15] It is worth noting that this process seems to affect malignant cells preferentially and is not frequently observed in their normal counterparts. Therefore, a potential therapeutic window might be available through blockade of mitochondrial transfer.

Fatty acid metabolism and bone marrow adipocytes in acute myeloid leukemia

Work from Dr. Tabe's and Dr. Andreeff's laboratories has revealed other metabolic changes in AML, particularly focused on the role of adipocytes and fatty acid metabolism. Fat cells are a predominant type of stromal cell in aged human bone marrow. BMSC can promote AML survival

through a metabolic shift from OXPHOS to fatty acid oxidation, which causes OXPHOS uncoupling.[16] In addition, leukemia stem cells express the fatty acid receptor CD36 and exhibit high levels of fatty acid oxidation, associated with cell quiescence and drug resistance.[17] However, a novel small molecule inhibitor of fatty acid oxidation, avocatin-B, selectively inhibits AML and leukemia stem cells without detectable toxicity in normal HSC. Avocatin-B increases fatty acid uptake and enhances the expression of fatty acid-binding protein-4 (FABP4) in adipocytes co-cultured with AML cells. However, concomitantly, avocatin-B increases glucose uptake and glycolysis in AML, thus contributing to AML survival.[18] Overall, these data highlight the limitations of targeting a single metabolic pathway, since leukemic cells may escape through metabolic adaptation. Accordingly, cytarabine-resistant AML cells exhibit increased fatty acid oxidation and OXPHOS. Fatty acid oxidation inhibition induces an energy shift from high to low OXPHOS that enhances anti-leukemia effects, but only in combination with cytarabine.[19] Inhibition of fatty acid oxidation additionally activates the endoplasmic reticulum stress activator transcription factor 4 (ATF4) and enhances cytarabine cytoxicity in AML cells co-cultured with bone marrow adipocytes.[20] These findings suggest that combined therapies containing inhibitors of fatty acid oxidation could be capable of targeting metabolic vulnerabilities in AML.

Inflammation and cell cycle

One hallmark of hematologic malignancies is a proinflammatory state whereby inflammatory cytokines affect the proliferation of normal and mutant cells. Inflammation is, therefore, one key trigger of the reshaped malignant microenvironment.

Impact of aged marrow macrophages on hematopoietic stem cells and their niche

Microenvironmental inflammation is another driver of hematopoietic aging. Previous studies have shown that aged CD41$^+$ LT-HSC accumulate during aging and their megakaryocyte bias results in increased circulating platelets in aged mice.[21-24] Calvi *et al.* have shown that aged bone marrow macrophages contribute to the expansion of platelet-based HSC through interleukin-1β.[25] Aged murine bone marrow macrophages exhibit an activated phenotype and defective phagocytic function, which causes reduced efferocytosis of senescent neutrophils. *In vitro* co-culture systems suggest that increased interleukin-1β and reduced Axl receptor tyrosine kinase and its associated protein growth arrest-specific 6 (Gas6) contribute to platelet skewing during aging.

Hematopoietic stem cells and their bone marrow niche under inflammatory stress

Inflammation can affect both HSC and their niches. Infection can cause stress and dysfunction in HSC responding to infection. Chemotherapy, transplantation or inflammatory cytokines, such as interferon (IFN)-α, can modify HSC quiescence and make HSC re-enter the cell cycle.[26-29] For example, acute or non-acute virus infections activate quiescent LT-HSC but also affect their function through IFN-I receptor signaling.[29] Non-acute murine cytomegalovirus infections alter the LT-HSC gene expression profile and impair HSC function upon transplantation. One mediator appears to be the extracellular matrix adaptor protein Matrilin-4 (Matn4), which is a candidate negative regulator of HSC proliferation under stress.[29] Under acute stress, Matn4 expression decreases, allowing for HSC expansion to replenish the blood system. Importantly, reduced expression of the Cxcl12/Sdf-1 receptor Cxcr4 in Matn4$^{-/-}$ HSC improves the reconstitution and expansion of HSC. On the non-hematopoietic side, endothelial cells proliferate after inflammatory stress or infection to maintain vessel integrity and permeability. The responses of endothelial cells to IFN-α *in vivo* are transient and dependent on the expression of IFN-α receptors. In this regard, vascular endothelial growth factor (VEGF) has emerged as one mediator of the activation of bone marrow endothelial cells by IFN-α-stimulated hematopoietic cells. In conclusion, as part of the dynamic crosstalk between HSC and their niches, inflammatory stress not only has an impact on HSC but also on their microenvironment and this altered bidirectional crosstalk affects the growth and function in each compartment.

The bone marrow microenvironment in myeloproliferative neoplasms

Associated with inflammation, bone marrow fibrosis is an extensive remodeling of the bone marrow extracellular matrix, which is typically observed in some myeloproliferative neoplasms. Previous studies found that damage to the bone marrow microenvironment contributes to the progression of myeloproliferative neoplasms.[30] However, the identification of fibrosis-driving cells and specific markers of a pre-fibrotic state are important therapeutic issues that remain only partially addressed. Schneider and colleagues described GLI family zinc finger 1 (Gli1)$^+$ mesenchymal stromal cells as fibrotic cells in different types of fibrosis. Gli1$^+$ cells appear to be myofibroblast precursors which contribute significantly to myelofibrosis. Accordingly, genetic ablation of Gli1$^+$ cells reduces fibrosis and improves hematopoiesis in experimental models.[31]

Regulation of dormant hematopoietic stem cells

Inflammation is only one of the mechanisms that can awaken dormant HSC, as shown in studies by Cabezas-Wallscheid and colleagues. Dormant HSC can now be identified with specific markers, such as Lineage$^-$Sca-1$^+$c-Kit$^+$ (LSK) CD150$^+$CD48$^-$CD135$^-$CD34$^-$ cells expressing the G protein-coupled receptor Gprc5c5.[32] Dormant HSC represent only a very small subset of bone marrow cells, but these cells harbor the highest long-term reconstituting potential. Dormant HSC are characterized by low levels of biosynthetic processes (transcription, mRNA processing and translation) which gradually increase as the HSC become activated. Retinoic acid/vitamin A-induced signaling is highly enriched in dormant HSC and contributes to maintain low levels of reactive oxygen species, protein translation and expression of the proto-oncogene c-myc in these cells. *In vivo*, pre-treatment with all-*trans* retinoic acid can preserve HSC quiescence upon stress induced by chemotherapy or lipopolysaccharide. These results suggest that retinoic acid might restrict HSC proliferation. In contrast, lack of vitamin A compromises HSC re-entry into dormancy after exposure to inflammatory stress.[32]

Molecular regulation and heterogeneity in the exit from quiescence by human hematopoietic stem cells

Not only the actual quiescence of HSC, but also the time that that these cells take to enter the cell cycle can be a

defining feature, as revealed by Laurenti and colleagues. In fact, LT-HSC take longer than short-term HSC to enter the cell cycle. Cyclin dependent kinase-6 (CDK6) expression controls the exit from quiescence in human HSC.[33] Consequently, enforced CDK6 expression can push LT-HSC to divide as quickly as short-term HSC. Human HSC heterogeneity and lineage commitment were dissected further in a subsequent study. The first lineage restriction appears to affect the $CD19^{-}CD34^{+}CD38^{-}CD45RA^{-}CD49f^{+}CD90^{+}$ HSC compartment's generation of myelo-lymphoid committed cells which are devoid of erythroid differentiation capacity. The expression of the C-type lectin domain family 9 member A (CLEC9A) and CD34 in these cells can be used to distinguish $CLEC9A^{hi}CD34^{lo}$ LT-HSC (with slow exit from quiescence) from $CLEC9A^{lo}$ $CD34^{hi}$ myelo-lymphoid-restricted HSC (with quicker entry into the cell cycle).[34] These results help identify human HSC subsets and will be very useful to study their interactions with bone marrow microenvironments.

Interaction of tumor cells with their microenvironment

Mapping the bone marrow microenvironment in sickness and in health

The development of single-cell technologies has made it possible to generate an atlas of different tissues at single-cell resolution. A recent study by Dr. Aifantis' group presented the transcriptional signatures of murine bone marrow vascular endothelial cells, perivascular cells and osteolineage/stromal cell populations under steady state or under stress (5-fluorocuracil), with a major emphasis on candidate cellular sources of key factors regulating hematopoiesis.[35] For example, the loss of the delta-like canonical Notch ligand 4 (DLL4) in endothelial cells caused profound transcriptional changes, which drove myeloid skewing of HSC/progenitors.

Targeting the microenvironment in smoldering myeloma

Like other hematologic malignancies, multiple myeloma involves a multistep transformation process[36] with concomitant remodeling of the BM microenvironment,[37] as shown by Ghobrial *et al.* However, studies on the human bone marrow microenvironment are frequently challenged by the scarcity and insufficient preservation of tissue biopsies for detailed studies. A potential way to replace bone marrow biopsies might be to combine whole-exome sequencing of circulating tumor cells and cell-free DNA, which might help our understanding of disease heterogeneity and evolution in multiple myeloma.[38] Cell-free DNA reveals a similar clonal structure as bone marrow biopsies,[39] potentially paving the path for less invasive mutational screening.

Investigating mechanisms regulating myeloma growth and dissemination using *in vivo* bone marrow imaging

Studies by Dr. Fooksman and others have showed the potential of intravital microscopy for studying the interactions of normal and mutant hematopoietic cells with their microenvironment. Antibody-secreting cells comprise mature plasma cells and more immature plasmablasts which can be identified by the expression of syndecan-1 (CD138), a marker with an unclear function until recently. CD138 has lately been found to promote the survival of antibody-secreting cells through IL-6 and A proliferation-inducing ligand (APRIL).[40] Therefore, ongoing studies are utilizing similar intravital imaging techniques to study the microenvironment in multiple myeloma and other hematologic malignancies.

The tumor microenvironment in chronic lymphocytic leukemia, plasma cell myeloma and myelodysplastic syndromes

Understanding and targeting tumor-microenvironment interactions in B-cell malignancies

Microenvironmental alterations can be putative therapeutic targets in B-cell malignancies, as revealed by Ringshausen *et al.* The expression of protein kinase C beta II (PKCβ2) and downstream activation of NF-kappa B (NFκB) in BMSC is required for the survival of malignant B cells.[41] Chronic lymphocytic leukemia (CLL) cells induce Notch2 signaling and complement C1q production by BMSC, which in turn inhibits glycogen synthase kinase 3 beta (GSK3β)-dependent degradation of β-catenin in CLL. Additionally, Notch2 activation in BMSC further stabilizes β-catenin in CLL through regulation of N-cadherin expression. Consequently, inhibition of Notch or Wnt pathways has therapeutic effects in experimental CLL models.[42]

The biological and clinical roles of the microenvironment in chronic lymphocytic leukemia

Work in Dr. Hallek's laboratory and others has illustrated how CLL becomes addicted to the microenvironment, and particularly to macrophages or nurse-like cells. A prominent example is the non-receptor tyrosine-protein kinase Lyn belonging to the SRC family, which is crucial both for B-cell receptor signaling and for microenvironmental support of the malignant cells.[43] Lyn-deficient mice present a reduced CLL burden. However, the loss of Lyn in B cells only reduces B-cell receptor signaling, but does not affect CLL progression. In fact, Lyn is required in microenvironmental cells (and particularly macrophages) for the expansion of CLL cells.

Pre-clinical modeling of myelodysplastic syndromes in murine xenograft models

The clinical heterogeneity and molecular complexity of myelodysplastic syndromes (MDS) make these diseases arduous to model and study. However, xenograft models have emerged as useful tools for studying MDS. Co-transplantation of $CD34^{+}$ cells with patient-derived BMSC has been reported in one study to increase long-term engraftment of human MDS in immunodeficient mice.[44] In that study, patient-derived hematopoietic cells prompted healthy BMSC to acquire MDS-BMSC-like features. Consequently, cytokines produced by MDS BMSC favored the propagation of MDS after orthotopic interfemoral transplantation into immunodeficient mice. However, this finding contrasts with that of another study which found similar engraftment of MDS regardless of the presence of human BMSC.[45] It is possible that technical differences and/or distinct diseases/stages underlie these divergent results. Moreover, due to recent advances in bioengineering and carrier materials, traditional xenotransplants are being progressively replaced by bioengineered humanized microenvironments. As one example, implantable scaffold

methods allow the study of multicellular interactions between human stromal cells and HSC.[46]

Targeting the tumor microenvironment

Targeting the tumor microenvironment in B-cell lymphomas

Other ways to target the tumor microenvironment in B-cell malignancies have been exemplified by research in Dr. Gribben's laboratory and take advantage of the fact that lymphoma cells live in an immune cell-enriched microenvironment. However, immune cells do not function normally because CLL or lymphoma cells reduce the F-actin immune synapse formation in tumor-infiltrating T cells. Nonetheless, impaired T-cell function can be therapeutically reverted by the immunomodulatory drug lenalidomide.[47] which has recently been approved for the treatment of lymphoma. In a subsequent study, the inhibitory B7-related molecules CD200, CD274 (PD-L1), CD276 (B7-H3) and VD270 (HVEM) were identified as key mediators of the T-cell synapse defect.[48] Consequently, the PD1-PDL1 axis has emerged as a highly promising target in CLL and lymphoma.[49,50] These results have been extrapolated to solid tumors, in which PD1 expression has become both a biomarker and a therapeutic target.

Engineering T cells to overcome the immunosuppressive tumor microenvironment

Engineered T cells can be used to overcome the immunosuppressive tumor microenvironment. Generating tumor-specific lymphocytes has proven challenging given that many tumors are not very immunogenic. A revolutionary approach in immunotherapy is to combine the variable regions of antibodies (which recognize epitopes shared by tumors) with the constant regions of the T-cell receptor to generate chimeric antigen receptor (CAR) T cells.[51] This approach has been improved recently by adding co-stimulatory domains. CD19-specific CAR-T cells have provided impressive results in acute lymphoblastic leukemia, with reported cure of chemorefractory disease. Some lessons learned from these studies are: (i) chemotherapy is essential; (ii) it is critical to include a co-stimulatory domain; (iii) targeting a single antigen may enable immune escape; and (iv) significant toxicities (neural, cytokine storm) should be avoided in the future by improving the specificity and efficacy of the approach (to reduce the number of CAR-T cells infused). However, despite the impressive positive results of CD19-specific CAR-T cells in acute lymphoblastic leukemia, AML has proven more difficult to treat. In this regard, integrated transcriptomics and proteomics have not identified single candidate targets in AML, although combinatorial strategies have been proposed.[52,53]

Targeting altered metabolism in the leukemia microenvironment

It is now clear that the bone marrow microenvironment rewires energy metabolism in AML; however, targeting metabolic vulnerabilities in AML has proven challenging given the high degree of metabolic adaptation in AML cells. One key driver of metabolic reprograming in the leukemic bone marrow microenvironment is hypoxia. Most tumors are typically hypoxic, as cancer cells avidly consume oxygen and blood vessels become progressively compressed or obstructed by the growing tumor mass. Cancerous tissue in both solid and liquid tumors develops chronic hypoxia, which is associated with resistance to therapy and immune suppression.[54] However, the role of (low) oxygen in the progression and chemoresistance of leukemia remains controversial. Recently, a hypoxia-activated prodrug (TH-302) was tested in models of AML *in vivo*.[55] TH-302 is able to eliminate cancer cells residing in hypoxic microenvironments. Hypoxic niches were increased in a syngeneic AML murine model, but AML cells surviving chemotherapy could be targeted by TH-302, which improved mouse survival. On the other hand, metabolic reprogramming was previously reported to become more dependent on glycolysis. However, recent findings have challenged this view by showing that many tumors rely primarily on OXPHOS. Although targeting OXPHOS clinically presents some obstacles, drugs such as IACS-010759, a highly effective and selective small-molecule inhibitor of complex I of the mitochondrial electron transport chain, can reduce tumor burden in experimental models of brain cancer and AML.[56]

Interferon in myeloproliferative neoplasms

Connected with the effects of IFN-α on HSC and their microenvironment described above, studies by Dr. Kiladjian and others have shown that IFN-α is one of very few drugs capable of reducing the mutant allele burden in myeloproliferative neoplasms. Ropeginterferon triggered a dose-dependent anti-proliferative effect in *JAK2*V617F-mutated cell lines, whereas it did not affect the differentiation of normal CD34$^+$ cells.[57] One possibility might be to combine IFN with JAK inhibition, since the latter does not seem to modify the allele burden, but does dampen inflammation. IFN has been shown to induce molecular histopathological responses in myelofibrosis but it also induces immune and inflammatory toxicity. Ruxolitinib may offset IFN toxicity and the combination of these two drugs might enhance the molecular and histopathological response rate. However, it is possible that the anti-JAK1 activity of ruxolitinib might antagonize IFN signaling. These issues remain to be investigated in future studies.

CXCR4 inhibitors

The CXCL12-CXCR4 axis regulates bone marrow homing, retention, proliferation and egress of HSC and also affects the traffic of leukocytes. In particular, CXCR4 expression in HSC is necessary to keep these cells in the CXCL12-enriched bone marrow microenvironment. Dr. Peled and others have shown that efficient blockade of CXCR4 mobilizes HSC from the bone marrow into the circulation. Plerixafor (AMD3100) is a first-generation CXCR4 antagonist which has low affinity for the receptor. It is approved for HSC mobilization (but only in combination with granulocyte colony-stimulating factor) for the treatment of multiple myeloma and non-Hodgkin lymphoma. The new-generation CXCR4 inhibitor BL8040 binds CXCR4 with higher affinity (1-2 nM) than AMD3100 (84 nM).[58] In addition, whereas AMD3100 rapidly dissociates from CXCR4, BL8040 behaves as an inverse agonist and has a slow off-rate, causing more sustained CXCR4 inhibition. CXCR4 directly or indirectly stimulates tumor growth and regulates stromal cell adhesion-mediated drug resistance to chemotherapy. BL8040 can induce the mobilization of AML cells into the circulation and promote AML differentiation and apoptosis. A synergistic effect can be observed in combination with FLT3 or BCL-2 inhibitors,[59] suggesting that combination therapies could be useful in AML.

New insights into early-stage bone colonization of disseminated cancer cells

Finally, solid cancers can metastasize into bone after hijacking the normal bone marrow microenvironment, as illustrated by the work of Dr Zhang and others. Upon colonization of the bone marrow, cancer cells dysregulate bone formation and degradation cycles and stimulate the release of factors that promote tumor growth in a vicious cycle. Ell & Kang stated that: "TGFβ, insulin-like growth factor (IGF), and calcium are released from the bone matrix during lysis, enhancing tumor proliferation and survival. TGFβ signaling in tumor cells enhances expression of bone metastasis proteins including parathormone-related protein (PTHrP), the Notch ligand Jagged1, connective tissue growth factor (CTGF), IL-11, and matrix metalloproteinases. Calcium signaling through the calcium-sensing receptor leads to increased proliferation and survival. Osteoblasts also secrete a number of proteins that positively regulate tumor growth, including IL-6, secreted protein acidic and cysteine rich (SPARC) and periostin. SPARC induces cancer migration and homing through the $\alpha_v\beta_5$ integrin, whereas periostin and IL-6 promote tumor survival".[60]

Whereas many molecules driving metastatic growth have been identified, there is an important lack of knowledge regarding mechanisms allowing cancer cell colonization and maintenance before expansion. The microenvironment of early-stage bone lesions appears to be primarily an osteogenic niche composed of alkaline phosphatase $(ALP)^+$ collagen-I $(ColI)^+$ cells which define a preosteolytic stage (osteoclasts are not yet predominant at this early stage). Cancer and osteogenic niche cells generate heterotypic adherent junctions formed by E-cadherin and N-cadherin. E-cadherin blockade can abolish spontaneous bone metastases in a manner dependent on mammalian target of rapamycin (mTOR) and p70.[61] Moreover, cancer cells and niche cells are connected by gap junctions formed by connexin (Cx)43, which is induced in cancer cells after bone marrow colonization. Cx43 allows for calcium transfer to cancer cells to drive mTOR-dependent metastatic growth. This pathway can be inhibited by danusertib or a combination of everolimus and arsenic trioxide.[62] This research illustrates how solid tumors may hijack normal bone marrow niches to drive metastatic growth.

Summary

Increasingly, the tumor microenvironment is the focus of studies addressing survival, growth and chemoresistance of solid tumors and hematologic malignancies since it plays critical roles in disease initiation, maintenance and relapse. A key challenge is the dual role of the microenvironment in regulating normal and malignant hematopoiesis, since inhibiting the development and maintenance of malignancies must be followed by the reestablishment of normal tissue function. Therapies targeting the tumor microenvironment (which not only comprises the immune system, but also the stromal and endothelial cells that interact with the malignant cells and the immune cells) must simultaneously eliminate chemoresistant cells and preserve/reestablish normal hematopoiesis. Multidisciplinary meetings uniting basic and clinical researchers concerned about the tumor microenvironment have proven a unique opportunity for cross-fertilization of scientific knowledge, ideas and approaches to identify key vulnerabilities of the malignant niches.

Acknowledgments

The authors apologize for the omission of relevant literature due to the focus of this review. The support of the European School of Hematology (ESH), Celgene, Janssen Oncology, Fluidigm and Cancer Research UK was critical for the organization of the Workshop on which this article is based. This work was supported by Bologna AIL and AIRC Associazione Italiana per la Ricerca sul Cancro with funding to DF, and core support grants from the Wellcome Trust and the Medical Research Council to the Cambridge Stem Cell Institute, National Health Service Blood and Transplant (United Kingdom), European Union's Horizon 2020 Research (ERC-2014-CoG-64765) and a Programme Foundation Award from Cancer Research UK to SM-F.

References

1. Lis R, Karrasch CC, Poulos MG, et al. Conversion of adult endothelium to immunocompetent haematopoietic stem cells. Nature. 2017;545(7655):439-445.
2. Cao Z, Ding BS, Guo P, et al. Angiocrine factors deployed by tumor vascular niche induce B cell lymphoma invasiveness and chemoresistance. Cancer Cell. 2014;25(3):350-365.
3. Cao Z, Scandura JM, Inghirami GG, et al. Molecular checkpoint decisions made by subverted vascular niche transform indolent tumor cells into chemoresistant cancer stem cells. Cancer Cell. 2017;31(1):110-126.
4. Kusumbe AP, Ramasamy SK, Adams RH. Coupling of angiogenesis and osteogenesis by a specific vessel subtype in bone. Nature. 2014;507(7492):323-328.
5. Kusumbe AP. Vascular niches for disseminated tumour cells in bone. J Bone Oncol. 2016;5(3):112-116.
6. Kusumbe AP, Ramasamy SK, Itkin T, et al. Age-dependent modulation of vascular niches for haematopoietic stem cells. Nature. 2016;532(7599):380-384.
7. Ho YH, Del Toro R, Rivera-Torres J, et al. Remodeling of bone marrow hematopoietic stem cell niches promotes myeloid cell expansion during premature or physiological aging. Cell Stem Cell. 2019 Jul 4. [Epub ahead of print]
8. Ergen AV, Boles NC, Goodell MA. Rantes/Ccl5 influences hematopoietic stem cell subtypes and causes myeloid skewing. Blood. 2012;119(11):2500-2509.
9. Guidi N, Sacma M, Standker L, et al. Osteopontin attenuates aging-associated phenotypes of hematopoietic stem cells. EMBO J. 2017;36(7):840-853.
10. Poulos MG, Ramalingam P, Gutkin MC, et al. Endothelial transplantation rejuvenates aged hematopoietic stem cell function. J Clin Invest. 2017;127(11):4163-4178.
11. Ye H, Adane B, Khan N, et al. Subversion of systemic glucose metabolism as a mechanism to support the growth of leukemia cells. Cancer Cell. 2018;34(4):659-673.
12. Spees JL, Olson SD, Whitney MJ, Prockop DJ. Mitochondrial transfer between cells can rescue aerobic respiration. Proc Natl Acad Sci U S A. 2006;103(5):1283-1288.
13. Marlein CR, Zaitseva L, Piddock RE, et al. NADPH oxidase-2 derived superoxide drives mitochondrial transfer from bone marrow stromal cells to leukemic blasts. Blood. 2017;130(14):1649-1660.
14. Moschoi R, Imbert V, Nebout M, et al. Protective mitochondrial transfer from bone marrow stromal cells to acute myeloid leukemic cells during chemotherapy. Blood. 2016;128(2):253-264.
15. Marlein CR, Piddock RE, Mistry JJ, et al. CD38-driven mitochondrial trafficking promotes bioenergetic plasticity in multiple myeloma. Cancer Res. 2019;79(9):2285-2297.
16. Samudio I, Harmancey R, Fiegl M, et al. Pharmacologic inhibition of fatty acid oxidation sensitizes human leukemia cells to apoptosis induction. J Clin Invest. 2010;120(1):142-156.
17. Ye H, Adane B, Khan N, et al. Leukemic stem cells evade chemotherapy by metabol-

ic adaptation to an adipose tissue niche. Cell stem cell. 2016;19(1):23-37.
18. Tabe Y, Saitoh K, Yang H, et al. Inhibition of FAO in AML co-cultured with BM adipocytes: mechanisms of survival and chemosensitization to cytarabine. Sci Rep. 2018;8(1):16837.
19. Farge T, Saland E, de Toni F, et al. Chemotherapy resistant human acute myeloid leukemia cells are not enriched for leukemic stem cells but require oxidative metabolism. Cancer Discov. 2017; 7(7):716-735.
20. Tabe Y, Yamamoto S, Saitoh K, et al. Bone marrow adipocytes facilitate fatty acid oxidation activating AMPK and a transcriptional network supporting survival of acute monocytic leukemia cells. Cancer Res. 2017;77(6):1453-1464.
21. Sanjuan-Pla A, Macaulay IC, Jensen CT, et al. Platelet-biased stem cells reside at the apex of the haematopoietic stem-cell hierarchy. Nature. 2013;502(7470):232-236.
22. Grover A, Sanjuan-Pla A, Thongjuea S, et al. Single-cell RNA sequencing reveals molecular and functional platelet bias of aged haematopoietic stem cells. Nat Commun. 2016;7:11075.
23. Gekas C, Graf T. CD41 expression marks myeloid-biased adult hematopoietic stem cells and increases with age. Blood. 2013;121(22):4463-4472.
24. Yamamoto R, Morita Y, Ooehara J, et al. Clonal analysis unveils self-renewing lineage-restricted progenitors generated directly from hematopoietic stem cells. Cell. 2013;154(5):1112-1126.
25. Frisch BJ, Hoffman CM, Latchney SE, et al. Aged marrow macrophages expand platelet-biased hematopoietic stem cells via interleukin1B. JCI Insight. 2019;5:pii 124213.
26. Essers MA, Offner S, Blanco-Bose WE, et al. IFNalpha activates dormant haematopoietic stem cells in vivo. Nature. 2009;458(7240):904-908.
27. Haas S, Hansson J, Klimmeck D, et al. Inflammation-induced emergency megakaryopoiesis driven by hematopoietic stem cell-like megakaryocyte progenitors. cell stem cell. 2015;17(4):422-434.
28. Walter D, Lier A, Geiselhart A, et al. Exit from dormancy provokes DNA-damage-induced attrition in haematopoietic stem cells. Nature. 2015;520(7548):549-552.
29. Hirche C, Frenz T, Haas SF, et al. Systemic virus infections differentially modulate cell cycle state and functionality of long-term hematopoietic stem cells in vivo. Cell Rep. 2017;19(11):2345-2356.
30. Arranz L, Sanchez-Aguilera A, Martin-Perez D, et al. Neuropathy of haematopoietic stem cell niche is essential for myeloproliferative neoplasms. Nature. 2014;512(7512):78-81.
31. Schneider RK, Mullally A, Dugourd A, et al. Gli1(+) mesenchymal stromal cells are a key driver of bone marrow fibrosis and an important cellular therapeutic target. Cell Stem Cell. 2017;20(6):785-800.e8.
32. Cabezas-Wallscheid N, Buettner F, Sommerkamp P, et al. Vitamin A-retinoic acid signaling regulates hematopoietic stem cell dormancy. Cell. 2017;169(5):807-823.
33. Laurenti E, Frelin C, Xie S, et al. CDK6 levels regulate quiescence exit in human hematopoietic stem cells. Cell Stem Cell. 2015;16(3):302-313.
34. Belluschi S, Calderbank EF, Ciaurro V, et al. Myelo-lymphoid lineage restriction occurs in the human haematopoietic stem cell compartment before lymphoid-primed multipotent progenitors. Nat Commun. 2018;9(1):4100.
35. Tikhonova AN, Dolgalev I, Hu H, et al. The bone marrow microenvironment at single-cell resolution. Nature. 2019;569(7755):222-228.
36. Hallek M, Bergsagel PL, Anderson KC. Multiple myeloma: increasing evidence for a multistep transformation process. Blood. 1998;91(1):3-21.
37. Mouhieddine TH, Weeks LD, Ghobrial IM. Monoclonal gammopathy of undetermined significance. Blood. 2019;133(23):2484-2494.
38. Manier S, Park J, Capelletti M, et al. Whole-exome sequencing of cell-free DNA and circulating tumor cells in multiple myeloma. Nat Commun. 2018;9(1):1691.
39. Mishima Y, Paiva B, Shi J, et al. The mutational landscape of circulating tumor cells in multiple myeloma. Cell Rep. 2017;19(1):218-224.
40. McCarron MJ, Park PW, Fooksman DR. CD138 mediates selection of mature plasma cells by regulating their survival. Blood. 2017;129(20):2749-2759.
41. Lutzny G, Kocher T, Schmidt-Supprian M, et al. Protein kinase c-beta-dependent activation of NF-kappaB in stromal cells is indispensable for the survival of chronic lymphocytic leukemia B cells in vivo. Cancer Cell. 2013;23(1):77-92.
42. Mangolini M, Gotte F, Moore A, et al. Notch2 controls non-autonomous Wnt-signalling in chronic lymphocytic leukaemia. Nat Commun. 2018;9(1):3839.
43. Nguyen PH, Fedorchenko O, Rosen N, et al. LYN kinase in the tumor microenvironment is essential for the progression of chronic lymphocytic leukemia. Cancer Cell. 2016;30(4):610-622.
44. Medyouf H, Mossner M, Jann JC, et al. Myelodysplastic cells in patients reprogram mesenchymal stromal cells to establish a transplantable stem cell niche disease unit. Cell Stem Cell. 2014;14(6):824-837.
45. Rouault-Pierre K, Mian SA, Goulard M, et al. Preclinical modeling of myelodysplastic syndromes. Leukemia. 2017;31(12):2702-2708.
46. Abarrategi A, Mian SA, Passaro D, et al. Modeling the human bone marrow niche in mice: from host bone marrow engraftment to bioengineering approaches. J Exp Med. 2018;215(3):729-743.
47. Ramsay AG, Clear AJ, Kelly G, et al. Follicular lymphoma cells induce T-cell immunologic synapse dysfunction that can be repaired with lenalidomide: implications for the tumor microenvironment and immunotherapy. Blood. 2009;114(21):4713-4720.
48. Ramsay AG, Clear AJ, Fatah R, Gribben JG. Multiple inhibitory ligands induce impaired T-cell immunologic synapse function in chronic lymphocytic leukemia that can be blocked with lenalidomide: establishing a reversible immune evasion mechanism in human cancer. Blood. 2012;120(7):1412-1421.
49. McClanahan F, Riches JC, Miller S, et al. Mechanisms of PD-L1/PD-1-mediated CD8 T-cell dysfunction in the context of aging-related immune defects in the Emicro-TCL1 CLL mouse model. Blood. 2015;126(2):212-221.
50. McClanahan F, Hanna B, Miller S, et al. PD-L1 checkpoint blockade prevents immune dysfunction and leukemia development in a mouse model of chronic lymphocytic leukemia. Blood. 2015;126(2):203-211.
51. Eshhar Z, Waks T, Gross G, Schindler DG. Specific activation and targeting of cytotoxic lymphocytes through chimeric single chains consisting of antibody-binding domains and the gamma or zeta subunits of the immunoglobulin and T-cell receptors. Proc Natl Acad Sci U S A. 1993;90(2):720-724.
52. Perna F, Berman SH, Soni RK, et al. Integrating proteomics and transcriptomics for systematic combinatorial chimeric antigen receptor therapy of AML. Cancer Cell. 2017;32(4):506-519.e5.
53. Bonifant CL, Velasquez MP, Gottschalk S. Advances in immunotherapy for pediatric acute myeloid leukemia. Expert Opin Biol Ther. 2018;18(1):51-63.
54. Baran N, Konopleva M. Molecular pathways: hypoxia-activated prodrugs in cancer therapy. Clin Cancer Res. 2017;23(10):2382-2390.
55. Benito J, Ramirez MS, Millward NZ, et al. Hypoxia-activated prodrug TH-302 targets hypoxic bone marrow niches in preclinical leukemia models. Clin Cancer Res. 2016;22(7):1687-1698.
56. Molina JR, Sun Y, Protopopova M, et al. An inhibitor of oxidative phosphorylation exploits cancer vulnerability. Nat Med. 2018;24(7):1036-1046.
57. Verger E, Soret-Dulphy J, Maslah N, et al. Ropeginterferon alpha-2b targets JAK2V617F-positive polycythemia vera cells in vitro and in vivo. Blood Cancer J. 2018;8(10):94.
58. Abraham M, Pereg Y, Bulvik B, et al. Single dose of the CXCR4 antagonist BL-8040 induces rapid mobilization for the collection of human CD34(+) cells in healthy volunteers. Clin Cancer Res. 2017;23(22):6790-6801.
59. Abraham M, Klein S, Bulvik B, et al. The CXCR4 inhibitor BL-8040 induces the apoptosis of AML blasts by downregulating ERK, BCL-2, MCL-1 and cyclin-D1 via altered miR-15a/16-1 expression. Leukemia. 2017;31(11):2336-2346.
60. Ell B, Kang Y. SnapShot: bone metastasis. Cell. 2012;151(3):690-690.
61. Wang H, Yu C, Gao X, et al. The osteogenic niche promotes early-stage bone colonization of disseminated breast cancer cells. Cancer Cell. 2015;27(2):193-210.
62. Wang H, Tian L, Liu J, et al. The osteogenic niche is a calcium reservoir of bone micrometastases and confers unexpected therapeutic vulnerability. Cancer Cell. 2018;34(5):823-839.

Proposed diagnostic criteria for classical chronic myelomonocytic leukemia (CMML), CMML variants and pre-CMML conditions

Peter Valent,[1,2] Attilio Orazi,[3] Michael R. Savona,[4] Mrinal M. Patnaik,[5] Francesco Onida,[6] Arjan A. van de Loosdrecht,[7] Detlef Haase,[8] Torsten Haferlach,[9] Chiara Elena,[10] Lisa Pleyer,[11] Wolfgang Kern,[9] Tea Pemovska,[12] Gregory I. Vladimer,[12] Julie Schanz,[8] Alexandra Keller,[1] Michael Lübbert,[13] Thomas Lion,[14] Karl Sotlar,[15] Andreas Reiter,[16] Theo De Witte,[17] Michael Pfeilstöcker,[2,18] Klaus Geissler,[19] Eric Padron,[20] Michael Deininger,[21] Alberto Orfao,[22] Hans-Peter Horny,[23] Peter L. Greenberg,[24] Daniel A. Arber,[25] Luca Malcovati[10] and John M. Bennett[26]

[1]Department of Internal Medicine I, Division of Hematology & Hemostaseology, Medical University of Vienna, Vienna, Austria; [2]Ludwig Boltzmann Institute for Hematology & Oncology, Vienna, Austria; [3]Department of Pathology, Texas Tech University Health Sciences Center, El Paso, TX, USA; [4]Department of Medicine, Vanderbilt University School of Medicine, Vanderbilt-Ingram Cancer Center, Nashville, TN, USA; [5]Division of Hematology, Department of Medicine, Mayo Clinic, Rochester, MN, USA; [6]Fondazione IRCCS Ca' Granda Ospedale Maggiore Policlinico, University of Milan, Milan, Italy; [7]Department of Hematology, Amsterdam UMC, location VU University Medical Center, Cancer Center Amsterdam, the Netherlands; [8]Clinic of Hematology and Medical Oncology, University Medical Center Göttingen, Göttingen, Germany; [9]MLL Munich Leukemia Laboratory, Munich, Germany; [10]Department of Molecular Medicine, University of Pavia, Pavia, Italy; [11]3rd Medical Department with Hematology and Medical Oncology, Hemostaseology, Rheumatology and Infectious Diseases, Paracelsus Medical University, Salzburg, Austria; [12]CeMM Research Center for Molecular Medicine of the Austrian Academy of Sciences, Vienna, Austria; [13]Department of Medicine I, Medical Center, Faculty of Medicine, University of Freiburg, Freiburg, Germany; [14]Children's Cancer Research Institute and Department of Pediatrics, Medical University of Vienna, Vienna, Austria; [15]Institute of Pathology, Paracelsus Medical University, Salzburg, Austria; [16]Department of Hematology and Oncology, University Hospital Mannheim, University of Heidelberg, Mannheim, Germany; [17]Department of Tumor Immunology-Nijmegen Center for Molecular Life Sciences, Radboud University Medical Center, Nijmegen, the Netherlands; [18]3rd Medical Department, Hanusch Hospital, Vienna, Vienna, Austria; [19]Sigmund Freud University, Vienna, Austria; [20]Malignant Hematology Department, H. Lee Moffitt Cancer Center & Research Institute, Tampa, FL, USA; [21]Huntsman Cancer Institute & Division of Hematology and Hematologic Malignancies, University of Utah, Salt Lake City, UT, USA; [22]Servicio Central de Citometría, Centro de Investigación del Cáncer (IBMCC, CSIC-USAL), CIBERONC and IBSAL, Universidad de Salamanca, Salamanca, Spain; [23]Institute of Pathology, Ludwig-Maximilians University, Munich, Germany; [24]Stanford University Cancer Institute, Stanford, CA, USA; [25]Department of Pathology, University of Chicago, Chicago, IL, USA and [26]Department of Pathology, Hematopathology Unit and James P Wilmot Cancer Institute, University of Rochester Medical Center, Rochester, NY, USA

Ferrata Storti Foundation

Haematologica 2019
Volume 104(10):1935-1949

Correspondence:

PETER VALENT
peter.valent@meduniwien.ac.at

Received: March 14, 2019.

Accepted: April 29, 2019.

Pre-published: May 2, 2019.

doi:10.3324/haematol.2019.222059

Check the online version for the most updated information on this article, online supplements, and information on authorship & disclosures: www.haematologica.org/content/104/10/1935

ABSTRACT

Chronic myelomonocytic leukemia (CMML) is a myeloid neoplasm characterized by dysplasia, abnormal production and accumulation of monocytic cells and an elevated risk of transforming into acute leukemia. Over the past two decades, our knowledge about the pathogenesis and molecular mechanisms in CMML has increased substantially. In parallel, better diagnostic criteria and therapeutic strategies have been developed. However, many questions remain regarding prognostication and optimal therapy. In addition, there is a need to define potential pre-phases of CMML and special CMML variants, and to separate these entities from each other and from conditions mimicking CMML. To address these unmet needs, an international consensus group met in a Working Conference in August 2018 and discussed open questions and issues around CMML, its variants, and pre-CMML conditions. The outcomes of this meeting are summarized herein and include diag-

nostic criteria and a proposed classification of pre-CMML conditions as well as refined minimal diagnostic criteria for classical CMML and special CMML variants, including oligomonocytic CMML and CMML associated with systemic mastocytosis. Moreover, we propose diagnostic standards and tools to distinguish between ´normal´, pre-CMML and CMML entities. These criteria and standards should facilitate diagnostic and prognostic evaluations in daily practice and clinical studies in applied hematology.

Introduction

Chronic myelomonocytic leukemia (CMML) is a myeloid stem cell disease characterized by an abnormal production and accumulation of monocytic cells, often in association with other signs of myeloproliferation, substantial dysplasia in one or more hematopoietic cell lineages, and an increased risk of transformation into secondary acute myeloid leukemia (AML).[1-5] As per definition, the Philadelphia chromosome and its related *BCR-ABL1* fusion gene are absent in CMML. Other disease-related drivers, such as the *JAK2* mutation V617F or the *KIT* mutation D816V, may be detected and may indicate a special variant of CMML, such as CMML associated with systemic mastocytosis (SM-CMML).[6-8] However, most somatic mutations identified in CMML patients, such as mutations in *SRSF2*, *TET2*, or *RAS*, are not disease-specific, but are also detected in myelodysplastic syndromes (MDS), myeloproliferative neoplasms (MPN), or AML.[8-11]

For many years, CMML was listed as a separate variant among the MDS in the classification of the French-American-British (FAB) working group.[2,12] However, in 2001, the World Health Organization (WHO) reclassified CMML into a newly created MDS/MPN overlap group, defined by the presence of both MDS-related and MPN-related morphological and clinical features.[13] Depending on the leukocyte count, CMML can be divided into a 'dysplastic' variant (leukocyte count ≤13x10^9/L) and a 'proliferative' variant (leukocyte count >13x10^9/L).[2] In 2001 and 2008, the WHO also proposed a split into CMML-1 and CMML-2, based on the percentage of blast cells in the blood and bone marrow (BM).[13,14] In the most recent updates of the WHO 2016 classification, CMML is again listed amongst the MDS/MPN overlap disorders.[15,16] Based on the percentage of blasts, CMML is now divided into CMML-0, CMML-1, and CMML-2.[15-19] Moreover, contrasting the 2008 WHO classification, the diagnosis of CMML now requires both an absolute monocytosis (≥1×10^9/L) and relative monocytosis (≥10% of leukocytes) in the peripheral blood (PB).[15-19] In the 2008 and 2016 update of the WHO classification, CMML can only be diagnosed per definition when rearrangements in *PDGFRA*, *PDGFRB* or *FGFR1* genes have been excluded, and in the 2016 update, the *PCM1-JAK2* fusion gene was added as an excluding criterion.[14-16,19] These molecular aberrations are commonly found in eosinophilia-associated neoplasms such as chronic eosinophilic leukemia.[20,21] However, CMML is also listed as an underlying variant in these molecular 'entities' in the WHO classification system.[20,21]

Over the past two decades, our knowledge about the molecular features and mechanisms in CMML has increased substantially.[4-11,22-26] Moreover, new diagnostic criteria, prognostic markers, and therapeutic concepts have been developed.[26-29] Nevertheless, a number of questions remain concerning basic diagnostic standards, prognostication, optimal management and therapeutic options. Furthermore, there is a need to define clinically relevant pre-phases of CMML and distinct CMML variants by clinical variables, histomorphological features, flow cytometric phenotypes, molecular markers and cytogenetic findings. It is also important to separate CMML and pre-CMML conditions from diverse mimickers. To address these unmet needs, an international consensus group discussed open questions and issues around CMML, its variants and pre-CMML entities in a Working Conference held in August 2018. The outcomes of this meeting are summarized in this article and include proposed diagnostic criteria and a classification of pre-CMML conditions as well as updated minimal diagnostic criteria for CMML and its variants. In addition, diagnostic standards and diagnostic algorithms are proposed. Details concerning the conference format, pre- and post-conference discussion and consensus-finding are described in the *Online Supplement*.

Definition of CMML and minimal diagnostic criteria

The diagnostic criteria of CMML, as defined by the WHO,[15,16] are depicted in *Online Supplementary Table S1*. Our faculty is of the opinion that these criteria are valid in general for the classical form of CMML, but need adjustments for special variants of CMML. Based on consensus discussion, the following concept is proposed.

The *classical* form of CMML is defined by the following pre-requisite criteria: (i) persistent (at least 3 months) absolute PB monocytosis (≥1×10^9/L) and relative monocytosis (≥10% of PB leukocytes); (ii) exclusion of *BCR-ABL1*$^+$ leukemia, classical MPN and all other hematologic neoplasms that may serve as a primary source of monocytosis; and (iii) a blast cell count of 0-19% in PB and/or BM smears and exclusion of all (other) histopathological, morphological, phenotypic, molecular and cytogenetic signs that qualify as evidence of AML. In addition, morphological and/or histopathological evidence for diagnostic dysplasia in one or more of the three major BM cell lineages (≥10% of megakaryocytes and/or erythroid precursor cells and/or neutrophilic cells) must be present. If dysplasia is absent or not diagnostic (<10%), the presence of cytogenetic or molecular lesions (mutations) typically found in CMML and/or the presence of CMML-related flow cytometry abnormalities may be employed as co-criteria and may lead to the diagnosis of CMML, provided that the pre-requisite criteria listed above are fulfilled. Pre-requisite criteria and co-criteria of the classical form of CMML are presented in Table 1.

The exclusion of various reactive states producing monocytosis (and sometimes even dysplasia) was also discussed and regarded as being of great importance. However, these mimickers cannot *a priori* exclude the presence of a concomitant CMML, but may indeed occur

Table 1. Minimal diagnostic criteria for classical chronic myelomonocytic leukemia.*

A. Prerequisite criteria (all must be fulfilled)
- Persistent (3 months) peripheral blood monocytosis ≥1x10^9/L and relative monocytosis of ≥10% of circulating peripheral blood leukoyctes
- Exclusion of *BCR-ABL1*$^+$ leukemia, classical MPN and all other bone marrow neoplasms that could serve as a primary source of chronic persistent monocytosis
- Blast cell count of <20% in peripheral blood and bone marrow smears and exclusion of all other histopathological, morphological, molecular and cytogenetic features that count as evidence of the presence of acute myeloid leukemia**
B. Morphological criterion = Dysplasia
- Dysplasia in at least 10% of all cells in one of the following lineages in the bone marrow smear: erythroid; neutrophilic; megakaryocytic
C. Co-criteria (for patients fulfilling A but not B, and otherwise showing typical clinical features of CMML such as splenomegaly)
- Typical chromosome abnormalities by conventional karyotyping or FISH***
- Abnormal findings in histological and/or immunohistochemical studies of bone marrow biopsy sections supporting the diagnosis of CMML****
- Abnormal immunophenotype of bone marrow and blood cells by flow cytometry, with multiple CMML-associated phenotypic aberrancies indicating the presence of an abnormal/dysplastic population of monocytic and other myeloid cells*****
- Evidence of a clonal population of myeloid cells determined by molecular (sequencing) studies revealing CMML-related mutations******

*The diagnosis of classical CMML can be established when all prerequisite criteria (A) and either morphological dysplasia (B) or one or more of the co-criteria (C) are fulfilled. **Examples: Auer rods, overt acute myeloid leukemia (AML) by histology and immunohistochemistry; presence of AML-specific diagnostic cytogenetic and/or molecular markers (e.g., inv16). ***Typical cytogenetic abnormalities found in CMML (*Online Supplementary Table S6*). ****Leukemic infiltration of CD14+ monocytes and exclusion of AML. *****Utilizing a cutoff value of >94% MO1 monocytes, phenotyping can identify CMML cases with a sensitivity of >90% and a specificity of >95%, and a decrease in MO3 monocytes is even as diagnostic as an increase in circulating MO1 cells.[127,129,131] ******Genes that are often mutated in the context of CMML/MDS include, among others, *TET2*, *SRSF2*, *ASXL1* and *SETBP1*. The minimal allele burden proposed to count as co-criterion: ≥10%. CMML: chronic myelomonocytic leukemia; MPN: myeloproliferative neoplasm(s); MDS: myelodysplastic syndrome(s); FISH: fluorescence *in situ* hybridization.

in CMML patients in the context of certain infections. Furthermore, most of these mimickers do not produce persistent monocytosis. Proof of clonality by molecular and cytogenetic studies, and other disease-specific parameters, together with global and specific laboratory (e.g., microbial screen) tests should easily lead to the conclusion that the patient is suffering from reactive monocytosis but not from (or also from) CMML.

The *a priori* exclusion of AML as a criterion should apply to both the classical and the special variants of CMML, whereas the *a priori* exclusion of other indolent hematopoietic neoplasms should only apply to the classical variant of CMML and oligomonocytic CMML but not to other special CMML variants. This is because several previous and more recent studies have shown that CMML may be accompanied by (or may accompany) other myeloid or lymphoid neoplasms, such as systemic mastocytosis. In several of these patients, the CMML clone is dominant and the additional sub-clone is smaller in size and usually not relevant clinically, even if these smaller clones express certain driver mutations, such as *KIT* D816V or a rearranged *PDGFRA* or *PDGFRB*. Rarely, a Philadelphia chromosome-positive chronic myeloid leukemia may develop as an additional small-sized (sub)clone in a patient with CMML. Our faculty is of the opinion that the presence of additional (chronic) myeloid, mast cell, or lymphoid neoplasms does not exclude a diagnosis of CMML, provided that diagnostic WHO criteria for CMML are fulfilled. Moreover, these concomitant neoplasms should not exclude a diagnosis of CMML even when the driver of the concomitant disease (e.g., *KIT* D816V) is detectable in CMML monocytes. Thus, whereas the occurrence of AML is always regarded as transformation of CMML, the occurrence of *indolent* myeloid, mast cell, or lymphoid neoplasms should be regarded as concomitant disorders. Co-existing myeloid neoplasms and CMML may be derived from the same original founder clone.

There are also patients in whom a certain driver of another BM neoplasm is present, such as a mutated *JAK2*, *PDGFRA/B*, or *FGFR1*, but only the diagnostic criteria for CMML (not those of the other BM neoplasm) are fulfilled. Our faculty concludes that these cases should also be regarded and diagnosed as special variants of CMML. This strategy is in line with the current WHO classification. In fact, whereas the primary molecular diagnosis is often based on a mutated form of *JAK2*, *PDGFRA/B* or other classical driver, the underlying or additional diagnosis may well be CMML.[20,21]

Grading of CMML

The grading system of CMML proposed by the WHO is regarded as standard in clinical hematology. Our faculty recommends the use of this grading system as the initial prognostic tool in classical CMML. In fact, classical CMML should be split into CMML-0, CMML-1 and CMML-2 based on the blast cell count (*Online Supplementary Table S2*).[15-19] In addition, CMML can be divided into a dysplastic variant and a proliferative variant based on leukocyte counts (threshold: 13x10^9/L) (*Online Supplementary Table S2*). The resulting grading system defines six distinct CMML variants with variable clinical outcome.[17] However, grading may sometimes be challenging. For example, blast cell counts obtained from BM smears may differ from those obtained in the PB so that the grade is questionable. Our faculty recommends that in patients in whom results from BM and PB smears would not fit into one distinct grade of CMML (e.g., BM blasts 4% and PB blasts 6%) grading should be based on the higher blast cell percentage (*Online Supplementary Table S2*). It is worth noting that initial prognostication by grading does not include all essential prognostic parameters.

Table 2. Overview of special variants of chronic myelomonocytic leukemia.

Special variant	Key diagnostic features that discriminate the variant from classical CMML
Oligomonocytic CMML	Absolute PB monocyte count <1x10⁹/L
SM with concomitant CMML = SM-CMML	WHO criteria for SM fulfilled; in most patients CMML monocytes exhibit *KIT* D816V
CMML with a concomitant myeloid neoplasm* expressing a classical MPN- driver, such as *JAK2* V617F, *BCR-ABL1* or rearranged *PDGFRA/B*** or *FGFR1*.	WHO criteria for a classical MPN, such as CML**, PMF, or a myeloid neoplasm with rearranged *PDGFRA/B* are fulfilled in addition to the criteria for CMML.
CMML with expression of a molecular MPN-driver – examples: CMML with *JAK2* V617F or CMML with a rearranged *PDGFRA/B* or CMML with rearranged *FGFR1*.	Molecular drivers of classical MPN, such as *JAK2* V617F**** or rearranged *PDGFRA/B**** are found but diagnostic criteria for such classical MPN are not fulfilled (only criteria for CMML are met)
CMML with a concomitant lymphoid/lymphoproliferative neoplasm	WHO criteria for a lymphoid neoplasm are fulfilled

*These conditions must be separated from MPN with concomitant monocytosis that do not fulfil the diagnostic criteria for CMML. **Unlike in SM-CMML, in which monocytes display *KIT* D816V or CMML with rearranged *PDGFRA*, the CMML monocytes must not express *BCR-ABL1* in patients with CML plus CMML. ***Several different translocations and fusion genes involving *PDGFRA* or *PDGFRB* may be detected, such as the t(5;12) associated with the *TEL-PDGFRB* fusion gene. ****JAK2 V617F itself counts as a feature of MPN; therefore, detection of *JAK2* V617F can confirm the diagnosis of CMML (as MPN/MDS overlap disease) when other signs of myeloproliferation are absent (e.g., no splenomegaly and no leukocytosis). CMML: chronic myelomonocytic leukemia; PB: peripheral blood; SM: systemic mastocytosis; WHO: World Health Organization; MPN: myeloproliferative neoplasm; CML: chronic myeloid leukemia; PMF: primary myelofibrosis.

We therefore recommend that in each case, deeper (full) prognostication should follow using multiparametric scoring systems (see later). It should be noted, however, that grading of CMML has only been validated in the classical form of CMML, not in special CMML variants. Therefore, although grading is also recommended for special CMML entities, it is not regarded standard and the result must be interpreted with caution in these patients.

Special variants of CMML: overview

As mentioned before, the classical form of CMML meets all pre-requisite criteria, and no signs (including molecular features) of an additional, concomitant BM neoplasm are detected. The special variants of CMML form a heterogeneous group of neoplasms comprising distinct clinical and biological entities. In one group of patients, the relative monocyte count (≥10%) is fulfilled without resulting in an absolute count ≥1×10⁹/L, precluding the diagnosis of 'classical CMML'. Most of these patients are diagnosed as having MDS or MPN/MDS-unclassified by WHO criteria. In another group of patients, a molecular signature suggestive of a different type of myeloid neoplasm is detected but only the criteria for CMML (not those for the other neoplasm) are met. Such an example is CMML with *JAK2* V617F (without definitive evidence of a concomitant MPN). In a third group, CMML co-exists with another BM neoplasm, such as MPN or mastocytosis. In these patients, additional blood count abnormalities (e.g., eosinophilia), an elevated serum tryptase level and/or BM fibrosis, may be detected.

All variants of CMML (classical and special) can occur as a primary CMML or as a secondary CMML following a 'mutagenic' event, such as chemotherapy (therapy-related CMML). In addition, our faculty is of the opinion, that the term secondary CMML may also be appropriate for those patients who develop CMML (months or years) after another indolent myeloid neoplasm, such as a MDS or systemic (indolent or aggressive) mastocytosis, had been diagnosed. In the following paragraphs, the clinical features and diagnostic criteria of special (atypical) variants of CMML are proposed and discussed. An overview of the special variants of CMML is provided in Table 2.

Oligomonocytic CMML

Over the past few years, more and more cases of cytopenic patients exhibiting relative monocytosis (≥10%) and moderately increased absolute blood monocytes not reaching the required threshold to diagnose classical CMML (1.0x10⁹/L) have been described. These cases have recently been referred to as oligomonocytic CMML.[30] According to the WHO classification most of these patients would be classified as having MDS (with monocytosis) or perhaps MPN/MDS-unclassifiable. However, most of these patients exhibit typical features of CMML, including a typical morphology of PB and BM cells, splenomegaly, and CMML-related molecular features (e.g. mutations in *TET2* and *SRSF2*).[30-32] Some of these patients have prominent BM monocytosis without diagnostic PB monocytosis at diagnosis.[30,32]

Whereas several of these cases remain stable without progression, the majority will develop 'overt' CMML or, eventually, secondary AML during follow-up. Therefore, oligomonocytic CMML may also be regarded as a potential pre-phase of classical CMML. Our faculty is of the opinion that the term oligomonocytic CMML should be used in clinical practice. Diagnostic pre-requisite criteria for oligomonocytic CMML are: (i) persistent (lasting at least 3 months) absolute peripheral monocytosis of 0.5-0.9×10⁹/L and relative blood monocytosis (≥10% of blood leukocytes); (ii) exclusion of *BCR-ABL1*⁺ leukemia, classical MPN and all other myeloid neoplasms that can explain monocytosis; and (iii) a blast cell count of 0-19% in PB and/or BM smears and exclusion of all histopathological, morphological, phenotypic, molecular and cytogenetic signs that count as proof of AML. Diagnostic dysplasia in one or more of the three major BM lineages (≥10%) must also be documented. If dysplasia is lacking or 'sub-diagnostic' (<10%), the presence of cytogenetic or molecular lesions (mutations) typically found in CMML and/or the presence of CMML-related flow cytometry abnormalities, may also lead to the conclusion that the patient has oligomonocytic CMML provided that the other diagnostic criteria described above are fulfilled and all other myeloid neoplasms have been excluded. The proposed criteria for oligomonocytic CMML are listed in

Table 3. **Proposed minimal diagnostic criteria for oligomonocytic chronic myelomonocytic leukemia.***

A. Prerequisite criteria (all must be fulfilled)
- Persistent (3 months) peripheral blood monocytosis 0.5-0.9x10^9/L and relative monocytosis of ≥10% of circulating peripheral blood leukoyctes
- Exclusion of *BCR-ABL1*$^+$ leukemia, classical MPN and all other bone marrow neoplasms that could serve as a primary source of chronic persistent monocytosis
- Blast cell count <20% in peripheral blood and bone marrow smears and exclusion of all other histopathological, morphological, molecular and cytogenetic features that count as evidence of the presence of acute myeloid leukemia**
B. Morphological criterion = Dysplasia
Dysplasia in at least 10% of all cells in one of the following lineages in the bone marrow smear: erythroid; neutrophilic; megakaryocytic
C. Co-criteria (for patients fulfilling A but not B, and otherwise showing typical clinical features of CMML such as splenomegaly)
- Typical chromosome abnormalities by conventional karyotyping or FISH***
- Abnormal findings in histological and/or immunohistochemical studies of bone marrow biopsy sections supporting the diagnosis of CMML****
- Abnormal immunophenotype of bone marrow and blood cells by flow cytometry, with multiple CMML-associated phenotypic aberrancies indicating the presence of an abnormal/dysplastic population of monocytic (and other myeloid) cells*****
- Evidence of a clonal population of myeloid cells determined by molecular (sequencing) studies revealing CMML-related mutations******

*The diagnosis of classical CMML can be established when all prerequisite criteria (A) and either morphological dysplasia (B) or one or more of the co-criteria (C) are fulfilled. **Examples: Auer rods, overt acute myeloid leukemia (AML) by histology and immunohistochemistry; presence of AML-specific diagnostic cytogenetic and/or molecular markers (e.g., inv16). ***Typical cytogenetic abnormalities found in CMML (*Online Supplementary Table S6*). ****Leukemic infiltration of CD14+ monocytes and exclusion of AML. *****Utilizing a cutoff value of >94% MO1 monocytes, phenotyping can identify CMML cases with a sensitivity of >90% and a specificity of >95%, and a decrease in MO3 monocytes is even as diagnostic as an increase in circulating MO1 cells.[127,129,131] ******Genes that are often mutated in the CMML/MDS context include, among other, *TET2*, *SRSF2*, *ASXL1* and *SETBP1*. Minimal allele burden proposed to count as a co-criterion: ≥10%. CMML: chronic myelomonocytic leukemia; MPN: myeloproliferative neoplasm(s); MDS: myelodysplastic syndrome(s); FISH: fluorescence *in situ* hybridization.

Table 3. Patients with oligomonocytic CMML should be managed and followed clinically in the same way as patients with classical CMML.

CMML associated with *KIT* D816V$^+$ systemic mastocytosis

According to WHO criteria, systemic mastocytosis (SM) can be divided into: (i) indolent SM (ISM), which is assocaiated with a normal life expectancy; (ii) smoldering SM (SSM), in which signs of BM dysplasia, myeloproliferation and/or splenomegaly are found but survival and prognosis are still favorable; and (iii) advanced SM, defined by a poor prognosis.[33-36] Advanced SM is further divided into aggressive SM (ASM), SM with an associated hematologic neoplasm (SM-AHN) and mast cell leukemia (MCL).[33-36] The most frequent AHN detected in patients with SM-AHN is CMML.[6-8,36] In these patients the SM component of the diseases may present as ISM, ASM or, rarely, as MCL. Our faculty concludes that diagnostic WHO criteria for SM and diagnostic criteria for classical CMML (except exclusion of SM) must be fulfilled to diagnose SM-CMML.

Patients with SM may present with monocytosis resembling oligomonocytic CMML. However, the clinical features of SSM and advanced SM overlap largely with those found in patients with oligomonocytic CMML. Especially in SSM, myeloproliferation, dysplasia and splenomegaly are diagnostic criteria.[33-35] Therefore, our faculty is of the opinion that such patients should be classified as having ISM, SSM or ASM with monocytosis rather than SM with oligomonocytic CMML.

In patients with CMML, a concomitant SM is often overlooked, especially when the disease does not present with cutaneous lesions. In other patients, CMML is diagnosed long before SM is detected by chance or after *KIT* D816V is identified: even though it is tempting to call these conditions CMML-SM, our faculty agreed that the classical terminology should be SM-CMML which is also in line with the WHO classification[34,35] and that the subtype of SM and of CMML should be defined in the final diagnosis (e.g., ISM-CMML-1 or ASM-CMML-2) with recognition that in the SM-context, CMML is always regarded as a secondary neoplasm.[6,36] Furthermore our faculty is of the opinion that it should be standard practice to examine BM and blood leukocytes for the presence of *KIT* D816V in all patients with (suspected) CMML. In almost all patients with SM-CMML, neoplastic monocytes display *KIT* D816V.[7] In these monocytes, mutated KIT is not expressed on the cell surface but acts as a cytoplasmic driver. In line with this hypothesis drugs targeting *KIT* D816V can sometimes induce a major decrease in monocyte counts in patients with ASM-CMML.[37]

Therapy of SM-CMML should be based on a bi-directional strategy: in fact the SM component of the disease should be treated as if no CMML was diagnosed and CMML should be treated as if no SM had been found, with recognition of drug-drug interactions and the possibility of drug-induced anaphylaxis.[33-35] In many cases (ISM-CMML) the SM component of the disease is only treated symptomatically.[33-35]

CMML associated with mutated *JAK2*, rearranged *PDGFRA/B* or other drivers

Patients with CMML may present with the *JAK2* mutation V617F, a rearranged *PDGFRA* or *PDGFRB*, often in the context of hypereosinophilia, or other drivers related to distinct hematopoietic neoplasms as defined by the WHO.[5,9-11,38-43]

CMML with rearranged *PDGFRA*, *PDGFRB*, *FGFR1* or *PCM1-JAK2*

In these patients, persistent substantial monocytosis (≥1.0x10^9/L) is detected and all other consensus criteria for classical CMML (see previous paragraphs) are also met, except the following specific exclusion criteria: CMML to be excluded in the presence of a well-characterized diagnosis of myeloid/lymphoid neoplasm with rearranged *PDGFRA*, *PDGFRB*, *FGFR1* or *PCM1-JAK2* (Table 2). Except for neglecting the above-mentioned criteria, our proposal is otherwise fully in agreement with all of the other tenets postulated by the WHO classification.[14,15] In relation to neoplasms with rearranged *PDGFRA/B*, *FGFR1* or *PCM1-JAK2*, the WHO's definition of 'myeloid/lymphoid neoplasms' is too generic and there is a clinical need to know whether the underlying myeloid neoplasm is an aggressive disease, like AML, or a chronic neoplasm such as CMML or chronic eosinophilic leukemia.[20,21] Our faculty is of the opinion that (unlike in previous times) the presence of one criterion-confirmed myeloid neoplasm should not *a priori* exclude the presence of another (second concomitant) myeloid or lymphoid neoplasm. Hence, when CMML is encountered in the context of another molecularly defined myeloid/lymphoid neoplasm (as a final diagnosis), it should be delineated as a specific subtype of the myeloid/lymphoid neoplasm with eosinophilia along with the specific associated gene rearrangement (*PDGFRA/B* or *FGFR1* or *PCM1-JAK2*).

CMML with *JAK2* V617F

In these patients the situation is different. First, *JAK2* V617F itself may be considered as a criterion of myeloproliferation in MDS/MPN, e.g. in cases with MDS/MPN with ring sideroblasts and thrombocytosis. In the context of CMML, the *JAK2* mutation is also typically associated with other signs of myeloproliferation (including BM fibrosis) and with the ´myeloproliferative variant´ of CMML.[39,42,43] Therefore, our faculty concludes that *JAK2* V617F should also count as a molecular co-criterion of MDS/MPN and thus for CMML. Second, the presence of a *JAK2*-mutated MPN does not exclude the presence of a concomitant CMML if diagnostic criteria for both neoplasms are fulfilled. If this is not the case because the size of the MPN-like clone carrying *JAK2* V617F is too small and/or other MPN features are clearly missing, the final diagnosis will be CMML with *JAK2* V617F. On the other hand, in patients in whom the *JAK2* allelic burden is high and clinical and laboratory features argue for an overt MPN rather than CMML (e.g., polycythemia and/or BM fibrosis without dysplasia and without molecular or flow cytometry-based signs of CMML) the final diagnosis will be *JAK2* V617F$^+$ MPN with monocytosis.[43] In a third group of patients, diagnostic criteria for both a distinct MPN and CMML are fulfilled and the mutation status confirms the presence of an overt *JAK2*-mutated MPN (usually with high allelic burden). These patients are suffering from both MPN and CMML or from a gray zone disease displaying hybrid features between MPN and CMML.[44,45] Our faculty concludes that it is therefore important to measure the *JAK2* V617F allele burden in all patients with CMML.[39,42,43] Other drivers, such as *BCR-ABL1*, are rarely found in patients with CMML. However, although in classical CMML, the presence of *BCR-ABL1* must be excluded, it may be detected in rare patients, suggesting the existence of a special variant of CMML (defined by a co-existing chronic myeloid leukemia). In some of these cases, the chronic myeloid leukemia clone may be small. In other patients, however, the chronic myeloid leukemia may even mask the CMML at the initial diagnosis.[46]

The management and therapy of patients with special variants of CMML depend on the subtype of the disease and the molecular driver involved, e.g., *FIP1L1/PDGFRA*, other gene abnormalities involving *PDGFRA* or *PDGFRB*, *KIT* D816V or *JAK2* V617F. Therefore, it is of crucial importance to screen for all these drivers in all patients with CMML. The type of therapy to consider in these patients depends on clinical features, the histopathological diagnosis, the size of the mutated clone(s) and the type of driver. The type of driver is of considerable importance since novel treatments directed against these drivers, are often extremely effective.[47-50] For example, imatinib can induce long-lasting molecular and hematologic complete remissions in patients with *FIP1L1/PDGFRA*-rearranged myeloid neoplasms with features of CMML or MPN.[47-49] Even in patients who develop CMML and secondary AML in the context of *FIP1L1/PDGFRA*, the disease may respond to imatinib.[50] It is, therefore, important to diagnose all patients based on molecular markers and to define the major drivers and therapeutic targets expressed by malignant cells in order to provide optimal management and therapy.

CMML associated with lymphoid neoplasms

In a small group of patients with CMML, a co-existing lymphoproliferative neoplasm is diagnosed, such as a lymphocytic leukemia, non-Hodgkin lymphoma or multiple myeloma.[51-60] In most patients, the lymphoid neoplasm is detected first, and CMML is considered to develop as treatment-induced, secondary, leukemia.[51,57] In other patients, CMML is diagnosed first and later a lymphoid neoplasm is detected during follow-up.[52-56] It is worth noting that in patients with CMML, polyclonal hypergammaglobulinemia is often recorded: this must be distinguished from the monoclonal gammopathy of concomitant myeloma, monoclonal gammopathies of undetermined significance and both low-count and high-count monoclonal B lymphocytoses which represent pre-malignant conditions.

The management and treatment of lymphoid neoplasms presenting with concomitant (secondary) CMML is a clinical challenge. In non-transplantable cases, both diseases require separate treatment plans. Because of the high risk of transformation to AML, allogeneic hematopoietic stem cell transplantation should be considered in young, fit patients, especially when it can be expected that the lymphoid neoplasm will also be eradicated by this approach.

Treatment-related CMML and other secondary forms of CMML

Our faculty concluded that both the classical form of CMML and the special variants of CMML should be divided into primary (*de novo*) CMML and secondary CMML. The latter group includes patients who (i) received chemotherapy and/or radiation therapy in the past (therapy-related CMML) or (ii) have a history of a preceding MDS, MPN or another indolent myeloid or mast cell neoplasm prior to their diagnosis of CMML.[51,57,58,61-64] Recent data suggest that patients with therapy-related secondary CMML may have shorter overall survival compared to that of patients with primary (*de*

novo) CMML.[65] Although progression-free survival may not be different in these patients compared to those with *de novo* CMML, some of these patients progress rapidly to secondary AML. It is also worth noting that patients with therapy-related secondary CMML have a higher frequency of karyotypic abnormalities compared to patients with *de novo* CMML.[66] Eligible patients in this group should be offered allogeneic hematopoietic stem cell transplantation.

Potential pre-phases of CMML

During the past few years evidence has accumulated suggesting that hematopoietic neoplasms, including MDS, MPN and MDS/MPN, develop in a step-wise manner. In the earliest phases of clonal development, patients present without overt signs or symptoms of a hematopoietic neoplasm but their leukocytes carry one or more somatic mutations, usually (early, passenger-type) mutations otherwise also found in overt myeloid neoplasms (for example *TET2* mutations).[67-70] In the context of MDS and other myeloid neoplasms, these cases have been referred to as clonal hematopoiesis of indeterminate potential (CHIP), or, when accompanied by cytopenia, as clonal cytopenia of unknown significance (CCUS).[69-73] Since these mutations are frequently detected in older individuals, the condition is also called age-related clonal hematopoiesis (ARCH).[70,73] In a few healthy individuals, *bona fide* oncogenic drivers (such as *BCR-ABL1*) are detected in a small subset of leukocytes. Because of the oncogenic potential of these drivers, these conditions are termed clonal hematopoiesis with oncogenic potential (CHOP).[71,73] CHIP, CCUS and CHOP may also be the earliest clonal conditions preceding CMML. For these cases, the definitions recently proposed for CHIP, CCUS and CHOP should apply.[69,71,73]

Apart from somatic mutations, other factors, such as epigenetic modifications, chronic inflammation or aging-related processes, may also trigger the selection and expansion of pre-malignant neoplastic clones in myeloid neoplasms including CMML.[74-76] Some of these conditions may present with persistent monocytosis without signs of an overt myeloid neoplasm and may represent pre-phases of overt CMML. In other patients, however, no or another hematopoietic neoplasm develops during follow-up. Therefore, our faculty concluded that this pre-phase should be termed idiopathic monocytosis of unknown significance, provided that the following criteria are met: (i) persistent (at least 3 months) relative (≥10%) *and* absolute (>0.5x10^9/L) monocytosis; (ii) no diagnostic dysplasia and no signs of myeloproliferation; (iii) no signs and criteria of a myeloid or other hematopoietic neoplasm fulfilled; (iv) no flow cytometric abnormalities or somatic mutations related to a myeloid, mast cell or lymphoid neoplasm detected in leukocytes; and (v) no reactive condition that would explain reactive monocytosis is detected (Table 4 and *Online Supplementary Table S3*). If CHIP-like mutations are found in such patients, but no hematopoietic neoplasm can be diagnosed using the WHO criteria, the final diagnosis changes to clonal monocytosis of unknown significance (*Online Supplementary Table S3*). It is also worth noting that idiopathic cytopenias of unknown significance can precede CMML.[64,77-79] Especially in patients with idiopathic thrombocytopenia of unknown significance, a CMML may be detected upon deeper investigations or during follow-up.[77-79] Finally, as mentioned before, oligomonocytic CMML, although proposed as a special variant of CMML, must also be regarded as a potential pre-phase of classical CMML. In this regard it is important to note that these patients should have a regular follow-up

Table 4. Overview of non-clonal and clonal conditions that may precede chronic myelomonocytic leukemia.

	Pre-CMML conditions and comparison to classical CMML						
Feature	IMUS	ICUS	CCUS	CHIP/CHOP	CMUS	O-CMML	CMML
Absolute monocytosis (≥0.5x10^9/L)	+	+/-	+/-	+/-	+	+	+
Substantial monocytosis (≥1x10^9/L)	+/-	-	-	-	+/-	-	+
Relative monocytosis (>10% of leukocytes)	+	-	-	-	+	+	+
Dysplasia*	-	-	-	-	-	+	+
Cytopenia(s)**	-	+	+	-	-	+/-	+/-
BM blasts	<5%	<5%	<5%	<5%	<5%	<20%	<20%
Flow abnormalities	-	-	+/-	+/-	-	++	++
Cytogenetic abnormality (≥1)	-***	-***	+/-	+/-	-***	++	++
Molecular aberration/s****	-	-	+	+	+****	++	++

*At least 10% of all cells in a given lineage (erythroid, neutrophilic, or megakaryocytic) are dysplastic. **Persistent cytopenia(s) recorded over a time-period of at least 4 months. ***In a subset of cases, a small clone is detectable by FISH. ****A molecular aberration is defined by CMML/MDS-related mutations and an allele burden of ≥2%. The working definition for pre-CMML conditions is also ≥2% allele burden, whereas the minimal allele burden to count as a co-criterion for CMML is 10%. In most patients with overt CMML, multiple gene mutations/aberrations are found. ****Here a CHIP-like mutation is detected – if more than one CHIP-like mutations are found the question is whether the final diagnoses changes to O-CMML. CMML: chronic myelomonocytic leukemia; IMUS: idiopathic monocytosis of unknown (undetermined) significance; ICUS: idiopathic cytopenia of undetermined significance; CCUS: clonal cytopenia of undetermined significance; CHIP: clonal hematopoiesis of indeterminate potential; CCUS, clonal cytopenia of undetermined significance; CMUS: clonal monocytosis of unknown (undetermined) significance; O-CMML: oligomonocytic CMML; MDS: myelodysplastic syndrome; BM: bone marrow; FISH: fluorescence *in situ* hybridization.

with repeated investigations of all disease-related parameters. A summary of non-clonal and clonal conditions potentially preceding CMML is shown in Table 4. With regard to criteria delineating non-clonal pre-diagnostic conditions, like idiopathic cytopenia of undetermined significance from the clonal conditions described above (CHIP, CCUS, CHOP), we refer the reader to the pertinent literature.[69,71,73]

Peripheral blood and bone marrow smears: proposed standards and recommendations

As in other myeloid neoplasms, a thorough examination of appropriately prepared and stained BM and PB smears is a crucial diagnostic approach in suspected CMML. It is standard to examine and count at least 100 leukocytes in the PB film and 200-500 nucleated cells in well-prepared thin BM films. BM cellularity, the erythroid-to-myeloid (E:M) ratio, and the percentage of blast cells (including monoblasts and promonocytes), monocytes, mast cells, and other myeloid cells must be recorded (reported) in each case. As in patients with MDS, at least 10% of cells in one of the major BM lineages (erythroid and/or neutrophilic and/or megakaryocytic) must be dysplastic to meet the dysplasia criterion for CMML.[13-18] It is also standard to study well-prepared and appropriately stained PB smears in CMML and to report the percentage of circulating monocytes, including normal (mature) and abnormal (immature) monocytes, blast cells, other immature myeloid cells, dysplastic (hypogranulated) neutrophils and other cell types in the PB. Overall, the same standards and recommendations that count for the evaluation of MDS by morphology (BM and PB stains)[12,80-83] also apply in cases with (suspected) CMML.[13-18] An important point is the classification of blast cells and monocytic cells in CMML (Table 5).[16,84] Blast cell types detectable in CMML include myeloblasts, monoblasts and also promonocytes (even if not named blast cells) (Table 5). Monocytes should be classified as normal (mature) or abnormal (immature).[16,84] The morphological criteria used to distinguish between these cell types are presented in Table 5. Together with morphology, cytochemical staining for non-specific esterase can also assist in the cytological delineation between monocytes, monoblasts and promononcytes.[16] An important aspect is that in many patients, megakaryocyte dysplasia is better documented and quantified in BM histology sections than in BM smears. Therefore, megakaryocyte dysplasia should only be recorded in BM smears when a sufficient number of these cells can be detected. Finally, the morphology of mast cells, when detected, should always be reported using established criteria and standards.[85]

Bone marrow histology and immunohistochemistry in CMML

A thorough investigation of an appropriately processed and stained BM biopsy section by histology and immunhistochemistry is standard in all cases with known or suspected CMML or a suspected pre-CMML condition.[14-16,30,86] Notably, BM histology and immunhistochemistry are essential approaches to confirm the diagnosis of CMML and to exclude AML and other CMML-mimickers. Moreover, BM histology and immunhistochemistry may provide important additional information, including that on BM fibrosis, focal accumulations of blast cells, increased angiogenesis, atypical (dysplastic) megakaryocytes, a hypocellular BM or concomitant mastocytosis (*Online Supplementary Table S4*).[33-35,86] The evaluation and enumeration of $CD14^+$ monocytes, $CD34^+$ progenitor cells and $CD117^+/KIT^+$ cells (progenitors and mast cells) by immunhistochemistry in BM biopsy sections represent an integral part of the diagnostic assessment. These approaches can also prevent diagnostic errors. For example, when the smear is of suboptimal quality, a preliminary diagnosis of CMML may change to AML based on BM histology and CD34 immunhistochemistry.

BM biopsy specimens are usually taken from the iliac crest and should be of adequate length (≥2 cm). The specimen should be fixed in neutral formalin (or alternative standard fixation), decalcified in EDTA (for at least 8 h) or by alternative standard decalcification, and embedded in paraffin-wax. Ideally 2-3 μm thin sections should be prepared. Routine stains include hematoxylin-eosin, Giemsa, Prussian blue, AS-D chloroacetate esterase, toluidine blue and silver impregnation (Gömöri's stain). BM cellularity should be measured and reported according to published standards.[87,88] For routine purposes, the pathologist should determine the cellularity as 'normocellular', 'hypocellular', or 'hypercellular', based on an age-adapted estimate.[89] The presence of variable degrees of BM fibrosis

Table 5. Classification of blast cells and monocytes in patients with chronic myelomonocytic leukemia.

Cell type	Nuclear shape	Chromatin	Cytoplasm	Size relative to mature monocytes
Blast cells:				
Myeloblast	Round/oval	Fine with nucleoli	Basophilic, rare or no granules	Smaller
Monoblast	Round/oval	Delicate/lace-like, nucleoli	Basophilic, rare azurophilic granules	Large (20-30 μM)
Promonocyte	Convoluted/indented*	Delicate/lace-like, nucleoli	Variably basophilic, variably azurophilic granules	Large
Monocytes:				
Abnormal/immature monocyte	Convoluted/indented	More condensed, rare nucleoli	Intermediate basophilic**	Smaller
Mature monocyte	Lobulated/ indented	Condensed, no nucleoli	Gray or pinkish with occasional azurophilic granules and vacuoles	=

*The most important feature discriminating promonocytes from monoblasts. **Less basophilic than promonocytes and more basophilic than mature monocytes.

(usually mild to moderate) has been reported in CMML cases, with several recent studies attempting to determine the prognostic value of this finding.[42,90,91] Indeed, although the data are not yet conclusive, the presence of marrow fibrosis in CMML seems to be of prognostic importance.[42,90,91]

The application of immunhistochemical markers is recommended in all patients with (suspected) CMML. The minimal immunohistochemistry panel includes CD14 (monocytes), CD34 (progenitors), CD117/KIT (progenitors and mast cells), tryptase (mast cells), and a megakaryocyte marker (CD41, CD42 or CD61) (*Online Supplementary Table S5*).[86,92,93] In unclear cases or when a co-existing (second) BM neoplasm is suspected, additional lineage-specific antibodies such as CD3, CD20, or CD25 (suspected mastocytosis) should be applied (*Online Supplementary Table S4*). When employing CD34 as a progenitor-related immunhistochemical marker, it is important to know that endothelial cells also express this antigen. Another important point is that blasts may sometimes be CD34-negative. In such cases, KIT/CD117 is applied as an alternative marker (*Online Supplementary Table S4*). For the immunohistochemical detection of monocytic cells, CD14 is a preferred antigen.[71,86] Tryptase and CD117 are useful immunhistochemistry markers for detecting and quantifying mast cells.[92,93] When spindle-shaped mast cells form compact clusters in the BM and express CD25, these cells usually also display *KIT* D816V – in these cases the final diagnosis is always SM-CMML.[93] In other cases, the pathologist will ask for *JAK2* V617F, based on an abnormal morphology and distribution of megakaryocytes. As in MDS, megakaryocytes may also express CD34 in patients with CMML.

Table 6. Commonly mutated genes detectable in patients with classical chronic myelomonocytic leukemia.

Gene name abbreviation	Gene class and function	Relative frequency in CMML	Clinical impact
ASXL1	Epigenetic regulation Histone modification	40%*	Poor prognosis** CHIP/ARCH***
EZH2	Epigenetic regulation Histone modification	5%	
TET2	Epigenetic regulation DNA methylation	60%*	CHIP/ARCH***
DNMT3A	Epigenetic regulation DNA methylation	5%	Poor prognosis** CHIP/ARCH***
IDH1	Epigenetic regulation	1%	Drug target
IDH2	Epigenetic regulation	5-10%	Drug target
CBL	Signaling	15%	RAS pathway
NRAS	Signaling	15%	Poor prognosis** RAS pathway
KRAS	Signaling	10%	RAS pathway
PTPN11	Signaling	5%	RAS pathway
FLT3	Signaling	<5%	AML-related Drug target
SRSF2	Pre–mRNA splicing	50%*	
SF3B1	Pre–mRNA splicing	5-10%	
U2AF1	Pre–mRNA splicing	5-10%	
ZRSR2	Pre–mRNA splicing	5%	
RUNX1	Gene transcription	15%	Poor prognosis** AML-related
SETBP1	Gene transcription	15%	Poor prognosis**
TP53	DNA damage	1%	Poor prognosis**
PHF6	Chromatin adaptor	5%	

*These mutations can be regarded as CMML-related mutations, but only *SRSF2* mutations do not, in addition, also count as classical CHIP/ARCH mutations. **Mutations in these genes are independent adverse prognostic factors regarding survival in CMML. ***These genes are frequently detected in individuals with clonal hematopoiesis of indeterminate potential (CHIP) also known as age-related clonal hematopoiesis (ARCH). Therefore, the diagnostic impact of these mutations may be regarded as somehow lower compared to that of other (CMML-related and other) mutations. CMML: chronic myelomonocytic leukemia; AML: acute myeloid leukemia.

Karyotyping in CMML: current recommendations and standards

Clonal cytogenetic abnormalities are detected in 20-30% of all patients with CMML. The most frequently identified aberrations are trisomy 8, abnormalities of chromosome 7 (especially monosomy 7 and deletion of 7q), and loss of the Y chromosome (–Y) (*Online Supplementary Table S6*).[94-97] Compared to MDS, isolated del(5q) and complex abnormal karyotypes are rarely detected in CMML. Our faculty is of the opinion that conventional karyotyping of BM cells should be performed in all patients with known or suspected CMML or a suspected pre-CMML condition. At least 20 metaphases should be examined.[98] In the case of a clear-cut result, even 10-20 metaphases may be sufficient to define the karyogram. Reporting of karyotypes should be performed using the International System for Human Cytogenetic Nomenclature (ISCN) guidelines.[99] A clone is defined by two or more metaphases showing the same gain or structural rearrangement (deletion, inversion, translocation) of chromosomal material or at least three metaphases showing a monosomy of the same chromosome.[99] Several of the cytogenetic anomalies in CMML may be difficult to detect by conventional karyotyping. Therefore, we are of the opinion that fluorescence *in situ* hybridization (FISH) should be performed in all patients with (suspected) CMML, at least in those in whom no karyotype anomaly was detected by conventional karyotyping. The FISH probes should cover all relevant regions, including 5q31, cep7, 7q31, 20q, cep8, cepY and p53. Special consideration should be directed to cryptic deletions of *TET2* (in 4q24), *NF1* (17q11), and *ETV6* (12p13) which can occur in up to 10% of CMML patients[10] and are only detectable by interphase FISH (*Online Supplementary Table S6*). It is worth noting that *NF1* deletions may occur during progression/karyotype evolution in CMML. The limitation of FISH is that is does not detect all karyotypic abnormalities. In some patients with CMML, clonal evolution is found. Subclones are defined by additional chromosomal defects (apart from the primary chromosomal defect) in at least two cells (or 3 cells for monosomies) and the absence of these additional chromosomal defects in the other clonal cells.[99] A complex karyotype is defined by at least three chromosome defects in one clone.[99] As in MDS, a complex karyotype in CMML is indicative of a poor prognosis. Overall, cytogenetic studies are of prognostic significance in CMML and have been used to optimize prognostic scoring systems.[97,100-102] In some patients with CMML, clonal evolution is observed over time and may then also be an adverse prognostic sign. Therefore, we recommend that chromosome analyses are performed each time a BM investigation is done in the follow-up in order to detect (or exclude) clonal evolution.

Mutation profiles in CMML: current standards and limitations

Somatic mutations are detectable in the vast majority of patients with CMML.[8,11,103-106] The clonal architecture, clone sizes and clonal evolution patterns vary from patient to patient.[106-108] In some cases, initially small clones expand over time. It is, therefore, standard to apply next-generation sequencing assays with sufficient sensitivity to identify *bona fide* somatic mutations associated with CMML. The most frequently detected somatic mutations in CMML are mutations in *TET2* (60%), *SRSF2* (50%), and *ASXL1* (40%) (Table 6).[31,103-110] The presence of a *SRSF2* mutation, particularly in combination with mutated *TET2*, correlates strongly with a CMML phenotype.[31,109,110] It is also worth noting that two of these mutations (*TET2*, *ASXL1*) are also known as CHIP/ARCH-related mutations. However, only mutated *ASXL1* has been associated with a poor prognosis in CMML.[104,109] An overview of somatic mutations recurrently detected in CMML is provided in Table 6. Somatic mutations with independent prognostic impact include several RAS-pathway mutations as well as mutations in *ASXL1*, *RUNX1* and *SETBP1* (Table 6).[31,103-111] RAS-pathway mutations trigger cell signaling and proliferation and have been associated with cytokine-independent growth of CMML progenitor cells, the proliferative variant of CMML, AML transformation and poor survival.[10,22,23,112-116] Other driver mutations involved in cell signaling, such as *JAK2* V617F or *KIT* D816V, are also major triggers of cellular differentiation (*Online Supplementary Table S7*). These drivers alone cannot induce transformation, but they may act together with other (e.g., 'RAS pathway') mutations to cause disease progression. Whereas *JAK2* V617F is a strong indicator of MPN-like differentiation, the presence of *KIT* D816V is almost always associated with concomitant mast cell differentiation and mastocytosis (SM-CMML).[6-8,32-36,39,42,43] The other mutations found in CMML act as modulators of epigenetic events and transcription (e.g., *ASXL1*) or DNA methylation (e.g., *TET2*), as regulators of the spliceosome machinery (e.g., *SRSF2*), or as modulators of the DNA damage response, such as *TP53* (Table 6). During progression of CMML to secondary AML and especially during therapy, the mutational landscape(s) and clonal architecture(s) may change.[109-113] For example initially small clones may expand and may be selected because of resistance-mediating molecular features. It is worth noting that several mutated gene products also serve as potential targets of therapy (Table 6).

Our faculty recommends that next-generation sequencing studies should be regarded as a standard approach in all patients with suspected or known CMML as well as in patients with idiopathic monocytosis of unknown significance and in those with persistent reactive monocytosis (in order to exclude an additional clonal component). When a CMML-related mutation is found in an individual with idiopathic monocytosis of unknown significance or reactive monocytosis, the diagnosis may change to clonal monocytosis of unknown significance or oligomonocytic CMML, depending on additional findings.

Our faculty also recommends that the next-generation sequencing assay should have sufficient sensitivity (to detect 2-5% clonal cells) and should cover all relevant lesions shown in Table 6. In the context of CHIP/ARCH, a cutoff variant allele frequency of 2% is considered diagnostic,[69] whereas in the context of CMML, we propose 10% as the variant allele frequency diagnostic cut off and thus marker to count as a co-criterion of CMML when, for example, no diagnostic morphological dysplasia can be documented (Tables 1 and 3), similar to the definition in MDS.[71,73] Determining the variant allele frequency is also useful for documenting the clinical impact of certain driver lesions in special CMML variants (e.g., with *JAK2* V617F or *KIT* D816V) and clone expansion during follow-up. Therefore, our faculty recommends that molecular studies in CMML should report variant allele frequencies with sufficient precision and sufficient sensitivity – in the same way as in MDS.[71,73] Finally, our faculty recommends that molecular markers should increasingly be used to optimize prognostic scoring systems in CMML.[117-120]

Flow cytometry in CMML: standards and limitations

Flow cytometry studies are an essential diagnostic tool in patients with (suspected) classical CMML, pre-CMML conditions and special CMML variants.[121-132] Therefore, our faculty is of the opinion that it is standard practice to perform multi-color flow cytometry (MFC) in the PB and BM in all cases with suspected or known CMML or a suspected pre-CMML condition. MFC studies are helpful to confirm the monocyte and blast cell counts in these patients and to exclude AML. In addition, MFC is useful to confirm the presence of distinct monocyte populations. Monocytes are defined as $CD14^+$ cells in these analyses. Based on the expression of CD14 and CD16, monocytes are further divided into classical (MO1) monocytes ($CD14^{bright}/CD16^-$), intermediate (MO2) monocytes ($CD14^{bright}/CD16^+$) and non-classical (MO3) monocytes ($CD14^{dim}/CD16^+$) (Table 7).[127,128,132] Compared to age-matched healthy donors[133] and patients with reactive monocytosis, but also myeloid neoplasms other than CMML (even MDS), the percentages of MO1 monocytes in the PB are higher and the percentage of MO3 monocytes is lower in patients with CMML.[127,131,132] When the absolute monocyte count is increased in the PB, a cutoff value of >94% MO1 monocytes, based on their

Table 7. Phenotypic classification of monocytes and distribution of monocyte subsets in patients with chronic myelomonocytic leukemia and in controls.*

Monocyte-subset	Defining phenotype	Typical relative frequency in: CMML	MDS or MPN	Reactive BM
Classical (MO1)	$CD14^{bright}/CD16^-$	≥94%	70-97%	<94%
Intermediate (MO2)	$CD14^{bright}/CD16^+$	<20%	5-20%	5-15%
Non-classical (MO3)	$CD14^{dim}/CD16^+$	<5%	5-10%	5-20%

*Data refer to published results presented in references #125 through #132. CMML: chronic myelomonocytic leukemia; MDS: myelodysplastic syndrome; MPN: myeloproliferative neoplasm; BM: bone marrow.

immunophenotype, can identify CMML with a sensitivity of >90% and a specificity of >95%.[127,129,131] Moreover, during successful therapy, the distribution of MO1, MO2, and MO3 monocytes changes back to near normal or normal.[128] Therefore, our faculty recommends that the percentages of MO1 monocytes are quantified in the PB by MFC in all cases with suspected or known CMML at diagnosis and during follow-up.

In many cases with CMML, neoplastic monocytes aberrantly display CD2, CD5, CD10, CD23, and/or CD56.[121-124] Of all aberrantly expressed surface markers, CD56 is most commonly detected on CMML monocytes.[121-124] CD5 is only (very) weakly expressed on neoplastic monocytes in most cases with CMML. The most frequently underexpressed antigens may be CD14 and CD15. Overall, however, the use of decreased expression of these markers as a diagnostic test in CMML is limited by a relatively low sensitivity. An abnormal monocyte immunophenotype is also seen in other myeloid neoplasms, including MDS. On the other hand, phenotypically aberrant monocytes (as described above) are typically neoplastic cells (unless the patient has been treated with growth factors). Therefore, our faculty recommends that MFC studies in patients with (suspected) CMML employ antibodies directed against aberrantly expressed surface markers, including CD2 and CD56. Additionally, as mentioned before, several surface markers are 'under-expressed' on CMML monocytes compared to their levels on normal blood monocytes. These antigens include, among others, CD13, CD14, CD15, CD33, CD38, CD45, and CD64.[121-124,129,131]

Other cell types may also express aberrant markers detectable by MFC in CMML. For example, myeloid progenitor cells may express CD56 in CMML and often exhibit the same phenotypic abnormalities as in MDS; this also holds true for neutrophils and erythroid cells (*Online Supplementary Table S8)*. Other cell types that may show aberrant phenotypes are dendritic cells and mast cells. Mast cells are of particular importance as these cells may be indicative of the presence of a concomitant mastocytosis (SM-CMML). In these cases, mast cells almost invariably express CD25 in MFC analyses (*Online Supplementary Table S8*).[134] Overall, our faculty is of the opinion that MFC studies should be performed on monocyte subsets, myeloid progenitors, neutrophils, erythroid cells and mast cells in (suspected) CMML. An overview of immunophenotypic aberrancies detectable in CMML is given in *Online Supplementary Table S8*.

Differential diagnoses of CMML: reactive and clonal mimickers

A number of conditions can mimick CMML and must be taken into account when patients with unexplained monocytosis are evaluated. Reactive disorders mimicking CMML include certain chronic bacterial infections (examples: tuberculosis or subacute endomyocarditis), fungal infections, chronic auto-immune processes and non-hematologic neoplasms. There are also hematologic malignancies that may present as a CMML-like disease. For example, Philadelphia chromosome-positive chronic myeloid leukemia usually presents with (absolute) monocytosis and can also show signs of dysplasia. Particularly high monocyte counts are recorded in chronic myeloid leukemia cases expressing *BCR-ABL1*$_{p190}$. When cryptic variants of *BCR-ABL1* are expressed by leukemic cells, it can be difficult to exclude CMML. Myeloid neoplasms (MDS or MPN) in progression and myelomonocytic or monocytic AML may also resemble CMML. The reactive and clonal mimickers of CMML are listed in *Online Supplementary Table S9*.

Scoring systems in CMML: recommended standards

Although several prognostic variables have been identified in CMML regarding survival and AML evolution, accurate prediction of the clinical course and survival remains a clinical challenge. A first step in prognostication is grading into CMML-0, CMML-1 and CMML-2. To delineate the prognosis in CMML more accurately, a number of scoring systems have been developed in the past.[29,117-121,135-138] Until 2012, the International Prognostic Scoring System (IPSS) served as the gold standard for prognostication in MDS and (dysplastic) CMML.[135]

However, a number of more specific scoring systemic taking CMML-related features into account have also been proposed.[117-120,136-138] During the past few years, researchers have successfully started to integrate cytogenetic and molecular variables into these scoring models.[117-121] Our faculty concludes that these novel approaches should be followed and developed into clinical application.

Management strategies and therapeutic options in CMML

Several new treatment strategies for CMML have been developed during the past 15 years. A detailed description of therapeutic options is beyond the scope of this article. The reader is referred to a series of excellent published review articles.[139-146] A disappointing fact is that all drug therapies are still non-curative. The only curative therapy in CMML remains allogeneic hematopoietic stem cell transplantation.[147,148] For most young and eligible patients with acceptable transplant-related risk, allogeneic hematopoietic stem cell transplantation is therefore recommended. All other forms of treatment are cytoreductive, experimental or palliative in nature. Some of these drugs, such as the hypomethylating agents (5-azacytidine, decitabine) may induce long-term disease control in a subset of patients with classical CMML.[139-145] In general, cytoreductive and palliative drugs should be used according to available recommendations provided by major societies.[145,148] Similarly, treatment response assessment should be performed in line with available (accepted) guidelines.[146,150]

Specific therapy may work in those patients who suffer from a special variant of CMML. For example, in CMML patients with a transforming *PDGFRA/B* mutation, treatment with imatinib or other similar tyrosine kinase inhibitor usually induces major responses or even long-lasting remissions.[47-49,151] In patients with SM-CMML, midostaurin may result in disease control, especially when the CMML portion of the disease exhibits *KIT* D816V. However, in many cases, relapses occur. Treatment options in CMML and its variants are summarized in *Online Supplementary Table S10*.

Concluding remarks and future perspectives

CMML is a unique and rare hematopoietic neoplasm with a complex biology and pathology. In the past 10

years, several different pre-CMML conditions and subvariants of CMML have been defined. In the current article, we propose minimal diagnostic criteria for classical CMML and for special CMML variants. These criteria should help in the diagnosis of pre-CMML conditions, classical CMML, special CMML variants, and conditions that mimick CMML. In addition, we propose standards and tools for the diagnosis, prognostication and management of CMML. Contemporary assays define all major histopathological, molecular, cytogenetic and flow cytometry-based features of neoplastic cells, and thereby cover all CMML variants, including oligomonocytic CMML and CMML associated with certain drivers or a concomitant myeloid neoplasm, such as mastocytosis. Different aberration profiles may also be found, resulting in a quite heterogeneous clinical picture and a variable clinical course. Although the course is often unpredictable, initial grading and consecutive application of CMML-directed prognostic scores are standard tools that support the prognostication of patients with CMML concerning survival and AML evolution. The application of criteria, tools and standards proposed herein should assist in the diagnosis, prognostication and management of patients with CMML.

Acknowledgments

We thank Sabine Sonnleitner, Sophia Rammler, Susanne Gamperl, Emir Hadzijusofovic and all other members of Peter Valent's research group involved for their excellent support in the organization of the Working Conference. This study was supported by Austrian Science Fund (FWF) grants F4701-B20 and F4704-B20, the Ludwig Boltzmann Institute for Hematology and Oncology (LBI HO) and a Stem Cell Research grant from the Medical University of Vienna.

References

1. Storniolo AM, Moloney WC, Rosenthal DS, Cox C, Bennett JM. Chronic myelomonocytic leukemia. Leukemia. 1990;4(11):766-770.
2. Bennett JM, Catovsky D, Daniel MT, et al. The chronic myeloid leukaemias: guidelines for distinguishing chronic granulocytic, atypical chronic myeloid, and chronic myelomonocytic leukaemia. Proposals by the French-American-British Cooperative Leukaemia Group. Br J Haematol. 1994;87 (4):746-754.
3. Bennett JM. Chronic myelomonocytic leukemia. Curr Treat Options Oncol. 2002;3(3):221-223.
4. Patnaik MM, Parikh SA, Hanson CA, Tefferi A. Chronic myelomonocytic leukaemia: a concise clinical and pathophysiological review. Br J Haematol. 2014;165(3):273-286.
5. Itzykson R, Duchmann M, Lucas N, Solary E. CMML: clinical and molecular aspects. Int J Hematol. 2017;105(6):711-719.
6. Sperr WR, Horny HP, Lechner K, Valent P. Clinical and biologic diversity of leukemias occurring in patients with mastocytosis. Leuk Lymphoma. 2000;37(5-6):473-486.
7. Sotlar K, Fridrich C, Mall A, et al. Detection of c-kit point mutation Asp-816 --> Val in microdissected pooled single mast cells and leukemic cells in a patient with systemic mastocytosis and concomitant chronic myelomonocytic leukemia. Leuk Res. 2002; 26(11):979-984.
8. Patnaik MM, Rangit Vallapureddy, Lasho TL, et al. A comparison of clinical and molecular characteristics of patients with systemic mastocytosis with chronic myelomonocytic leukemia to CMML alone. Leukemia. 2018;32(8):1850-1856.
9. McCullough KB, Patnaik MM. Chronic myelomonocytic leukemia: a genetic and clinical update. Curr Hematol Malig Rep. 2015;10(3):292-302.
10. Kohlmann A, Grossmann V, Klein HU, et al. Next-generation sequencing technology reveals a characteristic pattern of molecular mutations in 72.8% of chronic myelomonocytic leukemia by detecting frequent alterations in TET2, CBL, RAS, and RUNX1. J Clin Oncol. 2010;28(24):3858-3865.
11. Patnaik MM, Tefferi A. Cytogenetic and molecular abnormalities in chronic myelomonocytic leukemia. Blood Cancer J. 2016;6:e393.
12. Bennett JM, Catovsky D, Daniel MT, et al. Proposals for the classification of the myelodysplastic syndromes. Br J Haematol. 1982;51(2):189-199.
13. Vardiman JW, Imbert M, Pierre R, et al. Chronic myelomonocytic leukemia. In: World Health Organization Classification of Tumours – Pathology & Genetics: Tumours of the Haematopoietic and Lymphoid Tissues: Eds. Jaffe ES, Harris NL, Stein H, Vardiman JW. IARC Press Lyon 2001, pp 49-52.
14. Orazi A, Bennett JM, Germing U, Brunning RD, Bain B, Thiele J. Chronic myelomonocytic leukemia. In: WHO Classification of Tumours of Haematopoietic and Lymphoid Tissues: Eds. Swerdlow SH, Campo E, Harris NL, et al. International Agency for Research on Cancer - IARC Press Lyon 2008, pp 76-79.
15. Arber DA, Orazi A, Hasserjian R, et al. The 2016 revision to the World Health Organization classification of myeloid neoplasms and acute leukemia. Blood. 2016;127(20):2391-2405.
16. Orazi A, Bain B, Bennett JM, et al. Chronic myelomonocytic leukemia. In: WHO Classification of Tumours of Haematopoietic and Lymphoid Tissues: Eds. Swerdlow SH, Campo E, Harris NL, et al. International Agency for Research on Cancer – IARC Press Lyon 2017, pp 82-86.
17. Schuler E, Schroeder M, Neukirchen J, et al. Refined medullary blast and white blood cell count based classification of chronic myelomonocytic leukemias. Leuk Res. 2014;38(12):1413-1419.
18. Bennett JM. Changes in the updated 2016: WHO classification of the myelodysplastic syndromes and related myeloid neoplasms. Clin Lymphoma Myeloma Leuk. 2016;16 (11):607-609.
19. Moon Y, Kim MH, Kim HR, et al. The 2016 WHO versus 2008 WHO criteria for the diagnosis of chronic myelomonocytic leukemia. Ann Lab Med. 2018;38(5):481-483.
20. Bain BJ, Gilliland DG, Horny HP, Vardiman JW. Myeloid and lymphoid neoplasms with eosinophilia and abnormalities of PDGFRA, PDGFRB or FGFR1. In: WHO Classification of Tumours of Haematopoietic and Lymphoid Tissues: Eds. Swerdlow SH, Campo E, Harris NL, et al. International Agency for Research on Cancer - IARC Press Lyon 2008, pp 68-73.
21. Bain BJ, Horny HP, Arber DA, Tefferi A, Hasserjian RP. Myeloid/lymphoid neoplasms with eosinophilia and rearrangement of PDGFRA, PDGFRB or FGFR1, or with PCM1-JAK2. In: WHO Classification of Tumours of Haematopoietic and Lymphoid Tissues: Eds. Swerdlow SH, Campo E, Harris NL, et al. International Agency for Research on Cancer – IARC Press Lyon 2017, pp 72-79.
22. Parikh C, Subrahmanyam R, Ren R. Oncogenic NRAS rapidly and efficiently induces CMML- and AML-like diseases in mice. Blood. 2006;108(7):2349-2357.
23. Gelsi-Boyer V, Trouplin V, Adélaïde J, et al. Genome profiling of chronic myelomonocytic leukemia: frequent alterations of RAS and RUNX1 genes. BMC Cancer. 2008; 8:299.
24. Reinig E, Yang F, Traer E, et al. Targeted next-generation sequencing in myelodysplastic syndrome and chronic myelomonocytic leukemia aids diagnosis in challenging cases and identifies frequent spliceosome mutations in transformed acute myeloid leukemia. Am J Clin Pathol. 2016;145(4): 497-506.
25. Benton CB, Nazha A, Pemmaraju N, Garcia-Manero G. Chronic myelomonocytic leukemia: forefront of the field in 2015. Crit Rev Oncol Hematol. 2015;95(2):222-242.
26. Sallman DA, Padron E. Transformation of the clinical management of CMML patients through in-depth molecular characterization. Clin Lymphoma Myeloma Leuk. 2015;15S:S50-55.
27. Patnaik MM, Tefferi A. Chronic myelomonocytic leukemia: 2016 update on diagnosis, risk stratification, and management. Am J Hematol. 2016;91(6):631-642.
28. Onida F. Models of prognostication in chronic myelomonocytic leukemia. Curr Hematol Malig Rep. 2017;12(6):513-521.
29. Nazha A, Patnaik MM. Making sense of prognostic models in chronic myelomonocytic leukemia. Curr Hematol Malig Rep. 2018;13(5):341-347.

30. Geyer JT, Tam W, Liu YC, et al. Oligomonocytic chronic myelomonocytic leukemia (chronic myelomonocytic leukemia without absolute monocytosis) displays a similar clinicopathologic and mutational profile to classical chronic myelomonocytic leukemia. Mod Pathol. 2017;30(9):1213-1222.
31. Malcovati L, Papaemmanuil E, Ambaglio I, et al. Driver somatic mutations identify distinct disease entities within myeloid neoplasms with myelodysplasia. Blood. 2014;124(9):1513-1521.
32. Schuler E, Frank F, Hildebrandt B, et al. Myelodysplastic syndromes without peripheral monocytosis but with evidence of marrow monocytosis share clinical and molecular characteristics with CMML. Leuk Res. 2018;65:1-4.
33. Valent P, Horny HP, Escribano L, et al. Diagnostic criteria and classification of mastocytosis: a consensus proposal. Leuk Res. 2001;25(7):603-625.
34. Valent P, Akin C, Metcalfe DD. Mastocytosis: 2016 updated WHO classification and novel emerging treatment concepts. Blood. 2017;129(11):1420-1427.
35. Valent P, Akin C, Hartmann K, et al. Advances in the classification and treatment of mastocytosis: current status and outlook toward the future. Cancer Res. 2017;77(6): 1261-1270.
36. Sperr WR, Horny HP, Valent P. Spectrum of associated clonal hematologic non-mast cell lineage disorders occurring in patients with systemic mastocytosis. Int Arch Allergy Immunol. 2002;127(2):140-142.
37. Gotlib J, Kluin-Nelemans HC, George TI, et al. Efficacy and safety of midostaurin in advanced systemic mastocytosis. N Engl J Med. 2016;374(26):2530-2541.
38. Tefferi A, Gilliland DG. Oncogenes in myeloproliferative disorders. Cell Cycle. 2007;6(5):550-566.
39. Pich A, Riera L, Sismondi F, et al. JAK2V617F activating mutation is associated with the myeloproliferative type of chronic myelomonocytic leukaemia. J Clin Pathol. 2009;62(9):798-801.
40. Bacher U, Haferlach T, Schnittger S, Kreipe H, Kröger N. Recent advances in diagnosis, molecular pathology and therapy of chronic myelomonocytic leukaemia. Br J Haematol. 2011;153(2):149-167.
41. Bell GC, Padron E. Detection of a PDGFRB fusion in refractory CMML without eosinophilia: a case for broad spectrum tumor profiling. Leuk Res Rep. 2015;4(2):70-71.
42. Gur HD, Loghavi S, Garcia-Manero G, et al. Chronic myelomonocytic leukemia with fibrosis is a distinct disease subset with myeloproliferative features and frequent JAK2 p.V617F mutations. Am J Surg Pathol. 2018;42(6):799-806.
43. Hu Z, Ramos CB, Medeiros LJ, et al. Utility of JAK2 V617F allelic burden in distinguishing chronic myelomonocytic leukemia from primary myelofibrosis with monocytosis. Hum Pathol. 2019;85-209-298.
44. Chapman J, Geyer JT, Khanlari M, et al. Myeloid neoplasms with features intermediate between primary myelofibrosis and chronic myelomonocytic leukemia. Mod Pathol. 2018;31(3):429-441.
45. Patnaik MM, Pophali PA, Lasho TL, et al. Clinical correlates, prognostic impact and survival outcomes in chronic myelomonocytic leukemia patients with the JAK2V617F mutation. Haematologica. 2019;104(6):e236-239.
46. Khorashad JS, Tantravahi SK, Yan D, et al. Rapid conversion of chronic myeloid leukemia to chronic myelomonocytic leukemia in a patient on imatinib therapy. Leukemia. 2016;30(11):2275-2279.
47. Magnusson MK, Meade KE, Nakamura R, Barrett J, Dunbar CE. Activity of STI571 in chronic myelomonocytic leukemia with a platelet-derived growth factor beta receptor fusion oncogene. Blood. 2002;100(3):1088-1091.
48. Apperley JF, Gardembas M, Melo JV, et al. Response to imatinib mesylate in patients with chronic myeloproliferative diseases with rearrangements of the platelet-derived growth factor receptor beta. N Engl J Med. 2002;347(7):481-487.
49. Reiter A, Walz C, Cross NC. Tyrosine kinases as therapeutic targets in BCR-ABL negative chronic myeloproliferative disorders. Curr Drug Targets. 2007;8(2):205-216.
50. Shah S, Loghavi S, Garcia-Manero G, Khoury JD. Discovery of imatinib-responsive FIP1L1-PDGFRA mutation during refractory acute myeloid leukemia transformation of chronic myelomonocytic leukemia. J Hematol Oncol. 2014;7:26.
51. Ueki K, Sato S, Tamura J, et al. Three cases of multiple myeloma developing into melphalan-related chronic myelomonocytic leukemia. J Med. 1991;22(3):157-161.
52. Kouides PA, Bennett JM. Transformation of chronic myelomonocytic leukemia to acute lymphoblastic leukemia: case report and review of the literature of lymphoblastic transformation of myelodysplastic syndrome. Am J Hematol. 1995;49(2):157-162.
53. Yamamoto M, Nakagawa M, Ichimura N, et al. Lymphoblastic transformation of chronic myelomonocytic leukemia in an infant. Am J Hematol. 1996;52(3):212-214.
54. Gaulier A, Jary-Bourguignat L, Serna R, Pulik M, Davi F, Raphaël M. Occurrence of angioimmunoblastic T cell lymphoma in a patient with chronic myelomonocytic leukemia features. Leuk Lymphoma. 2000; 40(1-2):197-204.
55. Robak T, Urbańska-Ryś H, Smolewski P, et al. Chronic myelomonocytic leukemia coexisting with B-cell chronic lymphocytic leukemia. Leuk Lymphoma. 2003;44(11): 2001-2008.
56. Menter T, Schlageter M, Bastian L, Haberthür R, Rätz Bravo AE, Tzankov A. Development of an Epstein-Barr virus-associated lymphoproliferative disorder in a patient treated with azacitidine for chronic myelomonocytic leukaemia. Hematol Oncol. 2014;32(1):47-51.
57. Pemmaraju N, Shah D, Kantarjian H, et al. Characteristics and outcomes of patients with multiple myeloma who develop therapy-related myelodysplastic syndrome, chronic myelomonocytic leukemia, or acute myeloid leukemia. Clin Lymphoma Myeloma Leuk. 2015;15(2):110-114.
58. Hagihara M, Inoue M, Kodama K, Uchida T, Hua J. Simultaneous manifestation of chronic myelomonocytic leukemia and multiple myeloma during treatment by prednisolone and eltrombopag for immune-mediated thrombocytopenic purpura. Case Rep Hematol. 2016;2016: 4342820.
59. Saillard C, Guermouche H, Derrieux C, et al. Response to 5-azacytidine in a patient with TET2-mutated angioimmunoblastic T-cell lymphoma and chronic myelomonocytic leukaemia preceded by an EBV-positive large B-cell lymphoma. Hematol Oncol. 2017;35(4):864-868.
60. Soriano PK, Stone T, Baqai J, Sana S. A case of synchronous bone marrow chronic myelomonocytic leukemia (CMML) and nodal marginal zone lymphoma (NMZL). Am J Case Rep. 2018;19:1135-1139.
61. Wang SA, Galili N, Cerny J, et al. Chronic myelomonocytic leukemia evolving from preexisting myelodysplasia shares many features with de novo disease. Am J Clin Pathol. 2006;126(5):789-797.
62. Breccia M, Cannella L, Frustaci A, Stefanizzi C, D'Elia GM, Alimena G. Chronic myelomonocytic leukemia with antecedent refractory anemia with excess blasts: further evidence for the arbitrary nature of current classification systems. Leuk Lymphoma. 2008;49(7):1292-1296.
63. Ahmed F, Osman N, Lucas F, et al. Therapy related CMML: a case report and review of the literature. Int J Hematol. 2009;89(5):699-703.
64. Singh ZN, Post GR, Kiwan E, Maddox AM. Cytopenia, dysplasia, and monocytosis: a precursor to chronic myelomonocytic leukemia or a distinct subgroup? Case reports and review of literature. Clin Lymphoma Myeloma Leuk. 2011;11(3):293-297.
65. Subari S, Patnaik M, Alfakara D, et al. Patients with therapy-related CMML have shorter median overall survival than those with de novo CMML: Mayo Clinic long-term follow-up experience. Clin Lymphoma Myeloma Leuk. 2015;15(9):546-549.
66. Patnaik MM, Vallapureddy R, Yalniz FF, et al. Therapy related-chronic myelomonocytic leukemia (CMML): molecular, cytogenetic, and clinical distinctions from de novo CMML. Am J Hematol. 2018;93(1):65-73.
67. Busque L, Patel JP, Figueroa ME, et al. Recurrent somatic TET2 mutations in normal elderly individuals with clonal hematopoiesis. Nat Genet. 2012;44:1179-1181.
68. Genovese G1, Kähler AK, Handsaker RE, et al. Clonal hematopoiesis and blood-cancer risk inferred from blood DNA sequence. N Engl J Med. 2014;371(26):2477-2487.
69. Steensma DP, Bejar R, Jaiswal S, et al. Clonal hematopoiesis of indeterminate potential and its distinction from myelodysplastic syndromes. Blood. 2015;126(1):9-16.
70. Jaiswal S, Fontanillas P, Flannick J, et al. Age-related clonal hematopoiesis associated with adverse outcomes. N Engl J Med. 2014;371 (26):2488-2498.
71. Valent P, Orazi A, Steensma DP, et al. Proposed minimal diagnostic criteria for myelodysplastic syndromes (MDS) and potential pre-MDS conditions. Oncotarget. 2017;8(43):73483-73500.
72. Gibson CJ, Lindsley RC, Tchekmedyian V, et al. Clonal hematopoiesis associated with adverse outcomes after autologous stem cell transplantation for lymphoma. J Clin Oncol. 2017;35(14):1598-1605.
73. Valent P, Akin C, Arock M, et al. Proposed terminology and classification of pre-malignant neoplastic conditions: a consensus proposal. EBioMedicine. 2017;26:17-24.
74. Elbæk MV, Sørensen AL, Hasselbalch HC. Chronic inflammation and autoimmunity as risk factors for the development of chronic myelomonocytic leukemia? Leuk Lymphoma. 2016;57(8):1793-1799.
75. Grignano E, Mekinian A, Braun T, et al. Autoimmune and inflammatory diseases associated with chronic myelomonocytic leukemia: a series of 26 cases and literature review. Leuk Res. 2016;47:136-141.
76. Deininger MWN, Tyner JW, Solary E. Turning the tide in myelodysplastic/myelo-

proliferative neoplasms. Nat Rev Cancer. 2017;17(7):425-440.
77. Mainwaring CJ, Shutt J, James CM. Not all cases of idiopathic thrombocytopenic purpura (correction of pupura) are what they might first seem. Clin Lab Haematol. 2002;24(4):261-262.
78. Cai Y, Teng R, Lin Z, Zhang Y, Liu H. Chronic myelomonocytic leukemia presenting as relapsing thrombotic thrombocytopenic purpura. Aging Clin Exp Res. 2013;25(3):349-350.
79. Hadjadj J, Michel M, Chauveheid MP, Godeau B, Papo T, Sacre K. Immune thrombocytopenia in chronic myelomonocytic leukemia. Eur J Haematol. 2014;93(6):521-526.
80. Valent P, Horny HP, Bennett JM, et al. Definitions and standards in the diagnosis and treatment of the myelodysplastic syndromes: consensus statements and report from a working conference. Leuk Res. 2007;31(6):727-736.
81. Mufti GJ, Bennett JM, Goasguen J, et al. Diagnosis and classification of myelodysplastic syndrome: International Working Group on Morphology of Myelodysplastic Syndrome (IWGM-MDS) consensus proposals for the definition and enumeration of myeloblasts and ring sideroblasts. Haematologica. 2008;93(11):1712-1717.
82. Germing U, Strupp C, Giagounidis A, et al. Evaluation of dysplasia through detailed cytomorphology in 3156 patients from the Düsseldorf Registry on myelodysplastic syndromes. Leuk Res. 2012;36(6):727-734.
83. Della Porta MG, Travaglino E, Boveri E, et al. Minimal morphological criteria for defining bone marrow dysplasia: a basis for clinical implementation of WHO classification of myelodysplastic syndromes. Leukemia. 2015;29(1):66-75.
84. Goasguen JE, Bennett JM, Bain BJ, Vallespi T, Brunning R, Mufti GJ; International Working Group on Morphology of Myelodysplastic Syndrome. Morphological evaluation of monocytes and their precursors. Haematologica. 2009;94(7):994-997.
85. Sperr WR, Escribano L, Jordan JH, et al. Morphologic properties of neoplastic mast cells: delineation of stages of maturation and implication for cytological grading of mastocytosis. Leuk Res. 2001;25(7):529-536.
86. Orazi A, Chiu R, O'Malley DP, et al. Chronic myelomonocytic leukemia: the role of bone marrow biopsy immunohistology. Mod Pathol. 2006;19(12):1536-1545.
87. Tuzuner N, Bennett JM. Reference standards for bone marrow cellularity. Leuk Res. 1994;18(8):645-647.
88. Tuzuner N, Cox C, Rowe JM, Bennett JM. Bone marrow cellularity in myeloid stem cell disorders: impact of age correction. Leuk Res. 1994;18(8):559-564.
89. Schemenau J, Baldus S, Anlauf M, et al. Cellularity, characteristics of hematopoietic parameters and prognosis in myelodysplastic syndromes. Eur J Haematol 2015;95 (3):181-189.
90. Petrova-Drus K, Chiu A, Margolskee E, et al. Bone marrow fibrosis in chronic myelomonocytic leukemia is associated with increased megakaryopoiesis, splenomegaly and with a shorter median time to disease progression. Oncotarget. 2017;8(61):103274-103282.
91. Khan M, Muzzafar T, Kantarjian H, et al. Association of bone marrow fibrosis with inferior survival outcomes in chronic myelomonocytic leukemia. Ann Hematol. 2018;97(7):1183-1191.
92. Horny HP, Sotlar K, Valent P. Diagnostic value of histology and immunohistochemistry in myelodysplastic syndromes. Leuk Res. 2007;31(12):1609-1616.
93. Horny HP, Sotlar K, Sperr WR, Valent P. Systemic mastocytosis with associated clonal haematological non-mast cell lineage diseases: a histopathological challenge. J Clin Pathol. 2004;57(6):604-608.
94. Fugazza G, Bruzzone R, Dejana AM, et al. Cytogenetic clonality in chronic myelomonocytic leukemia studied with fluorescence in situ hybridization. Leukemia. 1995;9(1):109-114.
95. Haase D, Germing U, Schanz J, et al. New insights into the prognostic impact of the karyotype in MDS and correlation with subtypes: evidence from a core dataset of 2124 patients. Blood. 2007;110(13):4385-4395.
96. Wassie EA, Itzykson R, Lasho TL, et al. Molecular and prognostic correlates of cytogenetic abnormalities in chronic myelomonocytic leukemia: a Mayo Clinic-French Consortium Study. Am J Hematol. 2014;89(12):1111-1115.
97. Palomo L, Xicoy B, Garcia O, et al. Impact of SNP array karyotyping on the diagnosis and the outcome of chronic myelomonocytic leukemia with low risk cytogenetic features or no metaphases. Am J Hematol. 2016;91(2):185-192.
98. Steidl C, Steffens R, Gassmann W, et al. Adequate cytogenetic examination in myelodysplastic syndromes: analysis of 529 patients. Leuk Res. 2005;29(9):987-993.
99. ISCN: an International System for Human Cytogenetic Nomenclature (2016). Eds. McGowan-Jordan J, Simons A, Schmid M. Karger Basel, New York, 2016.
100. Such E, Cervera J, Costa D, et al. Cytogenetic risk stratification in chronic myelomonocytic leukemia. Haematologica. 2011;96(3):375-383.
101. Nomdedeu M, Calvo X, Pereira A, et al.; Spanish Group of Myelodysplastic Syndromes. Prognostic impact of chromosomal translocations in myelodysplastic syndromes and chronic myelomonocytic leukemia patients. A study by the Spanish Group of Myelodysplastic Syndromes. Genes Chromosomes Cancer. 2016;55(4): 322-327.
102. Hirsch-Ginsberg C, LeMaistre AC, Kantarjian H, et al. RAS mutations are rare events in Philadelphia chromosome-negative/bcr gene rearrangement-negative chronic myelogenous leukemia, but are prevalent in chronic myelomonocytic leukemia. Blood. 1990;76(6):1214-1219.
103. Kohlmann A, Grossmann V, Haferlach T. Integration of next-generation sequencing into clinical practice: are we there yet? Semin Oncol. 2012;39(1):26-36.
104. Smith AE, Mohamedali AM, Kulasekararaj A, et al. Next-generation sequencing of the TET2 gene in 355 MDS and CMML patients reveals low-abundance mutant clones with early origins, but indicates no definite prognostic value. Blood. 2010;116(19):3923-3932.
105. Patnaik MM, Tefferi A. Chronic myelomonocytic leukemia: 2018 update on diagnosis, risk stratification and management. Am J Hematol. 2018;93(6):824-840.
106. Jankowska AM, Makishima H, Tiu RV, et al. Mutational spectrum analysis of chronic myelomonocytic leukemia includes genes associated with epigenetic regulation: UTX, EZH2, and DNMT3A. Blood. 2011;118(14): 3932-3941.
107. Itzykson R, Kosmider O, Renneville A, et al. Clonal architecture of chronic myelomonocytic leukemias. Blood. 2013;121(12):2186-2198.
108. Patel BJ, Przychodzen B, Thota S, et al. Genomic determinants of chronic myelomonocytic leukemia. Leukemia. 2017; 31(12):2815-2823.
109. Gelsi-Boyer V, Trouplin V, Roquain J, et al. ASXL1 mutation is associated with poor prognosis and acute transformation in chronic myelomonocytic leukaemia. Br J Haematol. 2010;151(4):365-375.
110. Federmann B, Abele M, Rosero Cuesta DS, et al. The detection of SRSF2 mutations in routinely processed bone marrow biopsies is useful in the diagnosis of chronic myelomonocytic leukemia. Hum Pathol. 2014;45(12):2471-2479.
111. Bally C, Adès L, Renneville A, et al. Prognostic value of TP53 gene mutations in myelodysplastic syndromes and acute myeloid leukemia treated with azacitidine. Leuk Res. 2014;38(7):751-755.
112. Padua RA, Guinn BA, Al-Sabah AI, et al. RAS, FMS and p53 mutations and poor clinical outcome in myelodysplasias: a 10-year follow-up. Leukemia. 1998;12(6):887-892.
113. Ricci C, Fermo E, Corti S, et al. RAS mutations contribute to evolution of chronic myelomonocytic leukemia to the proliferative variant. Clin Cancer Res. 2010;16 (8):2246-2256.
114. Wang J, Liu Y, Li Z, et al. Endogenous oncogenic Nras mutation promotes aberrant GM-CSF signaling in granulocytic/monocytic precursors in a murine model of chronic myelomonocytic leukemia. Blood. 2010;116 (26):5991-6002.
115. Padron E, Painter JS, Kunigal S, et al. GM-CSF-dependent pSTAT5 sensitivity is a feature with therapeutic potential in chronic myelomonocytic leukemia. Blood. 2013;121 (25):5068-5077.
116. Geissler K, Jäger E, Barna A, et al. Chronic myelomonocytic leukemia patients with RAS pathway mutations show high in vitro myeloid colony formation in the absence of exogenous growth factors. Leukemia. 2016;30(11):2280-2281.
117. Itzykson R, Kosmider O, Renneville A, et al. Prognostic score including gene mutations in chronic myelomonocytic leukemia. J Clin Oncol. 2013;31(19):2428-2436.
118. Elena C, Gallì A, Such E, et al. Integrating clinical features and genetic lesions in the risk assessment of patients with chronic myelomonocytic leukemia. Blood. 2016;128 (10):1408-1417.
119. Palomo L, Garcia O, Arnan M, et al. Targeted deep sequencing improves outcome stratification in chronic myelomonocytic leukemia with low risk cytogenetic features. Oncotarget. 2016;7(35):57021-57035.
120. Onida F. Models of Prognostication in chronic myelomonocytic leukemia. Curr Hematol Malig Rep. 2017;12(6):513-521.
121. Xu Y, McKenna RW, Karandikar NJ, Pildain AJ, Kroft SH. Flow cytometric analysis of monocytes as a tool for distinguishing chronic myelomonocytic leukemia from reactive monocytosis. Am J Clin Pathol. 2005;124(5):799-806.
122. Lacronique-Gazaille C, Chaury MP, Le Guyader A, Faucher JL, Bordessoule D, Feuillard J. A simple method for detection of major phenotypic abnormalities in myelodysplastic syndromes: expression of CD56 in CMML. Haematologica. 2007;92 (6):859-860.
123. Kern W, Bacher U, Haferlach C, Schnittger S, Haferlach T. Acute monoblastic/monocytic leukemia and chronic myelomonocytic leukemia share common immunophenotypic features but differ in the extent of aber-

rantly expressed antigens and amount of granulocytic cells. Leuk Lymphoma. 2011;52(1):92-100.
124. Shen Q, Ouyang J, Tang G, et al. Flow cytometry immunophenotypic findings in chronic myelomonocytic leukemia and its utility in monitoring treatment response. Eur J Haematol. 2015;95(2):168-176.
125. Selimoglu-Buet D, Wagner-Ballon O, Saada V, et al; Francophone Myelodysplasia Group. Characteristic repartition of monocyte subsets as a diagnostic signature of chronic myelomonocytic leukemia. Blood. 2015;125(23):3618-3626.
126. Harrington AM, Schelling LA, Ordobazari A, Olteanu H, Hosking PR, Kroft SH. Immunophenotypes of chronic myelomonocytic leukemia (CMML) subtypes by flow cytometry: a comparison of CMML-1 vs CMML-2, myeloproliferative vs dysplastic, de novo vs therapy-related, and CMML-specific cytogenetic risk subtypes. Am J Clin Pathol. 2016;146(2):170-181.
127. Selimoglu-Buet D, Badaoui B, Benayoun E, et al; Groupe Francophone des Myélodysplasies. Accumulation of classical monocytes defines a subgroup of MDS that frequently evolves into CMML. Blood. 2017;130(6):832-835.
128. Picot T, Aanei CM, Flandrin Gresta P, et al. Evaluation by flow cytometry of mature monocyte subpopulations for the diagnosis and follow-up of chronic myelomonocytic leukemia. Front Oncol. 2018;8:109.
129. Hudson CA, Burack WR, Leary PC, Bennett JM. Clinical utility of classical and nonclassical monocyte percentage in the diagnosis of chronic myelomonocytic leukemia. Am J Clin Pathol. 2018;150(4):293-302.
130. Feng R, Bhatt VR, Fu K, Pirruccello S, Yuan J. Application of immunophenotypic analysis in distinguishing chronic myelomonocytic leukemia from reactive monocytosis. Cytometry B Clin Cytom. 2018;94(6):901-909.
131. Hudson CA, Burack WR, Bennett JM. Emerging utility of flow cytometry in the diagnosis of chronic myelomonocytic leukemia. Leuk Res. 2018;73:12-15.
132. Talati C, Zhang L, Shaheen G, et al. Monocyte subset analysis accurately distinguishes CMML from MDS and is associated with a favorable MDS prognosis. Blood. 2017;129(13):1881-1883.
133. Damasceno D, Teodosio C, van den Bossche WBL, et al, on behalf of the TiMaScan Study Group. Distribution of subsets of blood monocytic cells throughout life. J Allergy Clin Immunol. 2019;144(1):320-323.e5.
134. Escribano L, Garcia Montero AC, Núñez R, Orfao A; Red Española de Mastocitosis. Flow cytometric analysis of normal and neoplastic mast cells: role in diagnosis and follow-up of mast cell disease. Immunol Allergy Clin North Am. 2006;26(3):535-547.
135. Greenberg P, Cox C, LeBeau MM, et al. International scoring system for evaluating prognosis in myelodysplastic syndromes. Blood. 1997;89(6):2079-2088.
136. Onida F, Kantarjian HM, Smith TL, et al. Prognostic factors and scoring systems in chronic myelomonocytic leukemia: a retrospective analysis of 213 patients. Blood. 2002;99(3):840-809.
137. Such E, Germing U, Malcovati L, et al. Development and validation of a prognostic scoring system for patients with chronic myelomonocytic leukemia. Blood. 2013;121 (15):3005-3015.
138. Padron E, Garcia-Manero G, Patnaik MM, et al. An international data set for CMML validates prognostic scoring systems and demonstrates a need for novel prognostication strategies. Blood Cancer J. 2015;5:e333.
139. Padron E, Komrokji R, List AF. The clinical management of chronic myelomonocytic leukemia. Clin Adv Hematol Oncol. 2014;12(3):172-178.
140. Pleyer L, Germing U, Sperr WR, et al. Azacitidine in CMML: matched-pair analyses of daily-life patients reveal modest effects on clinical course and survival. Leuk Res. 2014;38(4):475-483.
141. Padron E, Steensma DP. Cutting the cord from myelodysplastic syndromes: chronic myelomonocytic leukemia-specific biology and management strategies. Curr Opin Hematol. 2015;22(2):163-170.
142. Solary E, Itzykson R. How I treat chronic myelomonocytic leukemia. Blood. 2017;130 (2):126-136.
143. Moyo TK, Savona MR. Therapy for chronic myelomonocytic leukemia in a new era. Curr Hematol Malig Rep. 2017;12(5):468-477.
144. Hunter AM, Zhang L, Padron E. Current management and recent advances in the treatment of chronic myelomonocytic leukemia. Curr Treat Options Oncol. 2018;19(12):67.
145. Diamantopoulos PT, Kotsianidis I, Symeonidis A, et al; Hellenic MDS Study Group. Chronic myelomonocytic leukemia treated with 5-azacytidine - results from the Hellenic 5-Azacytidine Registry: proposal of a new risk stratification system. Leuk Lymphoma. 2018;14:1-10.
146. Itzykson R, Fenaux P, Bowen D, et al, on behalf of the European Hematology Association, the European LeukemiaNet. Diagnosis and treatment of chronic myelomonocytic leukemias in adults: recommendations from the European Hematology Association and the European LeukemiaNet. HemaSphere. 2018;2(6): e150.
147. Eissa H, Gooley TA, Sorror ML, et al. Allogeneic hematopoietic cell transplantation for chronic myelomonocytic leukemia: relapse-free survival is determined by karyotype and comorbidities. Biol Blood Marrow Transplant. 2011;17(6):908-915.
148. de Witte T, Bowen D, Robin M, et al. Allogeneic hematopoietic stem cell transplantation for MDS and CMML: recommendations from an international expert panel. Blood. 2017;129(13):1753-1762.
149. Onida F, Barosi G, Leone G, et al. Management recommendations for chronic myelomonocytic leukemia: consensus statements from the SIE, SIES, GITMO groups. Haematologica. 2013;98(9):1344-1352.
150. Savona MR, Malcovati L, Komrokji R, et al; MDS/MPN International Working Group. An international consortium proposal of uniform response criteria for myelodysplastic/ myeloproliferative neoplasms (MDS/ MPN) in adults. Blood. 2015;125(12): 1857-1865.
151. Drechsler M, Hildebrandt B, Kündgen A, Germing U, Royer-Pokora B. Fusion of H4/D10S170 to PDGFRbeta in a patient with chronic myelomonocytic leukemia and long-term responsiveness to imatinib. Ann Hematol. 2007;86(5):353-354.

Ferrata Storti Foundation

Haematologica 2019
Volume 10410):1950-1961

Bone marrow endothelial cell-derived interleukin-4 contributes to thrombocytopenia in acute myeloid leukemia

Ai Gao,[1,2,#] Yuemin Gong,[1,2,3,#] Caiying Zhu,[1,2] Wanzhu Yang,[1,2] Qing Li,[1,2] Mei Zhao,[1,2] Shihui Ma,[1,2] Jianyong Li,[3] Sha Hao,[1,2,4,5,*] Hui Cheng[1,2,4,5,*] and Tao Cheng[1,2,4,5,*]

[1]State Key Laboratory of Experimental Hematology; [2]Institute of Hematology and Blood Disease Hospital, Chinese Academy of Medical Sciences and Peking Union Medical College, Tianjin; [3]Department of Hematology, the First Affiliated Hospital of Nanjing Medical University, Jiangsu Province Hospital, Jiangsu; [4]Center for Stem Cell Medicine, Chinese Academy of Medical Sciences, Tianjin and [5]Department of Stem Cell & Regenerative Medicine, Peking Union Medical College, Tianjin, China

#These authors contributed equally to this work.

ABSTRACT

Normal hematopoiesis can be disrupted by the leukemic bone marrow microenvironment, which leads to cytopenia-associated symptoms including anemia, hemorrhage and infection. Thrombocytopenia is a major and sometimes fatal complication in patients with acute leukemia. However, the mechanisms underlying defective thrombopoiesis in leukemia have not been fully elucidated. In the steady state, platelets are continuously produced by megakaryocytes. Using an *MLL-AF9*-induced acute myeloid leukemia mouse model, we demonstrated a preserved number and proportion of megakaryocyte-primed hematopoietic stem cell subsets, but weakened megakaryocytic differentiation via both canonical and non-canonical routes. This primarily accounted for the dramatic reduction of megakaryocytic progenitors observed in acute myeloid leukemia bone marrow and a severe disruption of the maturation of megakaryocytes. Additionally, we discovered overproduction of interleukin-4 from bone marrow endothelial cells in acute myeloid leukemia and observed inhibitory effects of interleukin-4 throughout the process of megakaryopoiesis *in vivo*. Furthermore, we observed that inhibition of interleukin-4 in combination with induction chemotherapy not only promoted recovery of platelet counts, but also prolonged the duration of remission in our acute myeloid leukemia mouse model. Our study elucidates a new link between interleukin-4 signaling and defective megakaryopoiesis in acute myeloid leukemia bone marrow, thereby offering a potential therapeutic target in acute myeloid leukemia.

Correspondence:

SHA HAO
haosha@ihcams.ac.cn

HUI CHENG
chenghui@ihcams.ac.cn

TAO CHENG
chengtao@ihcams.ac.cn

Received: December 14, 2018.

Accepted: February 20, 2019.

Pre-published: February 21, 2019.

doi:10.3324/haematol.2018.214593

Check the online version for the most updated information on this article, online supplements, and information on authorship & disclosures: www.haematologica.org/content/104/10/1950

Introduction

Historical data have revealed that the majority of patients with leukemia die of cytopenia-associated complications including infection and hemorrhage.[1,2] Progressive suppression of normal hematopoiesis is the major cause of cytopenias in leukemias and other malignancies.[3] Normal hematopoiesis is more seriously compromised than leukemic hematopoiesis in acute myeloid leukemia (AML), even with a low leukemia cell burden.[4] Maintenance of normal hematopoietic homeostasis depends on the bone marrow (BM) microenvironment, which is the site where hematopoietic stem cells (HSC) reside and are regulated through intercellular contacts and signaling molecules.[5] Interactions between leukemic cells and the BM microenvironment are attracting intense attention. Studies have shown that leukemia causes significant changes in a variety of cells and cytokines in the BM microenvironment, which impair the function of supporting normal

hematopoiesis.[3,6-9] Utilizing a congenic AML mouse model, we recently investigated dynamic changes in normal hematopoietic stem and progenitor cell (HSPC) numbers and cell cycling.[10] Our findings suggested that the AML microenvironment suppressed proliferation and differentiation of normal HSPC, in line with conclusions from another study based on a xenograft AML model.[11] Notably, from among all the HSPC subpopulations investigated, megakaryocytic-erythroid progenitors were the most affected. Subsequently, we observed the inhibitory effects of CCL3 from the AML microenvironment on erythropoiesis.[12] Strikingly, CCL3 acted on megakaryocytic-erythroid progenitors rather than HSC, and specifically suppressed erythropoiesis without affecting megakaryopoiesis.[12] How the path from HSC to megakaryocytes (MK) was influenced by the AML BM microenvironment remains to be defined.

Thrombocytopenia is a major and sometimes even fatal complication of acute leukemia.[3,13] It has been estimated that thrombocytopenia occurs in approximately 75% of all leukemia patients, with one-third of them having clinically significant bleeding.[14,15] In healthy individuals, functional platelets are produced on a daily basis by mature MK, which originate from multipotent HSPC. Thrombopoietin is recognized as the principal regulatory cytokine throughout the process of megakaryopoiesis.[16] An elegant study by Rauch *et al.*[17] attributed thrombocytopenia in AML patients to thrombopoietin scavenging by MPL^{hi} leukemic blasts and proposed the MPL^{hi} state as an indicator for more severe thrombocytopenia at diagnosis. However, despite its demonstrated effects in alleviating chemotherapy-associated thrombocytopenia in patients with solid tumors, thrombopoietin did not work well for acute leukemia patients who underwent chemotherapy or hematopoietic stem cell transplantation.[18] These phenomena suggest that the mechanism of thrombocytopenia is much more complicated in AML, and cannot be simply explained by chemotherapy-induced injury or a paucity of thrombopoietin. Thrombocytopenia may be a prolonged state due to the profound influence of leukemia on the process of megakaryopoiesis and thrombopoiesis, and on the BM microenvironment which tightly regulates hematopoiesis. In fact, recent studies have indicated that the perturbation of the BM microenvironment of leukemic hosts cannot be completely cured by current therapies, even if the leukemic burden is substantially reduced.[7,19] Thus, a thorough analysis of megakaryopoiesis and thrombopoiesis during leukemia development is required to search for detrimental factors in the leukemic microenvironment that could serve as potential therapeutic targets for these processes. In the classical hierarchical model of hematopoiesis, MK and erythrocytes share common progenitors.[20] However, recent studies suggest that MK can be generated directly by an upstream HSC subpopulation, independently of other lineage fates.[21,22] The alterations along the path from HSC to MK in AML are still unknown.

In the present study, we used an *MLL-AF9*-induced AML mouse model to analyze the dynamic changes of HSPC with MK potential. We found that thrombocytopenia in AML was caused primarily by reduced megakaryocytic differentiation of CD150^{+} HSC and defective maturation of MK. Furthermore, we detected elevated interleukin-4 (IL-4) levels in AML BM, which were found to inhibit megakaryopoiesis and thrombopoiesis *in vivo*. Finally, we observed that inhibition of IL-4 combined with chemotherapy attenuated leukemia progression as well as thrombocytopenia in our AML mouse model.

Methods

Mice

C57BL/6-Ly5.1 (Ly5.1) and C57BL/6-Ly5.2 (Ly5.2) mice were purchased from the State Key Laboratory of Experimental Hematology (SKLEH). R26-tdTomato mice[23] were purchased from Jackson Laboratory and actin-eGFP mice[24] were kindly provided by Dr. Bing Liu (Academy of Military Medical Sciences, Beijing, China). Mice experiments were approved by the Institutional Animal Care and Use Committee of SKLEH.

Flow cytometry

Details of the staining and enrichment procedures for flow cytometry have been described previously.[25] Intracellular von Willebrand factor (vWF) and Ki67 staining was performed using a BD IntraSure™ Kit (BD Biosciences, Franklin Lakes, NJ, USA). Cell surface markers for phenotypic analyses of hematopoietic and niche cells are listed in *Online Supplementary Table S1*. The antibodies used are listed in *Online Supplementary Table S2*.

Acquisition of bone marrow niche cells

Cells were isolated following a previously described protocol.[26] Immunophenotyping and antibodies are listed in *Online Supplementary Table S1* and *Online Supplementary Table S2*, respectively.

Bone sectioning and immunofluorescence imaging

Femora were fixed in 4% paraformaldehyde and dehydrated in 30% sucrose at 4°C prior to being embedded in optimal cutting temperature compound and frozen. For two-dimensional imaging, frozen femora were then cut into 5 μm sections using a cryostat and stained according to the Kawamoto method.[27] Images were acquired using a UltraView VOX confocal microscope (PerkinElmer, Waltham, MA, USA) and analyzed by Volocity.

Enzyme-linked immunosorbent assays

BM supernatants were prepared by flushing femora and tibiae of leukemic and control mice with 0.5 mL phosphate-buffered saline. Enzyme-linked immunosorbent assays for IL-4 (R&D Systems, Minneapolis, MN, USA) were performed according to the manufacturer's instructions. The concentrations were calculated using standard curves.

Isolation of bone marrow megakaryocytes

BM cells were flushed out and incubated with CD41-APC antibody for 15 min on ice. CD41^{+} cells were then enriched using anti-CD41 microbeads and incubated in Dulbecco modified Eagle medium supplemented with 10% fetal bovine serum and 10 μg/mL Hoechst 33342 at 37°C for 1 h. MK were sorted as SSC^{high}, CD41^{high}, ploidy ≥8N cells through a 100 μm nozzle.

Microarray analysis

The microarray was performed at Cnkingbio Company (Beijing, China). Gene set enrichment analysis was performed using GSEA v2.2.0. The microarray data have been deposited in the NCBI's Gene Expression Omnibus under accession number GSE112942.

Statistics

Unless otherwise stated, data are expressed as mean or mean ± standard error of the mean as indicated. *P* values were generated using an unpaired Student *t*-test and analysis of variance. GraphPad Prism and IBM SPSS Statistics software were used for the statistical analyses.

Results

Megakaryocytic differentiation from hematopoietic stem cells via both canonical and non-canonical routes was markedly inhibited in acute myeloid leukemia bone marrow

To elucidate the perturbation of the orchestrated process of thrombopoiesis in AML, we used a non-irradiated *MLL-AF9*-induced AML mouse model (*Online Supplementary Figure S1A*).[10] AML mice exhibited a progressive decrease of platelets during leukemia development. On day 14, when leukemic infiltration exceeded 80% of the whole BM, platelet counts were reduced to ~14% of the normal level (*Online Supplementary Figure S1B*). Meanwhile, we detected simultaneous loss of BM MK using a flow cytometry gating strategy introduced by Heazlewood *et al.*[28] (*Online Supplementary Figure S1C, D*). These results suggested that our AML mouse model could mimic the thrombocytopenic process that occurs in patients with AML.

The developmental landscape of BM MK has not been fully understood. It was estimated that approximately half of all MK progenitors (MkP) were from long-term (LT)-HSC which contributed little to other lineages[29] in native hematopoiesis, and the other half were from multipotent progenitors (MPP), especially MPP2.[21] Thus, we decided to measure the numbers and proportions of these MK-primed subpopulations during the progression of AML (Figure 1A).

For ease of comparison, we normalized the values of the AML group at indicated time points to that of healthy controls (day 0). All of these subpopulations decreased significantly as the leukemia developed, but to different extents. The changes of pre-megakaryocytic-erythroid (PreMegE) and MkP were much more dramatic: at the end stage of AML, the total number of residual PreMegE was less than 1% of normal level, and ~4.9% of MkP were left in leukemic BM (Figure 1B and *Online Supplementary Figure S2*). In contrast, ~17.2% of MPP2 and ~29.6% of LT-HSC were preserved in AML mice (Figure 1B and *Online Supplementary Figure S2*). Regarding their proportions in CD45.2$^+$ normal hematopoietic cells, the proportion of PreMegE dropped substantially and continuously, to about 1/10 of normal level; MkP declined at a moderate rate, to approximately 56% of that in the healthy state (Figure 1C). In contrast, the proportions of MPP2 and LT-HSC increased progressively ~3.4-fold and ~5.9-fold, respectively, as compared to the proportions in healthy controls at day 14 (Figure 1C).

We then assessed the apoptosis and cell cycle state of PreMegE and MkP to determine if the marked decrease of both subsets resulted from excessive cell death or growth arrest. We did not find significant changes in the rate of apoptosis of PreMegE during leukemia progression (*Online Supplementary Figure S3A*). In addition, their cycling was not inhibited in leukemia BM, and even displayed slightly active cycling in the mid-phase of disease (*Online Supplementary Figure S3B*), suggesting their active production of downstream populations. Correspondingly, PreMegE isolated from AML mice at the late stage yielded equal numbers of CD41$^+$ MK as the PreMegE isolated from healthy controls (*Online Supplementary Figure S3C, D*). As far as concerns MkP, their rate of apoptosis even declined in AML (*Online Supplementary Figure S3E, F*), and no significant alteration was detected in their cycling state (*Online Supplementary Figure S3G*). Additionally, the MK colony-forming capacity of MkP from AML hosts was comparable to that of MkP from healthy controls when cultured *in vitro* (*Online Supplementary Figure S3H*). Since MkP derived from the non-canonical pathway, or shortcut, comprised nearly 70% of the total MkP pool,[21] the severe reduction of their number (~95% lost) Figure 1B) and proportion in normal hematopoietic cells (~44% lost) (Figure 1C) suggests a major defect with the shortcut, or LT-HSC and MPP2.

We then sought to evaluate the MK differentiation potential of LT-HSC and MPP2 in AML BM, which was likely to be reflected by the expression of MK-specific proteins in these subsets. vWF is a protein involved in platelet aggregation and is abundant in MK and endothelial cells.[30] It has been reported that vWF$^+$ HSC have strikingly higher platelet reconstitution potential than vWF$^-$ HSC.[31] We, therefore, evaluated intracellular vWF protein levels in these subsets by flow cytometry using a verified antibody. The proportions of vWF$^+$ cells were significantly reduced in both LT-HSC (from ~21.1% to ~13.2%) and MPP2 (from ~19.1% to ~5.9%) in the late stage of AML (Figure 2A, B), indicating reduced MK differentiation from both subsets. Taken together, these data suggest that the scarcity of residual MkP in AML BM was due to severe blockade of MK differentiation in both the canonical and non-canonical routes.

We then investigated whether the decline of vWF expression indicated a prolonged impairment of the MK potential of MPP2 and LT-HSC. To do this, we used actin-eGFP mice as AML recipients and isolated eGFP$^+$ MPP2 and LT-HSC from AML (day 14) or healthy control BM to transplant into sub-lethally irradiated mice. We tracked the reconstitution rates of MPP2 and LT-HSC from day 10 to day 20 for maximum exhibition of donor-derived platelet potential. We observed lower levels of platelet reconstitution of both LT-HSC and MPP2 subsets from AML hosts as early as 14 days after transplantation (Figure 2C). However, the reconstitution of peripheral blood nucleated cells from AML and control groups at that time point showed no difference (Figure 2D). These results suggest that the specific impairment of MK differentiation induced by the AML BM microenvironment would not easily recover in a leukemia-free niche.

Megakaryocyte maturation was severely impaired in acute myeloid leukemia bone marrow

MkP should experience several cycles of endomitosis and cytoplasmic maturation before they become giant, multinucleated, platelet-producing MK.[32] Endomitosis leads to polyploidization of DNA content, which has been extensively demonstrated to be of vital importance for efficient platelet production.[33] Of note, it was reported that apoptosis and polyploidization are synchronous and intimately linked events during MK maturation; inhibition of apoptosis delays polyploidization and proplatelet formation.[34,35] We questioned whether the decreased

apoptotic rate of MkP in AML (*Online Supplementary Figure S3F*) was linked to a lack of maturation. Thus we assessed the polyploidization of MK in AML BM, and found that MK with high ploidy (≥32N) were reduced to a significantly greater extent than those with low ploidy (8-16N) (Figure 3A). As with their proportions in normal hematopoietic cells, the proportion of high-ploidy MK remained stable whereas the proportions of 8N and 16N MK progressively increased, especially the proportion of 8N ones (Figure 3B). MK in late-stage AML BM exhibited a clear left shift of ploidy distribution (Figure 3C). To gain further insight into the changes of MK function in AML, we isolated MK from AML and healthy control BM for microarray assay (*Online Supplementary Figure S4A*). The thrombopoietin-Mpl axis is a main regulator of thrombopoiesis, including MK maturation and platelet production. Our microarray data showed that the levels of Mpl expression in the two groups were similar (*Online Supplementary Figure S4B*). Gene expression data (GSE112942) showed downregulation of platelet signature genes and α-granule genes in MK from AML (Figure 3D), implying insufficient cytoplasmic maturation. In

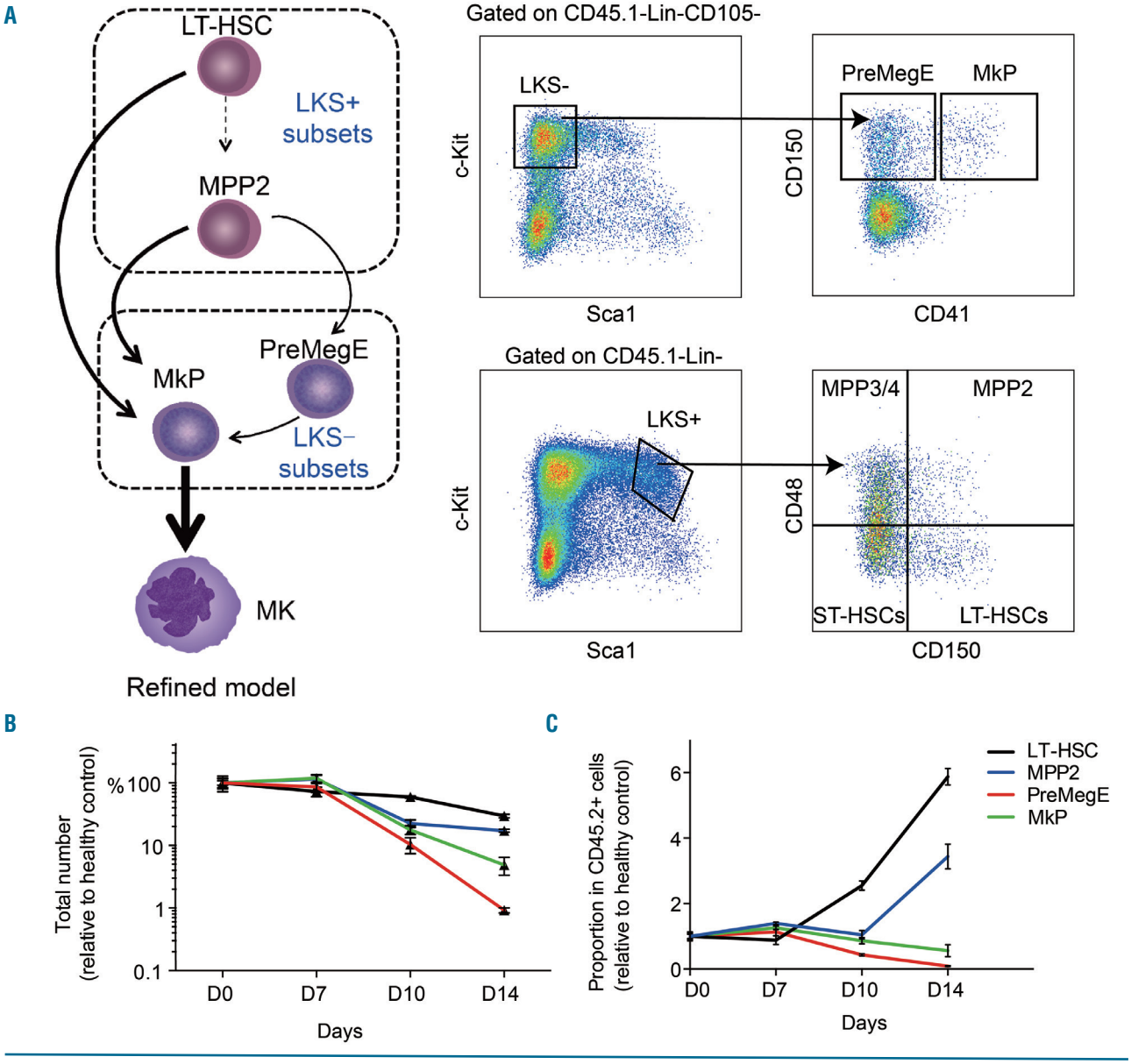

Figure 1. Dynamic changes of hematopoietic stem and progenitor cells with megakaryocyte potential in acute myeloid leukemia. (A) Left, refined model of native megakaryocytic differentiation from the canonical and non-canonical routes. Right, representative flow cytometric plots of hematopoietic stem and progenitor cell subpopulations involved in megakaryocytic differentiation. (B, C) Total numbers (B) and proportions (C) of LT-HSC, MPP2, PreMegE and MkP in normal hematopoietic cells in mice bone marrow at the indicated time points of AML. Data were normalized to the values in healthy controls and are presented as the percentage (B) or fold-increase (C) of controls. Four to five mice for each time point, three independent experiments. Error bars represent the standard error of mean. LT-HSC: long-term hematopoietic stem cells; LKS: Lin$^-$/c-Kit$^+$/Sca-1$^+$; MPP: multipotent progenitor, PreMegE: pre-megakaryocytic-erythroid; MkP: megakaryocyte progenitor; MK: megakaryocyte; ST-HSC: short-term hematopoietic stem cells.

addition, apoptosis-associated genes were significantly negatively enriched in MK from AML BM (Figure 3D). These data indicated that the maturation of MK was seriously impaired in AML BM.

The maturation of MK and their platelet-releasing activity have been proven to be dependent on their interaction with vascular endothelium.[36] We wondered if the defective maturation of MK in AML BM was caused by disrupted interaction with BM endothelial cells. As expected, a variety of genes involved in leukocyte migration, cell adhesion, cytokine-receptor interactions and chemokine signaling pathways were downregulated in MK from AML BM *versus* control BM (Figure 3E, F), indicating their weakened crosstalk with endothelial cells and the extracellular matrix. We then determined the location of MK with respect to blood vessels by *in situ* immunofluorescence imaging. In AML BM, we observed severe destruction of normal vasculature, including lack of typical sinusoid structure and vascular lumens (Figure 3G). Meanwhile, MK in AML BM were located closer to BM endothelial cells (Figure 3G, H), as a result of solid stress applied to them by overgrowing leukemia blasts. The compression of blood vessels and impaired blood perfusion in these areas might reduce the contribution of adjacent MK to the platelet pool.

Interleukin-4 signaling was upregulated in acute myeloid leukemia bone marrow and exerted inhibitory effects on multiple stages of megakaryocyte differentiation

As thrombopoietin is a key regulator of MK, we examined its concentration in the serum of control and AML mice. Thrombopoietin levels were similar in the two groups (*Online Supplementary Figure S5*), indicating that thrombopoietin is not the main cause of thrombocytopenia in our AML mouse model. To determine the factors in the leukemia microenvironment that had a negative impact on MK differentiation and maturation, we referred to our cytokine array data of AML *versus* control BM plasma.[12] Six cytokines (CCL3, CCL27, IL-4, Tnfrsf1a, Tnfrsf1b and Fcgr1) were upregulated in AML BM plasma. Among them, IL-4 has been reported to inhibit

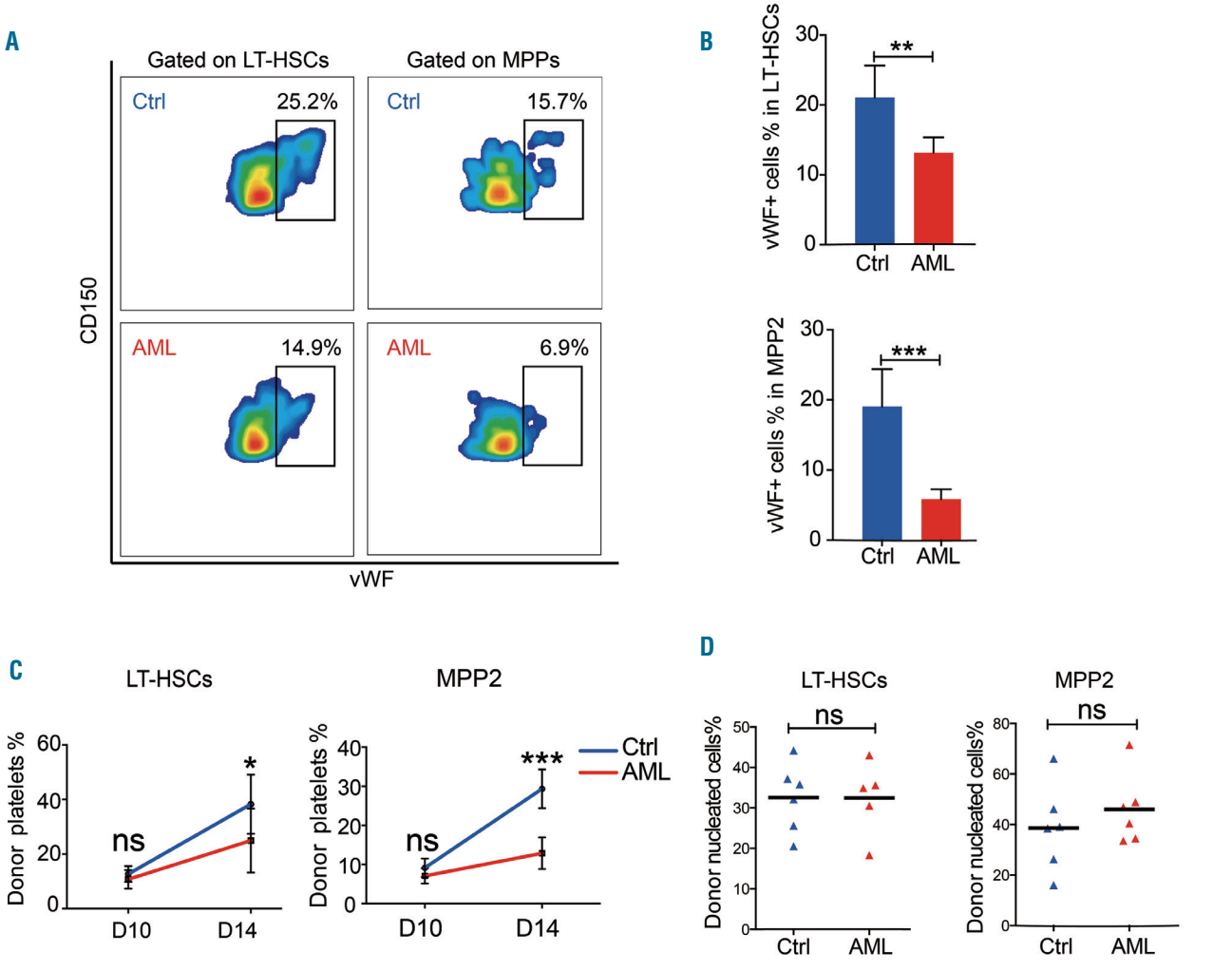

Figure 2. Reduced megakaryocyte differentiation of long-term hematopoietic stem cells and MPP2 from acute myeloid leukemia bone marrow. (A) Representative flow cytometric plots of vWF$^+$ cells in LT-HSC and MPP2 from healthy control and acute myeloid leukemia (AML) bone marrow (day 14). (B) Percentage of vWF$^+$ cells in LT-HSC and MPP2 from healthy control and AML bone marrow. Five to six mice, three independent experiments. (C, D) Percentage of donor-derived eGFP$^+$ platelets (C) and nucleated cells (D) in peripheral blood on day 14 after transplantation of 400 LT-HSC and 250 MPP2 isolated from control or AML bone marrow (day 14). Six mice, two independent experiments. *P<0.05, **P<0.01, ***P<0.001. ns, no significant difference. Error bars represent the standard error of mean. vWF: von Willebrand factor; LT-HSC: long-term hematopoietic stem cells; Ctrl: control; MPP: multipotent progenitor; eGFP: enhanced green fluorescent protein.

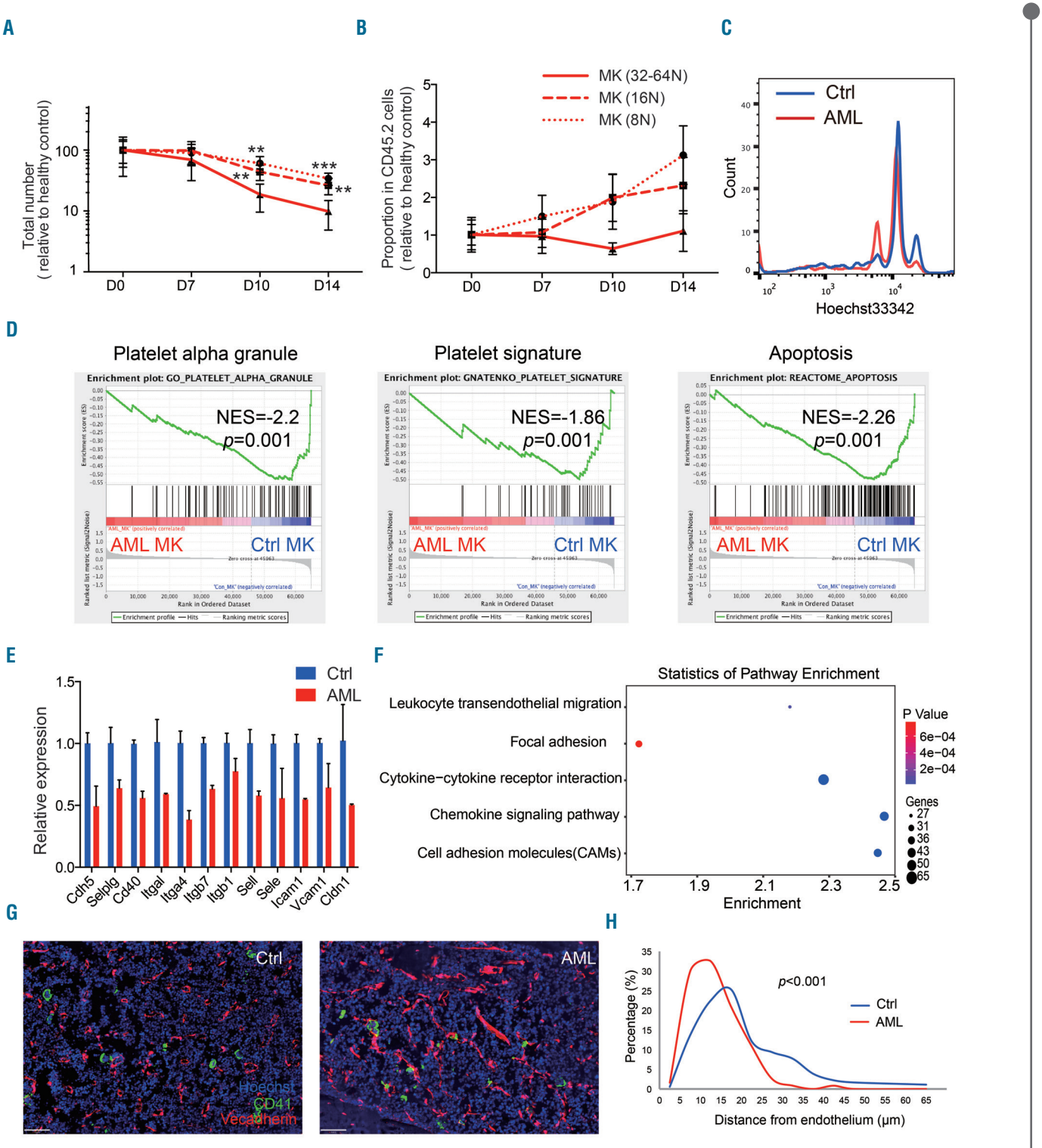

Figure 3. Insufficient maturation of megakaryocytes in acute myeloid leukemia bone marrow. (A) Total numbers of megakaryocytes (MK) with different ploidy in mice bone marrow at indicated time points of the development of acute myeloid leukemia (AML). Data were normalized to the values of healthy controls (Ctrl) and are presented as the percentages of control. Four or five mice for each time point, three independent experiments. (B) Proportions of MK with different ploidy in normal hematopoietic cells in mice bone marrow at the indicated time points of AML. Data were normalized to the values of healthy control and are presented as the folds of control. Four or five for each time point, three independent experiments. (C) Representative flow cytometric plot of MK ploidy distribution in healthy control and AML mice bone marrow (day 14). (D) Negative enrichment of platelet α-granule genes, platelet signature genes and apoptosis pathway in AML bone marrow-derived MK. NES: normalized enrichment score; P, family-wise error rate (FWER) *P*-value. (E) Significantly downregulated ($P<0.05$) genes encoding adhesion molecules in MK from AML bone marrow. Data are presented as fold-change of gene expression relative to the expression in healthy controls. (F) Significant enrichment of downregulated genes in cell-cell or cell-matrix interaction associated KEGG pathways in MK from AML bone marrow. (G) Representative confocal images of $CD41^+$ MK (green) and VE-cadherin$^+$ vasculature (red) in control and AML (day 14) mice femora. The scale bar represents 70 μm. (H) Quantification of the distance between MK (n=182 for controls, n=120 for AML) and endothelium. *P* values were calculated using a two-sample Kolmogorov–Smirnov test. $*P<0.05$, $**P<0.01$, $***P<0.001$. Error bars represent the standard error of mean.

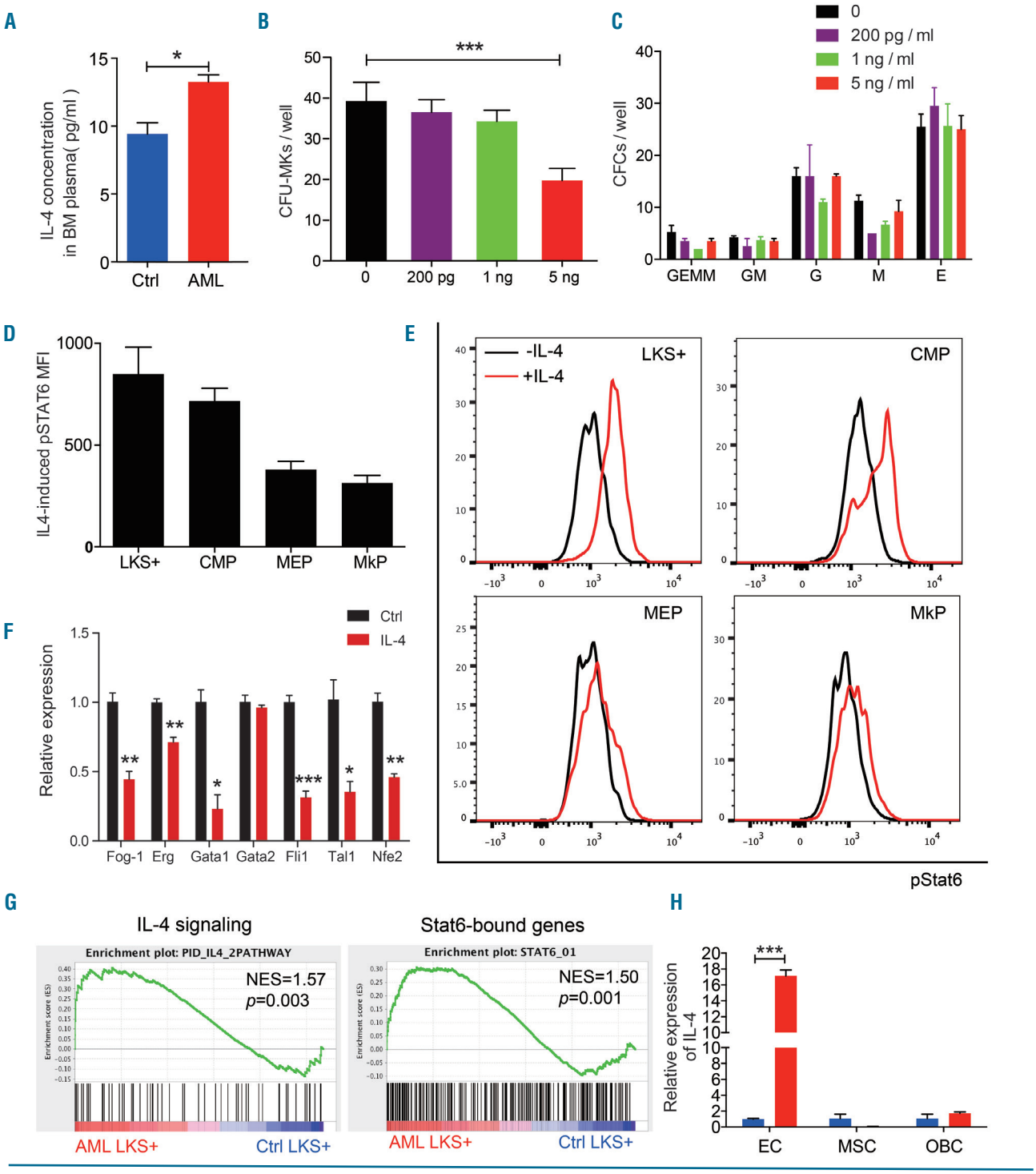

Figure 4. Elevated interleukin-4 level in acute myeloid leukemia bone marrow. (A) Interleukin-4 (IL-4) protein levels in bone marrow (BM) plasma of control (Ctrl) and acute myeloid leukemia (AML) mice based on enzyme-linked immunosorbent assay measurements. Five mice per group. (B) Number of megakaryocyte colonies (CFU-MK) formed from $5x10^4$ whole BM cells incubated with mIL-4 at the indicated concentrations. Four mice, two independent experiments. (C) Number of myeloid and erythroid colonies formed from $1x10^4$ whole BM cells incubated with mIL-4 at the indicated concentrations. Four mice, two independent experiments. CFC: colony-forming cells; GEMM: granulocyte, erythrocyte, monocyte, megakaryocyte; GM: granulocyte monocyte; G: granulocyte; M: monocyte; E: erythrocyte. (D) Mean fluorescence intensity (MFI) of phosphorylated Stat6 (pStat6) in FACS-sorted hematopoietic stem and progenitor cells (HSPC) upon exposure to mIL-4 (10 ng/mL) for 20 min, calculated by subtracting the MFI of non-treated controls. Three mice, two independent experiments. LKS: Lin$^-$/c-Kit$^+$/Sca-1$^+$; MPP: multipotent progenitor, CMP: common myeloid progenitor; MEP, megakaryocyte-erythroid progenitor; MkP: megakaryocyte progenitors. (E) Representative flow cytometric plots of pStat6 in FACS-sorted HSPC upon mIL-4 (10 ng/mL) exposure for 20 min. (F) Relative expression of megakaryocyte (MK)-associated transcription factors in LKS$^+$ cells upon mIL-4 (10 ng/mL) exposure for 24 h. Four mice, three independent experiments. (G) Positive enrichment of IL-4 signaling genes and Stat6-bound genes in LKS$^+$ cells from AML bone marrow. NES: normalized enrichment score; *P*, FWER *P*-value. (H) Relative expression of IL-4 mRNA in endothelial cells (EC), mesenchymal stem cells (MSC) and osteoblasts (OBC) isolated from AML and control mice BM. Four or five mice per group, three independent experiments. **P*<0.05, ***P*<0.01, ****P*<0.001. ns, no significant difference. Error bars represent the standard error of mean.

megakaryocytic colony formation of human CD34$^+$ BM cells[37] and to have relevance in the thrombocytopenic state of idiopathic thrombocytopenic purpura and allogeneic hematopoietic stem cell transplantation patients.[38,39] We confirmed the elevated level of IL-4 in the AML group using enzyme-linked immunosorbent assays (Figure 4A). Our *in vitro* colony-forming cell assays showed that IL-4 imposed a selective inhibitory effect on colony-forming unit-MK formation from BM cells (Figure 4B) without affecting other myeloid and erythroid lineages (Figure 4C). Interestingly, upon *in vitro* IL-4 stimulation, HSC-enriched LKS$^+$ cells exhibited an even more prominent response than myeloid progenitors (Figure 4D), as indicated by intracellular phosphorylation of Stat6 (Figure 4E) which has been recognized as a downstream transducer of IL-4 signaling.[40] In response to exposure to IL-4, all MK-associated transcription factors except for Gata2 were universally downregulated in LKS$^+$ cells (Figure 4f), suggesting the possible effects of this cytokine on MK differentiation of primitive hematopoietic cells. We next analyzed the transcriptome of LKS$^+$ cells from AML BM (GSE52506)[10] and found significant upregulation of IL-4 signaling genes and predicted Stat6-bound genes (Figure 4Gg). As BM immune cells have been reported to be the main source of IL-4,[41] we first quantified the IL-4 mRNA expression in T lymphocytes, B lymphocytes, monocytes, macrophages, natural killer cells and eosinophils. However, we did not detect upregulation of IL-4 in these cells from AML BM (*Online Supplementary Figure S6A*). The level of expression of IL-4 by AML blasts was similar to that by normal hematopoietic cells (*Online Supplementary Figure S6B*). We then quantified IL-4 expression in HSC niche cells including mesenchymal stem cells, endothelial cells and osteoblasts. We detected reproducible significant upregulation of IL-4 in endothelial cells but not in the other niche cells (Figure 4H). Thus, BM endothelial cells produced excessive IL-4 in AML to activate IL-4 signaling in HSC-enriched LKS$^+$ subsets.

To further understand the effects of IL-4 on MK differentiation, we intraperitoneally injected IL-4 into wildtype mice at 48 h intervals and analyzed the alterations of MK as well as HSPC with MK potential in mice BM (Figure 5A). In order to prolong the half-life of IL-4 and enhance its biological activity *in vivo*, we pre-associated the IL-4 with its specific monoclonal antibody as previously described[42] and injected the IL-4 complex (IL-4cx) into the mice. We observed a remarkable decrease of platelets in peripheral blood after the injection of two doses, while erythrocytes and leukocytes were barely affected (Figure 5B). Simultaneously, though the total number of BM cells was not changed (Figure 5C), the number of MK in the BM of IL-4-treated mice was severely reduced by ~84% (Figure 5D). The ploidy distribution of MK exhibited a left shift with high-ploidy (≥32N) cells being more severely decreased (Figure 5E), indicating that IL-4 treatment suppressed MK maturation. Among HSPC with MK potential, we observed an ~54% loss of PreMegE and ~37% loss of MkP (Figure 5F), whereas the proportion of LT-HSC was unaltered, and that of MPPs increased ~4 fold (Figure 5G). These results suggest that the downward differentiation of MPP2 was severely hampered by IL-4, especially in the route via PreMegE. As expected, vWF expression was significantly reduced in MPP2 from IL-4-treated mice (Figure 5H, I). Interestingly, we observed a remarkable increase of vWF$^+$ cells among LT-HSC (Figure 5H, I), indicating that IL-4 did not have an obvious inhibitory effect on their MK differentiation in our setting; on the contrary, LT-HSC gave rise to MK more actively as compensation for the reduced contribution of MPP2 to the MK pool, which limited the loss of MkP to a relatively small extent. Given the smaller reduction (~37%) of MkP and the considerable decrease of MK (~84%) (Figure 5D, F), thrombocytopenia induced by IL-4 administration was largely caused by a drastic inhibition of MkP maturation. Notably, IL-4 receptor (IL-4Rα) expression on MPP2 and MkP was higher than that on LT-HSC and PreMegE subsets (Figure 5J), in accordance with the more prominent response of MPP2 and MkP to *in vivo* IL-4 treatment.

Targeting interleukin-4 in conjunction with chemotherapy enhances platelet recovery in acute myeloid leukemia mice

Lastly, we tested whether targeting IL-4 could ameliorate thrombocytopenia in AML mice. To do this, AML mice were treated with anti-mIL-4 on days 7, 9, and 11 after injection of leukemic cells and were sacrificed on day 13 for analysis (*Online Supplementary Figure S7A*). Administration of anti-mIL-4 alone to leukemic mice neither significantly decreased leukemia load nor increased platelet count in the peripheral blood (*Online Supplementary Figure S7B, C*). Intensive induction chemotherapy is currently used for patients with AML as a general therapeutic strategy.[43,44] Because cytarabine (AraC) together with an anthracycline remains the mainstay of induction therapy,[44] we set up a treatment protocol in which AML mice were treated daily with 60 mg/kg of AraC for 1 week (*Online Supplementary Figure S7D*). This treatment significantly reduced the leukemic burden in the peripheral blood (*Online Supplementary Figure S7E*) and prolonged the survival of AML mice (*Online Supplementary Figure S7F*), but it was noted that the animals developed severe thrombocytopenia (*Online Supplementary Figure S7G*). To test the hypothesis that thrombocytopenia may be more mitigated by anti-IL-4 given during or after AraC treatment (*Online Supplementary Figure S7H*), we next established a treatment protocol in which AML mice were intraperitoneally injected daily with 10 mg/kg of anti-mIL-4 during AraC chemotherapy (Figure 6A). Interestingly, this treatment not only significantly reduced the leukemic burden (Figure 6B) but also enhanced the recovery of platelets (~4.7-fold increase) and erythrocytes (~1.9-fold increase). In contrast, leukocytes (Figure 6C) and serum thrombopoietin concentration (*Online Supplementary Figure S7I*) were not significantly affected. As a result, this new strategy of combining AraC with anti-IL-4 also significantly extended the duration of remission of AML mice (Figure 6D). Together, these data demonstrate that anti-mIL-4 combined with chemotherapy could improve the therapeutic response compared to that achieved with standard chemotherapy for AML.

Discussion

Thrombocytopenia is a frequent complication among AML patients: It can lead to a strong dependence on platelet transfusions and even fatal bleeding. Using an *MLL-AF9*-induced AML mouse model, we demonstrated that thrombocytopenia in AML was accompanied by a progressive loss of mature MK in the BM. A systematic

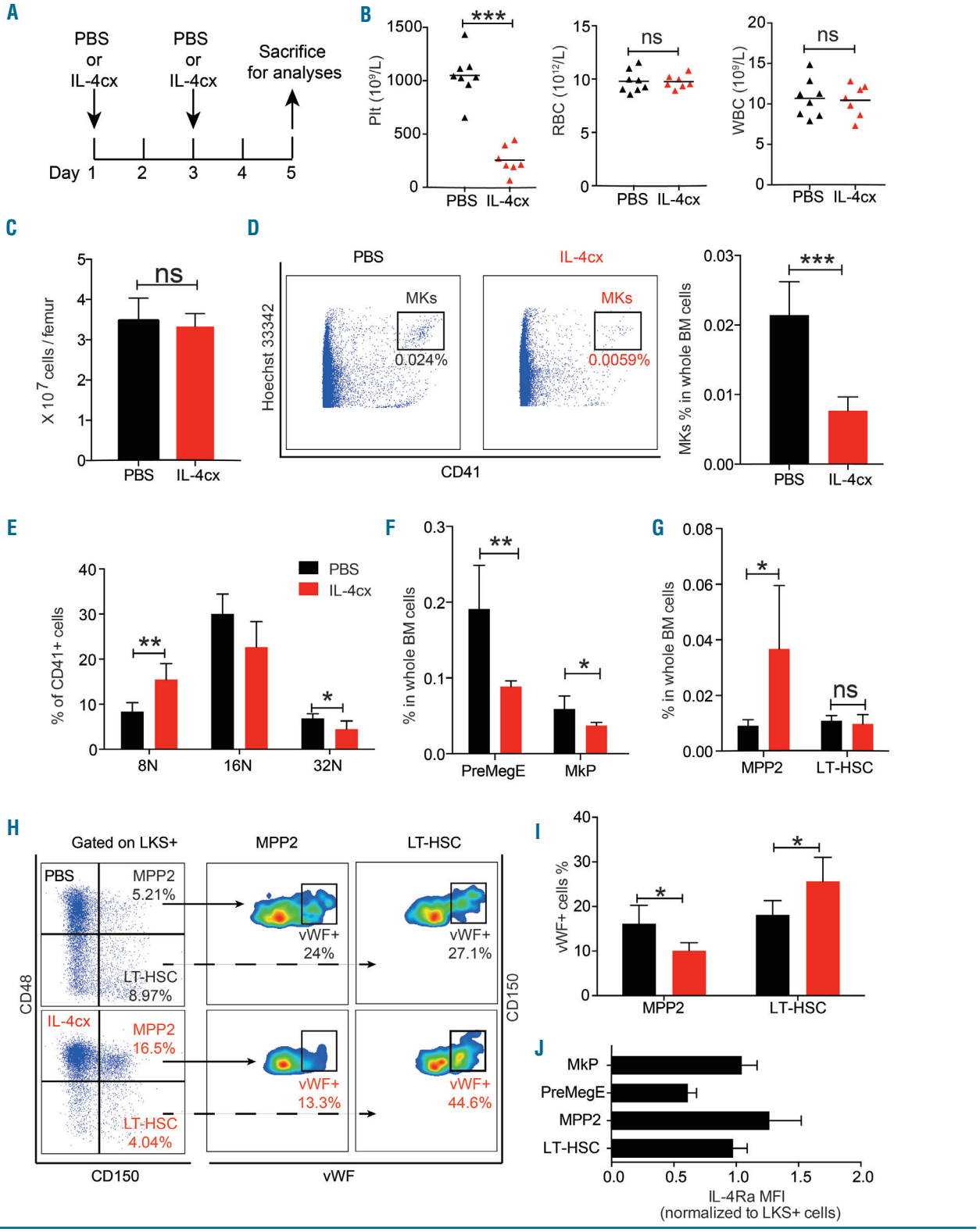

Figure 5. Inhibitory effects of interleukin-4 on megakaryopoiesis and thrombopoiesis *in vivo*. (A) Diagram of the experimental design: each mouse received intraperitoneal injections of 2 μg murine interleukin-4 (IL-4) complexed (cx) with 10 μg anti-mIL-4 (clone 11B11) or equivalent phosphate-buffered saline (PBS) on day 1 and day 3. Mice were sacrificed on day 5 for subsequent analyses. (B) Counts of platelets (Plt), erythrocytes (RBC) and leukocytes (WBC) in peripheral blood of mice injected with PBS or IL-4 complex (IL-4cx). Seven to eight mice per group; three independent experiments. (C) Total number of whole bone marrow cells per femur in mice injected with PBS or IL-4cx. Five mice per group; three independent experiments. (D) Representative flow cytometric plots (left) and percentage (right) of megakaryocytes (MK) in PBS or IL-4-treated mice bone marrow. Five mice per group, three independent experiments. (E) Percentages of MK with different ploidy among CD41$^+$ cells in the bone marrow of mice treated with PBS or IL-4. Five mice per group, three independent experiments. (F, G) Percentages of pre-megakaryocytic-erythroid (PreMegE) (F), megakaryocyte progenitors (MkP) (F), long-term hematopoietic stem cells (LT-HSC) (G) and multipotent progenitors (MPP2) (G) in the bone marrow of mice treated wih PBS or IL-4. Five mice per group, three independent experiments. (H, I) Representative flow cytometric plots (H) and percentages (I) of von Willebrand factor (vWF)$^+$ cells in LT-HSC and MPP2 in the bone marrow from mice treated with PBS or IL-4. Five mice per group, three independent experiments. (J) Mean fluorescence intensity (MFI) of IL4Rα on HSPC subsets, normalized to values in Lin/c-Kit$^+$/Sca-1$^+$ (LKS$^+$) cells. Four mice per group, two independent experiments. *P<0.05, **P<0.01, ***P<0.001. ns, no significant difference. Error bars represent the standard error of mean.

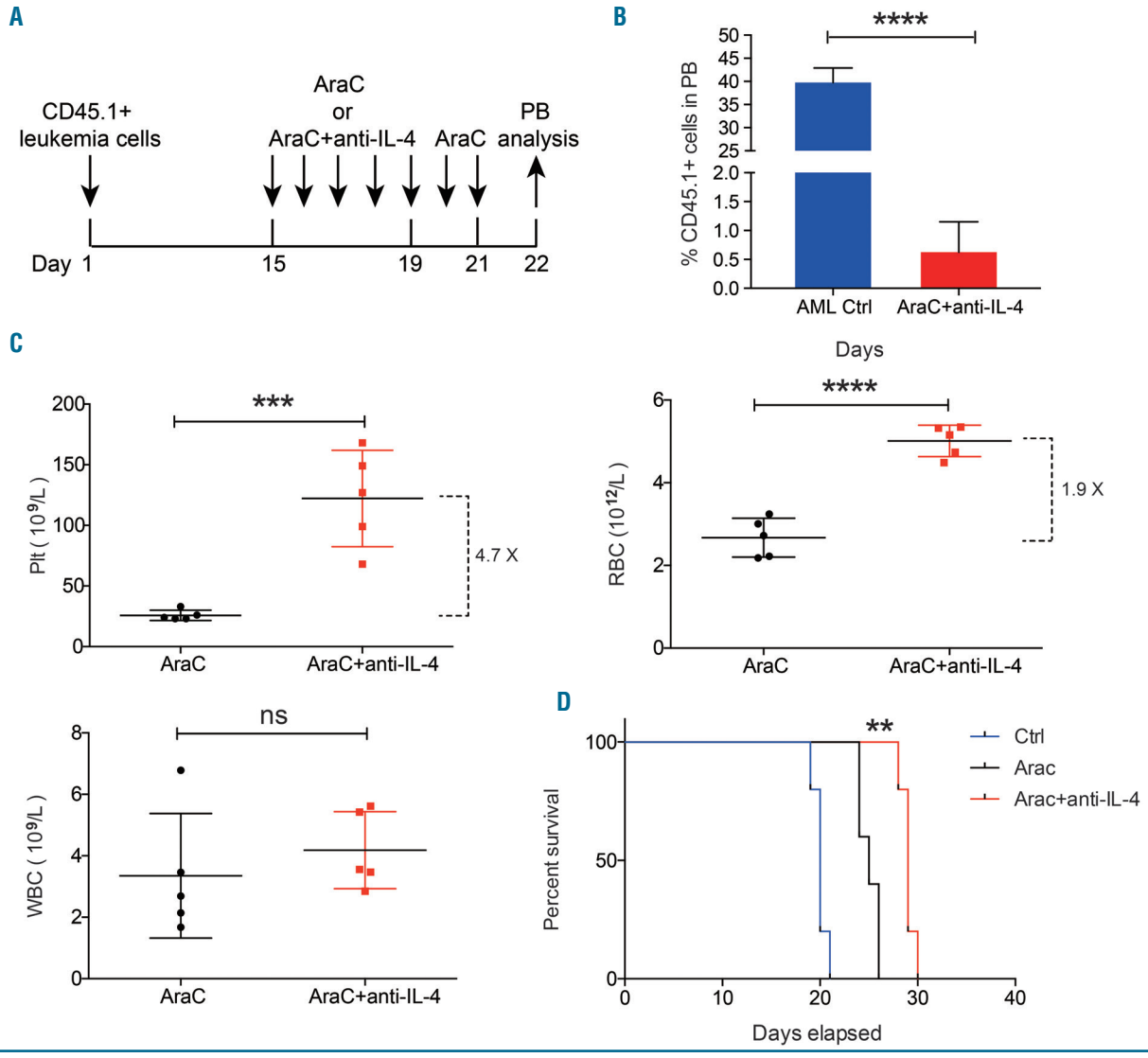

Figure 6. Targeting interleukin-4 cooperates with chemotherapy to enhance platelet recovery in acute myeloid leukemia mice. (A) Diagram of the experimental design: mice transplanted with CD45.1⁺ leukemic cells were treated with cytarabine (AraC) (60 mg/kg/day) for 1 week from day 15, with or without anti-interleukin-4 (anti-IL-4) (10 mg/kg/day) for 5 days. The peripheral blood (PB) analysis was performed on day 22. (B) Percentage engraftment of CD45.1⁺ leukemic cells in mice untreated (AML Ctrl) or treated as in (A): engraftment assessed in the PB. Five mice per group, three independent experiments. (C) Counts of platelets (Plt), erythrocytes (RBC) and leukocytes (WBC) in PB of mice injected with AraC alone or combined with anti-mIL-4. Five mice per group, three independent experiments. (D) Survival curves of recipient mice given different treatments as shown in (A). Five mice per group, three independent experiments. **P*<0.05, ***P*<0.01, ****P*<0.001, *****P*<0.0001. ns, no significant difference. Error bars represent the standard error of mean.

comparison of the megakaryocytic differentiation landscape between leukemia and healthy control mice revealed a marked reduction of MK differentiation from MPP2 and LT-HSC via both the canonical and non-canonical pathways, which was fundamentally responsible for the decreased MK in AML BM. Transcriptome analysis of MK from animals with AML showed severely impaired maturation and platelet-producing capacity. Additionally, we discovered an excessive production of IL-4 by BM endothelial cells and found that this had a striking role in suppressing MK differentiation from MPP2 and MK maturation *in vivo*, which might contribute to the thrombocytopenia of mice with AML. Finally, our preclinical data using pharmacological approaches to inhibit IL-4 in combination with AraC treatment showed that targeting IL-4 represents a promising strategy to improve the therapeutic responses in AML.

By performing colony assays on whole BM cells, Capitano *et al.*[45] recently found that IL-4, in synergy with transforming growth factor-β1, could inhibit hematopoietic progenitor cell colony formation. Our results further demonstrated that IL-4 had a unique inhibitory effect on colony-forming unit-MK formation without affecting other lineages, which was consistent with a previous study that assessed human CD34⁺ cells.[37] NF-E2 transcription factor has been identified as an essential factor for terminal MK maturation and normal platelet production.[46] It has been shown that IL-4 downmodulated the expression of NF-E2 transcription factor at both the mRNA and protein levels in normal maturing megakaryocytic cells

and in megakaryoblastic cell lines.[47] This suggests that the NF-E2 transcription factor might participate in the molecular mechanism of IL-4-induced defective MK differentiation and polyploidization in AML, but this requires further investigation.

Despite the marked response of LKS$^+$ cells to *in vitro* IL-4 stimulation, IL-4 appeared to act to a greater degree on the last step of MK differentiation, rather than on LT-HSC. Studies showed that MK could originate directly from an upstream HSC subpopulation, independently of other lineage fates.[21,22] Therefore, the increase of vWF$^+$ LT-HSC in IL-4-treated mice was more likely to be a compensation for MK reduction. In our AML mouse model, the number of PreMegE was dramatically reduced, while the decrease of MkP was less marked, which suggests that HSC compensated for the deficiency of MkP through the non-canonical route. In addition, the increase of vWF$^+$ LT-HSC in IL-4-treated mice was consistent with the phenomenon observed in MK-depleted mouse models,[48] suggesting the role of vWF$^+$ LT-HSC as MK reserves in native hematopoiesis and their relative resistance to stimuli. Thus, the blocked differentiation of LT-HSC in AML BM appears to result from a complex of factors, rather than IL-4 alone, including signals from niche cells, which require intensive research since they cannot be corrected easily by conventional cytotoxic therapy.

Studies have shown that leukemic cells impair the function of normal hematopoiesis by causing a significant change in a variety of niche cells and secreting cytokines in the BM microenvironment.[3,6-9] In our study, the administration of IL-4 inhibitors alone to leukemic mice did not increase platelet counts in the peripheral blood, likely due to the absence of a specific effect of IL-4 inhibitors on leukemic cells. Currently the standard treatment of leukemia is primarily chemotherapy.[43] It has been reported that AML patients given induction treatment with high-dose cytarabine had a considerably longer period of thrombocytopenia and received significantly more platelet transfusions in comparison to patients in the intermediate-dose group.[49] Thus, it is important to use hematopoietic growth factors to accelerate platelet recovery. In our study, anti-IL-4 was administered in combination with chemotherapy, with results suggesting that this has clinical potential for alleviating thrombocytopenia in AML. Additionally, anti-IL-4 has been shown to be safe when administered to patients with asthma,[50] implying that it could be applied in the treatment of AML. In our current study, all the data were generated based on a specific AML model and it is unclear whether results obtained can be generalized to other types of AML. More studies are, therefore, needed to expand this paradigm to other types of leukemia and to explore whether our findings in the mouse model can be translated to human AML.

In summary, our present study systemically describes defective megakaryopoiesis from HSC in AML and for the first time identifies BM endothelial cell-derived IL-4 as a candidate factor responsible for thrombocytopenia and a potential therapeutic target, in conjunction with chemotherapy, in patients with AML.

Acknowlegments

We thank Rong Guo (Cnkingbio Company) for technical support. This work was supported by grants from the National Key Research and Development Program of China (2016YFA0100600, 2017YFA0103400); the National Natural Science Foundation of China (81421002, 81730006, 81430004, 81670106, 81870086, 8181101081); CAMS Initiative for Innovative Medicine (2017-I2M-3-009, 2016-I2M-1-017); and the CAMS Fundamental Research Funds for Central Research Institutes (2016GH3100001, 2018PT31005).

References

1. Hersh EM, Bodey GP, Nies BA, Freireich EJ. Causes of death in acute leukemia: a ten-year study of 414 patients from 1954-1963. JAMA. 1965;193:105-109.
2. Chang HY, Rodriguez V, Narboni G, Bodey GP, Luna MA, Freireich EJ. Causes of death in adults with acute leukemia. Medicine (Baltimore). 1976;55(3):259-268.
3. Cheng H, Cheng T. 'Waterloo': when normal blood cells meet leukemia. Curr Opin Hematol. 2016;23(4):304-310.
4. Lichtman MA. Interrupting the inhibiton of normal hematopoiesis in myelogenous leukemia: a hypothetical approach to therapy. Stem Cells. 2000;18(5):304-306.
5. Morrison SJ, Scadden DT. The bone marrow niche for haematopoietic stem cells. Nature. 2014;505(7483):327-334.
6. Colmone A, Amorim M, Pontier AL, Wang S, Jablonski E, Sipkins DA. Leukemic cells create bone marrow niches that disrupt the behavior of normal hematopoietic progenitor cells. Science. 2008;322(5909):1861-1865.
7. Zhang B, Ho YW, Huang Q, et al. Altered microenvironmental regulation of leukemic and normal stem cells in chronic myelogenous leukemia. Cancer Cell. 2012;21(4):577-592.
8. Hoggatt J, Kfoury Y, Scadden DT. Hematopoietic stem cell niche in health and disease. Annu Rev Pathol. 2016;11:555-581.
9. Sanchez-Aguilera A, Mendez-Ferrer S. The hematopoietic stem-cell niche in health and leukemia. Cell Mol Life Sci. 2017;74(4):579-590.
10. Cheng H, Hao S, Liu Y, et al. Leukemic marrow infiltration reveals a novel role for Egr3 as a potent inhibitor of normal hematopoietic stem cell proliferation. Blood. 2015;126 (11):1302-1313.
11. Miraki-Moud F, Anjos-Afonso F, Hodby KA, et al. Acute myeloid leukemia does not deplete normal hematopoietic stem cells but induces cytopenias by impeding their differentiation. Proc Nati Acad Sci U S A. 2013;110(33):13576-13581.
12. Wang Y, Gao A, Zhao H, et al. Leukemia cell infiltration causes defective erythropoiesis partially through MIP-1alpha/CCL3. Leukemia. 2016;30(9):1897-1908.
13. Mukherjee S. "Blood feuds". Blood. 2015;126(11):1264-1265.
14. Colby-Graham MF, Chordas C. The childhood leukemias. J Pediatr Nurs. 2003;18 (2):87-95.
15. Webert K, Cook RJ, Sigouin CS, Rebulla P, Heddle NM. The risk of bleeding in thrombocytopenic patients with acute myeloid leukemia. Haematologica. 2006;91(11): 1530-1537.
16. de Sauvage FJ, Carver-Moore K, Luoh SM, et al. Physiological regulation of early and late stages of megakaryocytopoiesis by thrombopoietin. J Exp Med. 1996;183(2):651-656.
17. Rauch PJ, Ellegast JM, Widmer CC, et al. MPL expression on AML blasts predicts peripheral blood neutropenia and thrombocytopenia. Blood. 2016;128(18):2253-2257.
18. Kuter DJ, Begley CG. Recombinant human thrombopoietin: basic biology and evaluation of clinical studies. Blood. 2002;100 (10):3457-3469.
19. Passaro D, Tullio AD, Abarrategi A, et al. Increased vascular permeability in the bone marrow microenvironment contributes to disease progression and drug response in acute myeloid leukemia. Cancer Cell. 2017;32(3):324-341.
20. Akashi K, Traver D, Miyamoto T, Weissman IL. A clonogenic common myeloid progenitor that gives rise to all myeloid lineages. Nature. 2000;404(6774):193-197.
21. Rodriguezfraticelli AE, Wolock SL, Weinreb CS, et al. Clonal analysis of lineage fate in

native haematopoiesis. Nature. 2018;553 (7687):212-216.
22. Yamamoto R, Morita Y, Ooehara J, et al. Clonal analysis unveils self-renewing lineage-restricted progenitors generated directly from hematopoietic stem cells. Cell. 2013;154(5):1112-1126.
23. Madisen L, Zwingman TA, Sunkin SM, et al. A robust and high-throughput Cre reporting and characterization system for the whole mouse brain. Nat Neurosci. 2010;13(1):133-140.
24. Wright DE, Cheshier SH, Wagers AJ, Randall TD, Christensen JL, Weissman IL. Cyclophosphamide/granulocyte colony-stimulating factor causes selective mobilization of bone marrow hematopoietic stem cells into the blood after M phase of the cell cycle. Blood. 2001;97(8):2278-2285.
25. Cheng H, Liang PH, Cheng T. Mouse hematopoietic stem cell transplantation. Methods Mol Biol. 2013;976:25-35.
26. Houlihan DD, Mabuchi Y, Morikawa S, et al. Isolation of mouse mesenchymal stem cells on the basis of expression of Sca-1 and PDGFR-alpha. Nat Protoc. 2012;7(12):2103-2111.
27. Kawamoto T. Use of a new adhesive film for the preparation of multi-purpose fresh-frozen sections from hard tissues, whole-animals, insects and plants. Arch Histol Cytol. 2003;66(2):123-143.
28. Heazlewood SY, Neaves RJ, Williams B, Haylock DN, Adams TE, Nilsson SK. Megakaryocytes co-localise with hemopoietic stem cells and release cytokines that up-regulate stem cell proliferation. Stem Cell Res. 2013;11(2):782-792.
29. Sun J, Ramos A, Chapman B, et al. Clonal dynamics of native haematopoiesis. Nature. 2014;514(7522):322-327.
30. Denis C, Methia N, Frenette PS, et al. A mouse model of severe von Willebrand disease: defects in hemostasis and thrombosis. Proc Nati Acad Sci U S A. 1998;95(16):9524-9529.
31. Sanjuan-Pla A, Macaulay IC, Jensen CT, et al. Platelet-biased stem cells reside at the apex of the haematopoietic stem-cell hierarchy. Nature. 2013;502(7470):232-236.
32. Deutsch VR, Tomer A. Megakaryocyte development and platelet production. Br J Haematol. 2006;134(5):453-466.
33. Trakala M, Partida D, Salazar-Roa M, et al. Activation of the endomitotic spindle assembly checkpoint and thrombocytopenia in Plk1-deficient mice. Blood. 2015;126 (14):1707-1714.
34. Ryu KH, Chun S, Carbonierre S, et al. Apoptosis and megakaryocytic differentiation during ex vivo expansion of human cord blood CD34+ cells using thrombopoietin. Br J Haematol. 2001;113(2):470-478.
35. De BS, Sabri S, Daugas E, et al. Platelet formation is the consequence of caspase activation within megakaryocytes. Blood. 2002;100(4):1310.
36. Pitchford SC, Lodie T, Rankin SM. VEGFR1 stimulates a CXCR4-dependent translocation of megakaryocytes to the vascular niche, enhancing platelet production in mice. Blood. 2012;120(14):2787-2795.
37. Sonoda Y, Kuzuyama Y, Tanaka S, et al. Human interleukin-4 inhibits proliferation of megakaryocyte progenitor cells in culture. Blood. 1993;81(3):624-630.
38. Talaat RM, Elmaghraby AM, Barakat SS, El-Shahat M. Alterations in immune cell subsets and their cytokine secretion profile in childhood idiopathic thrombocytopenic purpura (ITP). Clin Exp Immunol. 2014;176 (2):291-300.
39. Elshal M, Takahashi Y, Chakrabarti S, et al. Complex alterations in serum cytokines and increased Il-4 levels characterize patients developing chronic thrombocytopenia after allogeneic hematopoietic cell transplantation. Blood. 2004;104(11):4985-4985.
40. Takeda K, Tanaka T, Shi W, et al. Essential role of Stat6 in IL-4 signalling. Nature. 1996;380(6575):627-630.
41. Wynn TA. Type 2 cytokines: mechanisms and therapeutic strategies. Nat Rev Immunol. 2015;15(5):271-282.
42. Woytschak J, Keller N, Krieg C, et al. Type 2 interleukin-4 receptor signaling in neutrophils antagonizes their expansion and migration during infection and inflammation. Immunity. 2016;45(1):172-184.
43. Dohner H, Estey EH, Amadori S, et al. Diagnosis and management of acute myeloid leukemia in adults: recommendations from an international expert panel, on behalf of the European LeukemiaNet. Blood. 2010;115(3):453-474.
44. Mayer RJ, Davis RB, Schiffer CA, et al. Intensive postremission chemotherapy in adults with acute myeloid leukemia. Cancer and Leukemia Group B. N Engl J Med. 1994;331(14):896-903.
45. Capitano M, Zhao L, Cooper S, et al. Phosphatidylinositol transfer proteins regulate megakaryocyte TGF-beta1 secretion and hematopoiesis in mice. Blood. 2018;132(10):1027-1038.
46. Shivdasani RA, Rosenblatt MF, Zucker-Franklin D, et al. Transcription factor NF-E2 is required for platelet formation independent of the actions of thrombopoietin/MGDF in megakaryocyte development. Cell. 1995;81(5):695-704.
47. Catani L, Amabile M, Luatti S, et al. Interleukin-4 downregulates nuclear factor-erythroid 2 (NF-E2) expression in primary megakaryocytes and in megakaryoblastic cell lines. Stem Cells. 2001;19(4):339-347.
48. Pinho S, Marchand T, Yang E, Wei Q, Nerlov C, Frenette PS. Lineage-biased hematopoietic stem cells are regulated by distinct niches. Dev Cell. 2018;44(5):634-641.e634.
49. Löwenberg B, Pabst T, Vellenga E, et al. Cytarabine dose for acute myeloid leukemia. N Engl J Med. 2011;364(11):1027-1036.
50. Hanania NA, Korenblat P, Chapman KR, et al. Efficacy and safety of lebrikizumab in patients with uncontrolled asthma (LAVOLTA I and LAVOLTA II): replicate, phase 3, randomised, double-blind, placebo-controlled trials. Lancet Respir Med. 2016;4(10): 781-796.

Ferrata Storti Foundation

Haematologica 2019
Volume 104(10):1962-1973

Pathogenic mutations identified by a multimodality approach in 117 Japanese Fanconi anemia patients

Minako Mori,[1,2] Asuka Hira,[1] Kenichi Yoshida,[3] Hideki Muramatsu,[4] Yusuke Okuno,[4] Yuichi Shiraishi,[5] Michiko Anmae,[6] Jun Yasuda,[7] Shu Tadaka,[7] Kengo Kinoshita,[7,8,9] Tomoo Osumi,[10] Yasushi Noguchi,[11] Souichi Adachi,[12] Ryoji Kobayashi,[13] Hiroshi Kawabata,[14] Kohsuke Imai,[15] Tomohiro Morio,[16] Kazuo Tamura,[6] Akifumi Takaori-Kondo,[2] Masayuki Yamamoto,[7,17] Satoru Miyano,[5] Seiji Kojima,[4] Etsuro Ito,[18] Seishi Ogawa,[3,19] Keitaro Matsuo,[20] Hiromasa Yabe,[21] Miharu Yabe[21] and Minoru Takata[1]

[1]Laboratory of DNA Damage Signaling, Department of Late Effects Studies, Radiation Biology Center, Graduate School of Biostudies, Kyoto University, Kyoto, Japan; [2]Department of Hematology and Oncology, Graduate School of Medicine, Kyoto University, Kyoto, Japan; [3]Department of Pathology and Tumor Biology, Graduate School of Medicine, Kyoto University, Kyoto, Japan; [4]Department of Pediatrics, Nagoya University Graduate School of Medicine, Nagoya, Japan; [5]Laboratory of DNA Information Analysis, Human Genome Center, The Institute of Medical Science, University of Tokyo, Tokyo Japan; [6]Medical Genetics Laboratory, Graduate School of Science and Engineering, Kindai University, Osaka, Japan; [7]Tohoku Medical Megabank Organization, Tohoku University, Sendai, Japan; [8]Department of Applied Information Sciences, Graduate School of Information Sciences, Tohoku University, Sendai, Japan; [9]Institute of Development, Aging, and Cancer, Tohoku University, Sendai, Japan; [10]Children's Cancer Center, National Center for Child Health and Development, Tokyo, Japan; [11]Department of Pediatrics, Japanese Red Cross Narita Hospital, Chiba, Japan; [12]Department of Pediatrics, Kyoto University Graduate School of Medicine, Kyoto, Japan; [13]Department of Pediatrics and Adolescence, Sapporo Hokuyu Hospital, Sapporo, Japan; [14]Department of Hematology and Immunology, Kanazawa Medical University, Uchinada-machi, Japan; [15]Department of Community Pediatrics, Perinatal and Maternal Medicine, Tokyo Medical and Dental University, Tokyo, Japan; [16]Department of Pediatrics and Developmental Biology, Tokyo Medical and Dental University, Tokyo, Japan; [17]Department of Medical Biochemistry, Graduate School of Medicine, Tohoku University, Sendai, Japan; [18]Department of Pediatrics, Hirosaki University Graduate School of Medicine, Hirosaki, Japan; [19]Department of Medicine, Center for Hematology and Regenerative Medicine, Karolinska Institute, Stockholm, Sweden; [20]Division of Molecular and Clinical Epidemiology, Aichi Cancer Center Research Institute, Nagoya, Japan and [21]Department of Innovative Medical Science, Tokai University School of Medicine, Isehara, Kanagawa, Japan

Correspondence:

MINORU TAKATA
mtakata@house.rbc.kyoto-u.ac.jp

MIHARU YABE
miharu@is.icc.u-tokai.ac.jp

Received: September 20, 2018.

Accepted: February 15, 2019.

Pre-published: February 21, 2019.

doi:10.3324/haematol.2018.207241

Check the online version for the most updated information on this article, online supplements, and information on authorship & disclosures: www.haematologica.org/content/104/10/1962

ABSTRACT

Fanconi anemia is a rare recessive disease characterized by multiple congenital abnormalities, progressive bone marrow failure, and a predisposition to malignancies. It results from mutations in one of the 22 known *FANC* genes. The number of Japanese Fanconi anemia patients with a defined genetic diagnosis was relatively limited. In this study, we reveal the genetic subtyping and the characteristics of mutated *FANC* genes in Japan and clarify the genotype-phenotype correlations. We studied 117 Japanese patients and successfully subtyped 97% of the cases. *FANCA* and *FANCG* pathogenic variants accounted for the disease in 58% and 25% of Fanconi anemia patients, respectively. We identified one *FANCA* and two *FANCG* hot spot mutations, which are found at low percentages (0.04-0.1%) in the whole-genome reference panel of 3,554 Japanese individuals (Tohoku Medical Megabank). *FANCB* was the third most common complementation group and only one *FANCC* case was identified in our series. Based on the data from the Tohoku Medical Megabank, we estimate that approximately 2.6% of Japanese are carriers of disease-causing *FANC* gene variants, excluding missense mutations. This is the largest series of subtyped Japanese Fanconi anemia patients to date and the results will be useful for future clinical management.

Introduction

Fanconi anemia (FA) is a rare recessive disease characterized by multiple congenital abnormalities, progressive bone marrow failure, and predisposition to malignancies. It results from mutations in one of the 22 known *FANC* genes.[1] These genes are summarized in *Online Supplementary Table S1*. The proteins encoded by these genes participate in a DNA interstrand cross-link repair pathway that deals with DNA damage due to endogenous aldehydes, which are particularly deleterious to hematopoietic stem cells.[2] However, more recent studies have shown that biallelic mutations in *FANCM* cause infertility and early onset cancer but not a typical FA phenotype, and some of the FA genes are actually 'FA-like' since the patients with mutations in these genes do not display hematologic defects (*Online Supplementary Table S1*). Molecular subtyping is critical for the accurate diagnosis and clinical management of the FA patients. However, finding causative mutations for a FA patient is not an easy task.[3,4]

In this study, we successfully subtyped 113 of the 117 Japanese FA patients and identified 215 mutant alleles through a comprehensive strategy starting from a simple genome polymerase chain reaction (PCR)-direct sequencing approach, then progressing to next generation sequencing. The co-ordinated strategies included whole-exome sequencing (WES) and targeted exome sequencing (targeted-seq). In some cases in which we could not reach a conclusive diagnosis, additional methods, such as array-comparative genomic hybridization (aCGH) or RNA-sequencing (RNA-seq) and whole-genome sequencing (WGS) analysis, were extremely useful in detecting deletions or splicing abnormalities, respectively. Similar to other ethnic groups, we found that the FA-A and FA-G groups are the most prevalent in Japan. The *FANCC* mutation is rare and, a little surprisingly, FA-B is the third most prevalent subtype in Japan. The patients with the rare complementation groups, such as FA-D1, E, F, I, N, P, and T, were detected in less than 5% of the cases. We noted striking genotype-phenotype correlation in Japanese FA-B, D1, I, and N cases. In addition, we report the allele frequency of FA-associated deleterious genetic variations in the general Japanese population using the 3.5KJPNv2 database from the Tohoku Medical Megabank Organization (ToMMo).

Methods

Patients and samples

We studied 117 Japanese FA patients from 104 families in total. They overlap with previously reported cases (*Online Supplementary Table S2*)[5-10] and an additional 13 new FA patients were recruited. The diagnosis of FA was confirmed on the basis of chromosomal breakage tests and clinical features. Informed consent was obtained from the family for all subjects involved in this study, and the study was approved by the Research Ethics Committees of all participating hospitals and universities, including Tokai University, Kyoto University, and Nagoya University. Genomic DNA or total RNA was isolated from peripheral blood or cultured fibroblasts using Puregene (Qiagen) or RNAeasy (Qiagen) kit, respectively. cDNA was synthesized with a PrimeScript RT reagent kit (Takara).

Mutation screening for *FANCA* and *FANCG*, and *ALDH2* genotyping

Mutation analyses by PCR of *FANCA* or *FANCG* genes, Multiplex Ligation-mediated Probe Amplification (MLPA) tests for *FANCA* (Falco Biosystems), and *ALDH2* genotyping were performed as previously described.[11,12]

Targeted-sequencing and whole-exome sequencing

Ten and 67 patients were examined by targeted-seq and WES, respectively, as previously described.[8] In targeted-seq, 184 genes, including 15 FA genes (*FANCA, B, C, D1, D2, E, F, G, I, J, L, M, N, O* and *P*), were covered. All the mutation variants identified by targeted-seq or WES were verified by PCR and Sanger sequencing.

Array-comparative genomic hybridization analysis

For 10 patients, aCGH was performed as previously described.[6] The probes covered 19 FA genes (*FANCA, B, C, D1, D2, E, F, G, I, J, L, M, N, O, P, Q, S, T, U*) as well as FA-related genes, including NBS1, three RAD51 paralogs (*XRCC3, RAD51B,* and *RAD51D*), *FAAP20, FAAP24,* and *FAAP100*.

RNA-sequencing

We performed RNA-seq for three patients (Cases 62, 98, and 104). Libraries for RNA-seq were prepared using the TruSeq RNA Sample Prep Kit (Illumina) at Macrogen, and sequenced using the Illumina HiSeq 2500 platform with a standard 126-bp paired-end read protocol. Exon skipping events were identified using Genomon-fusion[13] in which patient-specific spliced junctions were identified compared with those identified in a control sample.

Whole-genome sequencing

We performed WGS of DNA samples from one patient (Case 64) and his parents. The TruSeq DNA PCR-Free Library Preparation Kit (Illumina, San Diego, CA, USA) was used for library preparation. The prepared libraries were subjected to next-generation sequencing using a HiSeq X platform. We detected mutation variants as previously described.[8]

Estimating allele frequencies of the Fanconi anemia-associated deleterious genetic variations in the general Japanese population

We analyzed the 3.5KJPNv2 database, which was created with data generated by WGS of 3,554 individuals of the resident cohort of the ToMMo Project. The ToMMo project was established to develop a biobank that combines medical and genome information in the Tohoku area.[14] As of 5th November 2018, the allele frequencies, including indel variations, were released in the publicly accessible 3.5KJPNv2 database (*https://jmorp.megabank.tohoku.ac.jp/201811/*). Our analysis focused on nonsense mutations, frameshift mutations (indels) and splicing donor or acceptor site mutations with less than 1% allele frequencies.

Results

Genetic subtyping of 117 Japanese Fanconi anemia patients through a comprehensive mutation screening

We started mutation analysis of FA patients by direct sequencing of *FANCA* and *FANCG*, and MLPA analysis for *FANCA* in 2009. WES and targeted-seq analyses were initiated in 2012, and molecular diagnosis was successfully achieved in 107 (91.5%) of the 117 patients (Figure 1A). We also examined the *ALDH2* genotype which has been

Table 1. Allele frequency of FA-associated deleterious variants* in Japanese population.

Gene	Genomic location (hg19)	Reference allele/ Alternative allele	cDNA	Protein	Frequency
FANCA	chr16:89882954	CGGCCCAGGCCCTCCGGCGGCCCCCTG/C	c.77_102del	p.P15fs	0.0001
FANCA	chr16: 89833603	AG/A	c.2546delC	p.S849fs	0.0008
FANCA	chr16:89831476	T/A	c.2602-2A>T	aberrant splicing	0.0001
FANCA	chr16:89805357	TTTG/T	c.4189_4191del	p.T1397del	0.0001
FANCC	chr9:97897635	G/C	c.836C>G	p.S279X	0.0001
FANCC	chr9:97864024	G/A	c.1642C>T	p.R548X	0.0003
FANCD1 (BRCA2)	chr13:32903604	CTG/C	c.657_658del	p.Val220fs	0.0001
FANCD1 (BRCA2)	chr13:32911557	ATAACAT/A	c.3067_3072del	p.N1023_I1024del	0.0001
FANCD1 (BRCA2)	chr13:32911577	A/AT	c.3085_3086insT	p.M1029fs	0.0001
FANCD1 (BRCA2)	chr13:32913261	AGT/A	c.4770_4771del	p.C1591fs	0.0001
FANCD1 (BRCA2)	chr13:32914065	CAATT/C	c.5574_5577del	p.I1859fs	0.0003
FANCD1 (BRCA2)	chr13:32914209	ACT/A	c.5718_5719del	p.L1908fs	0.0001
FANCD1(BRCA2)	chr13:32914893	ATAACT/A	c.6402_6406del	p.N2135fs	0.0001
FANCD1 (BRCA2)	chr13:32920978	C/T	c.6952C>T	p.R2318X	0.0003
FANCD1 (BRCA2)	chr13:32930713	AG/A	c.7585delG	p.G2529fs	0.0001
FANCD1 (BRCA2)	chr13:32972800	C/T	c.10150C>T	p.R3384X	0.0004
FANCD2	chr3:10122879	T/TA	c.3072_3073insA	p.N1025fs	0.0001
FANCD2	chr3:10130510	A/C	c.3561-2A>C	aberrant splicing	0.0001
FANCE	chr6:35425734	GCTT/G	c.943_945del	p.L316del	0.0001
FANCG	chr9:35078714	AG/A	c.194delC	p.P65fs	0.0001
FANCG	chr9:35078601	C/G	c.307+1G>C	aberrant splicing	0.001
FANCG	chr9:35076439	G/A	c.1066C>T	p.Q356X	0.0004
FANCI	chr15:89801943	TCTC/T	c.94_96del	p.L33del	0.0001
FANCI	chr15:89803942	A/G	c.157-2A>G	aberrant splicing	0.0008
FANCI	chr15:89833476	G/GC	c.1854_1855insC	p.L619fs	0.0001
FANCI	chr15:89843085	GAA/G	c.2692_2693del	p.K898fs	0.0001
FANCI	chr15:89843605	C/CGGCAAT	c.2878_2879insGGCAAT	p.Q961_F962insWE	0.0004
FANCI	chr15:89850868	A/AC	c.3616_3617insC	p.L1208fs	0.0003
FANCJ (BRIP1)	chr17:59763487	G/C	c.2615C>G	p.S872X	0.0001
FANCJ (BRIP1)	chr17:59761334	AC/A	c.3072delG	p.S1025fs	0.0001
FANCJ (BRIP1)	chr17:59761166	C/CA	c.3240_3241insT	p.A1081fs	0.0003
FANCL	chr2:58456995	C/T	c.170G>A	p.W57X	0.0008
FANCL	chr2:58453870	ATCT/A	c.263_265del	p.K88del	0.0003
FANCL	chr2:58453867	AG/A	c.268delC	p.L90fs	0.0001
FANCL	chr2:58387305	C/CT	c.1044_1045insA	p.G349fs	0.0001
FANCM	chr14:45642287	A/ACT	c.2190_2191insCT	p.E735fs	0.0001
FANCM	chr14:45644477	TAAAC/T	c.2521_2522insAAAC	p.Q842fs	0.0001
FANCM	chr14:45650888	CGCAGA/C	c.4367_4371del	p.R1456fs	0.0001
FANCM	chr14:45658082	TGAA/T	c.4858_4860del	p.E1620del	0.0001
FANCM	chr14:45668139	G/A	c.6008+1G>A	aberrant splicing	0.0003
FANCN (PALB2)	chr16:23647568	AG/A	c.298delC	p.D101fs	0.0001
FANCN (PALB2)	chr16:23647395	G/A	c.472C>T	p.Q158X	0.0001
FANCN (PALB2)	chr16:23646369	AC/A	c.1497delG	p.L499fs	0.0001
FANCN (PALB2)	chr16:23646192	G/A	c.1675C>T	p.Q559X	0.0003
FANCN (PALB2)	chr16:23641004	CA/C	c.2470delT	p.C824fs	0.0001
FANCN (PALB2)	chr16:23635328	A/G	c.2834+2T>C	aberrant splicing	0.0001
FANCO (RAD51C)	chr17:56787352	G/C	c.837+1G>C	aberrant splicing	0.0001
FANCP (SLX4)	chr16:3651155	CAGA/C	c.985_987del	p.Ser329del	0.0001
FANCP (SLX4)	chr16:3647443	C/T	c.1620G>A	p.W540X	0.0001
FANCP (SLX4)	chr16:3644451	TA/T	c.2160+2delT	aberrant splicing	0.0003

cont. on the next page

continued from previous page

FANCP (SLX4)	chr16:3640407	CAGCTGG/C	c.3226_3231del	p.P1076_A1077del	0.0001
FANCP (SLX4)	chr16:3639742	CCT/C	c.3895_3896del	p.R1299fs	0.0001
FANCP (SLX4)	chr16:3639379	T/TG	c.4259_4260insC	p.I1421fs	0.0001
FANCQ (ERCC4)	chr16:14042182	C/G	c.2729C>G	p.S910X	0.0001
FANCR (RAD51)	chr15:40994106	C/T	c.328C>T	p.R110X	0.0003
FANCS (BRCA1)	chr17:41258497	A/T	c.188T>A	p.L63X	0.0003
FANCS (BRCA1)	chr17:41245553	G/GAAA	c.1995_1997insTTT	p.N665_L666insF	0.0001
FANCS (BRCA1)	chr17:41244748	G/A	c.2659C>T	p.Q887X	0.0001
FANCS (BRCA1)	chr17:41244333	AG/A	c.3214delC	p.L1072fs	0.0001
FANCS (BRCA1)	chr17:41226421	C/CA	c.4664_4665insT	p.E1556fs	0.0001
FANCT (UBE2T)	chr1:202304773	C/T	c.109+1G>A	aberrant splicing	0.0004
FANCU (XRCC2)	chr7:152346394	TA/T	c.175delT	p.T59fs	0.0001
FANCW (RFWD3)	chr16:74695317	G/A	c.31C>T	p.Q11X	0.0001
FANCW (RFWD3)	chr16:74685992	G/GA	c.546_547insT	p.Q183fs	0.0001
FANCW (RFWD3)	chr16:74678352	C/T	c.988-1G>A	aberrant splicing	0.0001
FANCW (RFWD3)	chr16:74660405	G/A	c.2017C>T	p.R673X	0.0001

These data were obtained from 3.5KJPNv2 database (*https://jmorp.megabank.tohoku.ac.jp/201811/*). *We focused on nonsense mutations, frameshift mutations, and splicing site mutations. Missense mutation variants were not included.

reported to affect FA phenotypes (see Discussion section) (*Online Supplementary Table S2*).[5,10] Unfortunately, mutations were found in only one allele in seven (six FA-A and one FA-G) of the 107 patients. Since the mutations in these patients were clearly pathogenic and rare, we assumed this was diagnostic, and did not perform further analysis.

For the remaining ten unclassified cases, we screened large deletions in FA and related genes using our custom-designed aCGH in 2014. It revealed large deletions in two FA-B cases and one FA-T case (Figure 1B). The *FANCB* deletions spanned the entire genic area of *FANCB* (complete loss), and the defects extended into neighboring genes *MOSPD2* and/or *GLRA2*. Reanalysis of the WES data suggested putative junctions, where were amplified and sequenced. While the junction in Case 60 had a 3 bp overlapping microhomology, implying microhomology-mediated end joining as the mechanism (see *Online Supplementary Figure S1* for further details), there was no such homologous sequence in the break point in Case 61, suggesting that the re-ligation was mediated by non-homologous end joining (Figure 1B).[15] Two cases of entire *FANCB* deletion have been described in the literature[16,17] without elucidation of the junctional sequence. All of these *FANCB* large deletions seem to be distinct, but uniformly accompany severe phenotypic malformations (see below). The FA-T case with a large deletion was previously described.[6]

After aCGH, seven FA cases remained unclassified. We performed WGS for Case 64, in which the parents' genome was available, and RNA-seq analysis was carried out for three cases (Cases 62, 98, and 104), in which the patients' fibroblast cell lines were available. Interestingly, these analyses identified three cases with aberrant splice site mutations. WGS revealed that Case 64 harbored a homozygous mutation (c.1154+5G>A) in intron 12 of the *FANCC* gene. Real-time PCR (RT-PCR) confirmed that the mutation caused a splicing abnormality, resulting in retention of 120bp of intron 12 and a subsequent in-frame nonsense codon (Figure 1C). In Case 62, RNA-seq analysis revealed skipping of *FANCB* exon 7 (Figure 1D). This was likely to be caused by a mutation in the first nucleotide of exon 7, which did not alter the encoded amino acid (p.Leu499Leu). This mutation was considered non-pathogenic when the WES results were originally evaluated. However, it has been increasingly recognized that similar synonymous mutations affect splicing and cause genetic disorders and cancer.[18,19] RNA-seq and WES also revealed that Case 98 had a homozygous mutation (c.3350+5G>A) in intron 12 of *PALB2/FANCN* gene, resulting in skipping of exon 12 (Figure 1D).

Collectively, 113 (97%) of 117 Japanese FA patients were subtyped, and a total of 215 mutant alleles were identified (*Online Supplementary Table S2* and Figure 2A and B). FA-A and FA-G accounted for 58% and 25% of FA patients, respectively (Figure 2A). Interestingly, *FANCB* was the third most common complementation group in our series (approx. 3%). In notable contrast to a previous report from the Rockefeller University Fanconi Anemia Mutation Database,[20] FA-C represented an extremely rare complementation group in Japan (*Online Supplementary Table S1*). In keeping with this, there was not a single record with an IVS4+4 mutation in the 3.5KJPN or the East Asian population represented in the Exome Aggregation Consortium (ExAC) database. In Europeans, the allele frequency of the mutation was relatively high (0.04%) in the ExAC database, which reflects a high frequency of the IVS4+4A>T mutation in Ashkenazi-Jewish FA-C cases.[21]

Characteristics of Japanese *FANCA* pathogenic variants

In 68 FA-A patients (from 59 unrelated families), 130 mutant alleles were identified that consisted of 55 different *FANCA* variants (listed in *Online Supplementary Table S3* and *Online Supplementary Figure S3A*). The mutant alleles included nine missense mutations, eight nonsense mutations, 16 small insertions/deletions (indels), 12 large

deletions, one large duplication, and nine splicing mutations. All of the nine missense mutations were rated as "damaging" by both SIFT and PolyPhen-2 prediction programs, including two novel variants (c.2723_2725TCT>GCC, p.LS908_909RP; c.3965T>G, p.V1322G). Three of the eight nonsense mutations, six of the 16 small indels, and four of the nine splicing mutations were novel (*Online Supplementary Table S3*). We consider that these 13 novel mutations are all pathogenic. The large duplication and all of the large deletions except one (c.3765+827_3814del) were detected by the MLPA assay. We did not identify the precise breakpoints of these *FANCA* deletions; therefore, it was unclear whether they were novel or not.

Similar to the previous reports from Western countries,[20,22,23] the mutational spectrum in Japanese FA patients was broad (Figure 2B). However, some mutations were recurrently detected. The *FANCA* c.2546delC mutation was the most frequent (41 of 130 alleles; 31.5%), and other mutations such as c.978_c.979delGA, c.2602-2A>T, and c.2602-1G>A were detected in at least three unrelated families. c.1303C>T, c.2170A>C, c.2840C>G, c.3720_3724del, c.4168-2A>G were each detected in two unrelated families. The 45 remaining mutation variants were unique and were detected in single patients. *FANCA* c.2546delC existed at 0.08% frequency among 3,554 individuals from 3.5KJPNv2 in the ToMMo (Table 1), but not in the ExAC database (0%). This mutation was also commonly identified in Korean FA-A patients,[24] and therefore seems to be a hotspot in the East Asian population.

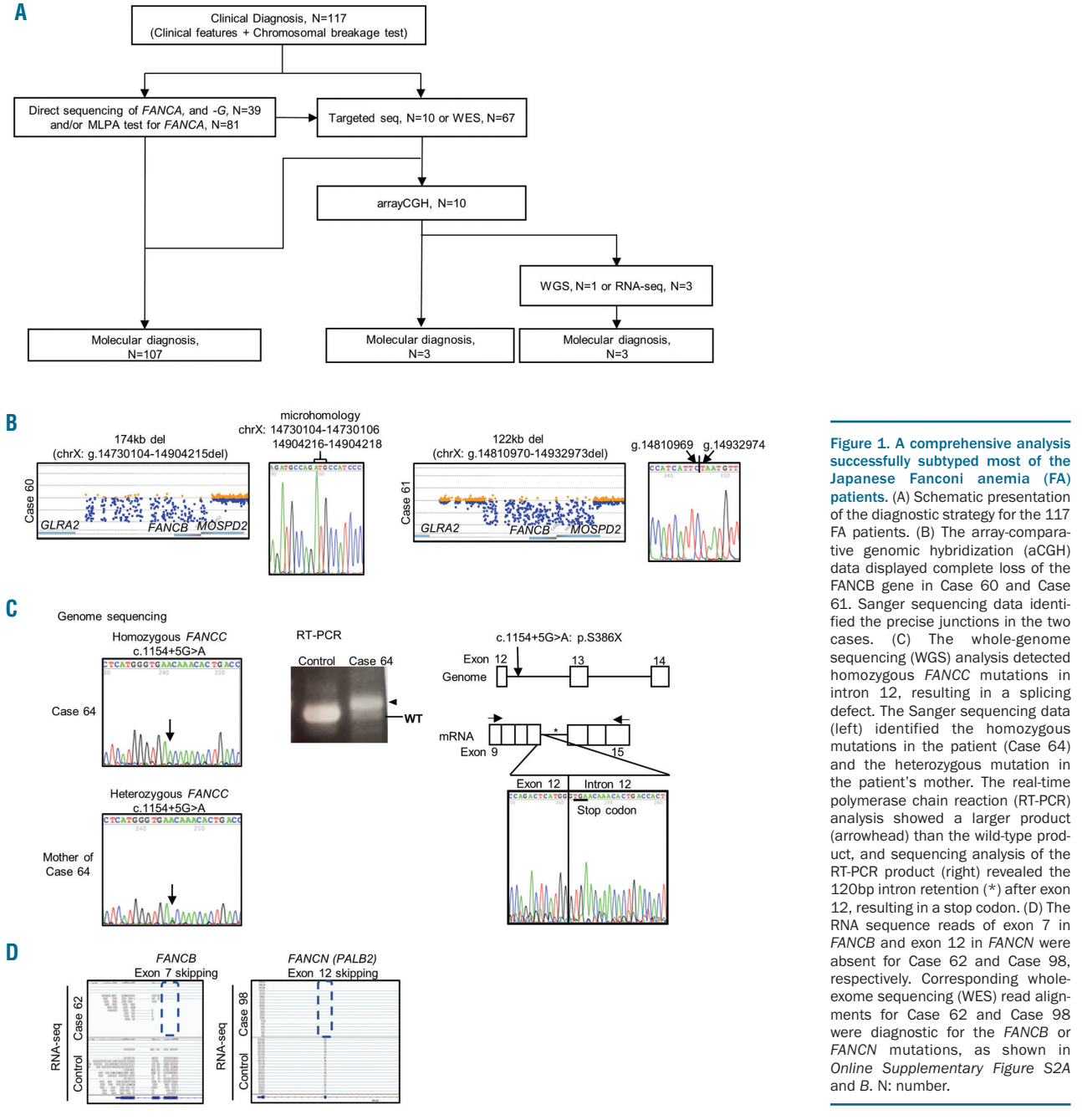

Figure 1. A comprehensive analysis successfully subtyped most of the Japanese Fanconi anemia (FA) patients. (A) Schematic presentation of the diagnostic strategy for the 117 FA patients. (B) The array-comparative genomic hybridization (aCGH) data displayed complete loss of the FANCB gene in Case 60 and Case 61. Sanger sequencing data identified the precise junctions in the two cases. (C) The whole-genome sequencing (WGS) analysis detected homozygous *FANCC* mutations in intron 12, resulting in a splicing defect. The Sanger sequencing data (left) identified the homozygous mutations in the patient (Case 64) and the heterozygous mutation in the patient's mother. The real-time polymerase chain reaction (RT-PCR) analysis showed a larger product (arrowhead) than the wild-type product, and sequencing analysis of the RT-PCR product (right) revealed the 120bp intron retention (*) after exon 12, resulting in a stop codon. (D) The RNA sequence reads of exon 7 in *FANCB* and exon 12 in *FANCN* were absent for Case 62 and Case 98, respectively. Corresponding whole-exome sequencing (WES) read alignments for Case 62 and Case 98 were diagnostic for the *FANCB* or *FANCN* mutations, as shown in *Online Supplementary Figure S2A* and *B*. N: number.

Table 2. Clinical phenotype of 10 Japanese Fanconi anemia patients with VACTERL-H association.

Individual	Affected gene	Mutation patterns	VACTERL-H features	FA-features	Family history of FA*	Birth weight SD score	DEB induced chromosome breakage (breaks /cell)	AL *** genotype
Case 18-1	*FANCA*	c.2546delC: p.S849FfsX40 c.4042_4043insC: p.I1348TfsX77	C: PDA R: Left renal agenesis L: Bilateral absent thumbs/ Bilateral radial hypoplasia	Short stature	+	-1.9	0.44	AA
Case 30	FANCA	c.2546delC: p.S849FfsX40 c.2546delC: p.S849FfsX40	V: scoliosis C: ASD/Persistent left superior vena E: Esophageal atresia	Skin pigmentation Deafness Right inguinal hernia Bicornuate uterus Short stature (-1.8SD)	–	-2.1	2.06	GG
Case 37	*FANCA*	c.2546delC: p.S849FfsX40 c.3295C>T: p.Q1099X	E: Esophageal atresia R: Right pelvic kidney L: Bilateral thumb hypoplasia	Jejunal atresia Strabismus Short stature (-4SD)	–	-2.3	0.12	GG
Case 60	*FANCB*	complete loss of *FANCB* gene (chrX g.14730104-14904216 del)	V: Spina bifida occulta/ Abnormal ribs A: Anal atresia C: PDA R: Right renal agenesis L: Right absent thumb/ Partial loss of left thumb	Skin pigmentation Microphthalmus/ Stenocephaly/Ptosis Duodenal stenosis Annular pancreas/ Hypospadias/ Undescended testis Short stature (-6SD)	–	-4.8	3.8	GG
Case 61	*FANCB*	complete loss of *FANCB* gene (chrX g.14810970-14932973 del)	V: Abnormal ribs/Scoliosis A: Anal atresia C: VSD/PS E: Duodenal atresia** R: Left renal agenesis L: Bilateral absent thumbs H: Hydrocephalus	Skin pigmentation Microphthalmus/ Deafness/ Ear canal stenosis Undescended testis (Short stature (-1SD))	–	-2.8	4.2	GA
Case 64	*FANCC*	c.1154+5G>A: p.S386X c.1154+5G>A: p.S386X	A: Anal atresia C: VSD, PDA E: Esophageal atresia	Skin pigmentation Deafness/Left aural stenosis/ Right aural atresia Cleft palate Short stature (-2SD)	–	-2.53	7.8	GG
Case 69	*FANCG*	c.307+1G>C c.1066C>T: p.Q356X	C: Coarctation complex R: Right renal agenesis/ Left renal cyst L: Bilateral absent thumbs/ Right radial hypoplasia	Skin pigmentation Short stature (-8SD)	–	-1.7	8.54	GA
Case 73-1	*FANCG*	c.307+1G>C c.307+1G>C	C: PDA R: Left renal agenesis L: Right absent thumb/ Bilateral radial hypoplasia	Skin pigmentation Bilateral aural atresia Short stature (-2.7SD)	+	-0.9	3.49	GA

continued on the next page

continued from previous page

Case 96	*FANCI*	c.158-2A>G:p.S54FfsX5 c.288G>A:p.C56FfsX8	A: Anal atresia C: VSD/PDA R: Right renal agenesis/ Left renal hypoplasia L: Bilateral absent thumb/ Bilateral absent radius H: Hydrocephalus	Skin pigmentation Microphthalmus Hypogenitalia Short stature (-8SD)	–	-3.9	0.52	GA
Case 99-1	*FANCP*	c.343delA: p.S115AfsX11 c.343delA: p.S115AfsX11	C: ASD/VSD/PS R: horseshoe kidney L: Bilateral floating thumbs/ bilateral radial hypoplasia	Intestinal malrotation Duodenal stenosis Short stature (-5.8SD)	+	-2.3	0.91	AA

*Case 18-1, 73-1, and 99-1 had a sibling with Fanconi anemia (FA). ** Duodenal atresia is considered to be a part of the VACTERL association by some reports.[27] ***ALDH2* wild type and the inactivating mutation (p.Glu504Lys) allele is referred to as G and A, respectively. ALDH2: aldehyde dehydrogenase-2; ASD: atrial septal defect; BM: bone marrow; DEB: diepoxybutane; PDA: patent ductus arteriosus; PS: pulmonary stenosis; SD: Standard Deviation; VACTERL-H: vertebral anomalies, anal atresia, cardiac anomalies, tracheal-esophageal fistula, esophageal atresia, renal structural abnormalities, limb anomalies, and hypocephalus; VSD: ventricular septal defect.

.

Characteristics of Japanese *FANCG* pathogenic variants

In 29 FA-G patients (from 27 unrelated families), 57 mutant alleles were identified, and seven different *FANCG* variants were detected (*Online Supplementary Table S4* and *Online Supplementary Figure S3B*). There were fewer unique mutation variants in FA-G compared with FA-A (Figure 2B). Three of the seven *FANCG* variants were novel. Of the three novel variants, two (c.907_908del and c.1386delC) were clearly pathogenic, whereas one mutation in intron 12 (c.1637-15G>A) was of uncertain significance. As previously reported, c.307+1G>C and 1066C>T accounted for most of the *FANCG* mutant alleles (49 of 57; 86%) in the Japanese FA-G patients.[25,26] Thirteen of the 29 FA-G patients were homozygous for c.307+1G>C, and eight were compound heterozygous with one c.307+G>C allele. Five of the eight remaining FA-G patients had homozygous c.1066C>T mutations. Four cases were compound heterozygous for the c.307+G>C and c.1066C>T mutations. In the 3.5KJPNv2 data, *FANCG* c.307+1G>C and c.1066C>T mutation variants were present with frequencies of 0.1% and 0.04%, respectively (Table 1). These mutations were similarly detected in Korean FA-G patients[24] but hardly ever observed in the other ethnic populations according to the ExAC database.

VACTERL-H phenotype caused by *FANCB*, *FANCI*, and other Fanconi anemia gene variants

We identified *FANCB* mutations in four affected males. The *FANCB* gene maps to the X-chromosome. Two of the four FA-B patients had a complete loss of the *FANCB* gene, as detected by aCGH (Figure 1B). In the remaining two patients, one harbored a nonsense mutation (c.516G>A/p.W172X) and one had a synonymous mutation (c.1497G>T/p.L499L) resulting in exon 7 skipping (Figure 1D and *Online Supplementary Figure S4A*). All four mutations were unique. The two FA-B cases with complete loss of *FANCB* displayed severe somatic abnormalities, consistent with VACTERL-H association (Table 2). The VACTERL-H association is defined as having three or more of the following defects: vertebral anomalies, anal atresia, cardiac anomalies, tracheal-esophageal fistula, esophageal atresia, renal structural abnormalities, limb anomalies, and hydrocephalus.[27] This set of anomalies has been reported in rare cases of FA, and is particularly associated with FA-B, I, J, N, or O cases.[28] The most frequent combination patterns in these patients with VACTERL-H association were cardiac-renal-limb anomalies (CRL), anal-renal-limb anomalies (ARL), and vertebral-renal-limb anomalies (VRL), which accounted for more than half of the patients. Cases 60 and 61 had five and seven features of the VACTERL-H anomalies, respectively.

Compared with these two FA-B cases, Case 62 with C-terminally truncated FANCB protein showed a less severe phenotype and experienced later onset of bone marrow failure (*Online Supplementary Figure S4A*). A recent biochemical study revealed that FANCB together with FAAP100 and FANCL are the central subcomplex components of the FA core complex, which is essential for ID2 complex monoubiquitination, a key activation event in the FA pathway. The FANCB:FAAP100 subunits form a scaffold that drives dimer formation of FANCL,[29] which is the E3 ligase component in the FA core complex. The truncated FANCB protein in Case 62 might, to some extent, maintain the ability to interact with FAAP100 or FANCL protein.[30] We were unable to obtain clinical information from another FA-B patient (Case 63).

Two FA-I cases were identified, and both had compound heterozygous mutations (*Online Supplementary Figure S4B*). Case 96, with N-terminal premature termination codons, had the five features of the VACTERL-H anomalies and died within two months after hematopoietic stem cell transplantation (HSCT) (Tables 2 and 3). On the other hand, Case 97, with C-terminal mutations, had only two features of the VACTERL-H and survived for more than 17 years after HSCT. In Case 96, a c.158-2A>G mutation in intron 3 and a c.288G>A mutation in the last codon of exon 4 caused splicing defects that resulted in a

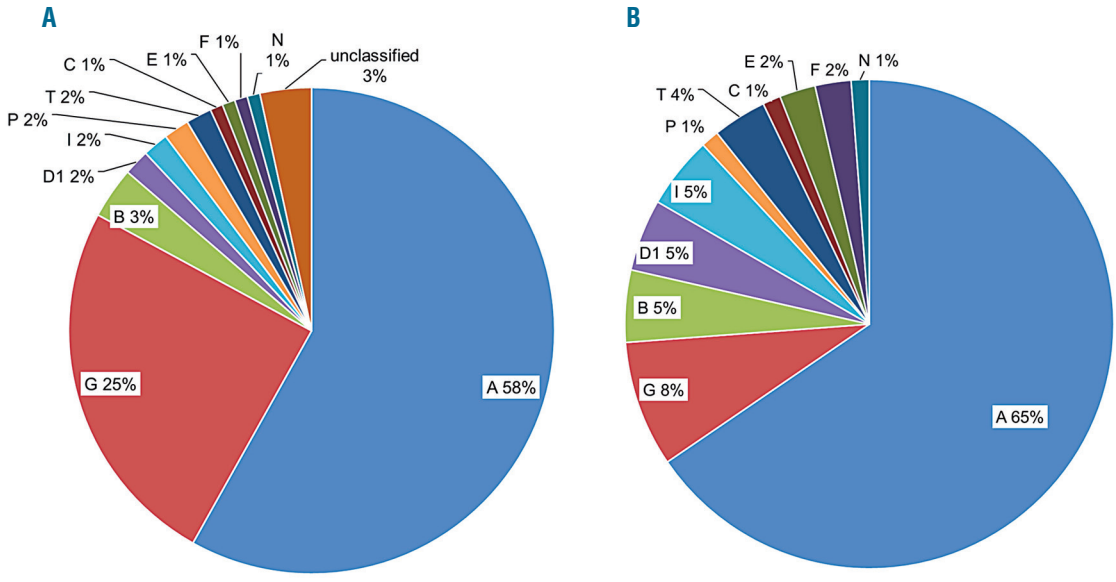

Figure 2. Frequency distribution of total (A) *versus* unique (B) Fanconi anemia (FA) gene mutations in the 117 Japanese FA patients. The frequency of the total FA gene mutation was based on subtyping of 117 FA cases, while frequency of unique FA gene mutations was derived from 84 genetic variants detected in the 117 FA patients.

Table 3. Hematologic findings and outcome of 10 Japanese Fanconi anemia patients with VACTERL-H association.

Individual	Onset of BMF (months)	BM status at HSCT	Karyotype of BM	Age at HSCT (months)	Outcome after HSCT (months)
Case 18-1	0	RCMD	46,XY,add(2)(q33)	13	Alive (105)
Case 30	70	SAA	46,XX	153	Dead/Esophageal cancer (165)
Case 37	49	RAEB1	46,XX, complex	192	Alive (66)
Case 60	58	SAA	46,XY	72	Alive (167)
Case 61	24	RCMD	46,XY,add(5)(p15)	51	Alive (160)
Case 64	40	SAA	46,XX	61	Alive (73)
Case 69	12	RCMD	46,XY	62	Alive (144)/Tongue SCC at 14 years old
Case 73-1	48	SAA	46,XY	88	Dead/Oral SCC (111)
Case 96	7	SAA	46,XY	45	Dead (2)
Case 99-1	0	RCMD	46,XY,+del(3)(q12)	13	Alive (59)

BM: bone marrow; BMF: bone marrow failure; FA: Fanconi anemia; HSCT: hematopoietic stem cell transplantation; RAEB: refractory anemia with excess of blasts; RCMD: refractory cytopenia with multilineage dysplasia; SAA: severe aplastic anemia; SCC: squamous cell carcinoma.

single nucleotide (guanine) insertion after exon 3 and skipping of exon 4, respectively (Figure 3). For Case 97, cells were not available and we could not verify the actual splicing defect caused by the c.3006+3A>G mutation. The patient's mother had only the c.3346_3347 insT mutation, while the father's genome was unavailable. The mutation at the +3 splice donor position was indicative of a potential splice defect[31] and we therefore considered that c.3006+3A>G would be a pathogenic mutation. This mutation was very rare and not reported as an SNV in the 3.5KJNv2 and ExAC database.

We also revisited available clinical data from 103 additional FA patients, and identified seven more cases with VACTERL-H (Tables 2 and 3). These include three FA-A, one FA-C case, two FA-G cases, and one FA-P case. All these seven cases met with VACTERL-H criteria with only three features. Four of the seven cases showed the CRL defect combination pattern. Compared with these cases, FA-B and FA-I cases with VACTERL-H association appeared to have higher number of malformations (from 5 to 7). We were unable to obtain detailed clinical information from the remaining nine patients. Thus, altogether there were ten VACTERL-H cases out of 108 cases with clinical data in our series, which seems slightly high compared to the previous report by Alter and Rosenberg (108 cases out of 2,245).[28]

Early-onset malignancies associated with the *FANCD1* (*BRCA2*) or *FANCN* (*PALB2*) complementation group

We identified two FA-D1 patients and one FA-N patient in our series. To the best of our knowledge, no FA-N cases and only one FA-D1 case (AP37P in Table 4) have been previously reported from Japan.[32,33] The two FA-D1 cases in our study had compound heterozygous mutations, of

which one was an N-terminal splice site mutation and the other was a nonsense or missense mutation (*Online Supplementary Figure S4C*). Both of the two *FANCD1* (*BRCA2*) splice site mutations (c.475+1G>A, c.517-2A>G) were regarded as deleterious. The one missense mutation (*FANCD1* c.7847C>T/p.S2616F) was rated as "damaging" by both SIFT and PolyPhen-2 prediction programs. It is notable that this missense mutation falls into the region termed "FA cluster" (amino acid position 2336-2729) where all of the five FA-D1-associated *BRCA2* missense mutations are found.[34] One FA-N patient had a homozygous splice mutation (c.3350+5C>T), resulting in skipping of exon 12 and C-terminal truncation (Figure 1D and *Online Supplementary Figure S4D*). This truncation may

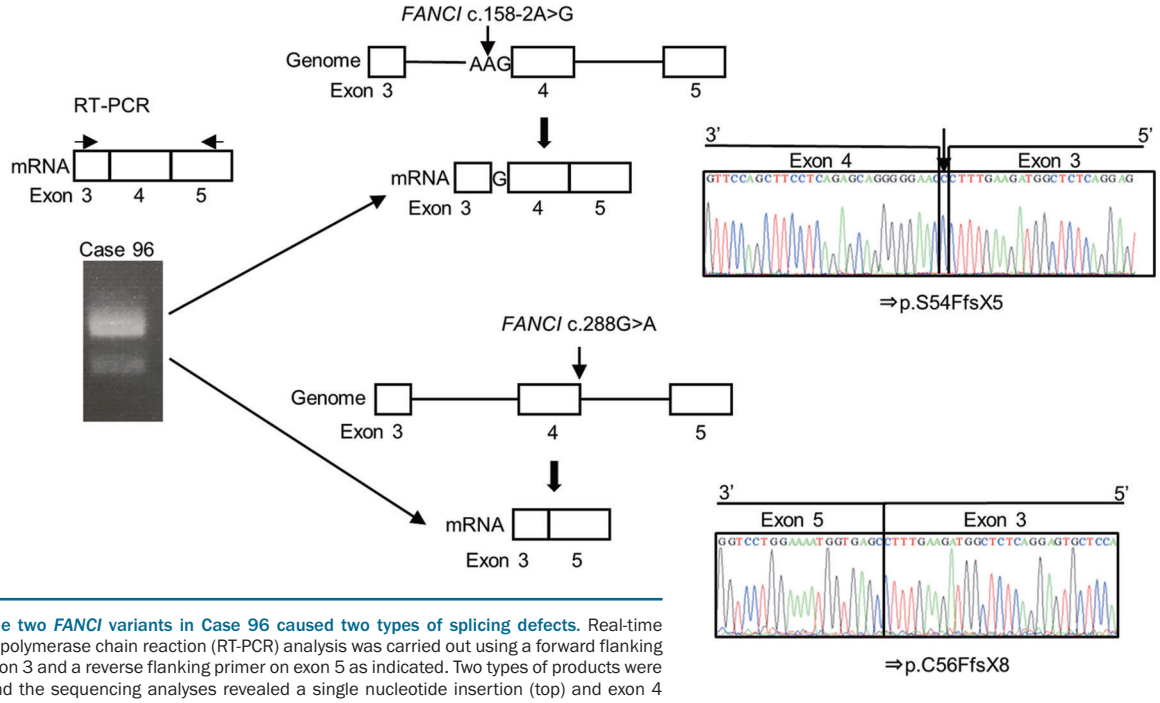

Figure 3. The two *FANCI* variants in Case 96 caused two types of splicing defects. Real-time quantitative polymerase chain reaction (RT-PCR) analysis was carried out using a forward flanking primer on exon 3 and a reverse flanking primer on exon 5 as indicated. Two types of products were obtained, and the sequencing analyses revealed a single nucleotide insertion (top) and exon 4 skipping (bottom).

Table 4. Clinical features of Japanese Fanconi anemia (FA)-D1 and FA-N cases.

Individual	Case 65	Case 66	Case 98	AP37P*
Sex	Female	Male	Male	Male
FA mutations	*FANCD1* c.517-2A>G, c.6952C>T: p.R2318X	*FANCD1* c.475+1G>A c.7847C>T:p.S2616F	*FANCN* c.3350+5C>T c.3350+5C>T	*FANCD1* c.-40+1G>A, c.8504C>A: p.S2835X
FA-features	Short stature Left thumb polydactyly Right renal agenesis Microphthalmus Microcephaly	Short stature Microcephaly	Short stature ASD, PDA Congenital absence of inferior vena cava, Congenital tracheal stenosis Microcephaly	Short stature Mid-face hypoplasia Sprengel's deformity Multiple café-au-lait spots
Chromosome breakage test	Positive (MMC)	Positive (MMC)	Positive (DEB)	Positive (MMC)
ALDH2 genotype	GG	GA	GA	GG
Hematologic abnormality (onset)	None	None	None	Acute myeloid leukemia (2 years old)
Solid tumors (onset)	Immature teratoma (9 months old)	T-lymphoblastic lymphoma, Adenosquamous lung carcinoma (23 years old)	Wilms tumor (1 year old)	None
Outcome	Alive with progressive teratoma at 1.7 years old	Died of lymphoma at 25.5 years old	Died of Wilms tumor at 1.5 years old	Died of leukemia at 2 years old

*a previously reported case.[32] MMC, mitomycin C, Other abbreviations are explained in Table 2 and 3.

affect *PALB2* interaction with *RNF168* or *BRCA2* which is mediated by the *PALB2* C-terminal WD40 domain.[35,36]

The three FA-D1 patients (including the previous Japanese case), as well as the one FA-N patient, all developed early-onset malignancies; this is in line with previous reports from Western countries (Table 4).[34,37,38] Although it is important to note that the first clinical manifestation in such cases could be onset of malignancy without prior clinical problems, Cases 65 and 98 had severe physical anomalies as well. Their malformations did not fully meet VACTERL-H criteria (Table 2). Alter *et al*. had previously reported that FA-D1 and FA-N patients were characterized by frequent VACTERL-H association and early-onset tumors, such as Wilms tumor, or acute myeloid leukemia (AML), with a cumulative incidence of malignancy as high as 97% by the age of 5.2 years.[34] Thus, Case 66 was highly unusual as a FA-D1 patient. He developed T-lymphoblastic lymphoma at 23 years of age, with a relatively short stature, and severe microcephaly (*Online Supplementary Appendix*). He received standard chemotherapy for the lymphoma, which caused prolonged pancytopenia. Then a mitomycin C-induced chromosome breakage test was performed, and he was diagnosed as FA. We list Case 66 as FA-D1, since he had biallelic, likely deleterious, *BRCA2* variants but no other FA gene mutations. This case may expand the clinical spectrum of FA-D1. Alternatively, for the moment, the possibility that hidden FA gene variants caused his FA phenotype cannot be excluded.

Allele frequency of pathogenic variations in 22 Fanconi anemia genes in the Japanese population

To estimate the frequency of pathogenic FA gene variations in the Japanese population, we analyzed WGS data for 22 FA genes from the 3.5KJPNv2 database. We identified 66 deleterious genetic variations (nonsense, frameshifts, and splicing site mutations) in 19 FA genes (Table 1). In addition to the three common *FANCA* [c.2546elC (0.08%)] and *FANCG* mutations [c.307+1G>C (0.1%); c.1066C>T (0.04%)], carriers with *FANCA* c.2602-2A>T, *FANCD1* c.6952C>T, *FANCG* c.194delC, or FANCI c.157-2A>G mutations were detected at low percentages (0.01-0.08%), and these variants were identified as causative mutations in Japanese FA patients. Allele frequencies of *FANCL* c.170G>A (p.W57X) variants were relatively high (0.08%); however, no patients with these variants were identified in our FA collection.

Monoallelic mutations in some FA genes, such as *BRCA1, BRCA2, BRIP1, PALB2* and *RAD51C*, cause adult-onset cancer predisposition[39-41] and we identified 25 deleterious variants in these genes (5 in *BRCA1*, 10 in *BRCA2*, 3 in *BRIP1*, 6 in *PALB2*, and 1 in *RAD51C*). *BRCA1* c.188T>A (p.L63X) and *BRCA2* c.6952C>T (p.R2318X) are well-known mutations in hereditary breast and ovarian cancer (HBOC) in Japan.[42] The *BRCA2* c.10150C>T (p.R3384X) was more prevalent than p.R2318X, but it has been classified as non-pathogenic because of its location near the 3'-end.[43] The *PALB2* c.2834+2T>C was recently identified in a Japanese female with bilateral breast cancer.[44]

From these analyses of allele frequency of FA-associated deleterious variants in 3,554 individuals, we estimated that approximately 2.6% of the Japanese could be considered to be carriers of pathogenic variations in FA genes.

Discussion

In this study, we report the largest series of subtyped Japanese FA patients to date by updating our previously reported cases with an additional 13 new cases (*Online Supplementary Table S2*). We employed various methods, including PCR-direct sequencing and next generation sequencing. WES and targeted exome sequencing were extremely useful in identifying mutations, as reported previously.[8] However, approximately half of the cases were undiagnosed even after these procedures.[8] When combined with the data generated by FANCA-MLPA, the diagnosis rate was much enhanced, since *FANCA* deletion was frequent, and WES/target-seq is not necessarily effective in identifying deletions. We also noted that mutations affecting splicing, such as intronic or synonymous variants, were difficult to detect by WES or targeted-seq. The former weak point was complemented by the use of aCGH, while RNA-seq was useful in detecting splicing abnormalities. We think the identification of two synonymous mutations affecting splicing is of great significance, since this type of mutations could have been easily overlooked. Thus, our approach ultimately achieved molecular diagnosis in most of the cases, and many private and novel mutations were identified in 11 of the 22 known FA genes.

Given the present results, we suggest that a molecular work-up of Japanese FA patients should start with screening for the three most-common mutations (*FANCA* c.2546delC, *FANCG* c.307+1G>C, and *FANCG* c.1066C>T) along with an MLPA assay for *FANCA*. As a next step, targeted-seq or WES analysis should be considered. For the remaining unclassified cases, aCGH, WGS, and RNA-seq analysis may be useful to identify large indels or splicing defects. Through these combined and comprehensive efforts, correct genetic diagnosis may be obtained in more than 90% of the Japanese FA patients.

Aldehyde dehydrogenase 2 (*ALDH2*) converts acetaldehyde to acetate, and potentially catalyzes other aldehydes as well. In East Asian countries, including Japan, a significant fraction (approx. 50%) of the population carries *ALDH2* variant *ALDH2*504Lys* which is encoded by the so-called A allele, and affects alcohol tolerance and some aspects of human health.[45] We have previously described a subset of severe FA cases that were homozygous for the *ALDH2*504Lys* variant (the AA genotype), and who experienced bone marrow failure and/or myelodysplastic syndrome (MDS) immediately after birth.[5,7] We also found several FA-B and FA-I cases that were accompanied by severe physical abnormalities, termed VACTERL-H. Two (Cases 18-1, 99-1) of the six previously reported FA cases carrying a homozygous *ALDH2* AA genotype also displayed these severe malformations[7] (Table 2), but, interestingly, their siblings (Cases 18-2, 99-2) with *ALDH2* GG genotype displayed relatively minor physical abnormalities (*Online Supplementary Table S2*). We note here that the FA-B or FA-I patients with VACTERL-H anomalies were carriers of the *ALDH2* GG or the GA genotype. The impact of endogenous aldehyde catabolism on bone marrow stem cells is very clear, and this effect also extends to the role of the FA proteins in preventing severe malformations. It has been suggested that the extent of physical abnormalities and severity of hematologic defects tend to be correlated.[46] In any event, FA-B and FA-I groups often exhibit severe malformations, as described previously[47,48] and confirmed here in Japanese cases. Since many of our

cases were referred to us in order to carry out HSCT, our data could be biased toward a proportion of patients with more severe malformations and may not reflect all individuals carrying FA gene variants. The relatively high incidence of VACTERL-H anomalies in our series could reflect this[46] and/or this may be due to the impact of the *ALDH2* genotype.

An important issue is how prevalent the FA-causing variants in the Japanese population are. We estimate that at least approximately 2.6% of the Japanese population might carry pathogenic variants in FA genes, using the 3.5KJPNv2 database. In Japan, approximately ten individuals with FA are born per one million births each year according to the report from the Japanese Society of Pediatric Hematology/Oncology.[49] FA-G accounted for 25% of Japanese FA patients according to our study and approximately two FA-G patients are estimated to be born each year in Japan. Our estimated allele frequency for *FANCG* (0.16%) from the 3.5KJPNv2 database is a reasonable one given the birth rate of the FA-G patients. Rogers *et al*. reported that at least one FA disease-causing variant among 16 FA genes (nonsense, splice altering, frame shifts, and a subset of missense variants that are judged to be highly deleterious) was identified in 4.3% of individuals from the ESP and 1KGP studies.[50] This estimate was substantially higher than ours, but our numbers may increase if we include deleterious missense mutation data in the future.

In conclusion, the molecular diagnostic strategy and data described in this study provide a basis for future molecular work-ups and clinical management for Japanese FA patients. In four cases, we failed to achieve a definitive subtyping; this could be due to technical problems or due to novel FA genes awaiting discovery. These remain as "unclassified", and could be of particular interest in further attempts to elucidate FA etiology.

Acknowledgments

The authors would like to thank patients and families for participating in the study, Dr. James Hejna (Kyoto University) for critical reading of the manuscript, and Akiko Watanabe and Fan Peng for technical and secretarial help.

Funding

This work was supported by JSPS KAKENHI Grant Number JP15H01738 [to MT], grants from the Ministry of Health, Labor, and Welfare [to SK and to EI], and grants from Uehara Memorial Foundation [to MT], and Astellas Foundation for Research on Metabolic Disorders [to MT].

References

1. Nalepa G, Clapp DW. Fanconi anaemia and cancer: an intricate relationship. Nat Rev Cancer. 2018;18(3):168-185.
2. Garaycoechea JI, Crossan GP, Langevin F, et al. Alcohol and endogenous aldehydes damage chromosomes and mutate stem cells. Nature. 2018;553(7687):171-177.
3. Chandrasekharappa SC, Lach FP, Kimble DC, et al. Massively parallel sequencing, aCGH, and RNA-Seq technologies provide a comprehensive molecular diagnosis of Fanconi anemia. Blood. 2013;121(22):e138-148.
4. De Rocco D, Bottega R, Cappelli E, et al. Molecular analysis of Fanconi anemia: the experience of the Bone Marrow Failure Study Group of the Italian Association of Pediatric Onco-Hematology. Haematologica. 2014;99(6):1022-1031.
5. Hira A, Yabe H, Yoshida K, et al. Variant ALDH2 is associated with accelerated progression of bone marrow failure in Japanese Fanconi anemia patients. Blood. 2013;122 (18):3206-3209.
6. Hira A, Yoshida K, Sato K, et al. Mutations in the Gene Encoding the E2 Conjugating Enzyme UBE2T Cause Fanconi Anemia. Am J Hum Genet. 2015;96(6):1001-1007.
7. Yabe M, Yabe H, Morimoto T, et al. The phenotype and clinical course of Japanese Fanconi Anaemia infants is influenced by patient, but not maternal ALDH2 genotype. Br J Haematol. 2016;175(3):457-461.
8. Muramatsu H, Okuno Y, Yoshida K, et al. Clinical utility of next-generation sequencing for inherited bone marrow failure syndromes. Genet Med. 2017;19(7):796-802.
9. Sekinaka Y, Mitsuiki N, Imai K, et al. Common Variable Immunodeficiency Caused by FANC Mutations. J Clin Immunol. 2017;37(5):434-444.
10. Yabe M, Koike T, Ohtsubo K, et al. Associations of complementation group, ALDH2 genotype, and clonal abnormalities with hematological outcome in Japanese patients with Fanconi anemia. Ann Hematol. 2019;98(2):271-280.
11. Tachibana A, Kato T, Ejima Y, et al. The FANCA gene in Japanese Fanconi anemia: reports of eight novel mutations and analysis of sequence variability. Hum Mutat. 1999;13(3):237-244.
12. Matsuo K, Wakai K, Hirose K, Ito H, Saito T, Tajima K. Alcohol dehydrogenase 2 His47Arg polymorphism influences drinking habit independently of aldehyde dehydrogenase 2 Glu487Lys polymorphism: analysis of 2,299 Japanese subjects. Cancer Epidemiol Biomarkers Prev. 2006;15(5): 1009-1013.
13. Shiraishi Y, Fujimoto A, Furuta M, et al. Integrated analysis of whole genome and transcriptome sequencing reveals diverse transcriptomic aberrations driven by somatic genomic changes in liver cancers. Creighton C, editor. PLoS One. 2014; 9(12):e114263.
14. Yasuda J, Kinoshita K, Katsuoka F, et al. Genome analyses for the Tohoku Medical Megabank Project toward establishment of personalized healthcare. J Biochem. 2019; 165(2):139-158.
15. Ceccaldi R, Rondinelli B, D'Andrea AD. Repair Pathway Choices and Consequences at the Double-Strand Break. Trends Cell Biol. 2016;26(1):52-64.
16. Umaña LA, Magoulas P, Bi W, Bacino CA. A male newborn with VACTERL association and Fanconi anemia with a FANCB deletion detected by array comparative genomic hybridization (aCGH). Am J Med Genet A. 2011;155A(12):3071-3074.
17. Flynn EK, Kamat A, Lach FP, et al. Comprehensive analysis of pathogenic deletion variants in Fanconi anemia genes. Hum Mutat. 2014;35(11):1342-1353.
18. Chamary JV, Parmley JL, Hurst LD. Hearing silence: non-neutral evolution at synonymous sites in mammals. Nat Rev Genet. 2006;7(2):98-108.
19. Supek F, Miñana B, Valcárcel J, Gabaldón T, Lehner B. Synonymous Mutations Frequently Act as Driver Mutations in Human Cancers. Cell. 2014;156(6):1324–1335.
20. Neveling K, Endt D, Hoehn H, Schindler D. Genotype-phenotype correlations in Fanconi anemia. Mutat Res. 2009;668(1-2):73-91.
21. Whitney MA, Saito H, Jakobs PM, Gibson RA, Moses RE, Grompe M. A common mutation in the FACC gene causes Fanconi anaemia in Ashkenazi Jews. Nat Genet. 1993;4(2):202-205.
22. Kimble DC, Lach FP, Gregg SQ, et al. A comprehensive approach to identification of pathogenic FANCA variants in Fanconi anemia patients and their families. Hum Mutat. 2018;39(2):237-254.
23. Castellà M, Pujol R, Callen E, et al. Origin, functional role, and clinical impact of Fanconi anemia FANCA mutations. Blood. 2011;117(14):3759-3769.
24. Park J, Chung N-G, Chae H, et al. FANCA and FANCG are the major Fanconi anemia genes in the Korean population. Clin Genet. 2013;84(3):271-275.
25. Yamada T, Tachibana A, Shimizu T, Mugishima H, Okubo M, Sasaki MS. Novel mutations of the FANCG gene causing alternative splicing in Japanese Fanconi anemia. J Hum Genet. 2000;45(3):159-166.
26. Yagasaki H, Oda T, Adachi D, et al. Two common founder mutations of the fanconi anemia group G gene FANCG/XRCC9 in the Japanese population. Hum Mutat. 2003;21(5):555.
27. Solomon BD, Pineda-Alvarez DE, Raam MS,

et al. Analysis of component findings in 79 patients diagnosed with VACTERL association. Am J Med Genet A. 2010;152A(9): 2236-2244.
28. Alter BP, Rosenberg PS. VACTERL-H Association and Fanconi Anemia. Mol Syndromol. 2013;4(1-2):87–93.
29. van Twest S, Murphy VJ, Hodson C, et al. Mechanism of Ubiquitination and Deubiquitination in the Fanconi Anemia Pathway. Mol Cell. 2017;65(2):247-259.
30. McCauley J, Masand N, McGowan R, et al. X-linked VACTERL with hydrocephalus syndrome: further delineation of the phenotype caused by FANCB mutations. Am J Med Genet A. 2011;155A(10):2370-2380.
31. Krawczak M, Thomas NST, Hundrieser B, et al. Single base-pair substitutions in exon-intron junctions of human genes: nature, distribution, and consequences for mRNA splicing. Hum Mutat. 2007;28(2):150-158.
32. Ikeda H, Matsushita M, Waisfisz Q, et al. Genetic reversion in an acute myelogenous leukemia cell line from a Fanconi anemia patient with biallelic mutations in BRCA2. Cancer Res. 2003;63(10):2688-2694.
33. Bakker JL, Thirthagiri E, van Mil SE, et al. A novel splice site mutation in the noncoding region of BRCA2: implications for Fanconi anemia and familial breast cancer diagnostics. Hum Mutat. 2014;35(4):442-446.
34. Alter BP, Rosenberg PS, Brody LC. Clinical and molecular features associated with biallelic mutations in FANCD1/BRCA2. J Med Genet. 2007;44(1):1-9.
35. Xia B, Sheng Q, Nakanishi K, et al. Control of BRCA2 cellular and clinical functions by a nuclear partner, PALB2. Mol Cell. 2006; 22(6):719-729.
36. Luijsterburg MS, Typas D, Caron M-C, et al. A PALB2-interacting domain in RNF168 couples homologous recombination to DNA break-induced chromatin ubiquitylation. Elife. 2017;6.
37. Reid S, Schindler D, Hanenberg H, et al. Biallelic mutations in PALB2 cause Fanconi anemia subtype FA-N and predispose to childhood cancer. Nat Genet. 2007;39(2): 162-164.
38. Wagner JE, Tolar J, Levran O, et al. Germline mutations in BRCA2: shared genetic susceptibility to breast cancer, early onset leukemia, and Fanconi anemia. Blood. 2004;103(8):3226-3229.
39. Prakash R, Zhang Y, Feng W, Jasin M. Homologous Recombination and Human Health: The Roles of BRCA1, BRCA2, and Associated Proteins. Cold Spring Harb Perspect Biol. 2015;7(4):a016600.
40. Katsuki Y, Takata M. Defects in homologous recombination repair behind the human diseases: FA and HBOC. Endocr Relat Cancer. 2016;23(10):T19-37.
41. Paulo P, Maia S, Pinto C, et al. Targeted next generation sequencing identifies functionally deleterious germline mutations in novel genes in early-onset/familial prostate cancer. PLoS Genet. 2018;14(4):e1007355.
42. Hirotsu Y, Nakagomi H, Sakamoto I, Amemiya K, Mochizuki H, Omata M. Detection of BRCA1 and BRCA2 germline mutations in Japanese population using next-generation sequencing. Mol Genet Genomic Med. 2015;3(2):121-129.
43. Borg A, Haile RW, Malone KE, et al. Characterization of BRCA1 and BRCA2 deleterious mutations and variants of unknown clinical significance in unilateral and bilateral breast cancer: the WECARE study. Hum Mutat. 2010;31(3):E1200-1240.
44. Nakagomi H, Hirotsu Y, Okimoto K, et al. PALB2 mutation in a woman with bilateral breast cancer: A case report. Mol Clin Oncol. 2017;6(4):556-560.
45. Gross ER, Zambelli VO, Small BA, Ferreira JCB, Chen C-H, Mochly-Rosen D. A personalized medicine approach for Asian Americans with the aldehyde dehydrogenase 2*2 variant. Annu Rev Pharmacol Toxicol. 2015;55:107-127.
46. Rosenberg PS, Huang Y, Alter BP. Individualized risks of first adverse events in patients with Fanconi anemia. Blood. 2004;104(2):350-355.
47. Holden ST, Cox JJ, Kesterton I, Thomas NS, Carr C, Woods CG. Fanconi anaemia complementation group B presenting as X linked VACTERL with hydrocephalus syndrome. J Med Genet. 2006;43(9):750-754.
48. Savage SA, Ballew BJ, Giri N, et al. Novel FANCI mutations in Fanconi anemia with VACTERL association. Am J Med Genet A. 2016;170A(2):386-391.
49. Yabe M, Yabe H. [Diagnosis and management of inherited bone marrow failure syndrome]. Rinsho Ketsueki. 2015;56(10):1914-1921.
50. Rogers KJ, Fu W, Akey JM, Monnat RJ. Global and disease-associated genetic variation in the human Fanconi anemia gene family. Hum Mol Genet. 2014;23(25):6815-6825.

Ferrata Storti Foundation

Haematologica 2019
Volume 104(10):1974-1983

Immunosuppressive therapy for pediatric aplastic anemia: a North American Pediatric Aplastic Anemia Consortium study

Zora R. Rogers,[1] Taizo A. Nakano,[2] Timothy S. Olson,[3] Alison A. Bertuch,[4] Winfred Wang,[5] Alfred Gillio,[6] Thomas D. Coates,[7] Anjulika Chawla,[8] Paul Castillo,[9] Peter Kurre,[10] Christopher Gamper,[11] Carolyn M. Bennett,[12] Sarita Joshi,[13] Amy E. Geddis,[14] Jessica Boklan,[15] Grzegorz Nalepa,[16] Jennifer A. Rothman,[17] James N. Huang,[18] Gary M. Kupfer,[19] Michaela Cada,[20] Bertil Glader,[21] Kelly J. Walkovich,[22] Alexis A. Thompson,[23] Rabi Hanna,[24] Adrianna Vlachos,[25] Maggie Malsch,[26] Edie A. Weller,[27] David A. Williams[28] and Akiko Shimamura[28]

[1]Pediatric Hematology/Oncology, University of Texas Southwestern Medical Center, Dallas, TX, USA; [2]Center for Cancer and Blood Disorders, Department of Pediatrics, Children's Hospital Colorado and the University of Colorado School of Medicine, Aurora, CO, USA; [3]Children's Hospital of Philadelphia, Philadelphia, PA, USA; [4]Baylor College of Medicine, Houston, TX, USA; [5]Department of Hematology, St. Jude Children's Research Hospital, Memphis, TN, USA; [6]Hackensack University Medical Center, Hackensack, NJ, USA; [7]Children's Hospital Los Angeles, Los Angeles, CA, USA; [8]Brown University, Providence, RI, USA; [9]University of Florida, Gainesville, FL, USA; [10]Oregon Health and Science University, Portland, OR, USA; [11]Johns Hopkins University, Baltimore, MD, USA; [12]Emory University, Atlanta, GA, USA; [13]Nationwide Childrens Hospital, Columbus, OH, USA; [14]Seattle Children's Hospital, Seattle, WA, USA; [15]Center for Cancer and Blood Disorders, Phoenix Children's Hospital, Phoenix, AZ, USA; [16]Indiana University School of Medicine, Indianapolis, IN, USA; [17]Duke Children's Hospital, Durham, NC, USA; [18]UCSF Benioff Children's Hospital, San Francisco, CA, USA; [19]Yale, New Haven, CT, USA; [20]Sick Kids Hospital, Toronto, Ontario, Canada; [21]Stanford University School of Medicine, Palo Alto, CA, USA; [22]University of Michigan, Ann Arbor, MI, USA; [23]Lurie Children's Hospital, Chicago, IL, USA; [24]Cleveland Clinic, Cleveland, OH, USA; [25]Hofstra Northwell School of Medicine, Hempstead, NY, USA; [26]Institutional Centers for Clinical and Translational Research, Boston Children's Hospital, Boston, MA, USA; [27]Division of Hematology and Oncology and Biostatistics and Research Design Center of the Institutional Centers for Clinical and Translational Research, Boston Children's Hospital, Boston, MA, USA and [28]Boston Children's Hospital and Dana Farber/Boston Children's Cancer and Blood Disorders Center, Boston, MA, USA

Correspondence:

AKIKO SHIMAMURA
akiko.shimamura@childrens.harvard.edu

Received: November 5, 2018.

Accepted: March 28, 2019.

Pre-published: April 4, 2019.

doi:10.3324/haematol.2018.206540

Check the online version for the most updated information on this article, online supplements, and information on authorship & disclosures: www.haematologica.org/content/104/10/1974

ABSTRACT

Quality of response to immunosuppressive therapy and long-term outcomes for pediatric severe aplastic anemia remain incompletely characterized. Contemporary evidence to inform treatment of relapsed or refractory severe aplastic anemia for pediatric patients is also limited. The clinical features and outcomes for 314 children treated from 2002 to 2014 with immunosuppressive therapy for acquired severe aplastic anemia were analyzed retrospectively from 25 institutions in the North American Pediatric Aplastic Anemia Consortium. The majority of subjects (n=264) received horse anti-thymocyte globulin (hATG) plus cyclosporine (CyA) with a median 61 months follow up. Following hATG/CyA, 71.2% (95%CI: 65.3,76.6) achieved an objective response. In contrast to adult studies, the quality of response achieved in pediatric patients was high, with 59.8% (95%CI: 53.7,65.8) complete response and 68.2% (95%CI: 62.2,73.8) achieving at least a very good partial response with a platelet count ≥50x10^{9}L. At five years post-hATG/CyA, overall survival was 93% (95%CI: 89,96), but event-free survival without subsequent treatment was only 64% (95%CI: 57,69) without a plateau. Twelve of 171 evaluable patients (7%) acquired clonal abnormalities after diagnosis after a median 25.2 months (range: 4.3-71 months) post treatment. Myelodysplastic syndrome or leukemia developed in 6 of 314 (1.9%). For relapsed/refractory disease, treatment with a hematopoietic stem cell transplant had a superior event-free survival compared to second immunosuppressive therapy treatment in a multivariate analysis (HR=0.19, 95%CI: 0.08,0.47; *P*=0.0003). This study highlights the need for improved therapies to achieve sustained high-quality remission for children with severe aplastic anemia.

Introduction

Acquired severe aplastic anemia (SAA) is a rare disorder characterized by peripheral bi- or pancytopenia and bone marrow (BM) hypoplasia. Initial therapy for younger patients with SAA is a matched sibling hematopoietic stem cell transplantation (HSCT) or immunosuppressive therapy (IST) if a matched sibling donor is not available.[1] There is a paucity of data for children with SAA treated during the modern era from the ethnically and geographically diverse population of North America. Pediatric studies from the National Institutes of Health,[2] the Japanese Childhood Aplastic Anemia Study Group,[3-6] Brazil,[7] and the Severe Aplastic Anemia Working Party of the European Group for Blood and Marrow Transplant (SAAWP-EBMT)[8,9] have been reported. However, diagnostic evaluation for constitutional disorders has been limited, and duration of follow up has often been variable and short. Many published studies report outcomes with rabbit anti-thymocyte globulin (rATG) due to the withdrawal of horse ATG (hATG) from some European and Asian markets in 2007; however, a large prospective study of upfront rATG *versus* hATG reported inferior response rates and lower survival with rATG.[10] Thus, contemporary data to inform therapeutic decisions in pediatric patients treated with IST in North America are of interest given international differences in treatment regimens, recent advances in diagnosis of genetic marrow failure disorders, improvements in HSCT outcomes, and better supportive care.

To facilitate collaborative clinical studies of pediatric aplastic anemia, a consortium of 25 institutions (now numbering 39) across North America, named the North American Pediatric Aplastic Anemia Consortium (NAPAAC), was formed in 2014.[11] The urgent need for evidence-based guidelines for patient management in pediatric SAA was highlighted by a NAPAAC survey of clinical practices of member institutions which revealed considerable variability in diagnostic evaluation and management.[11] Recognizing the challenges of performing a prospective trial to address these critical knowledge gaps, NAPAAC conducted a retrospective study of presentation and outcomes of pediatric patients diagnosed from 2002 to 2014 with SAA and treated with IST with a minimum of two years of follow up in member institutions. The objectives of the study were to determine the rates of response and survival following IST, to assess rates of clonal abnormalities, and to explore patient-specific factors contributing to survival, refractory disease, relapse, and clonal progression following IST. This NAPAAC effort represents the first large study of pediatric SAA reflecting the racially diverse population of children afflicted by SAA across multiple centers in North America. These contemporary data from a large number of pediatric patients will inform future studies of additional diagnostic or prognostic testing, and guide evidence-based clinical management.

Methods

Patients

A retrospective chart review was conducted by member institutions of all patients aged 1-20 years treated with IST as the first therapy for pediatric SAA between 1st January 2002 and 30th June 2014 for whom follow up was available for a minimum of 24 months or until death. This study was approved by the Institutional Review Board (IRB) at each participating institution or *via* a reliance agreement with the central study IRB at Boston Children's Hospital. Each site abstracted data from the local medical record and entered them into a central Red Cap database. The data included demographics, disease characteristics at diagnosis, treatment, and outcomes. When available, the original anonymized written reports of specific studies including BM aspirate and biopsy, cytogenetics, fluorescence *in situ* hybridization (FISH), clonal analysis for paroxysmal nocturnal hemoglobinuria (PNH), telomere flow-FISH analysis, immunological analyses, and autopsies were uploaded for central review.

Submitted cases were included only if the diagnostic BM was reported as hypocellular and the patient had at least two peripheral cytopenias: 1) absolute neutrophil count (ANC) < 0.5 $x10^9$/L; 2) platelet count (Plts) < $20x10^9$/L; 3) hemoglobin (Hb) < 8 g/dL. Central review of diagnostic marrow slides was not feasible but marrow pathology reports were reviewed to confirm that the marrow cellularity was <25% or hypocellularity was stated to be consistent with the diagnosis of SAA without a specified percentage cellularity. Patients with a local diagnosis of an inherited BM failure syndrome were excluded from this study, as were subjects with an HLA-matched sibling who went to transplant upfront. Date of diagnosis was considered to be the date of the BM biopsy. Date of treatment was considered the first day of IST, and all outcomes were timed from the first day of treatment. Structured reporting of status and blood counts was required at initiation of IST, as well as at 3, 6, 12, 24, 36, 48, and 60 months, and at last follow up.

Definitions

Overall survival (OS) was measured from the time from first day of IST until death or date last known alive. Event-free survival (EFS) was measured from the time from start of IST until an event (death or start of a second therapy for SAA, either HSCT or a second course of IST) or the date last known to be without an event.

Response[12] was defined using hemoglobin (Hb), absolute neutrophil count (ANC) and platelets (Plts). Complete response (CR), very good partial response (VGPR) and partial response (PR) required the indicated levels in all three lineages as noted below; no response (NR) was defined as failure in any lineage:

CR: Hb ≥10 g/dL and ANC ≥$1x10^9$/L and Plts ≥$100x10^9$/L
VGPR: Hb ≥8 g/dL and ANC ≥$0.5x10^9$/L and Plts ≥$50x10^9$/L
PR: Hb ≥8 g/dL and ANC ≥$0.5x10^9$/L and Plts ≥$20x10^9$/L
NR: Hb <8 g/dL or ANC <$0.5x10^9$/L or Plts <$20x10^9$/L

Patients receiving transfusions of packed red blood cells within six weeks or platelets or granulocyte-colony stimulating factor (G-CSF)/granulocyte/macrophage-colony stimulating factor (GM-CSF) within two weeks of evaluation were deemed to have had NR at that time point. An objective response (OR) was defined as at least a PR (PR+VGPR+CR) and a deep response (DR) was defined as at least a VGPR (VGPR+CR). Duration of response (DOR) was defined as time from start of response to an event (death or start of a second therapy for SAA, either HSCT or a second course of IST).

Statistical analysis

Summary statistics included median and range for continuous variables and frequency and proportion for binary variables. Fisher's exact test and Wilcoxon rank sum test were used to compare proportions and medians, respectively. The proportion of subjects with an OR, DR, and CR were reported along with the exact binomial 95% confidence interval (95%CI). OS, EFS and DOR were estimated using the Kaplan-Meier method (log-log transformation for Confidence Interval) and compared using the

log-rank test. A Cox proportional hazards model was used to compare EFS by treatment adjusting for co-variates of interest [age, gender, time from initial IST treatment to 2nd treatment, and lymphocytopenia (lymphocyte count <1x10^9/L)]. Reference groups in this model were: IST treatment, age at second treatment ≥10 years, male gender, lymphocyte count at diagnosis ≥1x10^9/L. An indicator variable was included in the model for missing lymphocyte data as these data were not provided for all subjects. The median follow up among all subjects was 62 months. There was 80% power to detect differences of at least 16% difference in proportions for 314 and 264 subjects, respectively (two-sided Fishers exact test, alpha=0.05). In terms of precision, the maximum Confidence Interval width of the exact binomial 95%CI for an observed proportion was 0.12 and 0.11, respectively, with n=314 and n=264. R language was used for analysis (R Core Team, 2016, Vienna, Austria; *https://www.R-project.org*).

Results

Patients' characteristics at diagnosis

A total of 314 pediatric patients treated with IST for SAA were identified by systematic retrospective chart review across 25 NAPAAC institutions. Table 1 summarizes baseline demographics of study subjects. Nine patients (0.03%) were 1-2 years of age. Gender was evenly distributed. The population was racially diverse, reflecting the ethnic diversity of North America. A family history of aplastic anemia, none of whom were first-degree relatives, was noted in four patients.

Hepatitis was noted prior to diagnosis in 43 (13.7%) patients, of whom 33 (12.5%) were treated with hATG/cyclosporine (CyA). Laboratory features at diagnosis are summarized in Table 2. PNH test results were available at diagnosis for 140 patients and a PNH clone

Table 1. Baseline demographics and characteristics.

	Study subjects All subjects	hATG/CyA
Total subjects (N)	314	264
Male gender (N, %)	162 (51.6%)	141 (53.4%)
Median age in years at diagnosis (Range)	9.8 (1-20.3)	9.6 (1-20.3)
Race (N,%)		
White*	183 (58.3%)	157 (59.5%)
Black or African American	52 (16.6%)	42 (15.9%)
Asian	23 (7.3%)	19 (7.2%)
Other	33 (10.5%)	24 (9.1%)
Native Hawaiian or Other Pacific Islander	11 (3.5%)	11(4.2%)
Native American or Alaska Native	1 (0.3%)	1 (0.4%)
Unknown	11 (3.5%)	10 (3.8%)

*Including Hispanic and Latino; hATG: horse anti-thymocyte globulin.; CyA: cyclosporin.

Table 2. Laboratory features at diagnosis.

	All subjects		hATG/CyA subjects	
	N Evaluable	Value	N Evaluable	Value
PNH clone detected, N (%)	140	55 (39.3%)	109	48(44%)
Median MCV, fL (IQR)	273	89.1 (83.1-97.8)	234	89.1 (83.0-98.8)
MCV > 100fL, N, (%)	273	55 (20.1%)	234	51 (21.8%)
Median absolute reticulocyte count x10^9/L (IQR)	231	19 (9,33)	190	20 (10, 33)
Median lymphocyte count/mL (IQR)	260	1210 (600-1890)	221	1260 (650-1950)
Lymphocyte count <1000/mL, N (%)	260	110 (42.3%)	221	89 (40.3)

PNH: paroxysmal nocturnal hemoglobinuria; MCV: mean red cell volume; fL: fentoliter; IQ: IQR: interquartile range.

Table 3. Treatment.

Treatment	N (%)
hATG+CyA	264 (84.1%)
hATG+Tacro	15 (4.8%)
rATG+CyA or Tacro	15 (4.8%)
CTX	19 (6.1%)
Unspecified ATG+CyA	1 (0.3%)

Tacro: tacrolimus, CTX: cyclophosphamide; hATG: horse anti-thymocyte globulin; rATG: rabbit anti-thymocyte globulin; CyA: cyclosporine.

was noted in 55 (39.3%). In most cases, the clone size was small [interquartile range (IQR): 0-0.12%]. Only 5 patients had PNH clones larger than 10% (range: 12.56-28.4%) in the granulocyte lineage and none had clinically evident hemolysis or thrombosis at diagnosis.

The most commonly investigated inherited BM failure syndromes at diagnosis were Fanconi anemia, Shwachman-Diamond syndrome, and dyskeratosis congenita. Fanconi anemia screening was negative for 292 patients (93%), 18 patients were not tested, and results were not available for four subjects. Genetic testing for Shwachman-Diamond syndrome was available for 46 patients (14.6%); all of these were negative. Perhaps reflecting the evolution of understanding the role of dyskeratosis congenita in BM failure over the past five years, telomere length was assessed at the time of diagnosis in only 115 patients (36.6%) and a report of a clinical telomere flow-FISH test was available for 93 patients (29.6%). No patient exhibited a pattern suspicious for a primary telomere disorder (telomeres <1st percentile in at least 3 different lymphocyte subsets).[13] However, telomere lengths <1st percentile were found in total lymphocytes in six patients, of whom only two had a complete 6-panel analysis.

The current diagnostic criteria for SAA includes an ARC (absolute reticulocyte count) of <20-60x10^9/L.12,14,15 Many institutions relied on hemoglobin (Hb) rather than the ARC as a more clinically relevant indicator of erythroid hypoplasia to inform diagnosis and treatment decisions. Comparison of ARC *versus* Hb for the 231 subjects with ARC <100 revealed a lack of concordance [(estimated Pearson correlation coefficient of 0.15 (95%CI: 0.02, 0.27)] between the commonly utilized diagnostic criteria of ARC of <60 x10^9/L and significant anemia defined as Hb <8 g/dL (Figure 1). A subset of patients meeting ARC criteria of ARC <60 x10^9/L had Hb >8 g/dL (12.7%, 28 of 220), and conversely, some patients who did not meet diagnostic criteria for ARC had Hb levels <8 g/dL (74%, 26 of 35).

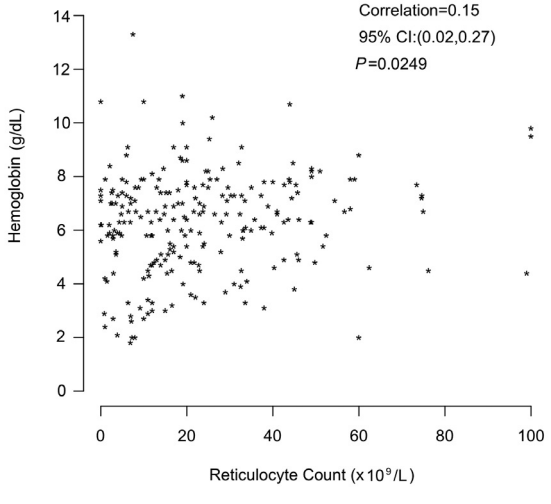

Figure 1. Correlation between absolute reticulocyte count and hemoglobin at diagnosis. Absolute reticulocyte counts <100x10^9/L (n=231) were plotted against the hemoglobin at diagnosis. CI: Confidence Interval.

Treatment

Treatment groups are outlined in Table 3. The majority of patients (n=264) received hATG plus CyA. Of these subjects, one patient received hATG but switched to rabbit ATG (rATG) due to an anaphylactic reaction. Overall, the demographics of the hATG/CyA population was similar to that of the entire group (Tables 1-3). The small number of subjects in groups treated with alternative IST regimens limited intergroup comparisons, and so only outcomes of the entire population and that of the hATG/CyA group were analyzed.

Of the 282 subjects who were treated with hATG,187 (71%) received 40 mg/kg/day for four days, 77 were dosed with a different regimen containing about the same total dose of hATG, and in 18 the dose was not available. CyA target trough levels were variable (100-400), with the majority 200-400. Following treatment with hATG/CyA, data regarding the cyclosporine taper were available for 194 patients. CyA was discontinued by six months for 13 subjects, between 6-12 months for 40 subjects, between 12-18 months for 34 subjects, between 18-24 months for 37 subjects, and after two years for 34 subjects. CyA was not discontinued at last follow up for 36 subjects.

Median time from diagnosis to treatment for all subjects was 24 days with an IQR of 12-40 days for the entire

Table 4. Best response to immunosuppressive therapy.

Response	All treatments		hATG/CyA	
	N	%	N	%
CR	189	60.2	158	59.8
VGPR	23	7.3	22	8.3
PR	10	3.2	8	3
NR	79	25.2	66	25
NE	13	4.1	10	3.8
Total	314	100	264	100

CR: complete response; VGPR: very good partial response; PR: partial response; NR: no response; NE: not evaluable.

Table 5. Response outcome in each treatment group.

Response Outcome	Treatment	Number of responses	Response Rate (%)	95% CI*
Objective Response (CR+VGPR+PR)	All	222	70.7	65.3, 75.7
	hATG/CyA	188	71.2	65.3, 76.6
Deep Response (CR+VGPR)	All	212	67.5	62.0, 72.7
	hATG/CyA	180	68.2	62.2, 73.8
Complete Response (CR)	All	189	60.2	54.5, 65.7
	hATG/CyA	158	59.8	53.7, 65.8

*95% exact binomial Confidence Interval.

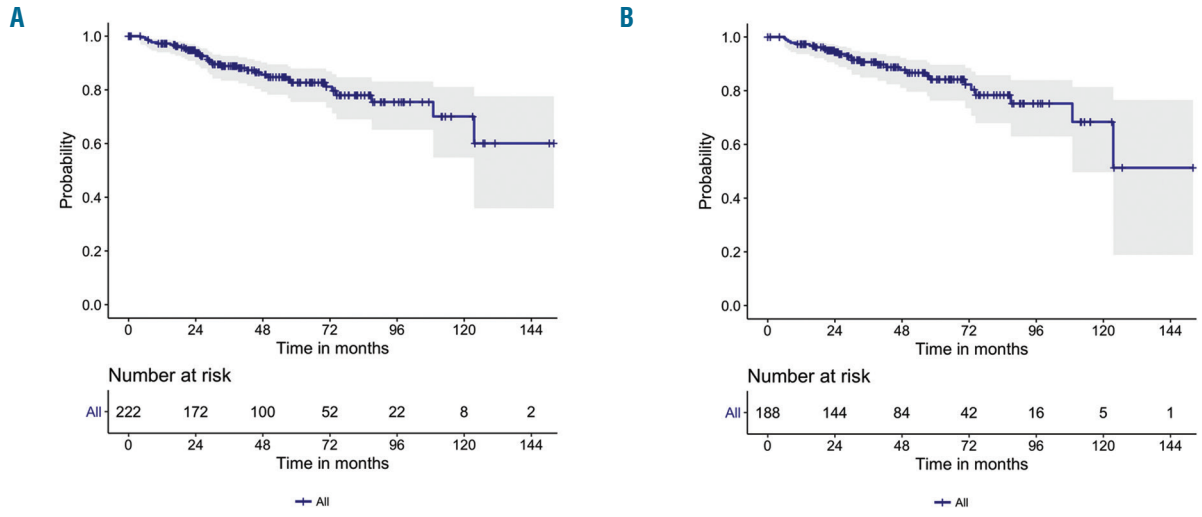

Figure 2. Duration of response. Kaplan-Meier analysis of duration of response for (A) all subjects or (B) subjects treated with horse anti-thymocyte globulin (rATG)/cyclosporine (CyA) who achieved at least a partial response.

cohort. Similar time to treatment was noted for the hATG/CyA group, with a median time from diagnosis of 23 days and an IQ range of 12-40 days.

Response

For the cohort of 314 patients and for the subset treated with hATG/CyA, median time to initial response was six months (range: 3-48 months; IQR: 3-12 months). Best responses for all patients and for the hATG/CyA group are summarized in Tables 4 and 5.

For the 264 subjects treated with hATG/CyA, OR was 71.2% (95%CI: 65.3,76.6), consistent with results from prior adult and pediatric studies.[8,9,16-20] The quality of response to hATG/CyA was good, with 59.8% (95%CI: 53.7,65.8) achieving a CR. Further, since the magnitude of a partial platelet response carries clinical implications for quality of life, the group attaining a deep response (Plts ≥50x10^9/L) was separately analyzed. A deep response was achieved by 68.2% (95%CI: 62.2,73.8). No response (NR) was noted in 66 subjects (25%) and 10 subjects (3.8%) were not evaluable (NE, Tables 4 and 5). Responses at six months post hATG/CyA were as follows: CR 21.6%, VGPR 19.7%, PR 8%, NR 47%, NE 3.7%.

The duration of response among subjects who had any initial response (CR, VGPR, or PR) is shown for all subjects (Figure 2A) and for those treated with hATG/CyA (Figure 2B). The estimated probability of sustained response for all subjects was 94% (95%CI: 89,96) at 24 months and 83% (95%CI: 76,88) at 60 months. For the subset of subjects treated with hATG/CyA, the estimated probability of sustained response was 94% (95%CI: 90,97) at 24 months and 84% (95%CI: 76,90) at 60 months. However, there was no plateau for loss of response observed over time even after five years post treatment.

Factors potentially affecting OR or DR for subjects treated with hATG/CyA were evaluated. No correlation with response was detected for telomere lengths <1st or <10th percentiles by flow-FISH, presence of a PNH clone, or red cell macrocytosis (mean corpuscular volume ≥100 fL) (P ≥0.17) (*Online Supplementary Table S1*). There was also no correlation between OR and median lymphocyte count (1.1 *vs.* 1.3;Wilcoxon rank sum test, P=0.51). There was no significant difference in median time from diagnosis to treatment between responders and non-responders (P≥0.29) (*Online Supplementary Table S1*).

Survival

The estimated overall survival is summarized in Figure 3. Median follow up amongst all 314 subjects was 62 months (59 months for those still alive) and 61 months among the hATG/CyA group (59 months for those still alive). At the time of this analysis, there were 29 (9.3%) deaths amongst all subjects; 21 (8%) amongst hATG/CyA-treated patients. Estimated OS (95%CI) for the entire cohort at 12, 24 and 60 months was 96% (95%CI: 94,98), 95% (92,97), and 92% (88,95), respectively (Figure 3A). Among the subjects who received hATG/CyA, estimated OS (95% CI) at 12, 24 and 60 months was 97% (94,99), 96% (93,98), and 93% (89,96), respectively (Figure 3B). Six individuals died after one treatment with hATG/CyA without receiving additional therapy.

Of the 314 subjects, 119 (38%) died or required an additional therapy. The estimated EFS (95%CI) for all subjects at 12, 24, and 60 months was 76% (95%CI: 70,80), 71% (95%CI: 66,76), and 62% (95%CI: 56,68), respectively (Figure 3C). The estimated median EFS for all subjects was 133 months. For patients treated with hATG/CyA, 98 of 264 subjects (37%) had an event. Median estimated EFS was 133 months (Figure 3D). Estimated EFS (95%CI) at 12, 24, and 60 months was 76% (95%CI: 70,81), 72% (95%CI: 66,77), and 64% (95%CI: 57,69), respectively, with events continuing to accrue even after five years post treatment.

No differences were detected in OS (P=0.13), EFS (P=0.26), or response (P>0.25) *versus* age at diagnosis for all subjects. No differences were detected in OS (P=0.09), EFS (P=0.22), or response (P>0.20) *versus* age at diagnosis for subjects treated with hATG/CyA.

Cytogenetics and clonal progression

Of the 271 patients in the cohort who had BM metaphase cytogenetics (n=254) and/or FISH (n=133)

Table 6. Clonal cytogenetic abnormalities at diagnosis and at follow up.

Acquired chromosomal abnormalities at diagnosis				
Abnormality	Status at follow up evaluation	Best response to initial therapy	Second therapy	Outcome
del(13)(q12q21)*	Decreased clone size	Relapse at two years	IST	Death, MVA
del(7q)	Not detected	CR by 12 months	None	Alive
add(11)(q23)*	N.A.	NR by 3 months	None	Alive
del(16)(q22)*	Not Detected	NR by 6 months	BMT	Alive
add(14)(q11.2)*	N.A.	CR by 3 months	None	Alive
del(13)(q12q14)*	Decreased clone size	CR by 6 months	None	Alive
+mar[2]*	N.A.	NR by 12 months	IST	Alive

*hATG/CyA subjects

Post-treatment acquisition of chromosomal abnormalities				
Abnormality	Time from diagnosis to first detection (months)	Best response to initial therapy	Second therapy	Outcome
del(13q)(q14q22)*	4.6	CR by 6 months	None	Alive
i(X)(p10)*	5.5	CR by 3 years	None	Alive
der(5)t(1;5)(q11;q11.2)*	66.5	NR by 12 months	IST	Alive
-7*	37.1	VGPR by 2 years	None	Alive
+14,-18*	4.5	CR by 12 months	None	Alive
-7	20	NR by 2 years	BMT	Death, PNA
-5,-7,del(7q),del(20p)*	4.3	NR by 6 months	BMT	Alive
8*	71	VGPR by 5 years	None	Alive
i(2q)*	67.7	Relapse at 2 years	IST	Alive
-7,del(7q)*	30.3	NR by 12 months	IST	Death, ALL
del(7q22)*	67	Relapse at 2 years	IST	Death, AML
-7*	8	NR by 6 months	IST	Alive

*hATG/CyA subjects

NR: no-response; N.A.: not available; VGPR: very good partial response; CR: complete response; IST: immunosuppressive therapy; BMT: bone marrow transplant; MVA: motor vehicle accident; PNA: pneumonia; ALL: acute lymphoblastic leukemia; AML: acute myeloid leukemia.

Table 7. Comparison of baseline cytogenetic clones with subsequent clonal abnormalities.

Baseline*	Follow Up						
	Normal		Abnormal		Not Evaluable		Total
	N	%	N	%	N	%	
Normal	137	51.9	12	4.6	115	43.6	264
Abnormal	3	42.9	2	28.6	2	28.6	7
Not Evaluable	16	37.2	1	2.3	26	60.5	43
Total	156	49.7	15	4.8	143	45.5	314

*Cytogenetics or fluorescence *in situ* hybridization at diagnosis.

assessments performed at diagnosis, seven (3%) had detectable clonal chromosomal abnormalities (Table 6). Six of these patients had follow-up cytogenetic assessments. Two patients had a del(13q) clone at diagnosis, which remained detectable through the duration of follow up (range: 33-49 months) but was not associated with acquisition of additional chromosomal abnormalities. In contrast, other small clones present at diagnosis, including del(7q) in one patient and del(16q) in one patient, were no longer detectable at follow-up assessment.

Of the 171 total patients who had follow-up BM metaphase cytogenetics (n=160) and/or FISH (n=109) assessment performed after IST initiation, 12 (7.0%) patients had evidence of new clonal chromosomal abnormalities (Table 7). One additional subject had a clonal abnormality [+der(14;21)(q10;q10)] at 143 months from the time of initial diagnosis; however, the baseline status was unknown. The most common genetic alteration after IST was loss of chromosome 7 [either -7 or del (7q)] occurring in six patients (3.5%), all of whom had normal cytogenetics at baseline. Three patients had a del(13q) clone detected during follow-up BM assessments of which one was acquired after treatment. Among those patients with

Table 8. Subsequent treatments.

Subsequent Treatment	All patients (N=314)		hATG/CyA (N=264)	
	N	%	N	%
2nd therapy	110	35	92	35
3rd therapy	35	11	33	13
4th therapy	3	1	3	1

no clonal abnormalities at presentation, but who subsequently developed abnormalities at follow up, the median time to observe an abnormality was 25.2 months (range: 4.3-71.0 months; IQ range: 5.3-66.6 months). Interestingly, only four patients had BM pathology reports confirming the diagnosis of myelodysplastic syndrome of whom two proceeded to HSCT prior to further clonal evolution. One patient developed acute lymphoblastic leukemia and three developed acute myeloid leukemia.

Complications

Complications following initiation of IST were common with bleeding (gastrointestinal, intracranial, hematuria or other significant hemorrhage) being most frequent and reported in 74 (23.6%) of all subjects (23.5% of hATG/CyA subjects). Infections, including bacteremia, fungal infections, cellulitis, meningitis, or pneumonia, were reported in 177 (56.4%) of all subjects (53.4% of hATG/CyA subjects). Renal failure requiring dialysis was reported in five patients (1.6%), all in the hATG/CyA group (1.9%). Causes of death classified by type of therapy and survival interval are detailed in *Online Supplementary Table S2*.

Outcomes after second-line therapy

Subsequent treatments following upfront hATG/CyA are summarized in Table 8.

Overall, 110 of 314 (35%) subjects received a second treatment, 35 of the 110 a third treatment, and three a fourth therapy.

Of the 38 patients undergoing HSCT for second-line therapy, response to initial treatment with hATG/CyA was as follows: 31 had refractory disease and seven had relapsed disease. Of the seven patients undergoing HSCT for relapsed disease, responses to initial hATG/CyA at three months and six months were as follows: one CR and six NR at three months; three CR, one VGPR, two NR, and one NE at six months. Of the 52 patients receiving a second IST treatment, response to initial treatment with hATG/CyA was as follows: 36 had refractory disease, 15 had relapsed disease, and one patient lacked available response data. Of the 15 patients undergoing second IST for relapsed disease, responses to initial hATG/CyA at three months and six months were as follows: one CR, one VGPR, one PR, and 12 NR at three months; one CR, four VGPR, five PR, and five NR at six months. Two additional patients received tacrolimus for relapsed disease.

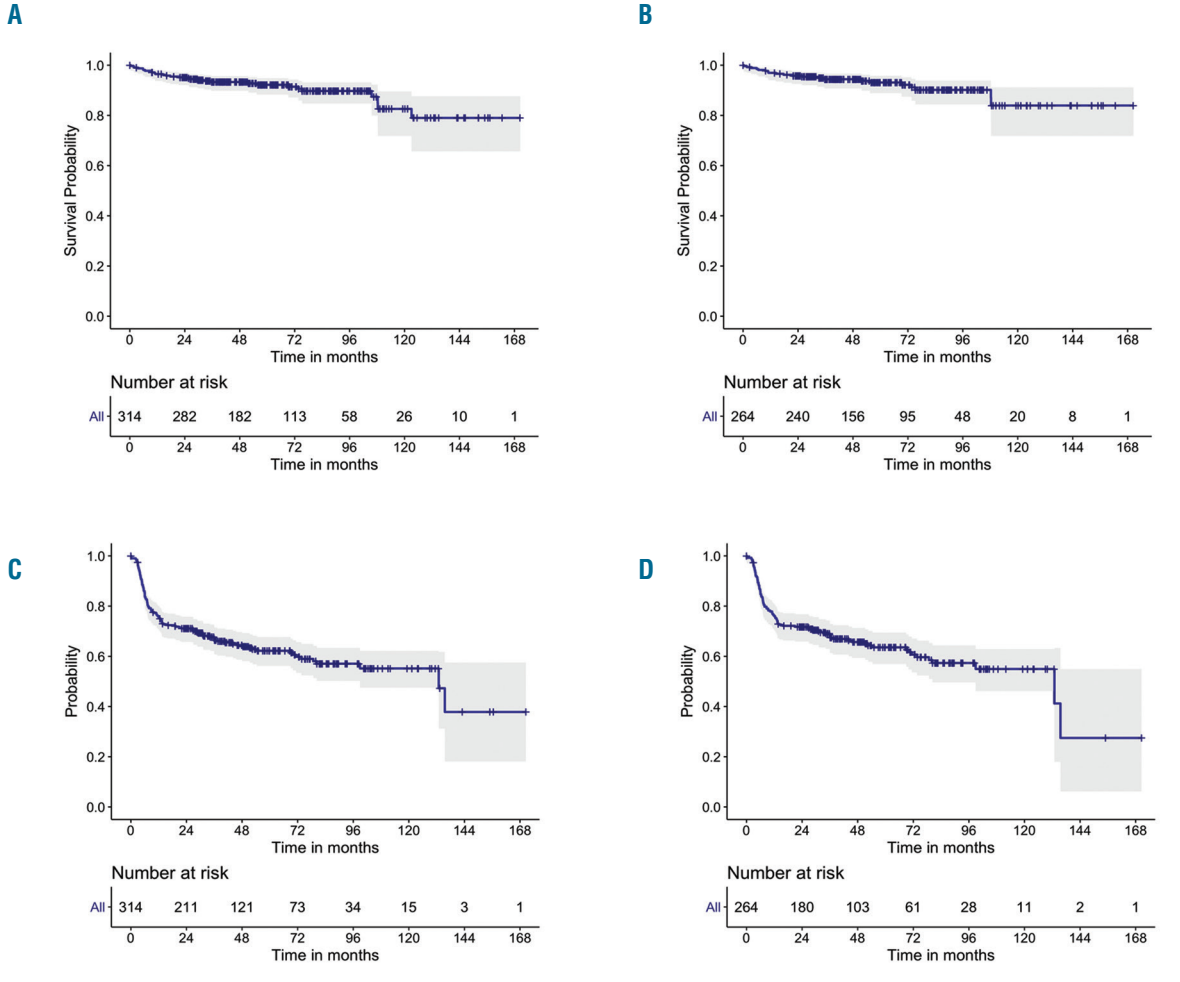

Figure 3. Immunosuppressive therapy: survival. Kaplan-Meier analysis of overall survival for (A) all subjects or (B) subjects treated with horse anti-thymocyte globulin (rATG) / cyclosporine (CyA). Kaplan-Meier analysis of event-free survival for (C) all subjects or (D) subjects treated with hATG/CyA.

Additional information is provided in the *Online Supplementary Table S1*.

For the 80 subjects who underwent second-line HSCT therapy, donors included 12 matched sibling donors, 61 matched unrelated donors (MUD), and 7 haplo-identical donors. Stem cell sources within the MUD cohort consisted of 42 from BM, five from peripheral blood, 12 from cord blood, and two without available data. Transplant preparative regimens varied widely both within and between institutions.

Overall survival for patients receiving a second treatment is shown in Figure 4A. Among all subjects (n=110) and the hATG/CyA group (n=92) who received second-line treatment, 20 (18.2%) and 15 (16.3%) died, respectively. In a Cox proportional hazards model, there was no significant effect of time from IST to second treatment on

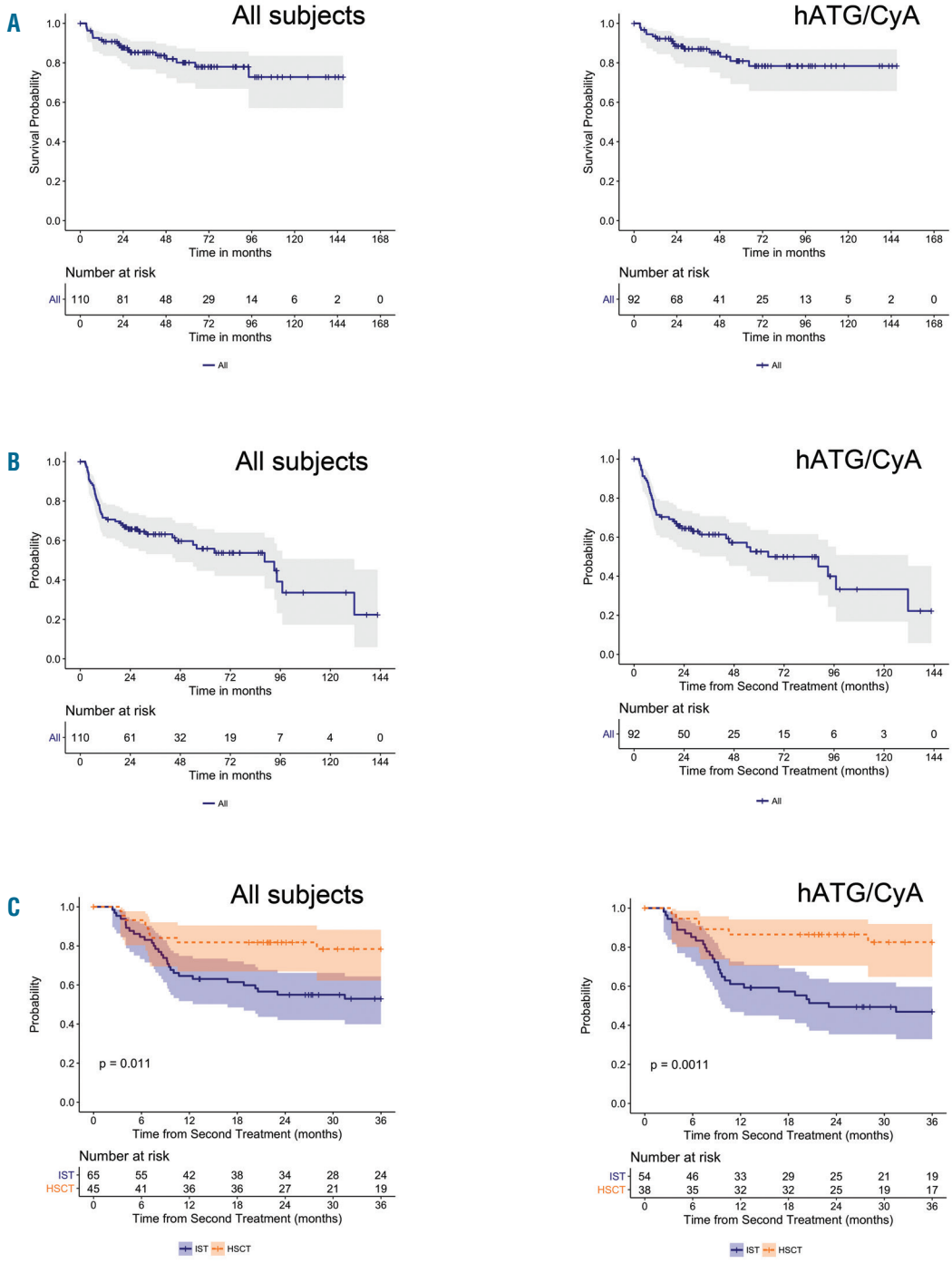

Figure 4. Outcomes after second-line therapy for relapsed/refractory disease. Kaplan-Meier analysis of (A) overall survival and (B) event-free survival for all subjects or subjects treated with horse anti-thymocyte globulin (rATG)/cyclosporine (CyA). (C) Log-rank test was used to compare event-free survival after second-line treatment with hematopoietic stem cell transplantation (HSCT) *versus* immunosuppressive therapy (IST) for all subjects or subjects treated with hATG/CyA.

OS for either the entire cohort (HR=1.0, 95%CI: 0.98,1.02; *P*=0.76) or the hATG/CyA group (HR=0.99, 95%CI: 0.98,1.03; *P*=0.69). EFS is shown in Figure 4B. Among all subjects receiving second-line treatment (n=110), 49 (44.6%) failed with a median time to failure of 88.5 months (95%CI: 45.6,131.5). Among the 92 subjects from the hATG/CyA group receiving second-line treatment, 43 (46.7%) failed with a median time to failure of 64.4 months (95%CI: 44.2,131.5)

Outcomes of second-line treatment with HSCT *versus* IST were compared for all subjects and for the hATG/CyA treatment group. Among all subjects receiving subsequent treatment (n=110), 45 received HSCT and 65 received IST. Among the hATG/CyA group receiving second-line treatment (n=92), 38 received HSCT and 54 received a second course of IST. Due to the significantly longer follow up with second-line IST as compared to bone marrow transplantation for both the entire cohort (69 *vs.* 36 months; log rank, *P*=0.05) and the hATG/CyA group (74 *vs.* 36 months; log rank, *P*=0.026), the data were censored at 36 months in the analysis to minimize the impact of differential follow up. The analysis shows that EFS is significantly longer with the second-line treatment of HSCT compared with IST (log rank, *P*≤0.011) (Figure 4C); this effect remains after adjusting for other variables (*Online Supplementary Figure S1*).

Discussion

We report a multi-institutional study of the presentation and outcomes of 314 North American pediatric SAA patients treated with IST. Although retrospective studies are limited by potential confounding factors and data availability, this multicenter study provides a contemporary analysis of the diagnostic evaluation and treatment outcomes for pediatric SAA. Since the natural history, risks, benefits, and outcomes of treatments are not identical between children versus adults with SAA, the study of rare diseases such as pediatric SAA requires collaborative effort through large consortia with the goal of improving diagnosis and treatment. As with any rare disease, national registries would greatly advance the prospective study of pediatric aplastic anemia.

Although traditionally reticulocytopenia has been used as a diagnostic criterion for SAA, in this large study, reticulocytopenia with an ARC <60x10^9/L did not correlate with a Hb <8 g/dL in a subset of patients. We found that the majority of clinicians were using clinically significant anemia and need for transfusion, rather than the ARC, to inform diagnosis and initiation of therapy. Indeed, in the setting of severe anemia without BM failure, the reticulocyte count would be expected to be markedly higher, so even an ARC within the normal range may be a sign of impaired erythropoiesis.

Red cell macrocytosis may be indicative of the time frame from evolution of reduced hematopoietic stem cell numbers and clinically significant cytopenias. In addition, red cell macrocytosis may be associated with dysplastic processes. However, no association between macrocytosis and likelihood of hematologic response or survival was observed. Lymphopenia in pediatric patients with other cytopenias may be seen with primary immunological disorders; however, no association with response was observed. Development of cytogenetically abnormal clones or overt hematologic clonal disease was rare, although post-treatment marrow surveillance was not uniformly conducted or captured due to the retrospective nature of this analysis.

A correlation between short leukocyte telomere length at diagnosis, measured by quantitative polymerase chain reaction, with increased risk of relapse, clonal evolution, and reduced survival has been reported.[21] Since current clinically available telomere length testing utilizes flow-FISH,[13] we explored whether the results of this clinical telomere length assay correlated with outcomes. We did not detect a correlation between telomere lengths less than either the 1st or 10th percentile for age with response to IST.

We observed some notable differences from reported outcomes for adult SAA patients treated with hATG/CyA. Since the magnitude of blood count recovery is especially important to support normal growth and activity in children, we examined the quality of response to IST. Of those pediatric patients who responded to hATG/CyA, the quality of response was high, with 59.8% achieving a CR and 68.2% achieving a DR. In contrast, typical rates of CR cited for adults is 10%.[12] In addition, a lower rate of clonal progression was noted for children in comparison to the 10-15% clonal progression reported in adults, although this observation is potentially limited by the retrospective nature of this study and short follow-up time.[22,23] However, EFS was low, with events continuing to accrue well past five years post IST without an apparent plateau. EFS is of particular concern for pediatric patients given their long future lifespan. Accordingly, both clinical decisions and evaluation of new therapies should be based on pediatric data whenever possible, rather than on extrapolation of data from adult cohorts. For patients with refractory or relapsed disease, EFS was superior for patients receiving second-line treatment with HSCT compared with IST even after adjusting for age, gender, time from initial IST to second treatment, and lymphocytopenia. A prospective study of 21 pediatric SAA patients receiving a second course of IST for refractory disease reported anaphylaxis in three patients and a trilineage response in only two (11%) of the remaining 18 patients, with a 5-year failure-free survival of only 9% at five years post second-line therapy.[6] Together with the excellent contemporary outcomes of MUD transplantation,[24-26] these data strongly suggest that allogeneic transplantation with a MUD is a superior second-line therapy for relapsed or refractory SAA after IST for pediatric patients. In addition, these data suggest a potential role for MUD HSCT as upfront therapy in young patients. A randomized pilot and feasibility trial comparing hATG/CyA *versus* MUD HSCT in newly diagnosed SAA patients lacking an HLA-matched family donor is currently underway.

Acknowledgments

The authors are grateful to Susan Kornetsky for her guidance and expertise. We also thank Tim Colby, Brian Sheehan, and Melissa Rose for their assistance with this project.

Funding

This project was supported by the Copeman Fund, Julian's Dinosaur Guild, and an NIH R24 DK 099808 to AS and DAW, the Rauch Family Foundation to TDC, the Campini Foundation to JNH and U54 DK106857 to GMK.

References

1. Young NS, Bacigalupo A, Marsh JC. Aplastic anemia: pathophysiology and treatment. Biol Blood Marrow Transplant. 2010;16(1 Suppl):S119-125.
2. Scheinberg P, Wu CO, Nunez O, Young NS. Long-term outcome of pediatric patients with severe aplastic anemia treated with antithymocyte globulin and cyclosporine. J Pediatr. 2008;153(6):814-819.
3. Kojima S, Horibe K, Inaba J, et al. Long-term outcome of acquired aplastic anaemia in children: comparison between immunosuppressive therapy and bone marrow transplantation. Br J Haematol. 2000; 111(1):321-328.
4. Yoshida N, Kobayashi R, Yabe H, et al. First-line treatment for severe aplastic anemia in children: bone marrow transplantation from a matched family donor versus immunosuppressive therapy. Haematologica. 2014;99(12):1784-1791.
5. Kamio T, Ito E, Ohara A, et al. Relapse of aplastic anemia in children after immunosuppressive therapy: a report from the Japan Childhood Aplastic Anemia Study Group. Haematologica. 2011;96(6):814-819.
6. Kosaka Y, Yagasaki H, Sano K, et al. Prospective multicenter trial comparing repeated immunosuppressive therapy with stem-cell transplantation from an alternative donor as second-line treatment for children with severe and very severe aplastic anemia. Blood. 2008;111(3):1054-1059.
7. Garanito MP, Carneiro JD, Odone Filho V, Scheinberg P. Outcome of children with severe acquired aplastic anemia treated with rabbit antithymocyte globulin and cyclosporine A. J Pediatr (Rio J). 2014; 90(5):523-527.
8. Dufour C, Pillon M, Passweg J, et al. Outcome of aplastic anemia in adolescence: a survey of the Severe Aplastic Anemia Working Party of the European Group for Blood and Marrow Transplantation. Haematologica. 2014;99(10):1574-1581.
9. Dufour C, Pillon M, Socie G, et al. Outcome of aplastic anaemia in children. A study by the severe aplastic anaemia and paediatric disease working parties of the European group blood and bone marrow transplant. Br J Haematol. 2015;169(4):565-573.
10. Scheinberg P, Nunez O, Weinstein B, Biancotto A, Wu CO, Young NS. Horse versus rabbit antithymocyte globulin in acquired aplastic anemia. N Engl J Med. 2011;365(5):430-438.
11. Williams DA, Bennett C, Bertuch A, et al. Diagnosis and treatment of pediatric acquired aplastic anemia (AAA): An initial survey of the North American Pediatric Aplastic Anemia Consortium (NAPAAC). Pediatr Blood Cancer. 2014;61(5):869-874.
12. Townsley DM, Scheinberg P, Winkler T, et al. Eltrombopag Added to Standard Immunosuppression for Aplastic Anemia. N Engl J Med. 2017;376(16):1540-1550.
13. Alter BP, Baerlocher GM, Savage SA, et al. Very short telomere length by flow fluorescence in situ hybridization identifies patients with dyskeratosis congenita. Blood. 2007;110(5):1439-1447.
14. Camitta BM, Storb R, Thomas ED. Aplastic anemia (first of two parts): pathogenesis, diagnosis, treatment, and prognosis. N Engl J Med. 1982;306(11):645-652.
15. Camitta BM, Storb R, Thomas ED. Aplastic anemia (second of two parts): pathogenesis, diagnosis, treatment, and prognosis. N Engl J Med. 1982;306(12):712-718.
16. Frickhofen N, Kaltwasser JP, Schrezenmeier H, et al. Treatment of aplastic anemia with antilymphocyte globulin and methylprednisolone with or without cyclosporine. The German Aplastic Anemia Study Group. N Engl J Med. 1991;324(19):1297-1304.
17. Rosenfeld SJ, Kimball J, Vining D, Young NS. Intensive immunosuppression with antithymocyte globulin and cyclosporine as treatment for severe acquired aplastic anemia. Blood. 1995;85(11):3058-3065.
18. Fuhrer M, Burdach S, Ebell W, et al. Relapse and clonal disease in children with aplastic anemia (AA) after immunosuppressive therapy (IST): the SAA 94 experience. German/Austrian Pediatric Aplastic Anemia Working Group. Klin Padiatr. 1998; 210(4):173-179.
19. Kojima S, Hibi S, Kosaka Y, et al. Immunosuppressive therapy using antithymocyte globulin, cyclosporine, and danazol with or without human granulocyte colony-stimulating factor in children with acquired aplastic anemia. Blood. 2000; 96(6):2049-2054.
20. Bacigalupo A, Bruno B, Saracco P, et al. Antilymphocyte globulin, cyclosporine, prednisolone, and granulocyte colony-stimulating factor for severe aplastic anemia: an update of the GITMO/EBMT study on 100 patients. European Group for Blood and Marrow Transplantation (EBMT) Working Party on Severe Aplastic Anemia and the Gruppo Italiano Trapianti di Midolio Osseo (GITMO). Blood. 2000;95(6):1931-1934.
21. Scheinberg P, Cooper JN, Sloand EM, Wu CO, Calado RT, Young NS. Association of telomere length of peripheral blood leukocytes with hematopoietic relapse, malignant transformation, and survival in severe aplastic anemia. JAMA. 2010;304(12):1358-1364.
22. Socie G, Rosenfeld S, Frickhofen N, Gluckman E, Tichelli A. Late clonal diseases of treated aplastic anemia. Semin Hematol. 2000;37(1):91-101.
23. Rosenfeld S, Follmann D, Nunez O, Young NS. Antithymocyte globulin and cyclosporine for severe aplastic anemia: association between hematologic response and long-term outcome. JAMA. 2003;289 (9):1130-1135.
24. Samarasinghe S, Steward C, Hiwarkar P, et al. Excellent outcome of matched unrelated donor transplantation in paediatric aplastic anaemia following failure with immunosuppressive therapy: a United Kingdom multicentre retrospective experience. Br J Haematol. 2012;157(3):339-346.
25. Anderlini P, Wu J, Gersten I, et al. Cyclophosphamide conditioning in patients with severe aplastic anaemia given unrelated marrow transplantation: a phase 1-2 dose de-escalation study. Lancet Haematol. 2015;2(9):e367-375.
26. Bacigalupo A, Giammarco S, Sica S. Bone marrow transplantation versus immunosuppressive therapy in patients with acquired severe aplastic anemia. Int J Hematol. 2016;104(2):168-174.

Ferrata Storti Foundation

Haematologica 2019
Volume 104(10):1984-1994

Deletion of a flippase subunit *Tmem30a* in hematopoietic cells impairs mouse fetal liver erythropoiesis

Fan Yang,[1*] Yumin Huang,[2*] Xianda Chen,[1*] Lu Liu,[1] Dandan Liao,[1] Huan Zhang,[3,4] Gang Huang,[5] Wenjing Liu,[6] Xianjun Zhu,[6,7] Wengong Wang,[8] Cheryl A. Lobo,[9] Karina Yazdanbakhsh,[10] Xiuli An[2,3,4] and Zhenyu Ju[1,11]

[1]Key Laboratory of Regenerative Medicine of Ministry of Education, Guangzhou Regenerative Medicine and Health Guangdong Laboratory, Institute of Aging and Regenerative Medicine, Jinan University, Guangzhou, China; [2]Department of Hematology, The First Affiliated Hospital of Zhengzhou University, Zhengzhou, China; [3]Laboratory of Membrane Biology, New York Blood Center, New York, NY, USA; [4]School of Life Science, Zhengzhou University, Zhengzhou, China; [5]Division of Pathology and Experimental Hematology and Cancer Biology, Cincinnati Children's Hospital Medical Center, Cincinnati, OH, USA; [6]The Sichuan Provincial Key Laboratory for Human Disease Gene Study, Institute of Laboratory Medicine, Sichuan Provincial People's Hospital, University of Electronic Science and Technology of China and Chengdu, Sichuan, China; [7]Chengdu Institute of Biology, Sichuan Translational Medicine Research Hospital, Chinese Academy of Sciences, Chengdu, China; [8]Department of Biochemistry and Molecular Biology, Beijing Key Laboratory of Protein Posttranslational Modifications and Cell Function, School of Basic Medical Sciences, Peking University Health Science Center, Beijing, China; [9]Laboratory of Blood-Borne Parasites, New York Blood Center, New York, NY, USA; [10]Laboratory of Complement Biology, New York Blood Center, New York, NY, USA and [11]Institute of Aging Research, School of Medicine, Hangzhou Normal University, Hangzhou, China

FY, YH and XC contributed equally to this work.

ABSTRACT

Transmembrane protein 30A (*Tmem30a*) is the β-subunit of P4-ATPases which function as flippase that transports aminophospholipids such as phosphatidylserine from the outer to the inner leaflets of the plasma membrane to maintain asymmetric distribution of phospholipids. It has been documented that deficiency of *Tmem30a* led to exposure of phosphatidylserine. However, the role of *Tmem30a in vivo* remains largely unknown. Here we found that Vav-Cre-driven conditional deletion of *Tmem30a* in hematopoietic cells led to embryonic lethality due to severe anemia by embryonic day 16.5. The numbers of erythroid colonies and erythroid cells were decreased in the *Tmem30a* deficient fetal liver. This was accompanied by increased apoptosis of erythroid cells. Confocal microscopy analysis revealed an increase of localization of erythropoietin receptor to areas of membrane raft microdomains in response to erythropoietin stimulation in Ter119$^-$ erythroid progenitors, which was impaired in *Tmem30a* deficient cells. Moreover, erythropoietin receptor (EPOR)-mediated activation of the STAT5 pathway was significantly reduced in *Tmem30a* deficient fetal liver cells. Consistently, knockdown of *TMEM30A* in human CD34$^+$ cells also impaired erythropoiesis. Our findings demonstrate that *Tmem30a* plays a critical role in erythropoiesis by regulating the EPOR signaling pathway through the formation of membrane rafts in erythroid cells.

Correspondence:

ZHENYU JU
zhenyuju@163.com

XIULI AN
xan@nybc.org

Received: August 7, 2018.

Accepted: February 27, 2019.

Pre-published: February 28, 2019.

doi:10.3324/haematol.2018.203992

Check the online version for the most updated information on this article, online supplements, and information on authorship & disclosures: www.haematologica.org/content/104/10/1984

Introduction

Hematopoietic stem cells (HSC) are long lived and able to differentiate into several lineages which are required throughout life.[1] There are two distinct waves of hematopoietic cells during mammalian embryogenesis. The first wave progenitors arise in the circulation of the yolk sac (YS) at embryonic day 7.25 (E7.25), and produce primitive erythrocytes which are essential for the survival of the embryo. The second wave HSC arise at embryonic day 10.5 in the dorsal aorta and differentiate

into mature blood cells in the fetal liver.[2] During embryogenesis, primitive erythroid cells (EryP) first arise from mesodermal progenitors and are detected within 'blood islands' at around E7.5. The maturation of erythroid precursors occurs in the blood circulatory system, where the nucleuses are condensed and embryonic hemoglobin is accumulated.[3] Definitive erythroid cells (EryD) rapidly outnumber the EryP in the growing fetal liver,[4,5] which are identified as β-globin switching and smaller enucleated erythroid cells.[6] The fetal liver is the key organ for definitive erythropoiesis during mid gestation. Definitive erythroid cells can be distinguished into five different sub-populations from R1 to R5 by double staining with the surface markers CD71 and Ter119.[7] Erythropoiesis comprises distinct differentiation stages including burst-forming unit-erythroid (BFU-E), colony-forming unit-erythroid (CFU-E), proerythroblast, basophilic erythroblast, polychromatic erythroblast, orthochromatic erythroblast, reticulocyte and erythrocyte. From the CFU-E stage onwards, the cell starts to express erythropoietin (EPO) receptor (EPOR). CFU-E and proerythroblat require EPO for survival.[8]

Erythroid differentiation occurs at the erythroblastic islands and is regulated by various cytokines and chemokines. EPO and stem cell factor (SCF) play essential roles in erythroid progenitor proliferation and differentiation. EPO is mainly synthesized in liver during embryo genesis and produced in the kidney in adult mammals. EPO/EPOR-mediated signaling transduction is crucial for primitive and definitive erythropoiesis both in the fetal liver (FL) and in the bone marrow.[9] EPO has two receptors: one is a homodimer of two EPO receptors (EPOR), another is a heterodimer consisting of EPOR and CD131.[10] The homodimeric EPO receptor exists in an unliganded state with the pre-bound tyrosine kinase JAK2.[11] Upon binding EPO, EPOR undergoes a conformational change that actives JAK2 which in turn phosphorylates tyrosine residues in the cytoplasmic tail of the EPOR.[12] This binding results in activation of STAT5, which leads to the activation of BCL-XL by direct STAT5 binding to the BCL-X promoter.[13] BCL-XL is a potent inhibitor of programmed cell death and inhibits activation of caspases in cells through direct interaction between caspases and BCL-XL.[14,15] The activation of the JAK2-STAT5 pathway through EPO/EPOR signaling is critical for sustaining the viability of erythroid cells in the fetal liver.[16]

Lipid rafts are small microdomains (10-200 nm) enriched in cholesterol and sphingolipids that can form larger platforms by protein-protein and protein-lipid interactions. The inner leaflet phosphatidylserine is essential for the coupling of actin with lipid-anchored proteins. The actin cytoskeleton clustering determines and immobilizes long saturated acyl chains phospholipids in the inner leaflet.[17] This immobilization engages in glycosylphosphatidylinositol (GPI)-anchored proteins in the outer monolayer interacted by cholesterol, which form the local raft domains. The most important role of lipid rafts is to separate and regulate specific membrane components with other components, thereby increasing the concentration of signaling molecules.

In eukaryotic cells, phospholipids are distributed asymmetrically between the inner and the outer layers of the plasma membrane.[18] Phosphatidylserine (PS) and phosphatidylethanolamine (PE) are mainly located in the inner monolayer while phosphatidylcholine (PC) is essentially present at the outer monolayer.[19,20] Lipids distributions are preserved by many of phospholipid transporters which can be separated into three groups including scramblases, flippases and floppases.[21] One of the most important transporters are the members of the Type-IV P-type ATPases (P4-ATPases) family which possess flippase activity that transports lipids from the outer to the inner leaflet to maintain phospholipid asymmetry. *Tmem30a* (also named CDC50A), the β-subunit of P4-ATPases, is essential for the formation of functional transporter complexes that act as flippase.[22] Maintenance of cell membrane asymmetry by flippase is critical as the loss of this asymmetry usually causes pathological phenotypes.[23]

To investigate the function of *Tmem30a* in embryonic hematopoiesis, we generated hematopoietic-specific *Tmem30a* deficient mice with conditional *Tmem30a* alleles and Cre recombinase expression controlled by the VAV promoter.[24] *Tmem30a* deficient mice (cKO) died *in utero* by E16.5 with severe anemia. Interestingly, *Tmem30a* is not essential for the maintenance of HSC homeostasis, but is essential for the definitive erythropoiesis. Moreover, *Tmem30a* deficiency impaired flippase activity, lipid rafts formation, and activation of EPOR/JAK2/STAT5/BCL-XL pathway. Our findings demonstrate the critical role of *Tmem30a* in erythropoiesis and uncover previously unknown mechanisms by which EPOR signal transduction pathway is initiated.

Methods

Mice

All mouse protocols were approved by the Institutional Animal Care and Use Committee of Jinan University, China. Tmem30a$^{WT/flox}$ mice were kindly provided by Prof. Xianjun Zhu and were back-crossed onto a C57/BL6 background. Exon 3 of the *Tmem30a* gene is flanked by loxP sites. The Vav-Cre line we used was B6.Cg-*Commd10*^{Tg}*(Vav*$^{1\text{-}icre}$*)*^{A2Kio} to generate hematopoietic deletion, as described previously.[25]

Flow cytometry

Cells were stained with APC-conjugated rat anti–mouse TER-119 (clone: Ter119, Biolegend) and PE conjugated rat anti-mouse CD71 (clone: RI7217, Biolegend) on ice for 30 minutes (min) in the dark. The cells were washed twice, followed by staining with fixable viability DAPI (0.25 μg/10^6 cells) and analyzed within 1 hour (h) of staining. For apoptosis, cells were additionally stained for 15 min in the dark with 10 μL of Annexin V-FITC in 100 μL 1xbinding buffer.[26] Cells were washed and cell pellets were re-suspended in 500 μL 1xbinding buffer containing 5 μL of 7AAD and immediately analyzed by a BD FACS Fortessa machine. Apoptosis was also assessed using TUNEL assay by flow cytometry using APO-BrdU TUNEL assay kit (Invitrogen, A23210).

Western blot analysis

Fetal liver cell samples were separated and then transferred to the polyvinylidene fluoride membrane. Primary antibodies to STAT5 (#9363, CST), Phospho-STAT5 (Tyr694) (#9351, CST), BCL-XL (54H6) (#2764, CST), Flotillin-2 (B-6) (SC-28320, Santa Cruz), TMEM30A (AV47410, Sigma-Aldrich), EPO-R (SAB4500780, Sigma-Aldrich) and β-Actin (A5316, Sigma-Aldrich) were used. The membrane was incubated with horseradish peroxidase enzyme conjugated secondary antibody for 1 h at RT. Clarity western ECL substrate solutions were dropped onto the membrane.

Erythroid differentiation *in vitro*

E14.5 fetal liver cells were labeled with APC-conjugated anti-mouse Ter119 antibody for 30 min followed by staining with anti-APC microbeads. Ter119- cells were purified and cultured in erythroid-differentiation medium containing Iscove modified Dulbecco medium, 15% FBS, 1% detoxified bovine serum albumin, 200 μg/mL recombinant human transferrin, 10 μg/mL recombinant human insulin, 10-4 M β-mercaptoethanol, and 2.5 U/mL recombinant human EPO. After culturing the cells for 24 h, the medium was replaced with IMDM, 20% FBS and 10^{-4} M β-mercaptoethanol for another 24 h. Q-VD-OPh hydrate (#SML0063, Sigma) was added to the erythroid-differentiation medium for every 24 h.

Knockdown of *TMEM30A* by lentivirus in human CD34$^+$ cells

Human CD34-positive ($^+$) cells were purified and harvested from cord blood. The CD34$^+$ cells were differentiated into erythroid cells and the differentiation was assessed by flow cytometry using GPA, Band 3 and α4 integrin as surface markers. pLKO1 vectors which express shRNA against the targeted gene of *TMEM30A* were purchased from Sigma-Aldrich. The sequences were as follows: sh-*TMEM30A*-1: GACAACCTGGAAGAACGATTT. sh-*TMEM30A*-2: GAGATTCTAGTGCTTTGCTTA. Lentivirus was prepared and transfected into CD34$^+$ cells on the culture day 2, as described previously. Knockdown efficiency was checked by real-time polymerase chain reaction (RT-PCR). The primers for TMEM30A were: forward primer-5'-GCGATGAACTATAACGCGAAGG-3'; reverse primer-5'-GCCAATGCCGATGGGAATGA-3'.

Statistical analysis

FACS analysis was performed using FlowJo software (BD, version 10). Statistical analysis was performed using GraphPad prism software (version 7). Band signal intensities were analyzed with ImageJ. The data were shown as the Mean±Standard Error of Mean (SEM). Differences among two groups were calculated by Student unpaired *t*-test. $P<0.05$ was considered statistically significant.

Details of the other methods used in this study are available in the *Online Supplementary Materials.*

Results

Tmem30a deficient mice are embryonic lethal with anemia at mid gestation

To investigate the function of *Tmem30a* in hematopoiesis, we crossed *Tmem30a*$^{flox/flox}$ mice with B6.Cg-Commd10Tg(Vav1-icre)A2Kio mice to generate hematopoietic-specific *Tmem30a*-deficient mice (*Online Supplementary Figure S1A and B*). The *Tmem30a*$^{flox/flox}$, VavCreTg/$^+$ (*Tmem30a* cKO) mice were not viable. The surviving *Tmem30a* cKO embryos at embryonic day 14.5 (E14.5) are pale (Figure 1A), suggesting a defect in fetal hematopoiesis. Genotyping of the progeny embryos showed that the living embryos roughly followed the expected Mendelian ratio with 25% *Tmem30a* cKO embryos up to E12.5, but that ratio dropped to 0% by E16.5 (Figure 1B). The *Tmem30a* cKO fetal liver was noticeably smaller (Figure 1D), and the number of fetal liver cells was significantly reduced in the cKO mice compared to that of control mice at E14.5 (Figure 1C). Hematoxylin & Eosin staining of *Tmem30a* fetal liver sections showed a severe atrophic phenotype (Figure 1E). Red blood cell (RBC) count, hematocrits and hemoglobin levels were significantly decreased in the peripheral blood of the E14.5 *Tmem30a* cKO embryos compared with controls (Figure 1F-H). Wright-Giemsa staining of peripheral blood smears showed a large fraction of nucleated erythrocytes (Figure 1I) in *Tmem30a* cKO blood compared to control. To explore the reasons of the impaired hematopoiesis in *Tmem30a*-deficient embryos, we first analyzed the maintenance of HSC in fetal livers by flow cytometry (*Online Supplementary Figure S1C*).[27] The total number of HSC (Lin$^-$Mac$^-$1lowSac-1$^+$ CD48$^-$CD150$^+$ cells) in cKO embryos was comparable to controls at E14.5 (*Online Supplementary Figure S1D*), indicating the impaired fetal hematopoiesis was not due to a defect in the FL HSC in cKO embryos, although *Tmem30a* is expressed in FL HSC as well as in T cells, B cells and erythroid cells (*Online Supplementary Figure S1E*). Interestingly, colony forming assay showed that the numbers of BFU-E and CFU-E colonies were drastically reduced in cKO embryos (Figure 1J and K). In contrast, no differences were seen in the colonies of CFU-G, CFU-M and CFU-GM between cKO and control (*data not shown*). These findings suggest that loss of *Tmem30a* in mice resulted in a severe mid gestation anemia, likely due to impaired fetal liver erythropoiesis.

Tmem30a is necessary for definitive erythropoiesis in the fetal liver

Next, we investigated fetal liver erythroid progenitor cells in the fetal liver. The number of EryP in cKO fetal livers was comparable with control (*Online Supplementary Figure S2A and B*). We also analyzed erythro-myeloid progenitors at embryo day 9.5 in the yolk sac by flow cytometry (*Online Supplementary Figure S2C*). The absolute number of progenitors in cKO was comparable with the control group (*Online Supplementary Figure S2D*). Finally, we analyzed definitive erythropoiesis using CD71 and Ter119 as surface markers (Figure 2A). The results showed that R3 erythroblast population (CD71^{hi}/Ter119^{hi}) was predominantly affected in the fetal livers of cKO embryos, suggesting a severe blockage in terminal erythroid differentiation from Ter119^{low} to Ter119^{hi} cells (Figure 2B). To further characterize terminal erythroid differentiation, we used FSC to separate Ter119^{hi} cells into three populations: S1 (large), S2 (medium), and S3 (small) (Figure 2C). The number of erythroblasts in S1 and S2 populations (basophilic to orthochromatic stages) and S3 population (reticulocytes) was decreased, suggesting a further defect at very late stage of erythroid maturation (Figure 2D). Next, we analyzed erythroblast enucleation in S1-S3 populations using live-cell nuclear staining with Syto-16 (Figure 2E). Most enucleation events occurred in the S3 population, and *Tmem30a* cKO fetal livers showed a significant reduction of enucleating efficiency in this population (Figure 2F).

Tmem30a deficiency leads to apoptosis of fetal liver erythroid cells

To explore the underlying mechanisms, we examined proliferation and apoptosis of the fetal liver cells. BrdU incorporation assays showed that the cell cycle profiles were comparable between *Tmem30a* cKO and control mice (*Online Supplementary Figure S3A and B*). We then investigated apoptosis, which is usually assessed by Annexin V binding to exposed PS. *Tmem30a* deficiency lead to increased Annexin V levels (Figure 3A and B). Since

Tmem30a deletion leads to PS exposure because of impaired PS translocation, it is difficult to determine whether the PS exposure is due to apoptotic or impaired PS translocation. Therefore, we employed the TdT-mediated dUTP nick end labeling (TUNEL) assay for determining the intrinsic cellular apoptosis, thereby analyzing the apoptosis-related DNA fragmentation. TUNEL staining showed that the cKO fetal liver cells displayed significantly higher TUNEL positive cells compared with controls (Figure 3C and D). Taken together, these data indicate that the defect of erythropoiesis in the Tmem30a deficient fetal liver is at least partly due to increased apoptosis.

Tmem30a deficiency impairs phosphatidylserine flippase activity in erythroid cells

Tmem30a is the β-subunit of the P4-ATPase, which functions as a flippase to maintain phospholipid asymmetry. Previous study showed that loss of *Tmem30a* resulted in impaired PS translocation.[22] Consistent with the previous study, our data showed that *Tmem30a* deficiency led to increased PS exposure in erythroid cells, as indicated by increased levels of Annexin V positive cells (Figure 4A and B). To examine if the increased PS exposure is at least partly due to impaired flippase activity, we analyzed the aminophospholipid flippase activity. NBD-PS fluorescence

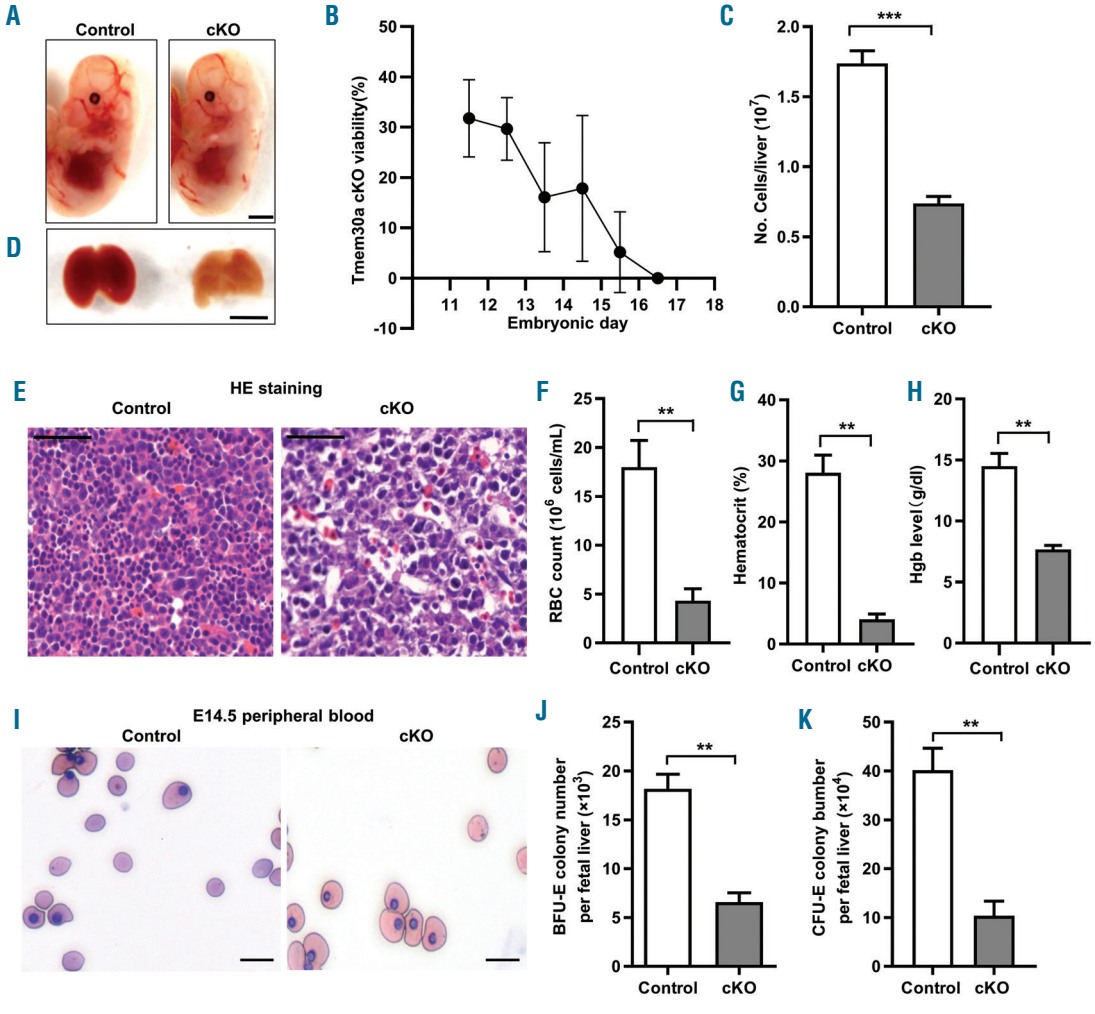

Figure 1. *Tmem30a*-deficient mice (cKO) are embryonic lethal with anemia. (A) Viability of *Tmem30a* embryos was determined. Scale bar represents 2 mm. (B) Timed matings of *Tmem30a*$^{WT/flox}$; VavCre$^{Tg/+}$ and Tmem30a$^{flox/flox}$; VavCre$^{-/-}$ were performed and embryos were harvested at stages E11.5 up to E16.5. The percentages reflect the numbers of living Tmem30a cKO embryos with respect to all embryos harvested in litters at each gestational stage. At least six pregnant mice have been checked at each time point and more than 35 embryos have been examined. (C) Gross appearance of E14.5 fetal livers. The cKO fetal livers were noticeably smaller than fetal livers of controls. Scale bar represents 2 mm. (D) The number of total fetal liver cells was counted in control and cKO embryos at E14.5. Data are presented as Mean ±Standard Error of Mean (SEM) for at least eight embryos per genotype. (E) Hematoxylin & Eosin staining of paraffin sections from *Tmem30a*$^{flox/flox}$; VavCre$^{-/-}$ and *Tmem30a*$^{flox/flox}$; VavCre$^{Tg/+}$ E14.5 fetal livers fixed in 4% formaldehyde solution. Scale bars represent 50 μm. (F) The red blood cell number was decreased in *Tmem30a* cKO peripheral blood. (G) Tmem30a cKO embryos exhibited reduced hematocrit compared with control mice at mid-gestation E14.5. (H) Hemoglobin levels were decreased in the peripheral blood in the cKO embryos. (I) Peripheral blood in Tmem30a cKO embryos reveals a large number of nucleated erythrocytes when sections underwent Wright-Giemsa staining. Scale bars represent 20 μm. (J) The BFU-E colony numbers were decreased in E14.5 cKO embryos compared with cKO. (K) CFU-E colony numbers per fetal liver of cKO were decreased at E14.5 *in vitro*. The graphs are representatives of three biological repeats. Data are indicated as Mean±SEM of three samples per each genotype. ***P*<0.01; ****P*<0.001.

increased rapidly in wild-type cells, but this increase was significantly blunted in cKO cells (Figure 4C and D). Interestingly, the flippase activity was mainly compromised in the R1 to R3 cell populations (Figure 4E and F), indicating correlation between flippase activity and cell development. We also analyzed the percentage of NBD-PS fluorescence positive cells in the S1 to S3 cell population and found that the flippase activity was mainly compromised in S1 and S2 cell populations (*Online Supplementary Figure S4A and B*). These data demonstrate that *Tmem30a* is crucial for phospholipid flipping in erythroid cells.

Tmem30a deficiency compromises lipid raft clustering upon erythropoietin treatment

The above data demonstrate that *Tmem30a* is required for phospholipid flipping. PS is essential for the coupling between actin and lipid anchored proteins, and thereby the formation of functional local raft-like domain at the plasma membrane. One of the most important roles of lipid rafts is to separate and regulate specific membrane components with other components and thereby increasing the concentration of signaling molecules. To examine whether depletion of *Tmem30* affects lipid raft formation

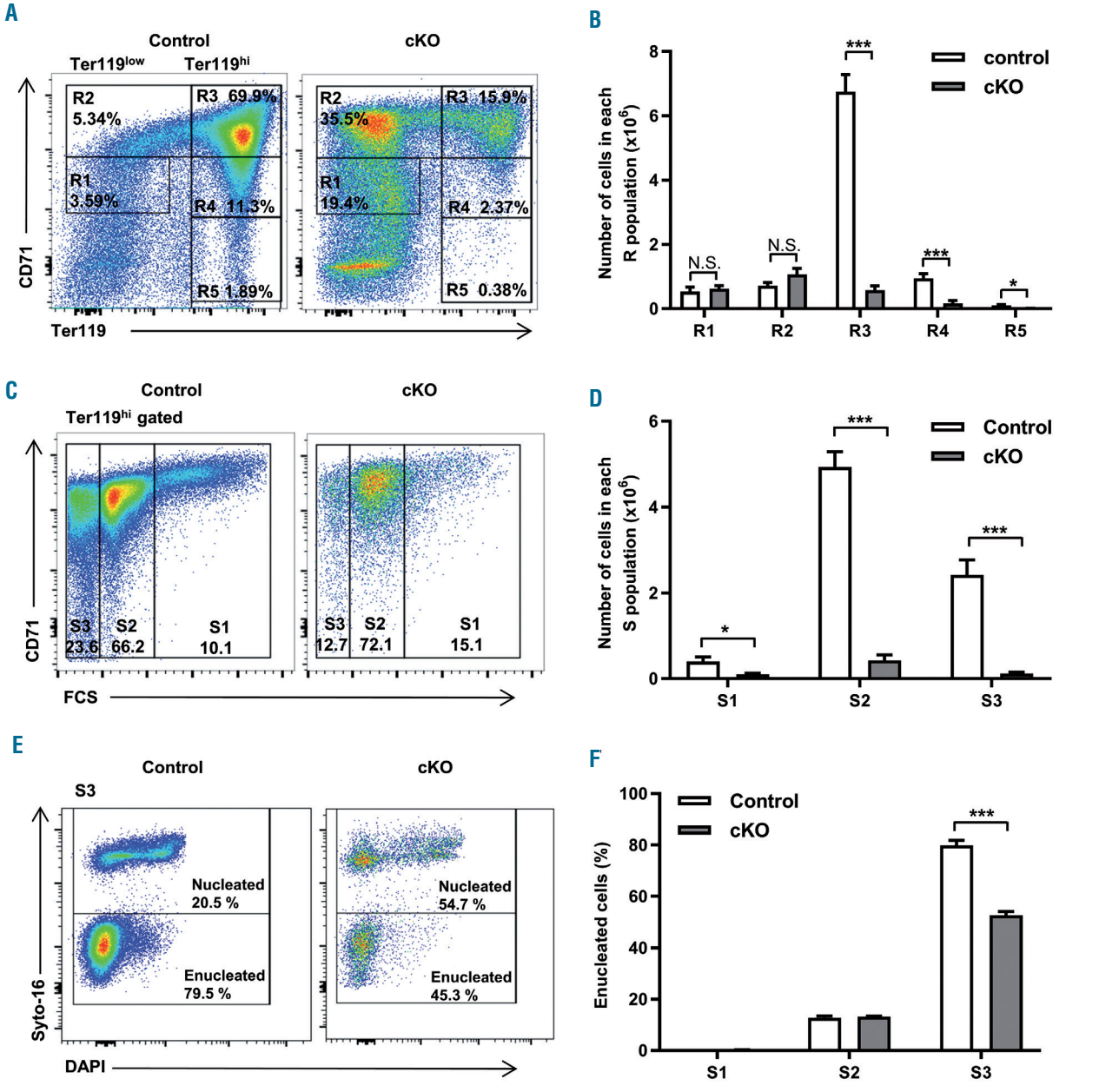

Figure 2. Tmem30a-deficient mice (cKO) embryos are defective in definitive erythropoiesis. (A) Representative flow cytometric profiles of control and *Tmem30a* cKO fetal liver single cells stained with CD71 and Ter119. Gates from R1 to R5 were set as indicated. (B) Absolute number of cells in each R population was calculated in the fetal liver from each embryo. Data are represented as mean±Standard Error of Mean (SEM) of the cell count of six fetal livers for each embryonic data set. (C) Representative CD71/FSC profiles of Ter119hi cells sorted into three populations according to cell size. The percentage of cells in each S population with respect to total Ter119hi cells are indicated for one representative fetal liver. (D) Comparison of the number of S1, S2, and S3 populations. (E) Representative flow cytometry of enucleated cells in the Ter119 hi population of fetal livers, using Syto-16 for nuclei and DAPI for cell viability. (F) Percentages of enucleated cells in the Ter119 hi populations. Data are presented as Mean±SEM of the cell count of six fetal livers for each embryonic data set. *P<0.05; **P<0.01; ***P<0.001.

and EPOR signaling, we analyzed the lipid raft distribution by using cholera toxin subunit B (CTxB) to label endogenous GM1 ganglioside, a component of lipid rafts. Co-staining of GM1 and EPOR on Ter119^{low} erythroid cells showed that EPO treatment stimulated the EPOR clustering and co-localized with the lipid rafts. Interestingly, *Tmem30a* deletion inhibited lipid raft clustering and EPOR co-localization with the lipid rafts (Figure 5A and B). The specificity of the EPOR antibody was demonstrated by immunofluorescence analysis omitting the primary anti-EPOR antibody as negative control (*Online Supplementary Figure S5A*). To further determine whether TMEM30A deficiency impedes the recruitment of EPOR to lipid raft, lipid rafts were separated from TER119 negative fetal liver cells upon EPO treatment. Western blot showed that the EPOR protein was presented in the extracted lipid rafts, but the level of EPOR was decreased in cKO cells (*Online Supplementary Figure S5B*). Taken together, these data suggest that the impaired lipid raft clustering upon EPO stimulation in *Tmem30a*-deficient fetal liver erythroid cells may compromise the EPO/EPOR signaling, which is essential for fetal liver erythropoiesis.

Tmem30a deficiency compromises STAT5 activation and down-regulates pro-survival protein BCL-X_L

It has been well documented that EPO/EPOR signaling activates the JAK2-STAT5 pathway to sustain the viability of erythroid cells in the fetal liver.[13] The above findings strongly suggest that the observed phenotypic changes of Tmem30a knockdown erythroid cells may be due to impaired EPO/EPOR signal transduction. To test this, we investigated the key components of the EPO/EPOR-JAK2-STAT5 signaling pathway. FACS analysis using EPOR antibody staining on living TER119$^-$ erythroid cells showed that the levels of EPOR expression on the cell surface were not reduced in cKO mice compared to control mice (*Online Supplementary Figure S5C*). Intriguingly, after EPO stimulation in culture, the activation of the JAK2-STAT5 signaling pathway was significantly impaired in *Tmem30a* deficient fetal liver cells, as demonstrated by the lack of phosphorylation of STAT5 in cKO cells upon EPO treatment (Figure 6A). In addition, the downstream transcriptional target genes of STAT5 signaling[28] such as Pim1, Socs3 and BCL-XL were significantly decreased after EPO exposure in *Tmem30a* deficient fetal livers compared to the controls (Figure 6B). Among these genes, BCL-X_L is essential for the survival of erythroid cells. Therefore, we further analyzed the protein levels of BCL-X_L by western blotting. The pro-survival protein BCL-X_L was dramatically decreased in cKO fetal liver although exposure to EPO did not increase BCL-X_L expression (Figure 6C). Perhaps 30-min exposure to EPO was not enough to increase the Bcl-X_L protein level. BCL-

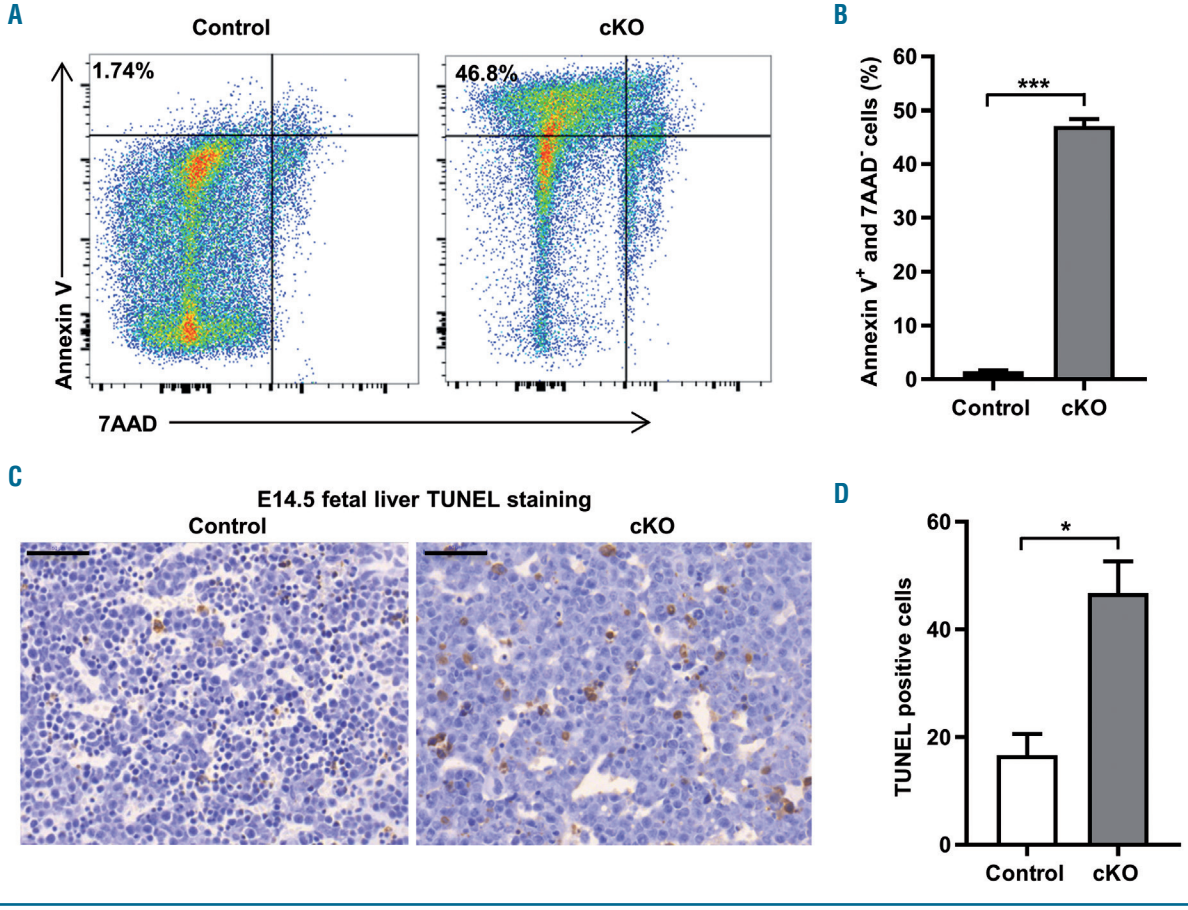

Figure 3. *Tmem30a*-deficient mice (cKO) fetal liver erythroid cells display a higher frequency of apoptosis. (A and B) Flow cytometric analysis of *Tmem30a* cKO fetal livers revealed increased percentages of Annexin V positive cells compared with wild-type littermate controls. (C) TUNEL staining of paraffin sections from fetal livers fixed in 4% formaldehyde solution. Scale bars represent 50 μm. (D) The number of TUNEL positive cells per $1.3*10^5$ square micrometers were calculated. All values are presented as Mean±Standard Error of Mean of three fetal livers per each embryonic data. *P<0.05; *** P<0.001.

X_L functions as a substrate to directly inhibit caspases before cleavage;[14] therefore, we measured caspase 3/7 activity using luminescent assays. Caspase 3/7 activity was increased in cKO fetal liver cells (Figure 6D). Next, we used Q-VD-OPh hydrate, a pan-caspase inhibitor to treat the Ter119^{low} erythroid cells in order to rescue the impaired definitive erythropoiesis in *Tmem30a* cKO erythroid cells (Figure 6E).[29] Interestingly, the presence of 50 μM Q-VD-OPh partially rescued erythroid cell maturation of *Tmem30a*-deficient erythroid cells (Figure 6F).

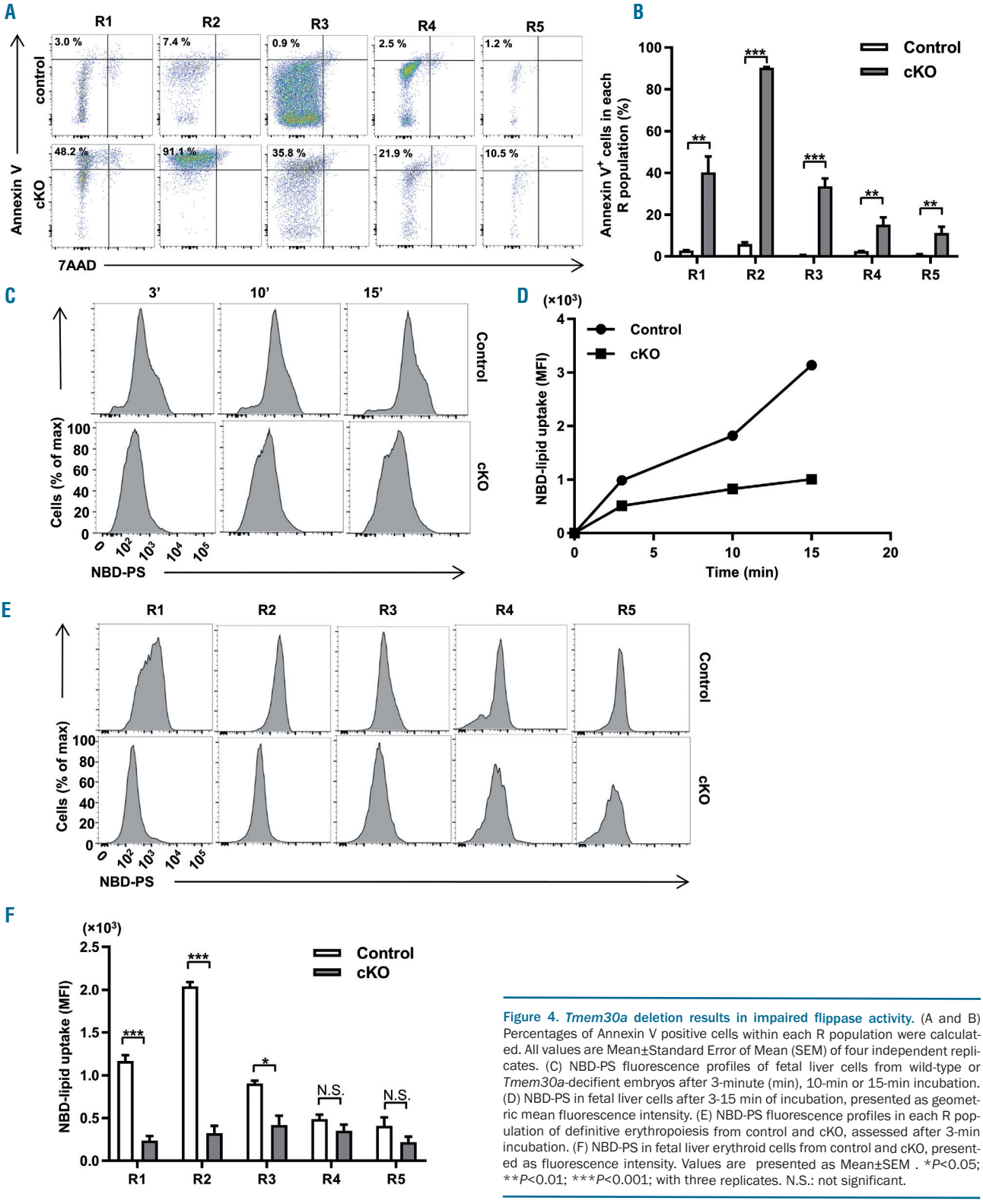

Figure 4. *Tmem30a* deletion results in impaired flippase activity. (A and B) Percentages of Annexin V positive cells within each R population were calculated. All values are Mean±Standard Error of Mean (SEM) of four independent replicates. (C) NBD-PS fluorescence profiles of fetal liver cells from wild-type or *Tmem30a*-decifient embryos after 3-minute (min), 10-min or 15-min incubation. (D) NBD-PS in fetal liver cells after 3-15 min of incubation, presented as geometric mean fluorescence intensity. (E) NBD-PS fluorescence profiles in each R population of definitive erythropoiesis from control and cKO, assessed after 3-min incubation. (F) NBD-PS in fetal liver erythroid cells from control and cKO, presented as fluorescence intensity. Values are presented as Mean±SEM . *P<0.05; **P<0.01; ***P<0.001; with three replicates. N.S.: not significant.

TMEM30A is required for human erythroid differentiation

To examine whether *TMEM30A* also plays a role in human erythropoiesis, we used shRNA-mediated knockdown approach in human cord blood CD34$^+$ cells.[30-32] *Online Supplementary Figure S6A* shows efficient knockdown of *TMEM30A*. As demonstrated by the decreased expression of GPA (*Online Supplementary Figure S6B*), delayed upregulation expression of band 3/downregulation of α4 integrin (*Online Supplementary Figure S6C*), *TMEM30A* knockdown impaired erythroid differentiation. Knockdown of *TMEM30A* also led to reduced cell growth (*Online Supplementary Figure S6D*). Moreover, similar to the murine data, *TMEM30A* knockdown also induced a significantly increase in the frequency of Annexin V positive cells (*Online Supplementary Figure S6E and F*). We further detected apoptosis of control and *TMEM30A* knockdown human erythroid cells by TUNEL assay. *TMEM30A* knockdown led to increased apoptosis (*Online Supplementary Figure S6G and H*). Finally, we examined the effect of *TMEM30A* on EPOR-mediated signal transduction in human erythroid cells. *TMEM30A* knockdown resulted in attenuated phosphorylation of EPOR downstream target STAT5 (*Online Supplementary Figure S6I and J*). Thus, *TMEM30A* plays a conserved function in both human and murine erythropoiesis.

Discussion

Studies over the past decade have clearly documented that *Tmem30a* is required for the flippase activity of P4-ATPases.[33] However, the function of *Tmem30a in vivo* remains largely unexplored. In the present study, we found that, unexpectedly, selective deletion of *Tmem30a* in hematopoietic cells severely impaired fetal liver erythropoiesis which contributes to the embryonic lethality of the mice. Our findings have, therefore, uncovered a novel role for *Tmem30a* in erythropoiesis.

In exploring the underlying mechanisms for the impaired erythropoiesis, we found that, while *Tmem30a* deletion did not affect cell cycle, it led to increased apoptosis of erythroid cells. Interestingly, the increased apoptosis is due to significantly impaired activation of JAK2-STAT5 signal transduction pathway, the essential pathway for survival of erythroid cells. Further examination revealed that *Tmem30a* deletion impaired lipid rafts formation accompanied with impaired EPOR clustering. Our findings provide new insights into the mechanisms by which EPO/EPOR signal transduction pathway is regulated.

The type 4 subfamily of P-type adenosine triphosphatases (P4-ATPases) actively transports phospholipids across the membrane bilayer. There are 14 P4-ATPases (ATP1-14) in eukaryotes whereas only three *Tmem30* (termed *Tmem30a*, *Tmem30b*, *Tmem30c*) homologs are identified, each *Tmem30* protein interacting with multiple P4-ATPases.[21,34] It is very interesting to note that, of the three Tmems, only *Tmem30a* is expressed in both murine and human erythroid cells. Since members of the *Tmem* family can compensate each other, the lack of expression of other Tmem family members in erythroid cells may explain the severe phenotypic changes of erythroid cells when *Tmem30a* is depleted. These findings imply the important role of flippase activity in erythropoiesis. Together with previous findings that ATP11C mutated mice showed a lower rate of PS translocation in pre-B cells and defective differentiation of B lymphocytes,[35] we suggest that flippase activity may play important roles in hematopoiesis in general, and this warrants future studies. It is likely that members of P4-ATPases family and Tmem family may contribute to hematopoiesis in a lineage-specific manner.

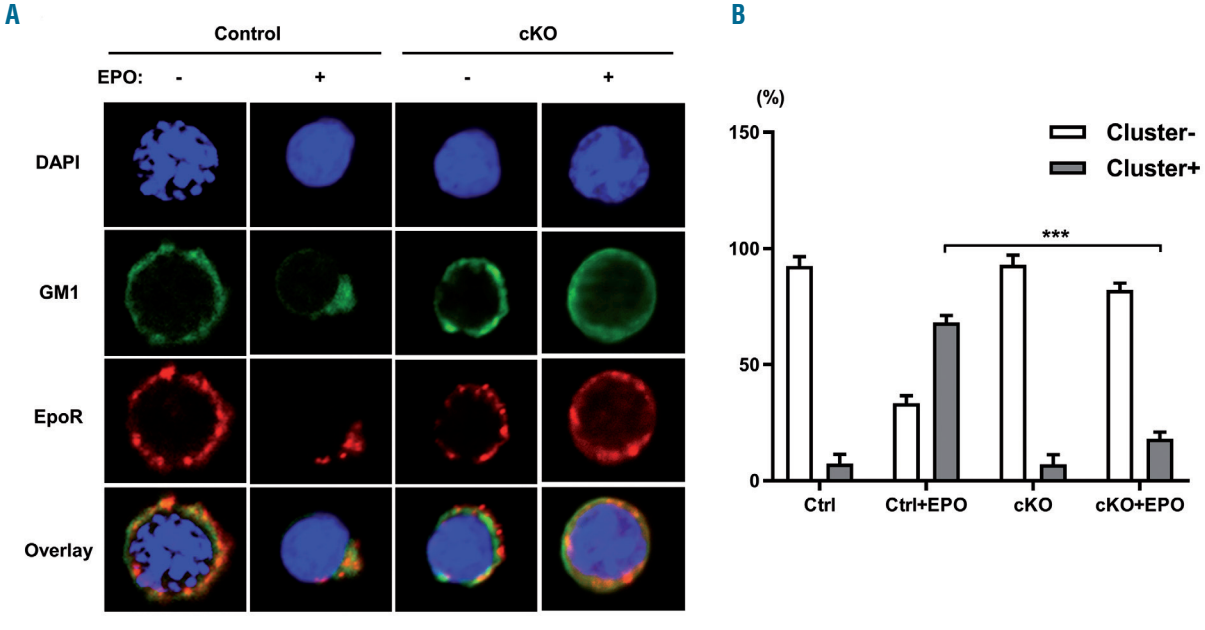

Figure 5. *Tmem30a* deletion impairs erythropoietin receptor (EPOR) clustering. (A) Isolated Ter119 low erythroid cells were stained with DAPI (blue) and with an anti-EPOR antibody (red). Lipid rafts were detected using GM1 ganglioside with FITC conjugated CTB (green). (B) Proportions of cells that showed lipid raft clustering are indicated as cluster+. Values are presented as Mean±Standard Error of Mean. ***P<0.001. N=3 slides per group.

The fact that EPO/EPOR mediated signal transduction pathway in erythroid cells is essential for erythropoiesis has been well documented.[36] However, how the pathway is initiated remains unclear. One striking finding of the current study is that EPO induces the clustering of EPOR at the areas of lipid raft domains on the plasma membrane. Importantly, disruption of lipid rafts formation due to *Tmem30a* deletion led to failure of EPOR clustering as well as impaired activation of JAK2-STAT5. These findings imply that initiation of EPOR signal pathway requires lipid rafts-mediated EPOR clustering. It has been shown that SCF receptor is essential for erythropoiesis because mutation of c-kit caused severe anemia.[37] Therefore, in addition to EPO receptor, other receptors may also be affected after *Tmem30a* deletion. Moreover, a recent study showed that *Tmem30a* plays an essential role in ensuring the survival of hematopoietic cells in adult mice,[38] suggesting that *Tmem30a* play different functions between embryo and adult hematopoiesis.

In summary, our study has uncovered a critical role of *Tmem30a* in erythropoiesis and identified the underlying mechanisms. As *Tmem30a* is required for the flippase activity, our findings suggest the role of flippase in erythropoiesis. Together with other findings, our study has

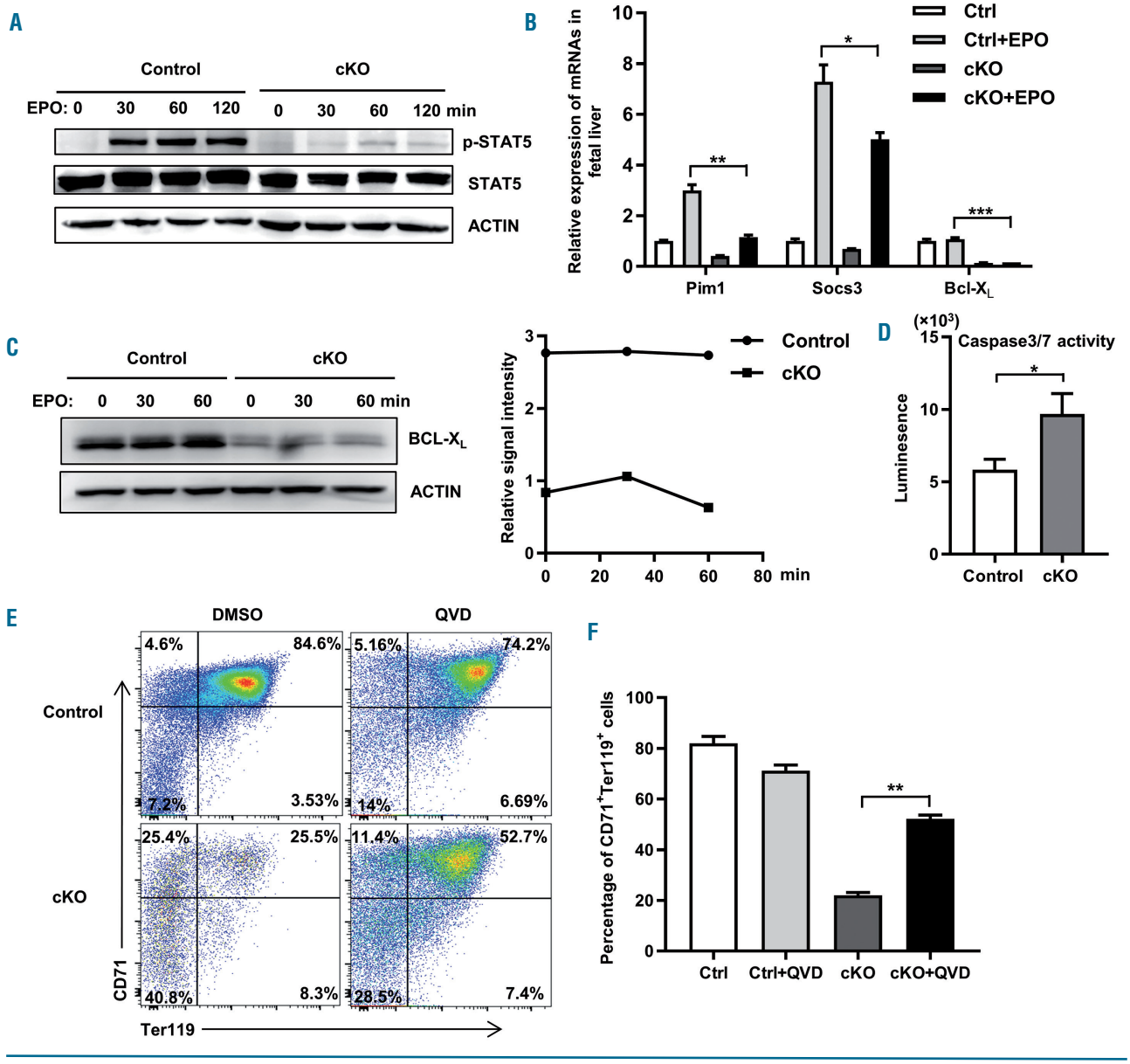

Figure 6. *Tmem30a* deficiency leads to decreased STAT5 phosphorylation. (A) STAT5 activation with or without erythropoietin (EPO) exposure, decreased STAT5 phosphorylation at Tyr694 which was demonstrated by western blotting of protein of fetal liver cells isolated from E14.5 cKO fetal livers compared with protein samples of fetal liver control cells. (B) Expression of STAT5 responsive genes in E14.5 control and cKO fetal liver cells measured by qualitative polymerase chain reaction (n=3 for each genotype). Data are presented as Mean±Standard Error of Mean (SEM) of fold-expression relative to control; expression normalized *versus* actin. **P*<0.05; ***P*<0.01; ****P*<0.001. (C) Decreased expression level of BCL-X_L after EPO exposure in cKO cells compared to control. (D) Levels of caspase-3/7 activity in total fetal liver cells were assessed. N=5 embryos for each group. (E) Enriched Ter119 negative fetal liver cells were cultured for 48 hours *in vitro* and stained with anti-CD71 and anti-Ter119 markers. (F) The pan-caspase inhibitor Q-VD-OPh partially reversed *Tmem30a* erythroid cell differentiation defects as analyzed by FACS.

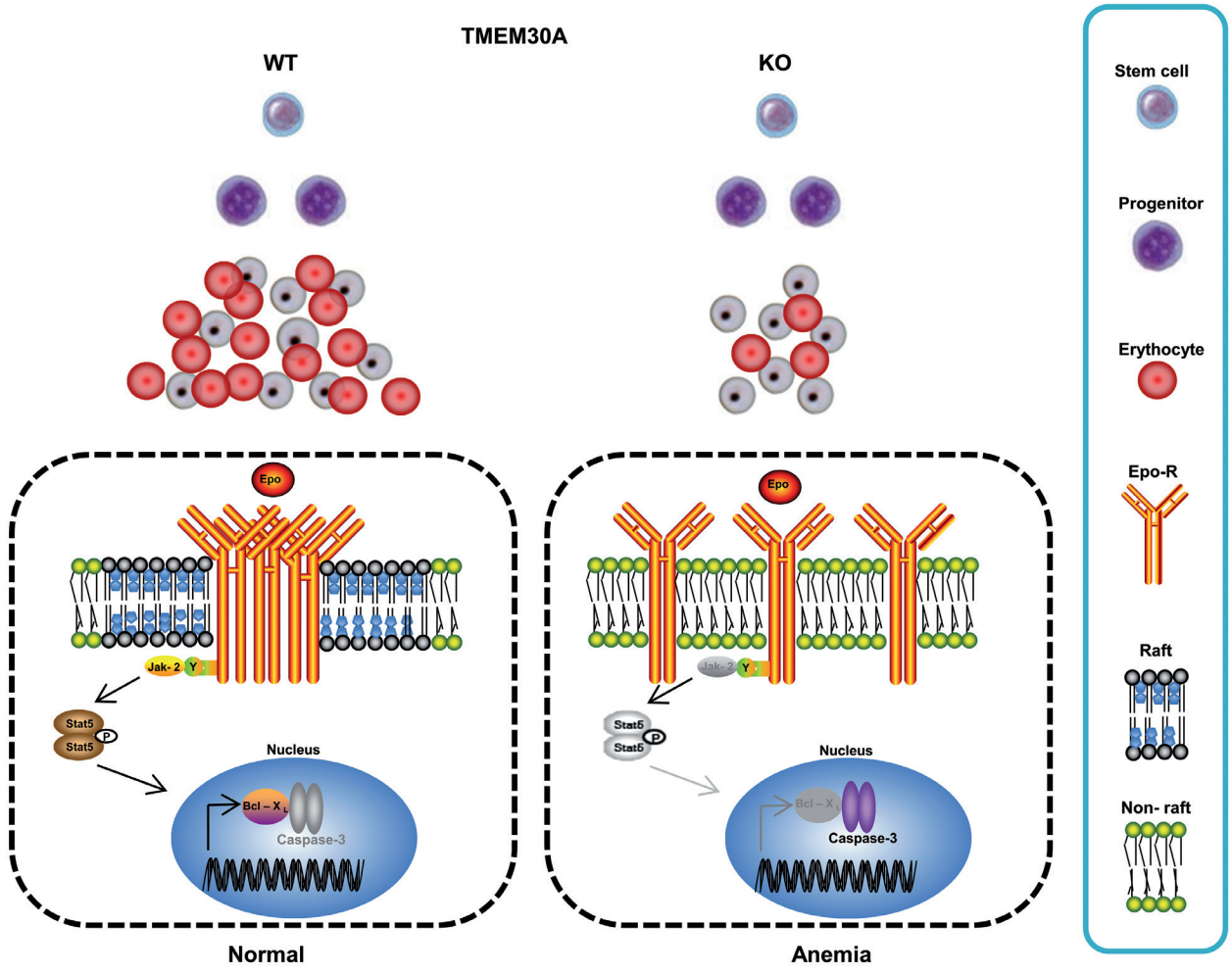

Figure 7. Model of *Tmem30a* function in erythropoiesis. Under normal conditions, upon erythropoietin (EPO) exposure, EPO-receptor (EPOR) localizes to lipid rafts and enhance EPOR-JAK2-STAT5-BCL-X_L-Caspase3 signal transduction which is essential for the survival of the embryos during erythropoiesis. In the absence of *Tmem30a*, lipid raft formation is disturbed, resulting in impaired downstream signal transduction.

elucidated a previously, unknown connection among membrane phospholipid partitioning, lipid raft clustering, receptor signal transduction, and erythroid differentiation (Figure 7).

Acknowledgments

The authors would like to thank the National Key Research and Development Program of China (grants 2016YFA0100602, 2017YFA0103302), National Natural Science Foundation of China (grants 91749203, 81525010, 81420108017 and 81530005), Program for Guangdong Introducing Innovative and Enterpreneurial Teams (2017ZT07S347), and by the Innovative Team Program of Guangzhou Regenerative Medicine and Health Guangdong Laboratory (grants 2018GZR110103002).

References

1. Sigurdsson V, Takei H, Soboleva S, et al. Bile Acids Protect Expanding Hematopoietic Stem Cells from Unfolded Protein Stress in Fetal Liver. Cell Stem Cell. 2016;18(4):522-532.
2. Baron MH, Isern J, Fraser ST. The embryonic origins of erythropoiesis in mammals. Blood. 2012;119(21):4828-4837.
3. Tober J, Koniski A, McGrath KE, et al. The megakaryocyte lineage originates from hemangioblast precursors and is an integral component both of primitive and of definitive hematopoiesis. Blood. 2007; 109(4): 1433-1441.
4. Orkin SH, Zon LI. Hematopoiesis: an evolving paradigm for stem cell biology. Cell. 2008;132(4):631-644.
5. Fang S, Nurmi H, Heinolainen K, et al. Critical requirement of VEGF-C in transition to fetal erythropoiesis. Blood. 2016;128(5):710-720.
6. Sankaran VG, Xu J, Orkin SH. Advances in the understanding of haemoglobin switching. Br J Haematol. 2010;149(2):181-194.
7. Fraser ST, Isern J, Baron MH. Maturation and enucleation of primitive erythroblasts during mouse embryogenesis is accompanied by changes in cell-surface antigen expression. Blood. 2007;109(1):343-352.
8. Kuhrt D, Wojchowski DM. Emerging EPO and EPO receptor regulators and signal transducers. Blood. 2015;125(23):3536-3541.
9. Suzuki N, Hirano I, Pan X, Minegishi N, Yamamoto M. Erythropoietin production in neuroepithelial and neural crest cells during primitive erythropoiesis. Nat Commun. 2013;4:2902.
10. Broxmeyer HE. Erythropoietin: multiple targets, actions, and modifying influences

for biological and clinical consideration. J Exp Med. 2013;210(2):205-208.
11. Livnah O, Stura EA, Middleton SA, Johnson DL, Jolliffe LK, Wilson IA. Crystallographic evidence for preformed dimers of erythropoietin receptor before ligand activation. Science. 1999;283 (5404): 987-990.
12. Witthuhn BA, Quelle FW, Silvennoinen O, et al. JAK2 associates with the erythropoietin receptor and is tyrosine phosphorylated and activated following stimulation with erythropoietin. Cell. 1993;74(2):227-236.
13. Socolovsky M, Fallon AE, Wang S, Brugnara C, Lodish HF. Fetal anemia and apoptosis of red cell progenitors in Stat5a-/-5b-/- mice: a direct role for Stat5 in Bcl-X(L) induction. Cell. 1999;98(2):181-191.
14. Clem RJ, Cheng EH, Karp CL, et al. Modulation of cell death by Bcl-XL through caspase interaction. Proc Natl Acad Sci U S A. 1998;95(2):554-559.
15. Vardaki I, Sanchez C, Fonseca P, et al. Caspase-3-dependent cleavage of Bcl-xL in the stroma exosomes is required for their uptake by hematological malignant cells. Blood. 2016;128(23):2655-2665.
16. Neubauer H, Cumano A, Muller M, Wu H, Huffstadt U, Pfeffer K. Jak2 deficiency defines an essential developmental checkpoint in definitive hematopoiesis. Cell. 1998;93(3):397-409.
17. Raghupathy R, Anilkumar AA, Polley A, et al. Transbilayer lipid interactions mediate nanoclustering of lipid-anchored proteins. Cell. 2015;161(3):581-594.
18. Devaux PF. Static and dynamic lipid asymmetry in cell membranes. Biochemistry. 1991;30(5):1163-1173.
19. Sprong H, van der Sluijs P, van Meer G. How proteins move lipids and lipids move proteins. Nat Rew Mol Cell Biol. 2001;2(7):504-513.
20. Leventis PA, Grinstein S. The distribution and function of phosphatidylserine in cellular membranes. Annu Rev Biophys. 2010;39:407-427.
21. Daleke DL, Lyles JV. Identification and purification of aminophospholipid flippases. Biochim Biophys Acta. 2000;1486(1): 108-127.
22. Segawa K, Kurata S, Yanagihashi Y, Brummelkamp TR, Matsuda F, Nagata S. Caspase-mediated cleavage of phospholipid flippase for apoptotic phosphatidylserine exposure. Science. 2014;344 (6188):1164-1168.
23. Zwaal RF, Comfurius P, Bevers EM. Surface exposure of phosphatidylserine in pathological cells. Cell Mol Life Sci. 2005;62(9): 971-988.
24. Kosan C, Saba I, Godmann M, et al. Transcription factor miz-1 is required to regulate interleukin-7 receptor signaling at early commitment stages of B cell differentiation. Immunity. 2010;33(6):917-928.
25. Wang H, Diao D, Shi Z, et al. SIRT6 Controls Hematopoietic Stem Cell Homeostasis through Epigenetic Regulation of Wnt Signaling. Cell Stem Cell. 2016;18(4):495-507.
26. Pietkiewicz S, Schmidt JH, Lavrik IN. Quantification of apoptosis and necroptosis at the single cell level by a combination of Imaging Flow Cytometry with classical Annexin V/propidium iodide staining. J Immunol Methods. 2015;423:99-103.
27. Gaudreau MC, Grapton D, Helness A, et al. Heterogeneous Nuclear Ribonucleoprotein L is required for the survival and functional integrity of murine hematopoietic stem cells. Sci Rep. 2016;6:27379.
28. Menon MP, Fang J, Wojchowski DM. Core erythropoietin receptor signals for late erythroblast development. Blood. 2006;107(7): 2662-2672.
29. Zhang J, Socolovsky M, Gross AW, Lodish HF. Role of Ras signaling in erythroid differentiation of mouse fetal liver cells: functional analysis by a flow cytometry-based novel culture system. Blood. 2003;102 (12):3938-3946.
30. Qu X, Zhang S, Wang S, et al. TET2 deficiency leads to stem cell factor-dependent clonal expansion of dysfunctional erythroid progenitors. Blood. 2018;132(22):2406-2417.
31. Yan H, Wang Y, Qu X, et al. Distinct roles for TET family proteins in regulating human erythropoiesis. Blood. 2017;129 (14):2002-2012.
32. Huang Y, Hale J, Wang Y, et al. SF3B1 deficiency impairs human erythropoiesis via activation of p53 pathway: implications for understanding of ineffective erythropoiesis in MDS. J Hematol Oncol. 2018;11(1):19.
33. Paulusma CC, Folmer DE, Ho-Mok KS, et al. ATP8B1 requires an accessory protein for endoplasmic reticulum exit and plasma membrane lipid flippase activity. Hepatology. 2008;47(1):268-278.
34. Paulusma CC, Oude Elferink RP. The type 4 subfamily of P-type ATPases, putative aminophospholipid translocases with a role in human disease. Biochim Biophys Acta. 2005;1741(1-2):11-24.
35. Siggs OM, Arnold CN, Huber C, et al. The P4-type ATPase ATP11C is essential for B lymphopoiesis in adult bone marrow. Nat Immunol. 2011;12(5):434-440.
36. Wu H, Liu X, Jaenisch R, Lodish HF. Generation of committed erythroid BFU-E and CFU-E progenitors does not require erythropoietin or the erythropoietin receptor. Cell. 1995;83(1):59-67.
37. Metcalf D. Hematopoietic cytokines. Blood. 2008;111(2):485-491.
38. Li N, Yang Y, Liang C, et al. Tmem30a Plays Critical Roles in Ensuring the Survival of Hematopoietic Cells and Leukemia Cells in Mice. Am J Pathol. 2018;188(6):1457-1468.

ARTICLE

Senescence-accelerated mice (SAMP1/TA-1) treated repeatedly with lipopolysaccharide develop a condition that resembles hemophagocytic lymphohistiocytosis

Isao Tsuboi,[1,3] Tomonori Harada,[1] Yoko Hirabayashi[2] and Shin Aizawa[1]

[1]Division of Anatomical Science, Department of Functional Morphology, Nihon University School of Medicine, Tokyo and [2]Cellular and Molecular Toxicology Division, National Center for Biological Safety and Research, National Institute of Health Science, Kawasaki, Japan

Ferrata Storti Foundation

Haematologica 2019
Volume 10410):1995-2005

ABSTRACT

Hemophagocytic lymphohistiocytosis is a life-threatening systemic hyperinflammatory disorder with primary and secondary forms. Primary hemophagocytic lymphohistiocytosis is associated with inherited defects in various genes that affect the immunological cytolytic pathway. Secondary hemophagocytic lymphohistiocytosis is not inherited, but complicates various medical conditions including infections, autoinflammatory/autoimmune diseases, and malignancies. When senescence-accelerated mice (SAMP1/TA-1) with latent deterioration of immunological function and senescence-resistant control mice (SAMR1) were treated repeatedly with lipopolysaccharide, SAMP1/TA-1 mice displayed the clinicopathological features of hemophagocytic lymphohistiocytosis such as hepatosplenomegaly, pancytopenia, hypofibrinogenemia, hyperferritinemia, and hemophagocytosis. SAMR1 mice showed no features of hemophagocytic lymphohistiocytosis. Lipopolysaccharide induced upregulation of proinflammatory cytokines such as interleukin-1β, interleukin-6, tumor necrosis factor-α, and interferon-γ, and interferon-γ-inducible chemokines such as c-x-c motif chemokine ligands 9 and 10 in the liver and spleen in both SAMP1/TA-1 and SAMR1 mice. However, upregulation of proinflammatory cytokines and interferon-γ-inducible chemokines in the liver persisted for longer in SAMP1/TA-1 mice than in SAMR1 mice. In addition, the magnitude of upregulation of interferon-γ in the liver and spleen after lipopolysaccharide treatment was greater in SAMP1/TA-1 mice than in SAMR1 mice. Furthermore, lipopolysaccharide treatment led to a prolonged increase in the proportion of peritoneal M1 macrophages and simultaneously to a decrease in the proportion of M2 macrophages in SAMP1/TA-1 mice compared with SAMR1 mice. Lipopolysaccharide appeared to induce a hyperinflammatory reaction and prolonged inflammation in SAMP1/TA-1 mice, resulting in features of secondary hemophagocytic lymphohistiocytosis. Thus, SAMP1/TA-1 mice represent a useful mouse model to investigate the pathogenesis of bacterial infection-associated secondary hemophagocytic lymphohistiocytosis.

Introduction

Hemophagocytic lymphohistiocytosis (HLH) is characterized by an unremitting activation of lymphocytes and macrophages that leads to an overwhelming inflammatory reaction resulting in organ damage.[1-3] HLH is broadly divided into primary HLH and secondary HLH (sHLH). Primary HLH is caused by mutations in genes such as *PFR1*, *UNC13D*, *STX11*, and *STXBP2*, which encode proteins involved in granule exocytosis.[4-8] sHLH is associated with viral, bacterial, parasitic, or fungal infections, which cause strong activation of the immune system.[1,2,9] sHLH also occurs in the context of autoimmune diseases such as systemic juvenile idiopathic arthritis, systemic lupus erythematosus, and Kawasaki disease and malignancies such as lymphoma.[10-14] HLH is characterized by high fever, lymphoadenopathy,

Correspondence:

ISAO TSUBOI
tsuboi.isao@nihon-u.ac.jp

Received: October 17, 2018.

Accepted: February 25, 2019.

Pre-published: February 28, 2019.

doi:10.3324/haematol.2018.209551

Check the online version for the most updated information on this article, online supplements, and information on authorship & disclosures: www.haematologica.org/content/104/10/1995

hepatosplenomegaly, pancytopenia, and coagulopathy.[9] The clinical entity of HLH is different from that of sepsis or inflammatory response syndrome.[15] However, these diseases show a common immunopathological state referred to as a cytokine storm.[9,15]

Senescence-accelerated mice, senescence-prone (SAMP) show early onset of a decline in immune function such as decreased natural killer-cell and T-cell activities and are susceptible to infection.[16-20] Thus, we investigated whether repeated lipopolysaccharide (LPS) treatment induces hyperinflammation by deterioration of the function of the immune system resulting in sHLH in the senescence-prone substrain, SAMP1/TA-1 mice.

Methods

Mice

SAMP1/TA-1 mice were bred and maintained in an experimental facility at Nihon University School of Medicine.[16,17] SAMR1/Ta Slc mice were purchased from Japan SLC Inc. (Hamamatsu, Japan). Eight- to 12-week old SAMR1 and SAMP1/TA-1 male mice were used.[16,17] All protocols involving laboratory mice were reviewed and approved by the Nihon University Animal Care and Use Committee (experiment codes AP15M033 and AP16M054). The approved experimental protocol was performed humanely in strict accordance with Nihon University rules concerning animal care and use.

Lipopolysaccharide treatment

Mice were injected intravenously with a single dose of 25 μg LPS three times at weekly intervals.[21,22] The body weight of non-treated SAMR1 and SAMP1/TA-1 mice was 29.6 ± 1.1 g and 31.2 ± 1.3 g, respectively. A control group of SAMR1 and SAMP1/TA-1 mice was treated with the same volume of pyrogen-free saline.

Progenitor cell colony assay

Myeloid progenitor (CFU-GM) cells were assayed using MethoCult M3231 (Stem Cell Technologies Inc., Vancouver, Canada) supplemented with 10 ng/mL recombinant murine granulocyte-macrophage colony-stimulating factor. B lymphoid-progenitor (CFU-preB) cells were assayed using MethoCult M3630. Erythroid progenitor (BFU-E) cells were assayed using MethoCult M3334 supplemented with 1 ng/mL recombinant murine interleukin (IL)-3. Megakaryocytic progenitors (CFU-Mk) were assayed using MegaCult-C supplemented with 50 ng/mL recombinant human thrombopoietin, 10 ng/mL recombinant murine IL-3, 20 ng/mL recombinant human IL-6, and 50 ng/mL recombinant murine IL-11. Cells were cultured in a humidified incubator at 37°C and 5% CO_2. CFU-GM, CFU-preB, and CFU-Mk cells were counted 7 days after plating the cells. BFU-E cells were counted 10 days after plating the cells.

Gene expression assay

The levels of gene expression of cytokines were determined with real-time polymerase chain reaction (PCR) using the Applied Biosystems 7500 Fast Sequence Detection System. Briefly, total RNA from splenic and liver cells was isolated using ISOGEN reagent (Nippongene Corp., Toyama, Japan). mRNA was reverse transcribed using Superscript III (Life Technologies, Carlsbad, CA, USA) and Oligo-dT (Promega Corp., Madison, WI, USA). The levels of gene expression were determined with real-time PCR using TaqMan™ Universal Fast PCR master mix (Applied Biosystems, Foster City, CA, USA) and specific primers. Specific primers and probes for murine IL-1β, IL-6, IL-10, tumor necrosis factor (TNF)-α, interferon (IFN)-γ, Cxcl9, Cxcl10, and GAPDH genes were purchased from Applied Biosystems as described elsewhere.[23,24]

Clinical laboratory tests and enzyme-linked immunosorbent assays

Plasma fibrinogen levels were measured by ACL ELITE PRO (Instrumentation Laboratory, Bedford, MA, USA). Serum ferritin levels were evaluated with an enzyme-linked immunosorbent assay kit (Abcam pic, Cambridge, UK).

Flow cytometry analysis for peritoneal macrophage polarization in SAMR1 and SAMP1/TA-1 mice

Peritoneal cells (2 x 10^5) were labeled using fluorescein isothiocyanate-conjugated rat anti-mouse CD11b monoclonal antibody and phycoerythrin-conjugated rat anti-mouse inducible nitric oxide synthase (iNOS) monoclonal antibody, or phycoerythrin-conjugated rat anti-mouse CD11b monoclonal antibody and fluorescein isothiocyanate-conjugated rat anti-mouse CD206 monoclonal antibody. Labeled cells were analyzed by flow cytometry (Cytomics FC500, Beckman Coulter, Brea, CA, USA) for direct detection of $CD11b^+/iNOS^+$ M1 macrophages and $CD11b^+/CD206^+$ M2 macrophages.

Statistical analysis

Data are expressed as the mean ± standard deviation (SD). Data sets were compared using the two-tailed unpaired Student *t* test and two-way analysis of variance. Differences were considered statistically significant at $P<0.05$.

Results

Repeated lipopolysaccharide treatment induced pancytopenia in SAMP1/TA-1 mice but not in SAMR1 mice

The numbers of peripheral white blood cells, red blood cells, and platelets were evaluated in SAMR1 and SAMP1/TA-1 mice after repeated LPS treatment (Figure 1A). The number of white blood cells in LPS-treated SAMR1 mice was slightly decreased until day 21 after the first LPS treatment compared with that of the non-treated control group (day 0). In contrast, the number of white blood cells in LPS-treated SAMP1/TA-1 mice was significantly decreased to 17.5% that of the non-treated control group by day 21 (SAMP1/TA-1; day 0 *vs*. day 7; $P<0.05$, day 0 *vs*. day 14; $P<0.005$, day 0 *vs*. day 21; $P<0.005$). The number of red blood cells in LPS-treated SAMR1 mice remained unchanged compared with that in the non-treated control group. In contrast, the number of red blood cells in LPS-treated SAMP1/TA-1 mice was significantly decreased to 44.7% that in the non-treated control group by day 21 (SAMP1/TA-1; day 0 *vs*. day 7; $P<0.005$, day 0 *vs*. day 14; $P<0.005$, day 0 *vs*. day 21; $P<0.005$). The numbers of platelets in LPS-treated SAMR1 mice on days 7, 14, and 21 were higher than those in the non-treated control group. In contrast, the number of platelets in LPS-treated SAMP1/TA-1 mice was significantly decreased to 9.9% that in the non-treated control group by day 21 (SAMP1/TA-1; day 0 *vs*. day 7; $P<0.005$, day 0 *vs*. day 14; $P<0.005$, day 0 *vs*. day 21; $P<0.005$).

Hemophagocytosis in hematopoietic tissues of lipopolysaccharide-treated SAMP1/TA-1 mice

Hemophagocytosis was observed in SAMP1/TA-1 mice

7 days after the first LPS treatment. Figure 1B shows hemophagocytic cells in peripheral blood, bone marrow, and the spleen.

Repeated lipopolysaccharide treatment induced hepatosplenomegaly in SAMP1/TA-1 mice but not in SAMR1 mice

The ratios of liver weight and spleen weight to whole body weight in SAMR1 and SAMP1/TA-1 mice after repeated LPS treatment were evaluated (Figure 2A). The ratio of liver weight to body weight in LPS-treated SAMR1 mice remained unchanged compared with that of the non-treated control group (day 0). In contrast, the ratio of liver weight to body weight in LPS-treated SAMP1/TA-1 mice increased continuously to 385.8% that of the non-treated control group by day 21 after the first LPS treatment (SAMP1/TA-1; day 0 *vs.* day 7; $P<0.001$, day 0 *vs.* day 14; $P<0.001$, day 0 *vs.* day 21; $P<0.001$).

The ratio of spleen weight to body weight in LPS-treated SAMR1 mice was slightly increased to 134.8% that of the non-treated control group (day 0) on day 7 after the first LPS treatment and remained unchanged thereafter. In contrast, the ratio of spleen weight to body weight in LPS-treated SAMP1/TA-1 mice was markedly increased to 548.2% that of the non-treated control group on day 7 and remained unchanged thereafter (SAMP1/TA-1; day 0 *vs.* day 7; $P<0.001$, day 0 *vs.* day 14; $P<0.001$, day 0 *vs.* day 21; $P<0.001$).

Figure 2B shows a photograph of the spleens and livers of SAMP1/TA-1 mice on day 21 after the first saline or LPS treatment. Repeated LPS treatment induced marked hepatosplenomegaly in SAMP1/TA-1 mice.

Liver and spleen histology in SAMP1/TA-1 mice after repeated lipopolysaccharide treatment

Figure 3A shows liver histology of SAMP1/TA-1 mice 21 days after the first treatment with saline or LPS. Figure 3B shows high-power liver histology of SAMP1/TA-1 mice 21 days after the first treatment with LPS. Congestion (Figure 3Ba) and microthrombi (Figure 3Bb) in the liver were observed in LPS-treated SAMP1/TA-1 mice.

Figure 4 shows splenic histology of SAMP1/TA-1 mice 21 days after the first treatment with saline or LPS. The red pulp region was expanded, and the structure of splenic pulp appeared somewhat chaotic in LPS-treated SAMP1/TA-1 mice compared with that in saline-treated SAMP1/TA-1 mice (Figure 4A *vs.* Figure 4B). Furthermore, decreased tissue staining of hemosiderin (ferric iron) was observed in LPS-treated SAMP1/TA-1 mice compared with that in saline-treated SAMP1/TA-1 mice (Figure 4C *vs.* Figure 4D).

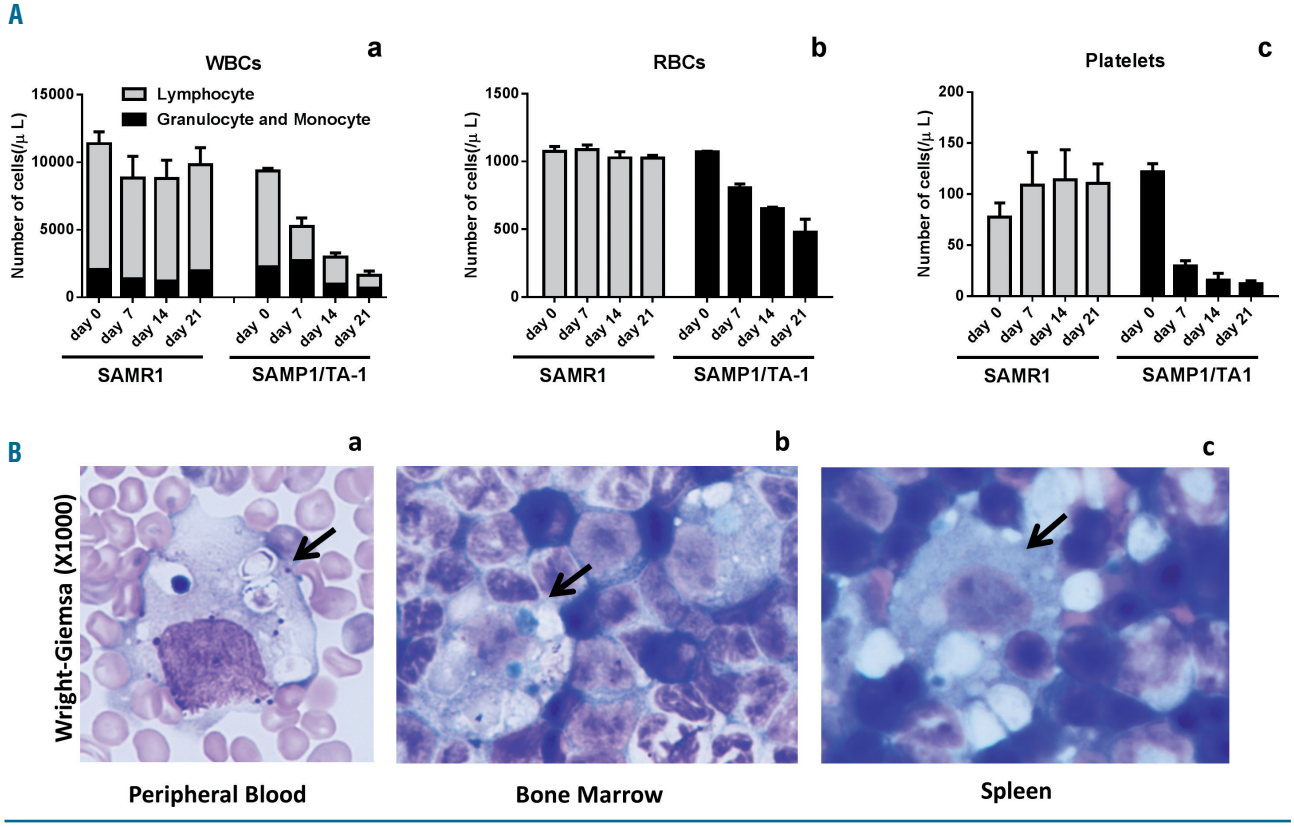

Figure 1. Repeated lipopolysaccharide treatment induced pancytopenia and hemophagocytosis in SAMP/TA-1 mice. (A) Numerical changes in white blood cell (WBC), red blood cell (RBC), and platelet counts in SAMR1 and SAMP1/TA-1 mice after treatment with lipopolysaccharide (LPS). Numerical changes in the counts of WBC (a), RBC (b), and platelets (c) in SAMR1 and SAMP1/TA-1 mice after repeated LPS treatment are shown. The samples of peripheral blood cells were obtained from non-treated control mice (day 0) and mice 7, 14, and 21 days after the first treatment with 25 μg LPS. Each bar represents the mean ± standard deviation obtained from three mice. (B) Hemophagocytosis in hematopoietic tissues of SAMP1/TA-1 mice after LPS treatment. A peripheral blood smear (a) and touch preparations of bone marrow (b) and spleen (c) were made on day 7 after the first treatment with 25 μg LPS. Cells were stained with Wright-Giemsa, and hemophagocytosis was evaluated.

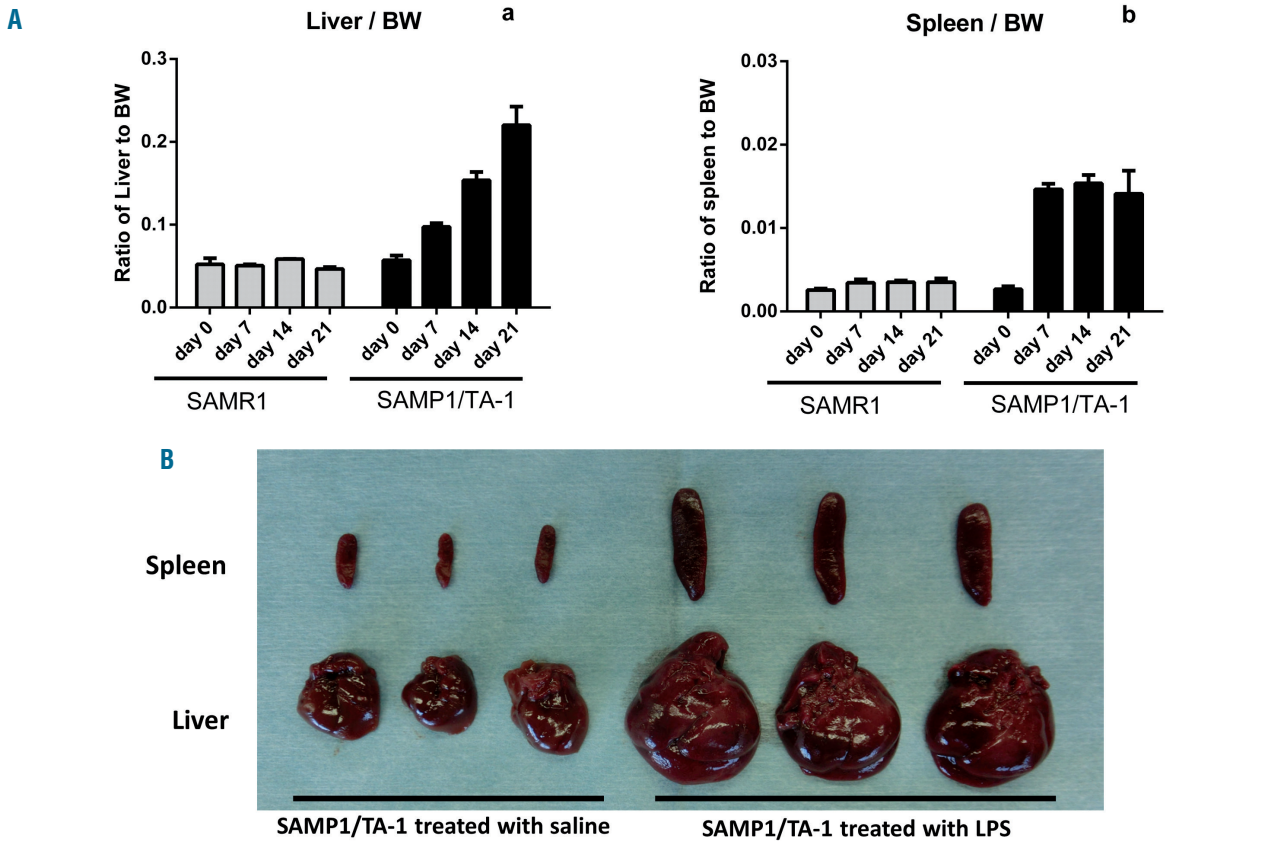

Figure 2. Repeated lipopolysaccharide treatment induced hepatosplenomegaly in SAMP/TA-1 mice. (A) Changes in the ratio of liver and spleen weight to total body weight (BW) in SAMR1 and SAMP1/TA-1 mice after treatment with lipopolysaccharide (LPS). Changes in the ratio of liver (a) and spleen weight (b) to total BW in SAMR1 and SAMP1/TA-1 mice after repeated LPS treatment are shown. The samples of spleen and liver obtained from non-treated control mice (day 0) and mice 7, 14, and 21 days after the first treatment with 25 μg LPS were weighed and expressed as a ratio of liver and spleen weight to total BW. Each bar represents the mean ± standard deviation obtained from three mice. (B) Photograph of spleen and liver specimens from SAMP1/TA-1 mice 21 days after the first treatment with saline or 25 μg LPS.

Lipopolysaccharide treatment induced hypofibrinogenemia and hyperferritinemia in SAMP1/TA-1 mice

The levels of fibrinogen in plasma in SAMP1/TA-1 mice 7 days after the first treatment with saline or LPS were 241 ± 55 mg/dL and 103 ± 13 mg/dL, respectively (Figure 5A). The levels of fibrinogen in the plasma of other strains of mice range from 200 to 400 mg/dL.[25] The levels of ferritin in serum in SAMP1/TA-1 mice 21 days after the first treatment with saline or LPS were 1680 ± 138 ng/mL and 3080 ± 1126 ng/mL, respectively (Figure 5B). The levels of ferritin in the serum of other strains of mice range from 750 to 1000 ng/mL.[26,27]

Numerical changes in hematopoietic progenitor cells in bone marrow from SAMR1 and SAMP1/TA-1 mice after repeated lipopolysaccharide treatment

The numbers of hematopoietic progenitor cells in femoral bone marrow were evaluated in SAMR1 and SAMP1/TA-1 mice after repeated LPS treatment (Figure 6).

The numbers of myeloid progenitor (CFU-GM) cells in both SAMR1 and SAMP1/TA-1 mice on days 7, 14, and 21 after the first LPS treatment were similar to those in the non-treated control group (day 0).

The numbers of B-cell progenitor (CFU-preB) cells in SAMR1 mice on days 7, 14, and 21 after the first LPS treatment were slightly decreased compared with those of the non-treated control group. In contrast, the numbers of CFU-preB cells in SAMP1/TA-1 mice on days 7, 14, and 21 after the first LPS treatment were significantly decreased compared with those of the non-treated control group.

The numbers of erythroid progenitor (BFU-E) cells in both SAMR1 and SAMP1/TA-1 mice on days 7, 14, and 21 after the first LPS treatment were decreased compared with those of the non-treated control group. The magnitude of the decrease in the number of BFU-E cells was greater in SAMP1/TA-1 mice than in SAMR1 mice (day 7; SAMR1 *vs.* SAMP1/TA-1 $P<0.05$, day 14; SAMR1 *vs.* SAMP1/TA-1 $P<0.05$, day 21; SAMR1 *vs.* SAMP1/TA-1 $P<0.05$).

The numbers of megakaryocytic progenitor (CFU-Mk) cells in SAMP1/TA-1 mice on days 7, 14, and 21 after the first LPS treatment were decreased compared with those of the non-treated control group, whereas the numbers of CFU-Mk cells in SAMR1 mice on days 7, 14, and 21 after the first LPS treatment were increased.

Changes in the levels of gene expression of cytokines and chemokines in the liver and spleen in SAMR1 and SAMP1/TA-1 mice after the first lipopolysaccharide treatment

Levels of gene expression of inflammatory cytokines, such as IL-1β, IL-6, TNF-α, and IFN-γ, anti-inflammatory

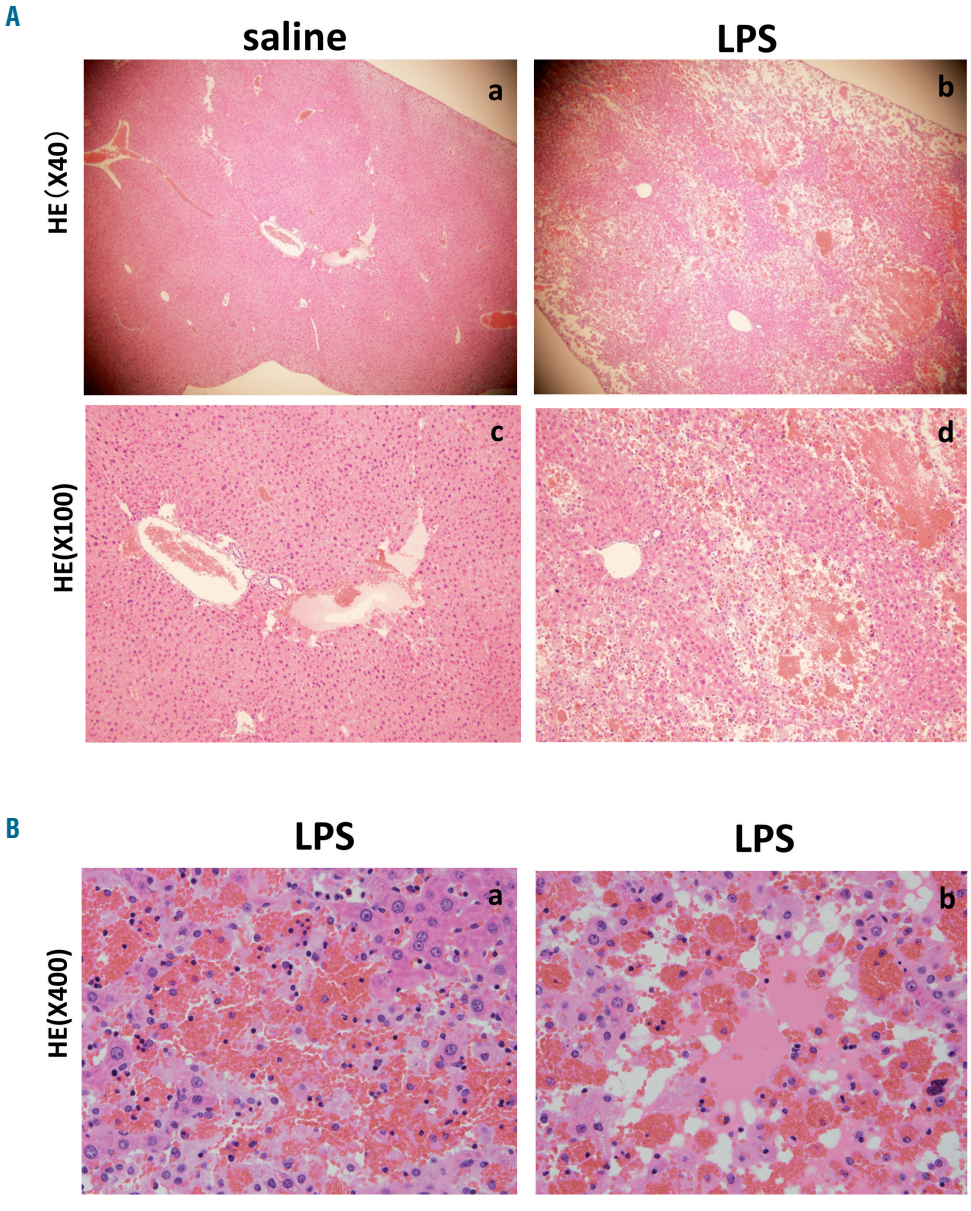

Figure 3. Changes in liver histology in SAMP1/TA-1 mice after lipopolysaccharide treatment. (A) Livers obtained from SAMP1/TA-1 mice 21 days after the first treatment with saline (a, c) or 25 μg lipopolysaccharide (LPS) (b, d) were sectioned and stained with hematoxylin & eosin (HE). (B) Changes in high-power liver histology in SAMP1/TA-1 mice after LPS treatment. Congestion (a) and microthrombi (b) were observed in the livers of LPS-treated SAMP1/TA-1 mice.

cytokines such as IL-10, and IFN-γ-induced chemokines such as Cxcl9 and Cxcl10 in the liver and spleen of SAMR1 and SAMP1/TA-1 mice after the first LPS treatment were evaluated (Figure 7).

Figure 7A shows the changes in levels of gene expression for cytokines in the liver in SAMR1 and SAMP1/TA-1 mice after the first LPS treatment. The levels of gene expression of IL-1β, IL-6, TNF-α, IFN-γ, IL-10, Cxcl9, and Cxcl10 in the liver of non-treated SAMP1/TA-1 mice were 401%, 253%, 146%, 380%, 694%, 353%, and 220% those of non-treated SAMR1 mice, respectively. The levels of gene expression of IL-1β, IL-6, TNF-α, IFN-γ, IL-10, Cxcl9, and Cxcl10 in the liver of both SAMR1 and SAMP1/TA-1 mice after the first LPS treatment were markedly upregulated during the first 6 h. Thereafter, the levels of gene expression of the cytokines and chemokines in the liver of SAMP1/TA-1 mice remained upregulated, whereas the levels of the cytokines and chemokines in the liver of SAMR1 mice promptly returned to pretreatment levels. Furthermore, the level of IFN-γ gene expression in the liver of SAMP1/TA-1 mice during the first 6 h after the first LPS treatment was markedly higher than that in SAMR1 mice.

Figure 7B shows the changes in the levels of gene expression of cytokines in the spleen in SAMR1 and SAMP1/TA-1 mice after the first LPS treatment. The levels of gene expression of IL-1β, IL-6, TNF-α, IFN-γ, IL-10, Cxcl9, and Cxcl10 in the spleen of non-treated SAMP1/TA-1 mice were 135%, 142%, 102%, 187%, 81%, 68%, and 71% those of non-treated SAMR1 mice, respectively. The levels of gene expression of IL-1β, IL-6, TNF-α, IFN-γ, IL-10, Cxcl9, and Cxcl10 in the spleen of SAMR1 mice after the first LPS treatment were markedly upregulated during the first 6 h, followed by prompt downregulation. The time courses of gene expression of

IL-1β, IL-6, TNF-α, IL-10, Cxcl9, and Cxcl10, but not IFN-γ, in the spleen of SAMP1/TA-1 mice after LPS treatment were similar to those in SAMR1 mice. The level of gene expression of IFN-γ in the spleen of SAMP1/TA-1 mice during the first 6 h after LPS treatment was markedly higher than that in SAMR1 mice.

Changes in the polarization of M1/M2 peritoneal macrophages in SAMR1 and SAMP1/TA-1 mice after the first lipopolysaccharide treatment

The polarization of M1/M2 peritoneal macrophages of SAMR1 and SAMP1/TA-1 mice after the first LPS treatment was evaluated. Figure 8 shows the changes in the

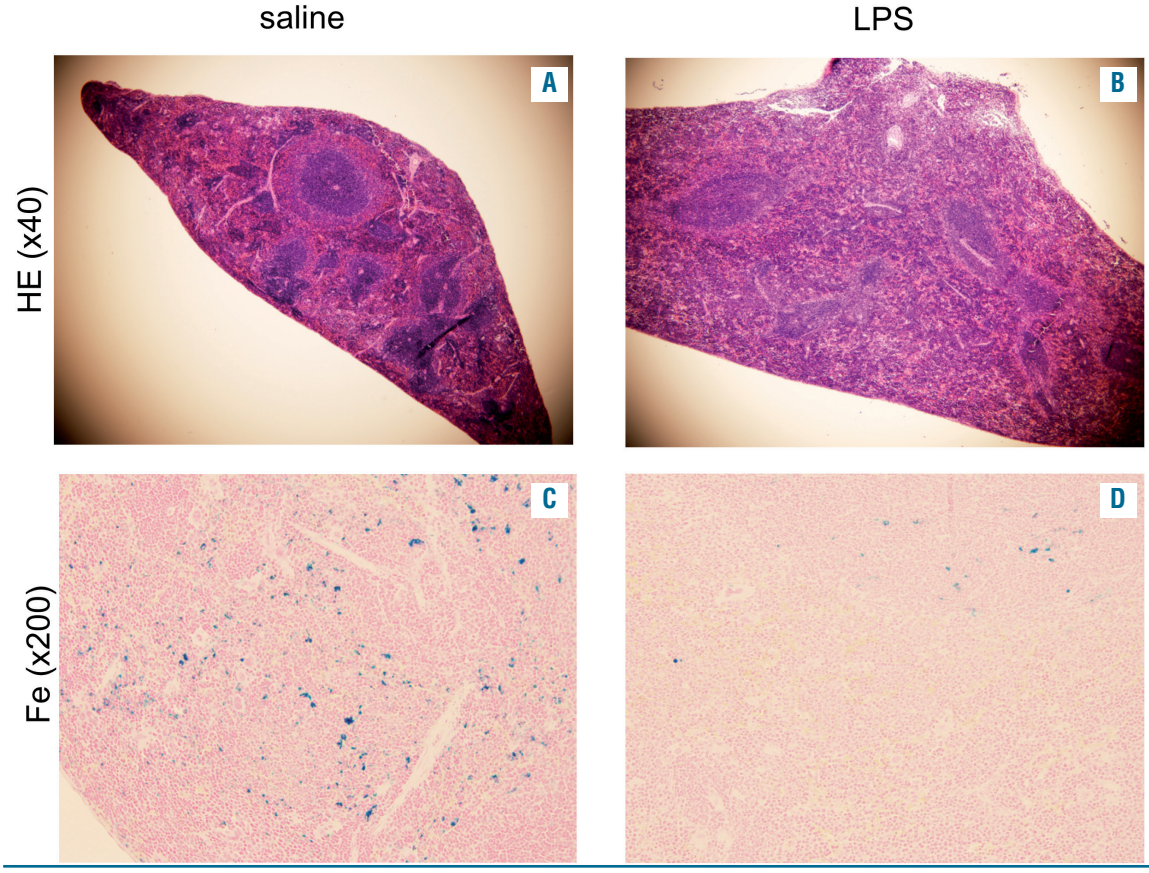

Figure 4. Changes in splenic histology in SAMP1/TA-1 mice after lipopolysaccharide treatment. (A-D) Spleens obtained from SAMP1/TA-1 mice 21 days after the first treatment with saline (A, C) or 25 μg lipopolysaccharide (LPS) (B, D) were sectioned and stained with hematoxylin & eosin (HE) (A, B) or Berlin blue to label trivalent iron (Fe) (C, D).

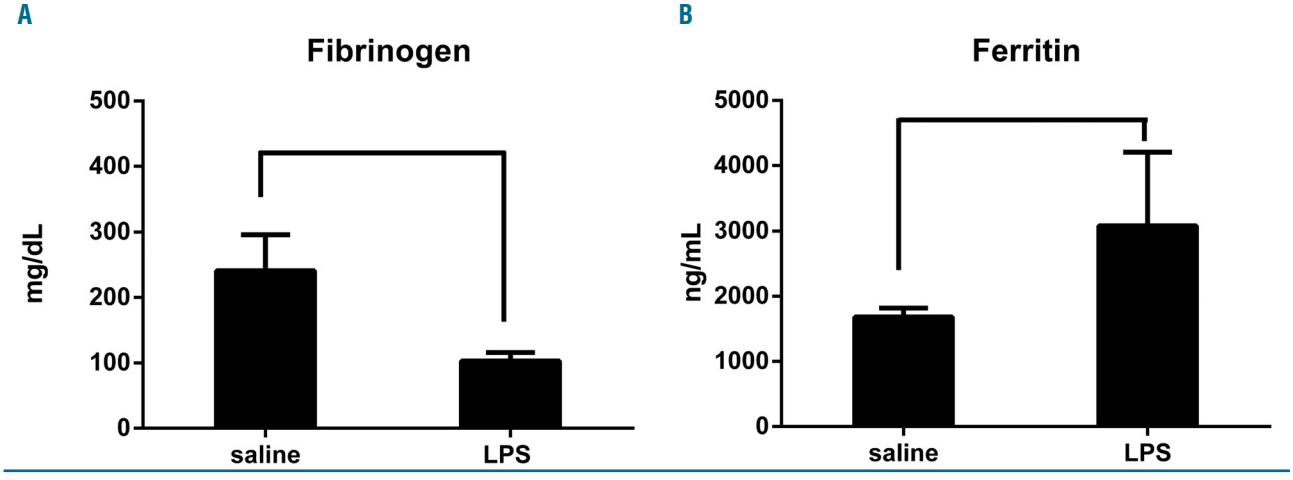

Figure 5. Changes in plasma fibrinogen levels and serum ferritin levels in SAMP1/TA-1 mice after lipopolysaccharide treatment. (A) Plasma fibrinogen levels were measured with ACL ELITE PRO in plasma obtained from SAMP1/TA-1 mice 21 days after the first injection of saline or 25 μg lipopolysaccharide (LPS). (B) Serum ferritin levels were evaluated with an enzyme-linked immunosorbent assay kit in serum obtained from SAMP1/TA-1 mice 7 days after the first treatment with saline or 25 μg LPS. Each bar represents the mean ± standard deviation obtained from three mice. *P<0.05 *vs.* saline-treated control.

proportions of M1 and M2 macrophages in SAMR1 and SAMP1/TA-1 mice after the first LPS treatment. The proportion of M2 macrophages ($CD11b^+/CD206^+$ cells) was higher than that of M1 macrophages ($CD11b^+/iNOS^+$ cells) in both non-treated SAMR1 and non-treated SAMP1/TA-1 mice. When treated with LPS, the proportions of M1 macrophages in SAMR1 and SAMP1/TA-1 mice were increased by day 2. Thereafter, although the proportions of M1 macrophages decreased in both SAMR1 and SAMP1/TA-1 mice, the magnitude of the decrease in the proportions of M1 macrophages on day 5 after LPS treatment differed between SAMR1 and SAMP1/TA-1 mice. Namely, the proportion of M1 macrophages in SAMP1/TA-1 mice remained high (8.0% of M1 cells) compared with that in SAMR1 mice (1.4% of M1 cells).

When treated with LPS, the proportions of M2 macrophages remained unchanged in both SAMR1 and SAMP1/TA-1 mice by day 2. Thereafter, the proportion of M2 macrophages in SAMP1/TA-1 mice decreased by day 5 (52.5% to 30.2%), whereas the proportion of M2 macrophages in SAMR1 mice remained high (57.2% to 58.4%).

Discussion

Several murine models of primary HLH and sHLH have been described. Murine models of primary HLH were generated by deletion of perforin and Rab27a genes, and mutation of the Unc13d gene, leading to defects in the granule exocytic pathway.[28-30] In contrast, sHLH can be induced by Epstein-Barr virus infection in humanized mice transplanted with human $CD34^+$ cells, *Salmonella enteritica* infection in Sv12956 mice, and cytomegalovirus infection in BALB/c mice.[25,31,32] Furthermore, C57BL/6 mice repeatedly given the toll-like receptor 9 agonist, CpG, and IL-6 transgenic mice given LPS also develop sHLH.[33,34]

Henter *et al.*[1] proposed that the diagnosis of HLH is based on eight criteria, including fever, splenomegaly bicytopenia, hypertriglyceremia and/or hypofibriogenemia, hemophagocytosis, low/absent natural killer-cell activity, hyperferritinemia, and high levels of soluble IL-2 receptor. Five of these eight criteria must be fulfilled for a diagnosis, unless a family history is present that is consistent with sHLH. When repeatedly treated with LPS, SAMP1/TA-1 mice showed hepatosplenomegaly, pancy-

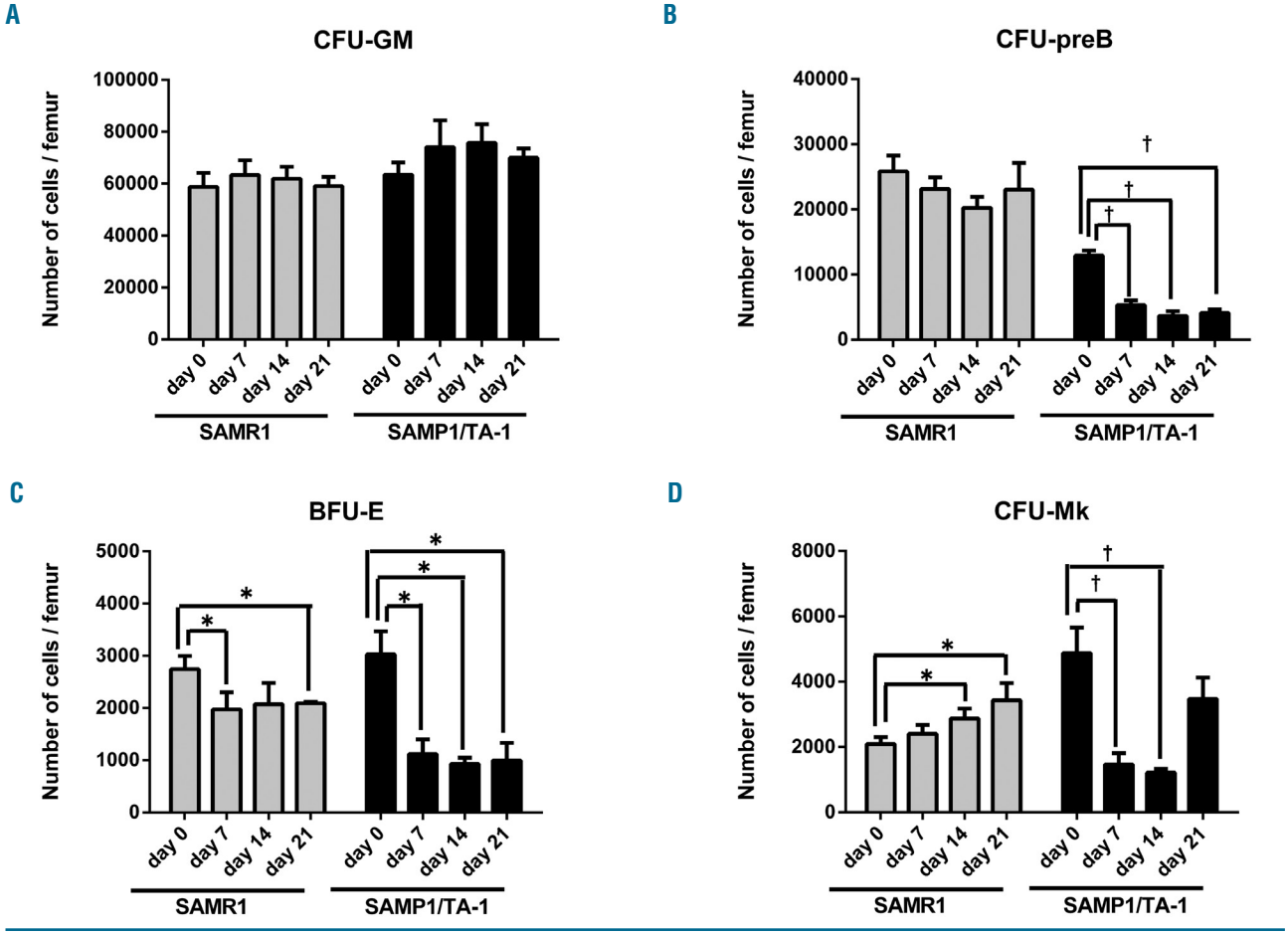

Figure 6. Numerical changes in hematopoietic progenitor cells in the bone marrow from SAMR1 and SAMP1/TA-1 mice after lipopolysaccharide treatment. (A-D) The numbers of hematopoietic progenitor cells in the femoral bone marrow of SAMR1 and SAMP1/TA-1 mice after repeated treatment with lipopolysaccharide (LPS) are shown: myeloid progenitors, CFU-GM (A); B lymphoid progenitors, CFU-preB (B); erythroid progenitors, BFU-E (C); and megakaryocytic progenitors, CFU-Mk (D). The samples of femoral bone marrow cells were obtained from non-treated control mice (day 0) and mice 7, 14, and 21 days after the first treatment with 25 μg LPS. Each bar represents the mean ± standard deviation obtained from three mice. *P<0.05, †P<0.005 *vs.* non-treated control.

topenia, hypofibrinogenemia, hyperferritinemia, and hemophagocytosis in peripheral blood, the bone marrow, and the spleen. These features are compatible with sHLH.

sHLH is a severe and potentially fatal condition that leads to overwhelming inflammation. Central to its pathogenesis is a cytokine storm with markedly increased levels of numerous proinflammatory cytokines such as IL-1β, IL-6, TNF-α, and IFN-γ. The levels of gene expression of IL-1β, IL-6, TNF-α, and IFN-γ were all markedly upregulated in the liver and spleen during the first 6 h after the first LPS treatment in both SAMR1 and SAMP1/TA-1 mice (Figure 7). However, the subsequent time course of gene expression for the cytokines in the liver and spleen were different between SAMR1 and SAMP1/TA-1 mice. Namely, the upregulation of IL-1β, IL-6, TNF-α, and IFN-γ in the liver of SAMP1/TA-1 mice was prolonged compared with that in SAMR1 mice (Figure 7A). These data suggest that prolonged overwhelming inflammation occurred in SAMP1/TA-1 mice but not in SAMR1 mice.

Macrophages commonly exist in two distinct subsets, M1 and M2 macrophages, which have opposite functions. M1 macrophages are proinflammatory, and M2 macrophages are anti-inflammatory. The M1/M2 macrophage balance governs the inflammation process.[35] LPS treatment resulted in a prolonged increase in the proportion of M1 macrophages and simultaneously a decrease in the M2 macrophage proportion in SAMP1/TA-1 mice on day 5, compared with SAMR1 mice (Figure 8). The proportions of M1 and M2 macrophages were analyzed using peritoneal macrophages, and these data also support the idea that prolonged overwhelming inflammation occurred in SAMP1/TA-1 mice.

In addition, the magnitude of the upregulation of IFN-γ in the liver and spleen was greater in SAMP1/TA-1 mice

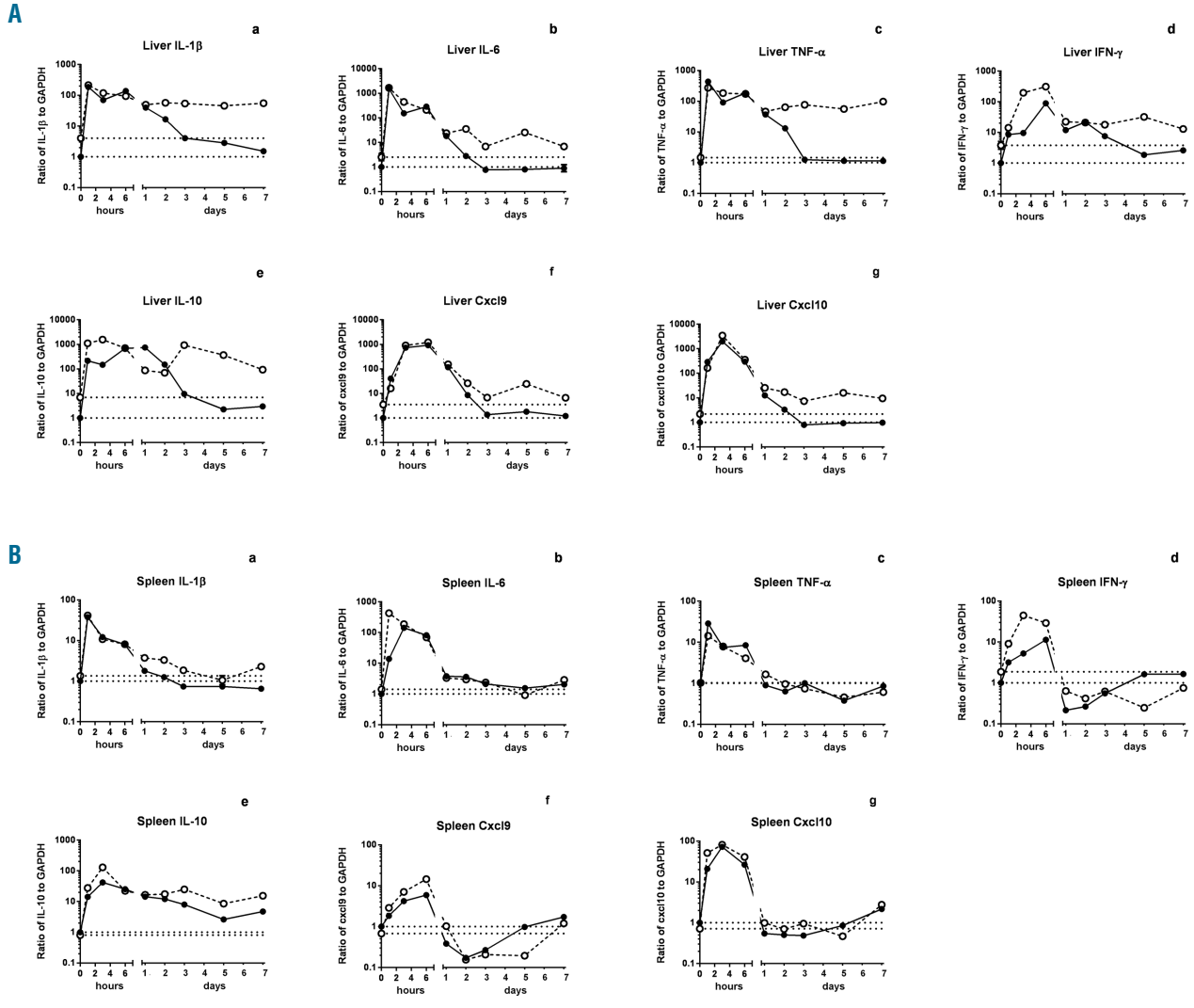

Figure 7. Changes in the levels of gene expression of cytokines and chemokines in the liver and spleen in SAMR1 and SAMP1/TA-1 mice after the first lipopolysaccharide treatment. (A, B) Changes in levels of gene expression of proinflammatory cytokines such as interleukin (IL)-1β, IL-6, tumor necrosis factor (TNF)-α, and interferon (IFN)-γ; anti-inflammatory cytokines such as IL-10; and IFN-γ-inducible chemokines such as Cxcl9 and Cxcl10 in the liver (A) and spleen (B) of SAMR1 and SAMP1/TA-1 mice after the first treatment with lipopolysaccharide (LPS). The expression levels of pro-inflammatory cytokines such as IL-1β (a), IL-6 (b), TNF-α (c), and IFN-γ (d); anti-inflammatory cytokines such as IL-10 (e); and IFN-γ-inducible chemokines such as Cxcl9 (f) and Cxcl10 (g) were evaluated in the liver (A) and spleen (B) of SAMR1 and SAMP1/TA-1 mice 1, 3, and 6 h and 1, 2, 3, 5, and 7 days after the first treatment with 25 μg LPS. Each value shown for SAMR1 (closed circles) and SAMP1/TA-1 (open circles) mice after LPS treatment is relative to the level in non-treated control SAMR1 mice. Each bar represents the mean ± standard deviation obtained from three mice.

than in SAMR1 mice (Figure 7Ad and 7Bd). The fluctuation of the expression of IFN-γ-inducible chemokine genes such as Cxcl9 and Cxcl10 in the liver and spleen of SAMP1/TA-1 mice paralleled that of IFN-γ, which indicated that functional IFN-γ was produced in the liver and spleen. In several animal models of sHLH, IFN-γ has been identified as a mediator of systemic inflammation and may play a pivotal role in the pathogenesis of sHLH, whereas the role of other cytokines is still not clear.[36,37] IL-1β, IL-6, and TNF-α are cytokines downstream of IFN-γ in a mouse model of sHLH.[36,37] Buatonis *et al.*[36] demonstrated that in an sHLH model induced by repeated toll-like receptor 9 treatment, total IFN-γ levels produced in tissues were 500- to 2,000-fold higher than those measured in blood, and they identified the liver and spleen as major sites of IFN-γ production. IFN-γ may be a critical factor in the pathogenesis of sHLH in SAMP1/TA-1 mice. However, investigation of a therapeutic approach using antibodies for proinflammatory cytokines such as IL-1β, IL-6, TNF-α, and IFN-γ in mice is necessary to clarify the central factor(s) in the pathogenesis of sHLH-like disease in LPS-treated SAMP1/TA-1 mice.

Acute systemic inflammation augments myelopoiesis but suppresses B lymphopoiesis and erythropoiesis.[22,38,39] Furthermore, acute systemic inflammation provokes rapid consumption of platelets, resulting in transient thrombocytopenia.[40,41] The numbers of peripheral white blood cells, red blood cells, and platelets in SAMP1/TA-1 mice after repeated LPS treatment decreased rapidly compared with those in SAMR1 mice (Figure 1A). When BALB/c

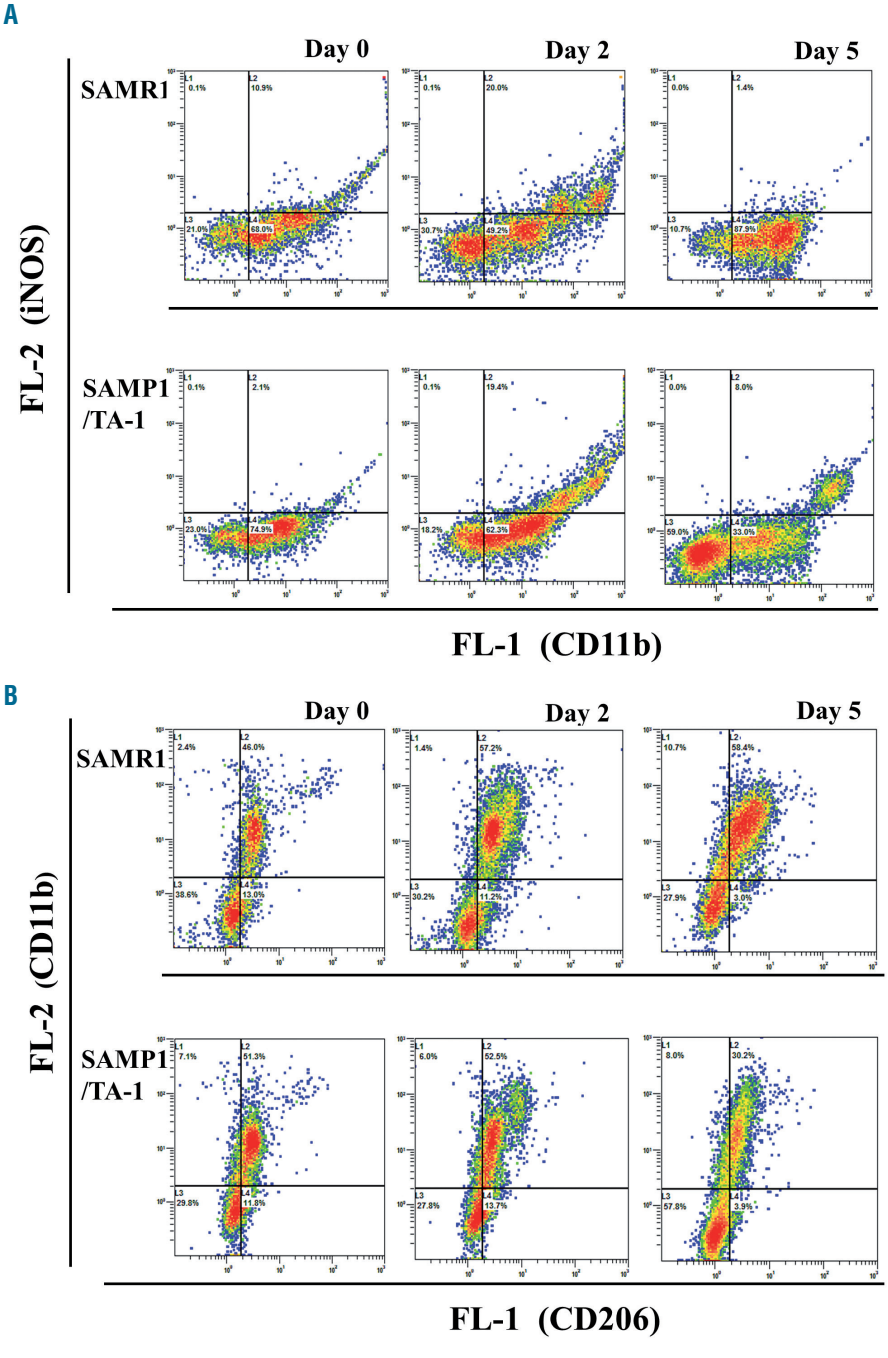

Figure 8. The proportions of M1 and M2 peritoneal macrophages in SAMR1 and SAMP1/TA-1 mice after lipopolysaccharide treatment. (A; B) The changes in the proportions of M1 cells ($CD11b^+/iNOS^+$ cells) (A) and M2 cells ($CD11b^+/CD206^+$ cells) (B) in SAMR1 and SAMP1/TA-1 mice after the first treatment with 25 μg lipopolysaccharide (LPS) were evaluated. The samples of peritoneal macrophages were obtained from non-treated control mice (day 0) and mice 2 and 5 days after the first treatment with 25 μg LPS.

mice were treated repeatedly with LPS, the numbers of white blood cells and platelets decreased rapidly after each treatment, followed by a prompt return to near or above pretreatment levels; the number of red blood cells remained unchanged.[22] Thus, the changes in the number of peripheral blood cells in SAMR1 mice after repeated LPS treatment were comparable with those in BALB/c mice after repeated LPS treatment.

The number of preB-cell progenitor cells in bone marrow was significantly decreased in SAMP1/TA-1 mice after LPS treatment, whereas the number of myeloid progenitor cells remained unchanged (Figure 6A,B). These results may indicate that the number of peripheral lymphocytes was more significantly decreased in SAMP1/TA-1 mice than in SAMR1 mice (Figure 1A). The number of erythroid progenitor cells was more significantly decreased in LPS-treated SAMP1/TA-1 mice than in LPS-treated SAMR1 mice (Figure 6C). Furthermore, the number of megakaryocyte progenitor cells in LPS-treated SAMP1/TA-1 mice was decreased, whereas the number of megakaryocyte progenitor cells in LPS-treated SAMR1 mice was increased (Figure 6D). These results suggest that severe anemia and thrombocytopenia in LPS-treated SAMP1/TA-1 mice may be in part due to profound and prolonged suppression of erythropoiesis and thrombopoiesis in the bone marrow. Taken together, the prolonged and tremendous cytokine storm induced by LPS may have disrupted the dynamics of hematopoiesis.

When repeatedly treated with LPS, ferric iron storage in the spleen of SAMP1/TA-1 mice was markedly decreased compared with that of non-treated SAMP1/TA-1 mice (Figure 4C *vs*. 4D). A similar phenomenon was observed in Typhimurium-infected mice, a model of sHLH, which showed increased erythropoiesis in the spleen.[25] When C57BL/6 mice are treated with an inflammatory compound, erythropoiesis in the spleen is accelerated, whereas erythropoiesis in the bone marrow is suppressed.[42,43] Taken together, splenic erythropoiesis in LPS-treated SAMP1/TA-1 mice may be accelerated to compensate for suppression of erythropoiesis, resulting in decreased ferric-iron storage in the spleen.

In this study, we demonstrated that SAMP1/TA-1 mice treated repeatedly with LPS develop an sHLH-like disease. SAMP1/TA-1 mice are susceptible to infection due to latent deterioration of immunological function. Bacterial infections are reported in 9% of adult cases of HLH.[44,45] LPS is a characteristic component of the wall of Gram-negative bacteria. Several cases of adult-onset sHLH associated with severe Gram-negative bacterial infection such as *Salmonella typhi, Escherichia coli, Klebsiella pneumoniae* and *Haemophils parainfluenzae* have been reported.[46-49] Thus, SAMP1/TA-1 mice are a useful model to investigate the pathogenesis of bacterial infection-associated sHLH.

Acknowledgments

The authors would like to thank Sonoko Araki and Miyuki Yuda for technical assistance. This work was supported in part by a Grant-in Aid for Scientific Research C from the Japan Society for the Promotion of Science, grant number JP18K06846.

References

1. Henter JI, Horne A, Aricó M, et al. HLH-2004: diagnostic and therapeutic guideline for hemophagocytic lymphohistiocytosis. Pediatr Blood Cancer. 2007;48(2):124-131.
2. Janka GE. Familial and acquired hemphagohistiocytosis. Annu Rev Med. 2012;(63):233-246.
3. Créput C, Galicier L, Buyse S, Azoulay E. Understanding organ dysfunction in hemophagocytic lymphohistiocytosis. Intensive Care Med. 2008;34(7):1177-1187.
4. Stepp SE, Dufourcq-Lagelouse R, Le Deist F, et al. Perforin gene defects in familial hemophagocytic lymphohistiocytosis. Science. 1999;286(5446):1957-1959.
5. Voskoboinik I, Smyth MJ, Trapani JA. Perforin-mediated target-cell death and immune homeostasis. Nat Rev Immunol. 2006;6(12):940-952.
6. Feldmann J, Callebaut I, Raposo G, et al. Munc13-4 is essential for cytolytic granules fusion and is mutated in a form of familial hemophagocytic lymphohistiocytosis (FHL3). Cell. 2003;115(4):461-473.
7. zur Stadt U, Rohr J, Seifert W, et al. Familiar hemophagocytic lymphohistiocytosis type 5 (FHL-5) is caused by mutations in Munc18-2 and impaired binding to syntaxin 11. Am J Hum Genet. 2009;85(4):482-492.
8. zur Stadt U, Schmidt S, Kasper B, et al. Linkage of familiar hemophagocytic lymphohistiocytosis (FHL) type-4 to chromosome 6q24 and identification of mutation in syntaxin 11. Hum Mol Genet. 2005;14(6):827-834.
9. Usmani GN, Woda BA, Newburger PE. Advances in understanding the pathogenesis of HLH. Br J Haematol. 2013;161(5):609-622.
10. Sawhney S, Woo P, Murray KJ. Macrophage activation syndrome: a potentially fatal complication of rheumatic disorders. Arch Dis Child. 2001;85(5):421-426.
11. Parodi A, Davi S, Pringe AB, et al. Macrophage activation syndrome in juvenile systemic lupus erythematosus. Arthritis Rheum. 2009;60(11):3388-3399.
12. Muise A, Tallett SE, Silverman ED. Are children with Kawasaki disease and prolonged fever at risk for macrophage activation syndrome? Pediatrics. 2003;112(6):e495-497.
13. Lehmberg K, Sprekels B, Nichols KE, et al. Malignancy-associated hemophagocytic lymphohistiocytosis in children and adolescents. Br J Haematol. 2015;170(4):539-549.
14. Ruscitti P, Rago C, Breda L, et al. Macrophage activation syndrome in Still's disease: analysis of clinical characteristic and survival in pediatric and adult patients. Clin Rheumatol. 2017;36(12):2839-2845.
15. Machowicz R, Janka G, Wiktor-Jedrzejczak W. Similar but not the same: differential diagnosis of HLH and sepsis. Crit Rev Oncol Hematol. 2017;114:1-12.
16. Takeda T, Hosokawa M, Takeshita S, et al. A new murine model of accelerated senescence. Mech Ageing Dev. 1981;17(2):183-194.
17. Tsuboi I, Morimoto K, Horie T, Mori KJ. Age-related changes in various hematopoietic progenitor cells in senescence-accelerated (SAM-P) mice. Exp Hematol. 1991;19(9):874-877.
18. Hosokawa T, Hosono M, Higuchi K, et al. Immune response in newly developed short-lived SAM mice I. Age-associated early decline in immune activity of cultured spleen cells. Immunology. 1987;62(3):419-423.
19. Hosokawa T, Hosono M, Hanada K, et al. Immune response in newly developed short-lived SAM mice II. Selectively impaired T–helper cell activity in in vitro antibody response. Immunology. 1987;62(3):425-429.
20. Dong L, Mori I, Hossain MJ, Kimura Y. The senescence-accelerated mouse shows aging-related defects in cellular but not humoral immunity against influenza virus infection. J Infect Dis. 2000;182(2):391-396.
21. Kumagai T, Morimoto K, Saitoh T, et al. Age-related changes in myelopoietic response to lipopolysaccharide in senescence-accelerated (SAM) mice. Mech Ageing Dev. 2000;112(2):153-167.
22. Tsuboi I, Harada T, Hirabayashi Y, Kanno J, Aizawa S. Differential regulation of lympho-myelopoiesis by stromal cells in the early and late phases in BALB/c mice repeatedly exposed to lipopolysaccharide. Biol Pharm Bull. 2016;39(12):1939-1947.
23. Tsuboi I, Hirabayashi Y, Harada T, et al. Predominant regeneration of B-cell lineage, instead of myeloid linage, of the bone marrow after 1 Gy whole-body irradiation in mice: role of differential cytokine expression

between B-cell stimulation by IL10,Flt3 ligand and IL7 and myeloid suppression by GM-CSF and SCF. Radiat Res. 2008;170 (1):15-22.
24. Tsuboi I, Hirabayashi Y, Harada T, et al. Role of hematopoietic microenvironment in prolonged impairment of B cell regeneration in age-related stromal-cell-impaired SAMP1 mouse: effects of a single dose of 5-fluorouracil. J Appl Toxicol. 2008;28(6):797-805.
25. Brown DE, McCoy MW, Pilonieta MC, Nix RN, Detweiler CS. Chronic murine typhoid fever is a natural model of secondary hemophagocytic lymphohistiocytosis. Plos One. 2010;5(2):e9441.
26. Reinhardt RL, Liang HE, Bao K, et al. A novel model for IFN-γ-mediated autoinflammatory syndrome. J Immunol. 2015;194 (5):2358-2368.
27. Girard-Guyonvarc'h C, Palomo J, Martin P, et al. Unopposed IL-18 signaling leads to severe TLR9-induced macrophage activation syndrome in mice. Blood. 2018;131(13):1430-1441.
28. Jordan MB, Hildeman D, Kappler J, Marrack P. An animal model of hemophagocytic lymphohistiocytosis (HLH):CD8+ T cells and interferon gamma are essential for the disorder. Blood. 2004;104(3):735-743.
29. Pachlopnik Schmid J, Ho CH, Chrétien F, et al. Neutralization of IFNgamma defeats hemophagocytosis in LCMV-infected perforin- and Rab27a-deficient mice. EMBO Mol Med. 2009;1(2):112-124
30. Crozat K, Hoebe K, Ugolini S, et al. Jinx, an MCMV susceptibility phenotype caused by disrupt of Unc13d: a mouse model of type 3 familial hemophagocytic lymphohistiocytosis. J Exp Med. 2007;204(4):853-863.
31. Sato K, Misawa N, Nie C, et al. A novel animal model of Epstein-Barr virus-associated hemophagocytic lymphohistiocytosis in humanized mice. Blood. 2011;117(21):5663-5673.
32. Brisse E, Imbrechts M, Put K, et al. Mouse cytomegalovirus infection in BALB/c mice resembles virus-associated secondary hemophagocytic lymphohyistiocytosis and shows a pathogenesis distinct from primary hemophagocytic lymphohistiocytosis. J Immunol. 2016;196(7):3124-3134.
33. Behrens EM, Canna SW, Slade K, et al. Repeated TLR9 stimulation results in macrophage activation syndrome–like disease in mice. J Clin Invest. 2011;121(6):2264-2277.
34. Strippoli R, Carvello F, Scianaro R, et al. Amplification of response to toll-like receptor ligands by prolonged exposure to interleukin-6 in mice. Arthritis Rheum. 2012;64(5):1680-1688.
35. Sica A, Mantovani A. Macrophage plasticity and polarization in vivo veritas. J Clin Invest. 2012;122(3):787-795.
36. Buatois V, Chatel L, Cons L, et al. Use of a mouse model to identify a blood biomarker for IFNγ activity in pediatric secondary hemophagocytic lymphohistiocytosis. Transl Res. 2017;180:37-52.e2.
37. Prencipe G, Caiello I, Pascarella A, et al. Neutralization of IFN-γ reverts clinical and laboratory features in a mouse model of macrophage activation syndrome. J Allergy Clin Immunol. 2018;141(4):1439-1449.
38. Aisaki K, Tsuboi I, Harada T, et al. Neopterin, inflammation–associated product, prolongs erythropoiesis suppression in aged SAMP1 mice due to senescent stromal-cell impairment. Exp Biol Med. 2012;237(3):279-286.
39. Taki M, Tsuboi I, Harada T, et al. Lipopolysaccharide reciprocally alters the stromal cells-regulated positive and negative balance between myelopoiesis and B-lymphopoiesis in C57BL/6 mice. Biol Pharm Bull. 2014;37(12):1872-1881.
40. Tacchini-Cottier F, Vesin C, Redard M, Buurman W, Piguet PF. Role of TNFR1 and TNFR2 in TNF-induced platelet consumption in mice. J Immunol. 1998;160(12):6182-6186.
41. Stohlawetz P, Folman CC, von dem Borne AE, et al. Effects of endotoxemia on thrombopoiesis in men. Thromb Haemost. 1999;81(4):613-617.
42. Tsuboi I, Harada T, Hirabayashi Y, et al. Inflammatory biomarker, neopterin, predominantly enhanced myelopoiesis, which suppressed erythropoiesis via activated stromal cells. Immunobiology. 2010;215(5):348-355.
43. Tsuboi I, Harada T, Oshima H, Aizawa S. Effect of neopterin on splenic erythropoiesis in mice. Pteridies. 2010;21(1):7-10.
44. Ramos-Casals M, Brito-Zerón P, López-Guillermo A, Khamashta MA, Bosch X. Adult hemophagocytic syndrome. Lancet. 2014;383(9927):1503-1516.
45. Brisse E, Wouters GH, Matthys P. Advances in the pathogenesis of primary and secondary haemophagocytic lymphohistiocytosis: differences and similarities. Br J Haematol. 2016;174(2):203-217.
46. Non LR, Patel RP, Esmaeeli PA, Despotovic V. Typhoid fever complicated by hemophagocytic lymphohistiocytosis and rhabdo. Am J Trop Med Hyg. 2015;93(5):1068-1069.
47. Chang KH, Tang LM, Lyu RK Spontaneous Escherichia coli meningitis associated with hemophagocytic lymphohistiocytosis. J Formos Med Assoc. 2006;105(9):756-759.
48. Liao YT, Ko PS, Lin YT. The first case of klebsiella pneumoniae liver abscess with hemophagocytic lymphohistiocytosis. J Microbiol Immuol Infect. 2019;52(2):363-364.
49. Costescu Strachinaru DI, Chaumont M, Gobin D, et al. Hemophagocytic lymphohistiocytosis associated to Haemophilus parainfluenzae endocarditis - a case report. Acta Clin Belg. 2018:73(3):220-223.

Ferrata Storti Foundation

Arrayed molecular barcoding identifies TNFSF13 as a positive regulator of acute myeloid leukemia-initiating cells

Marion Chapellier,[1] Pablo Peña-Martínez,[1] Ramprasad Ramakrishnan,[1] Mia Eriksson,[1] Mehrnaz Safaee Talkhoncheh,[2] Christina Orsmark-Pietras,[1] Henrik Lilljebjörn[1], Carl Högberg,[1] Anna Hagström-Andersson,[1] Thoas Fioretos,[1] Jonas Larsson,[2] and Marcus Järås[1]

[1]Department of Clinical Genetics and [2]Molecular Medicine and Gene Therapy, Lund Stem Cell Center, Lund University, Lund, Sweden

Haematologica 2019
Volume 104(10):2006-2016

ABSTRACT

Dysregulation of cytokines in the bone marrow (BM) microenvironment promotes acute myeloid leukemia (AML) cell growth. Due to the complexity and low throughput of *in vivo* stem-cell based assays, studying the role of cytokines in the BM niche in a screening setting is challenging. Here, we developed an *ex vivo* cytokine screen using 11 arrayed molecular barcodes, allowing for a competitive *in vivo* readout of leukemia-initiating capacity. With this approach, we assessed the effect of 114 murine cytokines on *MLL-AF9* AML mouse cells and identified the tumor necrosis factor ligand superfamily member 13 (TNFSF13) as a positive regulator of leukemia-initiating cells. By using *Tnfsf13*$^{-/-}$ recipient mice, we confirmed that TNFSF13 supports leukemia initiation also under physiological conditions. TNFSF13 was secreted by normal myeloid cells but not by leukemia mouse cells, suggesting that mature myeloid BM cells support leukemia cells by secreting TNFSF13. TNFSF13 supported leukemia cell proliferation in an NF-κB-dependent manner by binding TNFRSF17 and suppressed apoptosis. Moreover, TNFSF13 supported the growth and survival of several human myeloid leukemia cell lines, demonstrating that our findings translate to human disease. Taken together, using arrayed molecular barcoding, we identified a previously unrecognized role of TNFSF13 as a positive regulator of AML-initiating cells. The arrayed barcoded screening methodology is not limited to cytokines and leukemia, but can be extended to other types of *ex vivo* screens, where a multiplexed *in vivo* read-out of stem cell functionality is needed.

Correspondence:

MARCUS JÄRÅS
marcus.jaras@med.lu.se

Received: February 27, 2018.

Accepted: February 21, 2019.

Pre-published: February 28, 2019.

doi:10.3324/haematol.2018.192062

Check the online version for the most updated information on this article, online supplements, and information on authorship & disclosures: www.haematologica.org/content/104/10/2006

Introduction

Acute myeloid leukemia (AML) is characterized by an accumulation of immature myeloid blasts in the bone marrow (BM).[1] By providing cell-cell interactions and secreted factors, the BM niche supports AML and normal hematopoietic stem and progenitor cells (HSPC).[1,2] A dysregulation of cytokines in the BM microenvironment upon AML development contributes to the selective advantage of leukemia stem cells,[1] a self-renewing population of leukemia cells that constitutes a chemoresistant reservoir responsible for disease relapse.[3]

To identify factors that regulate AML cells, we recently developed an *in vitro* cytokine screen using fluorescently labeled c-Kit^{+} leukemia cells mixed with corresponding normal BM cells, allowing us to successfully identify both negative and positive regulators of AML cells.[4] However, to assess effects on leukemia stem cells, there is a strong demand to improve such screens to evaluate the impact of cytokines on the leukemia-initiating capacity of cells more directly using an *in vivo* readout. A major challenge for combining *ex vivo* screens with *in vivo* read-out of stem cell function is the large number of experimental animals needed to provide meaningful data. Hence, new methods that allow for a multiplexed *in vivo* read-out

of leukemia-initiating activity are needed. Molecular barcoding strategies, combined with next-generation sequencing (NGS), enable an *in vivo* readout of stem cell function in a competitive setting.[5-7] By using this strategy, the *in vivo* cell fate of multiple hematopoietic stem cells (HSC) or leukemia clones can be monitored on a clonal level.[5,8] However, because these approaches use pooled barcoded libraries, the *in vivo* cell fate of the genetically marked stem cell clones within mice cannot be traced to separate experimental conditions, such as cytokine stimulations.

In this study, we created a library of 11 arrayed molecular barcodes that were used to mark leukemia cells exposed to 114 separate cytokine conditions. The 11 barcoded leukemia cell populations were then pooled and injected into mice allowing for an *in vivo* competition read-out of leukemia-initiating activity. By using this methodology, we identified the tumor necrosis factor ligand superfamily member 13 (TNFSF13; also named, A proliferation-inducing ligand, APRIL) as a novel positive regulator of leukemia-initiating cells. TNFSF13 promoted AML cell growth by suppressing apoptosis and activating nuclear factor kappa B (NF-κB).

Methods

Murine leukemia model

MLL-AF9 (KMT2A-MLLT3) leukemias were generated on a *dsRed*$^+$ C57BL/6 transgenic background (6051; Jackson Laboratory, Bar Harbor, ME, USA), as previously described.[9,10] Experiments involving murine leukemia cells were performed using tertiary or quaternary transplanted leukemia cells serially propagated in sublethally irradiated (600 cGy) recipient mice. All animal experiments were conducted according to an Animal Care and Use Committee protocol approved by the Lund/Malmö Ethical Committee. Except for the propagation of leukemia cells, all experiments involving murine leukemia cells were performed using c-Kit$^+$ bone marrow cells. For details on the c-Kit$^+$ cells isolation and cell culture conditions, see the *Online Supplementary Methods.*

Generation of 11 lentiviral vectors containing molecular barcodes

To generate lentiviral vectors containing non-expressed molecular barcodes, we used a lentiviral pLKO.1 vector (Addgene #32684) that co-expressed a short hairpin RNA (shRNA) and a green fluorescent protein (GFP) marker gene.[11] The shRNA sequence, along with its promotor, was replaced by genetic barcodes (42 to 46 nucleotides) flanked by 23mer primer sequences using the *Nde1* and *EcoR1* restriction sites (*Online Supplementary Table S1*). Viral vectors with VSV-g pseudotyping were produced using standard protocols.

Ex vivo cytokine screening using barcoded leukemia cells

Freshly isolated c-Kit$^+$ dsRed$^+$ leukemia cells were transduced with the barcoded lentiviral vectors and exposed to the cytokine library of 114 cytokines (*Online Supplementary Table S2*) in 96-well plates. After 72 hours, cells from different wells were pooled, with each pool containing leukemia cells from up to 11 barcoded populations representing specific culture conditions, and injected into sublethally irradiated (600 cGy) recipient C57BL/6 mice *via* tail vein injection. After 7-12 days, mice were sacrificed, BM cells were harvested, and DNA was extracted (Qiagen Blood and Tissue DNA Extraction Kit). For details on the screen see the *Online Supplementary Methods*.

Sequencing of barcodes and bioinformatics analysis

Following BM cell extraction and DNA purification (DNAeasy Blood and Tissue Kit, Qiagen), the regions containing the barcodes were amplified using two-step polymerase chain reaction (PCR). Step one utilized pLKO.1-specific primers containing Nextera overhangs (*Online Supplementary Table S3*). The number of reads per barcode of each sample was extracted and normalized to the total read count within each sample. The mean of the three biological replicates was then calculated after normalization to the input (Day 0). For further details on the sequencing and bioinformatics, see the Online *Supplementary Methods*.

Tnfsf13$^{-/-}$ mouse model

The C57BL/6 *Tnfsf13*$^{-/-}$ mouse (#022971; B6.*Cg-Tnfsf13tm1Pod/J*)[12,13] was obtained from The Jackson Laboratory (Bar Harbor, Maine, USA) and further backcrossed (>5 generations) onto C57BL/6 wild-type mice. Genotyping was performed by PCR using protocols provided by the Jackson Laboratory.

Retroviral *MLL-AF9* expression in c-Kit$^+$ bone marrow cells and transplantations into sublethally irradiated mice

Murine stem cell virus gammaretroviral vectors co-expressing *MLL-AF9* and *GFP* (MIG-MLL-AF9)[14] were produced with an ecotropic envelope using standard protocols in 293T cells. c-Kit$^+$ BM cells were pre-stimulated for two days and spinoculated. Following overnight incubation at 37°C, transduced cells were injected into sublethally irradiated (600 cGy) recipient mice *via* tail vein injection. Each recipient mouse received cells corresponding to 250,000 initially seeded cells. Blood samples were taken after 40 days, and mice were sacrificed when they showed signs of disease. To assess leukemia development in sublethally irradiated (600 cGy) secondary recipient mice, 1,000 or 10,000 spleen leukemia cells from primary recipients were injected *via* the tail vein. For details on the transduction of c-Kit$^+$ BM cells, see the *Online Supplementary Methods.*

Flow cytometric analysis and cell sorting

The flow cytometric analyses were performed using a FACS Canto II (BD Biosciences, San Jose, CA, USA) or a FACS LSRFortessa (BD Biosciences), and cell sorting was performed using a FACS Aria II (BD Biosciences). For detailed information on antibodies used and staining for LSK and HSPC analysis, cell cycle, apoptosis and phosphoflow, see the *Online Supplementary Methods*.

Statistical analysis

Prism 6 (Graphpad) was used for the statistical analyses, including Student *t*-test and Kaplan-Meier survival analysis. Statistical significance is shown with asterisks: $^*P<0.05$; $^{**}P<0.01$; $^{***}P<0.001$; $^{****}P<0.0001$. Data are presented as mean±Standard Deviations (SD).

Results

Development of an *ex vivo* cytokine screen with a competitive *in vivo* read-out of leukemia-initiating activity using molecularly barcoded leukemia cells

To identify cytokines that regulate AML stem cells using a competitive *in vivo* read-out of leukemia-initiating activity, we generated lentiviral vectors harboring genetic barcodes in an arrayed setting. This approach allows for

labeling of leukemia cell populations with distinct molecular barcodes followed by exposure to separate experimental conditions. Each labeled cell population was stimulated with one cytokine *ex vivo* and after culture, leukemia cells from multiple cytokine conditions were pooled prior to *in vivo* competition. To trace the effects of the cytokines to the leukemia-initiating capacity of barcoded cells, the representation of individual barcodes *in vivo* was assessed using NGS (Figure 1A).

To allow for *in vivo* competition of up to 11 barcoded cell populations, we generated 11 lentiviral vectors with unique molecular barcodes and GFP as a marker gene (*Online Supplementary Table S1*). The barcodes were used to mark c-Kit$^+$ murine *MLL-AF9* AML cells generated on a dsRed transgenic background (Figure 1A and *Online Supplementary Figure S1A*). We have previously used these cells in screens because they have a well-defined leukemia-initiating cell population and initiate AML with a short latency, enabling rapid follow-up experiments in syngeneic hosts.[4,9,10,14,15]

To validate the robustness of the new methodology, 11 barcoded c-Kit$^+$ leukemia cell populations were exposed separately for three days to stem cell factor (SCF), which binds c-Kit and activates signaling that promotes leukemia-initiating cells.[16] Leukemia cells from the 11 barcoded cell populations were then pooled and injected into sublethally irradiated mice for *in vivo* competition of leukemia-initiating activity. Seven days post transplantation, mice were sacrificed, their BM was harvested, and DNA was extracted. We found that the 11 barcoded variants showed a similar distribution with less than 2-fold variability in the input pool relative to the *in vivo* pool (range: 0.51- to 1.65-fold), demonstrating that the arrayed barcoding methodology was robust in assessing the leukemia-initiating activity of the AML cells following *ex vivo* culture (Figure 1B).

Identification of TNFSF13 as a positive regulator of acute myeloid leukemia-initiating cells

To assess the impact of a library of 114 murine cytokines on c-Kit$^+$ MLL-AF9 leukemia cells, we performed two arrayed *ex vivo* cytokine screens, in which each cytokine was assessed in triplicate wells (*Online Supplementary Table S2*). After three days of *ex vivo* cytokine stimulation, up to 11 cytokine conditions of barcoded leukemia cells were pooled and injected into recipient mice (Figure 1A). As an internal positive control, for each pool, we stimulated one of the barcoded cell populations with SCF. The mice were sacrificed on day 7 (screen I) or day 12 (screen II) post transplantation, and engraftment of transduced leukemia cells was confirmed by assessing the frequency of GFP positive cells within dsRed$^+$ cells (*Online Supplementary Figure S1B and C*). As predicted, barcoded leukemia cells stimulated with SCF

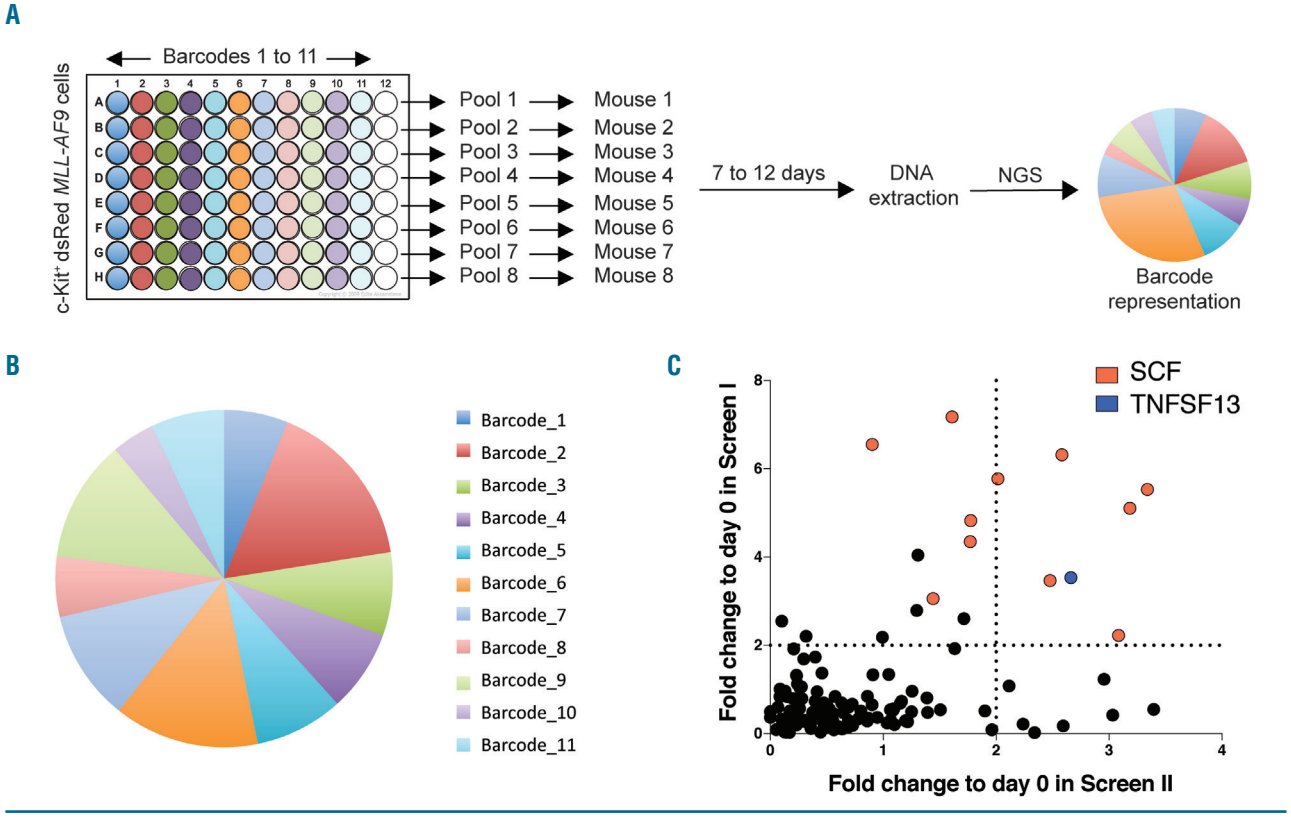

Figure 1. A barcoded cytokine screen identifies TNFSF13 as a positive regulator of acute myeloid leukemia (AML)-initiating cells. (A) Schematic flowchart depicting the arrayed barcoded *ex vivo* cytokine screen with AML cells. In total, 12 pools in triplicate were used to screen the entire cytokine library. After seven (screen I) or 12 (screen II) days, mice were sacrificed. Data were normalized to the input representation for each barcode. (B) Pie chart displaying the contribution of each barcoded cell population *in vivo* following *ex vivo* cultures with stem cell factor (SCF) only for all barcoded cell populations. (C) Scatter plot showing fold-change *in vivo versus* input of barcoded cell populations for the two screens. Dotted lines represent a fold-change threshold of 2 to identify cytokines that promote leukemia-initiating cells. Red dots: barcoded cell populations stimulated *ex vivo* with SCF as the positive control within each pool; blue dots: cells stimulated with TNFSF13. NGS: next-generation sequencing.

showed a relative increase within all pools *in vivo*, thus validating the new method (Figure 1C). Although a number of cytokines, such as interleukin-3 (IL3) and granulocyte-macrophage colony-stimulating factor (GM-CSF), that greatly expand (>20-fold over 3 days) AML cells in culture were included in the screen,[4] none of them expanded the leukemia-initiating cell population as assessed with *in vivo* read-out (*Online Supplementary Table S3*). This finding highlights the need for *in vivo* readout to assess the impact of cytokines on the leukemia-initiating capacity of the cells. Setting a threshold for 2-fold enrichment, TNFSF13 was the only cytokine, other than SCF, that scored in both screens (on average a 3.1-fold relative increase). In addition, the screens identified Interleukin 9 (IL9) as a candidate positive regulator (1.8 relative increase) of leukemia-initiating cells (*Online Supplementary Table S2*). Moreover, several negative regulators of leukemia-initiating cells were identified that were not further investigated in the present study (*Online Supplementary Table S2*).

Ex vivo stimulation with TNFSF13 or IL9 promotes leukemia-initiating cells

To validate the findings from the screen and first explore TNFSF13 as a regulator of primitive AML cells, we cultured c-Kit$^+$ *MLL-AF9* leukemia cells with increasing doses of TNFSF13. TNFSF13 supported the growth and survival of c-Kit$^+$ leukemic cells in culture (Figure 2A and *Online Supplementary Figure S2A*), but did not affect normal HSPC, as assessed by analyzing the effect of TNFSF13 on Lin$^-$Sca-1$^+$ c-Kit$^+$ (LSK) BM cells from healthy mice (Figure 2B). Moreover, *ex vivo* stimulation of c-Kit$^+$ leukemia cells with TNFSF13, followed by transplantation into sublethally irradiated mice, resulted in significantly higher levels of circulating leukemia cells in peripheral blood (mean 25.6% *vs.* 1.3% for non-stimulated cells; $P<0.0001$) (Figure 2C and D). Notably, the numbers of circulating leukemia cells were even higher than for mice that had received leukemia cells that were stimulated with SCF as a positive control (25.6% *vs.* 7.8%; $P<0.01$) (Figure 2D). Consistent with this finding, the TNFSF13-treated group exhibited reduced survival (median survival 29 *vs.* 38 days for the non-stimulated group; $P<0.0001$) (Figure 2E) and survival was even slightly shorter than for the SCF-treated group (Figure 2E). At the time of sacrifice, all except for one control mouse had a high leukemic burden, as confirmed by enlarged spleens and a high percentage of leukemia cells (>95% dsRed$^+$ cells) in their BM (*Online Supplementary Figure S2B and C*). Consistent with the findings in the

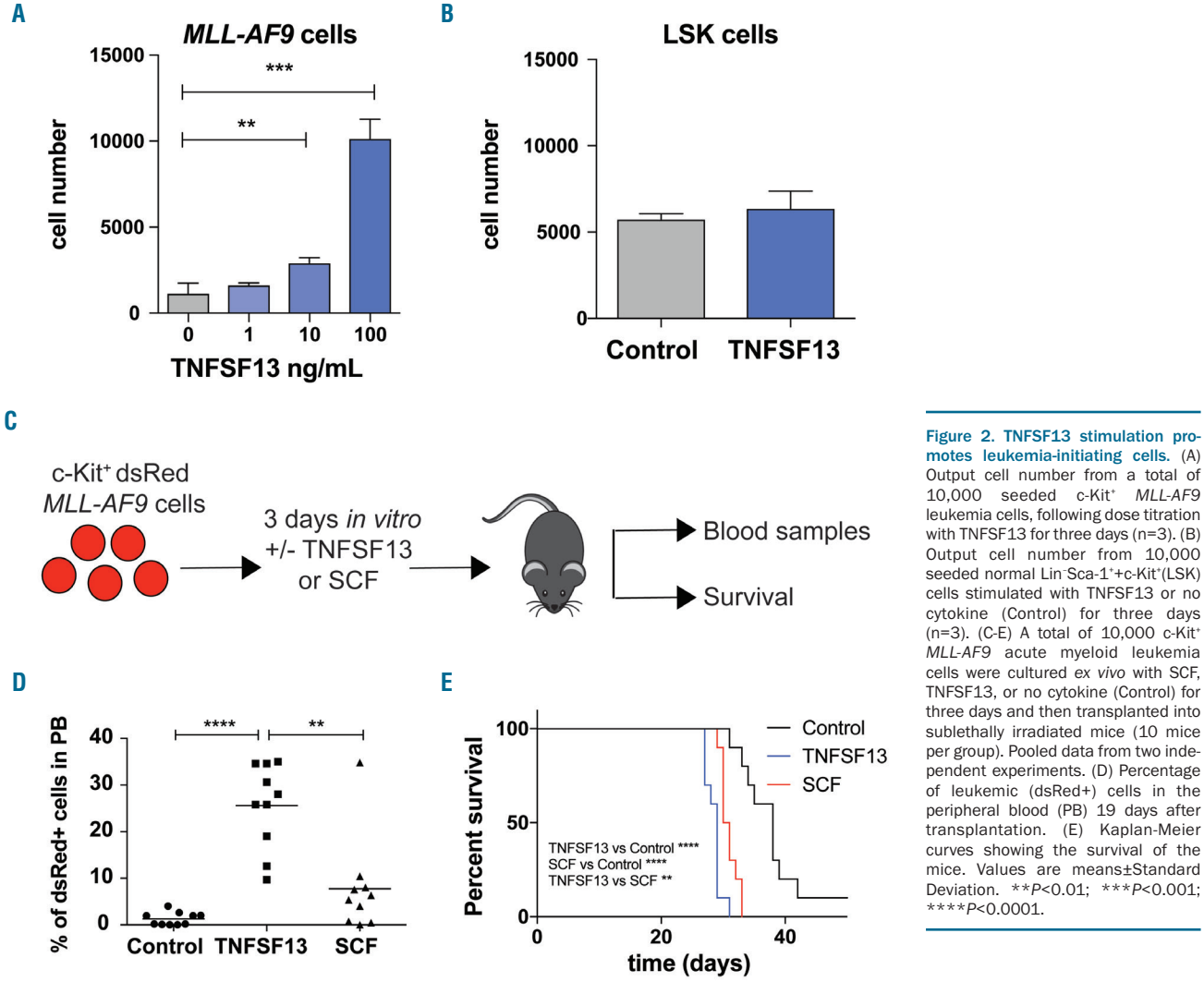

Figure 2. TNFSF13 stimulation promotes leukemia-initiating cells. (A) Output cell number from a total of 10,000 seeded c-Kit$^+$ *MLL-AF9* leukemia cells, following dose titration with TNFSF13 for three days (n=3). (B) Output cell number from 10,000 seeded normal Lin$^-$Sca-1$^+$+c-Kit$^+$(LSK) cells stimulated with TNFSF13 or no cytokine (Control) for three days (n=3). (C-E) A total of 10,000 c-Kit$^+$ *MLL-AF9* acute myeloid leukemia cells were cultured *ex vivo* with SCF, TNFSF13, or no cytokine (Control) for three days and then transplanted into sublethally irradiated mice (10 mice per group). Pooled data from two independent experiments. (D) Percentage of leukemic (dsRed+) cells in the peripheral blood (PB) 19 days after transplantation. (E) Kaplan-Meier curves showing the survival of the mice. Values are means±Standard Deviation. $^{**}P<0.01$; $^{***}P<0.001$; $^{****}P<0.0001$.

screen, IL9 also supported the growth of leukemic cells *in vitro* (*Online Supplementary Figure S3A*) and *ex vivo* stimulation of c-Kit$^+$ leukemia cells with IL9 prior to transplantation into mice resulted in elevated levels of leukemia cells in the blood and reduced survival compared to controls (*Online Supplementary Figure S3B and C*). Taken together, these observations validate our barcoded screening strategy and demonstrate that primarily TNFSF13, but also IL9, support AML-initiating cells.

Myeloid cells secrete TNFSF13

To assess the *in vivo* relevance of TNFSF13 in the context of AML, we measured TNFSF13 levels in the peripheral blood (PB) and BM of healthy control and leukemic mice. TNFSF13 was present at physiologically relevant levels in the PB and BM of both leukemic and healthy mice but at significantly higher levels in the blood of healthy control mice (Figure 3A and B). To determine whether TNFSF13 is secreted by AML cells or provided by cells in the microenvironment, normal c-Kit$^+$ cells and AML BM cells were cultured for three days in suspension cultures under conditions favoring myeloid (Gr-1$^+$CD11b$^+$) cell growth (Figure 3C), and *TNFSF13* expression in cells and TNFSF13 levels in the supernatants were analyzed. We found that normal myeloid BM cells expressed high levels of TNFSF13 (>240 ng/mL in supernatant), whereas leukemic cells did not (<10 ng/mL in supernatant), suggesting that non-leukemic myeloid cells support AML cells by secreting TNFSF13 (Figure 3D and E).

Tnfsf13$^{-/-}$ mice have myelopoiesis defects

To investigate the physiological role of TNFSF13 in an *in vivo* context, we used *Tnfsf13*$^{-/-}$ mice, which previously have mainly been characterized regarding cytokine regu-

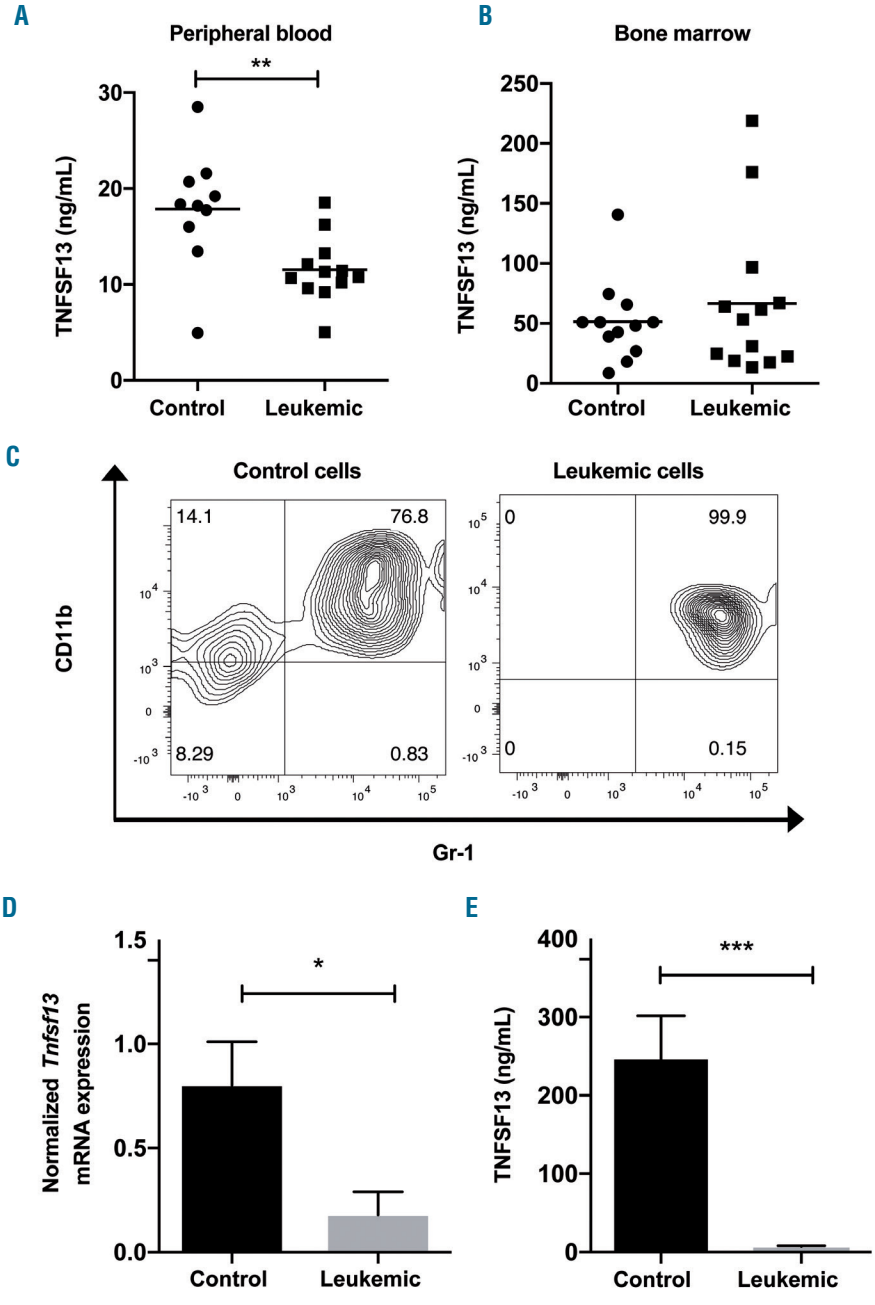

Figure 3. TNFSF13 is present in the bone marrow and peripheral blood and is secreted by myeloid cells. ELISA quantification of TNFSF13 in (A) blood plasma samples from healthy (10 mice) and leukemic mice (12 mice) and (B) bone marrow samples from healthy (12 mice) and leukemic mice (13 mice). (C-E) c-Kit$^+$ normal (control) and c-Kit$^+$ leukemic bone marrow cells were cultured for three days under conditions favoring myeloid cell growth. (C) Representative dot plots showing expression of CD11b and Gr-1 on control and leukemic bone marrow cells after three days of culture. (D) *Tnfsf13* mRNA expression in control and leukemic bone marrow cells determined by real-time polymerase chain reaction and normalized to a control sample after three days of culture (n=3 per group). (E) ELISA quantification of TNFSF13 in supernatants of normal or leukemic c-Kit$^+$ bone marrow cells cultured for three days (n=8 per group). Values are means±Standard Deviation. *P<0.05; **P<0.01; ***P<0.001.

lation and T-cell biology.[12,13] No change in white blood cell count, red blood cell count, or platelet levels was observed in *Tnfsf13*$^{-/-}$ mice (*Online Supplementary Table S4*). We then characterized their HSPC compartment and the lineage distribution in the BM and PB (*Online Supplementary Figure S4A and B*). Whereas long- and short-term HSC numbers were not affected, a significant decrease in granulocyte and macrophage progenitor (GMP) cells, accompanied by reduced numbers of monocytes, and a trend towards lower levels of granulocytes, was observed (Figure 4A-D, *Online Supplementary Table S4* and *Online Supplementary Figure S4A and B*). Moreover, a skewing towards more B cells and fewer T cells was detected in the BM, whereas in the PB, only T cells were significantly altered (*Online Supplementary Table S4*). These data indicate that TNFSF13 supports the formation of GMP cells and that it favors myeloid and T-cell development relative to B cells.

TNFSF13 is a ligand for two cell-surface receptors: TNF receptor superfamily member 13B (TNFRSF13B) and 17 (TNFRSF17).[17] Whereas TNFRSF17 was expressed on c-Kit^{+} leukemia cells, these cells were devoid of TNFRSF13B expression (Figure 4E and F). On normal HSPC, and in mature lineages of the BM and PB, TNFRSF17 was more broadly expressed than TNFRSF13B (Figure 4G and H and *Online Supplementary Figure S4C-G*). TNFRSF17 expression was detected in several mature blood cell lineages and multiple progenitor cell populations, with the lowest expression detected on long-term HSC (Figure 4G and H and *Online Supplementary Figure S4C and D*). These data suggest that TNFRSF17 is the primary receptor for TNFSF13 on murine AML cells and a putative receptor for TNFSF13 on normal murine myeloid progenitor cells and monocytes.

TNFSF13 promotes acute myeloid leukemia initiation by suppressing apoptosis and promoting active cell cycle progression

To assess whether TNFSF13 supports leukemia-initiation and progression *in vivo*, c-Kit^{+} *Tnfsf13*$^{-/-}$ BM cells were transduced with a gamma retroviral vector expressing MLL-AF9 and transplanted into sublethally irradiated *Tnfsf13*$^{+/+}$ or *Tnfsf13*$^{-/-}$ recipient mice (Figure 5A). A 2.1-fold-lower (P<0.01) leukemic burden was detected in the PB of *Tnfsf13*$^{-/-}$ recipient mice six weeks post transplantation, but no significant survival difference was observed between the two groups (Figure 5B and C and *Online Supplementary Figure S5A and B*). To study whether TNFSF13 supports AML maintenance *in vivo*, 10,000 or 1,000 leukemia cells harvested from spleens of primary recipients of each group were transplanted into corresponding *Tnfsf13*$^{+/+}$ or *Tnfsf13*$^{-/-}$ secondary recipient mice (Figure 5A). Interestingly, while no significant difference in survival was observed between the groups when transplanting 10,000 leukemia cells (*Online Supplementary Figure S5C*), *Tnfsf13*$^{-/-}$ recipients showed an extended survival compared to *Tnfsf13*$^{+/+}$ recipients when 1,000 leukemia cells were transplanted (mean of 28.5 *vs.* 34.5 days; P=0.0235) (Figure 5D). These data indicate that TNFSF13 supports AML initiation and maintenance under physiological conditions.

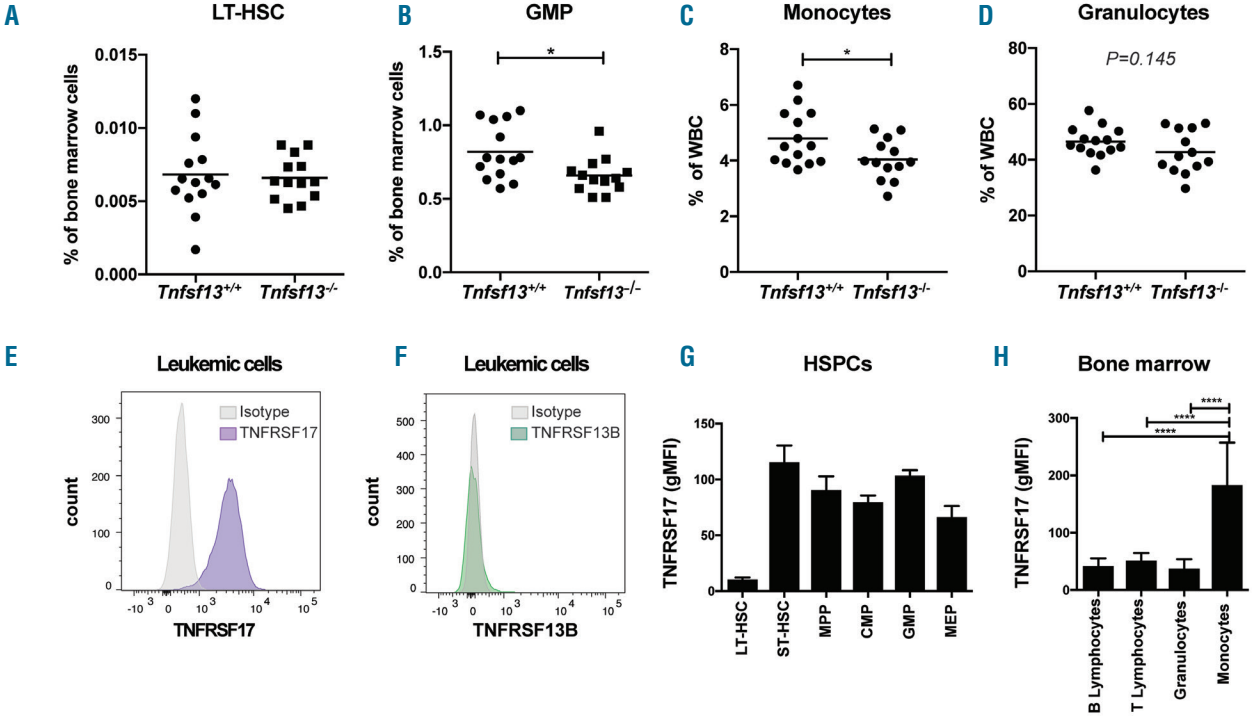

Figure 4. *Tnfsf13*$^{-/-}$ mice have myelopoiesis defects and acute myeloid leukemia cells express TNFRSF17. Frequency of (A) long-term hematopoietic stem cells (LT-HSC), (B) granulocyte and macrophage progenitor (GMP) cells, (C) monocytes, and (D) granulocytes in the bone marrow of *Tnfsf13*$^{+/+}$ (n=14) and *Tnfsf13*$^{-/-}$ (n=13) mice. Flow cytometric analysis showing (E) TNFRSF17 (purple) and (F) TNFRSF13B (green) expression on c-Kit^{+} MLL-AF9 leukemic cells. Isotype control is shown in light gray. TNFRSF17 geometric mean fluorescent intensity (gMFI) expression within (G) hematopoietic stem and progenitor cells (HSPC) (n=5) and (H) lineage populations (n=10) in the bone marrow of normal mice, after subtracting the signal using matching isotype control antibodies. Values are means±Standard Deviation. *P<0.05; ****P<0.0001. WBC: white blood cells.

To explore the biological mechanisms by which TNFSF13 promotes AML cells, we investigated whether TNFSF13 affects the apoptosis and cell cycle status of c-Kit$^+$ leukemia cells. We found that TNFSF13 stimulation had an anti-apoptotic effect, with both early and late apoptotic cells being reduced (Figure 6A and B). The anti-apoptotic effects were also accompanied by an increase in actively cycling cells (Figure 6C and D). Collectively, these data indicate that TNFSF13 supports AML cells by suppressing apoptosis and promoting active cell cycle progression.

TNFSF13 promotes human acute myeloid leukemia cells by suppressing apoptosis

To assess whether TNFSF13 also stimulates human AML cells, we analyzed the sensitivity of nine human myeloid leukemia cell lines to TNFSF13. Upon serum deprivation, we found that TNFSF13 significantly supported the growth and survival of six of the nine cell lines and TNFSF13 was confirmed to bind to the cell surface of the AML cells (Figure 7A and B and *Online Supplementary Figure S6A and B*). To efficiently bind to TNFRSF13B or TNFRSF17, TNFSF13 binds to heparan sulfate proteoglycans (HSPG), which facilitates TNFSF13 oligomerization.[18] In accordance with this, we detected expression of the proteoglycan SYNDECAN-1 (CD138) on Mono-Mac-6 cells (Figure 7C). Further, as previously described,[18,19] the binding of TNFSF13 to HSPG was blocked by heparin (Figure 7D). Moreover, consistent with the effect observed on murine c-Kit$^+$ leukemia cells, TNFSF13 stimulation suppressed apoptosis in the AML cell line Mono-Mac-6 (Figure 7E and *Online Supplementary Figure S6C*), but did not significantly affect the cell cycle (*Online Supplementary Figure S6D*). In accordance with murine AML cells, TNFRSF13B was not expressed on human AML cell lines, whereas TNFRSF17 was detected on 3 of 9 of the myeloid leukemia cell lines by flow cytometry, and in 7 of 9 of cell lines by real-time PCR, albeit at low levels (*Online Supplementary Figure S6E and H*).

To investigate which of the two receptors is the most prominent on AML patient cells, we analyzed their expression pattern in AML patient data from the TCGA database.[20] Similar to the c-Kit$^+$ murine leukemia cells and human cell line data, *TNFRSF17* was expressed at significantly higher levels than *TNFRSF13B* (*Online Supplementary Figure S6I*). In addition, we observed a higher relative expression of both *TNFRSF13B* and *TNFRSF17* in *RUNX1*-mutated (2.5- and 2.6-fold change, respectively) and *TP53*-mutated (3.5- and 3.2-fold change, respectively) AML patients, two genetic subtypes associated with a dismal outcome (*Online Supplementary Table S5*).[21-23] These findings demonstrate that TNFSF13 also promotes human AML cells *in vitro* by suppressing apoptosis, and suggest that TNFRSF17 is the primary receptor for TNFSF13 on human AML cells.

TNFSF13B promotes proliferation of human acute myeloid leukemia cells

We also evaluated the role of TNFSF13B (BAFF) in AML, another ligand for TNFRSF17. TNFSF13B levels were approximately 100-fold lower than TNFSF13 levels in the mouse BM (Figure 3B and *Online Supplementary Figure S7A*), whereas similar levels of the two cytokines were

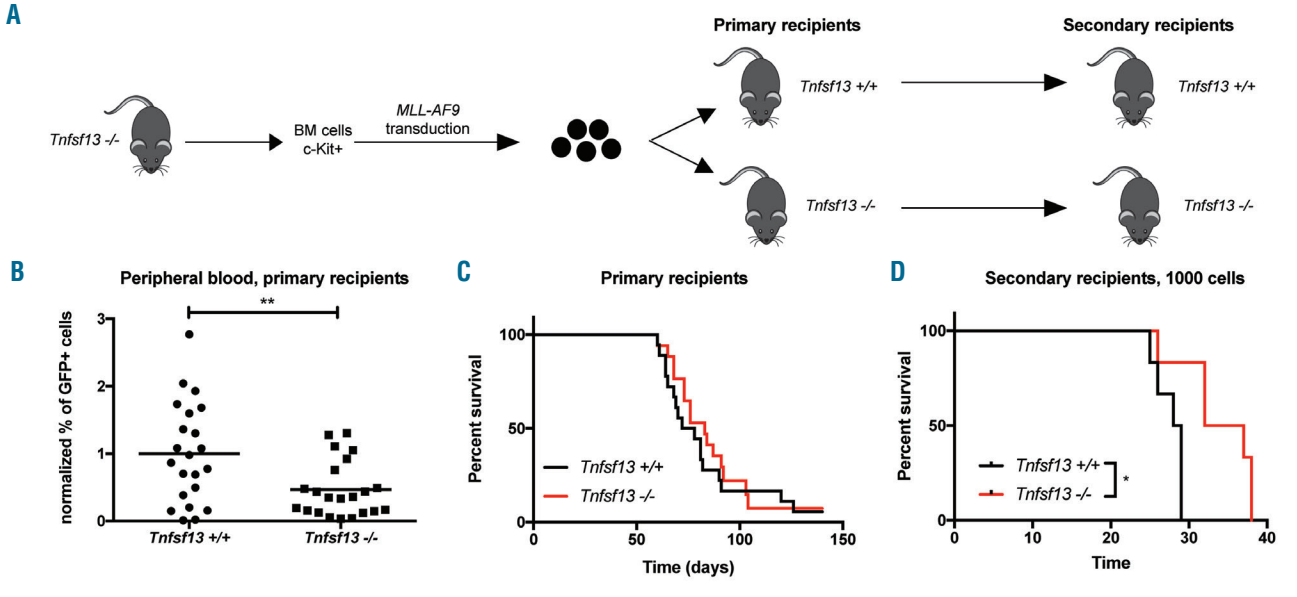

Figure 5. TNFSF13 supports leukemia development *in vivo*. A total of 250,000 c-Kit$^+$ bone marrow (BM) cells from *Tnfsf13*$^{-/-}$ mice were transduced with a MIG-*MLL-AF9* retroviral vector and transplanted into sublethally irradiated *Tnfsf13*$^{+/+}$ and *Tnfsf13*$^{-/-}$ primary recipient mice (22 mice per group, pooled from four independent experiments). 1,000 leukemia cells harvested from spleens of primary recipients were transplanted into secondary recipient mice with matching genetic background. (A) Schematic picture showing the experimental setup. (B) Percentage of leukemic (GFP$^+$) cells in the peripheral blood of the *Tnfsf13*$^{-/-}$ and *Tnfsf13*$^{+/+}$ recipient mice 40 days after transplantation, normalized to the mean of the control (*Tnfsf13*$^{+/+}$) group in each experiment. Horizontal lines show the mean values within groups. (C) Kaplan-Meier curves showing the survival of primary recipient mice. (D) Kaplan-Meier curves showing the survival of secondary recipient mice (6 mice per group; pooled data from 2 donors per group). *P<0.05; **P<0.01.

observed in plasma (Figure 3A and *Online Supplementary Figure S7B*). The c-Kit$^+$ murine leukemia cells did not show a significant response to TNFSF13B stimulation *in vitro* (*Online Supplementary Figure S7C*), but in human Mono-Mac-6 cells, TNFSF13B stimulation had similar effect as TNFSF13, resulting in increased cell number (*Online Supplementary Figure S7D*).

TNFSF13 supports acute myeloid leukemia cells in an NF-κB-dependent manner

To explore the molecular mechanism by which TNFSF13 promotes AML cell growth and survival, we generated RNA sequencing data of Mono-Mac-6 cells that had been stimulated with TNFSF13 for 24 hours. Consistent with TNFSF13 being a member of the tumor necrosis factor (TNF) superfamily, gene set enrichment analysis (GSEA) demonstrated an enriched TNF receptor activation signature upon TNFSF13 stimulation [false discovery rate (FDR) <0.10] (Figure 7F and *Online Supplementary Table S6*). Furthermore, an enriched NF-κB signature was evident in TNFSF13-stimulated cells (FDR<0.05) (Figure 7G and *Online Supplementary Table S6*) and phospho-flow cytometric analysis confirmed NF-κB activation upon TNFSF13 stimulation (Figure 7H). Consistent with this data, TNFSF13 stimulation resulted in a significant upregulation of the NF-κB target genes AGT, IRF1, IRF7, PTGDS, and VIM (*Online Supplementary Figure S8A*). By using a TNFRSF17 blocking antibody, TNFSF13-induced cell proliferation and NF-κB activation was hindered (Figure 7I and J), demonstrating that TNFSF13 activates NF-κB by binding to TNFRSF17. To assess whether TNFSF13 promotes cell proliferation by activating NF-κB, we inhibited NF-κB activation using TPCA1 and IKK-16, two selective inhibitors of IκB kinase (IKK).[24] Both TPCA1 and IKK-16 treatment inhibited NF-κB activation and reversed the effects of TNFSF13 in Mono-Mac-6 cells (Figure 7K and L and *Online Supplementary Figure S8B and C*). These data demonstrate that TNFSF13 supports the growth of human AML cells in an NF-κB-dependent manner.

Discussion

Although *in vivo* assays are critical to assess stem cell function, performing screens *in vivo* is challenging due to the large number of experimental animals needed to provide meaningful data. In this study, we developed arrayed molecular barcodes in lentiviral vectors, which enabled us to assess the effects of 114 cytokines on leukemia-initiat-

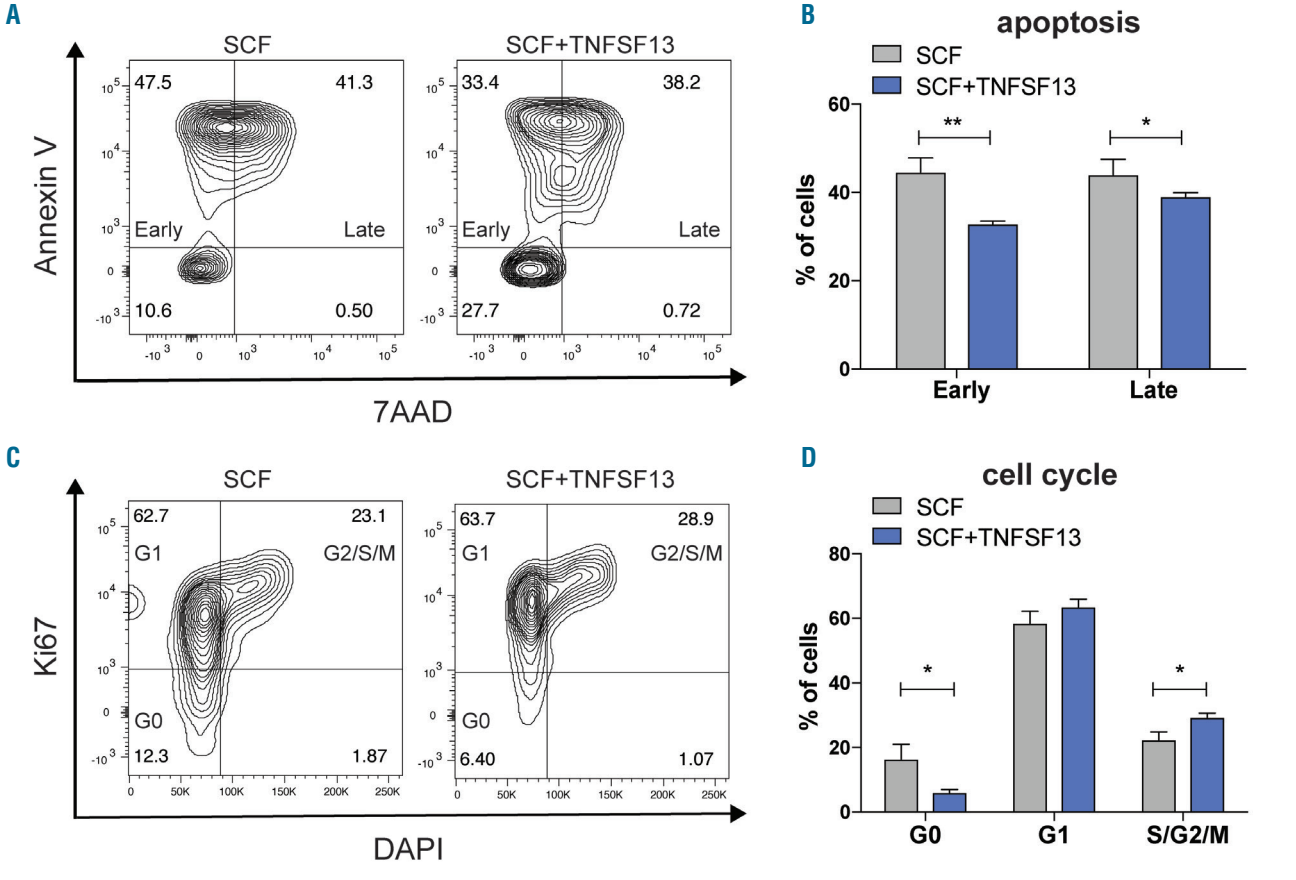

Figure 6. TNFSF13 maintains acute myeloid leukemia (AML) cells by suppressing apoptosis and promoting cell cycle progression. c-Kit$^+$ *MLL-AF9* AML cells were cultured for 3 days with stem cell factor (SCF) as a baseline and stimulated with TNFSF13 or no TNFSF13 (Control) prior to apoptosis and cell cycle analysis. (A) Representative contour plots showing Annexin-V and 7AAD staining. (B) Percentage of early (Annexin-V$^+$7AAD$^-$) and late (Annexin-V$^+$7AAD$^+$) apoptotic cells (n=3). (C) Representative contour plots showing Ki67 and DAPI staining. (D) Percentage of cells in G0, G1, or S/G2/M phase of the cell cycle (n=3) determined by Ki67 and DAPI staining. Values are means±Standard Deviation. *P<0.05; **P<0.01.

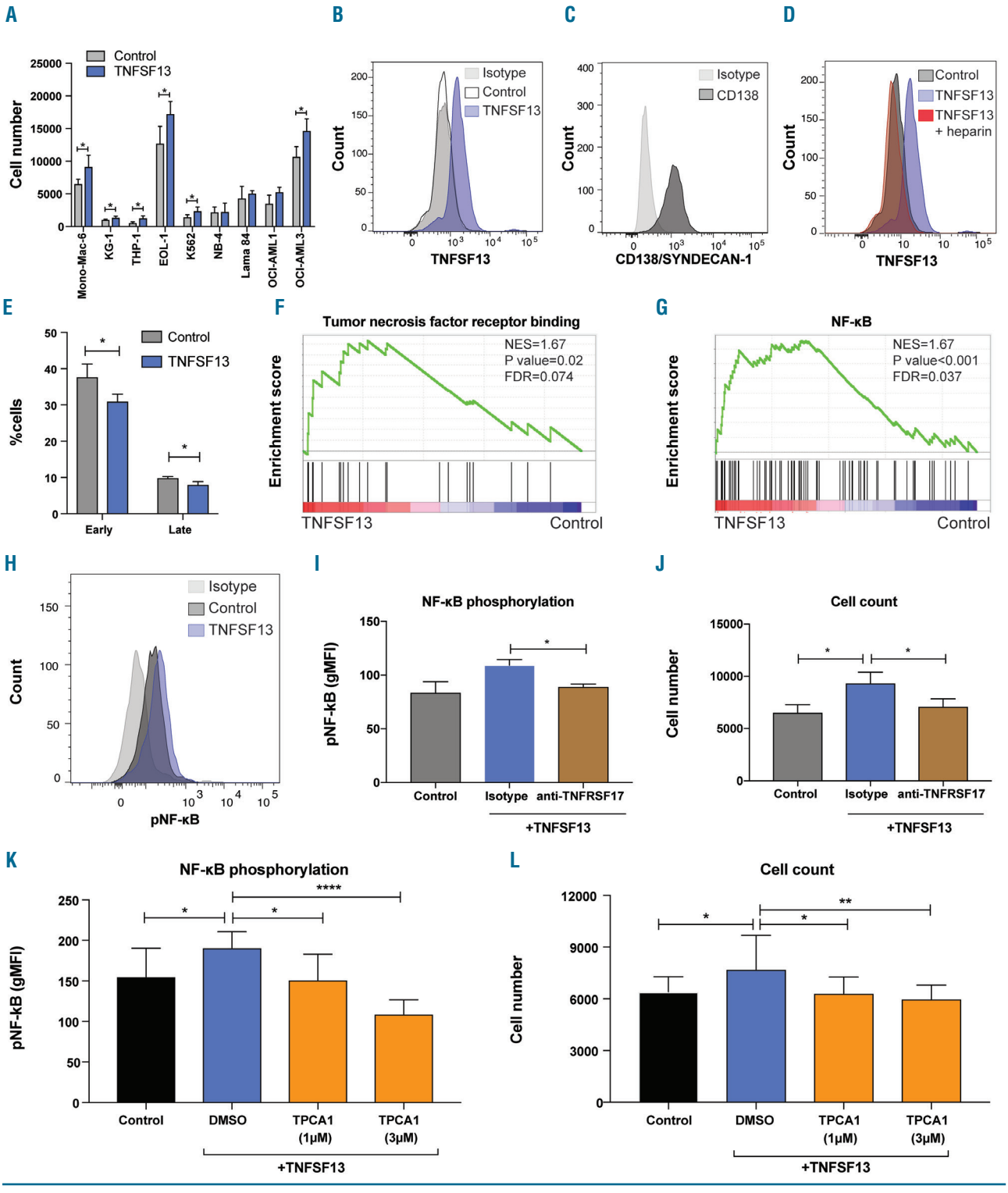

Figure 7. TNFSF13 promotes human acute myeloid leukemia cells in an NF-κB-dependent manner. (A) Output cell number of human myeloid leukemia cell lines cultured under serum-free conditions for three days with or without (Control) TNFSF13. A total of 1,000 cells were seeded per well (n=3). (B) Representative flow cytometric analysis showing staining of TNFSF13 on the cell surface of Mono-Mac-6 following 5-minute (min) stimulation with TNFSF13 (blue, 100 ng/mL) compared to non-stimulated cells (Control, white). Isotype control is shown in light gray. (C) Representative flow cytometric analysis showing SYNDECAN-1 (CD138) (dark gray) expression on Mono-Mac-6 cells. Isotype control is shown in light gray. (D) Representative flow cytometric analysis showing staining of TNFSF13 on the cell surface of Mono-Mac-6 following 5 min stimulation with TNFSF13 (100 ng/mL); with (red) or without (blue) heparin (4 IU/mL). Non-stimulated cells were used as control (white). (E) Percentage of early (Annexin-V$^+$7AAD$^-$) and late (Annexin-V$^+$7AAD$^+$) apoptotic Mono-Mac-6 cells following three days of stimulation with TNFSF13 (n=3). (F and G) Mono-Mac-6 cells were stimulated with TNFSF13 for 24 hours (h) prior to RNA sequencing. Gene Set Enrichment Analysis identified an enriched (F) TNF receptor signature (gene set from MsigDB, molecular signatures database) and an (G) NF-κB signature.[50] (H) Phospho-flow cytometric analysis of Mono-Mac-6 cells stimulated with TNFSF13 for 1 h. Isotype (light gray) and pNF-κB (Control, dark gray; TNFSF13, blue) staining. (I and J) Mono-Mac-6 cells were stimulated with TNFSF13 in the presence of a TNFRSF17 blocking antibody or corresponding isotype control, and analyzed for (I) pNF-κB expression after subtracting the signal using matching isotype control antibodies, and (J) output cell number after three days. (K and L) Mono-Mac-6 cells were treated with the IKK inhibitor TPCA1 at 1 or 3 μM during TNFSF13 stimulation and analyzed after three days for (K) pNF-κB expression after subtracting the signal using matching isotype control antibodies and (L) output cell number. Values are means±Standard Deviation. *P<0.05; **P<0.01; ****P<0.0001. FDR: false discovery rate; DMSO: dimethyl sulfoxide.

ing function using a competitive *in vivo* readout of leukemic cells. This approach significantly reduces the number of mice since leukemia cells from up to 11 different cytokine conditions can be pooled in each mouse. The arrayed barcoded approach is applicable to other types of *ex vivo* screens with *in vivo* readouts, as shown recently in a small-molecule screen using metastatic pancreatic cells.[25]

The barcoded cytokine screens identified IL9 and TNFSF13 as candidate positive regulators of leukemic-initiating cells. Validation experiments confirmed that both IL9 and TNFSF13 supported AML-initiating cells, but as TNFSF13 was more potent than IL9, we selected TNFSF13, a TNF superfamily ligand,[26] for further studies. The findings that *Tnfsf13*$^{-/-}$ recipient mice had lower leukemia burden and increased survival compared to controls following serial transplantations of leukemia cells suggest that TNFSF13 supports AML cells also under physiological condition. TNFSF13 has previously been shown to promote cancer-cell growth and survival of several types of solid tumors[27,28] and B-cell malignancies, such as acute lymphoblastic leukemia, Hodgkin lymphoma, and multiple myeloma.[26,29-32] In addition, elevated TNFSF13 levels have been found in multiple cancer types and are associated with a poor prognosis,[33] suggesting that TNFSF13 has broad tumor-promoting activity. Whereas the first *Tnfsf13*$^{-/-}$ mouse model generated did not reveal alterations in T- and B-cell development or *in vitro* function,[34] later studies of *Tnfsf13*$^{-/-}$ mice identified increased proliferation of T cells, changes in the secretion of immuno-cytokines, and impaired antibody class switching.[14,34]

In AML, TNFSF13 secretion has been linked to chemoresistance[36] and elevated TNFSF13 serum levels have been reported in patients,[36,37] but TNFSF13 has not previously been associated with AML stem cells or myelopoiesis. Given that the GMP cell stage is associated with AML initiation,[38] it was interesting to note that TNFRSF17 is expressed on myeloid progenitor cell populations and that *Tnfsf13*$^{-/-}$ mice have reduced numbers of GMP cells and monocytes, suggesting that TNFSF13 has a previously unrecognized role in myelopoiesis.

In agreement with previous studies showing that TNFSF13 is expressed by infiltrating neutrophils in solid tumors[39,40] and by myeloid BM cells in multiple myeloma,[41,42] we found that TNFSF13 was secreted by CD11b^{+}Gr-1^{+} myeloid cells but not by the corresponding murine AML cells. This finding suggests that mature myeloid BM cells support AML cells by secreting TNFSF13. In contrast to the findings in the murine MLL-AF9 AML model, TNFSF13 is expressed by leukemia cells in certain AML subtypes,[36,37] suggesting that TNFSF13 might play a more critical role for leukemia development and progression in these subtypes.

The anti-apoptotic effect induced by TNFSF13 is consistent with prior findings in B-cell malignancies[43-45] and glioma,[46] suggesting a similar mechanism induced by TNFSF13 in various types of cancers. Moreover, TNFSF13 promoted AML cells in an NF-κB-dependent manner, which is in agreement with studies showing that TNFSF13 activates NF-κB in multiple myeloma cells,[32] chronic lymphocytic leukemia,[30] and non-Hodgkin lymphoma B cells.[45] NF-κB signaling is elevated and critical for AML stem cells,[47,48] including MLL-rearranged AML cells, but the underlying mechanism causing NF-κB activation has not been clarified. Along with IL1-induced activation of NF-κB in primitive leukemia cells,[49] our findings suggest that TNFSF13 contributes to enhanced NF-κB activity in AML cells. Because AML cells from various AML subtypes lacking MLL rearrangements were also sensitive to TNFSF13, the effects of TNFSF13 stimulation are not restricted to MLL-rearranged AML.

In summary, we have established a cytokine screen using arrayed molecular barcoding of AML cells allowing for an *in vivo* competitive readout of leukemia-initiating activity. The screen provides a new strategy for studying the influence of secreted factors on AML-initiating cells. This approach identified TNFSF13 as a positive regulator of AML stem cells and showed that TNFSF13 promotes AML cells in an NF-κB-dependent manner. Moreover, we identified a role for TNFSF13 in normal myelopoiesis and showed that normal myeloid cells secrete TNFSF13. This study demonstrates the utility of using arrayed molecular barcoding as a new screening tool for identifying novel stem cell regulators.

Acknowledgments

This work was supported by the Swedish Cancer Society, the Swedish Childhood Cancer Foundation, the Crafoord Foundation, the Gunnar Nilsson Cancer Foundation, the Medical Faculty of Lund University, the Royal Physiographic Society of Lund, the Swedish Research Council, BioCARE, and FP7 Marie Curie.

References

1. Schepers K, Campbell TB, Passegué E. Normal and Leukemic Stem Cell Niches: Insights and Therapeutic Opportunities. Cell Stem Cell. 2015;16(3):254-267.
2. Morrison SJ, Scadden DT. The bone marrow niche for haematopoietic stem cells. Nature. 2014;505(7483):327-334.
3. Shlush LI, Mitchell A, Heisler L, et al. Tracing the origins of relapse in acute myeloid leukaemia to stem cells. Nature. 2017;547(7661):104-108.
4. Peña-Martinez P, Eriksson M, Ramakrishnan R, et al. Interleukin 4 induces apoptosis of acute myeloid leukemia cells in a Stat6-dependent manner. Leukemia. 2018;32(3):588-596.
5. Lu R, Neff NF, Quake SR, Weissman IL. Tracking single hematopoietic stem cells in vivo using high-throughput sequencing in conjunction with viral genetic barcoding. Nat Biotechnol. 2011;29(10):928-933.
6. Cheung AMS, Nguyen LV, Carles A, et al. Analysis of the clonal growth and differentiation dynamics of primitive barcoded human cord blood cells in NSG mice. Blood. 2013;122(18):3129-3137.
7. Grosselin J, Sii-Felice K, Payen E, Chretien S, Tronik-Le Roux D, Leboulch P. Arrayed lentiviral barcoding for quantification analysis of hematopoietic dynamics. Stem Cells. 2013;31(10):2162-2171.
8. Klauke K, Broekhuis MJC, Weersing E, et al. Tracing dynamics and clonal heterogeneity of Cbx7-induced leukemic stem cells by cellular barcoding. Stem Cell Rep. 2015;4(1):74-89.
9. Järås M, Miller PG, Chu LP, et al. Csnk1a1 inhibition has p53-dependent therapeutic efficacy in acute myeloid leukemia. J Exp Med. 2014;211(4):605-612.
10. Hartwell KA, Miller PG, Mukherjee S, et al. Niche-based screening identifies small-molecule inhibitors of leukemia stem cells. Nat Chem Biol. 2013;9(12):840-848.
11. Moffat J, Grueneberg DA, Yang X, et al. A lentiviral RNAi library for human and mouse genes applied to an arrayed viral high-content screen. Cell. 2006;124(6):1283-1298.
12. Xiao Y, Motomura S, Deyev V, Podack ER. TNF superfamily member 13, APRIL, inhibits allergic lung inflammation. Eur J Immunol. 2011;41(1):164-171.
13. Xiao Y, Motomura S, Podack ER. APRIL (TNFSF13) regulates collagen-induced

arthritis, IL-17 production and Th2 response. Eur J Immunol. 2008;38(12): 3450-3458.
14. Miller PG, Al-Shahrour F, Hartwell KA, et al. In Vivo RNAi Screening Identifies a Leukemia-Specific Dependence on Integrin Beta 3 Signaling. Cancer Cell. 2013; 24(1):45-58.
15. Puram RV, Kowalczyk MS, de Boer CG, et al. Core Circadian Clock Genes Regulate Leukemia Stem Cells in AML. Cell. 2016;165(2):303-316.
16. Wang Y-Y, Zhao L-J, Wu C-F, et al. C-KIT mutation cooperates with full-length AML1-ETO to induce acute myeloid leukemia in mice. Proc Natl Acad Sci U S A. 2011;108(6):2450-2455.
17. Bossen C, Schneider P. BAFF, APRIL and their receptors: Structure, function and signaling. Semin Immunol. 2006;18(5):263-275.
18. Ingold K, Zumsteg A, Tardivel A, et al. Identification of proteoglycans as the APRIL-specific binding partners. J Exp Med. 2005;201(9):1375-1383.
19. Hendriks J, Planelles L, de Jong-Odding J, et al. Heparan sulfate proteoglycan binding promotes APRIL-induced tumor cell proliferation. Cell Death Differ. 2005;12(6):637-648.
20. Ley TJ, Miller C, Ding L, et al. Genomic and epigenomic landscapes of adult de novo acute myeloid leukemia. N Engl J Med. 2013;368(22):2059-2074.
21. Papaemmanuil E, Gerstung M, Bullinger L, et al. Genomic Classification and Prognosis in Acute Myeloid Leukemia. N Engl J Med. 2016;374(23):2209–2221.
22. Gaidzik VI, Teleanu V, Papaemmanuil E, et al. RUNX1 mutations in acute myeloid leukemia are associated with distinct clinico-pathologic and genetic features. Leukemia. 2016;30(11):2160–2168.
23. Rucker FG, Schlenk RF, Bullinger L, et al. TP53 alterations in acute myeloid leukemia with complex karyotype correlate with specific copy number alterations, monosomal karyotype, and dismal outcome. Blood. 2012;119(9):2114-2121.
24. Podolin PL, Callahan JF, Bolognese BJ, et al. Attenuation of murine collagen-induced arthritis by a novel, potent, selective small molecule inhibitor of IkappaB Kinase 2, TPCA-1 (2-[(aminocarbonyl)amino]-5-(4-fluorophenyl)-3-thiophenecarboxamide), occurs via reduction of proinflammatory cytokines and antigen-induced T cell Proliferation. J Pharmacol Exp Ther. 2005;312(1):373-381.
25. Grüner BM, Schulze CJ, Yang D, et al. An in vivo multiplexed small-molecule screening platform. Nat Methods. 2016;13(10):883-889.
26. Hahne M, Kataoka T, Schroter M, et al. APRIL, a new ligand of the tumor necrosis factor family, stimulates tumor cell growth. J Exp Med. 1998;188(6):1185-1190.
27. García-Castro A, Zonca M, Florindo-Pinheiro D, et al. APRIL promotes breast tumor growth and metastasis and is associated with aggressive basal breast cancer. Carcinogenesis. 2015;36(5):574-584.
28. Wang R, Guo Y, Ma H, et al. Tumor necrosis factor superfamily member 13 is a novel biomarker for diagnosis and prognosis and promotes cancer cell proliferation in laryngeal squamous cell carcinoma. Tumour Biol. 2016;37(2):2635-2645.
29. Chiu A, Xu W, He B, et al. Hodgkin lymphoma cells express TACI and BCMA receptors and generate survival and proliferation signals in response to BAFF and APRIL. Blood. 2007;109(2):729-739.
30. Endo T, Nishio M, Enzler T, et al. BAFF and APRIL support chronic lymphocytic leukemia B-cell survival through activation of the canonical NF-kappaB pathway. Blood. 2007;109(2):703-710.
31. Quinn J, Glassford J, Percy L, et al. APRIL promotes cell-cycle progression in primary multiple myeloma cells: influence of D-type cyclin group and translocation status. Blood. 2011;117(3):890-901.
32. Tai Y-T, Acharya C, An G, et al. APRIL and BCMA promote human multiple myeloma growth and immunosuppression in the bone marrow microenvironment. Blood. 2016;127(25):3225-3236.
33. Moreaux J, Veyrune J-L, De Vos J, Klein B. APRIL is overexpressed in cancer: link with tumor progression. BMC Cancer. 2009; 9:83.
34. Varfolomeev E, Kischkel F, Martin F, et al. APRIL-deficient mice have normal immune system development. Mol Cell Biol. 2004;24(3):997-1006.
35. Castigli E, Scott S, Dedeoglu F, et al. Impaired IgA class switching in APRIL-deficient mice. Proc Natl Acad Sci U S A. 2004;101(11):3903-3908.
36. Bonci D, Musumeci M, Coppola V, et al. Blocking the APRIL circuit enhances acute myeloid leukemia cell chemosensitivity. Haematologica. 2008;93(12):1899-1902.
37. Bolkun L, Lemancewicz D, Jablonska E, et al. The impact of TNF superfamily molecules on overall survival in acute myeloid leukaemia: correlation with biological and clinical features. Ann Hematol. 2015; 94(1):35-43.
38. Krivtsov AV, Twomey D, Feng Z, et al. Transformation from committed progenitor to leukaemia stem cell initiated by MLL–AF9. Nature. 2006;442(7104):818-822.
39. Jablonska E, Wawrusiewicz-Kurylonek N, Garley M, et al. A proliferation-inducing ligand (APRIL) in neutrophils of patients with oral cavity squamous cell carcinoma. Eur Cytokine Netw. 2012;23(3):93-100.
40. Schwaller J, Schneider P, Mhawech-Fauceglia P, et al. Neutrophil-derived APRIL concentrated in tumor lesions by proteoglycans correlates with human B-cell lymphoma aggressiveness. Blood. 2007; 109(1):331-338.
41. Matthes T, Dunand-Sauthier I, Santiago-Raber M-L, et al. Production of the plasma-cell survival factor a proliferation-inducing ligand (APRIL) peaks in myeloid precursor cells from human bone marrow. Blood. 2011;118(7):1838-1844.
42. Matthes T, McKee T, Dunand-Sauthier I, et al. Myelopoiesis dysregulation associated to sustained APRIL production in multiple myeloma-infiltrated bone marrow. Leukemia. 2015;29(9):1901-1908.
43. Kern C, Cornuel J-F, Billard C, et al. Involvement of BAFF and APRIL in the resistance to apoptosis of B-CLL through an autocrine pathway. Blood. 2004;103 (2):679-688.
44. Moreaux J, Legouffe E, Jourdan E, et al. BAFF and APRIL protect myeloma cells from apoptosis induced by interleukin 6 deprivation and dexamethasone. Blood. 2004;103(8):3148-3157.
45. He B, Chadburn A, Jou E, Schattner EJ, Knowles DM, Cerutti A. Lymphoma B cells evade apoptosis through the TNF family members BAFF/BLyS and APRIL. J Immunol. 2004;172(5):3268-3279.
46. Roth W, Wagenknecht B, Klumpp A, et al. APRIL, a new member of the tumor necrosis factor family, modulates death ligand-induced apoptosis. Cell Death Differ. 2001;8(4):403-410.
47. Kuo H-P, Wang Z, Lee D-F, et al. Epigenetic roles of MLL oncoproteins are dependent on NF-kappaB. Cancer Cell. 2013;24(4): 423-437.
48. Bosman MCJ, Schepers H, Jaques J, et al. The TAK1-NF-kappaB axis as therapeutic target for AML. Blood. 2014;124(20):3130-3140.
49. Ågerstam H, Hansen N, von Palffy S, et al. IL1RAP antibodies block IL-1-induced expansion of candidate CML stem cells and mediate cell killing in xenograft models. Blood. 2016;128(23):2683-2693.
50. Pahl HL. Activators and target genes of Rel/NF-kappaB transcription factors. Oncogene. 1999;18(49):6853-6866.

ARTICLE

Hematopoietic niche drives FLT3-ITD acute myeloid leukemia resistance to quizartinib *via* STAT5- and hypoxia-dependent upregulation of AXL

Pierre-Yves Dumas,[1,2*] Cécile Naudin,[3*] Séverine Martin-Lannerée,[3] Brigitte Izac,[3] Luana Casetti,[3] Olivier Mansier,[4] Benoît Rousseau,[5] Alexandre Artus,[3] Mélody Dufossée,[1] Alban Giese,[6] Pierre Dubus,[6,7] Arnaud Pigneux,[1,2] Vincent Praloran,[1,2] Audrey Bidet,[4] Arnaud Villacreces,[1] Amélie Guitart,[1] Noël Milpied,[1,2] Olivier Kosmider,[3,8] Isabelle Vigon,[1] Vanessa Desplat,[1] Isabelle Dusanter-Fourt,[3] and Jean-Max Pasquet[1**]**

[1]Université de Bordeaux, Institut National de la Santé et de la Recherche Médicale INSERM U1035, F-33000 Bordeaux; [2]CHU Bordeaux, Service d'Hématologie Clinique et Thérapie cellulaire, F-33000, Bordeaux; [3]Université de Paris, Institut Cochin, Institut National de la Santé et de la Recherche Médicale INSERM U1016, Centre National de la Recherche Scientifique CNRS UMR8104, F-75014 Paris; [4]Service de Biologie des Tumeurs and Laboratoire d'Hématologie Biologique, Centre Hospitalo-Universitaire CHU Bordeaux, F-33000, Bordeaux; [5]Service Commun des Animaleries, Animalerie A2, Université de Bordeaux, Bordeaux; [6]Institut National de la Santé et de la Recherche Médicale INSERM U1218, and UMS005 TBM Core, Plateforme d'Histopathologie Expérimentale, Université de Bordeaux, F33000 Bordeaux; [7]Institut National de la Santé et de la Recherche Médicale, INSERM U1053, F33000 Bordeaux and [8]Service d'Hématologie Biologique, Assistance Publique-Hôpitaux de Paris, Hôpitaux Universitaires Paris Centre, Paris, France

**P-YD and CN contributed equally to this work. **ID-F and J-MP contributed equally as co-senior authors.*

Ferrata Storti Foundation

Haematologica 2019
Volume 104(10):2017-2027

ABSTRACT

Internal tandem duplication in Fms-like tyrosine kinase 3 (FLT3-ITD) is the most frequent mutation observed in acute myeloid leukemia (AML) and correlates with poor prognosis. FLT3 tyrosine kinase inhibitors are promising for targeted therapy. Here, we investigated mechanisms dampening the response to the FLT3 inhibitor quizartinib, which is specific to the hematopoietic niche. Using AML primary samples and cell lines, we demonstrate that convergent signals from the hematopoietic microenvironment drive FLT3-ITD cell resistance to quizartinib through the expression and activation of the tyrosine kinase receptor AXL. Indeed, cytokines sustained phosphorylation of the transcription factor STAT5 in quizartinib-treated cells, which enhanced AXL expression by direct binding of a conserved motif in its genomic sequence. Likewise, hypoxia, another well-known hematopoietic niche hallmark, also enhanced AXL expression. Finally, in a xenograft mouse model, inhibition of AXL significantly increased the response of FLT3-ITD cells to quizartinib exclusively within a bone marrow environment. These data highlight a new bypass mechanism specific to the hematopoietic niche that hampers the response to quizartinib through combined upregulation of AXL activity. Targeting this signaling offers the prospect of a new therapy to eradicate resistant FLT3-ITD leukemic cells hidden within their specific microenvironment, thereby preventing relapses from FLT3-ITD clones.

Introduction

The Fms-like tyrosine kinase 3 (FLT3) gene encodes a class III receptor tyrosine-kinase (RTK) that is well expressed in hematopoietic stem progenitor cells (HSPC) and strongly activates PI3K/AKT and MAPK pathways upon ligand binding.[1] Internal tandem duplication (ITD) in FLT3 is one of the most frequent mutations

Correspondence:

JEAN-MAX PASQUET
jean-max.pasquet@u-bordeaux.fr

ISABELLE DUSANTER-FOURT
isabelle.dusanter@inserm.fr

Received:
September 12, 2018.
Accepted: March 21, 2019.
Pre-published: March 28, 2019.
doi:10.3324/haematol.2018.205385

Check the online version for the most updated information on this article, online supplements, and information on authorship & disclosures: www.haematologica.org/content/104/10/2017

found in acute myeloid leukemia (AML).[2] Although the FLT3-ITD mutation is a late event in leukemogenesis,[3] it is an important target for the disease.[4] Indeed, FLT3-ITD mutation is associated with a poor prognosis,[5-7] and its frequent occurrence at relapse suggests that FLT3-ITD AML-initiating cells are key targets for long-lasting remission.

The FLT3-ITD mutation induces constitutive activity of the receptor and a distinct pattern of activated signaling pathways, the principal change being the activation of the transcription factor STAT5.[8] FLT3 tyrosine kinase inhibitors (FLT3-TKI), which were developed as ATP-competitive inhibitors, were initially tested in clinical trials and produced variable benefits according to the disease heterogeneity. Among these treatments, quizartinib (AC220), a FLT3-TKI specifically designed for FLT3, induces a hematologic improvement in monotherapy associated with approximately 50% of response.[9] However, bone marrow (BM) blasts show little noticeable cell apoptosis, but are associated with cell-cycle arrest and terminal differentiation.[10] Remissions are of short duration, with the emergence of resistance related to several mechanisms. Intrinsic mechanisms include the activation of bypass signaling pathways[11] and activation loop or gatekeeper mutations.[4] Extrinsic mechanisms include cell-to-cell interactions and secretion of cytoprotective factors.[12]

AXL belongs to the TAM receptor family, which also includes TYRO3 and MER.[13] This RTK is activated by homodimerization upon binding of its major ligand growth arrest-specific 6 (GAS6).[14] The GAS6/AXL pathway contributes to cell growth, survival, invasiveness, chemotaxis, apoptotic body clearance and immunity.[15] AXL is ectopically- or over-expressed in a wide variety of cancers and has always been associated with a poor prognosis.[16] We have reported resistance mechanisms involving AXL in chronic myeloid leukemia.[17] In AML, AXL and GAS6 levels of expression have been related to poor outcomes.[18,19] Paracrine AXL activation has been shown to induce AML resistance to conventional chemotherapies but also to FLT3-targeted therapy.[20-23] However, no information is available concerning the regulation of AXL expression in the context of the AML-supportive hematopoietic niche, which sustains AML resistance *in vivo*.

Indeed, AXL expression and function have been shown to be modulated by stress, nutrient deprivation and low oxygen (O_2) concentration in various solid tumors.[14,24] These characteristics are quite similar to those within the hematopoietic microenvironment of AML-initiating cells. We show here that the hematopoietic microenvironment educates AML cells to over-express AXL through a cytokine-dependent STAT5 activation and low O_2 concentration.

Methods

Cell culture, apoptosis and *AXL*, *GAS6* and *STAT5* gene expression knock-down using shRNA

All cell lines (MV4-11, MOLM-13, MOLM-14, UT7-mpl, K562, MS5, OP9, HS27a) were cultured in RPMI1640 or αMEM medium, supplemented with 10% fetal calf serum (FCS), 2 mM L-glutamine, 50 U/mL penicillin, and 50 µg/mL streptomycin. Hypoxia was induced by incubating cells in a specific O_2 chamber (BioSpherix). The UT7-mpl cell medium was supplemented with granulocyte-macrophage colony-stimulating factor (GM-CSF, 2.5ng/mL, Diaclone, France), as previously described.[25] UT7-mpl cells were pre-incubated for 18 hours (h) in the absence of GM-CSF, before being activated by cytokines. Where indicated, cells were cultured with vehicle or thrombopoietin peptide (Sigma), interleukin (IL)-3 (Miltenyi Biotec), AXL-Fc chimeric proteins (R&D Systems), AC220 (quizartinib) (LC laboratories), R428 (Selleckchem), Ly294002, pimozide, JAK inhibitor-I (Calbiochem/Merck). AC-4-130, a selective STAT5 inhibitor, was provided by JANPIX Ltd. (UK) under the license from Prof. Patrick Gunning's group (University of Toronto, Canada).[26] Cell apoptosis was assessed using an APC-conjugated Annexin V labeling detection kit coupled to flow cytometry and BDFACSDIVA™ software (BD Bioscience). For shRNA, viral supernatants were titrated by serial dilutions and a FACS analysis of GFP co-expressed marker in transduced K562 cells 72 h later (Accuri C6, Beckton Dickinson). Lentiviruses were added once, at a multiplicity of infection of 5-20 according to the cells. Transduced cells were sorted 2-3 days after transduction using GFP. Two different shRNA were used for all targets (*Online Supplementary Table S1*). To confirm silencing, AXL, GAS6 or STAT5 protein expressions were analyzed by immunoblotting.

Acute myeloid leukemia patient and cord blood donor biological samples

Acute myeloid leukemia samples were obtained from patients at the University Hospital of Bordeaux and University Hospital Paris Centre who gave written informed consent for the use of biological samples for research, in accordance with the Declaration of Helsinki. This allowed the collection of clinical and biological data in an anonymized database, registered at the "Commission Nationale de l'Informatique et des Libertés" (authorization n. 915285) and "Comité de Protection des Personnes" (authorization n. 2015-08-11D). For FLT3-ITD AML patient samples, selection criteria were high leukemic burden (blast cells level > 70%) and high FLT3-ITD/WT ratio (ITD/WT > 0.5) (*Online Supplementary Table S2*). Bone marrow mononuclear cells were co-cultured with MS5 stromal cells in H5100 medium (Stem Cell Technologies), unless otherwise stated. When indicated, AML cells were preincubated for 18 h in serum-free IMDM medium in the absence of MS5 before being incubated for 7 h in the presence of a cytokine cocktail that included IL-3 (20 ng/mL), GM-CSF (10 ng/mL) and TPO (20 nM). Human cord blood (CB) units were collected according to institutional guidelines. Cord blood $CD34^+$ were purified and cultured in a four-cytokine-supplemented serum-free IMDM medium, as previously described.[27]

Further details about the methods used are available in the *Online Supplementary Appendix*.

Results

Stromal protection of FLT3-ITD AML cells to quizartinib correlates with STAT5 activation

We first confirmed the protective effect of three stromal cell lines on MV4-11, MOLM-13 and MOLM-14 FLT3-ITD AML cell lines exposed to quizartinib (AC220), an ATP-competitive FLT3- inhibitor. Co-culture of AML cells with one human (HS27a) and two murine (OP9 or MS5) stromal cells decreased apoptosis triggered by FLT3-TKI treatment compared to AML cells cultured without stroma (Figure 1A and *Online Supplementary Figure S1A and B*). This decrease persisted at high AC220 concentra-

tions (10-20 nM) (*Online Supplementary Figure S1C*) and was not due to a decrease in active AC220 concentration by the metabolism of stromal cells (*Online Supplementary Figure S1D*). To investigate further the mechanism of such protection, stromal/AML cell co-cultures were performed with a transwell separating the two kinds of cells, thereby avoiding cell-to-cell contact. Transwell-separated stromal cells still protected FLT3-ITD AML cells from quizartinib-induced apoptosis, but the protective effect was weaker (Figure 1B), suggesting the involvement of both cell-to-cell contact and diffusible factors. We then analyzed signaling pathways in cells treated with AC220 in the presence or absence of stroma. Whereas AC220 treatment of FLT3-ITD AML cell lines (MV4-11, MOLM-14) decreased Y_{591}FLT3, T_{202}/Y_{204}ERK, Ser_{473}AKT and Y_{694}/Y_{699} STAT5 phosphorylation in the absence of stroma, the presence of co-cultured stromal cells (MS5, OP9, HS27A), along with AC220 treatment, specifically sustained Y_{694}STAT5A/Y_{699}STAT5B phosphorylation (hereafter referred to as pYSTAT5) (Figure 1C and *Online Supplementary Figure S1E*). STAT5 Tyr phosphorylation was still conserved at higher AC220 concentrations (*Online Supplementary Figure S1F*).

Therefore, stromal protection of FLT3-ITD AML cells is associated with an FLT3-ITD-independent conservation of STAT5 tyrosine phosphorylation.

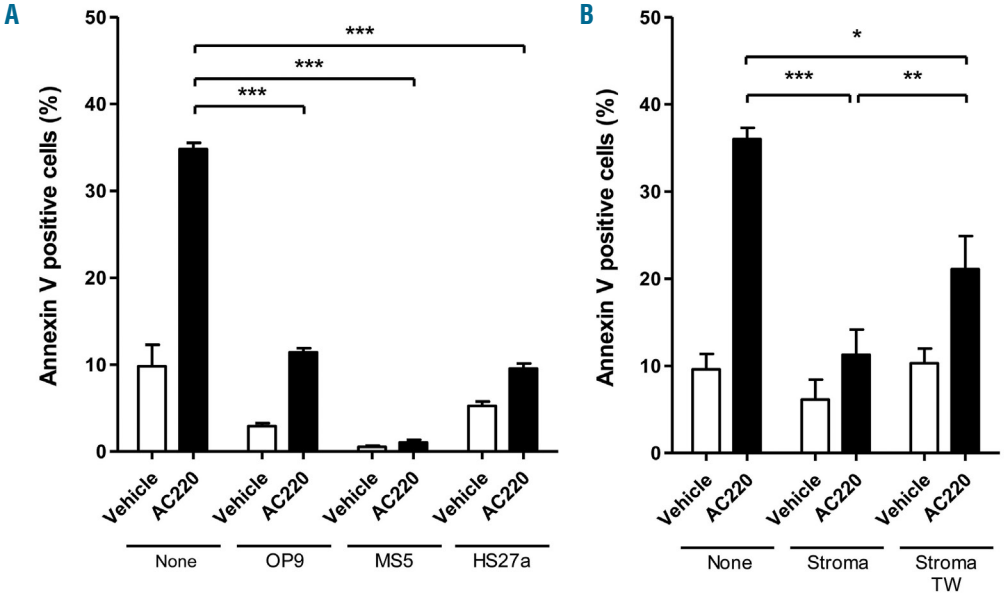

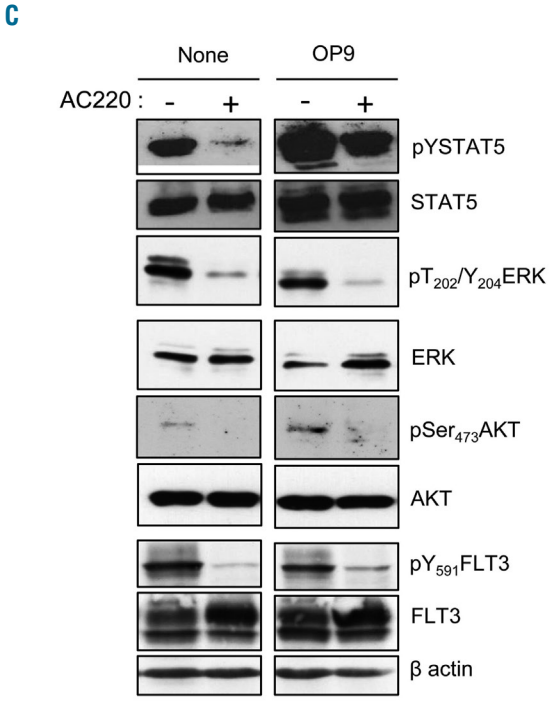

Figure 1. Stromal cells protect MV4-11 cells from AC220-induced apoptosis and correlate with enhanced STAT5 activation. (A) MV4-11 FLT3-ITD acute myeloid leukemia (AML) cell line was incubated in the absence (Vehicle) or presence of AC220 (3 nM) for 48 hours, without (None) or with the indicated murine (OP9 or MS5) or human (HS27a) stromal cell lines. Cell apoptosis was determined by Annexin V/DAPI labeling followed by flow cytometry analysis. (B) MV4-11 FLT3-ITD AML cell line was incubated in the absence (Vehicle) or presence of AC220 (3 nM) for 48 h, without (None) or with OP9 cells separated (Stroma TW) or not (Stroma) by transwells. Apoptosis induction was determined as in (A). (C) MV4-11 cells were incubated in the absence (Vehicle) or presence of AC220 (1 nM), without (none) or with OP9 stromal cells (Stroma) for 48 h. Upon cell lysis, immunoblot analysis of the indicated protein with β actin as a loading control, each of protein-dedicated immunoblot without (none) or with (stroma) OP9 co-culture was performed on the same membrane. Results shown are representative of three experiments. Graphs show the mean±Standard Error of Mean of results of at least three independent experiments. *P<0.05; **P<0.01; ***P<0.001.

AXL contributes to stromal cell-dependent FLT3-ITD AML resistance to FLT3-TKI

To determine how STAT5 contributes to TKI-resistance of AML cells by stromal cells, we looked for STAT5 target genes in myeloid cells. We searched for STAT5 regulated genes by conducting a comparative large-scale genome expression analysis of STAT5 knocked-down (KD) and control cells using normal human primitive $CD34^+$ $CD38^-$ HSPC. Among the top-ranked down-regulated transcripts upon STAT5 KD, we looked for mediators that might be involved in stromal protection. AXL was the only RTK down-regulated in these STAT5 KD cells (*Online Supplementary Table S3*) and was the only one reported in resistance to treatment in AML.[21,23] To examine the role of AXL in cancer resistance, we investigated whether there was a link between STAT5-dependent AXL regulation, stroma-dependent STAT5 tyrosine phosphorylation maintenance and stromal protection for AC220. We found that AXL mRNA and protein were both decreased in STAT5 KD HSPC (*Online Supplementary Figure S2A*). Like HSPC, STAT5 KD induced AXL loss in MV4-11 and MOLM-14 FLT3-ITD or UT7 FLT3 wt AML cell lines (Figure 2A and *Online Supplementary Figure S2B*). STAT5 is encoded by two highly similar genes, STAT5A and STAT5B, whose combined KD led to cell death. However, STAT5A-restricted KD did not affect AML cell survival; it allowed us to perform rescue experiments. Silencing of STAT5A followed by expression of either murine STAT5A or murine STAT5B enhanced AXL expression, thus providing evidence that both STAT5 regulated AXL expression (*Online Supplementary Figure S2B*). Finally, we found that stromal cells enhanced both STAT5 phosphorylation and AXL expression in MV4-11 and MOLM-14 cells (Figure 2B). These activities were both prevented when cells were incubated in the presence of the STAT5 inhibitor AC-4-130 (*Online Supplementary Figure S2C*). Overall, these data indicated that stroma supports STAT5 activation of AML cells, which enhances AXL expression of AML cells.

We thus analyzed the role of AXL in AML cell survival with a well-characterized and clinically investigated AXL-TKI compound, R428.[28] To determine whether AXL and FLT3-ITD pro-survival activity were connected, we first determined the minimal effective AC220 and R428 dose to induce apoptosis after 48 h of incubation (*Online Supplementary Figure S2D*). The minimal effective AC220 dose was 1-3 nM, depending on the FLT3-ITD AML cell line, whereas for R428 it was 0.3 μM for all. Using these doses, we observed that AXL and FLT3 co-inhibition triggered additive apoptosis (MOLM-13) and even a weak synergistic activity (MV4-11 and MOLM-14) as compared to single drug treatment (Figure 2C).

Next, we investigated whether such effects were observed in primary AML blasts. In all primary AML samples tested, HS27a stroma induced upregulation of AXL expression (AML#1, #2 in Figure 2D and *Online Supplementary Table S2*). However, this increase did not provide extra AML cell survival when AXL activity was inhibited. Instead, AXL and FLT3 co-inhibition induced a significantly stronger apoptosis than single drug treatments on primary AML blasts cultivated *ex vivo* on stromal cells (AML #3 to #9 in Figure 2E and *Online Supplementary Table S2*).

AXL is activated through the binding of its ligand GAS6, for which autocrine and paracrine activities have been reported in various contexts, including AML. Although both stromal and leukemic cells are known to secrete GAS6, stromal secretion was 10- to 20-fold more abundant than leukemia ones, as detected by species-specific ELISA (*Online Supplementary Figure S2E*).[29] We analyzed the contribution of GAS6 to the protective activity of stromal cells toward AC220-induced AML cell apoptosis. Protection of FLT3-ITD AML cells by stromal cells was significantly reduced yet was not suppressed in the presence of AXL-Fc, a well-known GAS6-neutralizing molecule[22] (Figure 2F). Moreover, GAS6-KD OP9 stromal cells provided weaker protection than parental OP9 (Figure 2G and *Online Supplementary Figure S2F*), confirming the results observed with AXL-Fc.

Taken together, using an AXL inhibitor (R428) or a GAS6-neutralizing molecule (AXL-Fc) and genetically engineered stromal cells (OP9 shGAS6), these results confirm that AXL activity contributes to the stromal protection of FLT3-ITD AML.

STAT5-activating cytokines up-regulate AXL expression and activity

Since AXL expression is associated with STAT5 activation, we wondered whether and how stroma activates STAT5. We first analyzed GAS6 activity but did not detect any STAT5 tyrosine phosphorylation upon GAS6 treatment in AML cells. We therefore wondered whether STAT5-activating cytokines, secreted by stromal cells, could trigger AXL overexpression. Therefore, we first used the UT7-mpl AML cell line (FLT3 wild type) which is highly sensitive to GM-CSF and TPO for its growth and survival.[25] Both GM-CSF and TPO activated STAT5 and enhanced AXL expression within a few hours (Figure 3A and B). These cytokines are known to activate STAT5 by binding to their receptors through subsequent activation of JAK2 kinase. In the presence of the STAT5 inhibitor pimozide (pi) or the JAK2 inhibitor-I (ji), GM-CSF and TPO no longer up-regulated AXL expression, whereas inhibition of the PI3K/AKT pathway by LY294002 (ly) had no effect (Figure 3B). We further observed that AXL activation was also induced by GM-CSF and TPO in AML cells, as assessed by Tyr779 AXL phosphorylation detection and by global Tyr phosphorylation in AXL immunoprecipitates (Figure 3B and C). Similar results were obtained using primary CB $CD34^+$ HSPC in the presence of interleukin (IL)-3 or TPO. However, this was not the case with the FLT3 ligand, which did not activate STAT5 (*Online Supplementary Figure S3A*). These results indicated that STAT5-activating cytokines can up-regulate both AXL expression and activation in normal HSPC and FLT3 wild-type AML.

FLT3-ITD AML cells are known to co-express cytokine receptors such as IL-3 and TPO receptors, whose activity remains ill-defined.[29,30] We wondered whether cytokines could trigger AXL upregulation, specifically in FLT3-ITD AML cells. Despite the presence of FLT3-ITD inhibitor AC220, IL-3 sustained STAT5 phosphorylation (Figure 3D). This activation was correlated with an increase in AXL protein expression (Figure 3E). Similarly, in primary AML samples, an IL-3/GM-CSF/TPO cytokine cocktail increased AXL RNA expression (AML#10-12 and #15-16 in Figure 3F and *Online Supplementary Table S2*) associated with STAT5 activation (AML#10-14 in Figure 3G and *Online Supplementary Table S2*).

To unravel how STAT5 up-regulates AXL transcript levels, we focused on the AXL genomic sequence. STAT5

transcription factors bind to TTCN3GAA STAT-Response Element (SRE) on their target genes. One SRE that is conserved among species including rat, mouse and human was identified within intron 16 and located at Chr19(+) [41,725,104-41,767,672] (*www.genome.ucsf.edu*). Oligonucleotide pull-down assays showed that this identified SRE was functional, since it bound STAT5 as efficiently as the control canonical SRE (ONc) from the IRF1 promoter sequence (*Online Supplementary Figure S3B*). Chromatin immunoprecipitation (ChIP) assays with STAT5 antibodies showed that STAT5-activation triggered binding to the AXL genomic sequence (Figure 3H). Together with STAT5 binding, recruitment of RNAPolII to the AXL gene was enhanced, as assessed by anti-RNAPolII

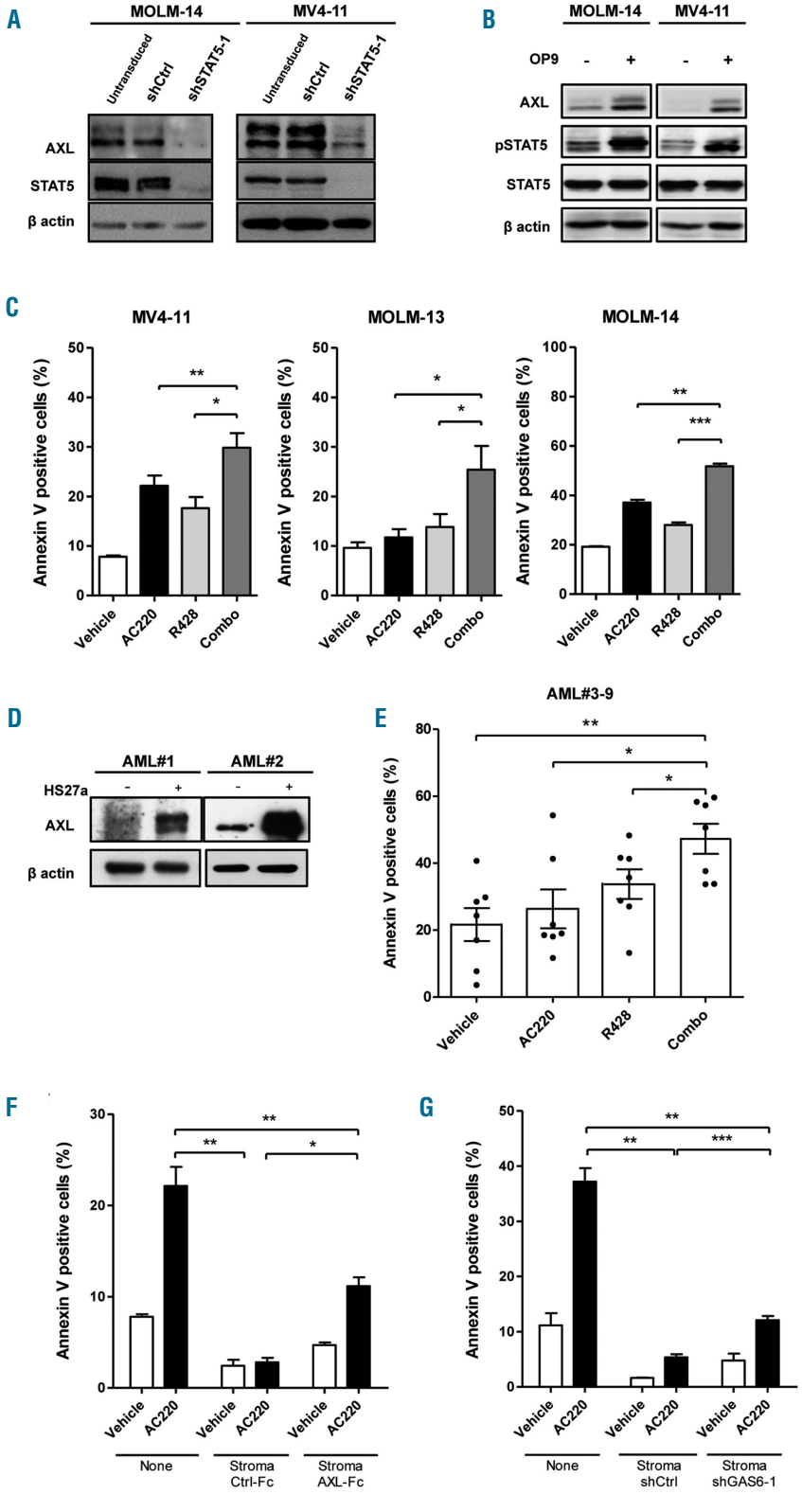

Figure 2. STAT5 up-regulates AXL which contributes to FLT3-ITD acute myeloid leukemia (AML) cell survival. (A) MOLM-14 and MV4-11 cells were transduced with the indicated shRNA encoding lentiviral vectors and lysed three days later. Immunoblot analysis of the indicated proteins was performed with β actin as a loading control. (B) MOLM-14 and MV4-11 cells were co-cultured in the absence (-) or presence (+) of OP9 stromal cells for 48 hours (h) before being isolated and lysed. The indicated proteins were analyzed by immunoblotting. (C) MV4-11, MOLM-13 and MOLM-14 cells were treated in the absence (Vehicle) or presence of minimal effective (MV4-11, MOLM-14) or suboptimal (MOLM-13) dose of AC220 (1 nM) and R428 (0.3 μM) or both (Combo) for 48 h. Apoptosis induction was determined as in Figure 1. (D) Primary FLT3-ITD AML blasts (n=2, AML#1-2) were cultured without (-) or with (+) human stromal cells (HS27a) for two days and lysed. Immunoblot analysis of the indicated proteins was performed with β actin as a loading control. (E) Primary FLT3-ITD AML blasts (n=7, AML#3-9) were co-cultured on MS5 stromal cells for 24 h, then co-incubated in the presence of AC220 (1 nM), R428 (0.3 μM) or both for 48 h. Apoptosis induction was assessed by Annexin V/DAPI labeling and flow cytometry analysis. Results are from seven AML samples treated in independent experiments. (F) MV4-11 cells were incubated with AC220 (1 nM), without (none) or with stromal cells (OP9) added with Ctrl-Fc or AXL-Fc (1 μg/mL). Cell apoptosis was determined as indicated in Figure 1. (G) MV4-11 cells were incubated in the absence (Vehicle) or presence of AC220 (3 nM), without (None) or with OP9 stromal cells that express shCtrl or shGAS6. Apoptosis induction was determined as described above. Graphs show the mean±Standard Error of Mean of results of at least three independent experiments. **P*<0.05; ***P*<0.01; ****P*<0.001.

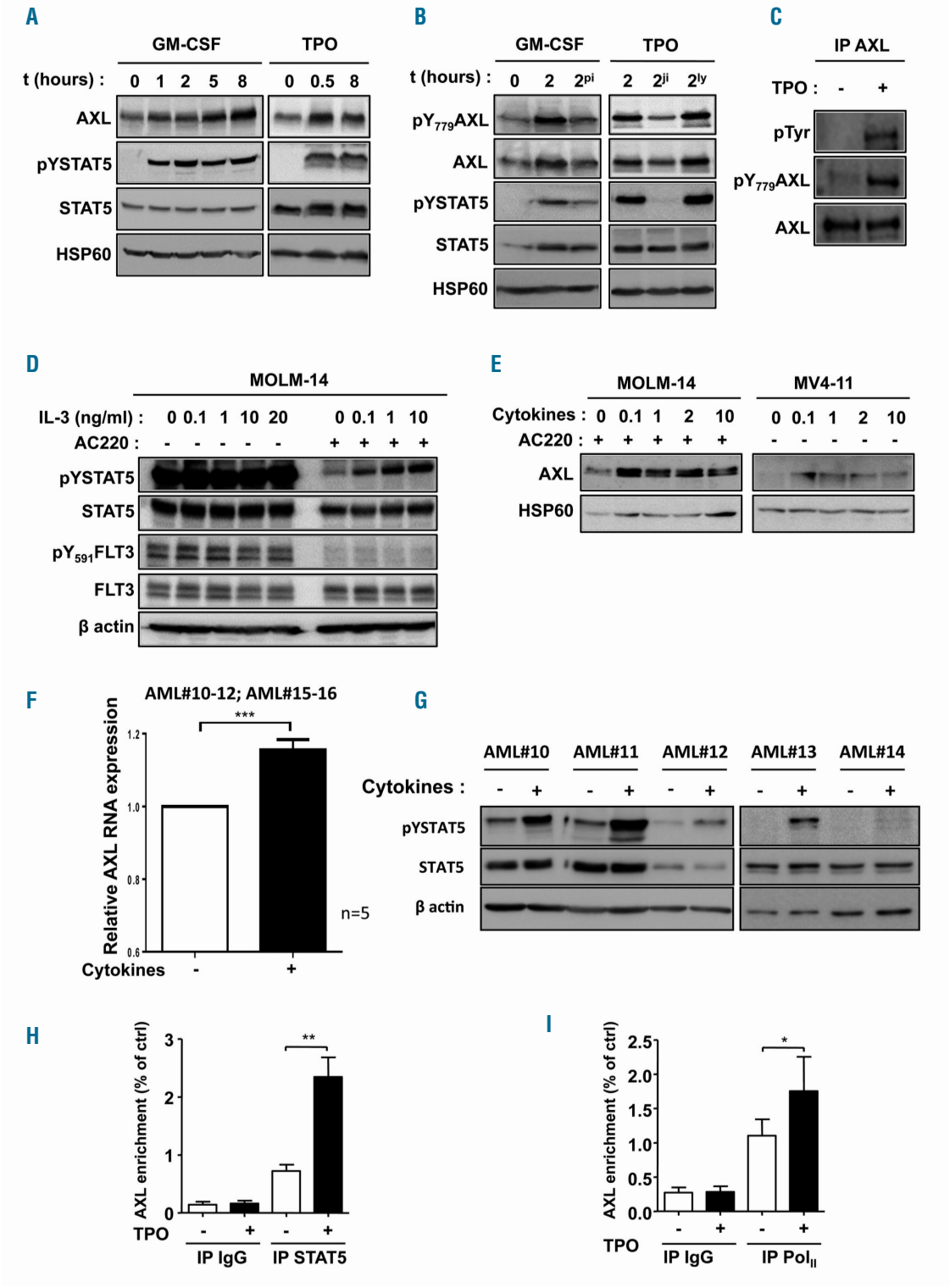

Figure 3. Activation of STAT5 up-regulates AXL gene expression and phosphorylation. (A) UT7-mpl acute myeloid leukemia (AML) cells were treated with GM-CSF (2.5 ng/mL) or TPO (20 nM) for the indicated time and lysed. Immunoblot analysis of the indicated proteins; HSP60 was used as a loading control. (B) UT7-mpl cells were treated with GM-CSF (2.5 ng/mL) or TPO (20 nM) for the indicated time in the absence or presence of pimozide (pi, 2 μM), JAK inhibitor-I (ji, 1 μM) or Ly294002 (ly, 20 μM). Total cell lysates were analyzed by western blotting with the indicated antibodies. HSP60 was used as a loading control. (C) UT7-mpl cells were incubated with (+) or without (-) TPO (20 nM) for one hour (h) before being lysed. AXL immunoprecipitates were prepared and analyzed by immunoblotting with the indicated antibodies. (D and E) MOLM-14 or MV4-11 cells were pre-incubated with (+) or without (-) AC220 (3 nM) for 3 h before adding IL-3 (ng/mL, MOLM-14) or TPO (nM, MV4-11) at the indicated concentration. Cells were incubated for 4 h before being lysed. (F and G) MS5 co-cultured AML primary blasts were maintained in serum-free medium without stroma for 18 h before being incubated in the presence of a IL-3 (20 ng/mL)/GM-CSF (10 ng/mL)/TPO (20 nM) cytokine cocktail for 7 h and then lysed for protein (F, n=6, AML#10-12 and 15-16) and mRNA (G, n=5, AML#10-14) purification. Immunoblot analysis of the indicated proteins using β actin or HSP60 as loading controls; real-time quantitative polymerase chain reaction (RT-qPCR) quantification of AXL mRNA levels in cytokine-treated and untreated primary AML cells, normalized to GAPDH expression, and expressed relative to untreated cells. (H and I) UT7-mpl cells were incubated with (+) or without (-) TPO (20 nM) for 30 minutes. Chromatin-immunoprecipitation (IP) assays were performed using control immunoglobulins (IP IgG), STAT5 (IP STAT5) or RNA polymerase II (IP PolII) antibodies. Immunoprecipitated DNA were analyzed by qPCR using primers spanning the conserved STAT5-responsive element of AXL gene sequence and expressed relative to total lysates (input). Graphs show the mean±Standard Error of Mean of at least three independent experiments. **P*<0.05; ***P*<0.01; ****P*<0.001; NS: not significant.

ChIP (Figure 3I). These data indicated that STAT5 binds to the AXL gene and increases AXL promoter activity.

Taken together, these data indicated that STAT5 mediates stroma-dependent AXL upregulation.

Low O_2 concentration enhances AXL expression

In addition to stromal cells and cytokines, the hematopoietic niche is also characterized by low O_2 concentrations, which have been linked to AXL expression in other cancer cells.[24,31] We thus assessed the contribution of low O_2 levels (1% O_2) in this model. Interestingly, hypoxia enhanced AXL expression in both FLT3-ITD AML cell lines and primary FLT3-ITD AML blasts (Figure 4A and AML#17 in Figure 4B and *Online Supplementary Table S2*). Several Hypoxia-Response Elements (HRE) have been described within a 2.4 kb fragment of the AXL promoter.[24] AXL transcript levels were thus assessed in hypoxic culture for both AML cell lines and primary AML blasts. In all cells, hypoxia enhanced AXL RNA expression, thereby indicating that O_2 levels affect AXL expression (Figure 4C and AML#18-20 in Figure 4D and *Online Supplementary Table S2*).

As AXL contributed to FLT3-ITD AML cell survival in normoxia (see Figure 2C), we then analyzed its involvement in AML cell survival in hypoxia by using the AXL-TKI R428. In the absence of stroma, R428-induced apoptosis was similar in hypoxia and normoxia. Conversely, in the presence of stroma, R428 triggered much stronger apoptosis under hypoxia (*Online Supplementary Figure S4*). Overall, these data indicate that both low O_2 concentrations and STAT5-activating stromal cytokines, in addition to GAS6, regulate AXL activity, thus mediating stronger AXL-dependent protection of AML cells.

AXL mediates microenvironment-dependent resistance of FLT3-ITD acute myeloid leukemia cells to AC220 treatment *in vivo*

Having shown that AXL mediates microenvironment-dependent protection against quizartinib *in vitro*, we analyzed the contribution of AXL *in vivo*. To better investigate the role of AXL on a long timescale, we generated stable AXL KD FLT3-ITD AML cells through lentivirus-mediated RNA interference (*Online Supplementary Figure S5A*). MV4-11 shCtrl and MV4-11 shAXL cells were engineered to stably express the firefly luciferase gene. They were xenografted by vein injection and leukemic cell engraftment was analyzed by bioluminescence imaging (BLI). BLI analysis did not evidence any significant difference in

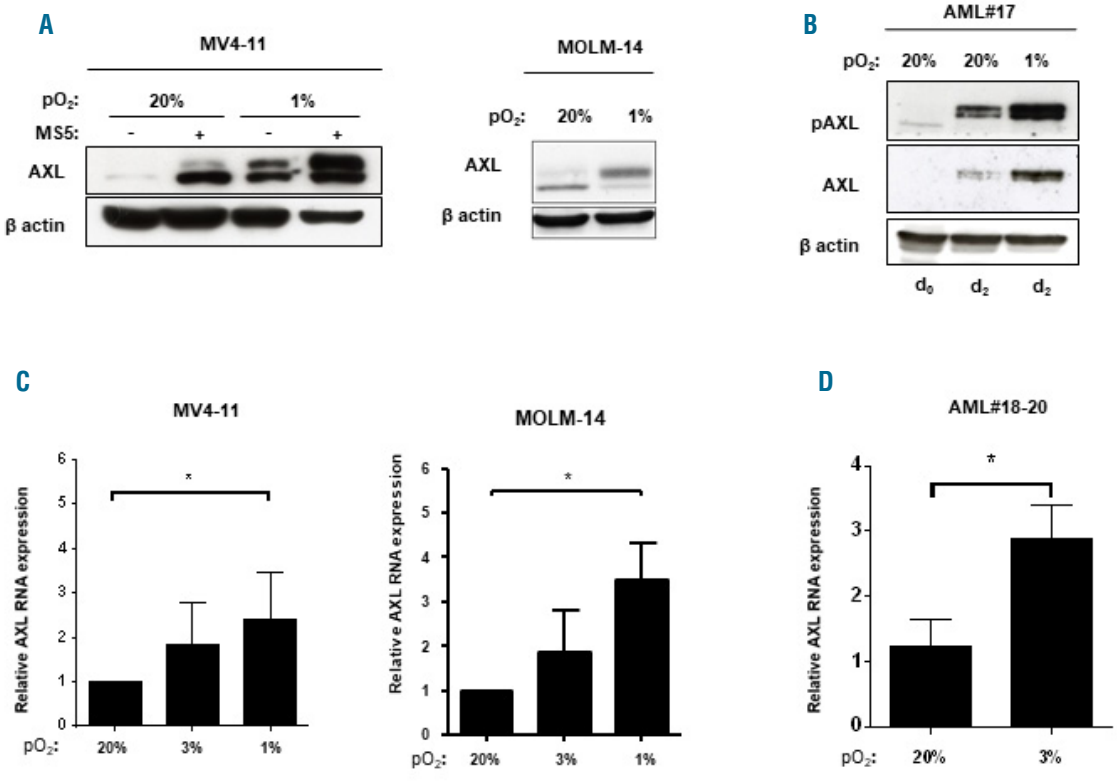

Figure 4. Low O_2 concentration up-regulates AXL expression of FLT3-ITD acute myeloid leukemia (AML) cells. (A) MV4-11 cells were incubated for 48 hours (h) at 20% or 1% O_2 with or without MS5 stromal cells as indicated; MOLM-14 cells were incubated for 48 h at 20% or 1% O_2 without stroma. Immunoblot analysis of the indicated proteins was performed with β actin as a loading control. (B) Primary FLT3-ITD AML blasts (AML#17) were cultured with HS27a stromal cells for two days in normoxia (20%) and hypoxia (1%). Samples were lysed at day zero and two days after growth on stromal cells. Immunoblot analysis of the indicated proteins was performed with β actin as a loading control. (C) MV4-11 and MOLM-14 cells were incubated for 48 h at 20%, 3%, 1% O_2. Real-time quantitative polymerase chain reaction (RT-qPCR) analysis of AXL mRNA was performed. Results are normalized to GUSB expression and expressed relative to 20% O_2 cultured cells. (D) Primary AML blasts (n=3, AML#18-20) were incubated for 48 h at 20% and 3% O_2. RT-qPCR analysis of AXL mRNA was performed as in (B). Graphs show the mean±Standard Error of Mean of results of at least three independent experiments. *P<0.05; **P<0.01; ***P<0.001.

engraftment (timing, intensity) between MV4-11 shCtrl and MV4-11 shAXL cells after seven days (*Online Supplementary Figure S5B*). Half of the mouse cohort was then treated with AC220 (5 mg/kg/day) by daily oral gavage for seven days, and response to treatment was assessed by BLI at day 14. The tolerance to treatment was checked by body weight control twice a week. A similar bioluminescence indicative of tumor progression was observed for MV4-11 shCtrl and MV4-11 shAXL cells in the vehicle-treated cohort (Figure 5A and B). In contrast, a significant decrease in total bioluminescent signal was observed in response to AC220 in MV4-11 shAXL-engrafted mice as compared to MV4-11 shCtrl-engrafted animals (P<0.01) (Figure 5B). To strengthen these data in the specific setting of the microenvironment, another set of experiments was performed with the same sequence of conditioning, engraftment and treatment, but BLI was performed upon treatment on femurs and tibias *ex vivo* at sacrifice. Again, a significant decrease in bioluminescence was observed in bones from AC220-treated MV4-11 shAXL-engrafted mice compared to bones from MV4-11 shCtrl-engrafted animals, whereas no significant difference was observed between these two cohorts in the absence of treatment (Figure 5C). Immunohistochemistry analysis of BM was then performed to trace human cells in the murine bone marrow tissue. Similar amounts of human cells were detected in MV4-11 shCtrl- and shAXL-injected mice in the absence of treatment (Figure 5D). In the AC220-treated cohort, as expected, lower amounts of human cells were detected in MV4-11 shCtrl-engrafted BM than in the untreated cohort. Interestingly, almost no human cells were detectable in MV4-11 shAXL-treated animal samples, so BLI detection was under the threshold in MV4-11 shAXL-treated animals (Figure 5D). Altogether, these results show that AXL plays a key role in the AC220 response of FLT3-ITD AML cells in the specific context of

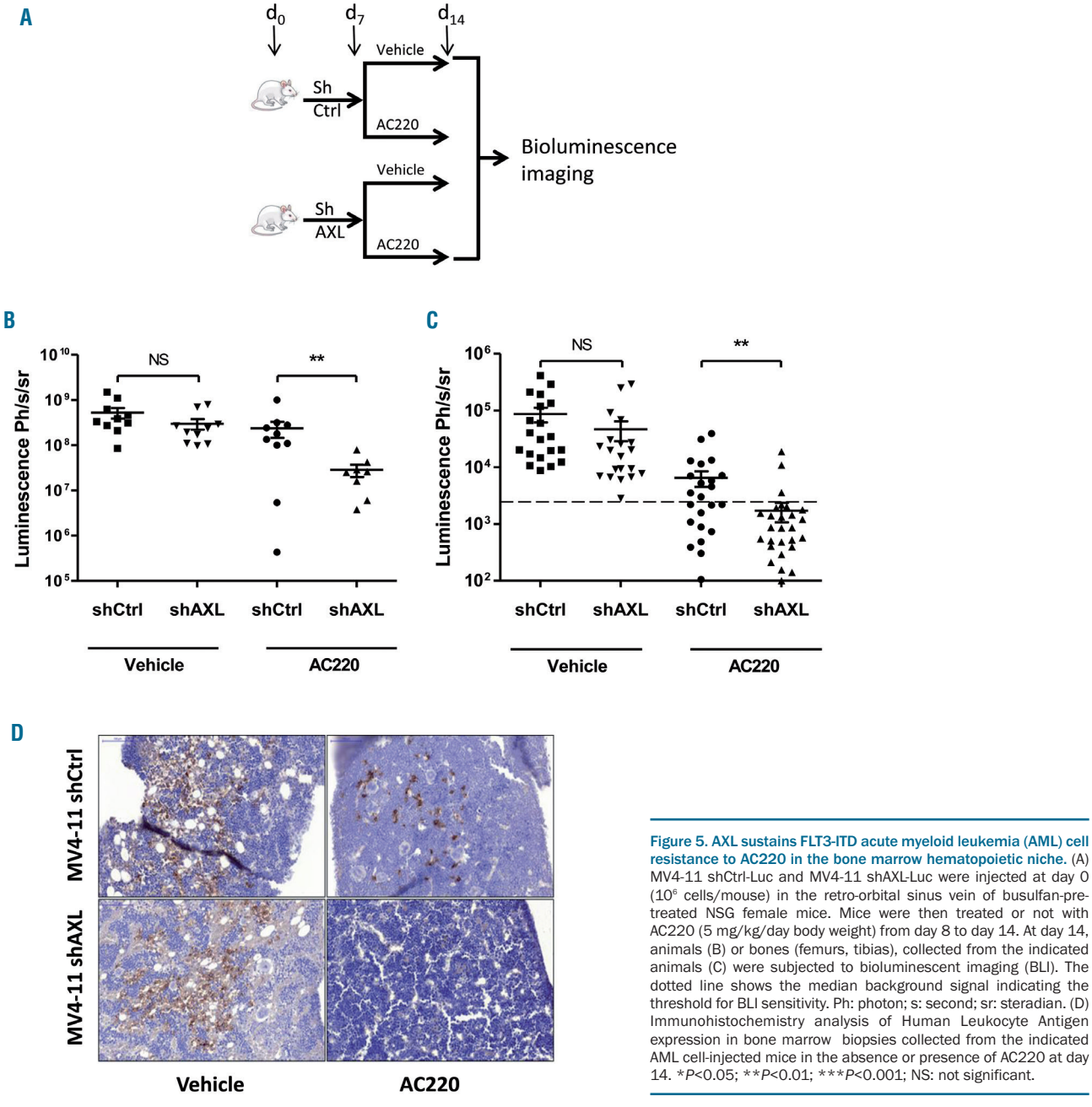

Figure 5. AXL sustains FLT3-ITD acute myeloid leukemia (AML) cell resistance to AC220 in the bone marrow hematopoietic niche. (A) MV4-11 shCtrl-Luc and MV4-11 shAXL-Luc were injected at day 0 (10^6 cells/mouse) in the retro-orbital sinus vein of busulfan-pre-treated NSG female mice. Mice were then treated or not with AC220 (5 mg/kg/day body weight) from day 8 to day 14. At day 14, animals (B) or bones (femurs, tibias), collected from the indicated animals (C) were subjected to bioluminescent imaging (BLI). The dotted line shows the median background signal indicating the threshold for BLI sensitivity. Ph: photon; s: second; sr: steradian. (D) Immunohistochemistry analysis of Human Leukocyte Antigen expression in bone marrow biopsies collected from the indicated AML cell-injected mice in the absence or presence of AC220 at day 14. *P<0.05; **P<0.01; ***P<0.001; NS: not significant.

the hematopoietic niche, thus confirming our *in vitro* and *ex vivo* data.

Next, we wondered whether the bone marrow niche protection of FLT3-ITD AML cells is specific to the hematopoietic niche conditions or if it would be similar in other microenvironments. We thus evaluated the impact of quizartinib on subcutaneous xenograft tumor growth using control (MV4-11 shCtrl) and AXL KD (MV4-11 shAXL) AML cells. Subcutaneous implantation of these cells into immunodeficient NSG mice resulted in solid tumors without any difference between MV4-11 shCtrl and MV4-11 shAXL cells (*Online Supplementary Figure S5C*). After 21 days, when tumors reached 300-500 mm^3, half of the mouse cohort received AC220 by daily oral gavage (5 mg/kg/day). This resulted in complete regression of the tumors after 14 days. We did not observe any difference between MV4-11 shCtrl and MV4-11 shAXL in terms of response to AC220 treatment regarding both the kinetic and intensity of tumor regression (*Online Supplementary Figure S5C*). The daily administration of AC220 was ceased after full tumor regression, allowing tumor regrowth 12 days after AC220 withdrawal. Again, a similar progression was observed post-relapse between MV4-11 shCtrl and MV4-11 shAXL-injected cohorts both in time to relapse and in tumor volumes, thus confirming the specific role of the hematopoietic niche (*Online Supplementary Figure S5C*). Similar tumor weights at sacrifice confirmed these observations (*Online Supplementary Figure S5D*).

The absence of any difference in subcutaneous tumor growth between MV4-11 shCtrl and MV4-11 shAXL-injected animals shows that the instrumental role of AXL in protecting AML cells against FLT3-targeted therapy *in vivo* is specifically mediated by the hematopoietic niche.

Discussion

These findings show that the bone marrow hematopoietic niche provides specific protection for FLT3-ITD AML cells against quizartinib by multiple signaling pathways converging to AXL upregulation and activation. In addition to the established role of the AXL canonical ligand GAS6, the bone marrow niche enhances AXL expression and the activity of AML cells through both STAT5-activating soluble factors and local hypoxic environment.

The microenvironment was already known to promote AML cell resistance *via* several mechanisms such as CXCL12-CXCR4 signaling,[32] adhesion molecules such as CD44 and selectins,[33] vasculature by VEGF,[34] and angiopoietins/TIE2 signaling[35] and well-reviewed by Brenner *et al.*[36] More recently, FLT3-ligand and FGF1/2 were also identified as protective molecules against FLT3-TKI *in vitro*.[37] Hypoxia, a key factor of the microenvironment, was also reported to drive pro-tumoral signaling in AML *via* a HIF1α/MIF/IL8 pathway that is also thought to play a role in chronic lymphocytic leukemia survival.[38] Stroma has also been shown to sustain AML cell resistance to cytarabine *via* activation of the AXL receptor upon AML cell-dependent education of stroma to secrete GAS6 *in vitro*.[21] We now provide evidence that several microenvironment messages converge to enhance AXL expression and activation, which sustain pro-survival signals to selectively protect FLT3-ITD AML cells from quizartinib treatment *in situ*. Beyond demonstrating the value of AXL as a therapeutic target for AML burden, our data suggest a more appealing approach in which prevention of AXL expression will be key to alleviating protection against treatment of the leukemic initiating cells provided by their hematopoietic niche.

The role of cytokines and growth factors inside the hematopoietic niche with regard to AML cell survival has long been debated. TPO receptor expression level has been shown in approximately 50% of AML patients.[30] In addition, primary human AML engrafts with higher efficacy in mice in which human versions of CSF1, CSF2, IL3 and TPO genes are knocked-in into murine loci, suggesting the central role of these cytokines.[39] The IL-3 receptor (CD123), whose expression carries a poor prognosis,[40] is thought to be a marker for AML-initiating cells[41] and to be closely related with FLT3-ITD mutation.[42] Our data now demonstrate a new survival mechanism provided by STAT5/hypoxia in the upregulation of AXL.

AXL expression is often up-regulated in solid tumors. Its activation has been mostly observed under stress conditions associated with metastatic disease or in situations where tumor cells are under severe nutrient deprivation. Knowledge about the extracellular messages that regulate AXL expression is limited. However, interferon-α has been reported to enhance AXL expression in monocytes through a STAT1-dependent pathway, but the mechanism by which this is achieved has not yet been investigated.[43] Our results show for the first time that the *AXL* gene exhibits a conserved SRE that binds cytokine-activated STAT5 which up-regulates AXL gene expression through enhanced recruitment of RNAPolII. All the cytokines studied (IL-3, GM-CSF and TPO) activated both STAT5A and STAT5B, but we observed that STAT5A-selective knockdown triggered massive AXL downregulation, whatever the levels of STAT5B expression and activation (*Dumas et al., 2019, personal communications*). These observations suggest that STAT5A plays a dominant role in AXL regulation, an observation that fits with major regulation by STAT5A of other genes like HIF2α or PHD3 that promote HSPC and leukemia cell maintenance, as we and others have observed.[44] Whether other STAT5-activating factors also enhance AXL expression and contribute to tumorigenesis and resistance of other myeloid leukemia, non-myeloid leukemia and/or solid tumors awaits further investigation.

The current findings show that STAT5-activating factors not only enhance AXL expression but also trigger AXL activation. Indeed, TK receptors such as EGFR or VEGFR, which activate Src kinases,[45] and FLT3, were shown to activate AXL.[22] AXL also functions as a docking site for non-receptor kinases such as Syk and Lyn,[46] which could be activated by hematopoietic niche signals. Whether other kinases mediate AXL activation remains to be studied.

AXL expression is known to be modulated by O_2 concentration in various solid tumors.[24,31] Our present data extend these observations to AML. Low O_2 concentrations are a well-known BM niche hallmark.[47] Hypoxia was shown to down-regulate FLT3 and FLT3-ITD signaling in AML cells.[48] Under such conditions, the PI3K/AKT pathway was shown to sustain AML cell survival, rescuing FLT3 activity,[49] while AXL is known to activate PI3K/AKT signaling in AML cells. We and others have previously shown that cytokine-activated STAT5 enhances HIF2α expression directly[44] but also indirectly by inhibiting one

of its destabilizers, the prolyl 4-hydroxylase domain protein 3 (PHD3) in both normal hematopoietic progenitors and leukemic cells.[27] Such activities might reinforce the hypoxia-induced message coming directly from the microenvironment and strengthen AXL overexpression.

Finally, our data show that the hematopoietic niche provides selective signals regulating AXL expression. This plays a pivotal role in the selective response of FLT3-ITD AML cells to quizartinib within the specific location of the bone marrow, where leukemic stem cells are well maintained. Our study suggests that, in addition to the dual inhibition of AXL and FLT3 through TKI combination or a dual TK inhibitor such as gilteritinib, targeting AXL upstream signaling steps could be investigated in targeting FLT3-ITD AML-initiating cells in the hematopoietic niche.[9,50]

Acknowledgments

We thank Mrs. Bernadette De Buhan and her family for their generous support. We thank the Cytometry and Genomic Facilities of Institut Cochin/Inserm U1016, the Cytometry Facility, Vectorology Facility, Animals Facility and Histology Facility of FR TransBioMed, Bordeaux University, for performing cell sorting, microarray screening and handling animals. We thank the Obstetric Unit at Orsay Hospital and the Cell Therapy Center at St-Louis hospital (Paris, France) for providing CB samples. P-YD was a recipient of the SIRIC Brio for research fellowship for one year, then the MD-PhD program from the University Hospital of Bordeaux for two years. CN and SM-L were fellows of the "Association pour la recherche contre le Cancer", "Ligue Nationale contre le Cancer" and Région Ile de France DIM-Biothérapies.We thank David Galeazzi for accurate data collection concerning patients at Bordeaux University Hospital. We also acknowledge the Centre de Ressources Biologiques Cancer, Bordeaux Biothèques Santé (BB-0033-00036) at Bordeaux University Hospital as well as the CRBP at the Hematology unit at Cochin Hospital (CPP: 2015-08-11 DC) for providing biological material.

Funding

AG was funded by the SIRIC Brio (grant INCa-DGOS-Inserm 6046) for his work at the UMS 005 TBM Core histopathology platform. This work was supported by grants from the Institut National de la Santé et de la Recherche Médicale (INSERM), Centre National de la Recherche Scientifique (CNRS), Paris-Descartes University, Agence Nationale de Recherche (ANR-2011-RPIB-009-04), Ligue Nationale contre le Cancer (RS13/75-6; EL2014-3), Ligue Régionale contre le Cancer (Comité Pyrénées Atlantique et comité Ile de Paris) and Cancéropôle Grand Sud-Ouest (2015-0389). We thank the data management unit at Toulouse University Hospital and the CAPTOR (Cancer Pharmacology of Toulouse Oncopole and Region) project (ANR-11-PHUC-001) for its financial support enabling e-CRF for the AML database. The funders had no role in study design, data collection or analysis, decision to publish or preparation of the manuscript. We thank Prof. D. Bouscary, Dr P. Auberger and Dr E. Lauret for their critical reading of the manuscript.

References

1. Gilliland DG, Griffin JD. The roles of FLT3 in hematopoiesis and leukemia. Blood. 2002;100(5):1532-1542.
2. Papaemmanuil E, Gerstung M, Bullinger L, et al. Genomic Classification and Prognosis in Acute Myeloid Leukemia. N Engl J Med. 2016;374(23):2209-2221.
3. Hirsch P, Zhang Y, Tang R, et al. Genetic hierarchy and temporal variegation in the clonal history of acute myeloid leukaemia. Nat Commun. 2016;7:12475.
4. Smith CC, Wang Q, Chin C-S, et al. Validation of ITD mutations in FLT3 as a therapeutic target in human acute myeloid leukaemia. Nature. 2012;485(7397):260-263.
5. Stirewalt DL, Kopecky KJ, Meshinchi S, et al. Size of FLT3 internal tandem duplication has prognostic significance in patients with acute myeloid leukemia. Blood. 2006; 107(9):3724-3726.
6. Schlenk RF, Dohner K, Krauter J, et al. Mutations and Treatment Outcome in Cytogenetically Normal Acute Myeloid Leukemia. N Engl J Med. 2008; 358(18):1909-1918.
7. Fischer M, Schnetzke U, Spies-Weisshart Br, et al. Impact of FLT3-ITD diversity on response to induction chemotherapy in patients with acute myeloid leukemia. Haematologica. 2017;102(4):e129-e131.
8. Choudhary C, Brandts C, Schwable J, et al. Activation mechanisms of STAT5 by oncogenic Flt3-ITD. Blood. 2007;110(1):370-374.
9. Cortes JE, Tallman MS, Schiller GJ, et al. Phase 2b study of 2 dosing regimens of quizartinib monotherapy in FLT3-ITD mutated, relapsed or refractory AML. Blood. 2018;132(6):598-607.
10. Sexauer A, Perl A, Yang X, et al. Terminal myeloid differentiation in vivo is induced by FLT3 inhibition in FLT3/ITD AML. Blood. 2012;120(20):4205-4214.
11. Green AS, Maciel TT, Hospital MA, et al. Pim kinases modulate resistance to FLT3 tyrosine kinase inhibitors in FLT3-ITD acute myeloid leukemia. Sci Adv. 2015;1 (8):e1500221.
12. Sato T, Yang X, Knapper S, et al. FLT3 ligand impedes the efficacy of FLT3 inhibitors in vitro and in vivo. Blood. 2011; 117(12):3286-3293.
13. Linger RMA, Keating AK, Earp HS, Graham DK. TAM Receptor Tyrosine Kinases: Biologic Functions, Signaling, and Potential Therapeutic Targeting in Human Cancer. Advances in Cancer Research. In: Klein GFVWaG, ed. Volume 100 ed: Academic Press, 2008:35-83.
14. Schoumacher M, Burbridge M. Key Roles of AXL and MER Receptor Tyrosine Kinases in Resistance to Multiple Anticancer Therapies. Curr Oncol Rep. 2017;19(3):19.
15. Graham DK, DeRyckere D, Davies KD, Earp HS. The TAM family: phosphatidylserine-sensing receptor tyrosine kinases gone awry in cancer. Nat Rev Cancer. 2014;14(12):769-785.
16. Verma A, Warner SL, Vankayalapati H, Bearss DJ, Sharma S. Targeting axl and mer kinases in cancer. Mol Cancer Ther. 2011; 10(10):1763-1773.
17. Gioia R, Leroy C, Drullion C, et al. Quantitative phosphoproteomics revealed interplay between Syk and Lyn in the resistance to nilotinib in chronic myeloid leukemia cells. Blood. 2011;118(8):2211-2221.
18. Rochlitz C, Lohri A, Bacchi M, et al. Axl expression is associated with adverse prognosis and with expression of Bcl-2 and CD34 in de novo acute myeloid leukemia (AML): results from a multicenter trial of the Swiss Group for Clinical Cancer Research (SAKK). Leukemia. 1999; 13(9):1352-1358.
19. Whitman SP, Kohlschmidt J, Maharry K, et al. GAS6 expression identifies high-risk adult AML patients: potential implications for therapy. Leukemia. 2014;28(6):1252-1258.
20. Hong CC, Lay JD, Huang JS, et al. Receptor tyrosine kinase AXL is induced by chemotherapy drugs and overexpression of AXL confers drug resistance in acute myeloid leukemia. Cancer Lett. 2008; 268(2):314-324.
21. Ben-Batalla I, Schultze A, Wroblewski M, et al. Axl, a prognostic and therapeutic target in acute myeloid leukemia mediates paracrine cross-talk of leukemia cells with bone marrow stroma. Blood. 2013; 122(14):2443-2452.
22. Park I-K, Mishra A, Chandler J, Whitman SP, Marcucci G, Caligiuri MA. Inhibition of the receptor tyrosine kinase Axl impedes activation of the FLT3 internal tandem duplication in human acute myeloid leukemia: implications for Axl as a potential therapeutic target. Blood. 2013;

121(11):2064-2073.
23. Park IK, Mundy-Bosse B, Whitman SP, et al. Receptor tyrosine kinase Axl is required for resistance of leukemic cells to FLT3-targeted therapy in acute myeloid leukemia. Leukemia. 2015;29(12):2382-2389.
24. Rankin EB, Fuh KC, Castellini L, et al. Direct regulation of GAS6/AXL signaling by HIF promotes renal metastasis through SRC and MET. Proc Natl Acad Sci U S A. 2014;111(37):13373-13378.
25. Porteu F, Rouyez MC, Cocault L, et al. Functional regions of the mouse thrombopoietin receptor cytoplasmic domain: evidence for a critical region which is involved in differentiation and can be complemented by erythropoietin. Mol Cell Biol. 1996;16(5):2473-2482.
26. Wingelhofer B, Maurer B, Heyes EC, et al. Pharmacologic inhibition of STAT5 in acute myeloid leukemia. Leukemia. 2018;32(5): 1135-1146.
27. Casetti L, Martin-Lanneree S, Najjar I, et al. Differential contributions of STAT5A and STAT5B to stress protection and tyrosine kinase inhibitor resistance of chronic myeloid leukemia stem/progenitor cells. Cancer Res. 2013;73(7):2052-2058.
28. Holland SJ, Pan A, Franci C, et al. R428, a selective small molecule inhibitor of Axl kinase, blocks tumor spread and prolongs survival in models of metastatic breast cancer. Cancer Res. 2010;70(4):1544-1554.
29. Angelini DF, Ottone T, Guerrera G, et al. A Leukemia-Associated CD34/CD123/CD25/CD99+ immunophenotype identifies FLT3-mutated clones in acute myeloid leukemia. Clin Cancer Res. 2015;21(17): 3977-3985.
30. Rauch PJ, Ellegast JM, Widmer CC, et al. MPL expression on AML blasts predicts peripheral blood neutropenia and thrombocytopenia. Blood. 2016;128(18):2253-2257.
31. Mishra A, Wang J, Shiozawa Y, et al. Hypoxia Stabilizes GAS6/Axl Signaling in Metastatic Prostate Cancer. Mol Can Res. 2012;10(6):703-712.
32. Braun M, Qorraj M, Buttner M, et al. CXCL12 promotes glycolytic reprogramming in acute myeloid leukemia cells via the CXCR4/mTOR axis. Leukemia. 2016;30(8):1788-1792.
33. Jin L, Hope KJ, Zhai Q, Smadja-Joffe F, Dick JE. Targeting of CD44 eradicates human acute myeloid leukemic stem cells. Nat Med. 2006;12(10):1167-1174.
34. Dias S, Hattori K, Zhu Z, et al. Autocrine stimulation of VEGFR-2 activates human leukemic cell growth and migration. J Clin Invest. 2000;106(4):511-521.
35. Schliemann C, Bieker R, Padro T, et al. Expression of angiopoietins and their receptor Tie2 in the bone marrow of patients with acute myeloid leukemia. Haematologica. 2006;91(9):1203-1211.
36. Brenner AK, Nepstad I, Bruserud O. Mesenchymal Stem Cells Support Survival and Proliferation of Primary Human Acute Myeloid Leukemia Cells through Heterogeneous Molecular Mechanisms. Front Immunol. 2017;8:106.
37. Traer E, Martinez J, Javidi-Sharifi N, et al. FGF2 from Marrow Microenvironment Promotes Resistance to FLT3 Inhibitors in Acute Myeloid Leukemia. Cancer Res. 2016;76(22):6471-6482.
38. Abdul-Aziz AM, Shafat MS, Sun Y, et al. HIF1alpha drives chemokine factor pro-tumoral signaling pathways in acute myeloid leukemia. Oncogene. 2018;37(20): 2676-2686.
39. Ellegast JM, Rauch PJ, Kovtonyuk LV, et al. inv(16) and NPM1mut AMLs engraft human cytokine knock-in mice. Blood. 2016;128(17):2130-2134.
40. Vergez F, Green AS, Tamburini J, et al. High levels of CD34+/CD38low/CD123+ blasts are predictive of an adverse outcome in acute myeloid leukemia: a Groupe Ouest-Est des Leucémies Aiguës et Maladies du Sang (GOELAMS) study. Haematologica. 2011;96(12):1792-1798.
41. Jordan CT, Upchurch D, Szilvassy SJ, et al. The interleukin-3 receptor alpha chain is a unique marker for human acute myelogenous leukemia stem cells. Leukemia. 2000;14(10):1777-1784.
42. Riccioni R, Diverio D, Riti V, et al. Interleukin (IL)-3/granulocyte macrophage-colony stimulating factor/IL-5 receptor alpha and beta chains are preferentially expressed in acute myeloid leukaemias with mutated FMS-related tyrosine kinase 3 receptor. Br J Haematol. 2009;144(3):376-387.
43. Rothlin CV, Ghosh S, Zuniga EI, Oldstone MB, Lemke G. TAM receptors are pleiotropic inhibitors of the innate immune response. Cell. 2007;131(6):1124-1136.
44. Fatrai S, Wierenga AT, Daenen SM, Vellenga E, Schuringa JJ. Identification of HIF2alpha as an important STAT5 target gene in human hematopoietic stem cells. Blood. 2011;117(12):3320-3330.
45. Ruan G-X, Kazlauskas A. Axl is essential for VEGF-A-dependent activation of PI3K/Akt. EMBO J. 2012;31(7):1692-1703.
46. Gioia R, Tregoat C, Dumas PY, et al. CBL controls a tyrosine kinase network involving AXL, SYK and LYN in nilotinib-resistant chronic myeloid leukaemia. J Pathol. 2015; 237(1):14-24.
47. Spencer JA, Ferraro F, Roussakis E, et al. Direct measurement of local oxygen concentration in the bone marrow of live animals. Nature. 2014;508(7495):269-273.
48. Sironi S, Wagner M, Kuett A, et al. Microenvironmental hypoxia regulates FLT3 expression and biology in AML. Sci Rep. 2015;5:17550.
49. Jin L, Tabe Y, Lu H, et al. Mechanisms of apoptosis induction by simultaneous inhibition of PI3K and FLT3-ITD in AML cells in the hypoxic bone marrow microenvironment. Cancer Lett. 2013;329(1):45-58.
50. Perl AE, Altman JK, Cortes J, et al. Selective inhibition of FLT3 by gilteritinib in relapsed or refractory acute myeloid leukaemia: a multicentre, first-in-human, open-label, phase 1-2 study. Lancet Oncol. 2017; 18(8):1061-1075.

Ferrata Storti Foundation

A systematic literature review and meta-analysis of minimal residual disease as a prognostic indicator in adult B-cell acute lymphoblastic leukemia

Renato Bassan,[1] Monika Brüggemann,[2] Hoi-Shen Radcliffe,[3] Elizabeth Hartfield,[4] Georg Kreuzbauer[5] and Sally Wetten[3]

[1]Complex Operative Unit of Haematology, dell'Angelo Hospital and Santissimi Giovanni and Paolo Hospital, Mestre and Venice, Italy; [2]Department of Medicine II, Schleswig-Holstein University Hospital, Kiel, Germany; [3]Amgen Ltd, Uxbridge, UK; [4]Oxford PharmaGenesis, Oxford, UK and [5]Amgen (Europe) GmbH, Zug, Switzerland

Haematologica 2019
Volume 104(10):2028-2039

ABSTRACT

Minimal (or 'measurable') residual disease in acute lymphoblastic leukemia appears to be a prognostic indicator, with potential value in informing individualized treatment decisions. Complete understanding of the strength of the association between minimal residual disease and long-term outcomes is, however, lacking. A systematic literature review and meta-analysis were performed to elucidate the clinical significance of minimal residual disease with respect to relapse-free survival and overall survival in precursor B-cell acute lymphoblastic leukemia. A total of 23 articles and abstracts, most published between 2012 and 2016, were identified for inclusion in the primary meta-analysis. Typically, patients were in their first complete remission at the time of minimal residual disease assessment; in two studies, all patients were in their second, or later, complete remission. The primary analysis revealed improved relapse-free survival across all studies for patients who achieved minimal residual disease negativity (random effects hazard ratio, 2.34; 95% confidence interval, 1.91–2.86). Improved overall survival for patients who achieved minimal residual disease negativity was also observed (hazard ratio, 2.19; 95% confidence interval, 1.63–2.94). There was no observed difference in the impact of minimal residual disease status in subgroups based on disease stage, minimal residual disease sensitivity threshold level, Philadelphia chromosome status, histological phenotype, risk group, minimal residual disease testing location, minimal residual disease timing after induction, or minimal residual disease detection method. Despite heterogeneity in study design and patient populations between the contributing studies, these data provide a compelling argument for minimal residual disease as a clinical tool for assessing prognosis and guiding treatment decisions in precursor B-cell acute lymphoblastic leukemia.

Correspondence:

RENATO BASSAN
renato.bassan@aulss3.veneto.it

Received: July 2, 2018.

Accepted: March 14, 2019.

Pre-published: March 19, 2019.

doi:10.3324/haematol.2018.201053

Check the online version for the most updated information on this article, online supplements, and information on authorship & disclosures: www.haematologica.org/content/104/10/2028

Introduction

Acute lymphoblastic leukemia (ALL) is a heterogeneous disease that derives from lymphoid cell populations.[1] Precursor B-cell ALL (B-ALL) is the most common immunological subtype,[2] and the most common genetic abnormality in B-ALL is the Philadelphia chromosome (Ph-positive ALL), found in approximately one-quarter of adult patients.[3] Genetic or molecular profiling can be used to characterize disease prognosis, predict response to therapy, and inform treatment decisions.[4,5]

The mainstay of treatment for patients with newly diagnosed B-ALL has historically involved induction chemotherapy, followed by consolidation and maintenance chemotherapies; allogeneic hematopoietic stem cell transplantation (HSCT) is recommended following consolidation in selected high-risk groups.[6] However,

for patients with Ph-positive disease in particular, outcomes with standard combination chemotherapy are poor.[3] The tyrosine kinase inhibitors imatinib, dasatinib, nilotinib, and ponatinib have shown efficacy in patients with Ph-positive disease, and there are some preliminary suggestions that they may also be efficacious in selected subsets of Ph-negative ALL.[6–8] Moreover, several targeted therapies have been developed for patients with B-ALL, such as the antibody-based therapies rituximab, inotuzumab ozogamicin and blinatumomab, these latter demonstrating greater effectiveness than salvage chemotherapy in the very high-risk setting of relapsed/refractory ALL, including both Ph-positive and Ph-negative patients.[9–11]

The introduction of targeted therapies, alongside advances in diagnostic procedures, have improved outcomes for patients with B-ALL.[12,13] However, despite a substantial proportion (74% to 91%) of patients achieving complete remission (CR), one-third or more will eventually relapse because of the presence of submicroscopic levels of leukemic cells in the bone marrow.[14–18] The presence of these remaining cancer cells is known as minimal residual disease (MRD; alternatively termed 'measurable residual disease').

MRD is increasingly being used in clinical practice as an independent prognostic marker for the duration of CR and long-term outcomes in patients with ALL, and for informing treatment decisions.[19–22] The European Society for Medical Oncology (ESMO) and National Comprehensive Cancer Network clinical practice guidelines for adult patients with ALL recommend the quantification of MRD whenever possible,[6,23,24] but it is not yet clear whether MRD status alone is sufficient to predict prognosis, or whether it should be combined with other parameters, such as patient-related (e.g., age) or disease-related (e.g., cytogenetics) risk factors. In drug development, MRD response has been considered as an early marker of efficacy in clinical studies, with potential use as a surrogate endpoint in registration studies for accelerated drug approval.[25,26] A full understanding of the prognostic significance of MRD is needed to guide its use across this broad range of settings.

A large number of studies have shown that achievement of MRD-negative status correlates positively with CR duration, reduced risk of relapse, and HSCT success.[22,27] The use of MRD testing is individualized within a given study protocol, and hence there is wide variation in the test method used, the timing and sensitivity of MRD assessment, the characteristics of the patients, and the treatments used before and after MRD was assessed. We conducted a systematic review to capture the evidence supporting the clinical significance of MRD on clinical outcomes and used this evidence to inform a meta-analysis with the aim of quantifying the impact of MRD status on relapse-free survival (RFS) and overall survival (OS). A recent meta-analysis suggested that event-free survival and OS were almost always better in patients with ALL who were MRD negative than in those who were MRD positive.[28] This meta-analysis included studies in children and adults, and in B-cell and T-cell phenotypes. Our meta-analysis focused on adult patients with B-ALL and includes 23 studies, 18 of which were not in the previous meta-analysis, which enabled us to explore the impact of MRD status within clinically important subgroups in this population.

Methods

Systematic literature review

Evidence base

We systematically reviewed published studies according to a prespecified protocol, using a process compliant with the 2009 Preferred Reporting Items for Systematic Reviews and Meta-Analyses (PRISMA) guidelines.[29] PubMed and Embase databases were searched (*Online Supplementary Table S1*) for studies in humans published in English between 1 January, 1995 and 1 March, 2016. Additional searches were conducted for congress proceedings [American Society of Clinical Oncology (ASCO), American Society of Hematology (ASH), European Hematology Association (EHA), and ESMO] published between 2012 and 2016.

Screening and data extraction

Titles or abstracts identified from the initial searches were evaluated against the prespecified inclusion criteria (*Online Supplementary Methods*). The full texts were obtained for all studies deemed eligible, and for studies whose eligibility was unclear during the title/abstract screening. The full texts were independently screened by two reviewers to confirm which studies should be included. Any discrepancies were resolved by a third reviewer. Data extraction is described in the *Online Supplementary Methods*.

Meta-analysis

Evidence base

Studies identified from the systematic literature review were excluded from the meta-analysis if RFS was not reported separately for patients who were MRD-negative and MRD-positive in status, or if insufficient data were reported to calculate a hazard ratio according to the methods outlined in Tierney *et al.*[30] For studies that included patients with B-ALL and T-cell ALL (T-ALL), hazard ratios were calculated only for the patients with B-ALL, if it was possible to do so.

Outcomes

The primary outcome was RFS – alternatively termed disease-free, event-free or leukemia-free survival in some publications. In studies that provided RFS definitions, RFS was mostly measured from CR until relapse or death. Other studies that provided a definition measured RFS from HSCT[31–33] or from the start of treatment.[34–36] For the purposes of the meta-analysis, we used the measure of RFS as provided in each study publication. The primary analysis set was based on studies that reported RFS according to MRD status. The secondary outcome was OS, determined from those studies in the primary analysis set that also reported OS according to MRD status.

Statistical analysis

The analysis of hazard ratios used unadjusted measures of treatment effect, where available. Meta-analysis was performed using the random effects model.[37,38] Heterogeneity between studies was assessed statistically using the I^2 and Cochran Q tests.[39,40] Meta-regression was performed to investigate the relationships between covariates (Ph status, median follow-up time, MRD cut-off sensitivity threshold, post-MRD treatment, disease stage, sex and age) and study-level hazard ratios.[38]

Results

Search results

The systematic literature search identified 1,899 records (1,252 full papers and 647 congress abstracts) for

title and abstract screening. An additional four full papers were included that were not identified during the systematic literature searches, giving a total of 1,903 records (Figure 1). Following screening of the title and abstract of each record, 278 records were included in the full text screen. Finally, 33 full papers and 21 congress abstracts were covered in the systematic review; these included 8,820 patients with B-ALL, 5,979 of whom had available MRD data. The study and patients' characteristics, together with clinical outcomes, are summarized in *Online Supplementary Tables S2–S7*. In total, 32 records (23 full texts and 9 congress abstracts) were eligible for the meta-analysis; of these, 23 records were included in the primary analysis set; the remaining papers were excluded because either the study populations overlapped with another, more recent, publication, and there were no unique data for inclusion in the meta-analysis, or inconsistencies in data reporting meant that it was not possible to calculate hazard ratios. A list of studies identified in the systematic review but not included in the meta-analysis, with reasons, is provided in *Online Supplementary Table S8*.

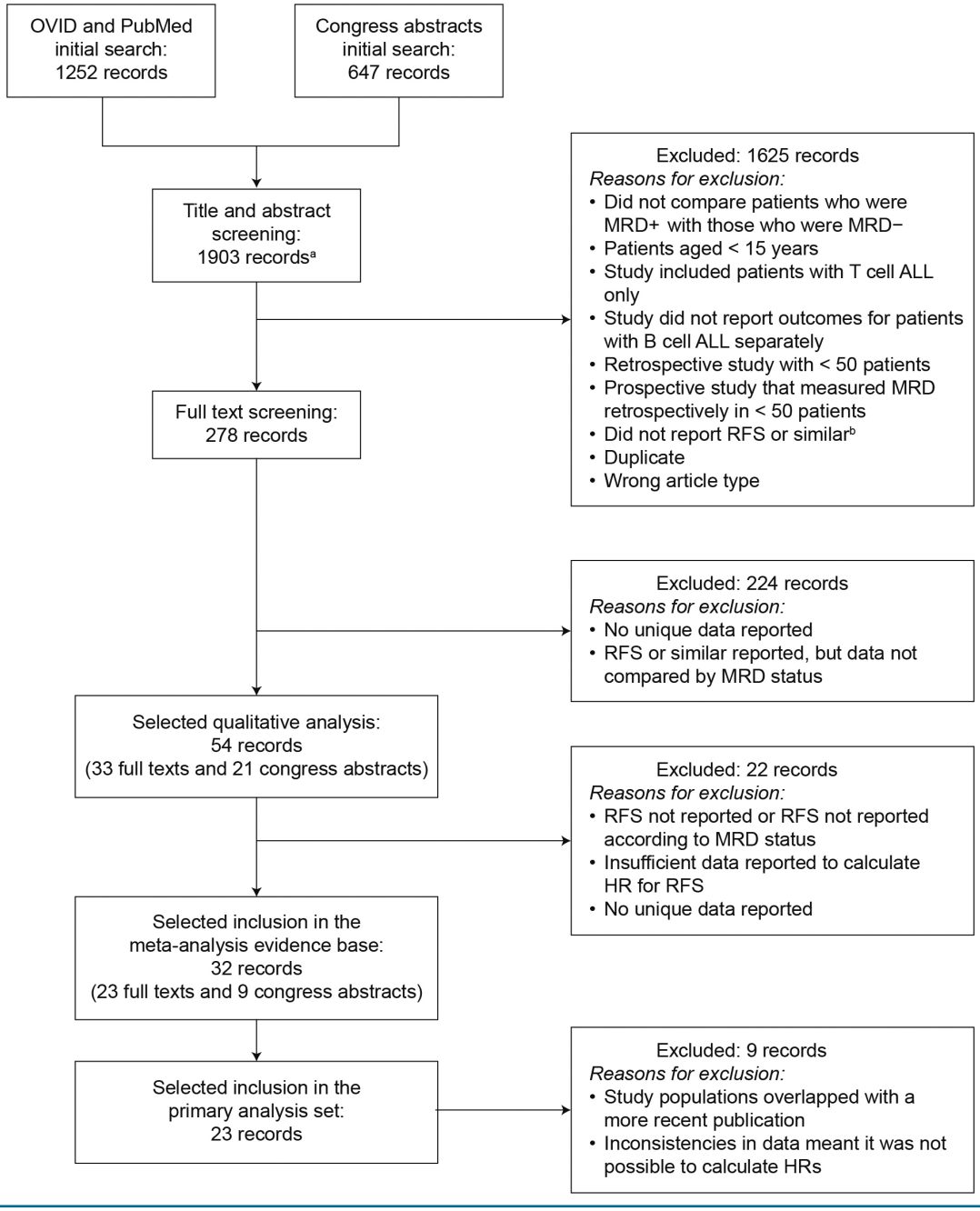

Figure 1. PRISMA flow diagram. [a]Includes four full text articles that were not identified during the systematic literature searches. [b]Protocol amendment. Includes disease-free survival, leukemia-free survival and duration of complete response or progression-free survival. ALL: acute lymphoblastic leukemia; B cell ALL/B-ALL: B-cell acute lymphoblastic leukemia; HR: hazard ratio; MRD: minimal residual disease; MRD−: minimal residual disease-negative status; MRD+: minimal residual disease-positive status; PRISMA: Preferred Reporting Items for Systematic Reviews and Meta-Analyses; RFS: relapse-free survival; T cell ALL/T-ALL: T-cell acute lymphoblastic leukemia.

Characteristics of studies and patients in the meta-analysis

Disease stage and treatment

Key characteristics of the studies included in the meta-analysis (Table 1) were considered in order to provide context when analyzing clinical outcomes according to MRD status.[20,31–36,41–56] Most studies assessing MRD status in adults with B-ALL were published from 2011 onwards, with the exception of a prospective study in Germany[35] and a Polish study.[47] Studies were mainly conducted in

Table 1. Characteristics of studies included in the meta-analysis.

First author	Year	Total number of patients (with MRD data)	Ph status	MRD method	MRD level	MRD test location	ALL phenotype	MRD timing	Disease stage at MRD	Pre-MRD tx	Post-MRD tx	Risk group
Included in primary analysis												
Lussana[56]	2016	106 (73)	Pos	PCR	10^{-5}	NA	B-cell	Pre-HSCT	CR1	Targeted	HSCT	NA
Gökbuget[41]	2015	116 (112)	Neg	PCR	10^{-4}	Central	B-cell	≤ 3 months from induction	CR1[a]	Targeted	Mix	NA
Chiaretti[42]	2015	63 (60)	Pos	PCR	NA	NA	B-cell	≤ 3 months from induction	CR1	Targeted	Mix	NA
Jabbour[43]	2017	78 (78)	NA	Flow (6 color)	10^{-4}	Local	B-cell	≤ 3 months from induction	CR2 or later	Targeted	Mix	NA
Nishiwaki[34]	2016	432 (432)	Pos	PCR	10^{-5}	Local	B-cell	Pre-HSCT	CR1	Targeted	HSCT	NA
Ravandi[44]	2016	340 (260)	Mix	Flow (6 color)	10^{-4}	Local	B-cell	≤ 3 months from induction	CR1	Targeted	Mix	NA
Bassan[49]	2014	159 (106)	Neg	PCR	10^{-4}	NA	Mix (79% B-cell)	≥ 3 months from induction	CR1	Chemo	Mix	Mix
Beldjord[46]	2014	860 (423)	Neg	PCR	10^{-4}	Central	B-cell	≤ 3 months from induction	CR1	Chemo	Mix	Mix
Gökbuget[20]	2012	1648 (580)	Neg	PCR	10^{-4}	Central	Mix (66% B-cell)	≤ 3 months from induction	CR1	Chemo	Mix	Mix
Holowiecki[47]	2008	131 (116)	Neg	Flow (3 color)	10^{-3}	Central	Mix (75% B-cell)	≤ 3 months from induction	CR1	Chemo	Mix	Mix
Patel[48]	2010	161 (161)	Neg	PCR	10^{-4}	NA	B-cell	≤ 3 months from induction	CR1	Chemo	Mix	Mix
Bassan[45]	2014	304 (141, [98 included in the analysis])	Neg	PCR	10^{-4}	NA	Mix (76% B-cell)	> 3 months from induction	CR1	Chemo	Mix	Mix
Gökbuget[36]	2014	189 (73)	Neg	PCR	10^{-4}	Central	B-cell	≤ 3 months from induction	CR2 or later	Targeted	Mix	Mix
Bachanova[31]	2014	197 (185)	Pos	PCR	NA	Local	B-cell	Pre-HSCT	CR1	Targeted	HSCT	NA
Giebel[32]	2010	123 (123)	Neg	Mix	10^{-3}	Local	B-cell	Pre-HSCT	CR1	Chemo	HSCT	High
Tucunduva[33]	2014	98 (98)	Pos	Mix	Mix	Local	B-cell	Pre-HSCT	CR1[b]	Targeted	HSCT	NA
Wassmann[35]	2005	27 (27)	Pos	PCR	NA	Central	B-cell	Post-HSCT	CR1[c]	HSCT	Targeted	NA
Weng[50]	2013	125 (106)	Mix	Flow (6 color)	10^{-4}	Local	B-cell	≤ 3 months from induction	CR1	Chemo	Mix	NA
Yanada[51]	2008	100 (85)	Pos	PCR	10^{-5}	Central	B-cell	≤ 3 months from induction	CR1	Targeted	Mix	NA
Wetzler[52]	2014	34 (13)	Pos	PCR	NA	Central	B-cell	Post-HSCT	CR1	Targeted	NA	NA
Yoon[53]	2016	173 (169)	Pos	PCR	10^{-4}	Central	B-cell	Pre-HSCT	CR1	Targeted	HSCT	NA
Lim[54]	2016	82 (78)	Pos	PCR	10^{-5}	Central	B-cell	≤ 3 months from induction	CR1	Targeted	Mix	NA
Short[55]	2016	202 (122)	Pos	PCR	10^{-4}	NA	B-cell	≤ 3 months from induction	CR1	Targeted	Targeted	NA
Included in subgroup analysis												
Ravandi[44,d]	2016	340 (260)	Mix	Flow	10^{-4}	Local	B-cell	> 3 months from induction	CR1	Targeted	Mix	NA
Gökbuget[20,d]	2012	1648 (580)	Neg	PCR	10^{-4}	Central	Mix (66% B-cell)	> 3 months from induction[e]	CR1	Chemo	Mix	Standard/ high
Holowiecki[47,d]	2008	131 (116)	Neg	Flow (3 color)	10^{-3}	Central	Mix (75% B-cell)	> 3 months from induction	CR1	Chemo	Mix	Mix
Patel[48,d]	2010	161 (161)	Neg	PCR	10^{-4}	NA	B-cell	> 3 months from induction/ pre-HSCT[e]	CR1	Chemo	HSCT/ Chemo	Standard/ high

[a]CR1 65%, CR2 34%, CR3 2%; [b]CR1 81%, CR2 19%; [c]CR1 78%, CR2 22%; [d]Study included in primary analysis with additional subgroups available for inclusion in subgroup analyses.
[e]Minimal residual disease was assessed at multiple time points, both ≤3 months and >3 months after induction. ALL: acute lymphoblastic leukemia; Central: central laboratory; CR1: first complete remission; CR2: second complete remission; CR3: third complete remission; Chemo: chemotherapy; Flow: flow cytometry; HSCT: hematopoietic stem-cell transplantation; Local: local laboratory; Mix: mixed; MRD: minimum residual disease; NA: not available; Neg: negative; PCR: polymerase chain reaction; Ph: Philadelphia chromosome; Pos: positive; R/R: relapsed and/or refractory; Targeted: targeted agent (e.g., tyrosine kinase inhibitor, blinatumomab, inotuzumab); tx: treatment.

Europe or East Asia, and almost all studies prospectively assessed MRD; only two studies included patients exclusively in second CR (CR2) or later, and the rest were in patients in first CR (CR1) at the time of MRD assessment (of these, three studies included a minority of patients in CR2 or later in combination with patients in CR1, and these were categorized as CR1 for the purposes of the meta-analysis). Approximately half were in Ph-positive patients (n=11), and these patients had typically received chemotherapy plus a tyrosine kinase inhibitor before their MRD assessment (*Online Supplementary Table S2*). Most patients with Ph-negative ALL received chemotherapy, with or without targeted agents. As mentioned, there were only two studies in which all patients were in CR2 or later, and these patients had received treatment with blinatumomab or inotuzumab ozogamicin, with or without chemotherapy, before MRD was assessed.[36,43] Two studies, in Ph-positive patients, examined the impact of MRD status following transplantation.[35,52]

Treatment received after MRD assessment varied across, and within, the studies; in most studies (n=14), pooled survival outcomes were reported for the mix of post-MRD treatments (targeted therapy, chemotherapy and HSCT) (Table 1). Six studies reported outcomes separately for patients who received an HSCT after their MRD assessment; a further two studies reported outcomes separately for post-MRD treatment with a targeted agent.

Minimal residual disease assessment methodology and timing

MRD was most commonly assessed at a central laboratory (n=10); other studies used a local reference laboratory (n=7) or did not specify whether centralized assessment was performed (n=6). A range of methodologies were used to assess MRD, although most (n=17) were polymerase chain reaction (PCR) based (Table 1). All but one of the studies of patients with Ph-negative ALL used PCR-based methodologies; three specified that they looked for immunoglobulin or T-cell receptor gene rearrangements (*Online Supplementary Tables S2* and *S3*). The remaining study used multiparameter flow cytometry (*Online Supplementary Table S2*). For patients who had Ph-positive ALL, all studies (n=11) used BCR-ABL as a marker of MRD; most (n=9) used real-time quantitative PCR, one study used molecular testing and one study used fluorescent *in-situ* hybridization. The most commonly used sensitivity limit was 1 in 10^4 cells for all methodologies, and sensitivities of 1 in 10^5 cells were only reported for PCR-based detection in studies of patients with Ph-positive status (Table 1). The three studies that included patients with mixed Ph status or did not report Ph status all used multiparameter flow cytometry (22%) (*Online Supplementary Tables S2* and *S3*). The number of colors used ranged from three to eight, and no trends in the number of colors used were observed over time in the studies.

MRD measurements were generally taken within 3 months of induction treatment (n=14) (*Online Supplementary Tables S2* and *S3*).

Clinical outcomes according to minimal residual disease status

Relapse-free survival

Figure 2 shows the meta-analysis results for the 23 studies included in the primary analysis. The overall results show improved RFS for patients who achieved MRD negativity [random effects hazard ratio (HR)=2.34; 95% confidence interval (CI): 1.91–2.86], and the effect was seen consistently across all studies.

The I^2 value was 59%, indicating moderate-to-high heterogeneity between the studies in the primary analysis. This effect was anticipated given the known variations between studies in the design, patients' characteristics and treatments received. For this reason, a predefined set of subgroups was examined to explore whether MRD negativity had a consistent effect in important subgroups of patients.

All subgroups showed an improved RFS in patients who achieved MRD negativity; no significant differential subgroup effects were observed (Figure 3). Although it should be noted that for some subgroups there were very few studies available, which contributed to overlapping confidence intervals, some trends were seen. The prognostic value of MRD appeared stronger in patients who received chemotherapy than in those who received targeted therapy before MRD assessment (HR=2.98; 95% CI: 2.12–4.20 and HR=0.90; 95% CI: 1.53–2.36, respectively), but the confidence intervals overlap. The subgroup that received HSCT before MRD assessment has a hazard ratio of 5.19 (95% CI: 1.95–13.8), but it should be noted that this is based on one study, and the confidence intervals are very wide. The prognostic value of MRD also seemed to be stronger in patients who received chemotherapy after their MRD assessment (HR=6.52; 95% CI: 2.43–17.5) than in those who received HSCT after MRD assessment (HR=1.73; 95% CI: 1.27–2.37), but again it should be noted that the data for chemotherapy after MRD assessment are from only one study.

The subgroup analysis was repeated separately according to Ph status and timing of MRD assessment (*Online Supplementary Figures S1* and *S2*). There was no difference in RFS improvement for patients who achieved MRD negativity between studies in the Ph-positive (HR=2.04; 95% CI: 1.53–2.73) and Ph-negative (HR=2.46; 95% CI: 2.02–2.98) groups. Hazard ratios in all subgroups favored MRD negativity, regardless of Ph status, with no apparent difference between Ph-positive and Ph-negative cases in any subgroup (*Online Supplementary Figure S1*). Similarly, there was no difference in RFS improvement for patients who achieved MRD negativity at early timepoints (within 3 months from induction: HR=2.60; 95% CI: 2.05–3.31) and later timepoints (more than 3 months from induction: HR=2.23; 95% CI: 1.67–2.97). Hazard ratios were more favorable in most subgroups at the early MRD timepoint compared with the later MRD timepoint group, but the subgroup confidence intervals overlapped between the early and later MRD timepoints (*Online Supplementary Figure S2*).

Overall survival

The meta-analysis results for the 14 studies included in the secondary (OS) analysis are summarized in Figure 4. The overall results show improved OS for patients who achieved MRD negativity (HR=2.19; 95% CI: 1.63–2.94). Individually, the results were consistently in favor of MRD negativity across all the studies with the exception of that by Bachanova *et al.*,[31] who reported a hazard ratio of 0.94, but with a confidence interval that crossed the null value (95% CI: 0.65–1.35). Four other studies also had confidence intervals that crossed the null value.[36,43,44,56]

The I^2 value was greater for the OS analysis (67%) than for the RFS analysis (59%), again confirming the extent of

the heterogeneity in the studies in terms of design, populations and treatment protocols. Reassuringly, a predefined analysis of key subgroups of interest showed a consistent improvement in OS in patients who achieved MRD negativity (Figure 5). As for RFS, no significant differential subgroup effects were seen. The prognostic value of MRD appeared to be greater in patients who received HSCT before MRD assessment (HR=8.02; 95% CI: 2.32–27.7) than those assessed after chemotherapy (HR=3.01; 95% CI: 2.08–4.37) or targeted therapy only (HR=1.65; 95% CI: 1.24–2.20). The prognostic value of MRD was less notable in patients who received HSCT treatment after MRD assessment (HR=1.24; 95% CI: 0.86–1.78) than those who received alternative interventions (HR=2.50; 95% CI: 1.88–3.33). As for RFS, the number of studies in some subgroups was small, and many of the confidence intervals overlapped.

Meta-regression

Meta-regression was explored to further investigate the heterogeneity between studies. The analysis was limited by the small number of studies that provided information for certain covariates (i.e. those used to define the subgroups), and for this reason we focused on RFS for which more studies were available. Heterogeneity remained even after adjustment for almost all covariates, as reflected by a significant within-group Q-statistic (Qw) (*Online Supplementary Table S9*). The exception was risk group; however, interpretation of the relevance of this covariate is limited by its inclusion in only three studies.

Of note, the Tierney method[30] used to calculate the hazard ratio for each study had no significant effect on the treatment difference.

Discussion

This systematic review and meta-analysis found that in adults with B-ALL, achieving MRD negativity was consistently associated with better survival outcomes than those of patients with MRD-positive status. In addition, the benefit of achieving MRD negativity was evident in all the

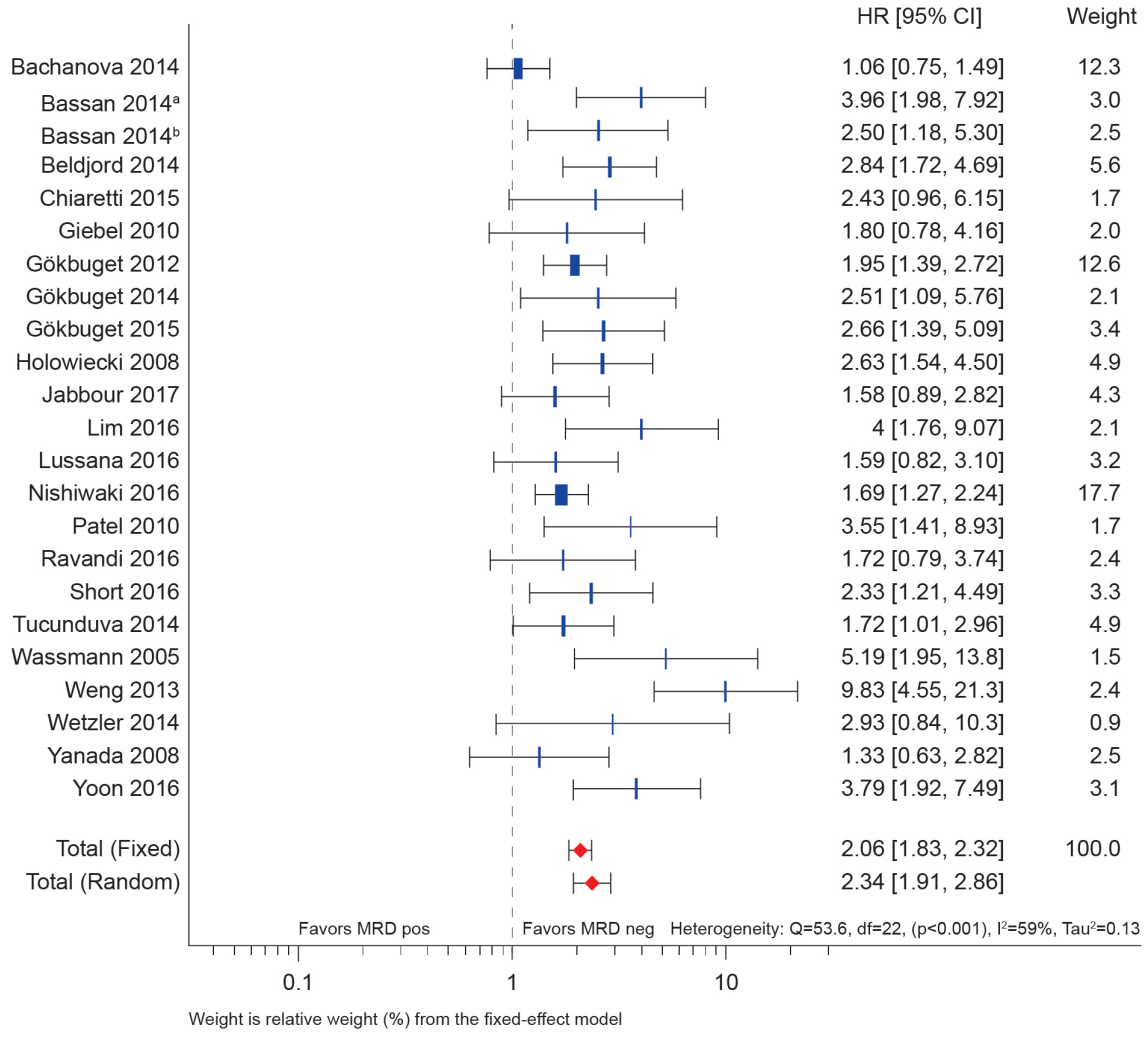

Figure 2. Forest plot of relapse-free survival hazard ratios for all studies included in the primary analysis. CI: confidence interval; HR: hazard ratio; MRD: minimal residual disease; MRD neg: minimal residual disease-negative status; MRD pos: minimal residual disease-positive status.

subgroups that we examined, highlighting its relevance for assessing prognosis and measuring treatment efficacy. There were some preliminary indications that MRD status may have a greater effect on outcomes in certain patient subgroups than in others. These data should be interpreted with caution, since no significant differential subgroup effects were seen, and most of the confidence intervals overlapped.

Our data build upon evidence from a recent meta-analysis of patients with B-ALL or T-ALL by Berry *et al.* that showed hazard ratios for event-free survival and OS almost uniformly favor MRD negativity, and that this

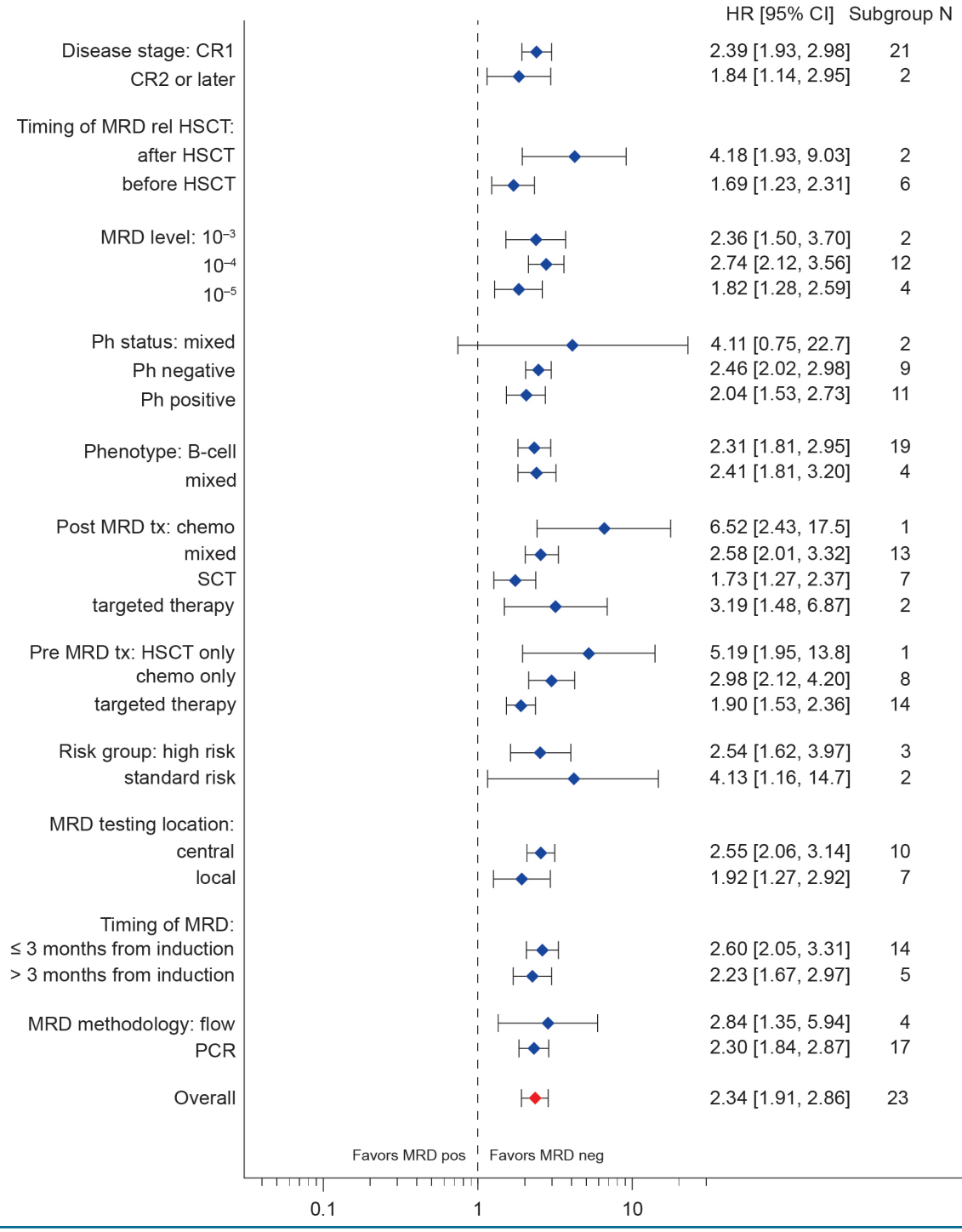

Figure 3. Forest plot of relapse-free survival hazard ratios by subgroup (random effects model). B cell ALL/B-ALL: B-cell acute lymphoblastic leukemia; CI: confidence interval; CR1: first complete remission; CR2: second complete remission; Chemo: chemotherapy; Flow: flow cytometry; HR: hazard ratio; HSCT: hematopoietic stem-cell transplantation; MRD: minimal residual disease; MRD neg: minimal residual disease-negative status; MRD pos: minimal residual disease-positive status; N: number of studies; PCR: polymerase chain reaction; Ph: Philadelphia chromosome; SCT: stem-cell transplantation; targeted: targeted agent (e.g., tyrosine kinase inhibitor, blinatumomab, inotuzumab); tx: treatment.

effect is retained within each of the subgroups.[28] The hazard ratio effect size appears slightly larger than in our meta-analysis, which could reflect differences in the studies included or the different analysis approach that was used (with a Bayesian rather than a random effects model). There was only partial overlap in studies between the two meta-analyses, with five studies included in both,[20,33,46–48] meaning that our study adds 18 studies and 2,245 patients to the combined evidence base. Only one of the adult studies in the analysis by Berry *et al.* was identified as concerning B-ALL,[48] but our efforts to extract data from the B-ALL populations wherever possible allowed us to conduct subgroup analyses specific for this phenotype with 19 studies of RFS and 12 studies of OS. Similarly, we calculated outcomes according to Ph status for a larger number of studies (20 *vs*. 8 in Berry *et al.*), enabling a more robust subgroup analysis and allowing further subgroup analyses to be conducted within each cytogenetic category. The lack of overlap between the two meta-analyses was likely due to differences in eligibility criteria: our study allowed for a larger range of methods to calculate hazard ratios (as described in Tierney *et al.*[30]), only excluding studies with small patient numbers if MRD was examined retrospectively, and included congress abstracts. Our study focused on a narrower population than that of Berry *et al.*, but a high degree of heterogeneity remained; this highlights the limitations of conducting meta-analyses according to MRD status and should encourage future research using pooled analysis of patient-level data.

In general, MRD evaluations are conducted in two different scenarios. The first is in patients who achieve morphological remission after receiving induction therapy, at the time of remission evaluation or shortly after, to evaluate the quality of the response. The second scenario is to use MRD monitoring as a predictor for pending relapse. We examined subgroups according to the timing of MRD assessment, either before or after 3 months from starting induction, or before or after HSCT. MRD assessments up to 3 months from induction were generally taken during or at the end of induction treatment – i.e. before consolidation or intensification therapy – and this subgroup therefore falls into the first scenario. In our analysis, there was little difference in the relative effect of MRD assessed at 3 months or later, and four studies that evaluated outcomes from multiple MRD timepoints showed a beneficial effect of MRD negativity at both earlier and later timepoints. Furthermore, subgroup analysis of RFS according to the timing of MRD assessment showed that there was no difference in RFS improvement for patients who achieved MRD negativity at early timepoints compared to those who achieved it at later timepoints. Measurement of MRD after HSCT may also fall into the second scenario, and the apparently large impact of MRD on RFS and OS in the post-HSCT subgroup may reflect the strong predictive ability of MRD to detect relapse in this setting.

Nevertheless, the timing of MRD measurement is an important consideration if the technique is to be used to support treatment decisions, and evidence exists to support early MRD testing. For example, in a study conducted in the USA that enrolled patients with Ph-negative B-ALL or T-ALL, MRD levels as early as 28 days following the initiation of induction therapy were used to predict out-

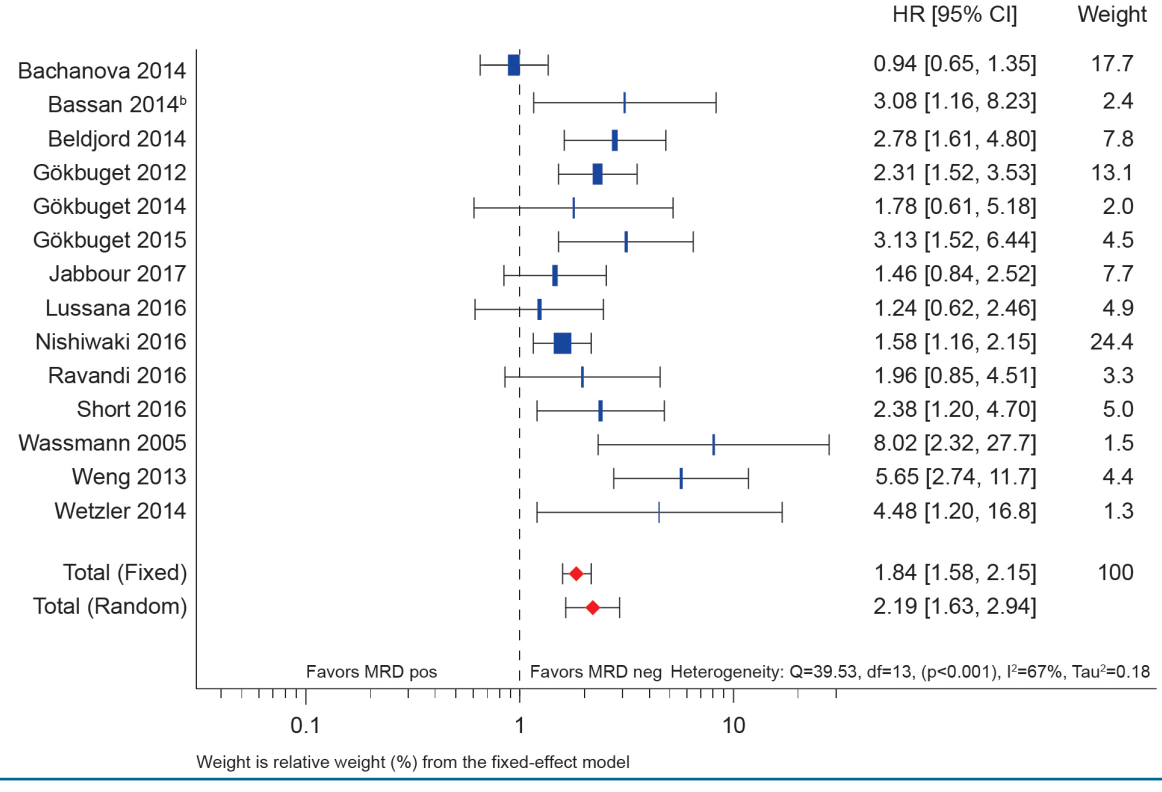

Figure 4. Forest plot of overall survival hazard ratios for all studies included in the primary analysis. CI: confidence interval; HR: hazard ratio; MRD: minimal residual disease; MRD neg: minimal residual disease-negative status; MRD pos: minimal residual disease-positive status.

comes.[57] In another study assessing patients with Ph-negative B-ALL or T-ALL, an early MRD response (day 11) was associated with the best prognosis.[58] In addition, in an analysis of patients with Ph-negative ALL from France, Belgium and Switzerland, lack of MRD response 6 weeks after induction initiation could identify patients who would benefit most from HSCT.[59] This highlights the importance of early testing if MRD status is to be used to influence treatment decisions.

Information from MRD testing could help to target highly effective immunotherapies, as well as therapies that are less well tolerated, such as HSCT, to those at high risk of relapse. In a study of Ph-negative patients from the GRAALL-2003 or -2005 trials, transplant was found to

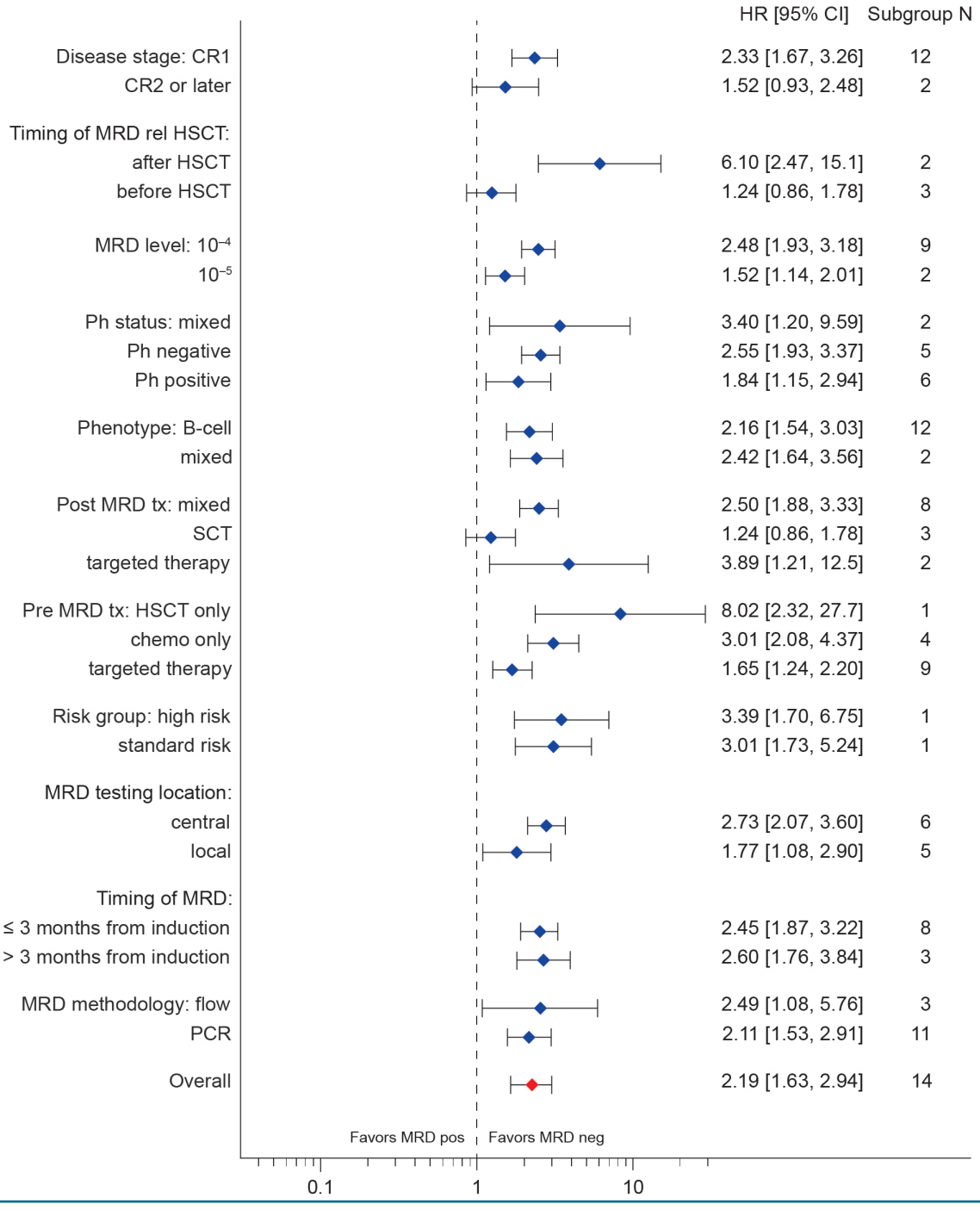

Figure 5. Forest plot of overall survival hazard ratios by subgroup (random effects model). B cell ALL/B-ALL: B-cell acute lymphoblastic leukemia; CI: confidence interval; CR1: first complete remission; CR2: second complete remission; chemo: chemotherapy; Flow: flow cytometry; HR: hazard ratio; HSCT: hematopoietic stem-cell transplantation; MRD: minimal residual disease; MRD neg: minimal residual disease-negative status; MRD pos: minimal residual disease-positive status; N: number of studies; PCR: polymerase chain reaction; Ph: Philadelphia chromosome; SCT: stem-cell transplantation; targeted: targeted agent (e.g., tyrosine kinase inhibitor, blinatumomab, inotuzumab); tx: treatment.

prolong RFS compared with chemotherapy among those who did not achieve an early MRD response, but was no better than chemotherapy in patients who did achieve an early MRD response.[59] Likewise, the PETHEMA ALL-AR03 trial used MRD to guide treatment decisions at the end of consolidation, and found that HSCT could be avoided in patients who reached MRD negativity without adversely affecting their prognosis.[60] Similarly, a study using the Northern Italy Leukemia Group trial protocol 10/07 implemented risk-stratification to define a cohort of patients with an MRD response who could achieve good outcomes with conventional maintenance instead of HSCT after induction therapy.[61] These studies provide evidence that MRD can play a role in sparing patients from the risks associated with transplantation, without negatively affecting survival outcomes.[6] New systemic therapies may offer alternatives to HSCT; for example, a phase II study (published in full since the literature review was conducted) found that blinatumomab could induce a complete MRD response in over three-quarters of patients with MRD-positive ALL in first-line treatment;[62] blinatumomab is now approved for use in patients with MRD-positive ALL in the USA.[63] There is a need to establish the role of MRD testing in guiding treatment in each subgroup of patients with ALL and to determine an evidence-based treatment protocol to optimize patients' outcomes.

Ph-positive and Ph-negative disease differ not just in terms of prognosis, but also in treatment regimens and method of MRD assessment. We analyzed RFS separately for Ph-positive and Ph-negative studies, and the prognostic ability of MRD negativity remained the same regardless of Ph status, with no discernible difference among subgroups. Subdividing the total population according to Ph status led to shrinkage or elimination of certain subgroups, but these results again point to the consistency of effect of MRD negativity across clinically relevant populations. It will be important in future research to further dissect the Ph-like subset of patients (who have a similar gene expression profile to Ph-positive ALL but without the targetable *BCR-ABL* translocation), given their poor prognosis and persistence of MRD.[64]

The question of how sensitive MRD assays need to be remains to be resolved. In a study of patients with untreated Ph-negative B-ALL or T-ALL, MRD levels of 10^{-3} or greater were associated with a poor prognosis.[45] In our study, no real differences in the association between MRD level and outcome were seen, regardless of whether the sensitivity threshold was 10^{-3}, 10^{-4} or 10^{-5}. Therefore, the threshold of 10^{-4} recommended by ESMO seems appropriate.[6]

The studies included in this systematic review and meta-analysis represent a broad range of patient subgroups and treatment regimens. Consequently, the findings should be generalizable across the whole B-ALL population. Nevertheless, these analyses have some limitations. Given the wide range of treatment regimens, follow-up times and methodologies for assessing MRD, the data should be interpreted with caution. Heterogeneity was high (as measured using I^2), but this was expected because it reflects the nature of studies included: they were not randomized and included different populations of patients, methods of analysis, follow-up times and study designs. In addition, treatments administered after MRD assessment, particularly HSCT, would be a major confounding factor when assessing the relationship between MRD and survival outcomes. We investigated sources of heterogeneity by using predetermined subgroup analyses of factors that might affect MRD and survival, and by using meta-regression. The subgroup analyses support the overall conclusion that MRD negativity is associated with better survival outcomes than MRD positivity. Heterogeneity remained high after accounting for key variables, indicating that there could be additional factors that affect the relative effect of MRD status on outcomes, which we were unable to account for in this analysis. Furthermore, for some subgroups very few studies were available, and data were sparse, meaning that the reliability of some of the subgroup results was suboptimal.

In some cases, time-to-event data were missing, and hazard ratios were calculated using published methodologies to account for this.[30] However, the meta-regression for RFS indicated that the Tierney method used to calculate hazard ratios was unlikely to influence the magnitude of the effect of MRD negativity.

It would be of interest to study the impact of MRD on bone marrow relapse. Although RFS is a good proxy for relapse, deaths in remission (e.g., following HSCT) may affect the results. This meta-analysis focused on MRD as a risk factor for systemic relapse and did not examine MRD as a predictor of extramedullary relapse or death from other causes, such as transplant-related mortality; therefore, different rates of death across subgroups from causes other than bone marrow relapse could confound the results. The extent of confounding due to HSCT-related mortality is unclear, however, and only two of the studies included in the meta-analysis comprised solely patients who did not undergo HSCT. Overall, the strong relationship observed in our study, and that by Berry *et al.*,[28] highlights the high prognostic value of MRD, despite this confounding factor.

In four studies, it was not possible to separate the B-cell and T-cell populations; however, the majority of patients in these studies had B-ALL (66% to 79%), and there was no difference in the prognostic value of MRD between the B-ALL and mixed studies for either RFS or OS. It should also be noted that our analysis only included two studies in CR2 or later; however, results in this subgroup were consistent with the overall findings.

In conclusion, this systematic review and subsequent meta-analysis have generated support for the use of MRD as a prognostic marker in the management of patients with ALL. Overall, and in all subgroups analyzed, MRD negativity was associated with better survival outcomes than MRD positivity. This finding appeared relatively unaffected by variation in the timing or sensitivity threshold of the MRD assay applied, though other factors – such as the window of opportunity for treatment before relapse – may need to be considered when refining MRD assessment methodology to optimize its value in practice. Detection of MRD offers a promising clinical tool that may help clinicians to harness the potential of emerging targeted therapies for ALL.

Acknowledgments

The authors would like to thank James O'Kelly PhD of Amgen Ltd who provided editorial support, and Kim Allcott PhD of Oxford PharmaGenesis who assisted with the systematic literature review and provided editorial support. This research was funded by Amgen.

References

1. Carroll W, Loh M, Biondi A, Willman C. The biology of acute lymphoblastic leukemia In: Reaman G, Smith F, eds. Childhood Leukemia: a Practical Handbook. Berlin and Heidelberg: Springer-Verlag. 2011:29–61.
2. Cancer Research UK. Types of acute lymphoblastic leukaemia. 2015. Available from: http://www.cancerresearchuk.org/about-cancer/acute-lymphoblastic-leukaemia-all/types (Accessed 24 May 2016).
3. Fielding AK. Current treatment of Philadelphia chromosome-positive acute lymphoblastic leukemia. Hematology Am Soc Hematol Educ Program. 2011;2011(1): 231–237.
4. Faderl S, Kantarjian HM, Talpaz M, Estrov Z. Clinical significance of cytogenetic abnormalities in adult acute lymphoblastic leukemia. Blood. 1998;91(11):3995–4019.
5. Iacobucci I, Mullighan CG. Genetic basis of acute lymphoblastic leukemia. J Clin Oncol. 2017;35(9):975–983.
6. Hoelzer D, Bassan R, Dombret H, Fielding A, Ribera JM, Buske C. Acute lymphoblastic leukaemia in adult patients: ESMO Clinical Practice Guidelines for diagnosis, treatment and follow-up. Ann Oncol. 2016;27(Suppl 5):v69–v82.
7. Parikh SA, Litzow MR. Philadelphia chromosome-negative acute lymphoblastic leukemia: therapies under development. Future Oncol. 2014;10(14):2201–2212.
8. Zhang H, Gu L, Liu T, Chiang KY, Zhou M. Inhibition of MDM2 by nilotinib contributes to cytotoxicity in both Philadelphia-positive and negative acute lymphoblastic leukemia. PLoS One. 2014;9(6):e100960.
9. Kantarjian H, Stein A, Gokbuget N, et al. Blinatumomab versus chemotherapy for advanced acute lymphoblastic leukemia. N Engl J Med. 2017;376(9):836–847.
10. Kantarjian HM, DeAngelo DJ, Stelljes M, et al. Inotuzumab ozogamicin versus standard therapy for acute lymphoblastic leukemia. N Engl J Med. 2016;375(8):740–753.
11. Martinelli G, Boissel N, Chevallier P, et al. Complete hematologic and molecular response in adult patients with relapsed/refractory Philadelphia chromosome-positive B-precursor acute lymphoblastic leukemia following treatment with blinatumomab: results from a phase II, single-arm, multicenter study. J Clin Oncol. 2017;35(16):1795–1802.
12. Bassan R, Hoelzer D. Modern therapy of acute lymphoblastic leukemia. J Clin Oncol. 2011;29(5):532–543.
13. Hoelzer D. Personalized medicine in adult acute lymphoblastic leukemia. Haematologica. 2015;100(7):855–858.
14. Annino L, Vegna ML, Camera A, et al. Treatment of adult acute lymphoblastic leukemia (ALL): long-term follow-up of the GIMEMA ALL 0288 randomized study. Blood. 2002;99(3):863–871.
15. Gökbuget N, Hoelzer D, Arnold R, et al. Treatment of adult ALL according to protocols of the German Multicenter Study Group for Adult ALL (GMALL). Hematol Oncol Clin North Am. 2000;14(6):1307–1325, ix.
16. Larson RA, Dodge RK, Burns CP, et al. A five-drug remission induction regimen with intensive consolidation for adults with acute lymphoblastic leukemia: Cancer and Leukemia Group B study 8811. Blood. 1995;85(8):2025–2037.
17. Rowe JM, Buck G, Burnett AK, et al. Induction therapy for adults with acute lymphoblastic leukemia: results of more than 1500 patients from the international ALL trial: MRC UKALL XII/ECOG E2993. Blood. 2005;106(12):3760–3767.
18. Thomas X, Boiron JM, Huguet F, et al. Outcome of treatment in adults with acute lymphoblastic leukemia: analysis of the LALA-94 trial. J Clin Oncol. 2004;22(20):4075–4086.
19. Chen X, Xie H, Wood BL, et al. Relation of clinical response and minimal residual disease and their prognostic impact on outcome in acute myeloid leukemia. J Clin Oncol. 2015;33(11):1258–1264.
20. Gökbuget N, Kneba M, Raff T, et al. Adult patients with acute lymphoblastic leukemia and molecular failure display a poor prognosis and are candidates for stem cell transplantation and targeted therapies. Blood. 2012;120(9):1868–1876.
21. Scheuring UJ, Pfeifer H, Wassmann B, et al. Serial minimal residual disease (MRD) analysis as a predictor of response duration in Philadelphia-positive acute lymphoblastic leukemia (Ph+ALL) during imatinib treatment. Leukemia. 2003;17(9):1700–1706.
22. Bassan R, Intermesoli T, Scattolin A, et al. Minimal residual disease assessment and risk-based therapy in acute lymphoblastic leukemia. Clin Lymphoma Myeloma Leuk. 2017;17S:S2–S9.
23. Brown PA, Shah B, Advani A, et al. NCCN clinical practice guidelines in oncology with NCCN evidence blocks. Acute lymphoblastic leukemia. Version I.2018 – December 13, 2018. Available from: https://www.nccn.org/professionals/physician_gls/pdf/all_blocks.pdf (Accessed 31 January 2019).
24. Short NJ, Jabbour E, Albitar M, et al. Recommendations for the assessment and management of measurable residual disease in adults with acute lymphoblastic leukemia: a consensus of North American experts. Am J Hematol. 2019;94(2):257–265.
25. European Medicines Agency. Guideline on the use of minimal residual disease as a clinical endpoint in multiple myeloma studies. 2018. Available from: https://www.ema.europa.eu/documents/scientific-guideline/draft-guideline-use-minimal-residual-disease-clinical-endpoint-multiple-myeloma-studies_en.pdf (Accessed 25 October 2018).
26. Food and Drug Administration. Hematologic malignancies: regulatory considerations for use of minimal residual disease in development of drug and biological products for treatment – guidance for industry. 2018. Available from: https://www.fda.gov/downloads/Drugs/GuidanceComplianceRegulatoryInformation/Guidances/UCM623333.pdf (Accessed 25 October 2018).
27. Bruggemann M, Kotrova M. Minimal residual disease in adult ALL: technical aspects and implications for correct clinical interpretation. Blood Adv. 2017;1(25):2456–2466.
28. Berry DA, Zhou S, Higley H, et al. Association of minimal residual disease with clinical outcome in pediatric and adult acute lymphoblastic leukemia: a meta-analysis. JAMA Oncol. 2017;3(7):e170580.
29. Liberati A, Altman DG, Tetzlaff J, et al. The PRISMA statement for reporting systematic reviews and meta-analyses of studies that evaluate health care interventions: explanation and elaboration. Ann Intern Med. 2009;339:b2700.
30. Tierney JF, Stewart LA, Ghersi D, Burdett S, Sydes MR. Practical methods for incorporating summary time-to-event data into meta-analysis. Trials. 2007;8:16.
31. Bachanova V, Marks DI, Zhang MJ, et al. Ph+ ALL patients in first complete remission have similar survival after reduced intensity and myeloablative allogeneic transplantation: impact of tyrosine kinase inhibitor and minimal residual disease. Leukemia. 2014;28(3):658–665.
32. Giebel S, Stella-Holowiecka B, Krawczyk-Kulis M, et al. Status of minimal residual disease determines outcome of autologous hematopoietic SCT in adult ALL. Bone Marrow Transplant. 2010;45(6):1095–1101.
33. Tucunduva L, Ruggeri A, Sanz G, et al. Impact of minimal residual disease on outcomes after umbilical cord blood transplantation for adults with Philadelphia-positive acute lymphoblastic leukaemia: an analysis on behalf of Eurocord, Cord Blood Committee and the Acute Leukaemia working party of the European Group for Blood and Marrow Transplantation. Br J Haematol. 2014;166(5):749–757.
34. Nishiwaki S, Imai K, Mizuta S, et al. Impact of MRD and TKI on allogeneic hematopoietic cell transplantation for Ph+ALL: a study from the adult ALL WG of the JSHCT. Bone Marrow Transplant. 2016;51(1):43–50.
35. Wassmann B, Pfeifer H, Stadler M, et al. Early molecular response to posttransplantation imatinib determines outcome in MRD+ Philadelphia-positive acute lymphoblastic leukemia (Ph+ ALL). Blood. 2005;106(2): 458–463.
36. Goekbuget N, Kantarjian H, Brüggemann M, et al. An evaluation of molecular response in a phase 2 open-label, multicenter confirmatory study in patients (pts) with relapsed/refractory B-precursor acute lymphoblastic leukemia (r/r ALL) receiving treatment with the BiTE® antibody construct blinatumomab Blood. 2014;124 (21):3704.
37. DerSimonian R, Laird N. Meta-analysis in clinical trials. Control Clin Trials. 1986;7(3): 177–188.
38. Whitehead A. Meta-Analysis of Controlled Clinical Trials. Chichester, UK: John Wiley & Sons, Ltd, 2003.
39. Hardy RJ, Thompson SG. Detecting and describing heterogeneity in meta-analysis. Stat Med. 1998;17(8):841–856.
40. Higgins JP, Thompson SG, Deeks JJ, Altman DG. Measuring inconsistency in meta-analyses. BMJ. 2003;327(7414):557–560.
41. Gökbuget N, Dombret H, Bonifacio M, et al. Long-term outcomes after blinatumomab treatment: follow-up of a phase 2 study in patients (pts) with minimal residual disease (MRD) positive B-cell precursor acute lymphoblastic leukemia (ALL). Blood. 2015;126(23):680 (abstract).
42. Chiaretti S, Vitale A, Elia L, et al. Multicenter total therapy Gimema LAL 1509 protocol for de novo adult Ph+ acute lymphoblastic leukemia (ALL) patients. Updated results and refined genetic-based prognostic stratification. Blood. 2015;126(23):81.
43. Jabbour E, Short NJ, Jorgensen JL, et al. Differential impact of minimal residual disease negativity according to the salvage status in patients with relapsed/refractory B-cell acute lymphoblastic leukemia. Cancer. 2017;123(2):294–302.
44. Ravandi F, Jorgensen JL, O'Brien SM, et al. Minimal residual disease assessed by multiparameter flow cytometry is highly prognostic in adult patients with acute lymphoblastic leukaemia. Br J Haematol.

2016;172(3):392–400.
45. Bassan R, Spinelli O, Oldani E, et al. Different molecular levels of post-induction minimal residual disease may predict hematopoietic stem cell transplantation outcome in adult Philadelphia-negative acute lymphoblastic leukemia. Blood Cancer J. 2014;4:e225.
46. Beldjord K, Chevret S, Asnafi V, et al. Oncogenetics and minimal residual disease are independent outcome predictors in adult patients with acute lymphoblastic leukemia. Blood. 2014;123(24):3739–3749.
47. Holowiecki J, Krawczyk-Kulis M, Giebel S, et al. Status of minimal residual disease after induction predicts outcome in both standard and high-risk Ph-negative adult acute lymphoblastic leukaemia. The Polish Adult Leukemia Group ALL 4-2002 MRD study. Br J Haematol. 2008;142(2):227–237.
48. Patel B, Rai L, Buck G, et al. Minimal residual disease is a significant predictor of treatment failure in non T-lineage adult acute lymphoblastic leukaemia: final results of the international trial UKALL XII/ECOG2993. Br J Haematol. 2010;148(1):80–89.
49. Bassan R, Masciulli A, Spinelli O, et al. Enhanced survival in adult Philadelphia-negative acute lymphoblastic leukemia (Ph-ALL) with an updated pediatric derived minimal residual disease (MRD)/risk-specific treatment strategy: NILG Study 10. Haematologica. 2014;99(Suppl 1):S726.
50. Weng XQ, Shen Y, Sheng Y, et al. Prognostic significance of monitoring leukemia-associated immunophenotypes by eight-color flow cytometry in adult B-acute lymphoblastic leukemia. Blood Cancer J. 2013;3:e133.
51. Yanada M, Sugiura I, Takeuchi J, et al. Prospective monitoring of BCR-ABL1 transcript levels in patients with Philadelphia chromosome-positive acute lymphoblastic leukaemia undergoing imatinib-combined chemotherapy. Br J Haematol. 2008;143 (4):503–510.
52. Wetzler M, Watson D, Stock W, et al. Autologous transplantation for Philadelphia chromosome-positive acute lymphoblastic leukemia achieves outcomes similar to allogeneic transplantation: results of CALGB Study 10001 (Alliance). Haematologica. 2014;99(1):111–115.
53. Yoon JH, Park S, Jeon YW, et al. Comparable long-term outcomes of reduced-intensity and myeloablative conditioning allogeneic hematopoietic cell transplantation by minimal residual disease kinetics during the tyrosine kinase inhibitor-based chemotherapy courses in adults with Philadelphia-chromosome positive acute lymphoblastic leukemia in first remission. Blood. 2016;128(22):3979.
54. Lim S, Joo YD, Sohn SK. Serial monitoring of BCR-ABL by real-time polymerase chain reaction in newly diagnosed Philadelphia chromosomepositive acute lymphoblastic leukemia treated with imatinib. Haematologica. 2016;101(suppl 1):E856.
55. Short NJ, Jabbour E, Sasaki K, et al. Impact of complete molecular response on survival in patients with Philadelphia chromosome-positive acute lymphoblastic leukemia. Blood. 2016;128(4):504–507.
56. Lussana F, Intermesoli T, Gianni F, et al. Achieving molecular remission before allogeneic stem cell transplantation in adult patients with Philadelphia chromosome-positive acute lymphoblastic leukemia: Impact on relapse and long-term outcome. Blood Marrow Transplant. 2016;22(11): 1983–1987.
57. Stock W, Luger SM, Advani AD, et al. Favorable outcomes for older adolescents and young adults (AYA) with acute lymphoblastic leukemia (ALL): early results of U.S. Intergroup Trial C10403. Blood. 2014; 124 (21):796.
58. Bruggemann M, Raff T, Flohr T, et al. Clinical significance of minimal residual disease quantification in adult patients with standard-risk acute lymphoblastic leukemia. Blood. 2006;107(3):1116–1123.
59. Dhèdin N, Huynh A, Maury S, et al. Role of allogeneic stem cell transplantation in adult patients with Ph-negative acute lymphoblastic leukemia. Blood. 2015;125(16): 2486–2496.
60. Ribera JM, Oriol A, Morgades M, et al. Treatment of high-risk Philadelphia chromosome-negative acute lymphoblastic leukemia in adolescents and adults according to early cytologic response and minimal residual disease after consolidation assessed by flow cytometry: final results of the PETHEMA ALL-AR-03 trial. J Clin Oncol. 2014;32(15):1595–1604.
61. Bassan R, Masciulli A, Intermesoli T, et al. Final results of Northern Italy Leukemia Group (NILG) trial 10/07 combining pediatric-type therapy with minimal residual disease study and risk-oriented hematopoietic cell transplantation in adult acute lymphoblastic leukemia (ALL). Blood. 2016;128 (22):176.
62. Gökbuget N, Dombret H, Bonifacio M, et al. Blinatumomab for minimal residual disease in adults with B-precursor acute lymphoblastic leukemia. Blood. 2018;131(14): 1522–1531.
63. Amgen Inc. BLINCYTO prescribing information. 2018. Available from: https://www.accessdata.fda.gov/drugsatfda_docs/label/2018/125557s013lbl.pdf (Accessed 01 May 2018).
64. Herold T, Gokbuget N. Philadelphia-like acute lymphoblastic leukemia in adults. Curr Oncol Rep. 2017;19(5):31.

Ferrata Storti Foundation

Haematologica 2019
Volume 104(10):2040-2052

p66Shc deficiency in the Eμ-TCL1 mouse model of chronic lymphocytic leukemia enhances leukemogenesis by altering the chemokine receptor landscape

Laura Patrussi,[1] Nagaja Capitani,[1,2] Cristina Ulivieri,[1] Noemi Manganaro,[1] Massimo Granai,[3] Francesca Cattaneo,[1] Anna Kabanova,[1] Lucia Mundo,[3] Stefania Gobessi,[4] Federica Frezzato,[5,6] Andrea Visentin,[5,6] Francesca Finetti,[1] Pier Giuseppe Pelicci,[7] Mario M. D'Elios,[2] Livio Trentin,[5,6] Gianpietro Semenzato,[5,6] Lorenzo Leoncini,[3] Dimitar G. Efremov[4] and Cosima T. Baldari[1]

[1]Department of Life Sciences, University of Siena, Siena; [2]Department of Clinical and Experimental Medicine, University of Florence, Florence; [3]Department of Human Biotechnologies, University of Siena, Siena; [4]International Center for Genetic Engineering and Biotechnology, Trieste; [5]Venetian Institute of Molecular Medicine, Padua; [6]Department of Medicine, Hematology and Clinical Immunology Branch, Padua University School of Medicine, Padua and [7]European Institute of Oncology, Milan, Italy

ABSTRACT

The Shc family adaptor p66Shc acts as a negative regulator of proliferative and survival signals triggered by the B-cell receptor and, by enhancing the production of reactive oxygen species, promotes oxidative stress-dependent apoptosis. Additionally, p66Shc controls the expression and function of chemokine receptors that regulate lymphocyte traffic. Chronic lymphocytic leukemia cells have a p66Shc expression defect which contributes to their extended survival and correlates with poor prognosis. We analyzed the impact of p66Shc ablation on disease severity and progression in the Eμ-TCL1 mouse model of chronic lymphocytic leukemia. We showed that Eμ-TCL1/p66Shc$^{-/-}$ mice developed an aggressive disease that had an earlier onset, occurred at a higher incidence and led to earlier death compared to that in Eμ-TCL1 mice. Eμ-TCL1/p66Shc$^{-/-}$ mice displayed substantial leukemic cell accumulation in both nodal and extranodal sites. The target organ selectivity correlated with upregulation of chemokine receptors whose ligands are expressed therein. This also applied to chronic lymphocytic leukemia cells, where chemokine receptor expression and extent of organ infiltration were found to correlate inversely with these cells' level of p66Shc expression. p66Shc expression declined with disease progression in Eμ-TCL1 mice and could be restored by treatment with the Bruton tyrosine kinase inhibitor ibrutinib. Our results highlight p66Shc deficiency as an important factor in the progression and severity of chronic lymphocytic leukemia and underscore p66Shc expression as a relevant therapeutic target.

Correspondence:

COSIMA T. BALDARI
baldari@unisi.it

LAURA PATRUSSI
patrussi2@unisi.it

Received: October 22, 2018.

Accepted: February 22, 2019.

Pre-published: February 28, 2019.

doi:10.3324/haematol.2018.209981

Check the online version for the most updated information on this article, online supplements, and information on authorship & disclosures: www.haematologica.org/content/104/10/2040

Introduction

Chronic lymphocytic leukemia (CLL) is characterized by the accumulation of long-lived mature CD5$^+$ B cells in peripheral blood, bone marrow and secondary lymphoid organs.[1] Leukemic cell survival is associated with defective apoptosis[2] and, moreover, is promoted by stromal cell-derived chemokines during their transit through secondary lymphoid organs,[3] where they also undergo proliferation within pseudofollicles.[1] Imbalanced expression of chemokine receptors regulating homing to (CCR7, CXCR4, CXCR5) and egress from (S1PR1) secondary lymphoid organs concurs to retain CLL cells in the lymphoid niche.[3]

The adaptor p66Shc participates in signaling pathways linking oxidative stress to apoptosis.[4] p66Shc promotes the production of reactive oxygen species (ROS) by interrupting the mitochondrial respiratory chain through cytochrome c binding and oxidation, causing activation of the apoptotic cascade. Additionally, it negatively

regulates B-cell survival by modulating the expression of several Bcl-2 family members and inhibiting the activation of the pro-survival kinase Akt.[5,6] p66Shc also participates in B-cell trafficking by controlling CCR7, CXCR4 and S1PR1 surface expression both transcriptionally and post-translationally.[7,8] Moreover, p66Shc attenuates CXCR4 and CXCR5 signaling.[9] CLL cells have a defect in the expression of p66Shc[6] and its transcription factor STAT4[10] which is causal to their extended survival,[6,7,11] suggesting a link between p66Shc deficiency and the pathogenesis of CLL.

Overexpression of *TCL1* driven by the IgM heavy chain enhancer (Eμ-*TCL1*) in mice results in the development of a B-cell leukemia that recapitulates aggressive CLL.[12] Here we have addressed the effect of p66Shc deficiency on the onset, development and outcome of CLL by generating a Eμ-TCL1/p66Shc$^{-/-}$ mouse. We showed that p66Shc deletion in Eμ-TCL1 mice resulted in accelerated leukemogenesis and enhanced disease aggressiveness, with enhanced nodal and extranodal infiltration. Our data provide direct evidence that p66Shc deficiency concurs to CLL pathogenesis and highlight p66Shc expression as a relevant disease target.

Methods

A detailed description of the methods is available in the *Online Supplementary Data* file.

Mice

Eμ-TCL1[12,13] and p66Shc$^{-/-}$ C57BL/6J (C57/p66$^{-/-}$)[14] mice were crossed to generate Eμ-TCL1/p66Shc$^{-/-}$ mice: the screening strategy is illustrated in *Online Supplementary Figures S1* and *S2*. C57BL/6J and C57/p66$^{-/-}$ mice were used as controls. Mice with ≥10% peripheral blood CD5^{+}CD19^{+} cells were considered to have developed leukemia. Overt leukemia was defined as reported elsewhere.[13]

Cell lines, patients and healthy donors

Transfectants generated using the CLL-derived B-cell line MEC1[15] and expressing human full-length p66Shc or the p66ShcQQ mutant were described previously.[8] *p66shc* silencing in an Epstein-Barr virus (EBV) B-cell line was performed as described elsewhere.[10] Peripheral blood samples were collected from 157 treatment-naïve CLL patients and five CLL patients subjected to pharmacological treatments (*Online Supplementary Table S1*). B cells from 15 buffy coats were used as healthy population controls. B cells were purified and transfected as described previously.[8]

Immunophenotyping of leukemic cells

Single-cell suspensions from mouse peripheral blood, peritoneal wash, spleen, bone marrow, lymph nodes, liver and lung were depleted of erythrocytes by hypotonic lysis and incubated with mouse Fc-Block for 15 min at 4°C. Murine leukemic cells and B cells purified from CLL patients and healthy donors were stained (antibodies and reagents listed in *Online Supplementary Table S2*) and subjected to flow cytometry (Guava Easy Cyte cytometer, Millipore).

RNA purification and polymerase chain reactions

Total RNA was extracted and retrotranscribed as described previously.[8] Real-time polymerase chain reactions (PCR) (primers listed in *Online Supplementary Table S3*) were performed using GoTaq Long PCR Master Mix (Promega) and results were processed and analyzed as described elsewhere.[11]

Cell treatment, apoptosis and reactive oxygen species measurement, immunoblot and chemotaxis assays

Freshly isolated normal and leukemic mouse B cells were treated with 50 μM H_2O_2 for 24 h, 1 μM ibrutinib for 48 h, or 35 μM fludarabine phosphate for 16 h. Dimethylsulfoxide was used as a control. Apoptosis was measured by flow cytometry on FITC-labeled annexin-V -stained CD5^{+}IgM^{+} cells. Intracellular ROS were measured by flow cytometry in cells labeled for 30 min at 37°C with 5 μM CM-H_2DCFDA.[8]

Immunoblots and chemotaxis assays (antibodies and chemokines listed in *Online Supplementary Table S2*) were carried out as reported previously.[16]

Histopathology and immunohistochemistry

Tissues, peripheral blood and peritoneal wash were collected and processed as detailed in the *Online Supplementary Methods*.

Statistical analyses

One-way analysis of variance (ANOVA) with a post-hoc Tukey test was used for experiments in which multiple groups were compared. Mann-Whitney rank-sum tests were performed to determine the significance of differences between two groups. Survival curves and medians were calculated within subgroups with the Kaplan-Meier method. A log-rank test was used to compare differences between estimated survival curves. Statistical analyses were performed using GraphPad Software (La Jolla, CA, USA). *P* values <0.05 were considered statistically significant.

Study approval

Experiments were approved by the Institutional Review Board and the local Ethics Committee.

Results

p66Shc expression decreases during leukemia progression in tumoral cells from Eμ-TCL1 mice

CLL cells have a profound reduction in p66Shc expression, which is more severe in patients with an unfavorable prognosis.[6] As Eμ-TCL1 mice are a model of aggressive CLL,[17] we investigated whether the p66Shc defect in CLL cells is recapitulated in leukemic Eμ-TCL1 cells. p66Shc mRNA was quantified in splenic leukemic cells from Eμ-TCL1 mice with overt leukemia (≥50% peripheral blood CD5^{+}CD19^{+} cells and a white blood cell count above the normal range; see *Online Supplementary Methods*).[13] The analysis was extended to B1a cells from C57BL/6 mice, the normal CD5^{+} B-cell counterpart,[18] and to the two other mature B-cell subsets, B1b and B2. While p66Shc was expressed at comparable levels in all normal B-cell subsets, tumoral B cells from mice with advanced disease expressed less p66Shc compared to normal B1a cells (Figure 1A). Interestingly, B1a cells from Eμ-TCL1 mice with milder disease (~20% peripheral blood CD5^{+}CD19^{+} cells) had intermediate levels of p66Shc (Figure 1B,C), indicating that p66Shc expression declines during disease progression, as further supported by a >78% inverse correlation between p66Shc mRNA levels in CD5^{+}CD19^{+} cells and the percentage of leukemic cells in peripheral blood from the same mouse (Figure 1D). STAT4, a key transcription factor for p66Shc that is defective in CLL cells,[10] was also downregulated in Eμ-TCL1 mice (Figure 1C,E).

The p66Shc expression defect in CLL cells can be rescued by *in vitro* or *in vivo* treatment with the Btk inhibitor ibrutinib, used for CLL treatment.[7,19] As for human CLL

cells, p66Shc expression increased in splenic leukemic cells from Eμ-TCL1 sick mice treated with 1 μM ibrutinib for 48 h, concomitant with increased STAT4 expression (Figure 1F,G) supporting the notion that the therapeutic effects of ibrutinib are associated with its STAT4/p66Shc-elevating activity.

p66Shc deficiency accelerates leukemogenesis in Eμ-TCL1 mice

Our results suggest that the p66Shc defect observed in leukemic CLL and Eμ-TCL1 cells may be implicated in disease pathogenesis. To test this hypothesis, we transferred the p66shc$^{-/-}$ allele into Eμ-TCL1 mice (*Online*

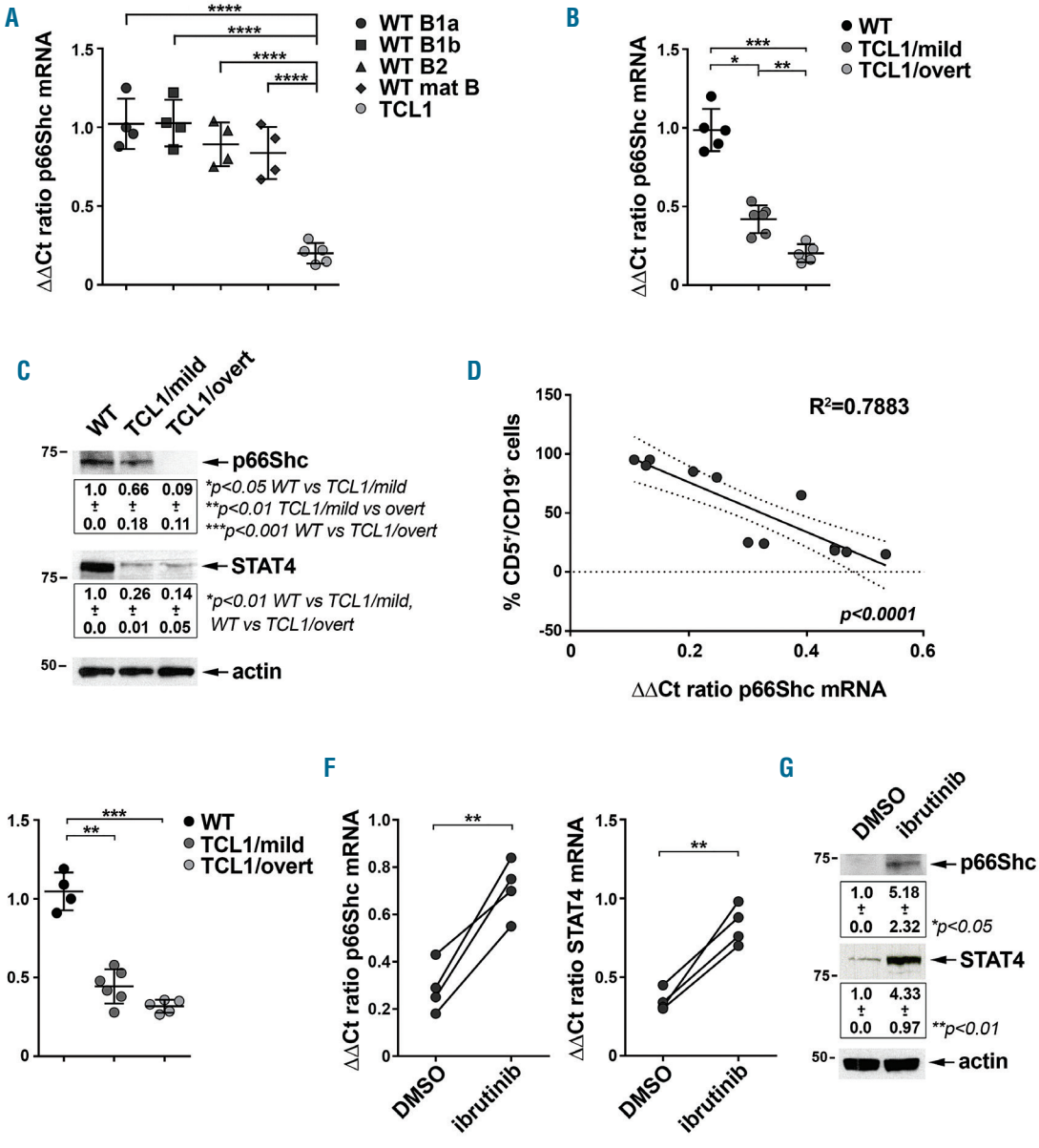

Figure 1. p66Shc expression decreases during leukemia progression in tumoral cells from Eμ-TCL1 mice and can be restored by ibrutinib treatment. (A) Quantitative real-time polymerase chain reaction (qRT-PCR) analysis of p66Shc mRNA in B1a, B1b, B2 and total mature B lymphocytes purified from four wildtype (WT) mice and in leukemic cells purified from five Eμ-TCL1 sick mice. The relative gene transcript abundance was determined on triplicate samples using the ΔΔCt method and normalized to *GAPDH*. (B, E). qRT-PCR analysis of p66Shc (B) and STAT4 (E) mRNA in B lymphocytes purified from five WT mice and in leukemic cells purified from Eμ-TCL1 mice with mild (~20% CD5$^+$CD19$^+$ cells in peripheral blood) (n=6) or overt leukemia (≥50% CD5$^+$CD19$^+$ cells and white cell count >10.7x10^6/mL in peripheral blood) (n=5). The relative gene transcript abundance was determined on triplicate samples using the ΔΔCt method. (C) Immunoblot analysis with anti-Shc and anti-STAT4 antibodies of postnuclear supernatants of leukemic cells purified from either WT (n=3) or Eμ-TCL1 mice with mild (n=3) or overt leukemia (n=3). The stripped filters were reprobed with anti-actin antibodies. (D) Correlation between the percentages of CD5$^+$CD19$^+$ cells and the mRNA levels of p66Shc in peripheral blood samples obtained from Eμ-TCL1 mice at different disease stages (n=12). (F) qRT-PCR analysis of p66Shc (left) and STAT4 (right) mRNA in leukemic cells purified from spleens of Eμ-TCL1 sick mice (n=4) incubated for 48 h with either dimethylsulfoxide (DMSO) (absolute cell viability: 88.4 ± 3.2% of annexin V/propidium iodide$^-$ cells) or 1 μM ibrutinib (absolute cell viability: 84.9 ± 2.9% of annexin V/propidium iodide$^-$ cells). The relative gene transcript abundance was determined on triplicate samples using the ΔΔCt method. (G) Immunoblot analysis with anti-Shc and anti-STAT4 antibodies of postnuclear supernatants of leukemic cells purified from spleens of Eμ-TCL1 sick mice (n=3) incubated for 48 h with either DMSO or 1 μM ibrutinib. The stripped filters were reprobed with anti-actin antibodies. Mean ± standard deviation. One-way analysis of variance (ANOVA), multiple comparisons. ****P≤0.0001; ***P≤0.001; **P≤0.01; *P≤0.05

Supplementary Figure S1A,B).[12] As expected, Eμ-TCL1/p66Shc$^{-/-}$ B cells did not express p66Shc (*Online Supplementary Figure S1C,D*) while expressing wildtype p53, similar to Eμ-TCL1 cells (*Online Supplementary Methods* and *Online Supplementary Table S3*).[20] Eμ-TCL1/p66Shc$^{-/-}$ mice developed a CLL-like disease similar to that occurring in Eμ-TCL1 mice. A large lymphocyte population, associated with the characteristic Gumprecht shadows, was evident in peripheral blood smears from sick mice (*Online Supplementary Figure S1E*). Flow cytometric analysis of peripheral blood samples from 6- and 9-month old mice revealed a discrete population of CD5^{+} B cells, which is the hallmark of disease development in Eμ-TCL1 mice (*Online Supplementary Figures S1F* and *S2*).[12] Similar to Eμ-TCL1 mice, leukemic Eμ-TCL1/p66Shc$^{-/-}$ mice eventually became visibly ill, showing labored breathing and splenomegaly (*Online Supplementary Figure S1G* and *Online Supplementary Table S4*) that necessitated euthanasia.

To address the impact of p66Shc deficiency on disease onset and progression, we followed leukemia development in 87 Eμ-TCL1 and 134 Eμ-TCL1/p66Shc$^{-/-}$ mice by immunophenotyping monthly peripheral blood samples. Eμ-TCL1/p66Shc$^{-/-}$ mice showed higher white blood cell counts and higher CD5^{+}CD19^{+} cell percentages in peripheral blood compared to those in Eμ-TCL1 mice (Figure 2A,B; *Online Supplementary Figure S1G*). Moreover disease progression, assessed as rate of increase in the percentage of CD5^{+}CD19^{+} cells, was faster in Eμ-TCL1/p66Shc$^{-/-}$ mice (Figure 2C).

Disease incidence, defined as the percentage of sick mice (>10% peripheral blood CD5^{+}CD19^{+} cells *vs.* ~5% in healthy C57BL/J6 mice) (*Online Supplementary Figure S3*) at defined time points, was significantly higher in Eμ-TCL1/p66Shc$^{-/-}$ mice than in Eμ-TCL1 mice (Figure 2D). Moreover, p66Shc deficiency led to an earlier onset of disease, which was detected ~2 months earlier in Eμ-TCL1/p66Shc$^{-/-}$ mice (Figure 2D) and resulted in a shorter lifespan (Figure 2E). Hence p66Shc deficiency in Eμ-TCL1 mice accelerates disease onset and development as well as its progression to an aggressive presentation.

p66Shc deficiency enhances leukemic cell chemoresistance

Consistent with the ability of p66Shc to modulate the expression of pro- and anti-apoptotic Bcl-2 family members,[6] leukemic Eμ-TCL1/p66Shc$^{-/-}$ cells expressed higher and lower levels of Bcl-2 and Bax, respectively, compared to levels in their Eμ-TCL1 counterparts (Figure 3A,B). At variance, Mcl-1 expression was comparable (*Online Supplementary Figure S4*). Accordingly, leukemic cells from sick Eμ-TCL1/p66Shc$^{-/-}$ mice were more resistant to fludarabine treatment, also when co-cultured with OP9 stromal cells to simulate the pro-survival stromal microenvironment (Figure 3C). Hence p66Shc deficiency in Eμ-TCL1 leukemic cells promotes these cells' survival, which likely contributes to the faster disease development and unfavorable outcome in Eμ-TCL1/p66Shc$^{-/-}$ mice. This is supported by the higher sensitivity to fludarabine of leukemic cells from Eμ-TCL1 mice with milder disease (<35% peripheral blood CD5^{+}CD19^{+} cells) compared to leukemic cells from mice at later disease stages (≥35% peripheral blood CD5^{+}CD19^{+} cells) (Figure 3D), which may be accounted for, at least in part, by their higher residual p66Shc expression (Figure 1B,C). Consistent with this notion, tumoral Eμ-TCL1/p66Shc$^{-/-}$ cells were less sensitive to fludarabine treatment, independently of disease stage (Figure 3D). Hence the reduction of p66Shc expression in Eμ-TCL1 mice during disease development contributes to the decreased chemosensitivity of leukemic cells.

p66Shc deficiency in Eμ-TCL1 mice is associated with nodal and extranodal leukemic cell accumulation

Leukemic cells accumulate in the peritoneal cavity of Eμ-TCL1 mice at early stages of disease, subsequently colonizing spleen, bone marrow and lymph nodes as well as extranodal sites.[12] p66Shc modulates the surface levels of receptors that regulate homing to and egress from secondary lymphoid organs,[8,7] suggesting that its deficiency might contribute to leukemic cell accumulation in secondary lymphoid organs and infiltration into non-lymphoid organs. The extent of organ infiltration by leukemic cells was measured in spleen, bone marrow and lymph nodes from Eμ-TCL1 and Eμ-TCL1/p66Shc$^{-/-}$ mice with ~60% leukemic cells in peripheral blood. The analysis was extended to liver and lung, as infiltration in these organs has been documented in CLL,[21,22] as well as to the peritoneal infiltrate.

Flow cytometric analysis of CD5^{+}CD19^{+} cells revealed higher percentages of leukemic cells in lymph nodes of Eμ-TCL1/p66Shc$^{-/-}$ mice than in those of Eμ-TCL1 mice (Figure 4A). This was confirmed by hematoxylin & eosin staining and immunohistochemical analysis of the same organs, which highlighted massive lymph node infiltration of Eμ-TCL1/p66Shc$^{-/-}$ mice by small lymphoid-like B220^{+} cells (Figure 4A). At variance, leukemic cell accumulation in spleen and bone marrow was comparable (*Online Supplementary Figure S5* and *Online Supplementary Table S4*), suggesting that Eμ-TCL1/p66Shc$^{-/-}$ tumoral cells show organ selectivity.

Leukemic cell infiltrates in the liver and lung were found to be more substantial in Eμ-TCL1/p66Shc$^{-/-}$ mice than in Eμ-TCL1 mice and were frequently associated with loss of organ architecture (Figure 4B,C). Increased peritoneal leukemic cell accumulation was also observed in Eμ-TCL1/p66Shc$^{-/-}$ mice (Figure 4D). Interestingly, flow cytometric analysis of the proliferation marker Ki-67 revealed a higher proliferation rate of leukemic Eμ-TCL1/p66Shc$^{-/-}$ cells in lymph nodes, liver and lung compared to their Eμ-TCL1 counterparts (*Online Supplementary Figure S6*), consistent with the anti-mitogenic function of p66Shc.[23]

Increased colonization of nodal and extranodal sites by Eμ-TCL1/p66Shc$^{-/-}$ cells is associated with higher expression of homing receptors

The chemokine receptors CXCR4 and CCR7 contribute to the pathogenesis of CLL by modulating leukemic B-cell homing to secondary lymphoid organs and bone marrow.[3,24,25] p66Shc modulates surface expression of homing and egress receptors both transcriptionally and post-translationally in normal and CLL B cells,[7,8] suggesting that the increased colonizing ability of leukemic Eμ-TCL1/p66Shc$^{-/-}$ cells may be caused by imbalanced expression of these receptors. Splenic leukemic cells from Eμ-TCL1 and Eμ-TCL1/p66Shc$^{-/-}$ mice with overt leukemia were analyzed by quantitative real-time PCR and flow cytometry for expression of chemokine receptors that regulate CLL cell homing to and residency in lymphoid organs, namely CXCR4, CCR7 and S1PR1. Splenic B cells from C57BL6/J and C57BL6/J/p66Shc$^{-/-}$ mice were used as controls.

Expression of CXCR4, which mainly guides B-cell homing to the bone marrow,[26] was comparable in leukemic cells from both mouse strains (Figure 5A), accounting at least in part for the comparable extent of tumoral cell infiltration in the spleen. Conversely, surface expression of CCR7, the main lymph node B-cell homing receptor,[27] was higher in Eμ-TCL1/p66Shc$^{-/-}$ cells (Figure 5B). Expression of S1PR1, which controls B-cell egress from secondary lymphoid organs,[28] was strongly downregulated in Eμ-TCL1/p66Shc$^{-/-}$ compared to Eμ-TCL1 cells (Figure 5C), in agreement with the causal relationship between p66Shc and S1PR1 expression in CLL cells.[8] Consistent with these results and the massive lymph node colonization (Figure 4A), leukemic Eμ-TCL1/p66Shc$^{-/-}$ cell chemotaxis towards the CCR7 ligand MIP-3β and the S1PR1 ligand S1P was enhanced and suppressed, respec-

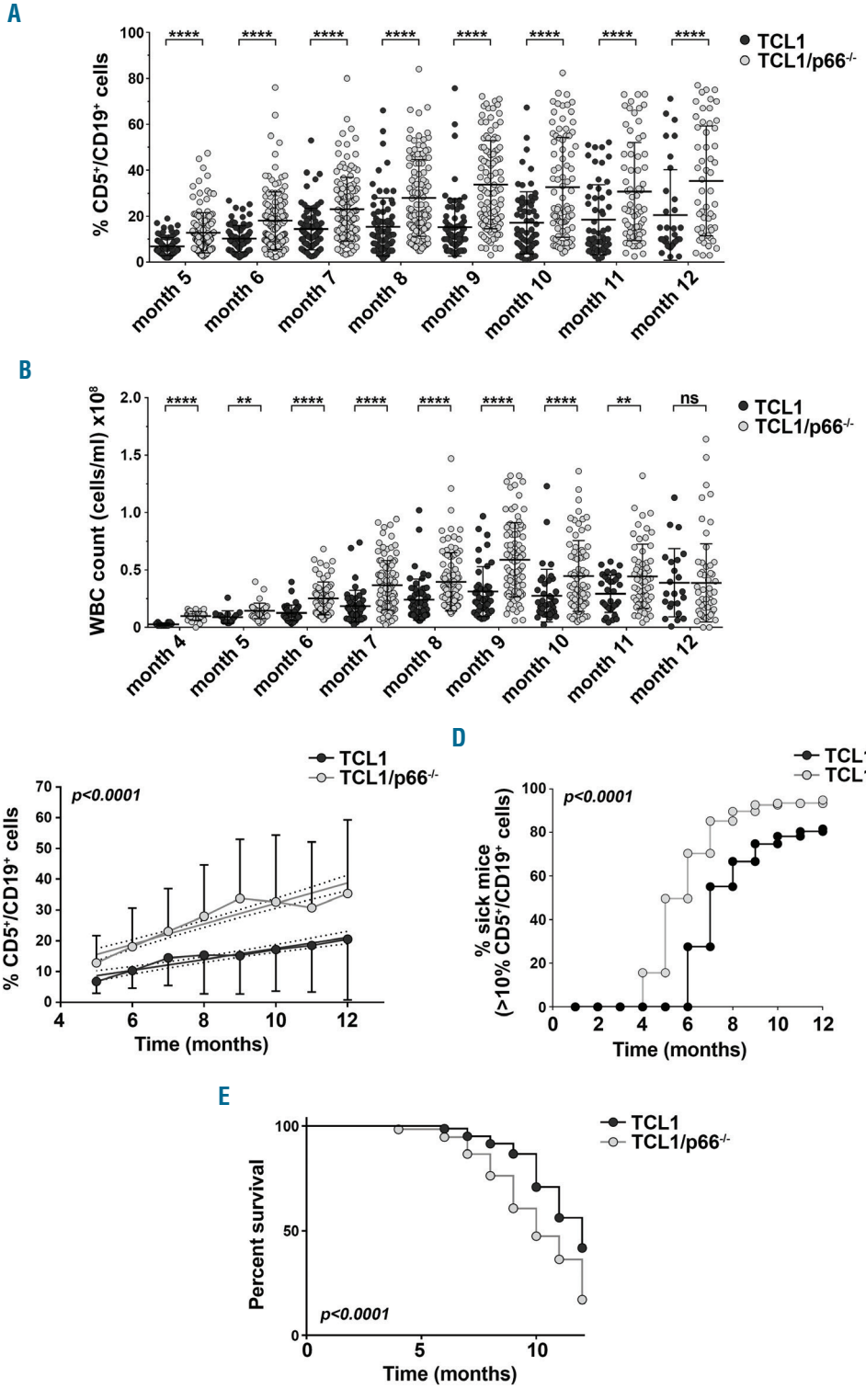

Figure 2. p66Shc deficiency accelerates leukemogenesis in Eμ-TCL1 mice. (A, B) Flow cytometric analysis of the percentages (A) and white blood cell (WBC) counts (B) of CD5$^+$CD19$^+$ cells in peripheral blood samples from either Eμ-TCL1 (n=87) or Eμ-TCL1/p66Shc$^{-/-}$ (n=134) mice collected at the indicated months. (C) Trend-lines calculated on the monthly average percentages of CD5$^+$CD19$^+$ cells in the Eμ-TCL1 and Eμ-TCL1/p66Shc$^{-/-}$ mice shown in (A). (D) Analysis of the percentages of sick mice, calculated as the percentage of mice with ≥10% CD5$^+$CD19$^+$ cells, calculated on the percentages of CD5$^+$CD19$^+$ cells shown in (A). (E) Log-rank survival analysis of the Eμ-TCL1 or Eμ-TCL1/p66Shc$^{-/-}$ mice shown in (A). Mean ± standard deviation. Mann-Whitney rank sum test. ****P≤0.0001; ***P≤0.001; **P≤0.01; ns: not significant.

tively, compared to that of leukemic Eμ-TCL1 cells, as assessed in transwell assays (*Online Supplementary Figure S7*). Although surface and mRNA levels of CXCR4 were similar in the two mouse strains, tumoral Eμ-TCL1/p66Shc$^{-/-}$ cell chemotaxis towards the CXCR4 ligand CXCL12 was enhanced (*Online Supplementary Figure S7*), consistent with the ability of p66Shc to negatively regulate CXCR4-dependent signaling[9] and CXCR4 recycling[7] in human B cells.

Lymphocyte homing to non-lymphoid organs is controlled by G protein-coupled receptors. B-cell homing to the liver is regulated by CCR1, CCR2, and CXCR3, while CCR2, CCR5, and CXCR3 have been implicated in B-cell homing to the lung.[29-34] CCR1 and CCR5 mRNA levels in leukemic cells were comparable in the two mouse strains (*Online Supplementary Figure S8*). Conversely, both surface and mRNA levels of CCR2 and CXCR3 were higher in leukemic Eμ-TCL1/p66Shc$^{-/-}$ cells

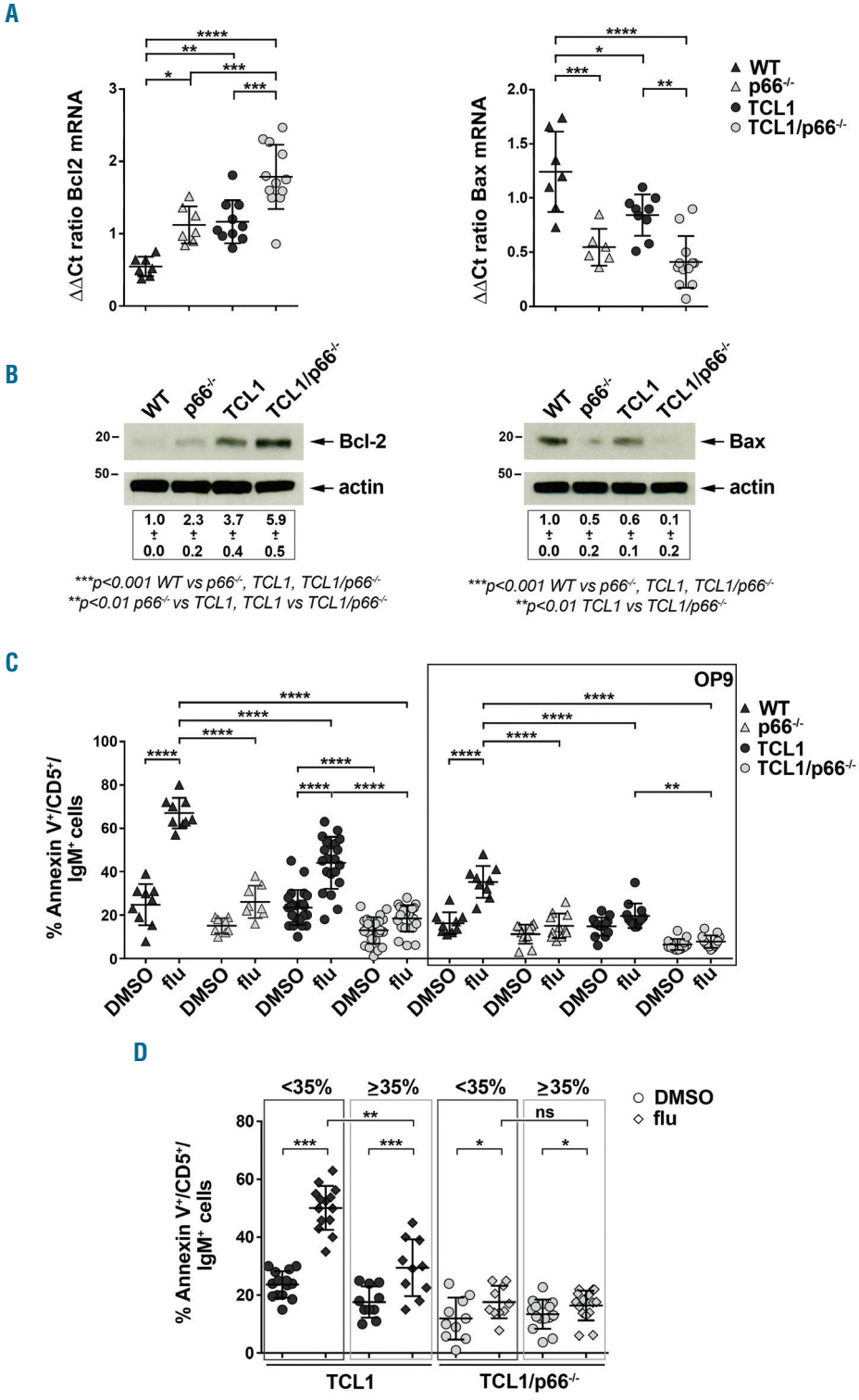

Figure 3. p66Shc deficiency in leukemic cells results in enhanced chemoresistance. (A) Quantitative real-time polymerase chain reaction analysis of Bcl-2 and Bax mRNA in leukemic cells purified from either wildtype (WT) (n=7) or p66Shc$^{-/-}$ (n=7) mice and from Eμ-TCL1 (n=10) or Eμ-TCL1/p66Shc$^{-/-}$ (n=12) mice with overt leukemia. The relative gene transcript abundance was determined on triplicate samples using the ΔΔCt method. (B) Immunoblot analysis with anti-Bcl-2 (left) and anti-Bax (right) antibodies of postnuclear supernatants of leukemic cells purified from either WT (n=3) or p66Shc$^{-/-}$ (n=3) mice and from Eμ-TCL1 (n=3) or Eμ-TCL1/p66Shc$^{-/-}$ (n=3) mice with overt leukemia. The stripped filters were reprobed with anti-actin antibodies. (C) Flow cytometric analysis of the percentages of annexin V$^+$CD5$^+$IgM$^+$ cells in peripheral blood from either WT (n=9) or p66Shc$^{-/-}$ (n=8) mice and from Eμ-TCL1 (n=20) or Eμ-TCL1/p66Shc$^{-/-}$ (n=22) mice. Samples were treated with either dimethylsulfoxide (DMSO) or 35 μM fludarabine (flu) for 16 h at 37°C. (D) Flow cytometric analysis of the percentages of annexin V$^+$CD5$^+$IgM$^+$ cells in peripheral blood from either Eμ-TCL1 (n=20) or Eμ-TCL1/p66Shc$^{-/-}$ (n=22) mice with <35% (black boxes) or ≥35% (gray boxes) CD5$^+$CD19$^+$ leukemic cells in peripheral blood, treated with either DMSO or 35 μM fludarabine for 16 h at 37°C. Mean ± standard deviation. One-way analysis of variance (ANOVA), multiple comparisons. ****P≤0.0001; ***P≤0.001; **P≤0.01; *P≤0.05

than in Eμ-TCL1 cells (Figure 5D,E). Consistent with these results and their enhanced liver and lung colonization (Figure 4B,C), chemotaxis towards the respective chemokines was enhanced in leukemic Eμ-TCL1/p66Shc$^{-/-}$ cells compared to leukemic Eμ-TCL1 cells (*Online Supplementary Figure S7*). Of note, similar effects, albeit less pronounced, were observed when mRNA and surface levels of these receptors, and the chemotactic responses thereof, were analyzed in B cells from C57BL6/J and C57BL6/J/p66Shc$^{-/-}$ mice (Figure 5 and *Online Supplementary Figure S7*), further supporting the central role of p66Shc in modulating expression of these receptors. Collectively, these results suggest that the more efficient colonization of and accumulation in extranodal sites by p66Shc$^{-/-}$ leukemic cells can be accounted for, at least in part, by the ability of p66Shc to modulate the expression of chemokine receptors that guide the cells' homing to those sites.

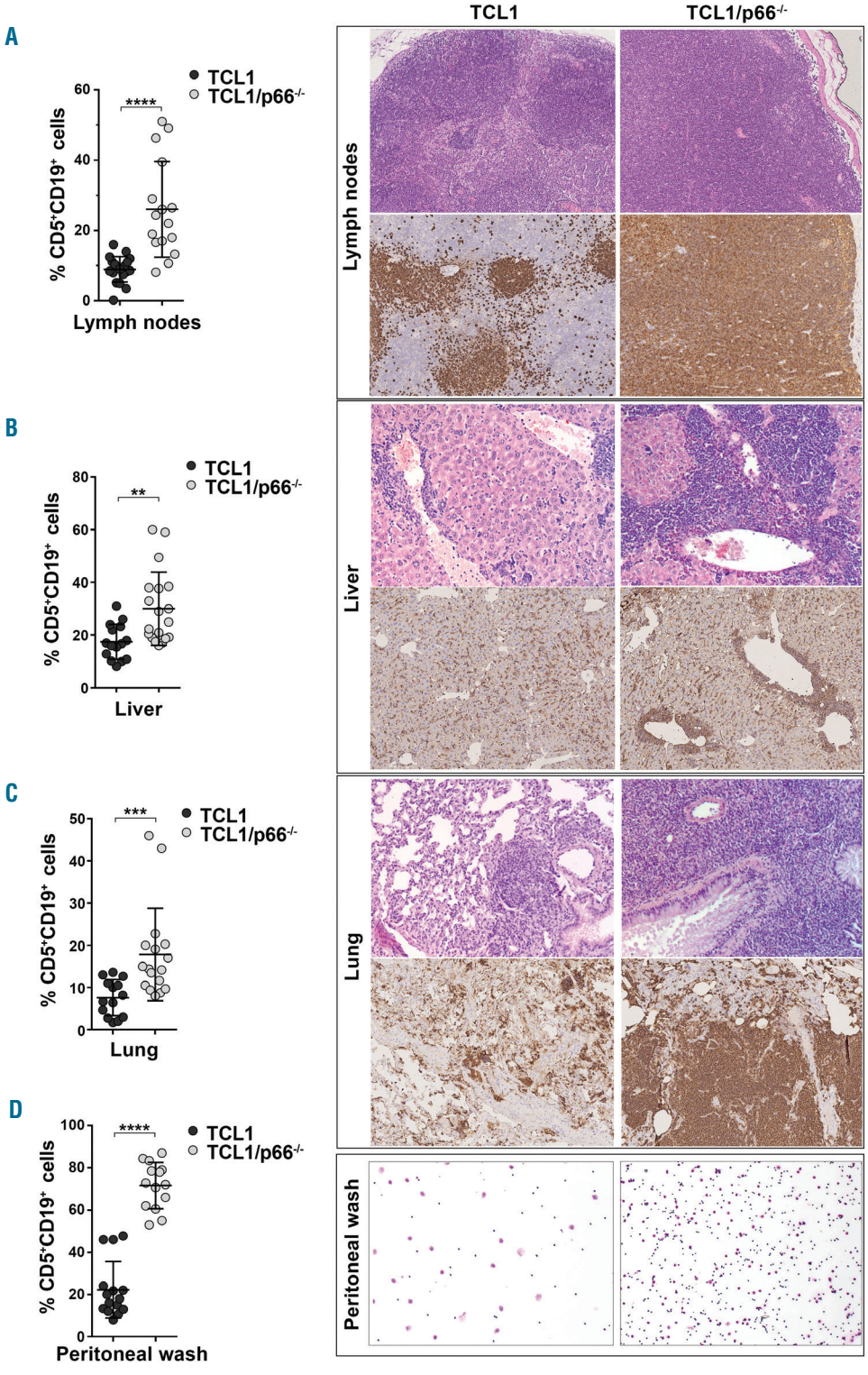

Figure 4. Nodal and extranodal accumulation of leukemic cells lacking p66Shc. (A-D) (Left) Flow cytometric analysis of the percentages of CD5^{+}CD19^{+} cells in lymph nodes (A), liver (B), lung (C) and peritoneal wash (D) from either Eμ-TCL1 (n=15) or Eμ-TCL1/p66Shc$^{-/-}$ (n=15) mice with overt leukemia. (Right) Hematoxylin & eosin staining (upper panels) and immunohistochemical analysis of B220 (lower panels) in lymph nodes (A), liver (B), lung (C) and peritoneal wash (D) from either Eμ-TCL1 (n=5) or Eμ-TCL1/p66Shc$^{-/-}$ (n=10) with overt leukemia. (Immunoperoxidase staining; original magnification, 5x, 10x and 20x). Mean ± standard deviation. Mann-Whitney rank sum test. ****P≤0.0001; ***P≤0.001; **P≤0.01.

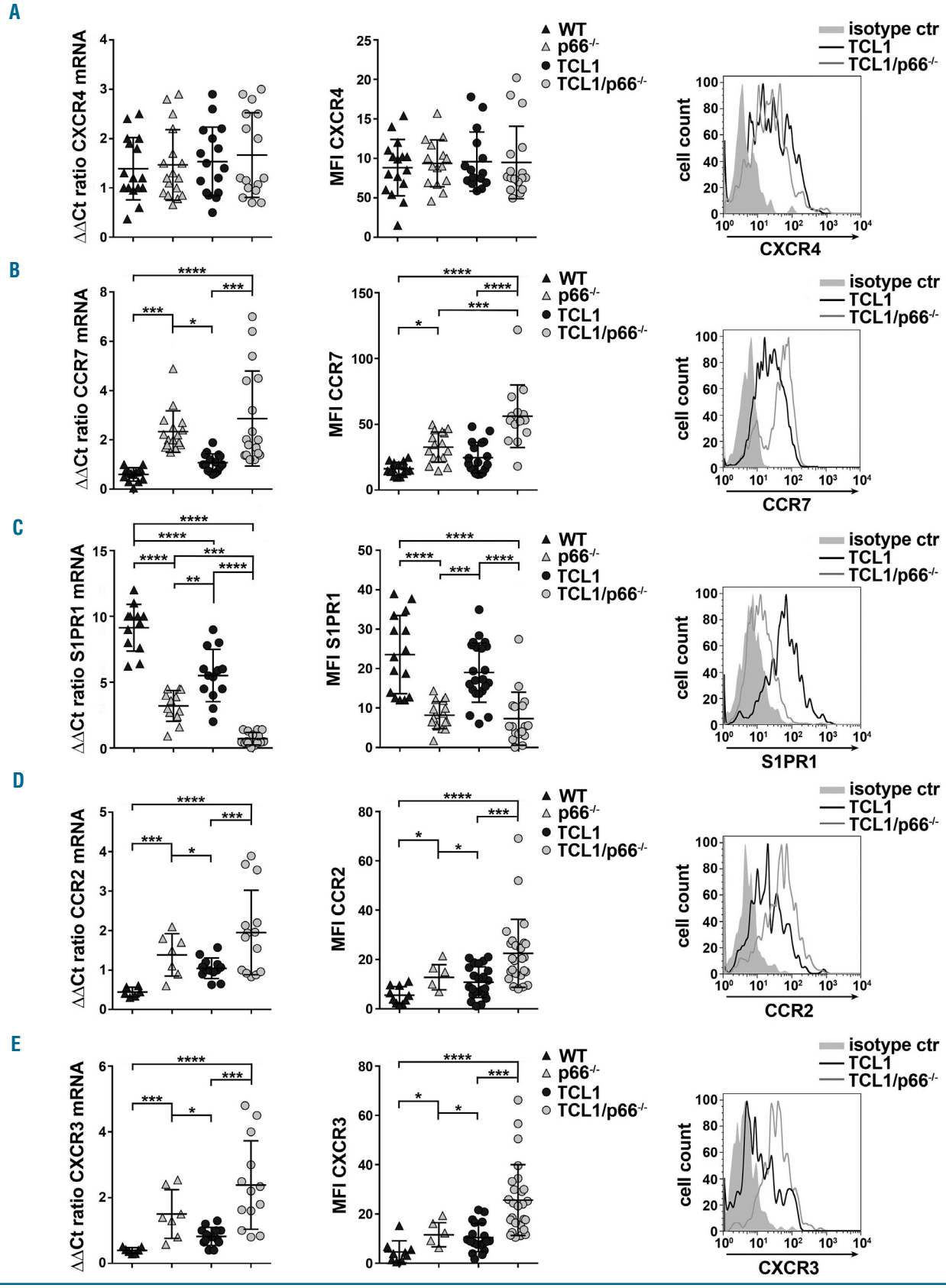

Figure 5. p66Shc deficiency in leukemic cells results in enhanced expression of homing receptors and reduced expression of the egress receptor S1PR1. (A-E) Quantitative real-time polymerase chain reaction analysis of the mRNA levels (left) and flow cytometric analysis of surface expression (right) of CXCR4 (A), CCR7 (B), S1PR1 (C), CCR2 (D) and CXCR3 (E) in $CD5^+CD19^+$ cells purified from either wildtype (WT) (n=16) or p66Shc$^{-/-}$ (n=15) mice (B1a cells) and from Eμ-TCL1 (n≥16) or Eμ-TCL1/p66Shc$^{-/-}$ (n≥16) mice with overt leukemia. The relative gene transcript abundance was determined on triplicate samples using the ΔΔCt method. Representative flow cytometric plots of the indicated stains are shown on the right. Chemotaxis toward the respective chemokines is shown in *Online Supplementary Figure S6*. Mean ± standard deviation. One-way analysis of variance (ANOVA), multiple comparisons. ****P≤0.0001; ***P≤0.001; **P≤0.01; *P≤0.05.

Reconstitution of p66Shc in chronic lymphocytic leukemia cells normalizes their CCR2 and CXCR3 expression

We translated these results to human CLL cells, in which a drastic reduction in p66Shc mRNA was observed compared to levels in healthy donor B cells, with lower residual levels in patients with unmutated IGHV (UM-CLL), who develop aggressive disease,[35] compared to patients with mutated IGHV (M-CLL) (Figure 6A,B).[6] No correlation with other genetic markers of CLL, namely 13q deletion or *TP53* deletion/mutation, was observed (*Online Supplementary Figure S9A,B*).

We investigated whether the residual levels of p66Shc in CLL cells could be correlated with the expression of the trafficking receptors found to be modulated by p66Shc deficiency in Eμ-TCL1 leukemic cells. As reported,[8] surface and mRNA levels of CCR7 and S1PR1 correlated inversely and directly, respectively, with p66Shc expression in CLL cells from the patients included in this study (Figure 6C,D and *Online Supplementary Figure S10A,B*).

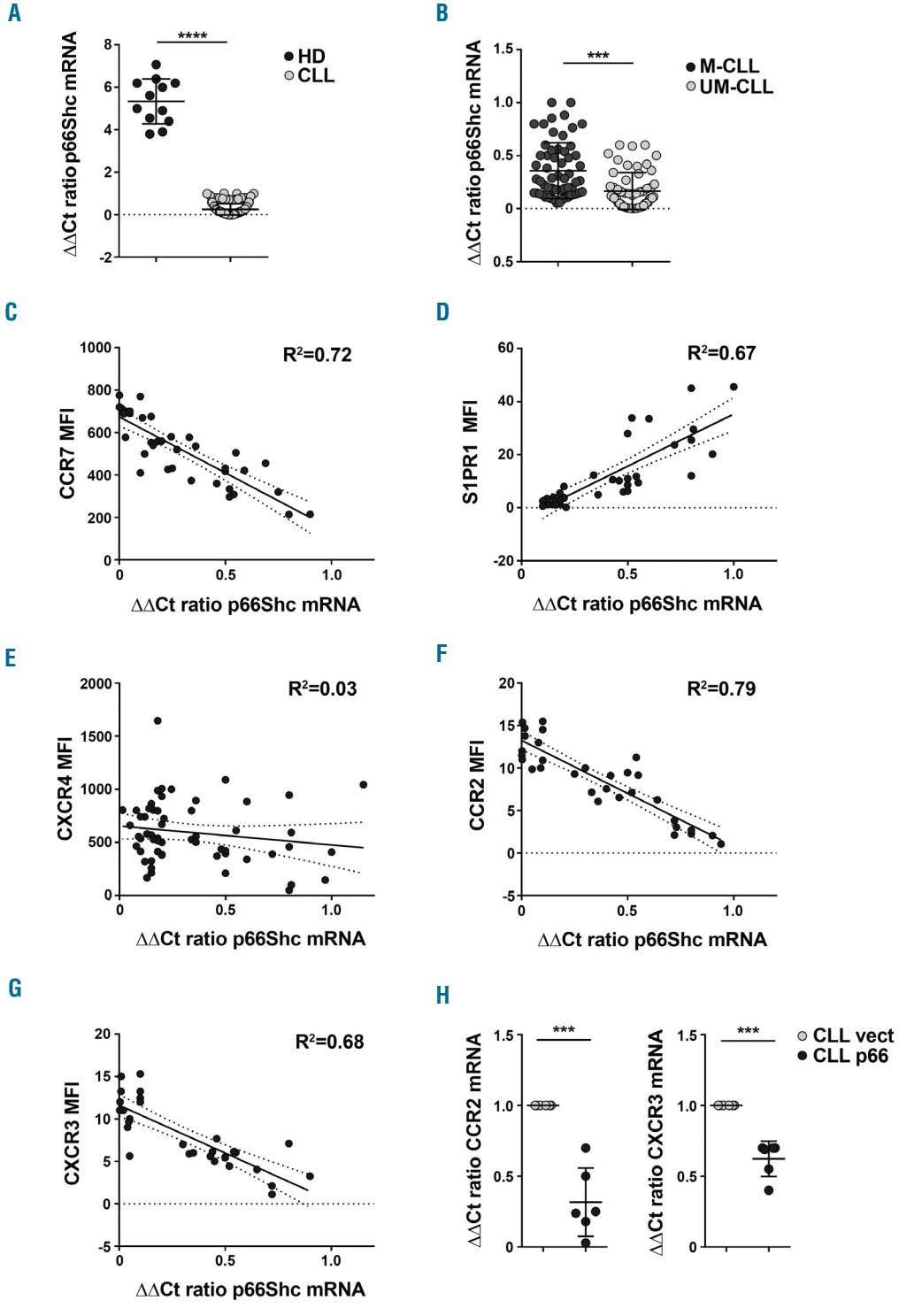

Figure 6. p66Shc deficiency is associated with abnormal expression of chemokine receptors and lymphadenopathy in human chronic lymphocytic leukemia. (A, B) Quantitative real-time polymerase chain reaction (qRT-PCR) analysis of p66Shc mRNA in B cells purified from either healthy donors (HD) (n=12) or patients with chronic lymphocytic leukemia (CLL) (n=157) (A), or B cells purified from CLL patients, grouped into those with mutated CLL (M-CLL) (n=67) or unmutated CLL (UM-CLL) (n=64) (B). (C-G) Correlation between mRNA levels of p66Shc and surface expression levels of CCR7 (C), S1PR1 (D), CXCR4 (E), CCR2 (F) and CXCR3 (G) in B cells purified from CLL patients (n≤89). (H) qRT-PCR analysis of CCR2 (left) and CXCR3 (right) mRNA in purified CLL B cells (n=6), nucleofected with either empty vector (CLL vect) or an expression construct encoding p66Shc (CLL p66). The relative gene transcript abundance was determined on triplicate samples using the ΔΔCt method. Mean ± standard deviation. Mann-Whitney rank sum test. ***$P \leq 0.001$" to "****$P \leq 0.0001$; ***$P \leq 0.001$".

Consistent with our finding that the upregulation of surface CXCR4 in CLL cells is mainly controlled post-translationally,[11] no correlation was observed between the mRNA levels of p66Shc and CXCR4 (Figure 6E and *Online Supplementary Figure S10C*).

The analysis was extended to CCR2 and CXCR3, which were selectively overexpressed in UM-CLL cells (*Online Supplementary Figure S9C,D*). Similar to CCR7, expression of these receptors was inversely correlated with that of p66Shc (Figure 6F,G and *Online Supplementary Figure S10D,E*), suggesting that p66Shc may negatively modulate their expression. p66Shc reconstitution in CLL cells did indeed result in a decrease in CCR2 and CXCR3 mRNA (Figure 6H and *Online Supplementary Figure S10F*).

Interestingly, infiltration of both nodal and extranodal areas, assessed by the number and size (cm) of infiltrated lymph nodes and the presence of spleen and/or liver enlargement, was significantly greater in patients whose leukemic cells had p66Shc mRNA levels below an arbitrarily set threshold (0.24, corresponding to the mean ΔΔCt p66Shc mRNA of all CLL patients) (*Online Supplementary Figure S11* and Table 1). These data provide evidence of a correlation of the severity of the p66Shc expression defect in CLL cells with their ability to infiltrate both nodal and extranodal districts, strongly supporting a role for p66Shc deficiency in disease presentation. Of note, p66Shc expression was enhanced in CLL patients showing a significant response to second-line ibrutinib treatment but not in CLL patients who failed to respond to ibrutinib therapy (Table 1 and *Online Supplementary Table S1*), suggesting that the response of CLL patients to therapeutic regimens results, at least in part, from the ability of leukemic cells to restore p66Shc expression.

Table 1. Pathological characteristics of patients with chronic lymphocytic leukemia and p66Shc mRNA levels in their respective leukemic cells during treatment.

	ΔΔCt p66Shc mRNA	
	>0.24±0.7 "above threshold"	≤ 0.24±0.7 "below threshold"
N. of CLL patients	30	34
N. of UM-CLL patients	6	19
% UM-CLL	20.00	55.88
N. of infiltrated lymph nodes	0.67±0.23	2.27±0.24 (***P<0.001 below *vs.* above threshold)
% LN >1.5 cm	53.33	88.23
% Spleen infiltration (> 13 cm)	13.33	70.59
% Liver infiltration (> 1 cm under arch)	3.33	29.41

	Patients responding to ibrutinib	Patients "failing" ibrutinib
Before CIT	0.8±0.2	0.14±0.06* (* P<0.05 "failing" *vs.* responding patients)
Follow-up CIT	5.8±2.3	0.35
Before ibrutinib	1.1±1.04	0.12±0.08
Follow-up ibrutinib	26.1±6.9	0.23±0.22** (**P<0.01 "failing" *vs.* responding patients)

Patients with chronic lymphocytic leukemia (CLL) were grouped according to p66Shc mRNA expression into either "above threshold" and "below threshold" (threshold 0.24, corresponding to the mean ΔΔCt p66Shc mRNA; n CLL=157), or according to response to ibrutinib into either "responding" or "failing" based on International Working Group CLL response criteria.[30] Mann-Whitney rank sum test. ***P≤0.001; **P≤0.01; *P≤0.05. LN: lymph nodes; CLL: chronic lymphocytic leukemia; UM-CLL: unmutated CLL; CIT: chemo-immunotherapy.

Modulation of CCR2 and CXCR3 expression by p66Shc is mediated by its pro-oxidant activity

p66Shc has a ROS-elevating activity that depends on its ability to interact with cytochrome c and interrupt the respiratory chain.[4] We quantified homeostatic ROS production in CLL cells loaded with the cell-permeant probe CM-H_2DCFDA. ROS production was profoundly decreased in CLL B cells compared to that in normal B cells, with the lowest levels in UM-CLL patients (Figure 7A), consistent with their lowest p66Shc levels.[6] Furthermore, we found a direct correlation between ROS production and p66Shc expression in CLL cells (Figure 7B). These findings were recapitulated in CM-H_2DCFDA-loaded Eμ-TCL1 cells which, similar to CLL cells, express low levels of p66Shc (Figure 1B) and in which ROS production was lower than that in B cells from control C57BL/6 mice (Figure 7C). ROS production was further impaired in Eμ-TCL1/p66Shc$^{-/-}$ cells (Figure 7C), confirming the pro-oxidant activity of p66Shc.

Transcription of both *ccr7* and *s1pr1* is controlled in opposite directions by the ROS-elevating activity of p66Shc.[8] To address the potential role of the pro-oxidant function of p66Shc in the regulation of CCR2 and CXCR3 expression we used the CLL-derived human B-cell line MEC1 stably transfected with a ROS-defective mutant carrying a E→Q substitution at positions 132-133 (p66QQ), which disrupts cytochrome c binding (Figure 7D,E).[8] The empty vector transfectant lacking p66Shc (ctr) and a transfectant expressing the wildtype protein (p66) were used as controls. Flow cytometric analysis of homeostatic ROS production in the CM-H_2DCFDA-loaded MEC1 transfectants showed enhanced ROS production in p66Shc-expressing cells, but not in cells expressing p66ShcQQ, compared to control cells (Figure 7F).

Mitochondrial redox signaling and apoptosis are also modulated by p53,[36] which is mutated in a large proportion of CLL patients[1] as well as in MEC1 cells.[37] To rule out a role for *TP53* mutations in the enhanced ROS production by p66Shc-expressing MEC1 cells, ROS were measured in EBV-immortalized B cells, which express wildtype p53,[38] transiently depleted of p66Shc by short interfering RNA-mediated knock-down. Similar to MEC1 cells, p66Shc deficiency in EBV-immortalized B cells resulted in a lower intracellular ROS content and enhanced CCR2 and CXCR3 expression (*Online Supplementary Figure S12*), underscoring the specific contribution of p66Shc to the ROS-dependent modulation of these receptors.

Surface and mRNA expression of CCR2 and CXCR3 was next measured in all transfectants. The wildtype p66Shc-expressing transfectant, but not the p66QQ transfectant, had lower mRNA and surface levels of both receptors compared to the levels in control cells (Figure 7G,I). Surface and mRNA expression of CCR2 and CXCR3 was also decreased in MEC1 cells after treatment with 50 μM H_2O_2, an exogenous ROS source (Figure 7H-J), indicating that the ability of p66Shc to modulate CCR2 and CXCR3 expression involves its ROS-elevating activity.

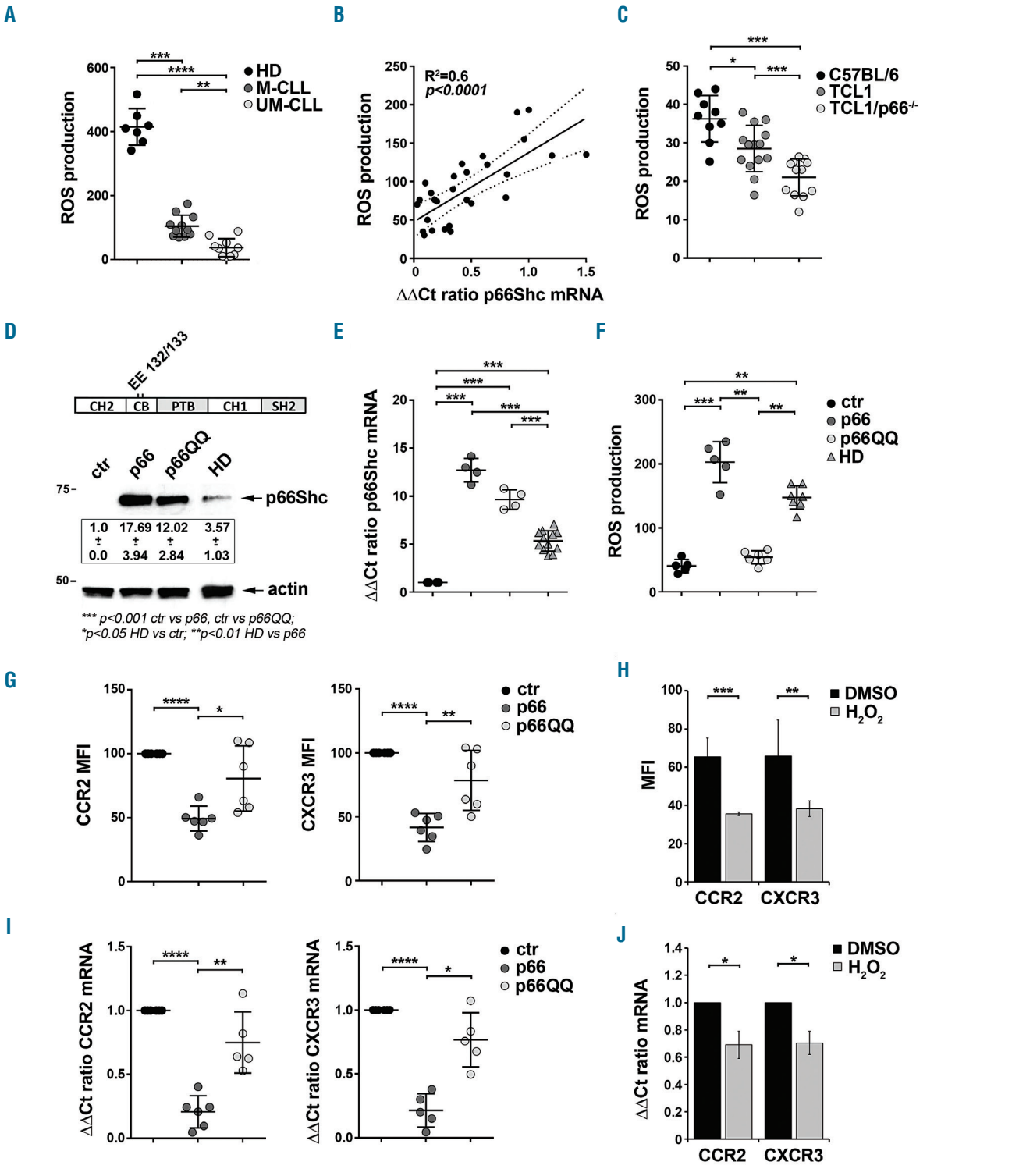

Figure 7. The pro-oxidant activity of p66Shc modulates CCR2 and CXCR3 expression. (A, C) Flow cytometric analysis of reactive oxygen species (ROS) production in B cells purified from either healthy donors (HD, n=7) or patients with chronic lymphocytic leukemia (CLL) grouped according to whether they had mutated CLL (M-CLL) (n=11) or unmutated CLL (UM-CLL) (n=9) (A) and in B1a cells from wildtype (C57BL/6, n=9) mice and from Eμ-TCL1 (n=13) or Eμ-TCL1/p66Shc$^{-/-}$ (n=12) sick mice (C), loaded with CM-H_2DCFDA. Data refer to duplicate samples from each patient/donor/mouse. (B) Correlation between mRNA levels of p66Shc and ROS production in B cells purified from CLL patients (n=28). (D, E) Immunoblot analysis of Shc expression (D) and quantitative real-time polymerase chain reaction (qRT-PCR) analysis of p66Shc mRNA (E) in MEC1 B cells stably transfected with empty vector (ctr) or an expression construct encoding either wildtype p66Shc (p66) or the EE132/133QQ (p66QQ) mutant, and in B cells purified from healthy donors (HD) (n=3). A control anti-actin blot of the stripped filter is shown below. The migration of molecular mass markers is indicated. The domain structure of p66Shc showing the localization of the amino acid residues substituted in the mutants is schematized at the top of the panel. (F) Flow cytometric analysis of ROS production in the MEC1 B-cell transfectants and in B cells purified from healthy donors (B cell, n=5) loaded with CM-H_2DCFDA. Data refer to duplicate samples from five independent experiments. (G, I). Flow cytometric analysis (G) and qRT-PCR analysis of the mRNA levels (I) of CCR2 (left) and CXCR3 (right) in MEC1 transfectants. Data refer to duplicate samples from five independent experiments. (H, J). Flow cytometric analysis (H) and qRT-PCR analysis of the mRNA levels (J) of CCR2 and CXCR3 in MEC1 cells treated for 24 h with either dimethylsulfoxide (DMSO) or 50 μM H_2O_2. Data refer to duplicate samples from four independent experiments. The relative gene transcript abundance was determined on triplicate samples using the ΔΔCt method. Mean ± standard deviation. Mann-Whitney rank sum test. ****P≤0.0001; ***P≤0.001**P≤0.01; *P≤0.05. MFI: mean fluorescence intensity.

Discussion

Here we used a genetic approach to specifically assess the outcome of p66Shc deficiency on CLL cell survival and disease onset and development. We showed that p66Shc deletion in Eμ-TCL1 mice results in accelerated leukemogenesis and enhanced disease aggressiveness, with massive nodal and extranodal infiltration. The enhanced ability of leukemic p66Shc$^{-/-}$ cells to infiltrate organs was associated with increased expression of chemokine receptors that drive homing to the organs. p66Shc expression declined with disease progression in Eμ-TCL1 cells, similar to human CLL. This defect could be restored by ibrutinib treatment which enhanced the cells' chemosensitivity. These results demonstrate *in vivo* that the p66Shc defect found in CLL cells concurs to CLL pathogenesis. Of note, p66Shc$^{-/-}$ mice spontaneously develop age-related autoimmunity,[5] a feature frequently associated with CLL.[1] Interestingly, p66Shc downregulation in CLL B cells induces the expression of the inhibitory molecule ILT3,[39] suggesting that compensatory mechanisms might be operational to restrain CLL cell responses.

The negative impact of p66Shc deletion on disease progression and outcome in Eμ-TCL1 mice can be accounted for, at least in part, by the extended survival and chemoresistance of leukemic cells, even when co-cultured with stromal cells as a surrogate pro-survival microenvironment. The p66Shc expression defect in CLL contributes to this biological behavior. p66Shc deficiency does indeed impinge on the Bcl-2 family balance in B cells, contributing to the shift of CLL cells towards survival, which correlates with chemoresistance and poor prognosis.[40] The ROS-elevating activity of p66Shc[4,14] underlies this latter's ability to modulate the genes, several of which are redox-sensitive.[41]

The survival of CLL cells depends to a major extent on their ability to home to the pro-survival microenvironment of bone marrow and secondary lymphoid organs. This process is orchestrated by homing receptors responding to local chemokines and egress receptors responding to lymph and blood S1P.[3] p66Shc is a central part of this circuitry which it affects by: (i) modulating CCR7 and S1PR1 expression in opposite directions in a ROS-dependent fashion;[8] (ii) modulating CCR7 and CXCR4 by slowing down their endosomal recycling;[7] and (iii) attenuating CXCR4 and CXCR5 signaling by recruiting the phosphatases SHP-1 and SHIP-1 close to the activated receptors.[9] The p66Shc defect in CLL cells has a major impact on these processes, resulting in enhanced responses to the chemokines of the lymphoid niche and impaired response to S1P.[7,8] This imbalance is expected to contribute to the lymphadenopathy and chemoresistance observed in a significant proportion of CLL patients, and indeed the levels of CCR7 are significantly higher and those of S1PR1 lower in CLL patients with clinical lymphadenopathy.[8] We showed that the levels of p66Shc in leukemic cells are inversely related to both the number and size of infiltrated lymph nodes in CLL patients. The results obtained in Eμ-TCL1/p66Shc$^{-/-}$ mice, showing massive lymph node accumulation during disease progression, provide experimental evidence that p66Shc deficiency promotes the nodal leukemic cell accumulation in CLL.

p66Shc deficiency also results in a striking extranodal accumulation of leukemic cells, with a preference for liver and lung, the most frequent extranodal target sites in CLL.[21,22] The ROS-related ability of p66Shc to modulate the expression and function of CCR2 and CXCR3, which drive neoplastic B-cell homing to liver and lung where the respective ligands are expressed,[42,43] may account for the enhanced ability of leukemic Eμ-TCL1/p66Shc$^{-/-}$ cells to colonize these organs. Interestingly, CCR2 and CXCR3 are overexpressed in CLL cells (as shown in this study and reported by Trentin *et al.*[44] for CXCR3). We show that p66Shc reconstitution in CLL cells reverts these abnormalities, validating in human CLL our finding that p66Shc deficiency contributes to CCR2 and CXCR3 overexpression in leukemic Eμ-TCL1/p66Shc$^{-/-}$ cells.

p66Shc expression declines during disease progression in Eμ-TCL1 mice, until its almost complete loss in mice with overt leukemia, paralleling the progressive decrease in fludarabine sensitivity of tumoral cells documented previously.[20] *p66shc* transcription is largely controlled in several primary and transformed cells, including T cells, by histone deacetylation and cytosine methylation in a CpG island within the promoter.[45,46] Although methylation increases in Eμ-TCL1 mice during disease development,[47] it is unlikely that methylation of the *p66shc* promoter caused its progressive silencing, as p66Shc expression is not epigenetically silenced in B cells.[6] Rather, in these cells *p66shc* is transcriptionally regulated by STAT4, which is defective in CLL cells.[10] Interestingly, p66Shc can be restored both in CLL cells[7] and in leukemic Eμ-TCL1 cells (Figure 1F,G) by treatment with ibrutinib, which also promotes STAT4 expression in leukemic Eμ-TCL1 cells (Figure 1F,G). Ibrutinib modulates the expression of genes downstream of Btk in the BCR and CXCR4 pathways,[48,49] which are implicated in CLL, suggesting that STAT4 and its target p66Shc may be regulated through these pathways. While this remains to be established, considering the pleiotropic role of p66Shc in B-cell survival and trafficking our finding suggests that direct or indirect STAT4 agonists that enhance the activity of residual STAT4 in CLL cells may normalize p66Shc expression and overcome chemoresistance in CLL. Our finding that interleukin-12, which activates STAT4, restores p66Shc expression in CLL cells[10] supports this hypothesis. Collectively, our findings underscore the pathological outcome of p66Shc deficiency in CLL and highlight the chemokine receptor network as a central target of its activity.

Acknowledgments

The authors thank Carlo M. Croce for providing Eμ-TCL1 mice and Sonia Grassini for technical assistance. This work was supported by grants from AIRC (IG-20148) and ITT-Regione Toscana to CTB, AIRC (IG-19236) to DGE, AIRC (IG-15286) to GS and AIRC (IG-15397) to LT.

References

1. Dighiero G, Hamblin TJ. Chronic lymphocytic leukaemia. Lancet. 2008;371(9617):1017–1029.
2. Ortiz-Maldonado V, Mozas P, Delgado J. The biology behind B-cell lymphoma 2 as a target in chronic lymphocytic leukemia. Ther Adv Hematol. 2016;7(6):321–329.
3. Burger JA. Nurture versus nature: the microenvironment in chronic lymphocytic leukemia. Hematol Am Soc Hematol Educ Progr. 2011;2011(1):96–103.
4. Giorgio M, Migliaccio E, Orsini F, et al. Electron transfer between cytochrome c and p66Shc generates reactive oxygen species that trigger mitochondrial apoptosis. Cell. 2005;122(2):221–233.

5. Finetti F, Savino MT, Baldari CT. Positive and negative regulation of antigen receptor signaling by the Shc family of protein adapters. Immunol Rev. 2009;232(1):115–134.
6. Capitani N, Lucherini OM, Sozzi E, et al. Impaired expression of p66Shc, a novel regulator of B-cell survival, in chronic lymphocytic leukemia. Blood. 2010;115(18):3726–3736.
7. Patrussi L, Capitani N, Cattaneo F, et al. p66Shc deficiency enhances CXCR4 and CCR7 recycling in CLL B cells by facilitating their dephosphorylation-dependent release from β-arrestin at early endosomes. Oncogene. 2018;37(11):1534–1550.
8. Capitani N, Patrussi L, Trentin L, et al. S1P1 expression is controlled by the pro-oxidant activity of p66Shc and is impaired in B-CLL patients with unfavorable prognosis. Blood. 2012;120(22):4391–4399.
9. Patrussi L, Capitani N, Cannizzaro E, et al. Negative regulation of chemokine receptor signaling and B-cell chemotaxis by p66Shc. Cell Death Dis. 2014;5(2):e1068.
10. Cattaneo F, Patrussi L, Capitani N, et al. Expression of the p66Shc protein adaptor is regulated by the activator of transcription STAT4 in normal and chronic lymphocytic leukemia B cells. Oncotarget. 2016;7(35):57086–57098.
11. Patrussi L, Capitani N, Martini V, et al. Enhanced chemokine receptor recycling and impaired S1P1 expression promote leukemic cell infiltration of lymph nodes in chronic lymphocytic leukemia. Cancer Res. 2015;75(19):4153–4163.
12. Bichi R, Shinton SA, Martin ES, et al. Human chronic lymphocytic leukemia modeled in mouse by targeted TCL1 expression. Proc Natl Acad Sci U S A. 2002;99(10):6955–6960.
13. Suljagic M, Longo PG, Bennardo S, et al. The Syk inhibitor fostamatinib disodium (R788) inhibits tumor growth in the Eμ-TCL1 transgenic mouse model of CLL by blocking antigen-dependent B-cell receptor signaling. Blood. 2010;116(23):4894–4905.
14. Migliaccio E, Giorgio M, Mele S, et al. The p66shc adaptor protein controls oxidative stress response and life span in mammals. Nature. 1999;402(6759):309–313.
15. Stacchini A, Aragno M, Vallario A, et al. MEC1 and MEC2: two new cell lines derived from B-chronic lymphocytic leukaemia in prolymphocytoid transformation. Leuk Res. 1999;23(2):127–36.
16. Patrussi L, Ulivieri C, Lucherini OM, et al. p52Shc is required for CXCR4-dependent signaling and chemotaxis in T cells. Blood. 2007;110(6):1730–1738.
17. Yan X, Albesiano E, Zanesi N, et al. B cell receptors in TCL1 transgenic mice resemble those of aggressive, treatment-resistant human chronic lymphocytic leukemia. Proc Natl Acad Sci U S A. 2006;103(31):11713–11718.
18. Dono M, Cerruti G, Zupo S. The CD5+ B-cell. Int J Biochem Cell Biol. 2004;36(11):2105–2111.
19. Byrd JC, Furman RR, Coutre SE, et al. Targeting BTK with ibrutinib in relapsed chronic lymphocytic leukemia. N Engl J Med. 2013;369(1):32–42.
20. Johnson AJ, Lucas DM, Muthusamy N, et al. Characterization of the TCL-1 transgenic mouse as a preclinical drug development tool for human chronic lymphocytic leukemia. Blood. 2006;108(4):1334–1338.
21. Kreiniz N, Beyar Katz O, Polliack A, Tadmor T. The clinical spectrum of hepatic manifestations in chronic lymphocytic leukemia. clin lymphoma myeloma leuk. 2017;17(12):863-869.
22. Carmier D, Dartigeas C, Mankikian J, et al. Serious bronchopulmonary involvement due to chronic lymphocytic leukaemia. Eur Respir Rev. 2013;22(129):416–419.
23. Pacini S, Pellegrini M, Migliaccio E, et al. p66SHC promotes apoptosis and antagonizes mitogenic signaling in T cells. Mol Cell Biol. 2004;24(4):1747–1757.
24. Till KJ, Lin K, Zuzel M, Cawley JC. The chemokine receptor CCR7 and alpha4 integrin are important for migration of chronic lymphocytic leukemia cells into lymph nodes. Blood. 2002;99(8):2977–2984.
25. Trentin L, Cabrelle A, Facco M, et al. Homeostatic chemokines drive migration of malignant B cells in patients with non-Hodgkin lymphomas. Blood. 2004;104(2):502–508.
26. Burger JA, Burger M, Kipps TJ. Chronic lymphocytic leukemia B cells express functional CXCR4 chemokine receptors that mediate spontaneous migration beneath bone marrow stromal cells. Blood. 1999;94(11):3658–3667.
27. López-Giral S, Quintana NE, Cabrerizo M, et al. Chemokine receptors that mediate B cell homing to secondary lymphoid tissues are highly expressed in B cell chronic lymphocytic leukemia and non-Hodgkin lymphomas with widespread nodular dissemination. J Leukoc Biol. 2004;76(2):462–471.
28. Cyster JG. Chemokines, sphingosine-1-phosphate, and cell migration in secondary lymphoid organs. Annu Rev Immunol. 2005;23:127–159.
29. Akram IG, Georges R, Hielscher T, Adwan H, Berger MR. The chemokines CCR1 and CCRL2 have a role in colorectal cancer liver metastasis. Tumor Biol. 2016;37(2):2461–2471.
30. Bigildeev AE, Shipounova IN, Svinareva DA, Drize NJ. Leukemia cells invading the liver express liver chemokine receptors and possess characteristics of leukemia stem cells in mice with MPD-like myeloid leukemia. Exp Hematol. 2011;39(2):187–194.
31. Zhao L, Lim SY, Gordon-Weeks AN, et al. Recruitment of a myeloid cell subset (CD11b/Gr1 mid) via CCL2/CCR2 promotes the development of colorectal cancer liver metastasis. Hepatology. 2013;57(2):829–839.
32. Rose CE, Sung S-SJ, Fu SM. Significant involvement of CCL2 (MCP-1) in inflammatory disorders of the lung. Microcirculation. 2003;10(3–4):273–288.
33. Jeyanathan M, Afkhami S, Khera A, et al. CXCR3 signaling is required for restricted homing of parenteral tuberculosis vaccine–induced T cells to both the lung parenchyma and airway. J Immunol. 2017;199(7):2555–2569.
34. Shetty S, Bruns T, Weston CJ, et al. Recruitment mechanisms of primary and malignant B cells to the human liver. Hepatology. 2012;56(4):1521–1531.
35. Hamblin TJ, Davis Z, Gardiner A, Oscier DG, Stevenson FK. Unmutated Ig V(H) genes are associated with a more aggressive form of chronic lymphocytic leukemia. Blood. 1999;94(6):1848–1854.
36. Gào X, Schöttker B. Reduction-oxidation pathways involved in cancer development: a systematic review of literature reviews. Oncotarget. 2017;8(31):51888–51906.
37. Pozzo F, Dal Bo M, Peragine N, et al. Detection of TP53 dysfunction in chronic lymphocytic leukemia by an in vitro functional assay based on TP53 activation by the non-genotoxic drug Nutlin-3: a proposal for clinical application. J Hematol Oncol. 2013;6:83.
38. Allday MJ, Sinclair A, Parker G, Crawford DH, Farrell PJ. Epstein-Barr virus efficiently immortalizes human B cells without neutralizing the function of p53. EMBO J. 1995;14(7):1382–1391.
39. Zurli V, Wimmer G, Cattaneo F, et al. Ectopic ILT3 controls BCR-dependent activation of Akt in B-cell chronic lymphocytic leukemia. Blood. 2017;130(18):2006–2017.
40. Robertson LE, Plunkett W, McConnell K, Keating MJ, McDonnell TJ. Bcl-2 expression in chronic lymphocytic leukemia and its correlation with the induction of apoptosis and clinical outcome. Leukemia. 1996;10(3):456–459.
41. Hildeman DA, Mitchell T, Aronow B, Wojciechowski S, Kappler J, Marrack P. Control of Bcl-2 expression by reactive oxygen species. Proc Natl Acad Sci U S A. 2003;100(25):15035–15040.
42. Marra F, Tacke F. Roles for chemokines in liver disease. Gastroenterology. 2014;147(3):577–594.e1.
43. Belchamber KBR, Donnelly LE. Macrophage dysfunction in respiratory disease. Results Probl Cell Differ. 2017;62:299–313.
44. Trentin L, Agostini C, Facco M, et al. The chemokine receptor CXCR3 is expressed on malignant B cells and mediates chemotaxis. J Clin Invest. 1999;104(1):115–121.
45. Ventura A, Luzi L, Pacini S, Baldari CT, Pelicci PG. The p66Shc longevity gene is silenced through epigenetic modifications of an alternative promoter. J Biol Chem. 2002;277(25):22370–22376.
46. Pezzicoli A, Ulivieri C, Capitani N, Ventura A, Pelicci P, Baldari CT. Expression in T-cells of the proapoptotic protein p66SHC is controlled by promoter demethylation. Biochem Biophys Res Commun. 2006;349(1):322–328.
47. Chen S-S, Raval A, Johnson AJ, et al. Epigenetic changes during disease progression in a murine model of human chronic lymphocytic leukemia. Proc Natl Acad Sci U S A. 2009;106(32):13433–13438.
48. Pavlasova G, Borsky M, Seda V, et al. Ibrutinib inhibits CD20 upregulation on CLL B cells mediated by the CXCR4/SDF-1 axis. Blood. 2016;128(12):1609–1613.
49. Seda V, Mraz M. B-cell receptor signalling and its crosstalk with other pathways in normal and malignant cells. Eur J Haematol. 2015;94(3):193–205.
50. Eichhorst B, Fink A-M, Bahlo J, et al. First-line chemoimmunotherapy with bendamustine and rituximab versus fludarabine, cyclophosphamide, and rituximab in patients with advanced chronic lymphocytic leukaemia (CLL10): an international, open-label, randomised, phase 3, non-inferiority trial. Lancet Oncol. 2016;17(7):928–942.

ARTICLE

Olaptesed pegol (NOX-A12) with bendamustine and rituximab: a phase IIa study in patients with relapsed/refractory chronic lymphocytic leukemia

Michael Steurer,[1‡] Marco Montillo,[2] Lydia Scarfò,[3] Francesca R. Mauro,[4] Johannes Andel,[5] Sophie Wildner,[1] Livio Trentin,[6] Ann Janssens,[7] Sonja Burgstaller,[8] Anna Frömming,[9] Thomas Dümmler,[9,10] Kai Riecke,[9] Matthias Baumann,[9,10] Diana Beyer,[9] Stéphanie Vauléon,[9] Paolo Ghia,[3] Robin Foà,[4] Federico Caligaris-Cappio[3] and Marco Gobbi[11]

[1]Division of Hematology and Oncology, Innsbruck Medical University, Innsbruck, Austria; [2]Department of Hematology, Niguarda Cancer Center, Niguarda Hospital, Milan, Italy; [3]Università Vita-Salute San Raffaele and IRCCS Istituto Scientifico San Raffaele, Milan, Italy; [4]Hematology, Department of Cellular Biotechnologies and Hematology, Sapienza University, Rome, Italy; [5]Medical Dept. 2, County Hospital, Steyr, Austria; [6]Department of Medicine, Hematology and Clinical Immunology Branch, University of Padua, Padua, Italy; [7]Department of Hematology, Universitaire Ziekenhuizen Leuven, Leuven, Belgium; [8]Department of Internal Medicine IV, Wels-Grieskirchen Hospital, Wels, Austria; [9]NOXXON Pharma, Berlin, Germany; [10]current affiliation: Mologen AG, Berlin, Germany and [11]Haematology Clinic, Department of Internal Medicine, University of Genoa, and Ospedale Policlinico S. Martino, Clinica Ematologica, Genoa, Italy

Ferrata Storti Foundation

Haematologica 2019
Volume 10410):2053-2060

‡This paper is dedicated to the memory of our colleague Prof. Michael Steurer, an extraordinary scientist and physician appreciated for his empathetic commitment to his patients, who recently passed away.

ABSTRACT

Olaptesed pegol (NOX-A12) is a pegylated structured L-oligoribonucleotide that binds and neutralizes CXCL12, a chemokine tightly regulating the life cycle of chronic lymphocytic leukemia cells. The resulting inhibition of CXCR4 and CXCR7 signaling reduces the protective activity of the bone marrow and lymph node microenvironment. CXCL12 inhibition mobilizes chronic lymphocytic leukemia cells into the circulation and prevents their homing into the protective niches. In this phase I/II study, 28 patients with relapsed/refractory chronic lymphocytic leukemia were treated with olaptesed pegol in combination with bendamustine and rituximab. Combination treatment was preceded by single escalating pilot doses of olaptesed pegol in the first ten patients for evaluation of safety and pharmacokinetics. Peak concentrations and systemic exposure of olaptesed pegol were dose-linear; plasma elimination was monophasic with a 53.2 h half-life. A rapid increase in circulating chronic lymphocytic leukemia cells was observed already 1 h after administration of olaptesed pegol and lasted for at least 72 h. Single-agent treatment was well tolerated and no dose-limiting toxicity was observed. The combination regimen yielded an overall response rate of 86%, with 11% of patients achieving a complete response and 75% a partial response. Notably, all ten high-risk patients, including four with a 17p deletion, responded to treatment. The median progression-free survival was 15.4 (95% confidence interval: 12.2, 26.2) months while the median overall survival was not reached with >80% of patients alive after a median follow-up of 28 months. Olaptesed pegol was well tolerated and did not result in additional toxicity when combined with bendamustine and rituximab (*ClinicalTrials.gov identifier: NCT01486797*). Further clinical development of this novel CXCL12 inhibitor is thus warranted.

Introduction

Olaptesed pegol (NOX-A12) is a novel, pegylated L-oligoribonucleotide, a so-called Spiegelmer®, which binds and neutralizes the chemokine CXCL12 (stromal cell-derived factor-1, SDF-1) with high affinity and specificity. As a result, it inhibits CXCL12 signaling through both of its receptors, CXCR4 and CXCR7.[1,2] In healthy

Correspondence:

MARCO GOBBI
gobbi@unige.it

Received: September 19, 2018.

Accepted: May 9, 2019.

Pre-published: May 16, 2019.

doi:10.3324/haematol.2018.205930

Check the online version for the most updated information on this article, online supplements, and information on authorship & disclosures: www.haematologica.org/content/104/10/2053

volunteers, single doses of olaptesed pegol mobilized white blood cells into peripheral blood; the mobilization was long-lasting and increased dose-dependently to more than 4 days at the highest dose in a phase I study.[1] Further analyzing the mode of action, it could be shown that olaptesed pegol detaches CXCL12 from cell surfaces leading to a disruption of the existing chemokine gradient.[3] CXCL12 facilitates homing and retention as well as trafficking of hematopoietic and immune cells via CXCR4.[4] This feature makes CXCL12 one of the key factors known to support survival of chronic lymphocytic leukemia (CLL) cells in the protective niches of the bone marrow and lymph node microenvironment which is an essential part of the pathogenesis and progression of the disease.[5] The CLL dissemination inside tissue microenvironments is actively coordinated by a crosstalk between leukemic cells and stroma, where CXCL12 not only mediates CLL cell chemotaxis, actin polymerization, and migration beneath and underneath CXCL12-secreting stromal cells but also protects CLL cells from spontaneous and drug-induced apoptosis.[6] Although surface expression of CXCR7 was not observed on CLL cells,[7] CXCR7-dependent angiogenic mononuclear cell trafficking was shown to support bone marrow angiogenesis[8] which plays a pathophysiological role in the leukemic microenvironment.[9] Interference with CXCL12 signaling by olaptesed pegol was shown to inhibit CLL cell chemotaxis and induce chemosensitization *in vitro* using primary CLL cells[3] as well as to remove CLL cells from the nurturing and protective microenvironment, prevent homing and make them more vulnerable to conventional therapy *in vivo* in an Eμ-TCL1 transgenic mouse model.[10] A similar phenomenon was recently demonstrated preclinically and clinically in multiple myeloma, in which olaptesed pegol was combined with bortezomib and dexamethasone.[2,11] In relapsed/refractory CLL patients, disease control becomes increasingly difficult due to increased resistance to therapy. Olaptesed pegol represents a novel paradigm of therapy that moves away from cancer cells to microenvironmental elements as the primary treatment target.

We report here the findings of a phase IIa study, meant to translate the novel concept of combining chemoimmunotherapy and CXCL12 inhibition into the clinic (*Online Supplementary Figure S1* delineates the anticipated mode of action), in which we assessed the pharmacokinetic, pharmacodynamic, safety and first efficacy data of olaptesed pegol in patients with relapsed/refractory CLL. The main objectives of the study were to assess the safety and tolerability of olaptesed pegol alone and in combination with bendamustine and rituximab (BR) in CLL patients, as well as to determine the response rates and remission duration.

Methods

The trial (EudraCT number 2011-004672-11, NCT01486797) was conducted in compliance with the Declaration of Helsinki and the International Conference on Harmonization Good Clinical Practices Guidelines. The clinical study protocol and its amendments, informed consent documents, and any other study-related documents were reviewed and approved by the applicable regional review boards or ethics committees. All authors had access to the primary clinical data.

Patients

Twenty-eight patients with relapsed/refractory CLL were enrolled out of 32 patients screened. Patients were eligible for this study if they were bendamustine-sensitive (having achieved at least a partial response lasting at least 6 months) or bendamustine-naïve. Patients were required to present with a World Health Organization (WHO) Performance Status ≤2 and a modified Cumulative Incidence Rating Scale (CIRS) score <7, to have a serum creatinine level ≤1.5 x the upper limit of normal (ULN) and/or calculated creatinine clearance ≥50 mL/min/1.73 m^2, and appropriate hematologic (platelet count ≥75x10^9/L, absolute neutrophil count >0.75x10^9/L) and liver parameters (bilirubin ≤1.5 x ULN, aspartate transaminase and/or alanine transaminase ≤2.5 x ULN).

Trial design and treatment

Initially, a single dose of olaptesed pegol was administered intravenously to ten patients in the pilot study phase to study safety, pharmacokinetics and pharmacodynamics of olaptesed pegol alone. Subsequently, olaptesed pegol was administered intravenously once per cycle in combination with BR as six cycles of 28 days to all 28 eligible patients including the initial ten pilot patients to study safety and efficacy of this novel combination. Details on drug administration are provided in the *Online Supplementary Information*.

Study assessments

Responses were assessed at the end of cycle 6 according to the 1996 National Cancer Institute-Working Group (NCI-WG) criteria updated in 2008 by the International Workshop on Chronic Lymphocytic Leukemia (IWCLL).[12] Adverse events were continuously monitored until 30 days after the last olaptesed pegol dose and were graded by National Cancer Institute's Common Terminology Criteria for Adverse Events (CTCAE) version 4.03.

Olaptesed pegol concentrations were measured in plasma at the indicated time points by a validated assay for pharmacokinetic analyses (see supplement to Vater *et al.*[1]). The pharmacodynamic activity of olaptesed pegol was studied by five-color flow cytometry analysis using a standard diagnostic panel based on CD5, CD19, CD45, 7-AAD plus beads on peripheral blood samples to study the mobilization of CLL cells. Additionally, CXCR4 expression was assessed on the detected CLL cells. Analyses were performed centrally by MLL GmbH (Munich, Germany). Minimal residual disease was not assessed.

A fluorescence *in situ* hybridization cytogenetics panel was used to investigate CLL cells unless this had been performed within the last 24 weeks prior to screening. Deletions of 11q22-q23, 13q14, 17p13 as well as a marker for trisomy 12 were assessed. IGHV status and *TP53* mutations were not assessed.

Serum for immunogenicity analyses was collected at screening, day -14, before first dosing at cycles 1 and 4 as well as at the final examination and 6 months thereafter. Further details can be found in the *Online Supplementary Information.*

Statistical analyses

Data management and biostatistics were performed by AMS Advanced Medical Services GmbH (Mannheim, Germany). All statistical analyses are descriptive and exploratory. Efficacy parameters were analyzed using SAS version 9.1.3 (SAS Institute Inc, Cary, NC, USA). Actuarial survival curves were estimated according to the Kaplan-Meier method.

Results

Patients' flow and characteristics

Thirty-two patients were screened. Ten patients were enrolled into the pilot group, which included a replacement for a patient withdrawn from the study after cycle 1. Eighteen more patients were enrolled after completion of the pilot group: these 18 patients started directly with combination treatment. Three patients discontinued therapy before completion of three treatment cycles because of chlamydial pneumonia, *E. coli* sepsis and one patient's decision and five more patients discontinued therapy before completion of six treatment cycles because of rash, multiple episodes of infection, start of a new therapy after progressive disease and personal decision by two patients (*Online Supplementary Figure S2*). The median number of olaptesed pegol + BR cycles administered was six (range, 1-6). All 28 enrolled patients constitute the intent-to-treat (ITT) population and all analyses presented further below were performed on the ITT population. One patient withdrew his consent for the study before any disease assessment, thus the remaining 27 patients constitute the full analysis set.

Table 1. Patients' demographics and baseline characteristics (n = 28).

Age (years)		Mean	66
BMI (kg/m^2)		Mean	25
Sex	Male	N (%)	16 (57%)
	Female	N (%)	12 (43%)
Ethnic origin	Caucasian	N (%)	28 (100%)
Disease stage (Binet)	Stage A	N (%)	6 (21%)
	Stage B	N (%)	11 (39%)
	Stage C	N (%)	11 (39%)
WHO Performance Status	0	N (%)	23 (82%)
	1	N (%)	5 (18%)
CIRS Performance Score	0	N (%)	6 (21%)
	1	N (%)	3 (11%)
	2	N (%)	4 (14%)
	3	N (%)	1 (3.6%)
	4	N (%)	4 (14%)
	5	N (%)	5 (18%)
	6	N (%)	5 (18%)
Risk status	High risk*	N (%)	10 (36%)
	Non-high-risk	N (%)	17 (61%)
	Not known	N (%)	1 (3.6%)
Hemoglobin (g / dL)		Mean (± SD)	12.432 (1.890)
Absolute lymphocyte counts (x10^9/L)		Mean (± SD)	47.309 (50.620)
Platelets (x10^9/L)		Mean (± SD)	145.89 (72.426)
Neutrophils (x10^9/L)		Mean (± SD)	4.249 (3.074)
Prior treatment with fludarabine and/or bendamustine		N (%)	23 (82%)
Prior treatment with rituximab		N (%)	19 (68%)
Prior treatment lines		Median (range)	1 (1-3)
Response to previous line of therapy	CR	N (%)	10 (36%)
	PR	N (%)	17 (61%)
	PD	N (%)	-
	n.a.	N (%)	1 (3.6%)

*Defined as having a deletion of 17p13 or who relapsed within less than 24 months after previous fludarabine or bendamustine-containing treatment regimens according to Stilgenbauer & Zenz.[13] BMI: body mass index; WHO: World Health Organization; CIRS: Cumulative Illness Rating Scale; SD: standard deviation.

The patients' demographic details and baseline characteristics are shown in Table 1. The median age was 66 years (range, 41 – 79) and 78% of patients had Binet stage B or C disease. High-risk CLL, defined as having a deletion of 17p13 or relapse within less than 24 months after previous fludarabine- or bendamustine-containing treatment regimens,[13] was found in ten patients (36%), of whom four (14%) presented with a 17p13 deletion (Table 2). Eighty-two percent of the patients had received prior treatment with fludarabine and/or bendamustine and 68% had been previously treated with rituximab. The median number of prior lines of therapy was one (range, 1-3) and the majority of patients (61%) had responded to their last therapy line with a partial response whereas 36% achieved a complete response. Eight patients (29%) presented with a deletion of 11q22-q23 and 13 patients (46%) a deletion of 13q14. Three patients (11%) had trisomy 12 (Table 2).

Pharmacokinetics

In patients enrolled into the pilot phase, peak plasma concentrations of olaptesed pegol increased in an approximately dose-linear way with mean peak levels of 1.76, 3.95 and 7.20 μmol/L at doses of 1, 2 and 4 mg/kg, respectively (Figure 1 and *Online Supplementary Table S1*). The terminal elimination half-life in patients receiving 4 mg/kg olaptesed pegol was 53.2 h, total body clearance was 36.1 mL/h and the volume of distribution at steady state was 2.9 L; similar figures were obtained for patients receiving 1 and 2 mg/kg olaptesed pegol (*Online Supplementary Table S1*). Peak plasma concentrations at cycles 1 and 4, when olaptesed pegol was administered in combination with BR were similar to the values for the agent given as a single dose (*Online Supplementary Table S2*).

Pharmacodynamics

CLL cell mobilization in the pilot group was evident already 1 h after olaptesed pegol treatment with 10,196 CLL cells/μL on average above baseline detected in peripheral blood (mean baseline level: 41,318 CLL cells/μL). A peak of 22,939 CLL cells/μL on average above

Table 2. Detailed cytogenetic abnormalities.

Parameter	Number (%) of patients	
Deletion of 17p13	Abnormal	4 (14%)
	Normal	23 (82%)
	Missing	1 (3.6%)
Deletion of 11q22-q23	Abnormal	8 (29%)
	Normal	19 (68%)
	Missing	1 (3.6%)
Trisomy 12	Abnormal	3 (11%)
	Normal	22 (79%)
	Missing	3 (11%)
Deletion of 13q14	Abnormal	13 (46%)
	Normal	14 (50%)
	Missing	1 (3.6%)
Number of cytogenetic abnormalities	0	6 (21%)
	1	14 (50%)
	2	7 (25%)
	Missing	1 (3.6%)

The fluorescence *in situ* hybridization panel analysis identified 21 (75%) patients with one or more cytogenetic abnormalities. IGHV status and *TP53* mutations were not assessed.

baseline, corresponding to a 200% increase, occurred at 24 h and CLL cell mobilization was effectively maintained for at least 72 h (Figure 2A,B). Simultaneously, CXCR4 expression on CLL cells gradually increased during the intravascular circulation of CLL cells peaking at 24 h (Figure 2C). In cycle 4, mobilization was evaluated in 24 patients and, similarly to the pilot phase, CLL cells were mobilized already 1 h after olaptesed pegol treatment with 187 CLL cells/μL above baseline (mean baseline level: 224 CLL cells/μL). Mobilized CLL cell numbers gradually increased, peaking at 24 h with 679 CLL cells/μL on average above baseline, corresponding to a >300% increase (Figure 2D,E) accompanied by a steady CXCR4 increase on CLL cells (Figure 2F).

Safety

Olaptesed pegol was safe and well tolerated as monotherapy with no serious adverse events reported in the pilot phase. All patients were escalated to the highest anticipated dose of 4 mg/kg olaptesed pegol, which was previously established in healthy volunteers as safe and efficacious in terms of lymphocyte mobilization.[1] Common adverse events (≥10%) observed in the trial are shown in Table 3. The most frequent adverse event observed on BR alone is neutropenia with grade 3/4 events recorded in up to 50% of the patients.[14-17] The triple regimen of olaptesed pegol in combination with BR does not seem to increase the incidence of grade 3/4 neutropenia, with a 50% incidence reported in this study. The incidences of grade 3/4 anemia and thrombocytopenia were low (14.3% each). There were very few non-hematologic grade 3/4 toxicities and these were mostly reported by single patients (nausea 3.6%, constipation 3.6%, abdominal pain 3.6%, pyrexia 3.6%, fatigue 3.6%, hyperuricemia 7.1% and cytokine release

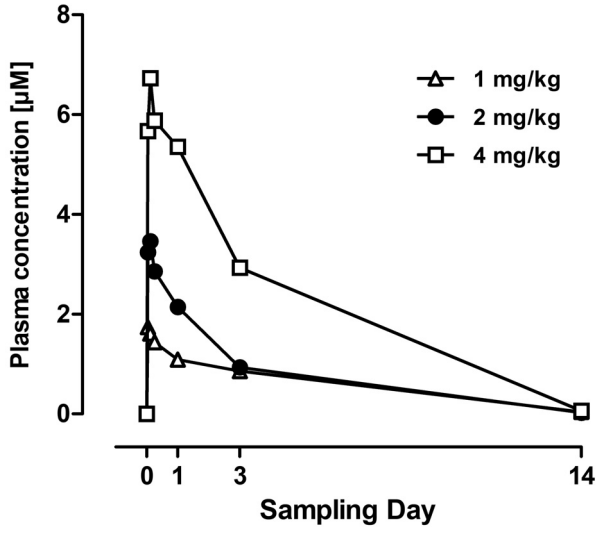

Figure 1. Plasma concentration-time curves of olaptesed pegol after administration of single intravenous doses (pilot phase, monotherapy). Data are shown as geometric means.

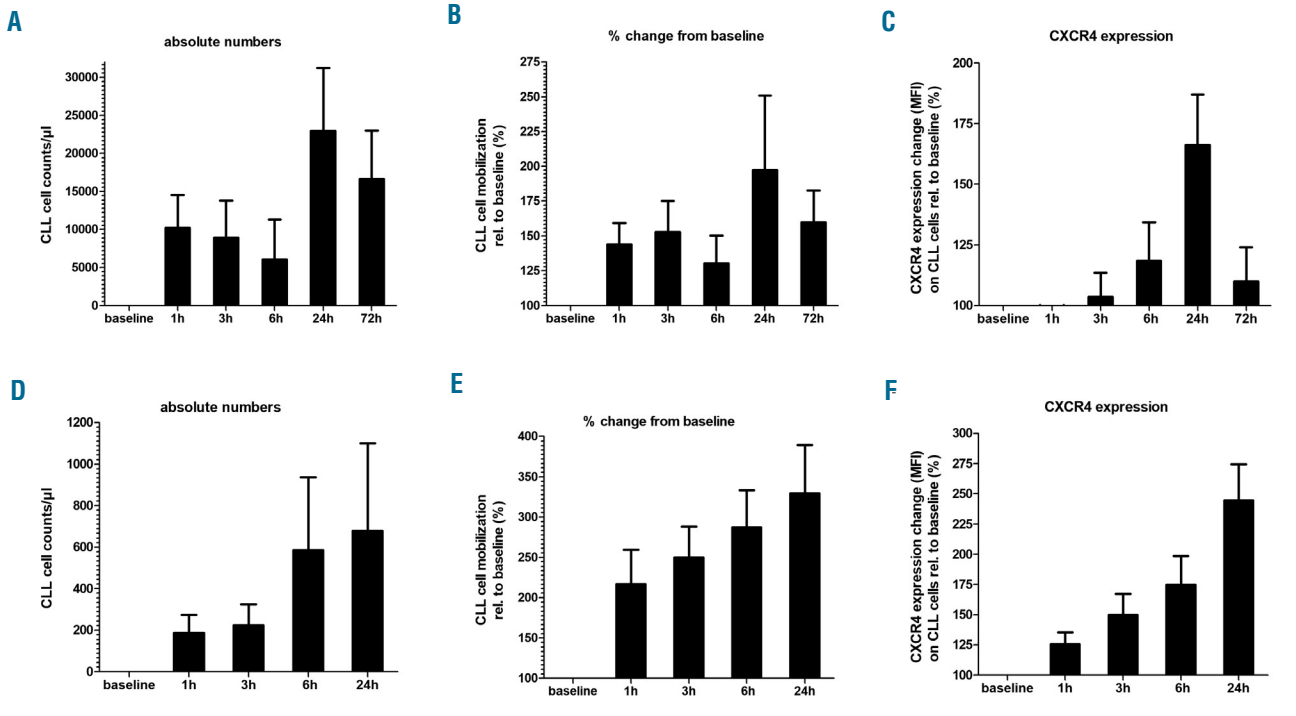

Figure 2. Mobilization kinetics of chronic lymphocytic leukemia cells and their CXCR4 expression levels after administration of olaptesed pegol. (A) Baseline values were set to 0 and chronic lymphocytic leukemia (CLL) cell counts above baseline are depicted as mean and standard error of mean (SEM) after administration of olaptesed pegol alone to ten patients in the pilot phase. (B) Baseline values were set to 100% and CLL cell mobilization above baseline is depicted in percent after administration of olaptesed pegol alone to ten patients in the pilot phase. (C) Mean fluorescence intensity (MFI) of CXCR4 expression on CLL cells was set to 100% at baseline and changes in MFI are depicted in percent for ten patients in the pilot group. (D) Baseline values were set to 0 and CLL cell counts above baseline are depicted as mean and SEM after administration of olaptesed pegol in combination with bendamustine and rituximab (BR) for 24 patients in cycle 4. (E) Baseline values were set to 100% and CLL cell mobilization above baseline is depicted in percent after administration of olaptesed pegol in combination with BR for 24 patients in cycle 4. (F) MFI of CXCR4 expression on CLL cells was set to 100% at baseline and changes in MFI are depicted in percent (whisker plots for 24 patients in cycle 4.

syndrome 3.6%). Grade 3/4 infections occurring during treatment were reported by single patients only (pneumonia 3.6%, cystitis 3.6%, infection 3.6%, lung infection 3.6%, chlamydial pneumonia 3.6% and sinusitis 3.6%) (*Online Supplementary Figure S3*). Of note, two (7.1%) patients experienced tumor lysis syndrome during the first treatment cycle, one laboratory (grade 1) and one clinical (grade 3) (*Online Supplementary Figure S3*).

Treatment response and survival

The overall response rate (ORR) defined as partial response or better, was assessed at the end of cycle 6. The ORR was 86% (24/28) in the ITT patient population, in which 75% (21/28) of the patients achieved a partial response and 10.7% (3/28) a complete response (Table 4). Similar response rates were observed in the full analysis set (ORR 89%; 24/27) and per-protocol population (ORR 91%; 19/21) (*Online Supplementary Table T3*). Notably, all ten patients who had a high-risk status responded to the treatment with a partial response (Table 4). Patients who had received two or more previous treatment lines had an ORR of 82% (9/11) and patients who had been pre-treated with fludarabine or bendamustine had an ORR of 83% (19/23) (Table 4). After an increase of lymphocytosis in the pilot group during olaptesed pegol monotherapy, a rapid reduction of lymphocytosis in peripheral blood, with normalization by treatment cycle 2 – 3, was observed (Figure 3A). The reduction of circulating CLL cells during the first treatment cycles also became evident by the significant improvement of the CLL to leukocyte ratio from cycle 1 to cycle 4 in the majority of the patients (Figure 3B). At screening, 24 out of 28 patients reported enlarged lymph nodes. A reduction of lymph node size by ≥50% at the end of treatment was achieved in 18 out of these 24 patients (Figure 3C). Hematologic parameters such as hemoglobin concentration and platelet count improved after an initial expected drop; neutrophil values stabilized throughout the treatment course (*Online Supplementary Figure S4*). After a median follow-up of 28 months, the median progression-free survival was 15.4 (95% confidence interval: 12.2, 26.2) months (Figure 4A) while the median overall survival was not reached: the 3-year survival rate was > 80% (Figure 4B) in the ITT population.

Table 3. Common adverse events (incidence ≥10%) observed in the trial.

Adverse event	Grade 1	Grade 2	Grade 3	Grade 4
Hematologic toxicity				
Neutropenia		10.7	32.1	17.9
Anemia		7.1	14.3	
Thrombocytopenia	3.6		7.1	7.1
Febrile neutropenia		3.6	7.1	
Leukopenia		10.7		
Non-hematologic toxicity				
Nausea	21.4	14.3	3.6	
Constipation	17.9	3.6	3.6	
Diarrhea	14.3	10.7		
Vomiting	10.7	7.1		
Abdominal pain upper	7.1		3.6	
Pyrexia	17.9	14.3	3.6	
Fatigue	10.7		3.6	
Asthenia	14.3			
Chills	10.7	3.6		
General physical health deterioration	7.1	3.6		
Mucosal inflammation	10.7			
Edema peripheral	7.1	3.6		
Hypokalemia	14.3	7.1		
Hyperuricemia	7.1		7.1	
Cough	10.7	7.1		
Pleural effusion		10.7		
Rash	3.6	7.1		
Cytokine release syndrome		10.7	3.6	

Discussion

The survival of CLL cells depends on periodic CXCL12-mediated migration into the bone marrow and other lymphoid tissue in order to establish an interactive network of cellular contacts within the microenvironment.[18] This interaction represents a novel and vulnerable therapeutic target which can be utilized in combination therapies.[19] The here-presented phase IIa study was meant to investigate the concept of simultaneously targeting CLL and its microenvironment. The study builds on the preclinical proof-of-concept regarding the significance of CXCL12 blockade in CLL[3,10] and on clinical phase I data in healthy subjects[1] as well as phase II data relating to targeting the multiple myeloma microenvironment.[11]

The pharmacokinetic data of olaptesed pegol observed in this study were very similar to those from healthy subjects and patients with multiple myeloma studied previously with regard to peak concentrations and terminal elimination half-life.[1,11] This indicates that the uptake, dis-

Table 4. Response rates in the intention-to-treat population (n=28) including subgroups.

	ITT	High risk#			Prior treatment lines		Fludarabine OR bendamustine pre-treatment	
*		yes	no	missing	1	2 or more	pre-treated	naïve
N (%)	28 (100%)	10 (36%)	17 (61%)	1 (3.6%)	17 (61%)	11 (39%)	23 (82%)	5 (18%)
CR	3 (10.7%)	0	3 (17.6%)	0	3 (17.6%)	0 (0%)	1 (4.3%)	2 (40%)
PR	21 (75%)	10 (100%)	11 (64.7%)	0	12 (70.6%)	9 (81.8%)	18 (78.3%)	3 (60%)
PD	3 (10.7%)	0	2 (11.8%)	1 (100%)	2 (11.8%)	1 (9.1%)	3 (13%)	0
NE	1 (3.6%)	0	1 (5.9%)	0	0	1 (9.1%)	1 (4.3%)	0
ORR	86%	100%	82%	0%	88%	82%	83%	100%

defined as having a deletion of 17p13 or who relapsed within less than 24 months after previous fludarabine or bendamustine-containing treatment regimens according to Stilgenbauer & Zenz.[13] *Response percentages are calculated based on the number of patients in the respective subgroup. CR: complete remission; PR: partial response; PD: progressive disease; NE: not evaluable; ORR: overall response rate (≥PR); ITT: intention-to-treat.

tribution and metabolism of olaptesed pegol were independent from disease and combination partner. Rapid increases in CLL cell numbers were observed, with a peak at 24 h, which were maintained for at least 72h. Interestingly, CXCR4 expression on CLL cells gradually increased during the intravascular circulation of CLL cells, also peaking at 24 h. The mobilization efficiency was maintained throughout the cycles with an up to 3-fold increase in CLL cell numbers above mean baseline level in cycle 4. The observed CXCR4 increase that accompanied mobilization reflects the extended circulation of CLL cells in the periphery as described by Calissano *et al.*[5] and represents a pharmacodynamic biomarker for the sustained blockade of CXCL12 by olaptesed pegol. Of note, continuous circulation of CLL cells ultimately leads to apoptosis, a phenomenon also called 'death by neglect'[20] due to the fact that CLL cells need to regularly receive their survival signals from the protective niches.[5]

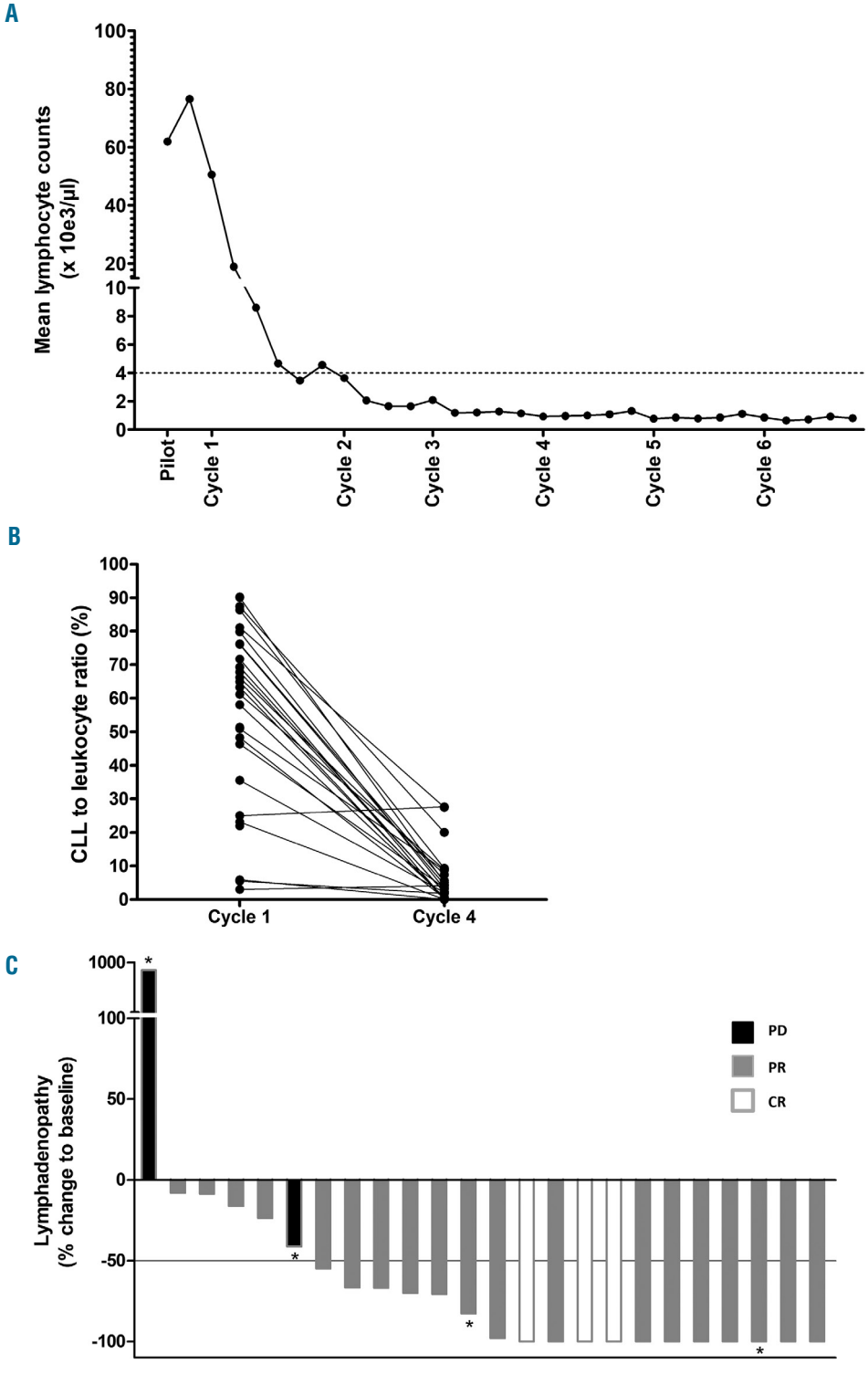

Figure 3. Mean lymphocyte counts, chronic lymphocytic leukemia to leukocyte ratio in cycle 1 *versus* cycle 4 and lymphadenopathy evaluation. (A) Mean lymphocyte counts (x 10^3/µL peripheral blood) evaluated at different time points during the pilot phase for ten patients (Pilot) and cycle 1 to cycle 6 for all 28 patients are depicted. (B) The chronic lymphocytic leukemia (CLL) cell to leukocyte ratio evaluated at cycle 1 and cycle 4 is depicted for each individual patient. (C) Lymphadenopathy at the end of treatment was assessed in 24 patients who presented with enlarged lymph nodes at screening. *For patients who discontinued treatment before cycle 6 the value at the end of cycle 3 is depicted. PD: progressive disease; PR: partial response; CR: complete response.

The triple regimen of olaptesed pegol in combination with BR was generally well tolerated with neutropenia recorded as the most frequent adverse event. The incidences of grade 3/4 anemia and thrombocytopenia were low. Non-hematologic toxicities, mostly nausea and pyrexia followed by mild diarrhea and constipation, were generally manageable. Altogether, the reported frequency and severity of adverse events were to be expected in a population of relapsed/refractory CLL patients during standard BR therapy.[14-17] Therefore, it does not appear that treatment with olaptesed pegol results in significant additional toxicities on top of BR.

Treatment with olaptesed pegol in combination with BR resulted in an ORR of 86% with 11% of patients achieving a complete response. Acknowledging the limitations of cross-trial comparisons due to different inclusion criteria of patients as well as the limited sample size of 28 patients in this study, the ORR of 86% compares favorably with responses to BR alone reported earlier with ORR ranging from 45-72%.[14-17] Although limited by the low numbers of patients, subgroup analyses showed that all ten high-risk patients, including four with a 17p deletion, achieved a partial response with the combination of olaptesed pegol and BR, even though 17p-deleted patients have been reported to respond poorly to BR alone.[15,17]

Other combinations with BR in relapsed/refractory CLL patients resulted in ORR of 84% for cytarabine + BR,[21] 82.7% for the BTK inhibitor ibrutinib + BR,[14] 70% for the PI3K inhibitor idelalisib + BR,[17] 67% for fludarabine + BR,[22] and 47% for lenalidomide + BR.[23] Of note, higher toxicity rates were reported for the addition of kinase inhibitors to BR regarding neutropenia, diarrhea and pneumonia[14,17] and very high incidences of grade 3/4 neutropenia and thrombocytopenia were reported if another chemotherapeutic drug was combined with BR.[21,22]

The median progression-free survival of 15.4 months in the ITT population is in the range of what is expected after BR treatment alone (11.1, 13.3, 14.7, and 17 months).[14-17] Seymour *et al.* reported a progression-free survival of 16.6 months for patients treated with BR only after one prior therapy line, which is slightly longer than the progression-free survival of 15.4 months in our study; however only 12.9% of the patients in the MURANO study had Rai stage III-IV CLL whereas 39% of patients in our study had Binet stage C disease.[16] Comparable progression-free survival values were achieved by the addition of another chemotherapy to BR such as fludarabine + BR or cytarabine + BR (19 and 16 months, respectively),[21,22] however much better progression-free survival results were reported for the combination of kinase inhibitors and BR (20.8 months for idelalisib[17] and not reached for ibrutinib[14]) . Notably, kinase inhibitors strongly interfere with CXCR4 downstream signaling and the resulting CLL cell displacement from their supportive microenvironment, followed by leukemia cell death due to 'death by neglect', is a central mechanism of action of kinase inhibitors.[20] In contrast to olaptesed pegol which was given once per 28-day cycle, however, the kinase inhibitors were administered daily or twice daily. Thus, the authors suggest studying whether longer progression-free survival could be achieved if olaptesed pegol were to be administered more often to fully exploit the 'death by neglect' mechanism indicated by the transient CXCR4-increase on peripheral CLL cells following olaptesed pegol treatment. Furthermore, kinase inhibitor treatment was sustained after completion of six BR cycles and could, therefore, further prolong the time to progression, whereas olaptesed pegol treatment was stopped after six BR-combination cycles. The median overall survival was not reached, resulting in a 3-year survival rate of >80% in the ITT population which compares favorably with other effective BR combinations (60% - 75%).[17,21,22]

A recent combination therapy utilizing bendamustine for initial debulking followed by obinutuzumab and venetoclax resulted in an ORR of 90% in a subgroup of 29 relapsed/refractory CLL patients.[24] A comparable ORR of 92% was achieved in 12 relapsed/refractory CLL patients when chemotherapy was omitted and obinutuzumab, ibrutinib and venetoclax were administered sequentially.[25] Another chemotherapy-free combination of rituximab and venetoclax produced an ORR of 92.3% in 194 relapsed/refractory CLL patients.[16] Interestingly, olaptesed pegol was reported to synergize with anti-CD20 antibodies such as rituximab or obinutuzumab by enhancing immune cell infiltration and antibody-dependent cellular

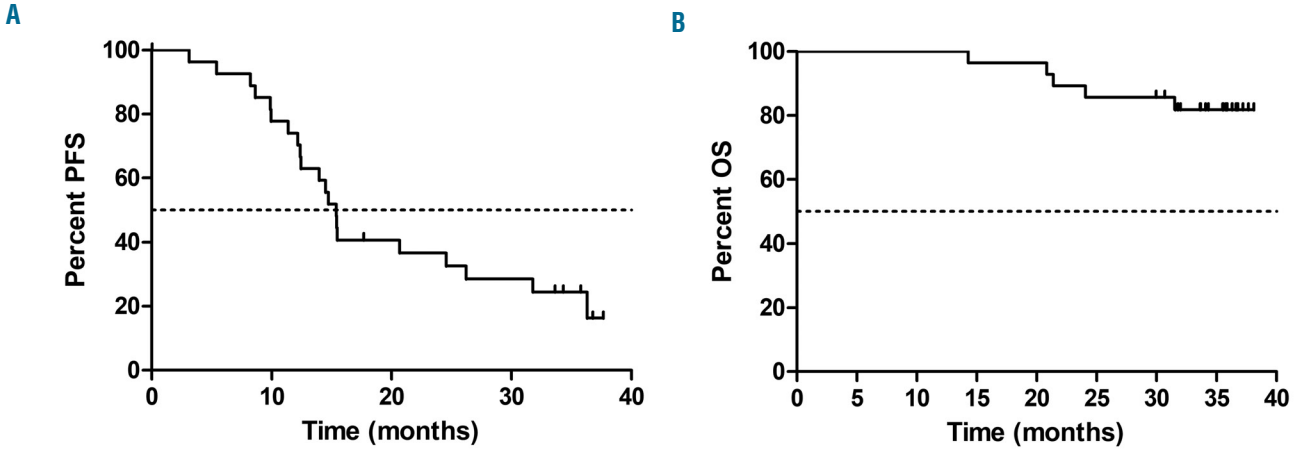

Figure 4. Progression-free survival and overall survival of patients. Kaplan-Meier analyses of (A) progression-free survival and (B) overall survival in the intent-to-treat population (n=28) are depicted. PFS: progression-free survival; OS: overall survival.

cytotoxicity.[26] Thus, combination therapies including anti-CD20 antibodies and novel agents, such as venetoclax together with olaptesed pegol, could be a viable option based on their complementary mechanisms of action in future clinical trials.

In conclusion, the data from our study demonstrate that treatment with olaptesed pegol results in the intended pharmacodynamic effect by effectively mobilizing CLL cells. The high response rate of 86% as well as 3-year overall survival rate of >80% compare favorably with those achieved by BR alone and in recent BR combination trials. These data together with the benign safety profile warrant further clinical development of this novel CXCL12 inhibitor in combination with targeted anti-CLL drugs in randomized studies.

Acknowledgments

The authors thank the patients who participated in the trial, the clinical staff and the Arbeitsgemeinschaft medikamentöse Tumortherapie (AGMT) for supporting the study in Austria.

References

1. Vater A, Sahlmann J, Kroger N, et al. Hematopoietic stem and progenitor cell mobilization in mice and humans by a first-in-class mirror-image oligonucleotide inhibitor of CXCL12. Clin Pharmacol Ther. 2013;94(1):150-157.
2. Roccaro AM, Sacco A, Purschke WG, et al. SDF-1 inhibition targets the bone marrow niche for cancer therapy. Cell Rep. 2014;9(1):118-128.
3. Hoellenriegel J, Zboralski D, Maasch C, et al. The Spiegelmer NOX-A12, a novel CXCL12 inhibitor, interferes with chronic lymphocytic leukemia cell motility and causes chemosensitization. Blood. 2014;123(7):1032-1039.
4. Scheiermann C, Kunisaki Y, Frenette PS. Circadian control of the immune system. Nat Rev Immunol. 2013;13(3):190-198.
5. Calissano C, Damle RN, Marsilio S, et al. Intraclonal complexity in chronic lymphocytic leukemia: fractions enriched in recently born/divided and older/quiescent cells. Mol Med. 2011;17(11-12):1374-1382.
6. Marasca R, Maffei R. NOX-A12: mobilizing CLL away from home. Blood. 2014;123(7):952-953.
7. O'Hayre M, Salanga CL, Kipps TJ, Messmer D, Dorrestein PC, Handel TM. Elucidating the CXCL12/CXCR4 signaling network in chronic lymphocytic leukemia through phosphoproteomics analysis. PLoS One. 2010;5(7):e11716.
8. Azab AK, Sahin I, Moschetta M, et al. CXCR7-dependent angiogenic mononuclear cell trafficking regulates tumor progression in multiple myeloma. Blood. 2014;124(12):1905-1914.
9. Li WW, Hutnik M, Gehr G. Antiangiogenesis in haematological malignancies. Br J Haematol. 2008;143(5):622-631.
10. Hinterseer E, Girbl T, Hutterer E, et al. The spiegelmer Nox-A12 abrogates homing of human CLL cells to bone marrow and mobilizes murine CLL cells in the Eμ-TCL1 transgenic mouse model Of CLL. Blood. 2013;122(21):4111-4111.
11. Ludwig H, Weisel K, Petrucci MT, et al. Olaptesed pegol, an anti-CXCL12/SDF-1 Spiegelmer, alone and with bortezomib-dexamethasone in relapsed/refractory multiple myeloma: a phase IIa study. Leukemia. 2017;31(4):997-1000.
12. Hallek M, Cheson BD, Catovsky D, et al. Guidelines for the diagnosis and treatment of chronic lymphocytic leukemia: a report from the International Workshop on Chronic Lymphocytic Leukemia updating the National Cancer Institute-Working Group 1996 guidelines. Blood. 2008;111(12):5446-5456.
13. Stilgenbauer S, Zenz T. Understanding and managing ultra high-risk chronic lymphocytic leukemia. Hematology Am Soc Hematol Educ Program. 2010;2010:481-488.
14. Chanan-Khan A, Cramer P, Demirkan F, et al. Ibrutinib combined with bendamustine and rituximab compared with placebo, bendamustine, and rituximab for previously treated chronic lymphocytic leukaemia or small lymphocytic lymphoma (HELIOS): a randomised, double-blind, phase 3 study. Lancet Oncol. 2016;17(2):200-211.
15. Fischer K, Cramer P, Busch R, et al. Bendamustine combined with rituximab in patients with relapsed and/or refractory chronic lymphocytic leukemia: a multicenter phase II trial of the German Chronic Lymphocytic Leukemia Study Group. J Clin Oncol. 2011;29(26):3559-3566.
16. Seymour JF, Kipps TJ, Eichhorst B, et al. Venetoclax-rituximab in relapsed or refractory chronic lymphocytic leukemia. N Engl J Med. 2018;378(12): 1107-1120.
17. Zelenetz AD, Barrientos JC, Brown JR, et al. Idelalisib or placebo in combination with bendamustine and rituximab in patients with relapsed or refractory chronic lymphocytic leukaemia: interim results from a phase 3, randomised, double-blind, placebo-controlled trial. Lancet Oncol. 2017;18(3):297-311.
18. Burger JA. The CLL cell microenvironment. Adv Exp Med Biol. 2013;792:25-45.
19. ten Hacken E, Burger JA. Microenvironment dependency in chronic lymphocytic leukemia: the basis for new targeted therapies. Pharmacol Ther. 2014;144(3):338-348.
20. Burger JA, Montserrat E. Coming full circle: 70 years of chronic lymphocytic leukemia cell redistribution, from glucocorticoids to inhibitors of B-cell receptor signaling. Blood. 2013;121(9):1501-1509.
21. Visco C, Finotto S, Pomponi F, et al. The combination of rituximab, bendamustine, and cytarabine for heavily pretreated relapsed/refractory cytogenetically high-risk patients with chronic lymphocytic leukemia. Am J Hematol. 2013;88(4):289-293.
22. Jain N, Balakrishnan K, Ferrajoli A, et al. A phase I-II trial of fludarabine, bendamustine and rituximab (FBR) in previously treated patients with CLL. Oncotarget. 2017;8(13):22104-22112.
23. Maurer C, Pflug N, Bahlo J, et al. Bendamustine and rituximab in combination with lenalidomide in patients with chronic lymphocytic leukemia. Eur J Haematol. 2016;97(3):253-260.
24. Cramer P, von Tresckow J, Bahlo J, et al. Bendamustine followed by obinutuzumab and venetoclax in chronic lymphocytic leukaemia (CLL2-BAG): primary endpoint analysis of a multicentre, open-label, phase 2 trial. Lancet Oncol. 2018;19(9):1215-1228.
25. Rogers KA, Huang Y, Ruppert AS, et al. Phase 1b study of obinutuzumab, ibrutinib, and venetoclax in relapsed and refractory chronic lymphocytic leukemia. Blood. 2018;132(15):1568-1572.
26. Zboralski D, Kruschinski A, Vater A. CXCL12 inhibition by Nox-A12 (olaptesed pegol) synergizes with the ADCC activity of CD20 antibodies by increasing NK cell infiltration in a 3D lymphoma model. Blood. 2016;128(22): 3021-3021.

ARTICLE

Histone deacetylase inhibition in combination with MEK or BCL-2 inhibition in multiple myeloma

Vijay G. Ramakrishnan,[1]* Kevin C. Miller,[2]* Elaine P. Macon,[1] Teresa K. Kimlinger,[1] Jessica Haug,[1] Sanjay Kumar,[1] Wilson I. Gonsalves,[1] S. Vincent Rajkumar[1] and Shaji K. Kumar[1]

[1]Division of Hematology, Department of Medicine, Mayo Clinic, Rochester, MN and [2]Mayo Clinic School of Medicine, Rochester, MN, USA

**VGR and KCM contributed equally to this work.*

Haematologica 2019
Volume 104(10):2061-2074

ABSTRACT

Despite recent advances in the treatment of multiple myeloma, patients with this disease still inevitably relapse and become refractory to existing therapies. Mutations in *K-RAS, N-RAS* and *B-RAF* are common in multiple myeloma, affecting 50% of patients at diagnosis and >70% at relapse. However, targeting mutated *RAS/RAF* via MEK inhibition is merely cytostatic in myeloma and largely ineffective in the clinic. We examined mechanisms mediating this resistance and identified histone deacetylase inhibitors as potent synergistic partners. Combining the MEK inhibitor AZD6244 (selumetinib) with the pan-histone deacetylase inhibitor LBH589 (panobinostat) induced synergistic apoptosis in *RAS/RAF* mutated multiple myeloma cell lines. Interestingly, this synergy was dependent on the pro-apoptotic protein BIM. We determined that while single-agent MEK inhibition increased BIM levels, the protein remained sequestered by anti-apoptotic BCL-2 family members. LBH589 dissociated BIM from MCL-1 and BCL-X_L, which allowed it to bind BAX/BAK and thereby initiate apoptosis. The AZD6244/LBH589 combination was specifically active in cell lines with more BIM:MCL-1 complexes at baseline; resistant cell lines had more BIM:BCL-2 complexes. Those resistant cell lines were synergistically killed by combining the BH3 mimetic ABT-199 (venetoclax) with LBH589. Using more specific histone deacetylase inhibitors, i.e. MS275 (entinostat) and FK228 (romidepsin), and genetic methods, we determined that concomitant inhibition of histone deacetylases 1 and 2 was sufficient to synergize with either MEK or BCL-2 inhibition. Furthermore, these drug combinations effectively killed plasma cells from myeloma patients *ex vivo*. Given the preponderance of *RAS/RAF* mutations, and the fact that ABT-199 has demonstrated clinical efficacy in relapsed/refractory multiple myeloma, these drug combinations hold promise as biomarker-driven therapies.

Introduction

Multiple myeloma (MM) is a cancer of differentiated plasma cells.[1] It evolves from a premalignant condition called monoclonal gammopathy of undetermined significance, which affects 5.3% of adults over the age of 70.[2] More than 30,000 people are projected to be diagnosed with MM in the USA in 2018.[3] Despite improvements in survival, MM remains incurable.[1,4] In addition, it is a clinically heterogeneous disease, with several major cytogenetic abnormalities that affect prognosis.[5,6] Nevertheless, most patients receive uniform up-front treatment.[1,6] Clearly, there is an unmet need for therapies that target particular drivers of the disease.

The RAS/RAF/MEK/ERK pathway is abnormally activated in MM through several mechanisms including oncogenic mutations and cytokines in the bone marrow microenvironment.[7,8] Activating mutations in *K-RAS, N-RAS* and *B-RAF* have been reported in 50% of MM patients at diagnosis.[7,9] Such mutations are present in <10% of patients with monoclonal gammopathy of undetermined significance,

Parts of this manuscript were presented in abstract form at the American Association for Cancer Research (AACR) Annual Meeting on April 17, 2018 in Chicago, IL, USA.

Correspondence:

VIJAY G. RAMAKRISHNAN
ramakrishnan.vijay@mayo.edu

Received: November 16, 2018.
Accepted: March 5, 2019.
Pre-published: March 7, 2019.

doi:10.3324/haematol.2018.211110

Check the online version for the most updated information on this article, online supplements, and information on authorship & disclosures: www.haematologica.org/content/104/10/2061

suggesting a role in disease progression.[7,10] Furthermore, >70% of patients have *RAS/RAF* mutations present at relapse.[11] It follows that directly targeting RAS/RAF/MEK/ERK in MM could be a promising strategy. However, MEK inhibition is merely cytostatic in MM *in vitro*.[12] Furthermore, a clinical trial evaluating MEK inhibitor monotherapy in MM showed limited efficacy.[13] Thus, it appears that for MEK inhibitors to be relevant in MM, they must be combined with other agents.

Recently, histone deacetylase (HDAC) inhibitors have shown significant activity in numerous tumor types, both *in vitro* and in the clinic.[14] In fact, the pan-HDAC inhibitor LBH589 (panobinostat) was recently approved for treating relapsed/refractory MM patients in combination with bortezomib.[15] As chemotherapeutic agents, HDAC inhibitors have been shown to inhibit cell survival and proliferation and enhance immune-mediated cytotoxicity.[14,15]

We hypothesized that LBH589 could induce enhanced apoptosis when combined with MEK inhibition in MM. Our hypothesis stemmed from two considerations: (i) MEK inhibitors induce apoptosis in several other *RAS/RAF* mutated cancers,[16,17] suggesting MM-specific resistance factors, and (ii) HDAC inhibitors kill MM cells through several known mechanisms, including modulation of the pro- and anti-apoptotic BCL-2 family members, which often mediate chemoresistance.[15,18-20]

In the present study, we show that MEK inhibition with AZD6244 (selumetinib), when combined with LBH589, synergistically drives intrinsic apoptotic cell death in MCL-1 "primed" *RAS/RAF* mutated MM cell lines. Mechanistically, MEK inhibition increases BIM levels; LBH589 acts as a *de facto* MCL-1 and BCL-X_L inhibitor, dissociating BIM:MCL-1 and BIM:BCL-X_L complexes. In contrast, we demonstrate that LBH589 synergizes with the BH3 mimetic ABT-199 (venetoclax) in BCL-2 "primed" cell lines, which are resistant to the AZD6244/LBH589 combination. Finally, we show that concomitant inhibition of HDAC1 and HDAC2 is sufficient to synergize with either MEK or BCL-2 inhibition in the same distinct MM cell lines.

Given that refractoriness to whole classes of drugs (e.g. proteasome inhibitors) is the final common endpoint for nearly all patients with MM,[21] the agents in this study are felicitous because they work via alternative mechanisms of action, are already approved or in clinical development, and offer the tantalizing prospect of targeted therapy guided by *RAS/RAF* mutational status and MCL-1/BCL-2 functional dependence.

Methods

Ethics

This study was approved by the Mayo Clinic Institutional Review Board. Patients' cells were collected after informed consent, in adherence to the Declaration of Helsinki.

Multiple myeloma cell lines and patients' cells

DOX40, H929, KMS11, KMS18, KMS28BM, MM1S, MM1R, OPM1, OPM2, RPMI8226 and U266 were obtained (see *Online Supplementary Methods*).[19,22] Briefly, all cell lines were cultured in RPMI 1640 medium (Mediatech Inc., Manassas, VA, USA) containing 10% fetal bovine serum (Mediatech, Inc.). Freshly obtained bone marrow aspirates from MM patients were collected after informed consent, then $CD138^+$ or bone marrow stromal cells were sorted and cultured as previously described.[19,22]

Reagents

ABT-199 was generously provided by Abbvie (Chicago, IL, USA). AZD6244, MEK162, SCH772984, SAHA, LBH589, MS275 and FK228 were purchased from Selleckchem (Houston, TX, USA). Tubacin was purchased from Sigma-Aldrich (St. Louis, MO, USA). Stock solutions were made in dimethylsulfoxide, aliquoted and stored at –20°C.

MTT, proliferation, and apoptosis assays

Cellular viability was measured using 3-(4, 5-dimethylthiazol-2-yl)-2, 5-diphenyl tetrasodium bromide (MTT) (Chemicon International Inc., Temecula, CA, USA) colorimetric assays at the indicated time points. Proliferation arrest assays were completed using ^{3}H-thymidine uptake as previously described.[23] Apoptosis of patients' cells was assayed using annexin/propidium iodide (PI) as previously described.[22,23] Briefly, cells were washed twice with annexin binding buffer (ABB: 10 mM HEPES pH 7.4, 140 mM NaCl, 2.5 mM $CaCl_2$) and then 100 μL cells (10^7/mL) were stained for 15 min at room temperature with 3 μL of annexin V-FITC (Caltag, Burlingame, CA, USA), then washed with ABB and re-suspended in 500 μL of ABB with 5 μL of 1 mg/mL PI (Sigma-Aldrich, St. Louis, MO, USA). The samples were then run on a Canto flow cytometer (BD Biosciences, San Jose, CA). All experiments with MM cell lines were performed in triplicate.

Western blotting

MM cell lines were lysed with NP40 buffer, 1 mM phenylmethyl-sulfonyl-fluoride (PMSF), protease inhibitor cocktail (PIC), and 1 mM HALT Phosphatase Inhibitor (Thermo Fisher Scientific, Rockford, IL, USA). Protein concentrations were measured using the BCA assay (Thermo Fisher). First, 20-25 μg were loaded on 4-20% Tris-Glycine gels and transferred onto polyvinylidene difluoride membranes (Bio-Rad, Hercules, CA , USA). Antibodies for acetylated histone 3, BAK, BAX, BCL-2, BCL-X_L, BIM, caspase 8, caspase 9, ERK, GAPDH, HDAC1, HDAC2, HDAC6, MCL-1, PARP, p-BCL-2 (S70), pERK, p-MCL-1 (S64), and p-MCL-1 (T163) were purchased from Cell Signaling Technology (Danvers, MA, USA) and used for probing as previously described.[19,22] All western blot experiments were performed in triplicate with a representative blot shown.

Immunoprecipitation

Proteins (100-150 μg) were incubated in a total volume of 500 μL of NP40 buffer, 1 mM PMSF, 1 mM PIC, 1 mM HALT Phosphatase Inhibitor (Thermo Fisher Scientific), and a 1:100 dilution of the following primary antibodies for 4 h: BAX 6A7 (Santa Cruz Biotechnology, Santa Cruz, CA, USA), BAX (Millipore Sigma, Burlington, MA, USA), and BCL-2, BCL-X_L, BIM and MCL-1 (Cell Signaling Technology). Samples were then incubated with ChIP-Grade Protein G Magnetic Beads (Cell Signaling Technology) for 12 h, washed five times, boiled in 2x Laemmli Sample Buffer dye (Bio-Rad) at 100 °C for 5 min, then loaded on 4-20% Tris-Glycine gels (Bio-Rad) and probed as described above. All experiments were performed in triplicate with a representative blot shown.

Short interfering RNA transfection

Short interfering (si)RNA for BIM, BAX, BAK, HDAC1, HDAC2 and HDAC6 were purchased from Thermo Fisher Scientific. ERK1 and ERK2 siRNA were purchased from Santa Cruz Biotechnology. siRNA were electroporated into MM cell lines using the Lonza nucleofector kit V (Lonza, Basel, Switzerland). The manufacturer's G-15 program was used for KMS18 and OPM2; O-23 was used for MM1S and KMS28. All experiments were performed in triplicate.

Isobologram analysis

The effects of combination treatments in MM cells were analyzed using the CalcuSyn™ software program (Biosoft, Ferguson, MO, USA), which is based on the Chou-Talalay method, as previously described.[19,24]

Results

Single-agent MEK inhibition does not induce cell death in multiple myeloma cell lines

Prior studies have documented the lack of induction of cytotoxicity by single-agent MEK inhibitors in MM.[12] We aimed to confirm these findings using a panel of MM cell lines that are wild-type or mutated for *RAS/RAF*. We treated cell lines with increasing doses of the MEK inhibitor AZD6244 (selumetinib) and observed a lack of significant cytotoxicity, with IC_{50} not reached at doses up to 1500 nM (*Online Supplementary Figure 1A*). AZD6244 was slightly more capable at inducing proliferation arrest in the same panel of cell lines, but still largely ineffective (*Online Supplementary Figure 1B*). These results were also confirmed by performing annexin/PI staining after treating two *RAS* mutant MM cell lines with 5000 nM of AZD6244, which is far above the concentrations at which the kinase activity of MEK is inhibited (*Online Supplementary Figure 1C*). Thus, it became clear that despite commonly occurring oncogenic mutations in *RAS* and *RAF*, MEK inhibitors have limited scope as single-agents in MM.

MEK + HDAC inhibition induces synergistic cell death in multiple myeloma cell lines

We examined the ability of the recently approved pan-HDAC inhibitor LBH589 (panobinostat) to enhance cell death induced by AZD6244 in MM cell lines. Low doses of the AZD6244/LBH589 drug combination induced potent synergistic cytotoxicity (Figure 1A). Interestingly, the synergy was observed in cell lines with mutations in *K-RAS* and *N-RAS* (i.e. H929, MM1R, MM1S, RPMI8226) and *B-RAF* (i.e. U266), but not in cell lines that are wild-type for *RAS* and *RAF* (i.e. KMS11, KMS18, OPM2). We also observed significantly more potent proliferation arrest when the drugs were used in combination (Figure 1B).

Components of the bone marrow microenvironment such as bone marrow stromal cells play an indispensable role in MM disease progression and resistance to therapies.[25] We therefore investigated whether AZD6244/LBH589 was able to overcome the protective effects of bone marrow stromal cells. To do this, we co-cultured MM1S cells with patient-derived bone marrow stromal cells and measured the proliferation rate after treatment with either single-agent AZD6244 or LBH589, or the drug combination. We observed that the AZD6244/LBH589 combination was able to inhibit the proliferation of MM1S even when co-cultured with bone marrow stromal cells (Figure 1C). We also noted synergistic cell death when we used another MEK inhibitor, MEK162 (binimetinib), or the ERK inhibitor SCH772984 in combination with LBH589 (*Online Supplementary Figure 1D*). Furthermore, AZD6244 synergistically killed MM cells when combined with the pan-HDAC inhibitor SAHA (*data not shown*).

To understand whether the cytotoxicity caused by the AZD6244/LBH589 combination occurred through the apoptotic pathway, we performed annexin/PI staining. The drug combination clearly induced apoptotic cell death by 72 h (Figure 2A). We also examined whether the combination induced the cleavage of caspases and PARP, both of which are markers of apoptosis. The AZD6244/LBH589 combination induced potent cleavage of caspase 9 and PARP, but not caspase 8, suggesting that the cell death occurred through the mitochondrial intrinsic apoptotic pathway (Figure 2B). Next, we examined whether the drugs, at the doses used above, were able to inhibit their target proteins. As expected, AZD6244 inhibited pERK and LBH589 caused an increase in acetylated histone H3 levels (Figure 2C). Finally, to confirm that MEK/ERK pathway inhibition contributed to the synergy with LBH589, and to examine whether both isoforms of ERK need to be inhibited for the synergy to occur, we nucleofected isoform-specific ERK siRNA into MM1S and treated the cells with LBH589. We observed that ERK1 or ERK2 knockdown individually enhanced the cell death induced by LBH589 (Figure 2D, E). However, simultaneous knockdown of both isoforms led to even more pronounced cell death when used in combination with LBH589, supporting an important survival role for both ERK isoforms in this context. Finally, we treated plasma cells obtained from MM patients with the drug combination. The characteristics of these patients are detailed in *Online Supplementary Table S*1. It is worth noting that several patients had high-risk features including *TP53* deletion, t(4;14) and refractoriness to multiple lines of therapy. We observed augmented apoptosis with the AZD6244/LBH589 drug combination compared to the effects of either drug alone (Table 1).

MEK + HDAC inhibitor-induced synergistic apoptosis is mediated by BIM

Given that the MEK/ERK pathway is known to phosphorylate the pro-apoptotic BH3-only protein BIM at serine 69 (S69) to mark it for proteasomal degradation,[26] we were not surprised to find that AZD6244 treatment increased BIM protein levels (Figure 3A). Although prior studies have shown that HDAC inhibition increases BIM expression in MM,[18,19] we did not observe increased levels of BIM with the several-fold lower doses of LBH589 that were used in this study (Figure 3A). Even so, given that MEK inhibition increased BIM and that the drug combination induced potent activation of intrinsic apoptotic markers, we hypothesized that BIM might play an important role in the observed synergy. To investigate this, we nucleofected MM1S cells with BIM siRNA and observed that BIM knockdown completely protected from the synergistic cell death induced by the MEK + HDAC inhibitor combination (Figure 3B).

HDAC inhibition dissociates BIM from MCL-1 and BCL-X_L

From the above results, it became clear that BIM plays an essential role in the synergistic apoptosis induced by the drug combination. Since BIM was upregulated by AZD6244, but not by LBH589, we reasoned that the increased levels of BIM induced by AZD6244 were unable to activate apoptosis due to sequestration by the anti-apoptotic BCL-2 family members (i.e. BCL-2, BCL-X_L and MCL-1). Thus, we hypothesized that the mechanism by which LBH589 synergizes with AZD6244 is by modulating the interactions of BIM with the anti-apoptotic BCL-2

A

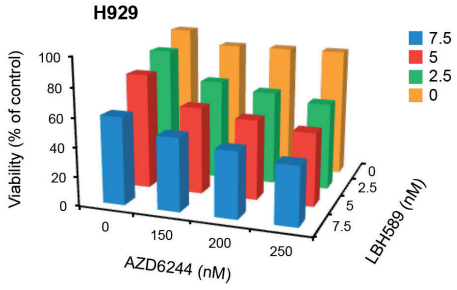

AZD6244 (nM)	LBH589 (nM)	Fa	CI
250	5	0.545	0.634

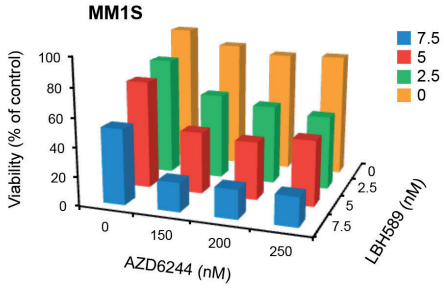

AZD6244 (nM)	LBH589 (nM)	Fa	CI
150	5	0.696	0.259

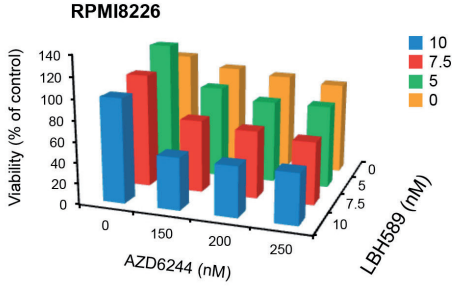

AZD6244 (nM)	LBH589 (nM)	Fa	CI
250	7.5	0.513	0.281

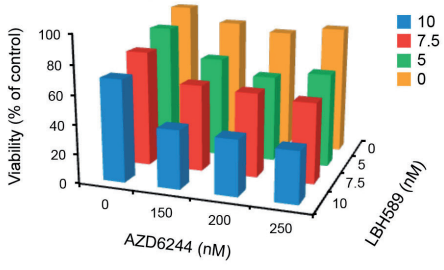

AZD6244 (nM)	LBH589 (nM)	Fa	CI
200	5	0.437	0.247

B

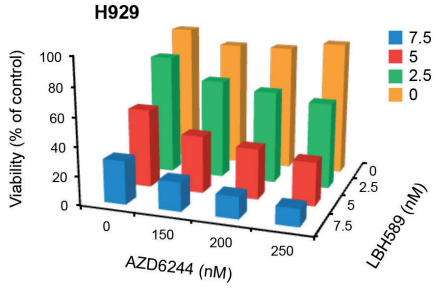

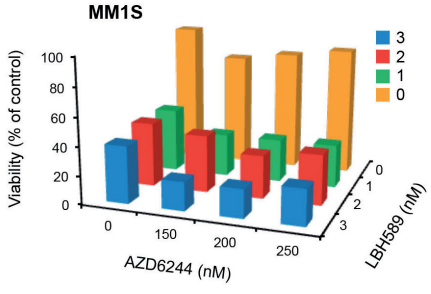

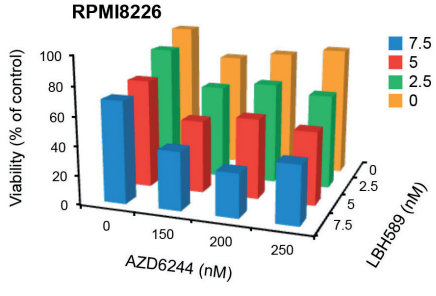

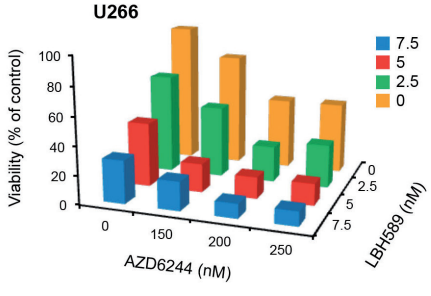

C

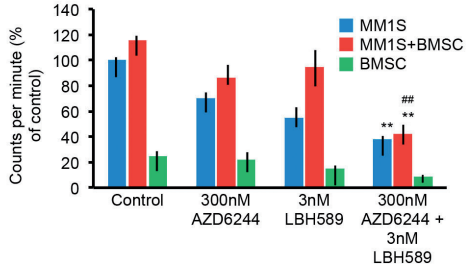

Figure 1. MEK inhibition in combination with histone deacetylase inhibition synergistically kills multiple myeloma cell lines *in vitro*. (A) AZD6244 and the pan-histone deacetylase (HDAC) inhibitor LBH589 induced synergistic cytotoxicity, assayed using MTT at 72 h in the *RAS*-mutated human multiple myeloma (MM) cell lines H929, MM1S, and RPMI8226, and the *RAF*-mutated human MM cell line U266. Viability is shown as percent of control on the Y-axis. Combination index (CI) values <1.0, indicating synergy, are shown for each cell line. (B) AZD6244 and LBH589 induced proliferation arrest, assayed with ^{3}H-thymidine incorporation, by 48 h in H929, MM1S, RPMI8226, and U266 cells, shown as percent of control on the Y-axis. (C) Bone marrow stromal cells (BMSC) derived from an MM patient were co-cultured with MM1S, and proliferation was assayed using ^{3}H-thymidine incorporation after treatment for 48 h with AZD6244, LBH5589, or the combination. Error bars represent the standard error of the mean of triplicate experiments. Differences between groups were calculated with the Student *t* test. $^{**}P<0.001$, $^{\#\#}P<0.01$. All experiments were performed in triplicate.

family proteins. In pursuit of demonstration of this, we immunoprecipitated BIM and examined its binding pattern with BCL-2, BCL-X_L and MCL-1 before and after drug treatment. AZD6244 increased the relative amount of BIM bound to all three anti-apoptotic proteins, which may partly explain why even though the drug markedly increases BIM levels, it has limited cytotoxic effects in MM as a single agent (Figure 3C). Interestingly, LBH589 dissociated BIM from MCL-1 and BCL-X_L, but not BCL-2 (Figure 3C). This effect was particularly evident when the anti-apoptotic proteins were "primed" with more BIM by AZD6244. We also noted this dissociation in the reciprocal experiment when pulling down with BCL-2 and MCL-1, and probing for BIM (Figure 3C). Furthermore, we observed increased BIM bound to both BAX and BAK after AZD6244 and LBH589 treatment individually, which was markedly increased after the combination treatment (Figure 3D). We also noted that LBH589 dissociated BAK from MCL-1 in a similar manner to BIM, which theoretically would facilitate increased BIM:BAK complexes in the presence of LBH589 to further activate the intrinsic apoptotic cascade (Figure 3D).

MCL-1/BCL-2 expression and BIM binding profile correlate with sensitivity to MEK + HDAC inhibition

In light of LBH589 dissociating BIM from MCL-1 and BCL-X_L, but not from BCL-2, we wondered if the cell lines that were resistant to the MEK+HDAC inhibitor combination expressed higher baseline levels of BCL-2. Western blots confirmed that this was partly true, but many of the AZD6244/LBH589-sensitive cell lines, including MM1R, MM1S, RPMI8226 and U266, had high expression of both BCL-2 and MCL-1 (Figure 4A). To interrogate the possibility that expression is a poor indication of functional dependence on either anti-apoptotic protein, we immunoprecipitated BIM and examined baseline levels of BIM:BCL-2, BIM:MCL-1 and BIM:BCL-X_L complexes in cell lines that were either sensitive or resistant to the MEK + HDAC inhibitor combination. Notably, BIM was mostly bound to MCL-1 in all of the cell lines which were sensi-

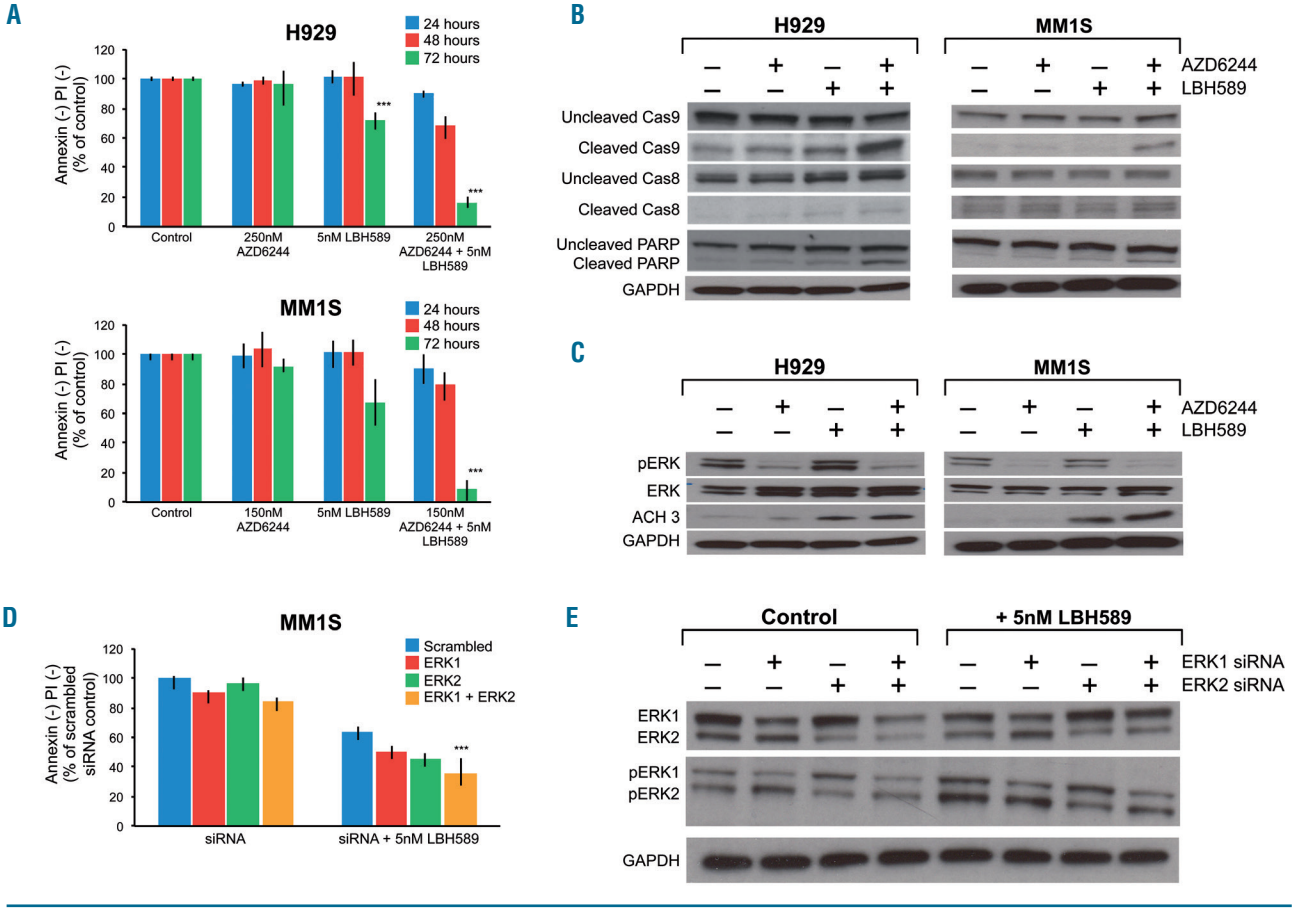

Figure 2. MEK + histone deacetylase inhibition drives synergistic apoptosis in multiple myeloma cell lines and inhibits target proteins. (A) Flow cytometric cell viability of the *RAS* mutant human multiple myeloma (MM) cell lines H929 and MM1S measured as the proportion of annexin$^-$/propidium iodide (PI)$^-$ cells, after 24, 48 and 72 h of treatment with AZD6244 and LBH589 at the indicated doses. Viability is shown as percent of control on the Y-axis. (B,C) H929 and MM1S were treated with AZD6244/LBH589 for 24 h, then whole-cell lysates were separated using sodium dodecylsulfate polyacrylamide gel electrophoresis (SDS-PAGE) and subjected to western blotting for the indicated proteins. (D) MM1S was electroporated with scrambled siRNA, ERK1, ERK2 siRNA or the combination, then left untreated or treated with 5 nM LBH589. At 72 h, cell viability was assessed using flow cytometry by analyzing the proportion of annexin$^-$/PI$^-$ cells, shown as percent of control on the Y-axis. (E) Whole-cell lysates from these cells were separated using SDS-PAGE and subjected to western blotting to confirm ERK1 and ERK2 silencing. Error bars represent the standard error of mean of triplicate experiments. Differences between groups were calculated with the Student *t* test. ***P*<0.001. All experiments were performed in triplicate.

tive to the MEK + HDAC inhibitor combination, including the aforementioned MM1R, MM1S, RPMI8226 and U266, suggesting that MCL-1 that is "BIM-primed" is critical for the observed synergy to occur (Figure 4A). On the other hand, cell lines with BIM mostly bound to BCL-2 were resistant to the MEK + HDAC inhibitor combination (Figure 4A). It was noteworthy that BCL-X_L was weakly expressed in most of the cell lines and there were few BIM:BCL-X_L complexes at baseline (Figure 4A).

BCL-2 + HDAC inhibition induces synergistic apoptosis in MEK + HDAC inhibitor-resistant, BCL-2-primed cell lines

Since cell lines with more BIM:BCL-2 complexes relative to BIM:MCL-1 complexes were resistant to the MEK + HDAC combination, we hypothesized that these BCL-2-primed cell lines would be sensitive to BCL-2 inhibition with the BH3 mimetic ABT-199 (venetoclax) when used in combination with LBH589. Remarkably, BCL-2 + HDAC inhibition caused synergistic proliferation arrest and cytotoxicity in nearly all the cell lines that were resistant to the MEK + HDAC combination, including DOX40, KMS18, KMS28 and OPM2 (Figure 4B and *data not shown)*. Pronounced induction of apoptosis was confirmed by annexin/PI staining (*Online Supplementary Figure S2*).

This coincided with cleavage of caspase 9/3 and PARP (Figure 4C). Immunoprecipitation experiments demonstrated that ABT-199 dissociated BIM from BCL-2, and LBH589 dissociated BIM from MCL-1 (Figure 4D). In addition, we found that ABT-199 and LBH589 both increased BIM bound to both BAX and BAK, an effect that was even more pronounced with the drug combination (Figure 4E). Moreover, BAX/BAK knockdown with siRNA protected from the ABT-199/LBH589-induced cytotoxicity, confirming that the observed synergistic cell death occurred via the mitochondrial intrinsic apoptotic pathway (Figure 4F).

Table 1. Changes in apoptosis of multiple myeloma patients' plasma cells exposed to various drug combinations. Plasma cells sorted from patients with multiple myeloma were exposed to AZD6244, LBH589, and the combination, or ABT-199, LBH589, and the combination for 72 h. The proportion of cells undergoing apoptosis was measured using flow cytometry, and the relative fold change in apoptosis is indicated. The upper part of the table summarizes the results from the 14 patients treated with the AZD6244/LBH489 combination, while the lower part summarizes the results for the nine patients treated with the ABT-199/LBH589 combination.

	Drug dose (nM)			Relative fold change in apoptosis		
Patient #	AZD6244	LBH589	Control	AZD6244	LBH589	AZD6244+ LBH589
MC1	500	10	1	1.35	3.15	5.96
MC2	500	5	1	1.71	3.43	4.07
MC3	500	5	1	1.07	3.47	4.47
MC4	500	7.5	1	0.62	2.14	2.62
MC5	300	5	1	4.21	3.07	20.71
MC6	500	7.5	1	1.07	7.41	15.19
MC7	500	2.5	1	1.67	1.54	9.44
MC8	500	2.5	1	4.67	4.33	9.56
MC9	500	2.5	1	1	1.38	2.85
MC10	500	1	1	2.75	4.75	11
MC11	500	1	1	2.78	1.78	6.78
MC12	500	2.5	1	2.85	1.23	4.08
MC13	500	2.5	1	2	3.75	7.5
MC14	500	2.5	1	2.3	2.1	5.6
Mean fold change in apoptosis			**1**	**2.15**	**3.11**	**7.85**

	Drug dose (nM)			Relative fold change in apoptosis		
Patient #	ABT-199	LBH589	Control	ABT-199	LBH589	ABT-199+ LBH589
MC10	500	1	1	2.75	4.75	13.5
MC11	500	2.5	1	1.78	4.89	6.22
MC12	500	2.5	1	2.15	1.23	3.23
MC13	500	2.5	1	3	3.75	12.75
MC14	500	1	1	2.2	2.1	4.6
MC15	1000	1	1	12.33	3.33	21.33
MC16	500	2.5	1	2.33	2	7.67
MC17	500	2.5	1	7.71	2	10.71
MC18	500	2.5	1	1.75	1.38	2.16
Mean fold change in apoptosis			**1**	**4**	**2.82**	**9.13**

Finally, we noted enhanced apoptosis after treating plasma cells from MM patients with the ABT-199/LBH589 combination (Table 1).

Notably, the ABT-199/LBH589 combination did not synergistically induce cell death in the *RAS/RAF* mutant, AZD6244/LBH589-sensitive cell lines (i.e. H929, MM1R, MM1S, RPMI and U266). This dovetails with the finding that while LBH589 dissociated BIM:MCL-1 complexes in all the cell lines we tested, it did not shift BIM onto BCL-2 in *RAS/RAF* mutant cell lines (e.g. MM1S) (Figure 3C). However, LBH589 did shift BIM onto BCL-2 in the *RAS/RAF* wild-type cell lines (e.g. OPM2) (Figure 4D), which jibes with its potent synergistic effect when combined with ABT-199. In summary, it appears that AZD6244/LBH589 and ABT-199/LBH589 target two distinct subgroups of MM cell lines with different BCL-2 family binding proclivities.

Baseline MCL-1/BCL-2 phosphorylation status correlates with sensitivity to MEK + HDAC or BCL-2 + HDAC inhibition

To determine why certain cell lines would preferentially have BIM bound to one anti-apoptotic protein over another, i.e. BCL-2 *versus* MCL-1, we examined several phosphorylation sites known to affect the binding capacity and stability of the BCL-2 family to see if there was any correlation. Interestingly, cell lines with higher p-BCL-2 at serine 70 (S70) tended to have more BIM bound to BCL-2 (Figure 5A). p-BCL-2 (S70) is known to increase the anti-apoptotic capacity of BCL-2, i.e. its ability to bind BAK and BH3-only proteins.[27]

On the other hand, cell lines with BIM mostly bound to MCL-1 tended to have relatively low expression of p-BCL-2 (S70), as well as relatively high expression of p-MCL-1 at threonine 163 (T163) (Figure 5A). p-MCL-1

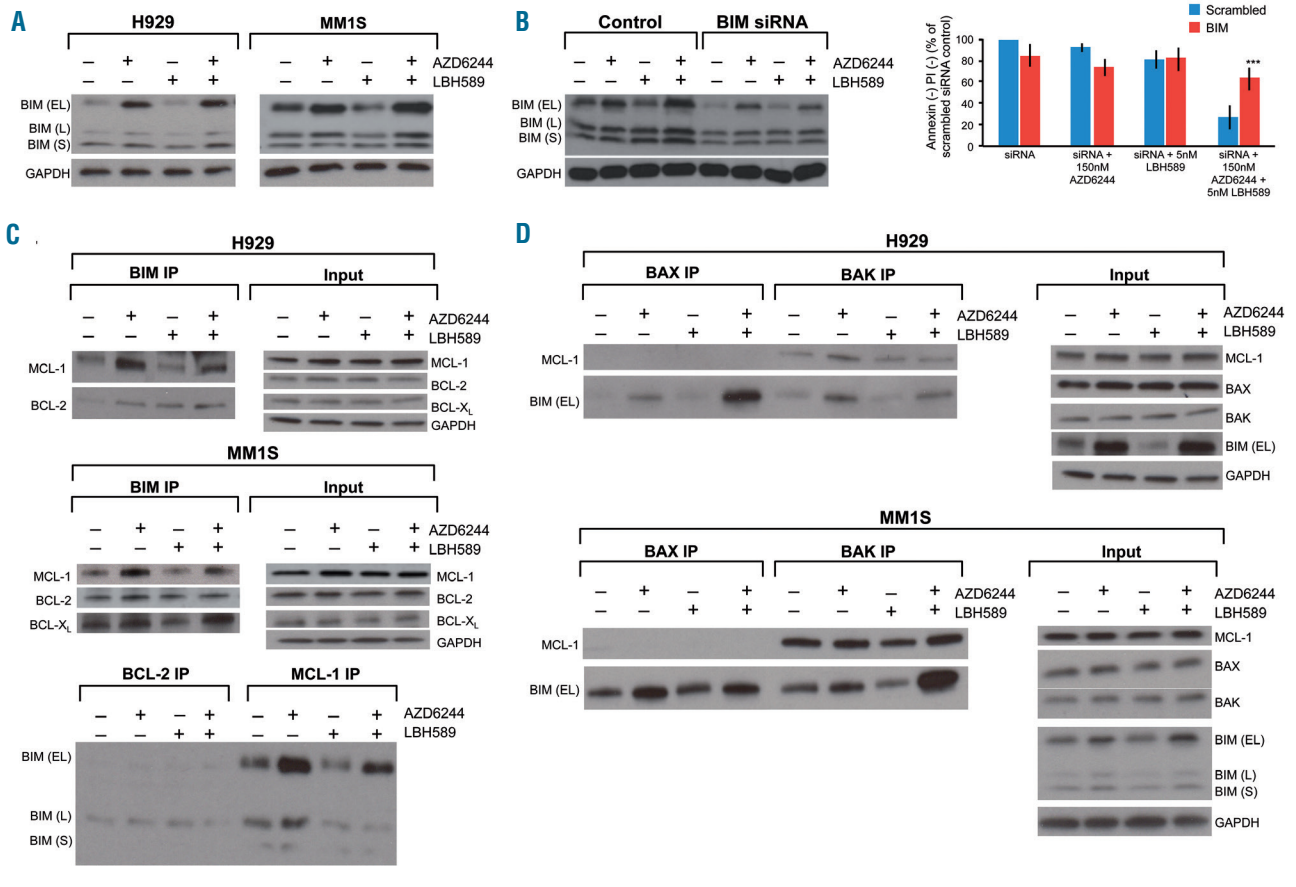

Figure 3. MEK + histone deacetylase inhibitor induced synergistic apoptosis is mediated by BIM. (A) The *RAS* mutant human multiple myeloma (MM) cell lines H929 and MM1S were treated with AZD6244/LBH589 for 24 h, then whole-cell lysates were blotted for the indicated proteins. (B) MM1S was electroporated with scrambled siRNA or BIM siRNA and then left untreated or treated with 5 nM LBH589. At 72 h, cell viability was assessed using flow cytometry by analyzing the proportion of annexin$^-$/propidium iodide (PI)$^-$ cells, shown as percent of control on the Y-axis. Furthermore, the whole-cell lysates were separated using sodium dodecylsulfate polyacrylamide gel electrophoresis (SDS-PAGE) and subjected to western blotting for the indicated proteins to confirm silencing. Error bars represent the standard error of mean of triplicate experiments. Differences between groups were calculated with the Student *t* test. $^{**}P<0.001$. (C) (Upper) H929 and MM1S were treated with AZD6244 (250 nM and 150 nM, respectively) and LBH589 (5 nM) for 24 h. BIM immunoprecipitates were separated using SDS-PAGE and subjected to western blotting to examine BCL-2, MCL-1 and BCL-X_L binding patterns. Whole cell lysates (input) were also separated and probed for the indicated proteins. (Lower) Immunoprecipitates from MM1S for BCL-2 and MCL-1 were also separated and probed to examine BIM binding. (D) H929 and MM1S were treated with AZD6244 (250 nM and 150 nM, respectively) and LBH589 (5 nM). BAX and BAK immunoprecipitation was performed and western blotting was used to examine levels of BIM and MCL-1 bound to BAX and BAK. Whole cell lysates (input) were also separated and probed for the indicated proteins. All experiments were performed in triplicate.

(T163) is a well-documented post-translational modification that stabilizes MCL-1, protecting it from proteasomal degradation.[28] However, we did not observe a correlation between p-MCL-1 at serine 64 (S64) and BIM binding preference (*data not shown*). p-MCL-1 (S64) increases the binding capacity of MCL-1, but not its stability.[29]

To our surprise, p-BCL-2 (S70) and p-MCL-1 (T163) were nearly perfect in predicting sensitivity to either MEK + HDAC or BCL-2 + HDAC inhibition (Figure 5A). This was particularly striking in the case of DOX40, a doxorubicin-resistant cell line derived from RPMI8226. DOX40 expressed more p-BCL-2 (S70) than p-MCL-1 (T163), and was sensitive to the ABT-199/LBH589 combination, whereas its parental cell line RPMI8226 did not express p-BCL-2 (S70), but did express p-MCL-1 (T163), and was sensitive to the AZD6244/LBH589 combination (Figure 5A). Interestingly, the only cell line we tested that was resistant to both drug combinations was KMS11, and this line has low expression of both p-BCL-2 (S70) and p-MCL-1 (T163) (Figure 5A).

RAS/RAF mutational status predicts sensitivity to MEK + HDAC or BCL-2 + HDAC inhibition

Since MEK inhibitors target the pathway downstream of *RAS/RAF*, we were curious to determine whether sensitivity to the AZD6244/LBH589 combination correlates with *RAS/RAF* mutational status. This is a felicitous prospect because the MEK/ERK pathway in part controls p-MCL-1 (T163).[28] Indeed, the *RAS*-mutated cell lines H929, MM1R, MM1S, RPMI8226, and the *RAF*-mutated

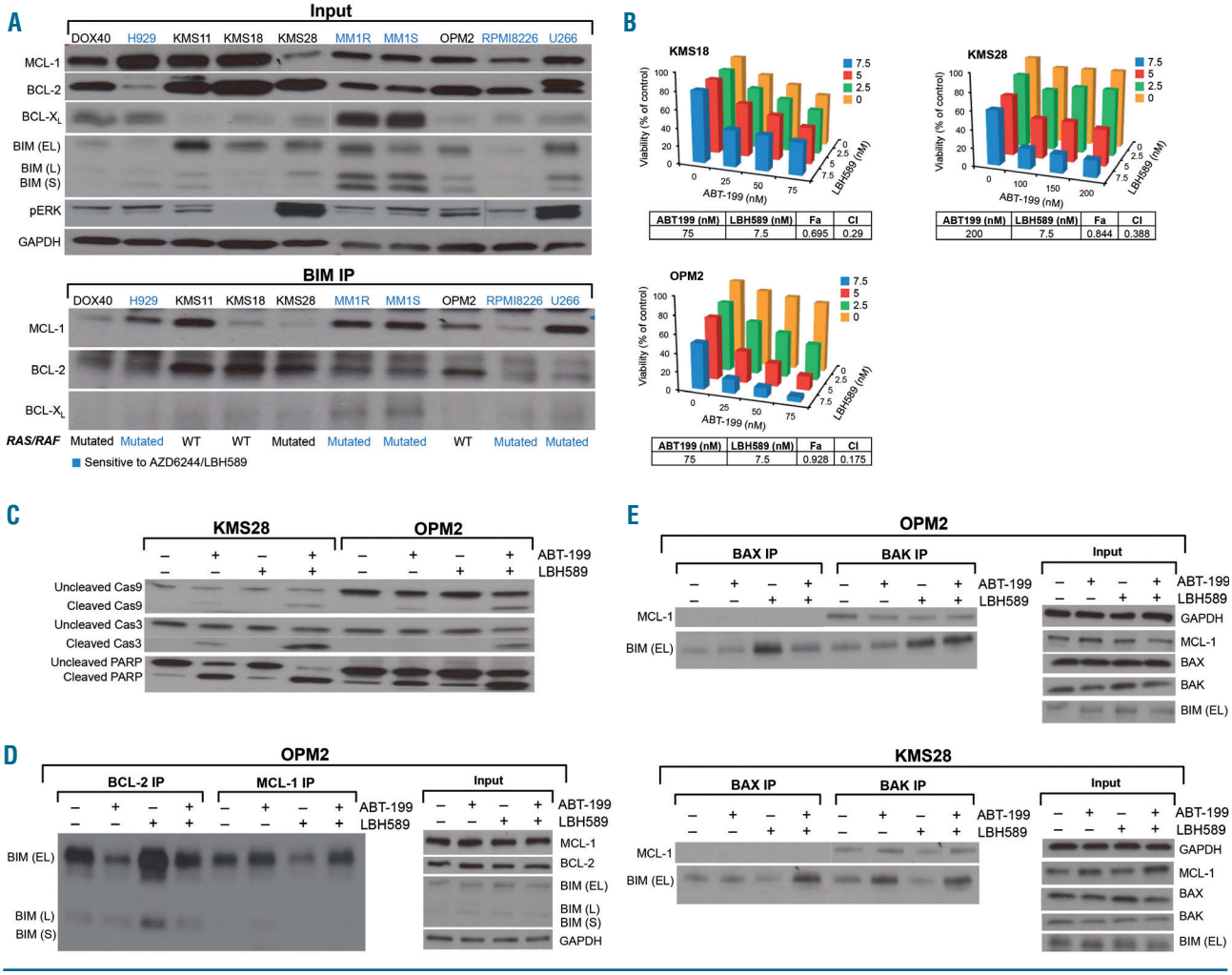

Figure 4. Predominance of BIM:MCL1 complexes correlates with sensitivity to MEK + histone deacetylase (HDAC) inhibition; MEK + HDAC inhibitor-resistant cell lines that had predominantly BIM:BCL-2 complexes were synergistically killed by BCL-2 + HDAC inhibition. (A) Whole-cell lysates from a panel of human multiple myeloma (MM) cell lines were immunoprecipitated with BIM. Subsequently, western blotting was performed to examine baseline levels of BIM:BCL-2, BIM:BCL-X_L and BIM:MCL-1 complexes. Whole cell lysates (input) were also separated with sodium dodecylsulfate polyacrylamide gel electrophoresis (SDS-PAGE) and probed for the indicated proteins. Cell lines sensitive to the AZD6244/LBH589 combination are indicated in blue. The mutational status of the cell lines, i.e. mutated or wild-type (WT) for *RAS/RAF*, is shown. (B) The BH3 mimetic ABT-199 and the pan-HDAC inhibitor LBH589 induced synergistic cytotoxicity (assessed using MTT) by 72 h in the human MM cell lines KMS18, OPM2 (*RAS/RAF* wild-type) and KMS28 (*RAS* mutant). Viability is shown as percent of control on the Y-axis. Combination index (CI) values <1.0, indicating synergy, are shown for each cell line. (C) KMS28 and OPM2 were treated with ABT-199/LBH589 for 24 h, then whole-cell lysates were separated using SDS-PAGE and probed for the indicated proteins. (D) OPM2 was treated with 50 nM ABT-199 and 5 nM LBH589 for 24 h, then immunoprecipitates for BCL-2 and MCL-1, and whole cell lysates (input) were separated using SDS-PAGE and probed for the indicated proteins. (E) OPM2 and KMS28 were treated with ABT-199 (50 nM and 250 nM, respectively) and LBH589 (5 nM) for 12 h. BAX and BAK immunoprecipitates and whole-cell lysates (input) were separated using SDS-PAGE and subjected to western blotting for the indicated proteins. All experiments were performed in triplicate.

cell line U266 were all sensitive to MEK + HDAC inhibition and had high baseline expression of p-MCL-1 (T163) (Figures 1A and 5A). On the other hand, the *RAS/RAF* wild-type cell lines KMS18 and OPM2 were resistant to MEK + HDAC inhibition, but sensitive to BCL-2 + HDAC inhibition. These cell lines also had high expression of p-BCL-2 (S70) (Figures 4B and 5A). However, the correlation between sensitivity to either drug combination and *RAS/RAF* mutational status was not perfect: DOX40 and KMS28 both have mutated *RAS*, but were sensitive to BCL-2 + HDAC inhibition rather than to MEK + HDAC inhibition. Finally, KMS11, which was resistant to both combinations, has wild-type *RAS/RAF*. Thus, we conclude that p-BCL-2 (S70), p-MCL-1 (T163) and *RAS/RAF* mutational status could all be useful biomarkers to predict for sensitivity to either the MEK + HDAC or BCL-2 + HDAC inhibitor combinations.

HDAC inhibition alters the phosphorylation of MCL-1

Given that HDAC inhibition dissociated BIM from MCL-1, we investigated whether LBH589 altered the expression of any BH3-only proteins that could theoretically bind to MCL-1 to displace BIM. However, at the doses at which we observed synergy, LBH589 did not appreciably alter the expression of any of the BH3-only proteins, including NOXA, PUMA, BAD, BID, BIK, BMF or HRK (*data not shown*). Since we found that baseline post-translational modifications on several of the anti-apoptotic BCL-2 family members correlated with sensitivity to either drug combination, we studied whether LBH589 altered any post-translational modifications on MCL-1 or BCL-X_L that could explain the BIM dissociation.

Interestingly, LBH589 down regulated p-MCL-1 (S64) in a time- and dose-dependent manner (Figure 5B). In addition, AZD6244 increased p-MCL-1 (S64), which may explain in part why MCL-1 becomes "primed" with BIM after AZD6244 treatment (Figure 5C). When the drugs were combined, LBH589 still decreased p-MCL-1 (S64) when compared to AZD6244 alone (Figure 5C). Taken together, it seems that LBH589 might facilitate apoptosis by decreasing the phosphorylation of MCL-1 at the S64 residue, making it less "sticky" to BIM, especially after it becomes primed with BIM in the context of MEK inhibitor treatment.[29]

p-MCL-1 (S64) is known to be driven by JNK,[29] and CDK1/2.[29,30] However, we were unable to replicate synergy when we used JNK or CDK inhibitors in combination with AZD6244 or ABT-199 (*data not shown*). Relatively less is known about the role of post-translational modifications on BCL-X_L, but similar to BCL-2 and MCL-1, phosphorylation has been documented to modulate the anti-apoptotic role of BCL-X_L.[20] However, LBH589 did not appreciably alter p-BCL-X_L (S62) levels (*data not shown*).

HDAC6 inhibition does not enhance apoptosis induced by MEK inhibition

Next, we wanted to identify which HDAC(s) must be inhibited for the observed synergy to occur with MEK or BCL-2 inhibitors. First, we examined the role of HDAC6 given the relevance of inhibiting the aggresome pathway in MM and early clinical results obtained using HDAC6 inhibition in the relapsed/refractory setting.[15,31] Treating cells with AZD6244 in combination with the HDAC6-specific inhibitor tubacin did not lead to synergistic cell

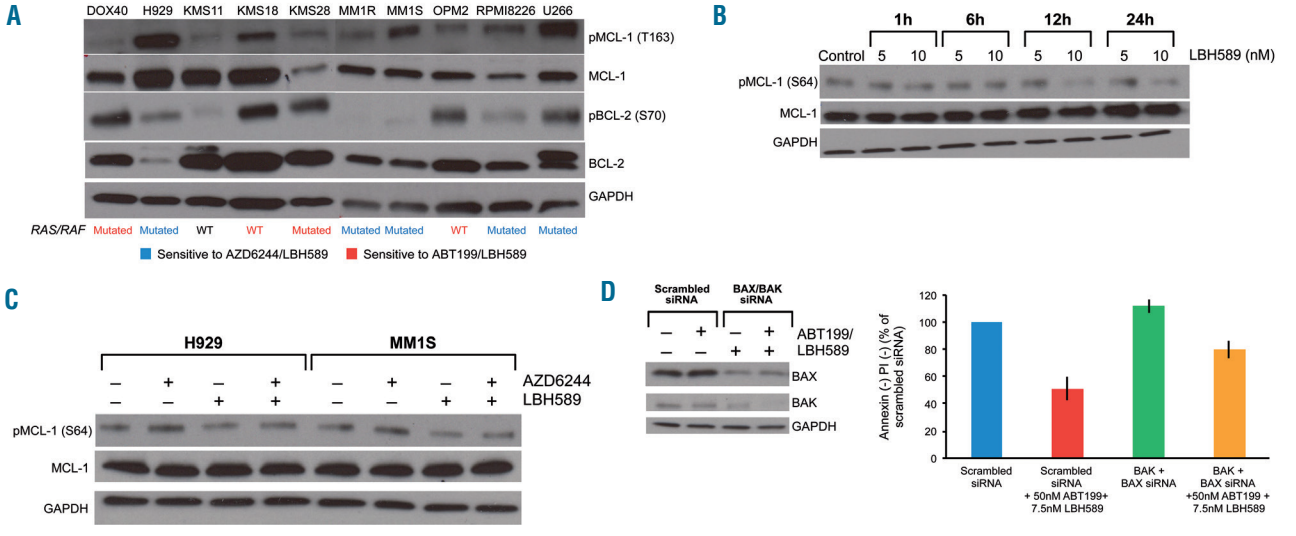

Figure 5. Phosphorylation status of MCL-1/BCL-2 correlates with sensitivity to MEK + histone deacetylase (HDAC) or BCL-2 + HDAC inhibition, and HDAC inhibition affects the phosphorylation of MCL-1. (A) Whole-cell lysates from a panel of human multiple myeloma (MM) cell lines were separated with sodium dodecylsulfate polyacrylamide gel electrophoresis (SDS-PAGE) and subjected to western blotting for the indicated proteins. Cell lines sensitive to the AZD6244/LBH589 combination are indicated in blue. Cell lines sensitive to the ABT-199/LBH589 combination are indicated in red. KMS11 was resistant to both drug combinations, and is indicated in black. Mutational status of the cell lines, either mutated or wild-type (WT) for *RAS/RAF*, is shown. (B) H929 was treated for 1, 6, 12, and 24 h with 5 and 10 nM LBH589. Whole cell lysates were separated with SDS-PAGE and subjected to western blotting for the indicated proteins. (C) H929 and MM1S were treated with AZD6244 (250 nM and 150 nM, respectively) and LBH589 (5 nM) for 24 h. Whole cell lysates from these cells were separated with SDS-PAGE and western blotting was performed for the indicated proteins. (D) KMS28 was electroporated with scrambled siRNA or BAX and BAK siRNA, then treated with 250 nM ABT-199 and 5nM LBH589. At 72 h, cell viability was assessed using flow cytometry by analyzing the proportion of annexin$^-$/propidium iodide (PI)$^-$ cells, shown as percent of control on the Y-axis. In addition, whole-cell lysates were separated using SDS-PAGE and probed for the indicated proteins to confirm silencing. Error bars represent the standard error of mean of triplicate experiments. All experiments were performed in triplicate.

death (*Online Supplementary Figure S3A*). These results were confirmed by knocking down HDAC6 using siRNA (*Online Supplementary Figure S3B*). Considering all the findings, we concluded that HDAC6 inhibition does not seem to be important for the synergistic cell death induced by the AZD6244/LBH589 combination.

Simultaneous inhibition of HDAC1 and HDAC2 is sufficient to enhance cell death induced by MEK or BCL-2 inhibition

We next examined whether inhibiting class I HDAC augmented cell death in combination with MEK or BCL-2 inhibitors. For this, we first used MS275 (entinostat), which inhibits HDAC1, 2 and 3. We observed potent synergy when MS275 was used with AZD6244 or ABT-199 in MM cell lines (*Online Supplementary Figure S4A, B*) and patients' cells (*Online Supplementary Table S2*) similar to the synergy observed with LBH589. This synergy occurred even at very low doses of MS275 (i.e. 150 nM), which would be unlikely to inhibit HDAC3 (the IC_{50} for HDAC3 is 1.7 μM).[32] To determine whether inhibiting HDAC1 and 2 would be sufficient to synergize with AZD6244 or ABT-199, we used the HDAC1 and 2 inhibitor FK228 (romidepsin) in combination with

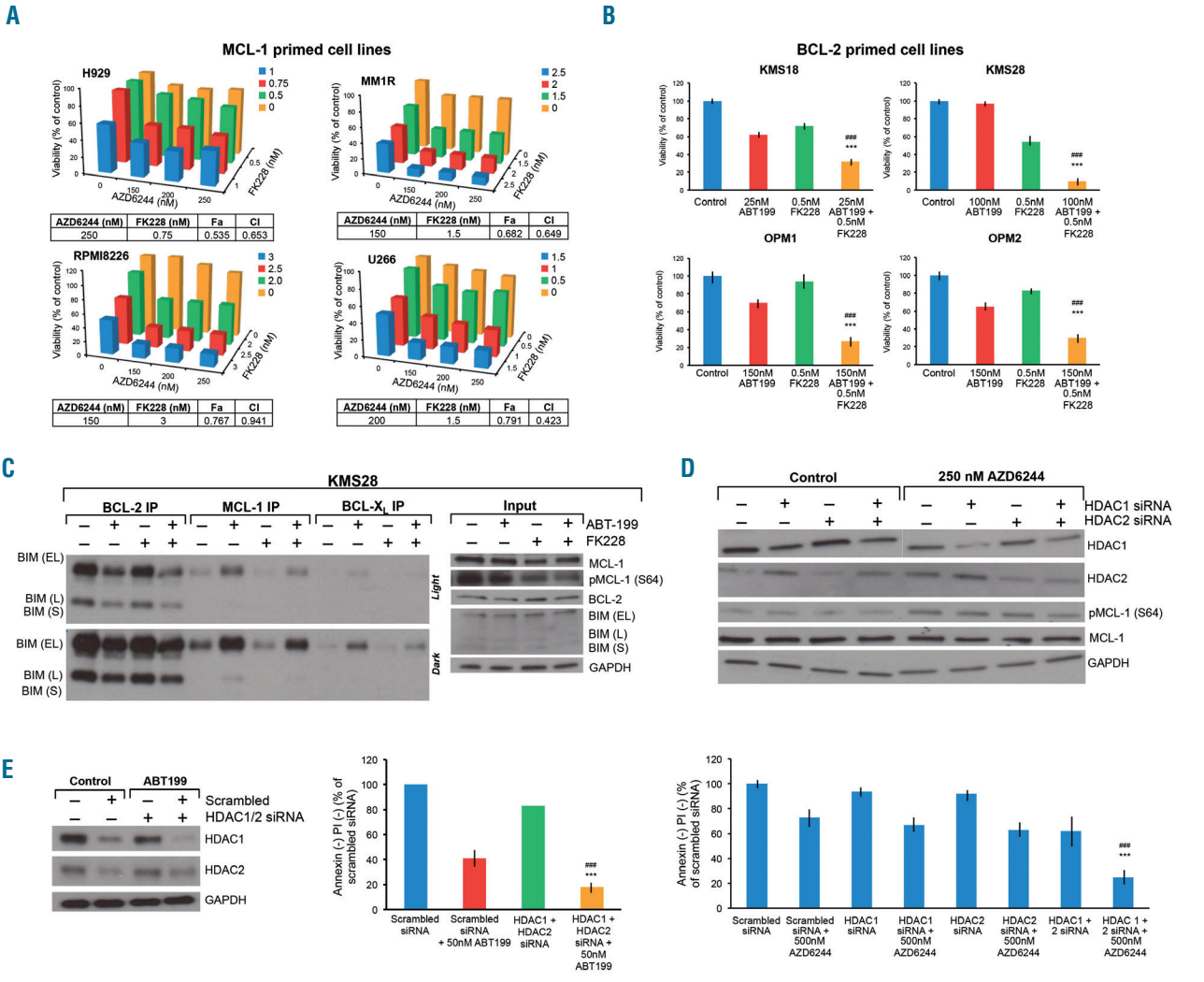

Figure 6. Concomitant inhibition of histone deacetylases 1 and 2 replicates synergy with MEK or BCL-2 inhibition in multiple myeloma cell lines. (A) The histone deacetylase (HDAC)-1 and -2 inhibitor FK228 (romidepsin) was combined with AZD6244 in increasing doses in the MCL-1 primed, *RAS/RAF* mutant human multiple myeloma (MM) cell lines H929, MM1R, RPMI8226 and U266. Cellular viability was assessed using MTT at 72 h. Viability is shown as percent of control on the Y-axis. Combination index (CI) values <1.0, indicating synergy, are shown for each cell line. (B) FK228 was combined with ABT-199 in increasing doses in the BCL-2-primed human MM cell lines KMS18, OPM1, OPM2 (*RAS/RAF* wild-type) and KMS28 (*RAS* mutant). Cellular viability was assessed using flow cytometry by analyzing the proportion of annexin$^-$/propidium iodide (PI)$^-$ cells, shown as percent of control on the Y-axis. (C) KMS28 was treated with 100 nM ABT-199 and 0.5 nM FK228 for 24 h, then immunoprecipitates for BCL-2, MCL-1 and BCL-X_L, or whole cell lysates (input) were separated using sodium dodecylsulfate polyacrylamide gel electrophoresis (SDS-PAGE) and probed for the indicated proteins. Light and dark film exposures are shown for the BCL-2, MCL-1 and BCL-X_L immunoprecipitates so the BIM:MCL-1 and BIM:BCL-X_L dissociations are apparent. (D) MM1S was electroporated with scrambled siRNA, HDAC1 siRNA, HDAC2 siRNA or HDAC1 and 2 siRNA, then left untreated or treated with 250 nM AZD6244. At 72 h, cell viability was assessed using flow cytometry by analyzing the proportion of annexin$^-$/PI$^-$ cells, shown as percent of control on the Y-axis. In addition, whole-cell lysates were separated using SDS-PAGE and probed for the indicated proteins to confirm silencing. (E) KMS18 was electroporated with scrambled siRNA or HDAC1 and HDAC2 siRNA, then left untreated or treated with 50 nM ABT-199. At 72 h, cell viability was assessed using flow cytometry by analyzing the proportion of annexin$^-$/PI$^-$ cells, shown as percent of control on the Y-axis. Also whole-cell lysates were separated using SDS-PAGE and probed for the indicated proteins to confirm silencing. Error bars represent the standard error of mean of triplicate experiments. Differences between groups were calculated with the Student *t* test. $^{**}P<0.001$, $^{\#\#}P<0.01$. All experiments were performed in triplicate.

AZD6244 or ABT-199 and observed marked synergy in MM cell lines (Figure 6A, B) and patients' cells (*Online Supplementary Table S2*). Using western blotting and immunoprecipitation, we also replicated the mechanistic finding that FK228 downregulates p-MCL-1 (S64) and causes BIM dissociation from MCL-1 and BCL-X_L in KMS28 (Figure 6C) and H929 (*Online Supplementary Figure S4C*). This strongly suggested that HDAC1 and 2 are involved in the mechanism. To confirm these results, we performed knockdown studies with HDAC1- and HDAC2-specific siRNA. Knocking down HDAC1 and HDAC2 individually in combination with AZD6244 or ABT-199 caused minor increases in apoptosis. However, simultaneous knockdown of both HDAC1 and HDAC2, when combined with AZD6244 or ABT-199, caused significantly more apoptosis (Figure 6D, E). Inhibiting HDAC3 in addition to HDAC1 and HDAC2 did not augment the synergy (*data not shown*). Dovetailing with our results with pharmacological HDAC inhibitors, we observed p-MCL-1 (S64) downregulation when HDAC1 and HDAC2 were silenced in tandem (Figure 6D). We also noted that knocking down either HDAC1 or HDAC2 individually caused a reciprocal upregulation of HDAC2 and HDAC1, respectively. We speculate that this could be the reason why inhibition of HDAC1 or HDAC2 individually was not sufficient to synergize with either MEK or BCL-2 inhibition (Figure 6D, E). Taken together, these results showed that simultaneous inhibition of HDAC1 and HDAC2 is sufficient to markedly enhance the apoptosis induced by AZD6244 or ABT-199 in MM.

Discussion

The sequestration of pro-apoptotic BCL-2 family proteins, such as BIM, by their anti-apoptotic counterparts, i.e. BCL-2 and MCL-1, is a pervasive survival strategy in cancer.[20] Hence, treatments that alter the pro/anti-apoptotic BCL-2 family member ratio or modulate their binding dynamics hold considerable promise, particularly in hematologic malignancies. In the present study, we identified two drug combinations, i.e. MEK + HDAC and BCL-2 + HDAC inhibition, which target two distinct subgroups of MM: MCL-1 or BCL-2 primed, respectively (summarized in Figure 7). In support of these being discrete phenotypes, none of the MM cell lines that we tested was sensitive to both drug combinations. Furthermore, sensitivity aligned mostly based on *RAS/RAF* mutational status.

Mutations in the *RAS/RAF* pathway are present in nearly half of all malignant tumor types.[33] In lieu of a direct way to inhibit RAS, MEK inhibitors have shown significant clinical benefit in several *RAS/RAF*-mutated cancers.[34] Herein, we identified that *RAS/RAF*-mutated MM

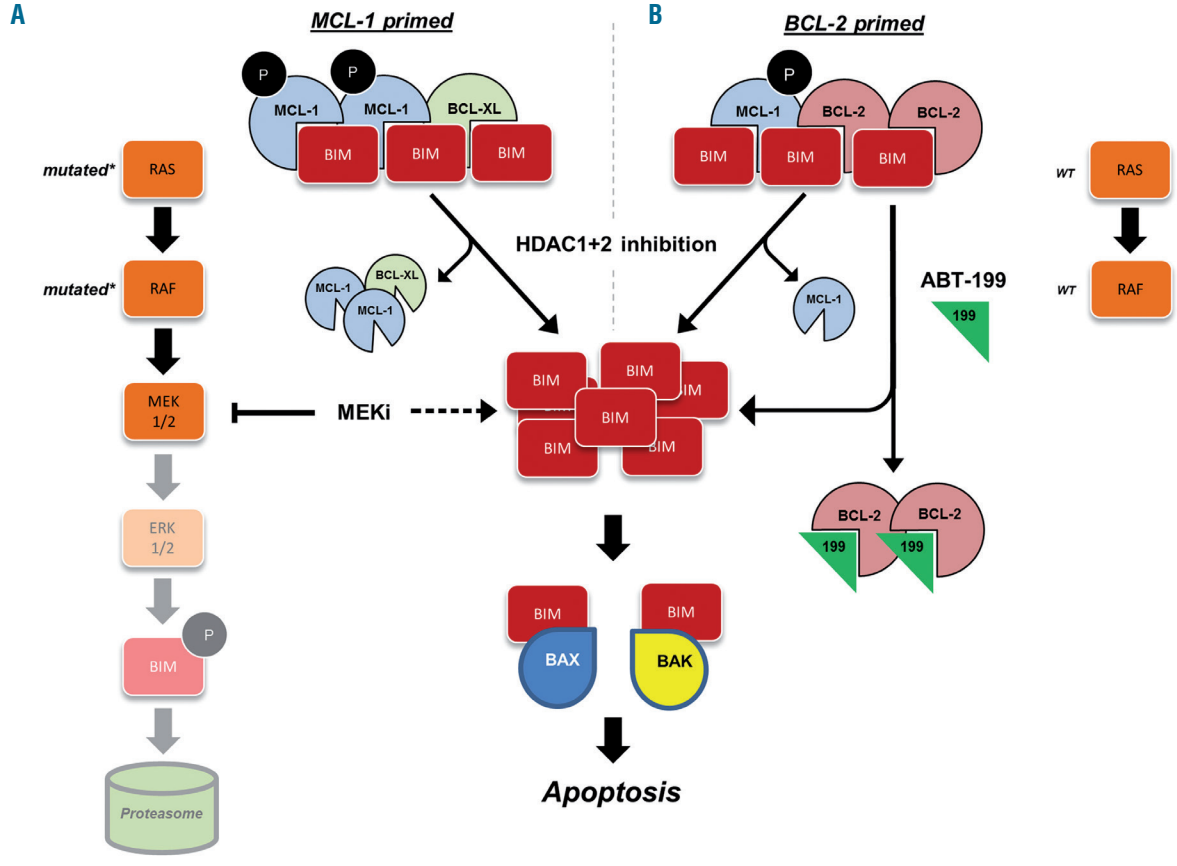

Figure 7. Proposed mechanism of MEK or BCL-2 inhibition in combination with histone deacetylase inhibition in multiple myeloma. (A) MCL-1-primed lines, which all had mutated *RAS/RAF*, were sensitive to the MEK + histone deacetylase (HDAC) inhibitor combination. MEK inhibition increased BIM levels, and HDAC1+2 inhibition dissociated BIM:MCL-1 and BIM:BCL-X_L complexes, the former perhaps by means of downregulation of p-MCL-1 (S64). (B) BCL-2-primed cell lines tended to be wild-type (WT) for *RAS/RAF*, and were sensitive to the BCL-2+HDAC inhibitor combination. Likewise, HDAC1+2 inhibition dissociated BIM:MCL-1 complexes. Both drug combinations in effect increased free BIM levels, which we found were able to engage BAX and BAK, ultimately leading to synergistic apoptotic cell death.

cells are particularly sensitive to MEK inhibition when this is used in combination with pan-HDAC or class I HDAC inhibitors. Our results demonstrate that while single-agent MEK inhibition increased BIM, this protein remained sequestered by anti-apoptotic BCL-2 family members. Concomitant HDAC inhibition, specifically of class I HDAC, dissociated BIM:MCL-1 and BIM:BCL-X_L complexes, but not BIM:BCL-2 complexes, thereby freeing BIM to activate apoptotic cell death (Figure 7A).

Given the prevalence of *RAS/RAF* mutations in MM, we anticipate that this combination could be highly clinically effective. While we did not investigate specific differences between *N-RAS* and *K-RAS* mutations here, a prior study showed different response durations after standard therapy, i.e. bortezomib, between these two subgroups; future research should examine the significance of these isoforms in the context of MEK + HDAC inhibition.[35] In addition, given the marked intra-tumoral heterogeneity of MM, the impact of the variant allele frequency of *RAS/RAF* mutations must be evaluated in future studies.

Our mechanistic studies identified that MEK + HDAC inhibitor-sensitive MM cell lines expressed high levels of p-MCL-1 (T163), a post-translational modification that enhances the stability of MCL-1 and is driven in part by ERK.[36] MCL-1 is unique among the anti-apoptotic BCL-2 family because of its short half-life, but is often upregulated or stabilized in numerous cancers, including MM.[37,38] Although p-MCL-1 (T163) does not affect the binding capacity of MCL-1, stability of the anti-apoptotic BCL-2 family proteins is part and parcel of their function.[39]

Interestingly, we identified for the first time that the pan-HDAC inhibitor LBH589 and class I HDAC inhibitors MS275 and FK228 act as MCL-1 and BCL-X_L inhibitors at relatively low doses. Furthermore, we suggest that the downregulation of p-MCL-1 at the S64 residue may be responsible for the former observation.[29] Unlike other studies using several-fold higher doses of HDAC inhibitors in their experiments,[18,40] HDAC inhibition did not increase levels of BIM, NOXA, or any other BH3-only proteins in our experiments. Thus, HDAC inhibitor-driven upregulation of BH3-only proteins does not appear to mediate synergy with MEK or BCL-2 inhibition, at least in MM. However, we were unable to elucidate specifically how HDAC inhibition downregulated p-MCL-1 (S64), or functionally prove that this was responsible for the observed BIM dissociation. In addition, further studies are required to determine how LBH589 dissociates BIM from BCL-X_L.

MM cell lines that were resistant to MEK+HDAC inhibition had markedly more BIM:BCL-2 complexes at baseline. Combining ABT-199 (venetoclax) with HDAC inhibitors synergistically killed these cell lines (Figure 7B). ABT-199 is a highly potent BCL-2 inhibitor which, in just a few years, has altered the treatment landscape of chronic lymphocytic leukemia.[41] It has also produced promising clinical responses in many other hematologic malignancies and several non-Hodgkin lymphomas.[42] More relevant to our study, single-agent ABT-199 recently produced encouraging clinical responses in patients with relapsed/refractory MM, particularly those with t(11;14) who had high *BCL2* expression.[43] It is conceivable that HDAC inhibition could either expand the pool of patients who would be sensitive to BCL-2 inhibition, or deepen the responses of partially sensitive patients.

However, it should be noted that concomitant HDAC inhibition did not sensitize all MM cell lines to BCL-2 inhibition, as evidenced by the *in vitro* resistance of *RAS/RAF* mutant, MCL-1-primed MM cell lines to BCL-2 + HDAC inhibition. Even so, it is well documented that increased sequestration of BH3-only proteins by MCL-1 and BCL-X_L is a major resistance mechanism of BH3 mimetics.[44] Perhaps then, HDAC inhibition could re-sensitize patients, who relapse after ABT-199 treatment, to BCL-2 inhibition. It is also worth noting that several specific MCL-1 inhibitors are actively being developed for use in MM.[45] Speculatively, cells that acquire resistance to MCL-1 inhibition could be investigated to determine whether they become more BCL-2-dependent, and thereby sensitive to the ABT-199/LBH589 combination.

Notably, we demonstrated markedly increased apoptosis in plasma cells sorted from MM patients with a wide variety of clinical characteristics after treatment with the MEK + HDAC and BCL-2 + HDAC inhibitor combinations *ex vivo*. However, there were too few patients' samples to discern if the type or number of prior lines of therapy, or particular cytogenetic abnormalities predicted for sensitivity to either combination. Even so, it is conceivable that readily discernible subgroups of patients, beyond the subgroups formed on the basis of *RAS/RAF* mutational status, may be identified and that these subgroups could be more likely to respond to either combination therapy, akin to patients with t(11;14) treated with ABT-199.[43]

Using both pharmacological and genetic methods, we determined that simultaneous inhibition of HDAC1 and HDAC2 was sufficient to induce apoptosis when combined with either MEK or BCL-2 inhibition. This is of interest because the clinical utility of the pan-HDAC inhibitor LBH589 in MM has been limited by toxicities, mostly related to diarrhea, fatigue, lymphopenia and thrombocytopenia,[15] which could perhaps be avoided with more specific HDAC inhibition. MS275 (entinostat), an HDAC1, 2, and 3 inhibitor, is actively being investigated in clinical trials for numerous tumor types.[46] Moreover, FK228 (romidepsin), which mostly inhibits HDAC1 and HDAC2, has been approved by the Food and Drug Administration for the treatment of several T-cell lymphomas.

Specific HDAC1+2 inhibition has previously been shown to drive apoptosis in lymphoid cell lines.[47] In MM, a prior study showed that the apoptosis induced by HDAC inhibitors is mainly mediated by HDAC class I inhibition.[48] Interestingly, elevated HDAC1 expression has been correlated with poor prognosis in MM.[49] In our study, we observed that both HDAC1 and HDAC2 must be inhibited for the synergistic effect with AZD6244 or ABT-199. Given the genetic and functional similarity between HDAC1 and 2, we think that it will be important to target both of these proteins simultaneously to attain meaningful clinical responses. It must be noted that while our approach using HDAC inhibition holds considerable promise in MM and other cancers, the pharmacological specificities of HDAC inhibitors have been inconsistently described to date, and often do not include specificity for particular HDAC1/2-containing multiprotein complexes such as CoREST.[14] Speculatively, perhaps inhibition of these complexes is important for the mechanisms described in the present study, rather than inhibition of the isolated enzymatic activity of HDAC1 and 2. If so, compounds with greater specificity for CoREST or

other HDAC1/2-containing complexes could achieve greater efficacy with potentially less toxicity.[50]

Acknowledgments

We thank Dr. Scott Kaufmann, M.D., Ph.D. for helpful discussions and commentary during the writing of this manuscript. We also thank the patients and their families for the gracious donation of their bone marrow aspirates to our laboratory. This work was funded by the Predolin Foundation, Mayo Clinic Hematology Small Grants Program, International Myeloma Foundation, CTSA grant number TL1TR002380 from the National Center for Advancing Translational Sciences (NCATS), Mayo Clinic Multiple Myeloma SPORE, Wendy Will Case Cancer Fund, Mayo Clinic Development Funds from the Myeloma, Amyloidosis and Dysproteinemia Disease Oriented Group (MADDOG), and the Mayo Clinic Office of Translation to Practice. Additionally, we would like to thank the American Association for Cancer Research for a Scholar-in-Training Award, and the American Society of Hematology for an HONORS award.

References

1. Rajkumar SV. Treatment of multiple myeloma. Nat Rev Clin Oncol. 2011;8(8):479-491.
2. Kyle RA, Therneau TM, Rajkumar SV, et al. Prevalence of monoclonal gammopathy of undetermined significance. N Engl J Med. 2006;354(13):1362-1369.
3. Noone AM, Howlader N, Krapcho M, et al. SEER Cancer Statistics Review, 1975-2015, National Cancer Institute. Bethesda, MD, https://seer.cancer.gov/csr/1975_2015/, based on November 2017 SEER data submission, posted to the SEER web site, April 2018.
4. Kumar SK, Dispenzieri A, Lacy MQ, et al. Continued improvement in survival in multiple myeloma: changes in early mortality and outcomes in older patients. Leukemia. 2014;28(5):1122-1128.
5. Sonneveld P, Avet-Loiseau H, Lonial S, et al. Treatment of multiple myeloma with high-risk cytogenetics: a consensus of the International Myeloma Working Group. Blood. 2016;127(24):2955-2962.
6. Kumar SK, Rajkumar SV. The multiple myelomas — current concepts in cytogenetic classification and therapy. Nat Rev Clin Oncol. 2018;15(7):409-421.
7. Chng WJ, Gonzalez-Paz N, Price-Troska T, et al. Clinical and biological significance of RAS mutations in multiple myeloma. Leukemia. 2008;22(12):2280-2284.
8. Lentzsch S, Chatterjee M, Gries M, et al. PI3-K/AKT/FKHR and MAPK signaling cascades are redundantly stimulated by a variety of cytokines and contribute independently to proliferation and survival of multiple myeloma cells. Leukemia. 2004;18(11):1883-1890.
9. Walker BA, Boyle EM, Wardell CP, et al. Mutational spectrum, copy number changes, and outcome: results of a sequencing study of patients with newly diagnosed myeloma. J Clin Oncol. 2015;33(33):3911-3920.
10. Rasmussen T, Kuehl M, Lodahl M, Johnsen HE, Dahl IM. Possible roles for activating RAS mutations in the MGUS to MM transition and in the intramedullary to extramedullary transition in some plasma cell tumors. Blood. 2005;105(1):317-323.
11. Kortüm KM, Mai EK, Hanafiah NH, et al. Targeted sequencing of refractory myeloma reveals a high incidence of mutations in CRBN and Ras pathway genes. Blood. 2016;128(9):1226-1233.
12. Ramakrishnan V, D'Souza A. Signaling pathways and emerging therapies in multiple myeloma. Curr Hematol Malig Rep. 2016;11(2):156-164.
13. Holkova B, Zingone A, Kmieciak M, et al. A phase 2 trial of AZD6244 (selumetinib, ARRY-142886), an oral MEK1/2 inhibitor, in relapsed/refractory multiple myeloma. Clin Cancer Res. 2016;22(5):1067-1075.
14. West AC, Johnstone RW. New and emerging HDAC inhibitors for cancer treatment. J Clin Invest. 2014;124(1):30-39.
15. Laubach JP, Moreau P, San-Miguel JF, Richardson PG. Panobinostat for the treatment of multiple myeloma. Clin Cancer Res. 2015;21(21):4767-4773.
16. Meng J, Fang B, Liao Y, Chresta CM, Smith PD, Roth JA. Apoptosis induction by MEK inhibition in human lung cancer cells is mediated by Bim. PLoS One. 2010;5(9):e13026.
17. Wang YF, Jiang CC, Kiejda KA, Gillespie S, Zhang XD, Hersey P. Apoptosis induction in human melanoma cells by inhibition of MEK is caspase-independent and mediated by the Bcl-2 family members PUMA, Bim, and Mcl-1. Clin Cancer Res. 2007;13(16):4934-4942.
18. Chen S, Dai Y, Pei XY, Grant S. Bim upregulation by histone deacetylase inhibitors mediates interactions with the Bcl-2 antagonist ABT-737: evidence for distinct roles for Bcl-2, Bcl-xL, and Mcl-1. Mol Cell Bio. 2009;29(23):6149-6169.
19. Ramakrishnan V, Kimlinger T, Timm M, Haug J, Rajkumar SV, Kumar S. Multiple mechanisms contribute to the synergistic anti-myeloma activity of the pan-histone deacetylase inhibitor LBH589 and the rapalog RAD001. Leuk Res. 2014;38(11):1358-1366.
20. Correia C, Lee S-H, Meng XW, et al. Emerging understanding of Bcl-2 biology: Implications for neoplastic progression and treatment. Biochim Biophys Acta. 2015;1853(7):1658-1671.
21. Kumar SK, Dimopoulos MA, Kastritis E, et al. Natural history of relapsed myeloma, refractory to immunomodulatory drugs and proteasome inhibitors: a multicenter IMWG study. Leukemia. 2017;31(11):2443-2448.
22. Ramakrishnan V, Ansell S, Haug J, et al. MRK003, a γ-secretase inhibitor exhibits promising in vitro pre-clinical activity in multiple myeloma and non-Hodgkin's lymphoma. Leukemia. 2012;26(2):340-348.
23. Kumar S, Raje N, Hideshima T, et al. Antimyeloma activity of two novel N-substituted and tetraflourinated thalidomide analogs. Leukemia. 2005;19(7):1253-1261.
24. Chou T-C, Talalay P. Quantitative analysis of dose-effect relationships: the combined effects of multiple drugs or enzyme inhibitors. Adv Enzyme Regul. 1984;22:27-55.
25. Ghobrial IM, Detappe A, Anderson KC, Steensma DP. The bone-marrow niche in MDS and MGUS: implications for AML and MM. Nat Rev Clin Oncol. 2018;15(4):219-233.
26. Cragg MS, Jansen ES, Cook M, et al. Treatment of B-RAF mutant human tumor cells with a MEK inhibitor requires Bim and is enhanced by a BH3 mimetic. J Clin Invest. 2008;118(11):3651-3659.
27. Dai H, Ding H, Meng XW, Lee SH, Schneider PA, Kaufmann SH. Contribution of Bcl-2 phosphorylation to Bak binding and drug resistance. Cancer Res. 2013;73(23):6998-7008.
28. Domina AM, Vrana JA, Gregory MA, Hann SR, Craig RW. MCL1 is phosphorylated in the PEST region and stabilized upon ERK activation in viable cells, and at additional sites with cytotoxic okadaic acid or taxol. Oncogene. 2004;23(31):5301-5315.
29. Kobayashi S, Lee S-H, Meng XW, et al. Serine 64 phosphorylation enhances the antiapoptotic function of Mcl-1. J Biol Chem. 2007;282(25):18407-18417.
30. Choudhary GS, Tat TT, Misra S, et al. Cyclin E/Cdk2-dependent phosphorylation of Mcl-1 determines its stability and cellular sensitivity to BH3 mimetics. Oncotarget. 2015;6(19):16912-16925.
31. Yee AJ, Bensinger WI, Supko JG, et al. Ricolinostat plus lenalidomide, and dexamethasone in relapsed or refractory multiple myeloma: a multicentre phase 1b trial. Lancet Oncol. 2016;17(11):1569-1578.
32. Tatamiya T, Saito A, Sugawara T, Nakanishi O. Isozyme-selective activity of the HDAC inhibitor MS-275. Cancer Res. 2004;64(7):567.
33. Sanchez-Vega F, Mina M, Armenia J, Chatila WK, et al. Oncogenic signaling pathways in The Cancer Genome Atlas. Cell. 2018;173(2):321-37.e10.
34. Zhao Y, Adjei AA. The clinical development of MEK inhibitors. Nat Rev Clin Oncol. 2014;11(7):385-400.
35. Mulligan, G, Lichter, DI, Di Bacco, A, et al. Mutation of NRAS but not KRAS significantly reduces myeloma sensitivity to single-agent bortezomib therapy. Blood. 2004;123(5):632-639.
36. Domina AM, Vrana JA, Gregory MA, Hann SR, Craig RW. MCL1 is phosphorylated in the PEST region and stabilized upon ERK activation in viable cells, and at additional sites with cytotoxic okadaic acid or taxol. Oncogene. 2004;23(31):5301-5315.
37. Wuilleme-Toumi S, Robillard N, Gomez P, et al. Mcl-1 is overexpressed in multiple myeloma and associated with relapse and shorter survival. Leukemia. 2005;19(7):1248-1252.
38. Gores GJ, Kaufmann SH. Selectively targeting Mcl-1 for the treatment of acute myel-

ogenous leukemia and solid tumors. Genes Dev. 2012;26(4):305-311.
39. Rooswinkel RW, van de Kooij B, de Vries E, et al. Antiapoptotic potency of Bcl-2 proteins primarily relies on their stability, not binding selectivity. Blood. 2014;123(18): 2806-2815.
40. Torres-Adorno AM, Lee J, Kogawa T, et al. Histone deacetylase inhibitor enhances the efficacy of MEK inhibitor through NOXA-mediated MCL1 degradation in triple-negative and inflammatory breast cancer. Clin Cancer Res. 2017;23(16):4780-4792.
41. Roberts AW, Davids MS, Pagel JM, et al. Targeting BCL2 with venetoclax in relapsed chronic lymphocytic leukemia. N Engl J Med. 2016;374(4):311-322.
42. Davids MS, Roberts AW, Seymour JF, et al. Phase I first-in-human study of venetoclax in patients with relapsed or refractory non-Hodgkin lymphoma. J Clin Oncol. 2017;35(8):826-833.
43. Kumar S, Kaufman JL, Gasparetto C, et al. Efficacy of venetoclax as targeted therapy for relapsed/refractory t(11;14) multiple myeloma. Blood. 2017;130(22):2401-2409.
44. Bose P, Gandhi V, Konopleva M. Pathways and mechanisms of venetoclax resistance. Leuk Lymphoma. 2017;58(9):1-17.
45. Caenepeel, S, Brown, SP, Belmontes B, et al. AMG 176, a selective MCL1 inhibitor, is effective in hematologic cancer models alone and in combination with established therapies. Cancer Discov. 2018;8(12):1582-1597.
46. Surolia I, Bates SE. Entinostat finds a path: a new study elucidates effects of the histone deacetylase inhibitor on the immune system. Cancer. 2018;124(24):4597-4600.
47. Stubbs MC, Kim W, Bariteau M, et al. Selective inhibition of HDAC1 and HDAC2 as a potential therapeutic option for B-ALL. Clin Cancer Res. 2015;21(10):2348-2358.
48. Mithraprabhu S, Khong T, Jones SS, Spencer A. Histone deacetylase (HDAC) inhibitors as single agents induce multiple myeloma cell death principally through the inhibition of class I HDAC. Br J Haematol. 2013;162(4):559-562.
49. Mithraprabhu S, Kalff A, Chow A, Khong T, Spencer A. Dysregulated class I histone deacetylases are indicators of poor prognosis in multiple myeloma. Epigenetics. 2014;9(11):1511-1520.
50. Kalin JH, Wu M, Gomez AV, et al. Targeting the CoREST complex with dual histone deacetylase and demethylase inhibitors. Nat Commun. 2018;9(1):53.

ARTICLE

Anti-apoptotic *BCL2L2* increases megakaryocyte proplatelet formation in cultures of human cord blood

Seema Bhatlekar,[1] Indranil Basak,[1] Leonard C. Edelstein,[2] Robert A. Campbell,[1] Cory R. Lindsey,[2] Joseph E. Italiano Jr.,[3] Andrew S. Weyrich,[1] Jesse W. Rowley,[1] Matthew T. Rondina,[1,4] Martha Sola-Visner[5] and Paul F. Bray[1,6]

[1]Program in Molecular Medicine and Department of Internal Medicine, University of Utah, Salt Lake City, UT; [2]Cardeza Foundation for Hematologic Research, Thomas Jefferson University, Philadelphia, PA; [3]Brigham and Women's Hospital, Harvard University, Boston, MA; [4]George E. Wahlen VAMC GRECC, Salt Lake City, UT; [5]Boston Children's Hospital, Harvard University, Boston, MA and [6]Division of Hematology and Hematologic Malignancies, Department of Internal Medicine, University of Utah, Salt Lake City, UT, USA

Ferrata Storti Foundation

Haematologica 2019
Volume 104(10):2075-2083

ABSTRACT

Apoptosis is a recognized limitation to generating large numbers of megakaryocytes in culture. The genes responsible have been rigorously studied *in vivo* in mice, but are poorly characterized in human culture systems. As CD34-positive ($^+$) cells isolated from human umbilical vein cord blood were differentiated into megakaryocytes in culture, two distinct cell populations were identified by flow cytometric forward and side scatter: larger size, lower granularity (LLG), and smaller size, higher granularity (SHG). The LLG cells were CD41a^{High} CD42a^{High} phosphatidylserine^{Low}, had an electron microscopic morphology similar to mature bone marrow megakaryocytes, developed proplatelets, and displayed a signaling response to platelet agonists. The SHG cells were CD41a^{Low}CD42a^{Low}phosphatidylserine^{High}, had a distinctly apoptotic morphology, were unable to develop proplatelets, and showed no signaling response. Screens of differentiating megakaryocytes for expression of 24 apoptosis genes identified *BCL2L2* as a novel candidate megakaryocyte apoptosis regulator. Lentiviral *BCL2L2* overexpression decreased megakaryocyte apoptosis, increased CD41a$^+$ LLG cells, and increased proplatelet formation by 58%. An association study in 154 healthy donors identified a significant positive correlation between platelet number and platelet *BCL2L2* mRNA levels. This finding was consistent with the observed increase in platelet-like particles derived from cultured megakaryocytes over-expressing *BCL2L2*. *BCL2L2* also induced small, but significant increases in thrombin-induced platelet-like particle αIIbβ3 activation and P-selectin expression. Thus, *BCL2L2* restrains apoptosis in cultured megakaryocytes, promotes proplatelet formation, and is associated with platelet number. *BCL2L2* is a novel target for improving megakaryocyte and platelet yields in *in vitro* culture systems.

Introduction

Hematopoietic stem cells (HSC) are essential for reconstituting hematopoiesis in the setting of bone marrow (BM) transplantation and are of great value for studies of the basic biology of hematopoiesis. Differentiating HSC into megakaryocytes (MK) in culture has become a standard approach to study megakaryocytopoiesis (MKpoiesis). MK culture systems are also powerful tools for the functional assessment of novel platelet genes, gene variants, protein-coding transcripts, and microRNA associated with platelet reactivity and clinical hemorrhagic or thrombotic disorders. Recent advancements in MKpoiesis research have opened up a new, promising field of *ex vivo* manufacturing of platelets,[1-4] with the ultimate goal of infusing these products into patients with thrombocytopenia or qualitative

Correspondence:

PAUL F. BRAY
paul.bray@hsc.utah.edu

Received: August 16, 2018.

Accepted: January 30, 2019.

Pre-published: February 7, 2019.

doi:10.3324/haematol.2018.204685

Check the online version for the most updated information on this article, online supplements, and information on authorship & disclosures: www.haematologica.org/content/104/10/2075

platelet disorders. Improvements in this technology may also allow 'designer' platelets to be engineered that overcome immunological incompatibility and infection issues.[5]

A major limitation of all MK culture systems is the relatively short time period for which the differentiating MK can be kept viable before they die through apoptosis.[6] The role of apoptosis during MKpoiesis is somewhat controversial,[7] with some data supporting a role for the intrinsic pathway of apoptosis in platelet production,[8-10] while other studies show that MK must restrain apoptosis to survive and progress safely through proplatelet formation and platelet generation.[11-13] However, the apoptosis regulators of human cord blood-derived (CB)-MK cultures remain poorly understood. During the course of our studies with cultured CB MK, we observed two distinct populations of cells by forward and side scatter flow cytometry. The aims of the current study were to determine: (i) whether there were viability and apoptosis differences between these two populations; and (ii) molecular mechanism(s) of apoptosis regulation during Mkpoiesis. We also wanted to begin to identify approaches that would reduce MK apoptosis in order to produce greater yields of MK and platelet in cultures. We demonstrate that the anti-apoptosis Bcl2 family member *BCL2L2* (encoding Bcl-w) regulates cultured MK apoptosis, promotes proplatelet formation, and is associated with human platelet number.

Methods

Primary megakaryocyte cultures

Human umbilical cord CB was obtained from the New York Blood Center (New York, NY, USA) under institutional review board (IRB) approval (00108527). $CD34^+$ hematopoietic stem and progenitor cells (HSPC) were isolated from human umbilical vein CB and cultured in serum free expansion media supplemented with 25 ng/mL of stem cell factor (SCF) and 20 ng/mL of thrombopoietin (TPO) (Peprotech, Rocky Hill, NJ, USA) for six days. Cells were cultured with 50 ng/mL TPO only from days 6-13.[14] Adult granulocyte-macrophage colony-stimulating factor (GM-CSF) mobilized $CD34^+$ HSPC were purchased from the Utah Cell Therapy and Regenerative Medicine Center (Salt Lake City, UT, USA) under the University of Utah IRB approval (00108527).

Megakaryocyte proplatelet formation assay

Day 9 transduced cells were plated at $2x10^4$ cells/mL in 60μ-Dish Grid-500 plates (Ibidi, Fitchburg, WI, USA) using fresh medium supplemented with 50 ng/mL TPO. On day 13, the proplatelet forming (PPF) MK, defined as displaying at least one filamentous pseudopod, were scored with a light microscope blinded as to experimental group. Images were taken at room temperature under 40x objective, numerical aperture 1.35, using FV1000 confocal laser scanning microscope (Olympus, Center Valley, PA, USA). The percentage of PPF MK was calculated as the number of PPF MK compared to the total number of round cultured cells analyzed. An average 200 cells were counted per condition.

Integrin αIIbβ3 activation assessment

Cells were resuspended in Tyrode's buffer (138 mM NaCl, 5.5 mM dextrose, 12 mM $NaHCO_3$, 0.8 mM $CaCl_2$, 0.4 mM $MgCl_2$, 2.9 mM KCl_2, 0.36 mM Na_2HPO_4, 20 mM Hepes, pH 7.4). Integrin αIIbβ3 activation was quantified with FITC-labeled PAC1 (1:100) (BD Pharmingen) in response to stimulation[15] with no agonist (resting), 100 μM PAR4-AP [GL Biochem (Shanghai) Ltd., China], 250 nM thrombin (Enzyme Research, South Bend, IN, USA) or 10 μg/mL CRP (synthesized at Baylor College of Medicine and cross-linked with glutaraldehyde) for 20 minutes (min) at 37°C, followed by 4% paraformaldehyde fixation at room temperature. Cells were analyzed on a Cytoflex or BD Accuri C6 flow cytometer.

Statistical analysis

All statistical analyses were performed using GraphPad Prism 6 software version 10.1 (La Jolla, CA, USA) and reported as Mean±Standard Error of Mean (SEM). Fold changes for *BCL2L2* levels over time in cultures and for lentiviral overexpression were presented as $\log_2$ (fold change) compared to their respective controls (day 6 for changes in *BCL2L2* levels over time and empty vector control for overexpression) and analyzed by a one-sample t-test. Log_2 transformation was adopted to have a normally distributed fold-change data, determined by Kolmogorov-Smirnov normality test. The relationship between platelet *BCL2L2* mRNA expression levels and platelet counts in the 154 healthy human donors in the Platelet RNA Expression Study 1 (PRAX-1) was assessed by Pearson's correlation with 95% Confidence Interval (95%CI). For all other analyses, statistical significance was assessed using paired Student *t*-test. $P<0.05$ was considered statistically significant.

See *Online Supplementary Appendix* for further details of the experiments.

Results

Subsets of cultured megakaryocytes show differing viability

$CD34^+$ cells were isolated from human umbilical vein CB and cultured to generate MK as described previously.[14] By day 13, $CD34^+$ cells were differentiated into MK, as demonstrated by the expression of mature MK markers (*Online Supplementary Figure S1A-D*). Day 13 MK were larger than day 0 HSC (*Online Supplementary Figure S1E*) and demonstrated polyploid MK (*Online Supplementary Figure S1F and G*). Thus, these culture conditions promoted generation of mature, polyploid MK.

Flow cytometric analysis of day 13 cultures revealed distinct cell populations differing by forward scatter (FSC) and side scatter (SSC) characteristics (Figure 1A): larger MK with lower granularity [larger, lower granular (LLG)] and smaller MK with higher granularity [smaller, higher granular (SHG)]. Peripheral blood (PB) mobilized adult $CD34^+$ cells cultured under the same conditions also generated similar subpopulations of MK (*Online Supplementary Figure S2*). Approximately 80% of LLG MK expressed both CD41a/CD42a and CD41a/CD42b markers, while only 20-30% SHG MK were double positive for mature MK markers (Figure 1B). Lower surface expression of CD42b (GPIbα) in day 13 SHG cells compared to LLG cells is consistent with mitochondrial damage[16] as observed in apoptotic adult mobilized HSPC-derived MK.[17]

Since the numbers of SHG MK showed less differentiation towards mature MK than the LLG MK, and because SHG MK showed reduced CD42b expression, we considered whether SHG MK may have undergone (or be undergoing) apoptosis. Figure 1C shows few $CD41a^+$ LLG MK-bound annexin V [termed phosphatidylserine $(PS)^{Low}$], a marker of apoptosis-induced phosphatidylserine expression, whereas a significantly higher percentage of $CD41a^+$ SHG MK bound annexin V (termed PS^{High}). Anti-annexin

V microbeads were used to separate day 13 PS^{Low} LLG MK from PS^{High} SHG MK (purity shown in *Online Supplementary Figure S3*). Transmission electron microscopy revealed that PS^{Low} LLG MK exhibited many typical features of BM MK, including large cells with multi-lobed nuclei, mitochondria, granules and surface protrusions (Figure 2A). In contrast, most of the PS^{High} SHG MK were apoptotic, displaying membrane blebbing, highly condensed or absent nuclei, and few or no granules (Figure 2B). $CD41a^{+}$ LLG MK showed a substantial increase in mitochondrial membrane potential compared to $CD41a^{+}$ SHG MK (Figure 1D), further supporting viability of the former.

Several approaches to characterize the functionality of the LLG and SHG MK were undertaken. The signaling capacity of these different MK populations was assessed and LLG, but not SHG, were able to activate integrin αIIbβ3 in response to agonist stimulation (Figure 3A). In addition, thrombin-induced Ca^{2+} mobilization was observed only in LLG cells but not in SHG cells (Figure 3B). Importantly, by day 13 we observed MK proplatelet formation (PPF). After separating LLG from SHG based on PS exposure, we observed more PPF in PS^{Low} LLG MK than in PS^{High} SHG MK (Figure 3C).

Next, we sought to address whether the LLG population was the origin of the SHG cells. Day 13 PS^{Low} LLG MK were isolated and labeled with lipophilic cell tracking dye DiO[18,19] and cultured for an additional 48 hours (h) to follow the 'movement' of the DiO label to SHG MK (Figure 3D). We observed an increase in DiO^{+} LLG MK at day 15 (Figure 3E). More importantly for this experiment, significantly more SHG MK contained tracking dye after an additional two days in culture (Figure 3E). These data indicate that CB-derived MK cultures represent a continuum of cells transitioning from mature viable $CD41a^{High}$ $CD42a^{High}$ PS^{Low} functional LLG MKs into $CD41a^{Low}$ $CD42a^{Low}$ PS^{High} apoptotic SHG MK.

BCL2L2 regulates megakaryocyte apoptosis and larger, lower granular megakaryocyte number

To begin to understand the molecular mechanisms regulating cultured MK apoptosis, we screened 24 genes with established roles in intrinsic and extrinsic apoptosis pathways whose expression changed as MK matured in culture. Because the percentages of SHG MK substantially increased between day 6 and day 13 (*Online Supplementary Figure S4*), we performed gene expression profiling on CD61-purified MK at these time points and observed a 3-fold and 12-fold increase, respectively, in *BCL2L1* and *BCL2L2*, two anti-apoptotic Bcl-2 family members (Figure 4A). *BCL2L1* encodes Bcl-xL and has an established role

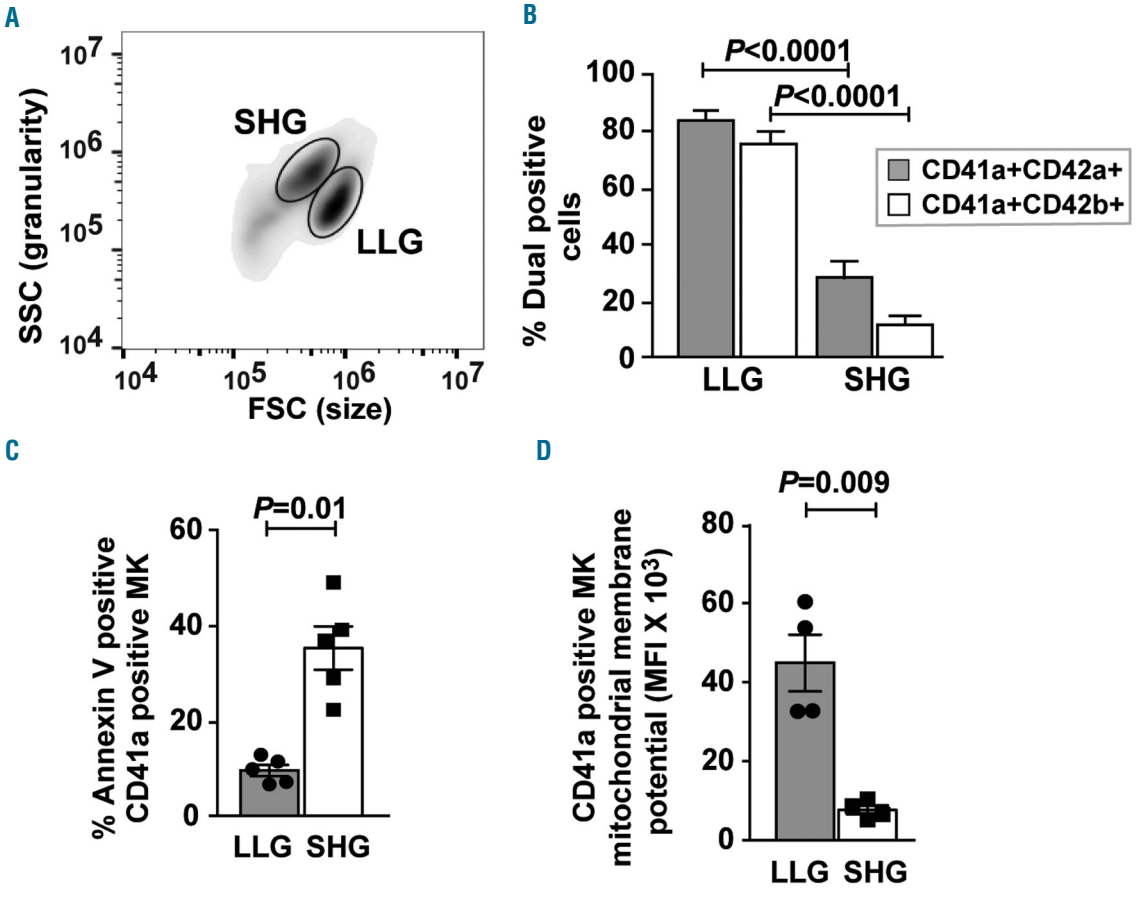

Figure 1. Two distinct populations emerge during cultured megakaryocytopoiesis. (A) Forward scatter (FSC) and side scatter (SSC) flow cytometric analysis of day 13 cultures showing the distinct larger size, lower granularity (LLG) and smaller size, higher granularity (SHG) populations of megakaryocytes (MK). (B) LLG and SHG cells were quantified for dual MK markers CD41aCD42a (n=10) and CD41aCD42b (n=10) by flow cytometry. (C) LLG and SHG MK were analyzed by flow cytometry using PE-labeled annexin V and APC-labeled anti-CD41a (n=5). (D) LLG and SHG MK were stained with APC-labeled anti-CD41a and TMRM to detect mitochondrial membrane potential and analyzed by flow cytometry (n=4). Error bars indicate mean±SEM. All assays performed on day 13 cultures.

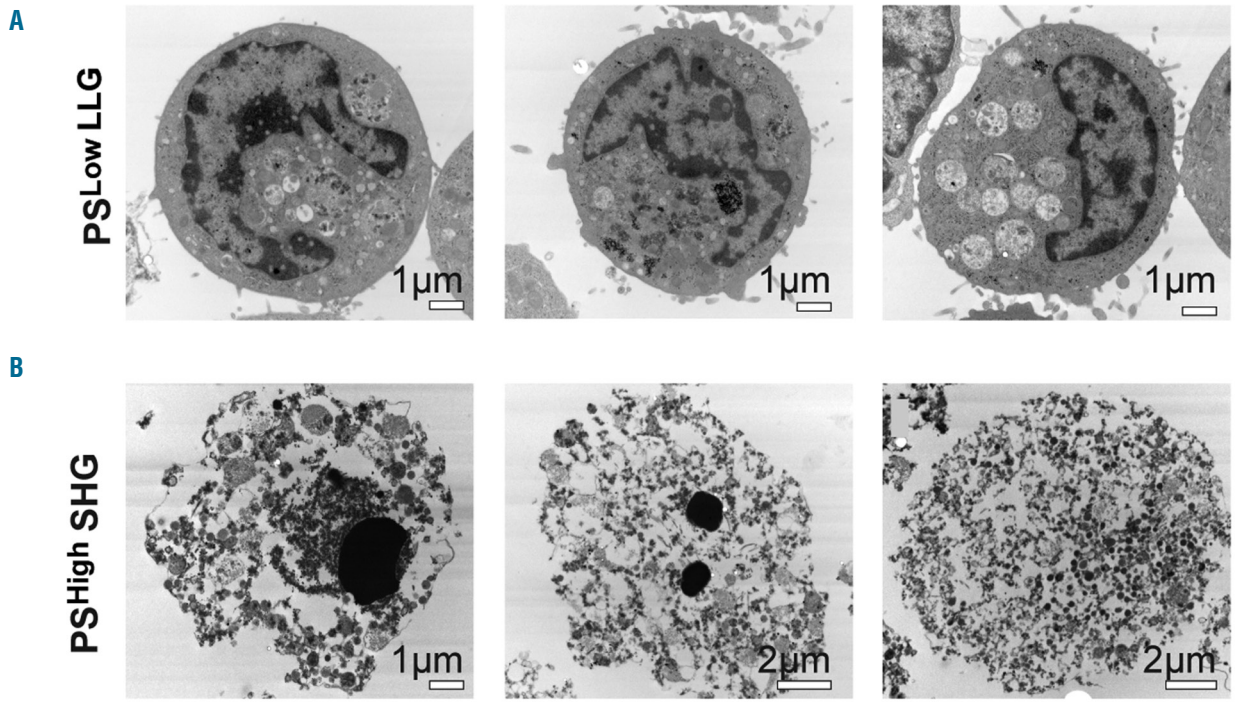

Figure 2. Transmission electron microscopy images of cultured megakaryocytes (MK). (A) Three representative annexin V microbead-isolated PS^{Low} larger size, lower granularity MK. (B) Three representative annexin V microbead-isolated PS^{High} smaller size, higher granularity MK.

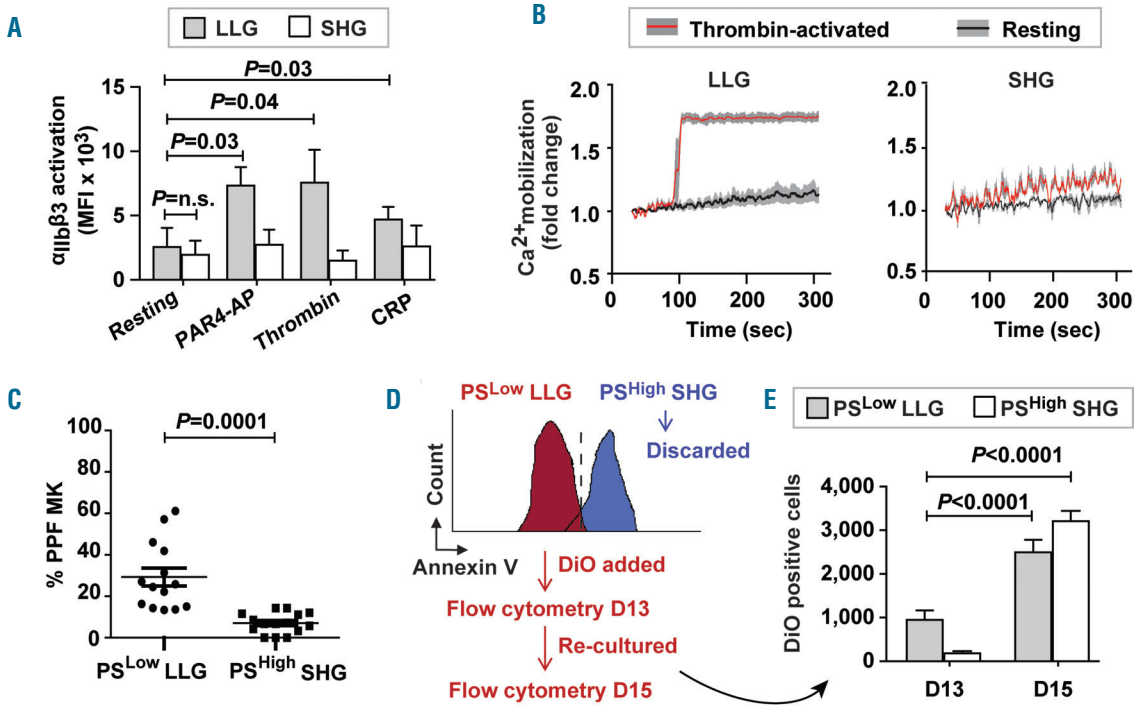

Figure 3. Larger size, lower granularity (LLG) and smaller size, higher granularity (SHG) megakaryocytes (MK) are viable and apoptotic, respectively. Assays performed on day 13 cultures for (A-C). (A) LLG and SHG MK were stimulated with PAR4-AP, thrombin, collagen related peptide (CRP) or no agonist (resting), and PAC1 binding (marker of integrin αIIbβ3 activation) was quantified by flow cytometry (n=4). n.s.: not significant. (B) LLG and SHG were stimulated with thrombin (red line) or no agonist (resting; black line) and calcium mobilization was measured (gray lines represent Standard Error of Mean for 3 separate experiments). (C) Quantification of proplatelet forming (PPF) MK blinded as to whether samples were PS^{Low} LLG or PS^{High} SHG cells. Data were collected from five independent cords and each data point represents the percentage of PPF MK counted from randomly selected objective field image. An average 200 cells were counted per cord sample. (D) Schematic outlining for DiO labeling experiment. Day 13 PS^{Low} LLG MK were separated from PS^{High} SHG MKs using annexin V microbeads. PS^{Low} LLG MK were labeled with Vybrant DiO cell tracking dye and re-cultured for two days. (E) Bar graph showing numbers of DiO-positive PS^{Low} LLG MKs and PS^{High} SHG MK at day 13 and day 15 (48 hours post DiO addition) (n=6).

in MKpoiesis.[12,13,20] However, *BCL2L2* (encoding Bcl-w) has not been studied in Mkpoiesis and became the focus of further investigation. The increase in expression of *BCL2L2* observed by RNA sequencing was verified by qPCR on RNA isolated from CD61-purified MK (Figure 4B). This led to the hypothesis that those MK with increasing levels of anti-apoptotic *BCL2L2* would be the LLG, whereas those MK with stable or decreasing levels of anti-apoptotic *BCL2L2* would be the SHG. LLG MK and SHG MK were purified by cell sorting and analyzed for changes in *BCL2L2* expression over time in culture. There was no difference between LLG and SHG cells for *BCL2L2* expression at days 6 and 9, but a significant difference was observed by day 13 due to a fall in *BCL2L2* in SHG cells and concomitant rise in LLG cells (Figure 4C).

We next considered the effects of *BCL2L2* on cultured MK apoptosis and number. Initially, we used the general Bcl-2 family inhibitor, ABT-263, to screen for an effect on CD41a$^+$ LLG MK numbers, and observed a significant reduction (*Online Supplementary Figure S5*). Since ABT-263 inhibits all Bcl-2 family members, we specifically tested the effects of *BCL2L2* on the cultured MK. CB-derived MK cultures were transduced with lentiviral vectors containing *BCL2L2*, and both mRNA and protein increased by day 13 (Figure 5A-C). *BCL2L2* overexpression significantly reduced the percentage of annexin V$^+$ CD41a$^+$ MK (Figure 5D) and increased the number of CD41a$^+$ LLG MK by 19% ($1.36x10^5$ to $1.61x10^5$; P=0.049).

BCL2L2 regulates megakaryocyte proplatelet formation

Megakaryocyte PPF is believed to be a critical process in thrombopoiesis. By day 13 we observed MK PPF primarily in LLG MK (Figure 3C), and asked whether Bcl-w might affect PPF. Importantly, when we scored MK PPF blinded to lentiviral transduction treatment group, we found that *BCL2L2* overexpression induced a significant 58% increase in PPF MK (Figures 5E and F).

Relationship between *BCL2L2* expression and platelet number

Megakaryocyte PPF is tightly linked to PB platelet count,[10,21,22] raising the possibility that *BCL2L2* may regulate platelet number as well as MKpoiesis. Because we had previously performed genome-wide platelet gene expression profiling in 154 healthy individuals,[14] we were able to query this dataset for such an association. Platelet *BCL2L2* mRNA levels were positively correlated with platelet count in the PRAX1-1 study (Figure 6A).

As is typical of MK culture systems, the day 13 cultures also contained a population of small, hypogranular particles that overlapped the forward and side scatter properties of normal human platelets (Figure 6B). These particles are typically referred to as platelet-like particles (PLP), and we assessed the effect of MK *BCL2L2* overexpression on PLP number and function. Compared to control lentiviral transduction, *BCL2L2* overexpression induced a modest but significant increase in CD41a$^+$ PLP from approximate-

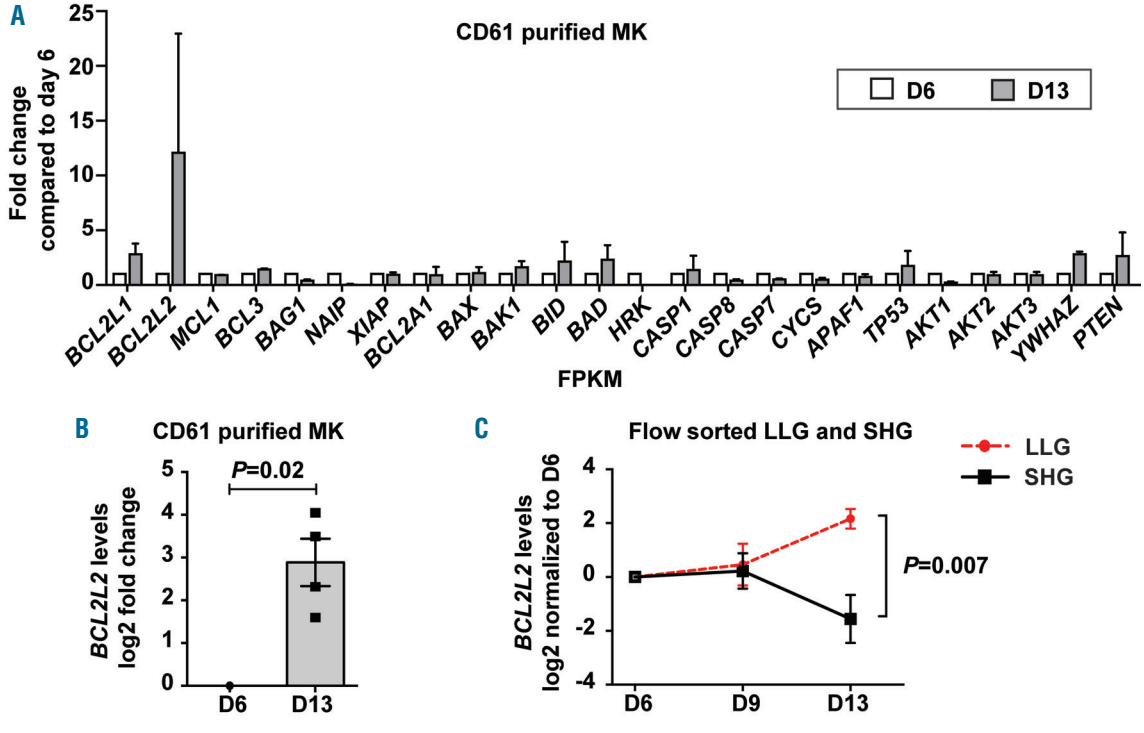

Figure 4. Expression of the anti-apoptotic gene *BCL2L2* increases functional megakaryocytes (MK). CD61$^+$ MK RNA was isolated from day 6 and day 13 cultures for analyses in (A) and (B). (A) CD61-positive ($^+$) MK expression of 24 apoptosis-related genes was assessed by RNA sequencing (n=3). Average fold changes in expression for day 13 *versus* day 6 are shown. (B) CD61$^+$ MK *BCL2L2* quantification by quantitative polymerase chain reaction (qPCR) (n=4). (C) Larger size, lower granularity (LLG) and smaller size, higher granularity (SHG) MK were flow cytometrically sorted and *BCL2L2* expression was quantified by qPCR. Fold changes were determined for LLG and SHG MK compared to their respective day 6 expression (n=4 for day 6 and day 13; n=6 for day 9).

ly 10% to approximately 19% (Figure 6C), suggesting *BCL2L2* enables mature platelet production.

Platelet-like particles were stimulated with thrombin to assess their ability to activate αIIbβ3 and release α-granules. PLP from both control and *BCL2L2* lentiviral constructs demonstrated cell activation above background (Figure 5D and E, and flow cytometry plots in *Online Supplementary Figure S6*); the signal was small but consistent in PLP with control lentivirus. Importantly, among these CD41a$^+$ and CD42a$^+$ PLP, MK *BCL2L2* overexpression enhanced thrombin-induced activation compared to control lentivirus (Figure 6D and E, and flow cytometry plots in *Online Supplementary Figure S6*). PAC1 binding and P-selectin expression in PLP treated with buffer instead of thrombin were not altered by *BCL2L2* overexpression (*data not shown*).

Discussion

There has been exciting progress in the generation of MK and platelets *via* the use of induced pluripotent stem cells, immortalized MK cell lines, and bioreactors,[1,23,24] but cultured human CB MK remain an important tool for gaining a deeper understanding of MKpoiesis and platelet production. Apoptosis of MK in a culture system remains a major obstacle to progress in the *in vitro* generation of MK and platelets.[6] A great deal of our understanding about the apoptosis genes regulating MKpoiesis and PB platelet number is derived from work in murine systems,[12,20,25-27] while relatively less is known about *in vitro* cultured MK apoptosis. The major finding in the current study is that the pro-survival gene *BCL2L2* restrains apoptosis in cultured human MK, regulates PPF, and is associated with platelet number in healthy humans. We also found that suspensions of CB-derived MK are a useful system for assessing candidate gene function by flow cytometric analysis, and that *BCL2L2* overexpression induced increases in agonist-induced signaling responses in PLP. *BCL2L2* thus becomes another potential target for enhancing MK yields *in vitro*, which may benefit both basic research on MKpoiesis and the long-term goal of producing platelets for transfusion into patients.

Two distinct populations of cells invariably emerged during our CB MK cultures that were easily distinguished by flow cytometry logarithmic scale forward and side scatter measures. Electron microscopic analysis of the LLG MK (Figure 2) demonstrated they were most similar to primary BM MK, and resembled those observed by Cramer *et al.*[28] and Chantelot-Bellanne *et al.*[29] In contrast, the SHG population represented primarily apoptotic cells resembling the senescent MK observed by Radley *et al.*, where the nucleus fragmented but the cells appeared to change shape and 'round up' rather than fragment.[30] Membrane degradation during apoptosis likely contributed to the loss of MK markers (Figure 1B). The most important functional differences between LLG and SHG were the ability to form proplatelets and 'signal' in response to platelet ago-

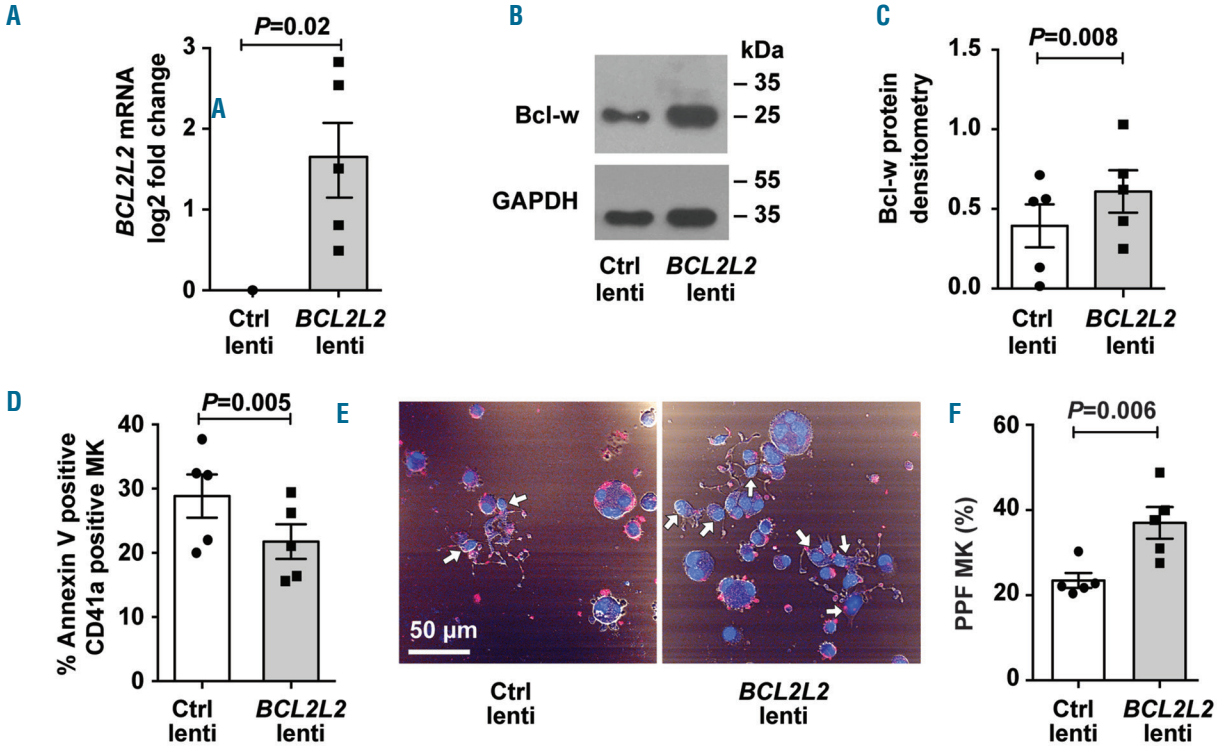

Figure 5. *BCL2L2* overexpression reduces megakaryocyte (MK) apoptosis. (A-F) Transduction of MK cultures with empty lentiviral vector (Ctrl lenti) or lentiviral vector containing *BCL2L2*. (A) Overexpression of *BCL2L2* mRNA was confirmed by quantitative polymerase chain reaction (qPCR). Fold change of *BCL2L2* mRNA levels was determined compared to Ctrl lenti (n=5). (B) Representative western blot image for Bcl-w protein (encoded by BCL2L2 gene) for *BCL2L2* overexpression compared to Ctrl. (C) Densitometric analysis of western blots for *BCL2L2* overexpression compared to Ctrl (n=5). Glyceraldehyde-3-phosphate dehydrogenase (GAPDH) was used as a normalizer for densitometric analysis. (D) The percentage of annexin V-positive (+) CD41a$^+$ MK was determined for *BCL2L2* over-expressed and Ctrl cells by flow cytometry (n=5). (E) Representative image of proplatelet formation in Ctrl and *BCL2L2* over-expressed cells. Image shows α-tubulin staining (red) and nuclear stain, DAPI (blue). White arrows show proplatelet-forming MK. (F) Quantification of proplatelet forming (PPF) MK amongst total cells blinded to treatment group (n=5).

nists (Figure 2A-C). It is worth noting that although PS-positivity marked apoptotic SHG MK, some fraction of LLG MK were also capable of PS exposure in response to thrombin stimulation (*Online Supplementary Figure S7*), perhaps akin to collagen and thrombin activated (COAT) platelets.[31-33] Thus, simple gating on flow cytometric forward and side scatter measurements, without the need for fluorescently-labeled antibodies, identified functional MK and can improve signal-to-noise read-outs that test the functionality of candidate MK/platelet genes.

Apoptosis was established as a mechanism for platelet lifespan by the Kile laboratory when they showed that the balance between Bcl-xL and Bak regulate murine lifespan *in vivo*.[20] The pro-survival Bcl-2 family member Bcl-xL degrades in aging platelets, thus allowing apoptosis to proceed. In addition to Bcl-xL, the Bcl-2 family includes Bcl-2, Mcl-1 and Bcl-w, which are encoded by *BCL2, MCL1* and *BCL2L2*, respectively. Altered murine expression of pro-survival Bcl-2 family members has shown variable effects on platelet number. Global chimeric vav-Bcl2 overexpression resulted in normal MK numbers but an approximately 50% reduction in platelet counts,[34] whereas MK-specific deletion of *Bcl2* had no effect on platelet number.[35] MK-specific deletion of *Bcl2l1* deletion caused MK apoptosis, loss of platelet shedding, and a macrothrombocytopenia.[12] MK-specific deletion of *Mcl1* did not affect MK number or morphology, or platelet count or volume.[13] Print *et al*. globally inactivated *Bcl2l2* to study its importance in murine physiology.[36] Although Mkpoiesis was not a major focus of their study, they reported that three *Bcl2l2*$^{-/-}$ mice displayed numbers of MK colony-forming cells and platelets comparable to three wild-type littermates. This latter report appears to differ from our finding in primary human MK and platelets, where *BCL2L2* increased during MK differentiation, overexpression of *BCL2L2* increased the numbers of both the viable CD41a^{+} LLG MK and MK PPF (Figure 4E and F), and *BCL2L2* levels correlated with platelet number (Figure 5A). This apparent discrepancy between human and mouse regarding the effect of *BCL2L2* on MKpoiesis and platelet production could be due to a compensatory upregulation of other Bcl-2 family members in the *Bcl2l2* null mice. Alternatively, small numbers of mice and different conditions may have led to a chance finding in the Print *et al*. study,[36] but there also may be species differences in the relative importance of *BCL2L2* because human platelets contain 3.6-fold higher levels of *BCL2L2* transcripts than mouse platelets.[37]

We showed that the SHG MK were derived from the LLG MK (Figure 2D and E), supporting a process by which viable LLG avoid apoptosis long enough to mature and acquire mature MK markers, but an unknown trigger induces some cells to become dying SHG. The day 9 to day 13 increase in *BCL2L2* is expected to restrain apoptosis in LLG cells, whereas *BCL2L2* reduction should enable apoptosis to proceed in SHG cells (Figure 3C). Perhaps a yet-to-be-defined switch regulates *BCL2L2* levels after day 9 in cultured cells. CB-derived LLG MK began to develop proplatelet extension around day 12 and peaked at days 13-15, similar to what had been reported by Balduini *et al*.[38] Because SHG appear days before PPF MK (*Online*

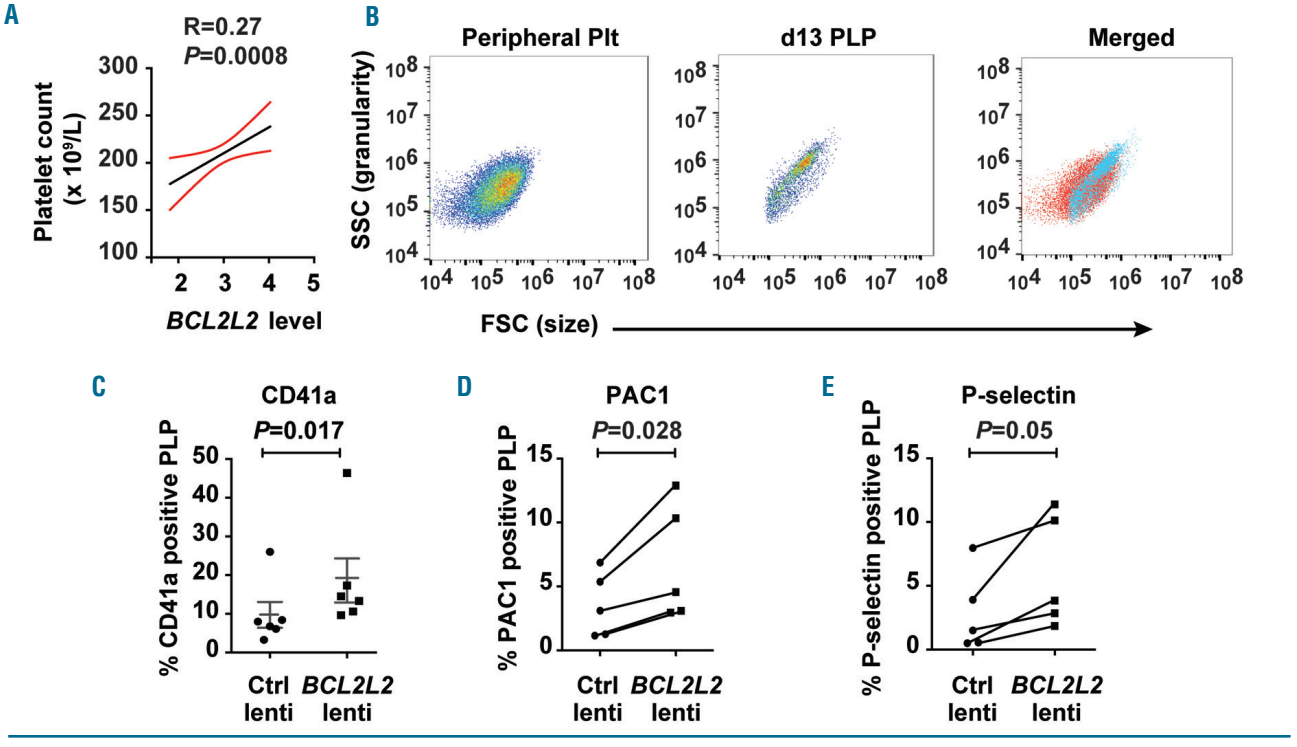

Figure 6. Relationship of *BCL2L2* to blood platelet number and cultured platelet-like particles (PLP). (A) *BCL2L2* is positively associated with peripheral blood platelet counts in 154 healthy individuals in the PRAX1 study. (B) Forward scatter and side scatter flow cytometric analysis of human peripheral blood platelets (Peripheral Plts), day 13 PLP and the merged image. (C-E) Flow cytometric assessment of cultured PLP after MK transduction with empty lentiviral vector (Ctrl lenti) or lentiviral vector containing *BCL2L2*. PLP were defined by forward scatter, side scatter and presence of platelet-specific surface marker (see Methods). (C) The percentages of day 13 PLP that were CD41a-positive (+) (n=6). (D) The percentages of day 13 PLP that bound PAC1 after stimulation with 250 nM thrombin (n=5). (E) The percentages of day 13 PLP that expressed P-selectin after stimulation with 250 nM thrombin (n=5).

Supplementary Figure S4), they do not seem to be 'exhausted' MK post release of proplatelets.

Sim *et al*. used adult mobilized HSPC to culture MK that also gave rise to populations of functional and apoptotic MK.[17] Our work differs from this primarily by studying the molecular mechanism of apoptosis. We are unaware of direct comparisons among any source of MK (neonatal, adult, murine, embryonic stem cells, etc.) in terms of the degree of apoptosis in culture, but it is reasonable to consider that some molecular mechanisms will be shared. In this regard, our data show no statistically significant difference between *BCL2L2* levels in neonatal and adult MK (P>0.47), and adult MK also display more PPF with *BCL2L2* overexpression (*Online Supplementary Figure S8*). As with MK, there is no statistically significant difference between *BCL2L2* levels in neonatal and adult platelets.[39]

The finding of a significant positive correlation between human platelet *BCL2L2* levels and PB platelet counts (Figure 5A) supports a mechanism whereby Bcl-w increases MK PPF which causes increased blood platelets. Numerous apoptosis genes have been studied for effects on Mkpoiesis.[8-13,19,40,41] We observed that pro-apoptotic genes *BAX* and *BAK1* showed little to no change in expression from day 6 to day 13 in MK cultures (*Online Supplementary Figure S9A and B*). However, similar to *BCL2L2*, anti-apoptotic gene *BCL2L1* showed increased expression in LLG over time, and was higher at day 13 in LLG compared to SHG (*Online Supplementary Figure S9C*). Taken together, these studies suggest *BCL2L1* and *BCL2L2* restrain apoptosis and that this may be the key mechanism for prolonging MK survival in the late stages of differentiation in culture. We cannot exclude a role for other apoptosis genes in Mkpoiesis and platelet production. It is also reasonable to consider that, like Bcl-xL and Bak, Bcl-w may also impact the life span of the human PB platelet.[20] However, additional studies are needed to address this possibility.

The *BCL2L2*-induced increase in MK PPF led to experiments assessing production of PLP. *BCL2L2* overexpression roughly doubled the number of $CD41a^+$ PLP and increased the ability of these PLP to show a functional response when activated with thrombin (Figure 5C-E). However, we did not observe any significant correlation between *in vivo BCL2L2* expression with other platelet agonists such as ADP, PAR1-AP and PAR4-AP (*www.Plateletomics.com*, as reported by Simon *et al.*[40]). Nevertheless, we would emphasize that the percentages of functional PLP were small, although consistent and statistically significant.

Our findings have several research and clinical implications. Firstly, we have shown that simple gating on flow cytometric forward and side scatter measurements allows the identification of the subset of viable and functional MK. This approach represents a substantial improvement in the signal-to-noise read-outs to test the functionality of candidate MK/platelet genes identified in GWAS. Secondly, promotion of apoptosis by inhibiting of Bcl-2 family members is under investigation for the treatment of a variety of malignancies;[41-43] a limiting toxicity has been thrombocytopenia.[42,43] Bcl-2 family members, *MCL1* and *BCL2L1* are the most frequently amplified in 26 tumor types,[44,45] whereas *BCL2L2* amplification is rare.[46] Perhaps selective targeting of Bcl-2 family members that spares Bcl-w could minimize thrombocytopenia. Lastly, progress toward the manufacture of *in vitro* platelets may benefit from the pro-survival benefits on MK generation and PPF of Bcl-w. *BCL2L2* overexpression may have synergistic or additive effects when used in combination with an antagonist of the aryl hydrocarbon receptor (StemRegenin 1), *BCL2L1* overexpression, abscisic acid, and other factors that have been shown to increase numbers of proplatelet-forming MK in culture.[1,47,48]

Funding

This study was supported by a grant from the National Institutes of Health National Heart, Lung and Blood Institute (HL116713) and funding from the Cardeza Foundation of Hematologic Research. The authors thank Ms. Lin Ma, Thomas Jefferson University, and Ms. Sarah Hugo, University of Utah for their help isolating cord blood stem cells; Dr. Xianguo Kong, Thomas Jefferson University for designing lentiviral vectors; Ms. Diana Lim, Molecular Medicine Program from University of Utah, for drafting the figures and consultation on data display.

Acknowledgments

The authors also thank the University of Utah Flow Cytometry Facility in addition to the National Cancer Institute through Award Number 5P30CA042014-24.

References

1. Ito Y, Nakamura S, Sugimoto N, et al. Turbulence Activates Platelet Biogenesis to Enable Clinical Scale Ex Vivo Production. Cell. 2018;174(3):636-648.e18.
2. Moreau T, Evans AL, Vasquez L, et al. Large-scale production of megakaryocytes from human pluripotent stem cells by chemically defined forward programming. Nat Commun. 2016;7:11208.
3. Nakamura S, Takayama N, Hirata S, et al. Expandable megakaryocyte cell lines enable clinically applicable generation of platelets from human induced pluripotent stem cells. Cell Stem Cell. 2014;14(4):535-548.
4. Thon JN, Dykstra BJ, Beaulieu LM. Platelet bioreactor: accelerated evolution of design and manufacture. Platelets. 2017;28(5):472-477.
5. Zhang N, Zhi H, Curtis BR, et al. CRISPR/Cas9-mediated conversion of human platelet alloantigen allotypes. Blood. 2016;127(6):675-680.
6. Zauli G, Vitale M, Falcieri E, et al. In vitro senescence and apoptotic cell death of human megakaryocytes. Blood. 1997;90(6):2234-2243.
7. Kile BT. The role of apoptosis in megakaryocytes and platelets. Br J Haematol. 2014;165(2):217-226.
8. Morison IM, Cramer Borde EM, Cheesman EJ, et al. A mutation of human cytochrome c enhances the intrinsic apoptotic pathway but causes only thrombocytopenia. Nat Genet. 2008;40(4):387-389.
9. Kaluzhny Y, Yu G, Sun S, et al. BclxL overexpression in megakaryocytes leads to impaired platelet fragmentation. Blood. 2002;100(5):1670-1678.
10. De Botton S, Sabri S, Daugas E, et al. Platelet formation is the consequence of caspase activation within megakaryocytes. Blood. 2002;100(4):1310-1317.
11. Kodama T, Takehara T, Hikita H, et al. BH3-only activator proteins Bid and Bim are dispensable for Bak/Bax-dependent thrombocyte apoptosis induced by Bcl-xL deficiency: molecular requisites for the mitochondrial pathway to apoptosis in platelets. J Biol Chem. 2011;286(16):13905-13913.
12. Josefsson EC, James C, Henley KJ, et al. Megakaryocytes possess a functional intrinsic apoptosis pathway that must be restrained to survive and produce platelets. J Exp Med. 2011;208(10):2017-2031.
13. Debrincat MA, Josefsson EC, James C, et al. Mcl-1 and Bcl-x(L) coordinately regulate megakaryocyte survival. Blood. 2012;119(24):5850-5858.

14. Edelstein LC, Simon LM, Montoya RT, et al. Racial differences in human platelet PAR4 reactivity reflect expression of PCTP and miR-376c. Nat Med. 2013;19(12):1609-1616.
15. Faraday N, Rade JJ, Johns DC, et al. Ex vivo cultured megakaryocytes express functional glycoprotein IIb-IIIa receptors and are capable of adenovirus-mediated transgene expression. Blood. 1999;94(12):4084-4092.
16. Bergmeier W, Burger PC, Piffath CL, et al. Metalloproteinase inhibitors improve the recovery and hemostatic function of in vitro-aged or -injured mouse platelets. Blood. 2003;102(12):4229-4235.
17. Sim X, Jarocha D, Hayes V, et al. Identifying and enriching the platelet-producing human stem cell-derived megakaryocytes using factor V uptake. Blood. 2017;130(2):192-204.
18. Parish CR. Fluorescent dyes for lymphocyte migration and proliferation studies. Immunol Cell Biol. 1999;77(6):499-508.
19. Ragnarson B, Bengtsson L, Haegerstrand A. Labeling with fluorescent carbocyanine dyes of cultured endothelial and smooth muscle cells by growth in dye-containing medium. Histochemistry. 1992;97(4):329-333.
20. Mason KD, Carpinelli MR, Fletcher JI, et al. Programmed anuclear cell death delimits platelet life span. Cell. 2007;128(6):1173-1186.
21. Beauchemin H, Shooshtarizadeh P, Vadnais C, Vassen L, Pastore YD, Moroy T. Gfi1b controls integrin signaling-dependent cytoskeleton dynamics and organization in megakaryocytes. Haematologica. 2017;102(3):484-497.
22. Machlus KR, Johnson KE, Kulenthirarajan R, et al. CCL5 derived from platelets increases megakaryocyte proplatelet formation. Blood. 2016;127(7):921-926.
23. Thon JN, Mazutis L, Wu S, et al. Platelet bioreactor-on-a-chip. Blood. 2014; 124(12):1857-1867.
24. Sugimoto N, Eto K. Platelet production from induced pluripotent stem cells. J Thromb Haemost. 2017;15(9):1717-1727.
25. McArthur K, Chappaz S, Kile BT. Apoptosis in megakaryocytes and platelets: the life and death of a lineage. Blood. 2018;131(6):605-610.
26. Schoenwaelder SM, Jarman KE, Gardiner EE, et al. Bcl-xL-inhibitory BH3 mimetics can induce a transient thrombocytopathy that undermines the hemostatic function of platelets. Blood. 2011;118(6):1663-1674.
27. White MJ, Schoenwaelder SM, Josefsson EC, et al. Caspase-9 mediates the apoptotic death of megakaryocytes and platelets, but is dispensable for their generation and function. Blood. 2012;119(18):4283-4290.
28. Cramer EM, Norol F, Guichard J, et al. Ultrastructure of platelet formation by human megakaryocytes cultured with the Mpl ligand. Blood. 1997;89(7):2336-2346.
29. Bellanne-Chantelot C, Schmaltz-Panneau B, Marty C, et al. Mutations in the SRP54 gene cause severe congenital neutropenia as well as Shwachman-Diamond-like syndrome. Blood. 2018;132(12):1318-1331.
30. Radley JM, Haller CJ. Fate of senescent megakaryocytes in the bone marrow. Br J Haematol. 1983;53(2):277-287.
31. Alberio L, Safa O, Clemetson KJ, Esmon CT, Dale GL. Surface expression and functional characterization of alpha-granule factor V in human platelets: effects of ionophore A23187, thrombin, collagen, and convulxin. Blood. 2000;95(5):1694-1702.
32. Dale GL, Friese P, Batar P, et al. Stimulated platelets use serotonin to enhance their retention of procoagulant proteins on the cell surface. Nature. 2002;415(6868):175-179.
33. Jobe SM, Leo L, Eastvold JS, et al. Role of FcRgamma and factor XIIIA in coated platelet formation. Blood. 2005; 106(13):4146-4151.
34. Ogilvy S, Metcalf D, Print CG, Bath ML, Harris AW, Adams JM. Constitutive Bcl-2 expression throughout the hematopoietic compartment affects multiple lineages and enhances progenitor cell survival. Proc Natl Acad Sci U S A. 1999;96(26):14943-14948.
35. Debrincat MA, Pleines I, Lebois M, et al. BCL-2 is dispensable for thrombopoiesis and platelet survival. Cell Death Dis. 2015;6:e1721.
36. Print CG, Loveland KL, Gibson L, et al. Apoptosis regulator bcl-w is essential for spermatogenesis but appears otherwise redundant. Proc Natl Acad Sci U S A. 1998; 95(21):12424-12431.
37. Rowley JW, Oler AJ, Tolley ND, et al. Genome-wide RNA-seq analysis of human and mouse platelet transcriptomes. Blood. 2011;118(14):e101-111.
38. Balduini A, Pallotta I, Malara A, et al. Adhesive receptors, extracellular proteins and myosin IIA orchestrate proplatelet formation by human megakaryocytes. J Thromb Haemost. 2008;6(11):1900-1907.
39. Caparros-Perez E, Teruel-Montoya R, Lopez-Andreo MJ, et al. Comprehensive comparison of neonate and adult human platelet transcriptomes. PLoS One. 2017; 12(8):e0183042.
40. Simon LM, Edelstein LC, Nagalla S, et al. Human platelet microRNA-mRNA networks associated with age and gender revealed by integrated plateletomics. Blood. 2014;123(16):e37-45.
41. Oltersdorf T, Elmore SW, Shoemaker AR, et al. An inhibitor of Bcl-2 family proteins induces regression of solid tumours. Nature. 2005;435(7042):677-681.
42. Roberts AW, Seymour JF, Brown JR, et al. Substantial susceptibility of chronic lymphocytic leukemia to BCL2 inhibition: results of a phase I study of navitoclax in patients with relapsed or refractory disease. J Clin Oncol. 2012;30(5):488-496.
43. Wilson WH, O'Connor OA, Czuczman MS, et al. Navitoclax, a targeted high-affinity inhibitor of BCL-2, in lymphoid malignancies: a phase 1 dose-escalation study of safety, pharmacokinetics, pharmacodynamics, and antitumour activity. Lancet Oncol. 2010; 11(12):1149-1159.
44. De Blasio A, Vento R, Di Fiore R. Mcl-1 targeting could be an intriguing perspective to cure cancer. J Cell Physiol. 2018; 233(11):8482-8498.
45. Beroukhim R, Mermel CH, Porter D, et al. The landscape of somatic copy-number alteration across human cancers. Nature. 2010;463(7283):899-905.
46. Cerami E, Gao J, Dogrusoz U, et al. The cBio cancer genomics portal: an open platform for exploring multidimensional cancer genomics data. Cancer Discov. 2012;2(5): 401-404.
47. Malara A, Fresia C, Di Buduo CA, et al. The Plant Hormone Abscisic Acid Is a Prosurvival Factor in Human and Murine Megakaryocytes. J Biol Chem. 2017;292 (8):3239-3251.
48. Strassel C, Brouard N, Mallo L, et al. Aryl hydrocarbon receptor-dependent enrichment of a megakaryocytic precursor with a high potential to produce proplatelets. Blood. 2016;127(18):2231-2240.

Ferrata Storti Foundation

Haematologica 2019
Volume 104(10):2084-2090

Complications of whole-exome sequencing for causal gene discovery in primary platelet secretion defects

Marcin M. Gorski,[1,2] Anna Lecchi,[1] Eti A. Femia,[1] Silvia La Marca,[1] Andrea Cairo,[1] Emanuela Pappalardo,[1,2] Luca A. Lotta,[1] Andrea Artoni[1] and Flora Peyvandi[1,2]

[1]Fondazione IRCCS Ca' Granda Ospedale Maggiore Policlinico, Angelo Bianchi Bonomi Hemophilia and Thrombosis Center, Milan and [2]Università degli Studi di Milano, Department of Pathophysiology and Transplantation and Fondazione Luigi Villa, Milan, Italy

ABSTRACT

Primary platelet secretion defects constitute a heterogeneous group of functional defects characterized by reduced platelet granule secretion upon stimulation by different agonists. The clinical and laboratory heterogeneity of primary platelet secretion defects warrants a tailored approach. We performed a pilot study in order to develop DNA sequence analysis pipelines for gene discovery and to create a list of candidate causal genes for platelet secretion defects. Whole-exome sequencing analysis of 14 unrelated Italian patients with primary secretion defects and 16 controls was performed on Illumina HiSeq. Variant prioritization was carried out using two filtering approaches: identification of rare, potentially damaging variants in platelet candidate genes or by selecting singletons. To corroborate the results, exome sequencing was applied in a family in which platelet secretion defects and a bleeding diathesis were present. Platelet candidate gene analysis revealed gene defects in 10/14 patients, which included *ADRA2A, ARHGAP1, DIAPH1, EXOC1, FCGR2A, ITPR1, LTBP1, PTPN7, PTPN12, PRKACG, PRKCD, RAP1GAP, STXBP5L*, and *VWF*. The analysis of singletons identified additional gene defects in *PLG* and *PHACTR2* in two other patients. The family analysis confirmed a missense variant p.D1144N in the *STXBP5L* gene and p.P83H in the *KCNMB3* gene as potentially causal. In summary, exome sequencing revealed potential causal variants in 12 of 14 patients with primary platelet secretion defects, highlighting the limitations of the genomic approaches for causal gene identification in this heterogeneous clinical and laboratory phenotype.

Correspondence:

FLORA PEYVANDI
flora.peyvandi@unimi.it

Received: August 21, 2018.

Accepted: February 22, 2019.

Pre-published: February 28, 2019.

doi:10.3324/haematol.2018.204990

Check the online version for the most updated information on this article, online supplements, and information on authorship & disclosures: www.haematologica.org/content/104/10/2084

Introduction

Disorders of platelet function are characterized by highly variable mucocutaneous bleeding manifestations and excessive hemorrhage following surgical procedures or trauma.[1-4] Primary platelet secretion defects (PSD) are the most common platelet functional defects[5] and display both clinical and laboratory heterogeneity.[6] From a clinical standpoint, PSD may be associated with a mild to severe bleeding tendency.[7] Thus, given the heterogeneous nature of PSD, laboratory testing is limited to specialized laboratories and accurate mechanistic diagnosis remains challenging.

Platelet aggregation and secretion studies with lumi-aggregometry, in which dense granule secretion is assessed in parallel with traditional light transmission aggregometry, provide evidence for platelet dysfunction.[8,9] PSD is characterized by reduced or absent δ-granule secretion upon stimulation by one or more platelet aggregation agonists either at low or high doses.[8,9] However, lumi-aggregometry, the gold standard technique for platelet function studies, is not always predictive of the molecular mechanisms, rendering the mechanistic differentiation of primary PSD difficult.

Multiple inherited alterations of platelet function have been described, including forms with different patterns of inheritance.[2,4,10] When the laboratory phenotype is

not discriminatory, genotyping using next-generation DNA sequencing (NGS) could be a comprehensive and cost-effective strategy for the diagnosis of platelet function disorders.[11-13] Indeed, NGS-based approaches, based on whole-exome sequencing (WES) or custom gene panels, proved to be successful for the diagnosis of inherited platelet defects.[11,13,14] Leo *et al.* applied WES to study 329 candidate genes involved in platelet function defects and identified gene variants in patients with defects in Gi signaling and with platelet secretion abnormalities.[15] WES was also successful in identifying causal mutations in the *RASGRP2* gene, which encodes a protein required for signaling and platelet activation,[16,17] and in identifying a causal mutation displaying autosomal dominant inheritance located in the *THBD* gene.[18] However, a standardized pipeline or procedure linking the identified gene defects to the specific sub-phenotype of diverse platelet function disorders is still lacking.

Given the positive experience acquired with the use of WES in identifying potentially pathogenic genetic variants in platelet function defects, the use of NGS-based diagnostics provides a great opportunity to improve causal gene identification and understand the underlying clinical phenotype.[19-22] For this reason, we decided to apply exome sequencing in a well-characterized group of patients with primary PSD and clinically relevant bleeding.[5] The aim of our pilot study was to test whether WES could be an adequate diagnostic tool for causal gene discovery in a heterogeneous group of platelet function defects such as primary PSD.

Methods

Study population

Fourteen unrelated patients with a diagnosis of primary PSD were enrolled from among 360 individuals with suspected platelet function disorders referred to our outpatient clinic at Ospedale Maggiore Policlinico (Milan, Italy).

The patients' inclusion criteria were: (i) European ancestry; (ii) platelet count >120x10^9/L; (iii) impaired platelet ATP secretion after stimulation with two or more agonists measured by lumi-aggregometry; (iv) normal expression of platelet glycoprotein (GP) Ib/IX/V and GPIIb/IIIa to exclude Bernard-Soulier syndrome and Glanzmann thrombasthenia; (v) absence of any other known platelet disorder; and (vi) absence of von Willebrand disease. Four family members of one patient (C740) were also included and studied.

All studied subjects abstained from taking drugs that affect platelet function for 2 weeks before blood sampling. All platelet function results were compared with our internal normal ranges.

The study was approved by the local Ethical Committee of the Ospedale Maggiore Policlinico and carried out according to the Declaration of Helsinki. All participants signed informed consent.

Platelet phenotyping

Personal and family histories and results of blood tests including a complete blood count, prothrombin time and activated partial thromboplastin time determined by standard methods, von Willebrand factor antigen and von Willebrand factor ristocetin cofactor determined by an automated latex enhanced immunoassay (Instrumentation Laboratory, Milan, Italy)[23] were collected (*Online Supplementary Methods*). The bleeding severity score (BSS) was calculated for each patient according to Tosetto *et al.*[24] (normal values: children <2; men <5; women <6).

Blood samples were drawn into trisodium citrate for coagulation, von Willebrand factor measurement, and platelet function studies and into K–EDTA for DNA extraction[25] and blood cell counts.

Platelet aggregation and ATP secretion induced by ADP (4 and 20 μM), collagen (2 μg/mL), thrombin receptor activator peptide-14 (10 μM), and thromboxane A2 analog U46619 (1 μM) were measured in platelet-rich plasma by lumi-aggregometry (Chronolog 560, Mascia Brunelli, Milan, Italy).[26] Platelet-rich plasma was prepared as previously reported.[27] Intraplatelet ADP, ATP, serotonin, and fibrinogen content were measured as previously reported[28,29] (*Online Supplementary Methods*).

Whole-exome sequencing

Individual exomes were enriched using a SeqCap EZ Human Exome Library Kit v2.0 (Roche NimbleGen) and paired-end sequencing was carried out on the HiSeq2000 (Illumina, San Diego, CA, USA) at the Beijing Genomics Institute (www.bgi.com).

The Short Oligonucleotide Analysis Package aligner (soap2.21)[30] was used to align reads to the reference human genome (hg19/GRCh37) and produce individual binary alignment map (BAM) files. The Genome Analysis Tool Kit was used for quality recalibration, duplicate read marking, insertions/deletions (indels) realignment, and BAM sorting to produce a merged, sample-level variant calling file (VCF) (*Online Supplementary Methods*).

Variant filtering and candidate gene discovery

Variant filtering and candidate gene discovery were performed on the project level, merged VCF file containing 14 unrelated Italian PSD patients and 16 healthy controls by using two different filtering strategies: selection of singletons and filtering for the single nucleotide variants (SNV) reported by Leo *et al.*[15] (*Online Supplementary Methods*).

Variant pathogenicity was assigned according to the American College of Medical Genetics and Genomics (ACMG) pathogenicity classification.[31] Platelet gene expression was evaluated using the Human Proteome Map (HPM).[32] (*Online Supplementary Methods*).

Results

Clinical characteristics of patients with platelet secretion defects

Of 360 patients with suspected platelet disorders investigated at our center, 14 unrelated patients (12 females and 2 males; median age 23 years) fulfilled the study inclusion criteria (Table 1). The patients' BSS ranged between 0 and 15 and 64% of the cases resulted abnormal (Table 1). Prothrombin time, activated partial thromboplastin time, plasma fibrinogen, and von Willebrand factor levels were within the normal ranges (*data not shown*). Platelet count was normal in all PSD patients (median 258 x10^9/L, minimum-maximum 120-357; normal values 150-450), except for patient C749 who had a slightly low platelet count (120 x10^9/L).

Platelet functions studies

Platelet aggregation was lower than the normal range in the majority of the patients with all agonists tested (Figure 1A) and rapidly reversible in 60% of the cases when induced by ADP (4 μM). Platelet ATP secretion was absent after stimulation by ADP (4 μM) in all patients and lower than the normal range in response to the other agonists in the majority of cases (Figure 1B). In particular, platelet

secretion was impaired with two stimuli in 4/14 patients, with three stimuli in 4/14, and with more than three stimuli in 6/14 (Table 1). These findings confirmed the diagnosis of primary PSD in all patients.

The concentrations of total serotonin, ADP, and ATP were normal in all patients as was the ATP/ADP ratio, which is considered a diagnostic hallmark for δ-storage pool deficiency (*Online Supplementary Table S1*). Similarly, fibrinogen from platelet α-granules was normal. All together, these data excluded that the secretion defect of these patients was attributable to the presence of α- or δ-storage pool deficiency.

Exome sequencing and candidate gene discovery

NGS data analysis revealed 101,562 variants that passed quality control and were sequenced with an average read depth of 51 over each site. Of those, 96,432 were single SNV and 5,130 were indels. The number of singletons, defined as private variants occurring exclusively in a single individual, was 11,430 (mean, 762) in PSD cases and 23,564 (mean, 1,473) in controls. In addition, we identified 30,973 rare variants with a minor allele frequency (MAF) ≤1% and 11,187 of these variants were considered novel, i.e., not listed in the Database of Single Nucleotide Polymorphisms (dbSNP) or any other variant database.

Table 1. Clinical and biological characteristics of 14 unrelated patients with platelet secretion defects.

ID	Sex	Age	BSS	Parents consang.	First-grade family Bleeding history	Platelet secretion stimulus				
						ADP 4 μM	ADP 20 μM	Collagen 2 μg/mL	U46619 1 μM	TRAP 10 μM
C696	F	34	4	no	No	+	-	-	+	-
C708	F	36	5	no	Mother (mild PSD)	+	+	+	+	-
C729	F	3	2	no	No	+	+	-	-	n/p
C732	F	25	15	no	No	+	+	-	+	-
C739	M	5	0	no	Mother	+	+	-	-	n/p
C740	M	19	10	no	Father (mild PSD), Sister (mild bleeding diathesis without PSD)	+	+	+	+	+
C749	F	55	9	no	Mother and sister with thrombocytopenia	+	+	+	-	+
C783	F	63	13	no	Mother	+	+	-	-	-
C797	F	31	5	no	No	+	+	-	+	-
C831	F	20	7	no	Mother	+	-	+	-	+
C847	F	19	7	no	Mother	+	+	-	+	+
C862	F	3	7	no	No	+	+	-	+	n/p
C1075	F	52	15	no	Brother	+	+	+	-	+
C1107	F	60	8	no	No	+	+	-	+	+

ID: patient identity; BSS: bleeding severity score; U46619: a thromboxane A2 analog; TRAP: thrombin receptor activator peptide. F: female; M: male; PSD: platelet secretion defect; (+) indicates defective platelet secretion response to the stimulus; (-) indicates response within the normal range; n/p: data not present.

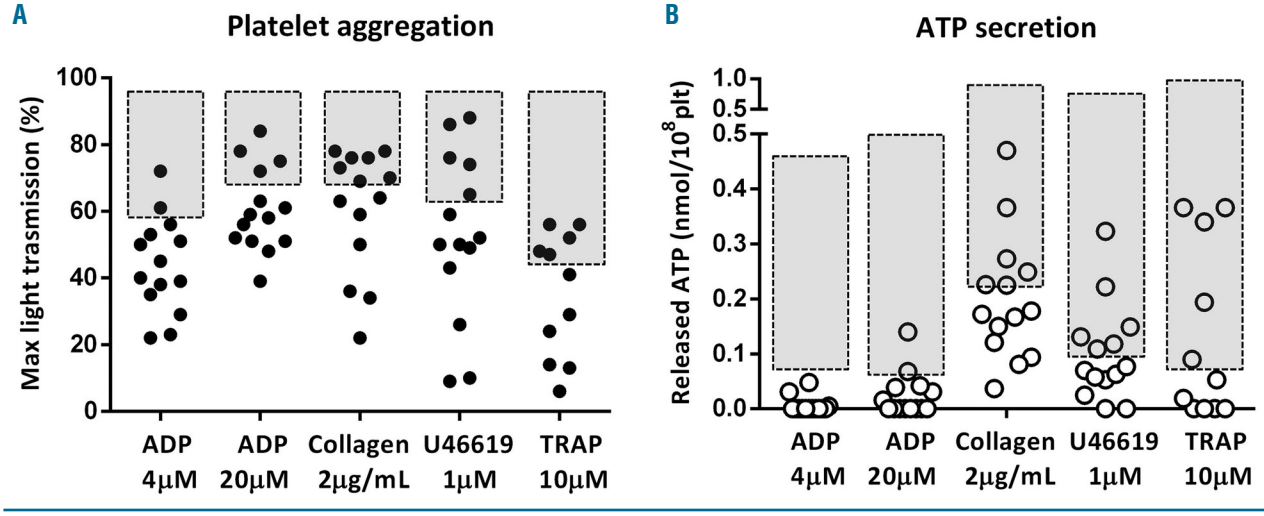

Figure 1. Platelet aggregation and secretion of 14 unrelated patients with platelet secretion defects. Dot plots of platelet (A) aggregation and (B) secretion. Boxes indicate our internal range of normality (5th-95th percentiles). U46619: thromboxane A2 analog; TRAP: thrombin receptor activator peptide.

Platelet candidate gene filtering approaches

Candidate gene discovery was carried out by two independent filtering approaches: by identification of variants in platelet candidate genes and by selecting singletons (*Online Supplementary Figure S1*). In the former approach, we selected from PSD patients all rare, potentially deleterious variants located in the coding regions of 329 candidate platelet genes listed by Leo *et al.*[15] This prioritizing strategy revealed 37 gene defects, of which six were novel (*Online Supplementary Table S2*). Since this variant prioritizing strategy yielded multiple SNV for the following patients, C729 (5 SNV), C732 (4 SNV), C739 (4 SNV), C740 (7 SNV), and C831 (4 SNV), we used the ACMG variant pathogenicity classification,[31] which revealed 14 gene defects classified as variants of uncertain significance (VUS) in eight patients. To provide functional analysis of these genes, we assessed their expression patterns in platelets using the HPM, which integrates mass spectrometry analysis of different human tissues and cell types as part of the human proteome project.[32] This evaluation identified potential gene defects in seven PSD patients, with the genes involved being: *EXOC1* (C732), *DIAPH1* (C739), *STXBP5L* and *PRKACG* (C740), *PTPN12* (C749), *VWF* (C831), *PRKCD* (C1075), *PTPN7* and *PRKCD* (C1107).

Singleton filtering approach

Given that the first approach failed to identify gene defects in six patients, we decided to apply another filtering strategy based on the isolation of singletons. To this end, we selected from all 14 patients private variants, which were rare and possibly deleterious and we obtained 2,875 SNV in 2,162 genes. To prioritize these SNV for their putative role in PSD, we performed functional annotation using the Database for Annotation, Visualization and Integrated Discovery (DAVID).[33] Significantly associated Gene Ontology (GO) annotations were found for gene clusters in the following functional categories: biological process - extracellular matrix organization for 48 genes (P=2.1x10^{-7}, Bonferroni P=9.9x10^{-4}); cellular component - basal lamina containing 10 genes (P=5.7x10^{-6}, Bonferroni P=4.4x10^{-3}); molecular function - extracellular matrix structural constituent comprising 22 genes (P=5.6x10^{-6}, Bonferroni P=8.3x10^{-3}). In addition, Kyoto Encylopedia of Genes and Genomes (KEGG) pathway analysis (*www.genome.jp/kegg/pathway.html*) revealed once again a cluster of 26 genes with functional annotation associated with extracellular matrix-receptor interactions (P=2.9x10^{-6}, Bonferroni P=7.9x10^{-4}). The extracellular matrix functional category can be defined as any material produced by cells and secreted into the surrounding medium, includiing collagen, laminin, fibronectin proteins and glycosaminoglycans (*http://www.uniprot.org/keywords/?query=Extracellular%20matrix*), indicating that our prioritizing method had indeed identified genes potentially affected in PSD.

Functional overlap between the above-mentioned gene clusters was achieved by enriching for variants present in genes exhibiting GO terms such as platelets and secretion, platelets and granules, platelets and signaling.

In this way, we identified 70 potential gene defects, of which 68 were missense variants. We also found a STOP gain variant in the *PHF14* gene (c.G298T, p.E100X) in patient C749 and a frameshift deletion in the *TBXAS1* gene (c.151_152delGT, p.V51fs) present in patient C831. Importantly, all 37 missense variants identified by filtering for gene defects in platelet candidate genes were also found in the list of singletons, which together produced a list of 107 candidate gene defects presented in *Online Supplementary Table S2*.

Similar to the previous filtering strategy, the singleton approach revealed an excess of potential gene defects in several patients (*Online Supplementary Table S2*). To be able to assign causality, a further reduction in the number of SNV was necessary. To this end, we once again used the ACMG variant pathogenicity classification,[31] which resulted in the identification of 22 putative gene defects classified as VUS in ten patients with primary PSD. However, only 13 of these variants were located in genes expressed in human platelets according to the HPM[32] (Table 2). In summary, this variant prioritization approach provided candidate gene defects for four patients, C696, C708, C797 and C847, for whom the previous strategy was ineffective. It is interesting to note that several of these gene defects were missing from the list of Leo *et al.*,[15] indicating that these genomic loci could potentially become novel candidate genes associated with PSD.

Family analysis of patient C740

Only one notable pedigree, case C740, was investigated. The distribution of the PSD phenotype and BSS in his relatives are reported in Figure 2 (father C1300, mother C1301, and two sisters C1302 and 1304). WES was performed in all four individuals and the variant filtering steps were based on MAF ≤1%, selecting SNV with potentially damaging consequences and assuming disease transmission present in affected and absent in unaffected family members (*Online Supplementary Figure S2*). Upon classification according to the ACMG,[31] four SNV were confirmed in a heterozygous state in PSD-affected C740 and father C1300, suggesting an autosomal dominant transmission of the disease. Two of the SNV, p.D1144N in the *STXBP5L* gene and p.P83H in the *KCNMB3* gene, classified as VUS (Table 3) may be involved in the secretion process, thus being the most probable gene defects responsible for the PSD phenotype in this family.

Discussion

In this pilot study, we performed WES in 14 unrelated Italian patients diagnosed with primary PSD and 16 healthy controls. We selected a group with a common phenotype characterized by impaired platelet aggregation and secretion with two or more stimuli as assessed with lumi-aggregometer and a normal platelet content of the granules, confirming the diagnosis of PSD. In our previous study, we demonstrated that a PSD was present in almost one fifth of patients with a mild bleeding diathesis.[5]

To identify causal genes underlying these defects, we carried out two prioritizing approaches, which were based on the identification of rare, potentially deleterious variants present in 329 platelet candidate genes listed by Leo *et al.*[15] or by selecting singletons (*Online Supplementary Figure S1*). These strategies revealed a number of plausible candidate gene defects explaining the phenotypic defects of primary PSD. For instance, patient C740 carries a missense variant p.D1144N in the *STXBP5L* gene (Table 2). In a recent report, another missense variant was identified in this gene as being potentially causal in platelet secretion

abnormalities.[15] Since STXBP5, a paralog of STXBP5L, promotes platelet secretion,[34,35] perhaps STXBP5L may also play a role in this process. Another interesting candidate is the *KCNMB3* gene that carries the p.P83H missense variant. This gene encodes the Calcium-Activated Potassium Channel Subunit Beta-3 protein involved in a pathway activated in response to elevated platelet cytosolic Ca^{2+}.

For patient C732, a gene defect was found in *EXOC1*, which is another candidate gene that influences platelet granule exocytosis. This gene encodes the Exocyst Complex Component 1 protein that functions as part of the exocyst complex and is required for targeting exocytic vesicles to specific docking sites on the plasma membrane.[36]

We also found a missense variant, p.A464P, in the *RAP1GAP* gene in patient C831. This variant has been classified as likely benign and for this reason, it was excluded from Table 2. Importantly, the Rap1GAP protein plays a regulatory role in platelet aggregation,[37] suggesting that this missense variant may actually have a functional role.

As previously reported, PSD can be associated with proteins acting at different levels: signal transduction, platelet activation, degranulation, or exocytosis.[4] Indeed, we found potential gene defects in proteins involved in all of these processes (Table 2). Importantly, several patients in our study had multiple defects in the above-mentioned genes and gene pathways, which may explain the com-

Table 2. Putative causal variants identified by whole-exome sequencing in 12/14 patients with primary platelet secretion defects according to the classification of Leo *et al.*[15] or by selecting singletons (*Online Supplementary Figure S1*). All variants were heterozygous.

ID	Gene	Nucleotide change	dbSNP	Amino acid change	MAF 1000G	MAF ESP	MAF ExAC	SIFT	Poly phen2	Mutation Taster	CADD C score	Platelet expression (*)	Assess. (**)
C696	*COL24A1*	c.G4673A	-	p.G1558E	-	-	-	D	D	D	25	-	VUS
C708	*TTN*	c.G106955A	rs200497615	p.R35652Q	-	0.0007	0.0003	B	B	D	25	+	VUS
	CSRNP1	c.C673T	rs142034027	p.R225W	-	0.0007	0.0001	D	D	D	32	-	VUS
	NRP1	c.G620A	rs148308681	p.R207H	-	0.0001	0.0001	D	D	D	33	-	VUS
C729	*TTN*	c.C104564A	-	p.S34855Y	-	-	-	D	D	D	20	+	VUS
	ITGA2	c.G305A	rs41392746	p.S102N	-	-	3.01E-05	B	B	B	20	+	VUS
	MYO3A	c.T1525C	rs150793986	p.Y509H	-	0.0003	0.0002	D	D	D	27	-	VUS
	MUC2	c.G6931A	rs200823008	p.V2311I	-	0.0001	0.0008	-	-	-	-	-	VUS
C732	*EXOC1*	c.G2009A	rs35001804	p.G670E	0.003	0.0086	0.009	D	D	D	32	+	VUS
C739	*DIAPH1*	c.T3227G	rs143763573	p.F1076C	-	-	0.0001	D	D	D	26	+	VUS
	ITPR3	c.C5720T	-	p.T1907M	-	-	-	D	D	D	33	+	VUS
C740	*TTN*	c.C72358T	rs372309164	p.L24120F	-	0.0002	0	B	D	D	18	+	VUS
	TTN	c.G1895A	rs150231219	p.G632D	-	0.0002	0	D	B	B	19	+	VUS
	SLC2A7	c.C670T	rs35776221	p.R224C	0.006	0.01	0.008	D	D	D	27	-	VUS
	STXBP5L	c.G3430A	rs139176240	p.D1120N	-	0.0001	0.0001	B	D	D	25	+	VUS
	KCNMB3	c.C248A	rs61734056	p.P83H	-	1.50E-05	0.0001	D	D	D	27	-	VUS
	LCN1	c.G298C	rs117638349	p.G100R	0.006	0.008	0.004	D	D	B	23	-	VUS
	PRKACG	c.C280T	-	p.R94C	-	-	-	D	D	B	23	+	VUS
	MUC2	c.G2594A	-	p.S865N	-	-	-	-	-	-	-	-	VUS
	MUC2	c.A5038G	rs371137719	p.T1680A	0.01	0.0024	0	-	-	-	-	-	VUS
C749	*LYST*	c.G8806A	rs2753327	p.V2936I	0.001	0.0009	0.0009	B	B	D	22	-	VUS
	TTN	c.G49413T	rs202094100	p.W16471C	-	0.0008	0.0006	D	D	D	24	+	VUS
	PHF14	c.G298T	-	p.E100X	-	-	-	-	-	D	38	-	VUS
	PTPN12	c.C1066T	rs752211731	p.P356S	-	-	0	D	D	D	27	+	VUS
C797	*TTN*	c.C17T	rs201490999	p.P6L	-	-	-	D	D	D	24	+	VUS
	EGF	c.G3073A	-	p.A1025T	-	-	-	B	B	D	15	+	VUS
C831	*TTN*	c.T15768A	rs138826545	p.H5256Q	-	0.0002	0.0002	B	B	D	12	+	VUS
	EGF	c.G1723A	rs115396821	p.G575R	0.008	0.0024	0.0027	D	D	D	26	+	VUS
	TBXAS1	c.151_152del	-	p.V51fs	-	-	-	-	-	-	-	+	VUS
	VWF	c.G8171A	-	p.C2724Y	-	-	-	D	D	D	26	+	VUS
C847	*TTN*	c.C91384T	rs373623340	p.R30462W	-	-	3.01E-05	D	D	D	26	+	VUS
	PHACTR2	c.G1360C	-	p.D454H	-	-	-	D	D	D	26	+	VUS
	NOS3	c.C3385T	rs774447524	p.R1129C	-	-	2.31E-05	D	D	D	34	-	VUS
C1075	*PRKCD*	c.A1043G	rs33911937	p.N348S	-	0.0015	0.0016	B	B	D	15	+	VUS
C1107	*PTPN7*	c.G425A	rs115136927	p.R142Q	0.003	0.0072	0.0062	B	D	D	27	+	VUS
	PRKCD	c.G868T	-	p.A290S	-	-	-	B	D	D	25	+	VUS
	MMRN1	c.G3680T	rs147451161	p.R1227L	0.003	0.0031	0.0036	D	D	D	28	+	VUS

dbSNP: Database of Single Nucleotide Polymorphisms v.138; MAF: minor allele frequency (MAF from European populations is shown); 1000G: the 1000 Genomes Project; ExAC: the Exome Aggregation Consortium; ESP: the Exome Sequencing Project; SIFT: Sorting Intolerant From Tolerant; PolyPhen2: Polymorphism Phenotyping v.2; Mutation Taster, prediction scores, D: damaging; B: benign; CADD C score: Combined Annotation Dependent Depletion score;[41] VUS: variant of uncertain significance. (*) Platelet gene expression evaluated by the Human Proteome Map (HPM) (*http://www.humanproteomemap.org*);[32] (**) Assess. – Assessment of variant pathogenicity assigned according to the American College of Medical Genetics and Genomics pathogenicity classification.[31]

Table 3. Putative causal variants identified by whole-exome sequencing in the family of patient C740 (*Online Supplementary Figure S2*).

Gene	dbSNP	Nucl. change	Amino acid change	C740	C1300	C1301	C1302	C1304	MAF 1000G	MAF ExAC	MAF ESP	SIFT	Poly phen2	Mutation Taster	CADD C score	Plt Exp. (*)	Assess (**)
SLC2A7	rs35776221	c.C670T	p.R224C	het	het	-	-	-	0.006	0.01	0.008	D	D	D	27	-	VUS
STXBP5L	rs139176240	c.G3430A	p.D1144N	het	het	-	-	-	-	0.0004	0.0001	B	D	D	25	+	VUS
KCNMB3	rs61734056	c.C248A	p.P83H	het	het	-	-	-	-	1.50E-05	0.0001	D	D	D	27	-	VUS
LCN1	rs117638349	c.G298C	p.G100R	het	het	-	-	-	0.006	0.008	0.004	D	D	B	23	-	VUS

dbSNP: Database of Single Nucleotide Polymorphisms v.138; MAF: minor allele frequency (MAF from European populations is shown); 1000G: the 1000 Genomes Project; ExAC: the Exome Aggregation Consortium; ESP: the Exome Sequencing Project; SIFT: Sorting Intolerant From Tolerant; PolyPhen2: Polymorphism Phenotyping v.2; Mutation Taster, prediction scores, D: damaging; B: benign; CADD C score: Combined Annotation Dependent Depletion score;[41] VUS: variant of uncertain significance. (*) Platelet gene expression evaluated by the Human Proteome Map (HPM) (*http://www.humanproteomemap.org*);[32] (**) Assess. – Assessment of variant pathogenicity assigned according to the American College of Medical Genetics and Genomics pathogenicity classification.[31]

plex and heterogeneous nature of primary PSD. This indicates that an in-depth functional analysis of platelet receptor and signaling pathways will be necessary to discriminate differences in clinical and laboratory phenotypes of affected individuals.

Study limitations

Following a positive experience with the application of WES to identify gene defects underlying inherited platelet function disorders,[19-22] we chose to investigate primary PSD using the same technique, hoping that a genomic approach could be effective in identifying causal variants in a heterogeneous clinical and phenotype such as primary PSD. However, exome sequencing followed by two independent variant prioritization approaches yielded inconclusive results. The primary reason for this is undoubtedly the heterogeneous clinical and laboratory phenotype of primary PSD, which may have led to the identification of genes not necessarily associated with the disease. For instance, 20 missense variants were detected in the *TTN* gene in 11 PSD patients, of which eight are VUS. However, *TTN* is one of the most frequently mutated genes in the human genome,[38] implying that the variations found in this gene are probably due to the size of its coding regions (363 exons).

Another limitation of this study was perhaps the choice of the variant prioritization strategy. We applied a generally accepted filtering method based on the selection of rare (MAF ≤1%), potentially damaging variants. This approach revealed a great abundance of variants for most patients, which required further selection based on the ACMG pathogenic classification of SNV (Table 2). This revealed 34 putative gene defects classified as VUS in 12 patients with primary PSD, of which 24 were located in genes expressed in human platelets according to the HPM (Table 2). However, it is possible that many potentially causal SNV, which were classified as likely benign or benign, were excluded due to lack of supporting evidence or because the gene defects may only manifest at the level of megakaryocyte development or platelet maturation.

In addition, some of the functional defects might have been located in the non-coding parts of the genome such as promoters, intronic sequences or enhancers, which were not covered by exome sequencing. Finally, since the identification of gross chromosomal aberration such as copy number variations from the WES data remains a technical challenge, it is likely that these structural variants would not have been detected. Although several bioinformatics methods have been developed for copy number variation analysis from WES data, they require uniform coverage and high resolution of the sequencing data across all exons/coding regions as well as a specialized bioinformatics pipeline of data analysis validated against the whole-genome data.[39] For this reason, whole-genome sequencing is the only sure means for identifying the copy number variations alongside SNV and small indels.

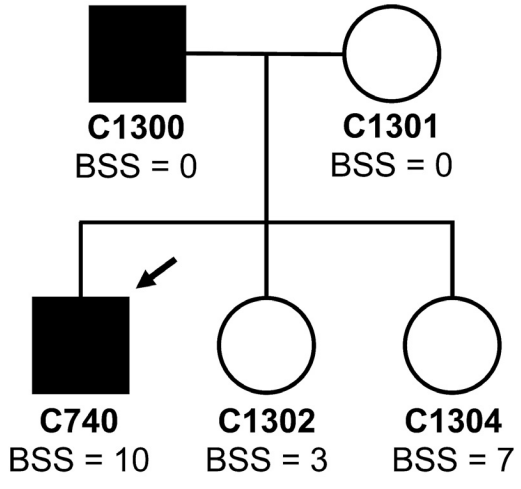

Figure 2. Pedigree of patient C740. Black and white symbols indicate subjects affected by platelet secretion defects and unaffected family members, respectively. The arrow indicates the proband C740. BSS: bleeding severity score.

In conclusion, we carried out exome sequencing in 14 patients with primary PSD and 16 healthy controls, followed by two variant prioritization strategies. Our analysis identified potential gene defects in 12 patients, implying that the NGS-based diagnostic strategies for causal gene identification in such a heterogeneous clinical and laboratory phenotype as primary PSD may be ineffective. In this case, a well-defined, common disease phenotyping and properly established pipeline for variant analysis are necessary. The difficulty in assigning causality can be overcome by genetic screening of affected and unaffected family members, which allows the identification of gene defects that segregate with the clinical phenotype, or by functional studies.

The perils of genetic data sharing with patients may involve ethical concerns, lack of confidence in assessing the causality of identified variants, and the implication of some inherited platelet pathologies with other risks.[40] For these reasons, sharing genetic data with patients is still an open issue that requires further discussion.

Acknowledgments

This study was supported by Bayer Hemophilia Award Program (BHAP) 2011- Special Project Award to Flora Peyvandi and by BHAP 2012 - Early Career Award to Luca A. Lotta. We thank Prof. Pier Mannuccio Mannucci for his critical revision of the manuscript.

References

1. Cattaneo M. Inherited platelet-based bleeding disorders. J Thromb Haemost. 2003;1 (7):1628-1636.
2. Hayward CP, Rao AK, Cattaneo M. Congenital platelet disorders: overview of their mechanisms, diagnostic evaluation and treatment. Haemophilia. 2006;12(Suppl 3):128-136.
3. Hayward CP, Rivard GE. Quebec platelet disorder. Expert Rev Hematol. 2011;4(2): 137-141.
4. Nurden A, Nurden P. Advances in our understanding of the molecular basis of disorders of platelet function. J Thromb Haemost. 2011;9 (Suppl 1):76-91.
5. Lotta L, Maino A, Tuana G, et al. Prevalence of disease and relationships between laboratory phenotype and bleeding severity in platelet primary secretion defects. PLoS One. 2013;8(4):e60396.
6. Rao AK, Jalagadugula G, Sun L. Inherited defects in platelet signaling mechanisms. Semin Thromb Hemost. 2004;30(5):525-535.
7. Quiroga T, Goycoolea M, Panes O, et al. High prevalence of bleeders of unknown cause among patients with inherited mucocutaneous bleeding. A prospective study of 280 patients and 299 controls. Haematologica. 2007;92(3):357-365.
8. Cattaneo M. Light transmission aggregometry and ATP release for the diagnostic assessment of platelet function. Sem Thromb Hemost. 2009;35(2):158-167.
9. Pai M, Wang G, Moffat KA, et al. Diagnostic usefulness of a lumi-aggregometer adenosine triphosphate release assay for the assessment of platelet function disorders. Am J Clin Pathol. 2011;136(3):350-358.
10. Cattaneo M. Molecular defects of the platelet P2 receptors. Purinergic Signal. 2011;7(3):333-339.
11. Bastida JM, Lozano ML, Benito R, et al. Introducing high-throughput sequencing into mainstream genetic diagnosis practice in inherited platelet disorders. Haematologica. 2018;103(1):148-162.
12. Peyvandi F, Hayward CP. Genomic approaches to bleeding disorders. Haemophilia. 2016;22 (Suppl 5):42-45.
13. Simeoni I, Stephens JC, Hu F, et al. A high-throughput sequencing test for diagnosing inherited bleeding, thrombotic, and platelet disorders. Blood. 2016;127(23):2791-2803.
14. Leinoe E, Zetterberg E, Kinalis S, et al. Application of whole-exome sequencing to direct the specific functional testing and diagnosis of rare inherited bleeding disorders in patients from the Oresund Region, Scandinavia. Br J Haematol. 2017;179(2): 308-322.
15. Leo VC, Morgan NV, Bem D, et al. Use of next-generation sequencing and candidate gene analysis to identify underlying defects in patients with inherited platelet function disorders. J Thromb Haemost. 2015;13 (4):643-650.
16. Lozano ML, Cook A, Bastida JM, et al. Novel mutations in RASGRP2, which encodes CalDAG-GEFI, abrogate Rap1 activation, causing platelet dysfunction. Blood. 2016;128(9):1282-1289.
17. Sevivas T, Bastida JM, Paul DS, et al. Identification of two novel mutations in RASGRP2 affecting platelet CalDAG-GEFI expression and function in patients with bleeding diathesis. Platelets. 2018;29(2):192-195.
18. Maclachlan A, Dolan G, Grimley C, Watson SP, Morgan NV, on behalf of the Uk Gapp Study Group. Whole exome sequencing identifies a mutation in thrombomodulin as the genetic cause of a suspected platelet disorder in a family with normal platelet function. Platelets. 2017;28(6):611-613.
19. Bariana TK, Ouwehand WH, Guerrero JA, Gomez K. Dawning of the age of genomics for platelet granule disorders: improving insight, diagnosis and management. Br J Haematol. 2017;176(5):705-720.
20. Heremans J, Freson K. High-throughput sequencing for diagnosing platelet disorders: lessons learned from exploring the causes of bleeding disorders. Int J Lab Hematol. 2018;40 (Suppl 1):89-96.
21. Lentaigne C, Freson K, Laffan MA, Turro E, Ouwehand W. Inherited platelet disorders: toward DNA-based diagnosis. Blood. 2016;127(23):2814-2823.
22. Westbury SK, Mumford AD. Genomics of platelet disorders. Haemophilia. 2016;22 (Suppl 5):20-24.
23. Lotta LA, Lombardi R, Mariani M, et al. Platelet reactive conformation and multimeric pattern of von Willebrand factor in acquired thrombotic thrombocytopenic purpura during acute disease and remission. J Thromb Haemost. 2011;9(9):1744-1751.
24. Tosetto A, Rodeghiero F, Castaman G, et al. A quantitative analysis of bleeding symptoms in type 1 von Willebrand disease: results from a multicenter European study (MCMDM-1 VWD). J Thromb Haemost. 2006;4(4):766-773.
25. Lotta LA, Wang M, Yu J, et al. Identification of genetic risk variants for deep vein thrombosis by multiplexed next-generation sequencing of 186 hemostatic/pro-inflammatory genes. BMC Med Genomics. 2012;5(7):1-8.
26. Cattaneo M, Cerletti C, Harrison P, et al. Recommendations for the standardization of light transmission aggregometry: a consensus of the Working Party from the Platelet Physiology Subcommittee of SSC/ISTH. J Thromb Haemost. 2013;11 (6):1183-1186.
27. Femia EA, Pugliano M, Podda G, Cattaneo M. Comparison of different procedures to prepare platelet-rich plasma for studies of platelet aggregation by light transmission aggregometry. Platelets. 2012;23(1):7-10.
28. Cattaneo M, Bettega D, Lombardi R, Lecchi A, Mannucci PM. Sustained correction of the bleeding time in an afibrinogenaemic patient after infusion of fresh frozen plasma. Br J Haematol. 1992;82(2):388-390.
29. Cattaneo M, Lecchi A, Lombardi R, Gachet C, Zighetti ML. Platelets from a patient heterozygous for the defect of P2CYC receptors for ADP have a secretion defect despite normal thromboxane A2 production and normal granule stores: further evidence that some cases of platelet 'primary secretion defect' are heterozygous for a defect of P2CYC receptors. Arterioscler Thromb Vasc Biol. 2000;20(11):101-106.
30. Li R, Yu C, Li Y, et al. SOAP2: an improved ultrafast tool for short read alignment. Bioinformatics. 2009;25(15):1966-1967.
31. Richards S, Aziz N, Bale S, et al. Standards and guidelines for the interpretation of sequence variants: a joint consensus recommendation of the American College of Medical Genetics and Genomics and the Association for Molecular Pathology. Genet Med. 2015;17(5):405-424.
32. Kim MS, Pinto SM, Getnet D, et al. A draft map of the human proteome. Nature. 2014;509(7502):575-581.
33. Huang DW, Sherman BT, Tan Q, et al. DAVID bioinformatics resources: expanded annotation database and novel algorithms to better extract biology from large gene lists. Nucleic Acids Res. 2007;35(Web Server issue):W169-W175.
34. Ye S, Huang Y, Joshi S, et al. Platelet secretion and hemostasis require syntaxin-binding protein STXBP5. J Clin Invest. 2014;124(10): 4517-4528.
35. Zhu Q, Yamakuchi M, Ture S, et al. Syntaxin-binding protein STXBP5 inhibits endothelial exocytosis and promotes platelet secretion. J Clin Invest. 2014;124(10):4503-4516.
36. Lipschutz JH, Mostov KE. Exocytosis: the many masters of the exocyst. Curr Biol. 2002;12(6):212-214.
37. Schultess J, Danielewski O, Smolenski AP. Rap1GAP2 is a new GTPase-activating protein of Rap1 expressed in human platelets. Blood. 2005;105(8):3185-3192.
38. Shyr C, Tarailo-Graovac M, Gottlieb M, Lee JJ, van KC, Wasserman WW. FLAGS, frequently mutated genes in public exomes. BMC Med Genomics. 2014;7(64):1-11
39. Eilbeck K, Quinlan A, Yandell M. Settling the score: variant prioritization and Mendelian disease. Nat Rev Genet. 2017;18(10):599-612.
40. Greinacher A, Eekels JJM. Diagnosis of hereditary platelet disorders in the era of next-generation sequencing:"primum non nocere". J Thromb Haemost. 2019; 10.1111/jth.14377
41. Kircher M, Witten DM, Jain P, O'Roak BJ, Cooper GM, Shendure J. A general framework for estimating the relative pathogenicity of human genetic variants. Nat Genet. 2014;46(3):310-315.

ARTICLE

Defective AP-3-dependent VAMP8 trafficking impairs Weibel-Palade body exocytosis in Hermansky-Pudlak Syndrome type 2 blood outgrowth endothelial cells

Ellie Karampini,[1,*] Maaike Schillemans,[1,*] Menno Hofman,[1] Floris van Alphen,[2] Martin de Boer,[3] Taco W. Kuijpers,[3,4] Maartje van den Biggelaar,[1] Jan Voorberg[1,5] and Ruben Bierings[1,6]

[1]Molecular and Cellular Hemostasis, Sanquin Research and Landsteiner Laboratory, Amsterdam UMC, University of Amsterdam, Amsterdam; [2]Research Facilities, Sanquin Research and Landsteiner Laboratory, Amsterdam UMC, University of Amsterdam, Amsterdam; [3]Blood Cell Research, Sanquin Research and Landsteiner Laboratory, Amsterdam UMC, University of Amsterdam, Amsterdam; [4]Pediatric Hematology, Immunology and Infectious Disease, Amsterdam UMC, University of Amsterdam, Amsterdam; [5]Experimental Vascular Medicine, Amsterdam UMC, University of Amsterdam, Amsterdam and [6]Hematology, Erasmus University Medical Center, Rotterdam, the Netherlands

EK and MS contributed equally to this work.

Ferrata Storti Foundation

Haematologica 2019
Volume 104(10):2091-2099

ABSTRACT

Weibel-Palade bodies are endothelial secretory organelles that contain von Willebrand factor, P-selectin and CD63. Release of von Willebrand factor from Weibel-Palade bodies is crucial for platelet adhesion during primary hemostasis. Endosomal trafficking of proteins like CD63 to Weibel-Palade bodies during maturation is dependent on the adaptor protein complex 3 complex. Mutations in the *AP3B1* gene, which encodes the adaptor protein complex 3 β1 subunit, result in Hermansky-Pudlak syndrome 2, a rare genetic disorder that leads to neutropenia and a mild bleeding diathesis. This is caused by abnormal granule formation in neutrophils and platelets due to defects in trafficking of cargo to secretory organelles. The impact of these defects on the secretory pathway of the endothelium is largely unknown. In this study, we investigated the role of adaptor protein complex 3-dependent mechanisms in trafficking of proteins during Weibel-Palade body maturation in endothelial cells. An *ex vivo* patient-derived endothelial model of Hermansky-Pudlak syndrome type 2 was established using blood outgrowth endothelial cells that were isolated from a patient with compound heterozygous mutations in *AP3B1*. Hermansky-Pudlak syndrome type 2 endothelial cells and CRISPR-Cas9-engineered *AP3B1*$^{-/-}$ endothelial cells contain Weibel-Palade bodies that are entirely devoid of CD63, indicative of disrupted endosomal trafficking. Hermansky-Pudlak syndrome type 2 endothelial cells have impaired $Ca2^{+}$-mediated and cAMP-mediated exocytosis. Whole proteome analysis revealed that, apart from adaptor protein complex 3 β1, also the μ1 subunit and the v-SNARE VAMP8 were depleted. Stimulus-induced von Willebrand factor secretion was impaired in CRISPR-Cas9-engineered VAMP8$^{-/-}$ endothelial cells. Our data show that defects in adaptor protein complex 3-dependent maturation of Weibel-Palade bodies impairs exocytosis by affecting the recruitment of VAMP8.

Introduction

Weibel-Palade bodies (WPB) are the storage and secretory compartment of endothelial cells and play an important role in hemostasis, inflammation and angiogenesis.[1] Secretion of their main cargo, the hemostatic protein von Willebrand factor (vWF), promotes platelet adhesion at the site of injury.[2] Apart

Correspondence:

RUBEN BIERINGS
r.bierings@erasmusmc.nl

Received: October 7, 2018.

Accepted: January 9, 2019.

Pre-published: January 10, 2019.

doi:10.3324/haematol.2018.207787

Check the online version for the most updated information on this article, online supplements, and information on authorship & disclosures: www.haematologica.org/content/104/10/2091

from vWF, WPB also store angiopoietin-2, IGFBP7 and various chemokines, along with the transmembrane protein P-selectin and the integral membrane protein CD63.[1,3] Simultaneous release of this cocktail of inflammatory and angiogenic mediators from WPB also promotes extravasation of leukocytes and vessel repair mechanisms. Weibel-Palade bodies belong to the lysosome-related organelles (LRO), a heterogeneous group of subcellular organelles that share features with lysosomes through acquisition of recycled cargo and/or membrane components from the endo-lysosomal system.[4] Biogenesis and subsequent degranulation of LRO is fundamental to the function of a wide variety of (circulating) cells, including granulocytes, T cells, platelets and endothelial cells. Although their function and cargo differ between cell types, the mechanisms and core components that control LRO biogenesis, maturation and degranulation are shared and operate in all cells with LRO. In endothelial cells, biogenesis of WPB starts at the trans-Golgi Network (TGN) and is driven by the biosynthesis of vWF. At this point, other soluble cargo, as well as P-selectin, are also included in newly forming WPB. In a subsequent post-Golgi step during WPB maturation, additional key components, such as CD63, are transferred from adaptor protein complex 3 (AP-3)-positive endosomes to maturing WPB.[5-7] AP-3 is a heterotetrameric complex, consisting of four subunits: β1, δ1, β1 and σ1, previously also referred to as β3A-, δ3-, μ3A- and σ3A-adaptins, respectively.[8] The AP-3 μ1 subunit is known to interact with membrane proteins through linear sequences of amino acid residues in their cytoplasmic tail, such as the di-leucine ([DE]XXX[LI]) and the tyrosine (YXXØ) motifs,[9,10] the latter of which is also present in CD63 (G**Y**EV**M**).[11] When its tyrosine motif is altered or the expression of AP-3β1 is down-regulated, CD63 shows impaired trafficking to WPB, suggestive of a direct interaction between the AP-3 complex and CD63.[7]

Defective formation and degranulation of LRO is at the basis of a number of poorly understood congenital storage pool disorders (SPD) that affect secretory responses of cells. Since the mechanisms of LRO formation and degranulation are shared between different cell types, SPD are often polysystemic, affecting many cell types at the same time which leads to complex disease symptoms. Hermansky-Pudlak syndrome (HPS) is a group of autosomal recessive disorders characterized by hypopigmentation and platelet storage pool deficiency, due to defective maturation of melanosomes and platelet dense granules, respectively.[12] HPS-2, a subtype of HPS, affects the expression and functionality of the AP-3 complex by mutations in the *AP3B1* gene, which encodes the AP-3 complex β1 subunit.[13] Apart from the shared HPS features of platelet dysfunction and albinism, HPS-2 is also uniquely characterized by $CD8^+$ cytotoxic T-cell dysfunction and neutropenia.[14-16]

Given the polysystemic nature of SPD, we sought to determine how genetic deficiencies in the AP-3 sorting machinery impact the secretory function of endothelial cells. Here we show, using blood outgrowth endothelial cells (BOEC) from an HPS-2 patient, that defects in AP-3 dependent maturation of WPB impairs the exocytotic potential of WPB by affecting the recruitment of the WPB-localized member of the SNARE fusion machinery VAMP8.

Methods

Cell culture and isolation of blood outgrowth endothelial cells

Blood outgrowth endothelial cells were isolated as previously described and cultured in EGM-2 (Lonza, Basel, Switzerland, CC-3162) supplemented with 18% fetal calf serum (FCS) (Bodinco, Alkmaar, the Netherlands) (EGM-18).[17] HPS-2 BOEC were isolated from venous blood from a patient diagnosed with HPS-2 (described by de Boer *et al.*[16]), caused by compound heterozygote *AP3B1* mutations (c.177delA, p.K59Nfs*4 and c.1839-1842delTAGA, p.D613Efs*38). The study was performed according to national regulations regarding the use of human materials. The patient's parents signed an informed consent form allowing participation. Control BOEC were isolated from healthy, anonimized donors participating in the voluntary internal blood donor system of Sanquin Blood Supply following written consent. The study was approved by the Medical Ethical Committee of the Academic Medical Center in Amsterdam and was conducted in accordance with the Declaration of Helsinki.

DNA constructs

The mEGFP-LIC and LVX-mEGFP-LIC vectors have been described before.[18,19] The EGFP-AP-3β1 plasmid encoding AP-3β with EGFP fused to its aminoterminus was a gift from Dr. Adolfo Saiardi.[20] To construct LVX-mEGFP-AP3-β1, a 3317 bp fragment containing the AP-3β1 coding sequence was cut from EGFP-AP-3β1 using BsrGI and SacII and pasted in frame behind mEGFP using the same sites in mEGFP-LIC. In a second step, the AP-3β1 coding sequence was excised from mEGFP-AP-3β1 using BsrGI and NotI and pasted in frame behind mEGFP in the LVX-mEGFP-LIC vector.

CRISPR genome engineering

gRNA were designed to target exon 1 of the *AP3B1* gene and exon 1 and 2 of the VAMP8 gene using the CRISPR Design tool (*http://crispr.mit.edu*). gRNAs [(AP3B1 exon 1: gRNA-4: TACAATGAGCAGTCCGGAGG and gRNA-5: ACAATGAGCAGTCCGGAGGA); (VAMP8 exon 1: gRNA-4: GAATGTGGAGCGGATCCTGG and gRNA-5: AGA ATGTGGAGCGGATCCTG; exon 2: gRNA-3: CTGGAGCGACTCGAGATGCG)] were selected based on the specificity score with the minimum amount of off-target effects and were subsequently cloned as hybridized oligos [(AP3B1: gRNA-4: RBNL306 5'-CA CCGTACAATGAGCAGTCCGGAGG-3' and RBNL307 5'-AAACCCTCCGGACTGCTCA TTGTAC-3'; gRNA-5: RBNL308 5'-CACCGACAATGAGCAGTCCGGAGGA-3' and RBNL309 5'-AAACTCCTCCGGACTGCTCATTGT C-3'), (VAMP8: gRNA-3: RBNL318 5'-CACCGGTGGAGGAAATGATCGTGTG-3' and RBNL319 5'-AAACCACACGATCATT TCCTCCACC-3'; gRNA-4: RBNL320 5'-CACCGATTCACTTACTGACCGGCCT-3' and RBNL321 5'-AAACAGGCCGGTCAGTAAGTGAATC-3'; gRNA-5: RBNL322 5'-CACCGA TTCACTTACTGACCGGCCT-3' and RBNL323 5'-AAACGGCCGGTCTCAGTAAGTGAA TTC-3')] into BsmBI-digested LentiCRISPR_v2 vector (a gift from Dr. Feng Zhang; Addgene #52961). A detailed protocol on transduction and clonal selection of knockout BOEC has been previously described.[21]

CD63 and CD62P membrane exposure

Endothelial cells were cultured in gelatin-coated 6-well plates until confluency for 3-4 days prior to the experiment. In order to measure CD63 surface exposure in WT and HPS-2 BOEC under steady conditions, cells were washed twice with phosphate buffered saline (PBS), detached with Accutase (Sigma, A6964),

and stained with FITC-conjugated anti-CD63 antibody at 4°C for 30 minutes (min) in the dark. After incubation, cells were washed with PBS, spun down at 250xg, 4°C for 2 min and suspended in PBS containing 0.01% (v/v) NaN3. Samples were measured by flow cytometry (BD FACSCANTO II, BD Biosciences). In order to measure CD62P levels on the plasma membrane upon stimulation, cells were pre-incubated in release medium for at least 30 min. Stimulation was performed in RM supplemented with 100 µM histamine for 5 min. After stimulation, cells were treated with ice-cold PBS and detached by Accutase. Staining for CD62P exposure was performed at 4°C in the dark with a PE-conjugated anti-CD62P antibody for 20 min. Cells were centrifuged at 4°C at 250xg for 2 min and subsequently resuspended in PBS containing 0.01% (v/v) NaN_3.

Further details on materials and methods are available in the *Online Supplementary Appendix*.

Results

AP3B1 deficient endothelial cells exhibit impaired intracellular protein trafficking from endosomes to Weibel-Palade bodies

To study the role of the AP-3 complex in primary endothelial cells, we isolated BOEC from peripheral blood mononuclear cells of an HPS-2 patient with mutations in the AP3B1 gene that encodes for the β1 subunit of the heterotetrameric AP-3 complex. The patient, who has previously been described by de Boer *et al.*,[16] is a compound heterozygote with both mutations (exon 2: c.177delA, p.K59Nfs4; exon 17: c.1839-1842delTAGA, p.D613Efs*38) leading to a frame shift and a premature stop codon (Figure 1A). As expected, western blot analysis of lysates of BOEC confirmed that the expressed levels of AP-3 β1 were not detectable (Figure 1B). The truncated AP-3β1 protein products, generated in the HPS-2 BOEC, are most likely rapidly degraded as previously reported in HPS-2 fibroblasts.[13] In order to test whether there is any remaining functionality of the AP-3 complex in HPS-2 BOEC, we determined the localization of proteins that are subject to AP-3 dependent trafficking. Both the tetraspanin CD63 and the leukocyte receptor CD62P continuously cycle between plasma membrane and WPB.[5,6] However, after endocytic retrieval, CD63 is incorporated in maturing WPB through transfer from AP-3 positive endosomes, while P-selectin diverges to the trans-Golgi network where it is incorporated in nascent WPB.[7] Therefore, we stained HPS-2 and healthy control BOEC for vWF and CD63 or P-selectin. We observed that CD63 is not detectable in WPB in HPS-2 BOEC and can only be observed in round endosome-like structures (Figure 1E, left). Quantitative evaluation of our imaging data showed that in WT BOEC, nearly a third of cellular CD63 is associated with WPB (Figure 1 right top), and that on average about 60% of the WPB are CD63 positive (1E right bottom), numbers that are both in close accordance with previous studies.[7,22] We observed a sharp reduction in these parameters in HPS-2 BOEC pointing to a defect in CD63 trafficking. P-selectin trafficking to WPB is unaffected by the lack of AP-3 β1 (*Online Supplementary Figure S1A*). We also measured CD63 surface expression in HPS-2 and healthy control BOEC under steady state conditions using flow cytometry. We observed that CD63 surface levels were significantly increased in HPS-2 BOEC (*Online Supplementary Figure S1B*). Taken together these data point to defective AP-3 dependent trafficking mechanisms in HPS-2 BOEC.

To further corroborate the role of AP-3 in trafficking of CD63, we also generated AP3B1 knock-out primary endothelial cells using CRISPR-Cas9 gene editing. Using lentiviral transduction of cord blood BOEC (cbBOEC), with guide (gRNA) targeting the first exon of the AP3B1 gene, we generated 3 clonal cbBOEC lines containing indels that led to frame shifts and subsequent premature stop codons in the AP3B1 gene (Figure 1C). This resulted in complete abolishment of AP-3β1 expression in all three clonal lines (Figure 1D). Similar to what we observed in HPS-2 BOEC, and to what has been reported in endothelial cells after siRNA-mediated AP-3 β1 silencing,[7] WPB of *AP3B1*$^{-/-}$ cbBOEC did not contain CD63 (Figure 1F and *Online Supplementary Figure S2*).

AP3B1-deficient HPS-2 blood outgrowth endothelial cells have an unstable AP-3 complex and lack the Weibel-Palade body v-SNARE VAMP8

To better understand the phenotypic effect of loss of AP-3 β1 expression, we performed a comparative analysis of the whole proteome between HPS-2 and healthy control BOEC by means of label-free LC-MS/MS. We identified 5812 proteins, from which 4323 were quantifiable following the selection criteria. To include the natural variation in our analysis, we compared HPS-2 BOEC to four independent healthy control donors. Z-scored LFQ values of the proteins with the highest variation between samples (S0=0.4, FDR = 0.05) are shown in the heatmap in Figure 2A. Following this approach, we were able to confirm the AP-3 β1 depletion in HPS-2 BOEC (Figure 2B). Moreover, we observed that the expression of AP-3 µ1, an AP-3 subunit encoded by *AP3M1*, was also significantly reduced. However, expression levels of AP-3δ1 and AP-3 σ1, the other two subunits of the AP-3 complex, were not significantly different and only modestly reduced (Figure 2B). A similar observation has previously been made in HPS-2 fibroblasts[23] and in murine pe fibroblasts (pearl, *pe*, mouse model of HPS-2), where δ1 and σ1 subunits remained as a heterodimer and showed cytosolic rather than membrane-associated localization.[24] The tight correlation of β1 and µ1 expression levels suggests that loss of AP-3 β1 and consequential disintegration of the AP-3 complex destabilizes the AP-3µ1 subunit. This was supported by the observation that lentivirally expressed mEGFP-AP-3 β1 was able to rescue the expression of AP-3 µ1 in HPS-2 BOEC (Figure 2C).

Interestingly, among the down-regulated proteins, we discovered that the expression of the WPB-localized SNARE protein VAMP8 is severely diminished (Figure 2A and *Online Supplementary Figure S3*). This was specific for VAMP8 as the expression levels of other SNARE proteins that have been implicated in WPB exocytosis were not significantly altered (*Online Supplementary Figure S3*). Western blot analysis also revealed a complete depletion of VAMP8 expression in HPS-2 BOEC compared to healthy controls (Figure 2D). Moreover, immunofluorescent staining in healthy control and HPS-2 BOEC for VAMP8 and vWF, showed that WPB in HPS-2 BOEC lack VAMP8 immunoreactivity (Figure 2E). In addition, in the *AP3B1* knockout BOEC lines, VAMP8 was strongly reduced when compared to the control cbBOEC (*Online Supplementary Figure S4*).

Ex vivo HPS-2 endothelial cells have impaired stimulus-induced Weibel-Palade body exocytosis

To investigate the contribution of AP-3 dependent maturation on the degranulation efficiency of WPB in endothelial cells, we measured the stimulus-induced vWF release in HPS-2 BOEC. We observed that, under unstimulated conditions, the release of vWF is unaffected in the HPS-2 BOEC compared to WT (Figure 3A). However, upon stimulation, HPS-2 BOEC showed a clear defect in vWF release with both $Ca2^{+}$ (histamine) and cAMP-mediated (forskolin) secretagogues (Figure 3B). As an alternative measurement of WPB exocytosis, we also investigated how other WPB proteins respond to histamine treatment. We stimulated WT and HPS-2 BOEC and measured CD62P exposure on the plasma membrane (Figure 3D). We found that significantly less CD62P was expressed on HPS-2 BOEC plasma membrane when compared to healthy control BOEC upon histamine stimulation. The reduction in the stimulus-induced surface expression of CD62P and release of vWF in HPS-2 BOEC suggests that defects in the AP-3 dependent maturation of WPB alter the exocytotic potential of these organelles in endothelial cells.

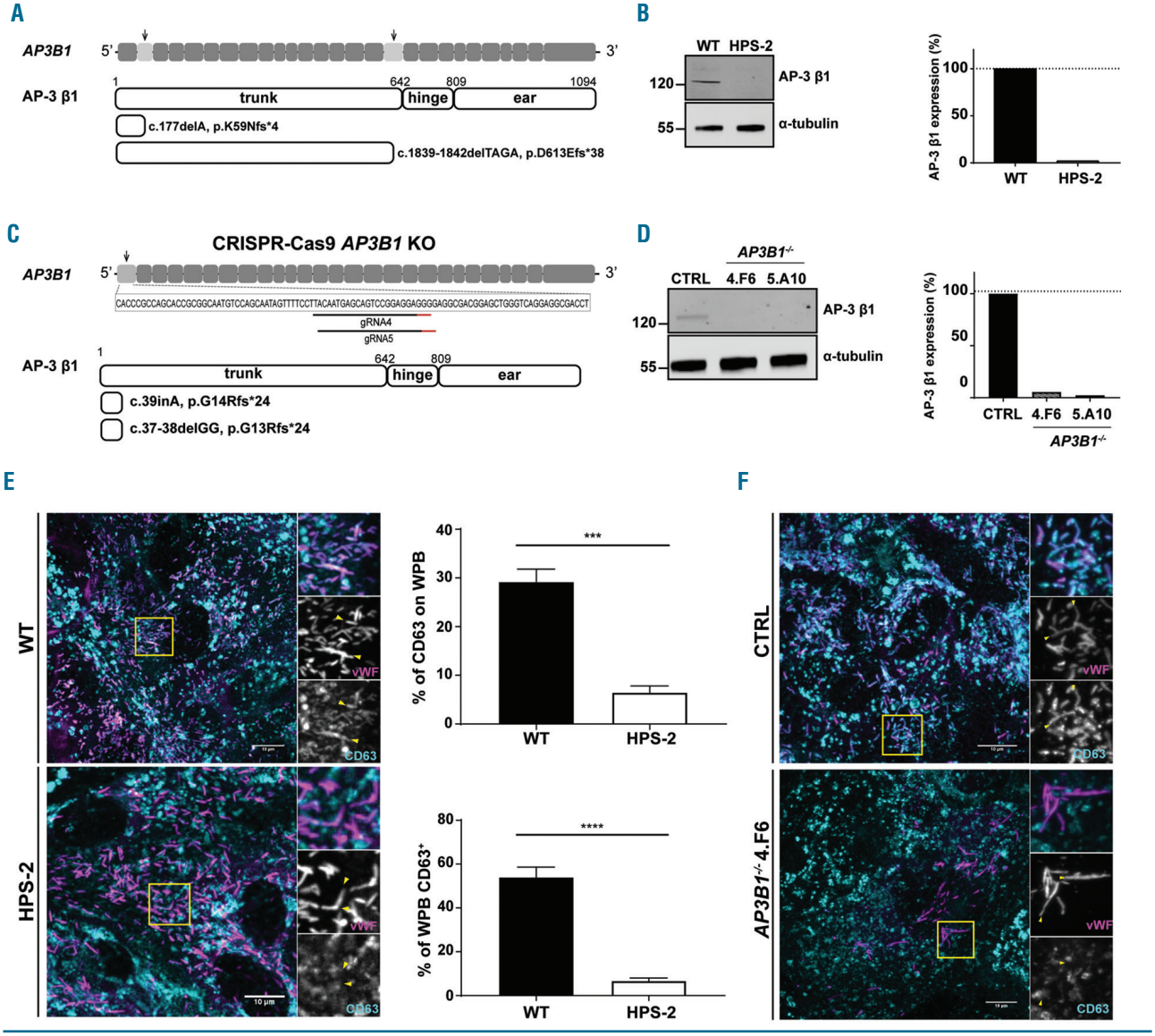

Figure 1. Disrupted trafficking of CD63 to Weibel-Palade bodies in *ex vivo* patient-derived HPS-2 BOEC and CRISPR/Cas9-engineered AP3B1$^{-/-}$ BOEC. (A) Cartoon depicting the mutations of the HPS-2 patient in the *AP3B1* gene and the corresponding predicted truncated protein products relative to the full length AP-3β1 domain structure. (B) Expression of AP-3β1 in WT and HPS-2 BOEC. (B) Healthy WT and HPS-2 BOEC lysates were separated with SDS-PAGE and were immunoblotted for AP-3β1; α-tubulin was used as a loading control. Molecular weight standards are indicated on the left (kDa) and quantification of relative AP-3β1 expression in HPS-2 BOEC normalized to AP-3β1 in healthy WT BOEC (right). (C) Cartoon representation of the CRISPR\Cas9-engineering strategy to generate AP3B1$^{-/-}$ BOEC lines. Guide RNA (gRNA4 and gRNA5) are shown underneath a fragment of AP3B1 exon 1 sequence with their protospacer adjacent motif (PAM) indicated in red. The mutations and the corresponding predicted truncated protein products of 2 AP3B1$^{-/-}$ clones (4.F6 and 5.A10, respectively) are shown relative to the full length AP-3β1 domain structure. (D) Loss of AP-3β1 expression in AP3B1$^{-/-}$ BOEC. (D) Lysates of clonal CTRL BOEC and 2 clonal AP3B1$^{-/-}$ BOEC lines (4.F6 and 5.A10) were separated with SDS-PAGE and were immunoblotted for AP-3β1; α-tubulin was used as a loading control (left) and quantification of relative AP-3β1 expression in clonal AP3B1$^{-/-}$ BOEC lines normalized to AP-3β1 in clonal CTRL BOEC (right). (E-F) Immunostaining of BOEC for vWF (magenta) and CD63 (cyan) in WT *versus* HPS-2 BOEC (E left) and CTRL *versus* AP3B1$^{-/-}$ 4.F6 BOEC (F), respectively. Boxed areas are magnified in the right part. Yellow arrowheads indicate the position of WPB in both channels. Scale bars represent 10 μm. (E) Proportion of CD63 immunoreactivity that is found on WPB (right, top) and proportion of WPB that contain CD63 immunoreactivity (right, bottom). Student *t*-test, ***P<0.001, ****P<0.0001.

Weibel-Palade bodies v-SNARE protein VAMP8 promotes Weibel-Palade body exocytosis

Expression of the SNARE protein VAMP8 is reduced in the absence of AP-3 β1, in HPS-2 patient BOEC as well as in CRISPR-Cas9 engineered *AP3B1* knockout endothelial cells. SNARE proteins are key regulators of intracellular membrane fusion events, such as during exocytosis or during fusion between organelles. To further investigate the role of VAMP8 in endothelial cells, we first studied the intracellular localization of VAMP8 with confocal microscopy in HUVEC/healthy control BOEC. In line with previous reports, VAMP8 was localized on a subset of WPB and on spherical organelles of the endosomal system (*Online Supplementary Figure S5*).[21,25] Interestingly, VAMP8-positive WPB and VAMP8-positive endosomes both contained CD63, suggesting their shared itinerary may be indicative of a common AP-3 dependent trafficking pathway.

To explore the role of VAMP8 in endothelial cells we generated clonal CRISPR-Cas9 knockout BOEC by introducing a mutation in the first and second exon (Figure 4A) and evaluated the knockout efficiency by western blot (Figure 4B) and immunofluorescence (*Online Supplementary Figure S6A*). We investigated both AP-3-dependent intracel-

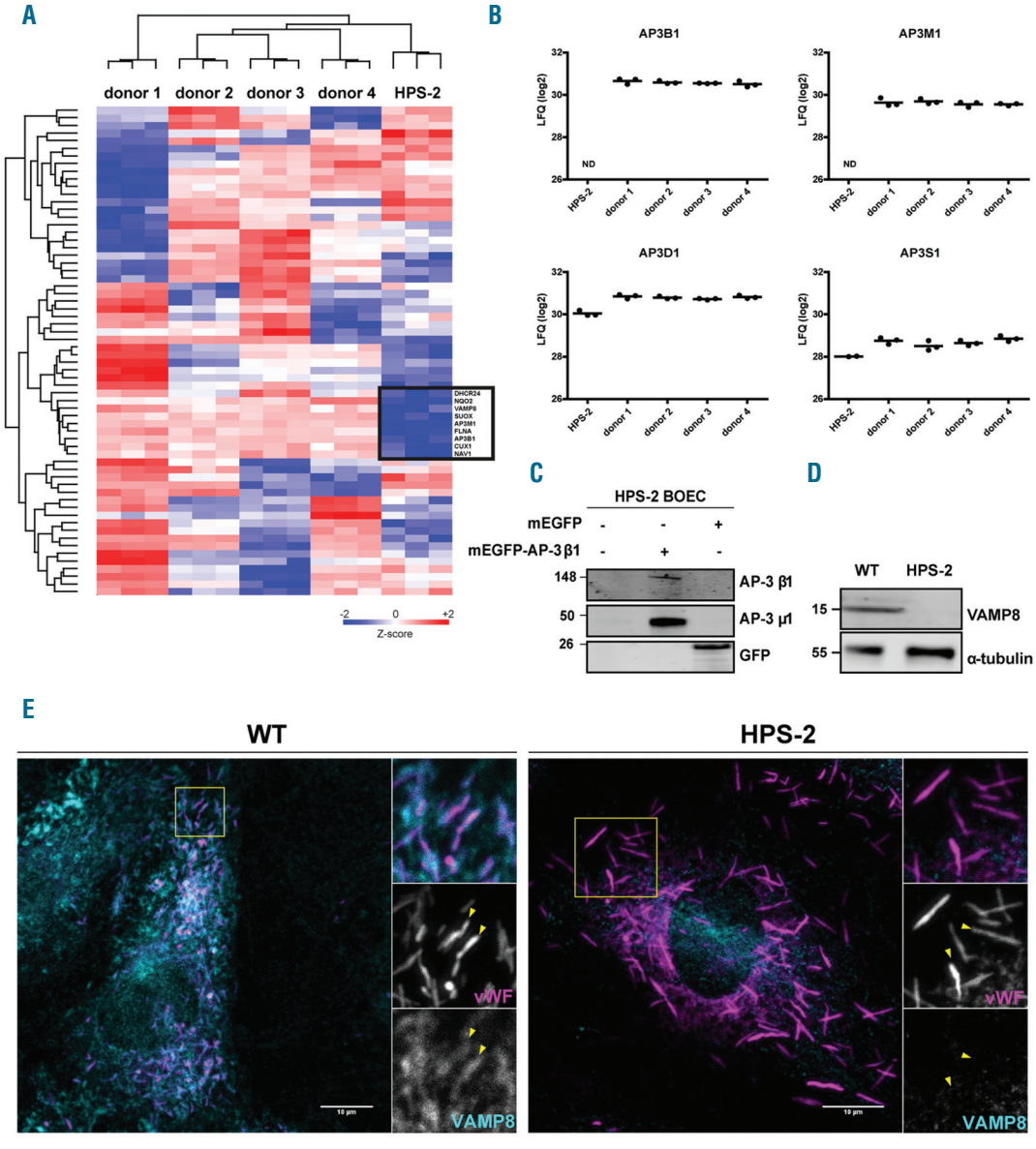

Figure 2. HPS-2 BOEC lack components of the AP-3 complex and the WPB v-SNARE VAMP8. (A and B) Whole proteome analysis of HPS-2 BOEC. (A) Heatmap of Z-scored LFQ (log_2) values of the proteins with the highest variation between BOEC derived from 4 individual healthy donors and HPS2 derived BOEC (ANOVA S0=0.4, FDR = 0.05) (B) Graph representing LFQ (log_2) values for AP3B1, AP3D1, AP3M1 and AP3S1. (C) HPS-2 BOEC lentivirally transduced with mEGFP-AP-3β1 and mEGFP (control). Lysates were separated with SDS-PAGE and were immunoblotted for AP-3β1, AP-3μ1 and GFP; molecular weight standards are indicated on the left (kDa). (D) Immunoblot analysis of VAMP8 in lysates of HPS-2 and WT BOEC; α-tubulin was used as a loading control.(E) Immunofluorescent stainings for von Willebrand factor (magenta) and VAMP8 (cyan) in healthy WT and HPS-2 BOEC. Boxed areas are magnified in the right part. Yellow arrowheads indicate the position of WPB in both channels. Scale bars represent 10 μm.

lular protein trafficking as well as the efficiency of WPB to exocytose upon stimulation in two clonal VAMP8$^{-/-}$ BOEC lines. To assess the involvement of VAMP8 in a fusion step between WPB and the endosomal compartment during CD63 recruitment, we checked the localization of CD63 in control and VAMP8-deficient cell lines. Immunofluorescent staining of CD63 and vWF in the VAMP8$^{-/-}$ lines exhibit a similar pattern when compared to the control cell lines, with CD63 being found on endosome-like structures as well as WPB (*Online Supplementary Figure S6B*). This suggests that membrane transfer between endosomes and WPB during CD63 trafficking does not depend on VAMP8. We next examined the involvement of VAMP8 in WPB exocytosis by testing stimulus-induced vWF release in CRISPR-edited VAMP8$^{-/-}$ BOEC. Our data show that the intracellular levels of vWF are similar for VAMP8-deficient and control cell lines (Figure 4C), showing that the process of CRISPR-Cas9 genetic modification and clonal selection does not affect vWF biosynthesis and/or WPB biogenesis. However, upon $Ca2^{+}$-mediated stimulation of WPB release with histamine, VAMP8 knockout endothelial cells secreted significantly less vWF when compared to the control lines (Figure 4D). These findings demonstrate that VAMP8 promotes stimulus-induced vWF secretion and establish VAMP8 as a novel component of the WPB exocytotic machinery.

Discussion

The AP-3 complex regulates the formation and maturation of lysosome-related organelles in many different cell types.[8] In this study, we show that mutations in the *AP3B1* gene that lead to HPS-2 result in loss of AP-3 β1 and rapid degradation of the AP-3 μ1 subunit of the AP-3 complex. While the δ1 and σ1 subunits are still expressed, the consequential destabilization of the AP-3 complex leads to a failure to traffic proteins to the WPB. Two of these, CD63 and VAMP8, normally co-reside on endosomes and WPB. However, in the absence of AP-3-dependent sorting, their fates differ radically. Blockade of the route from the endosomal compartment to the WPB causes an increase of CD63 on the cell surface, possibly caused by a global redistribution of CD63 in the absence of its storage compartment. This has previously been reported for other cell types derived from HPS-2 patients, such as cytotoxic T lymphocytes and fibroblasts.[13-15,23] VAMP8 expression is severely reduced in both HPS-2 BOEC and in CRISPR-engineered AP3B1 KO BOEC, for which we currently do not have an explanation. Contrary to CD63, VAMP8 does not contain any of the known sorting motifs that would allow it to directly interact with the AP-3 complex.[9,10] VAMP7, a v-SNARE that is found on a number of LRO, has been shown to interact with the AP-3 complex on

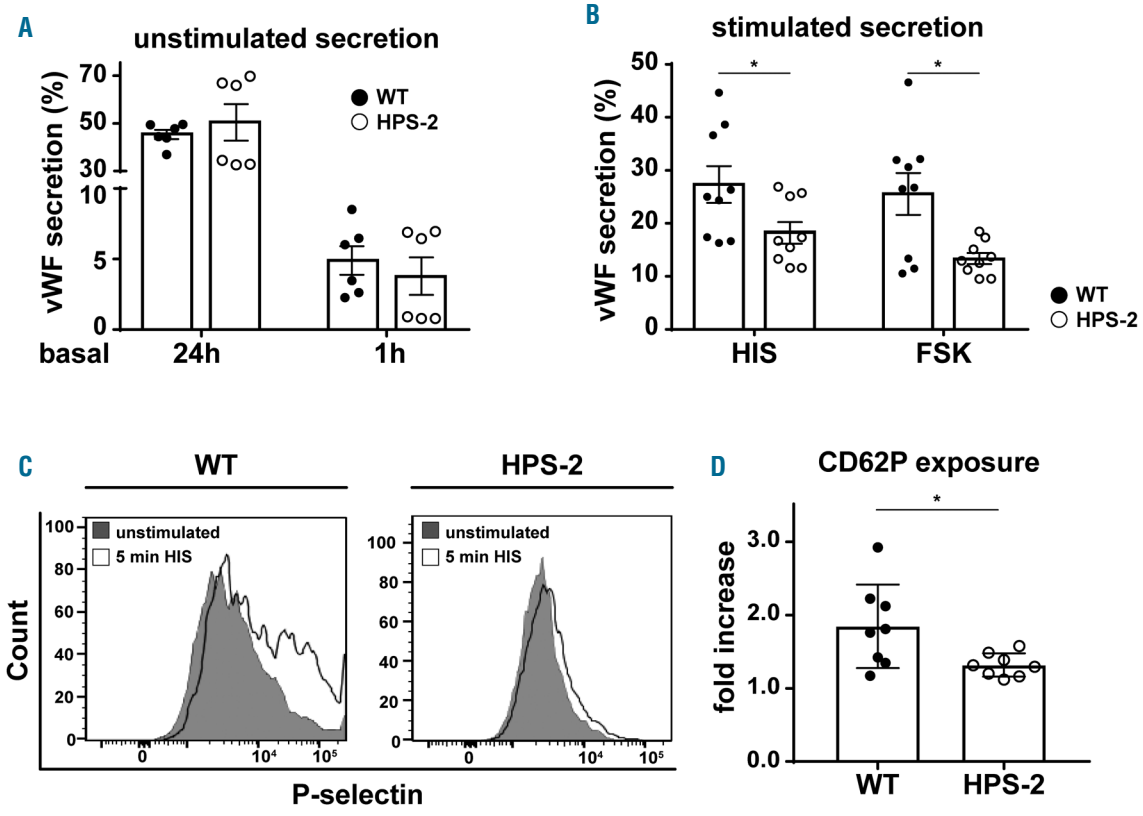

Figure 3. Impaired stimulus-induced von Willebrand Factor (vWF) secretion and P-selectin cell surface exposure in HPS-2 blood outgrowth endothelial cells (BOEC). (A) Basal (unstimulated) secretion of vWF in conditioned media after 24 hours and 1 hour from WT HPS-2 (black) and HPS-2 (white) BOEC (n=6). (B) Stimulated vWF secretion after 30 minutes treatment with 100 μM histamine (HIS) or 10 μM forskolin + 100 μM IBMX (FSK) from WT (black) and HPS-2 (white) BOEC. Secretion is expressed as relative proportion of intracellular vWF in unstimulated cells (n=9). (C) Representative histograms of P-selectin (CD62P) cell surface expression before (close gray) and after 5 minutes stimulation with 100 μM histamine (open black line) (D) CD62P exposure after histamine stimulation expressed as fold increase over unstimulated cells (n=8). Two tailed Student *t*-test, **P*<0.05.

early endosomes *via* a direct interaction between the AP-3 δ1 subunit and the N-terminal longin domain of VAMP7.[26,27] Destabilization of the AP-3 complex, such as in mocha mice which lack the δ1 subunit of AP-3, leads to mistargeting of VAMP7.[27] It has also been suggested that AP-3 indirectly traffics STX13 to maturing melanosomes *via* VAMP7.[28] Although VAMP8 does not contain a longin domain, it may be possible that during WPB maturation there is a similar mechanism by which VAMP8 latches on to the back of another AP-3 interacting partner.

In this study, we further explored the effect of WPB maturation on regulated secretion and identify VAMP8 as a novel component of the exocytotic fusion machinery. Previous studies have found that WPB contain the v-SNAREs VAMP3 and VAMP8, but so far only VAMP3 has been implicated in $Ca2^{+}$-dependent WPB exocytosis.[25] We had previously established that VAMP8 is a direct interactor of both syntaxin-3 (STX3) and syntaxin-4 (STX4).[21] STX4, which is found at the plasma membrane, has been implicated in thrombin-induced release of WPB through the formation of a complex with WPB-localized VAMP3.[25,29] We have recently shown that STX3 is localized on WPB and that absence of STX3 from endothelial cells results in impaired basal and hormone-evoked vWF secretion.[21] The decrease in histamine-evoked vWF secretion in VAMP8 knock-out endothelial cells indicates an active involvement of VAMP8 in stimulus-induced WPB exocytosis. Based on its ability to interact with STX4 and STX3, VAMP8 can potentially support exocytosis *via* direct (WPB-plasma membrane) or homotypic (WPB-WPB) fusion modes. Further research on this topic should address the involvement of VAMP8 in the different modes of fusion.

In vivo, *VAMP8*$^{-/-}$ mice show delayed and decreased thrombus formation.[30] Although, in their study, Graham *et al.* found that defective thrombus formation correlated with impaired dense granule release from *VAMP8*$^{-/-}$ platelets, they did not test whether lack of VAMP8 in endothelial cells also contributed to defects in thrombus formation. A more pronounced defect in thrombus formation was also observed in ruby eye mice, a murine model for HPS-6, which lack platelet dense granules.[31]

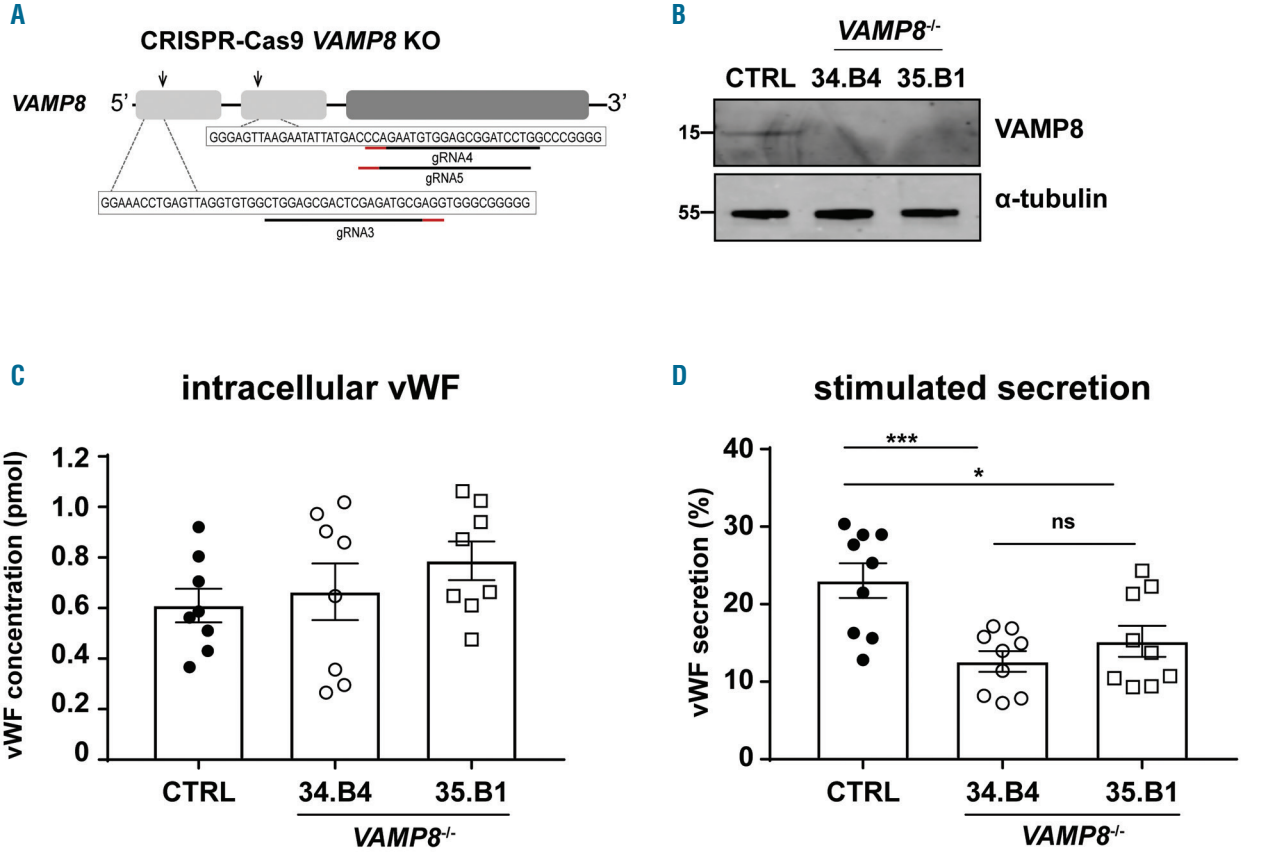

Figure 4. CRISPR-Cas9-engineered *VAMP8*$^{-/-}$ blood outgrowth endothelial cells (BOEC) have decreased histamine-induced von Willebrand Factor (vWF) secretion. A and B) Generation of clonal VAMP8 deficient BOEC lines using CRISPR/Cas9 genome-editing. (A) Cartoon representation of the CRISPR/Cas9-engineering strategy to generate VAMP8$^{-/-}$ BOEC lines. Guide RNA targeting exon 1 and exon 2 (gRNA3 and gRNA4&5, respectively) are shown underneath fragments of VAMP8 exon 1 and 2 sequences with their protospacer adjacent motif (PAM) indicated in red. (B) Loss of VAMP8 expression in clonal VAMP8$^{-/-}$ BOEC. Lysates of clonal CTRL BOEC and 2 clonal VAMP8$^{-/-}$ BOEC lines (34.B4 and 35.B1) were separated with SDS-PAGE and were immunoblotted for VAMP8; α-tubulin was used as a loading control. Molecular weight standards are indicated on the left (kDa). (C) Intracellular levels of vWF in lysates from control and 2 clonal VAMP8$^{-/-}$ KO BOEC lines (34.B4 and 35.B1) as determined by ELISA (n=9). (D) Stimulated VWF secretion after 30 minutes treatment with 100 μM histamine (HIS) from CTRL (close black) and 2 clonal VAMP8$^{-/-}$ KO BOEC lines (34.B4 and 35.B1) (open circle and square respectively). Secretion of vWF in supernatant from control and 2 clonal VAMP8$^{-/-}$ KO BOEC lines (34.B4 and 35.B1). Secretion is expressed as relative proportion of intracellular vWF in unstimulated cells (n=9). Two tailed Student *t*-test, ns: $P>0.05$; *$P<0.05$; ***$P<0.001$.

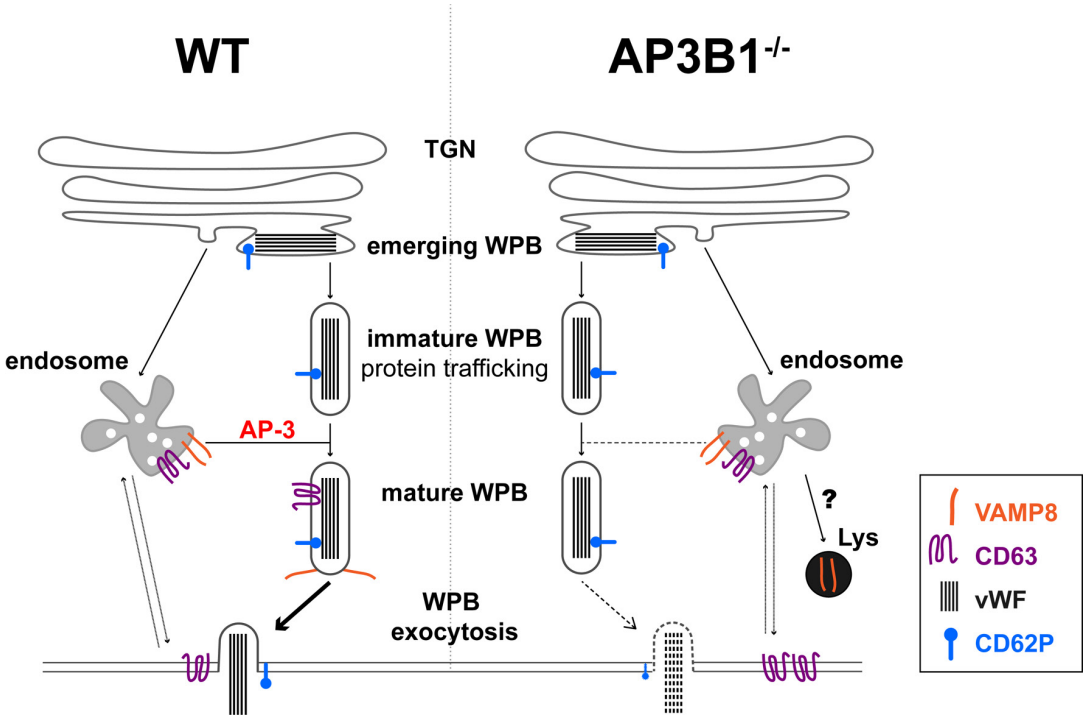

Figure 5. Proposed model of (defective) AP-3 dependent acquisition of VAMP8 during Weibel-Palade bodies (WPB) maturation. WPB in normal endothelial cells (WT, left) emerge from the *trans*-Golgi network (TGN) and mature by acquisition of recycled membrane proteins, such as CD63 and VAMP8, through endosomal trafficking to the WPB membrane *via* an AP-3 dependent pathway. Recruitment of VAMP8 promotes the secretion competence of WPB by supporting the formation of trans-SNARE complexes with STX3 and STX4,[21] which will allow WPB to undergo exocytosis upon cellular activation. After membrane fusion, CD63 and VAMP8 are retrieved and, *via* the early endosome (EE), make their way to another WPB. In the absence of a function AP-3 complex (right), such as in HPS-2 or *AP3B1*$^{-/-}$ BOEC, WPB fail to recruit CD63 from the early endosomes. This leads to a global redistribution of cellular CD63, increasing its presence on the cell surface during steady state conditions. WPB also fail to acquire (part of) their fusion machinery such as VAMP8, resulting in attenuated WPB exocytosis in response to cellular activation. Following its failure to transfer to the WPB membrane, VAMP8 is possibly rerouted to the lysosome where it is degraded.

Contributing to this phenotype was: (i) the inability to secrete protein disulfide isomerase (PDI) from so called T-granules, a tubular secretory compartment in platelets that contains VAMP8;[32] and (ii) defective thrombin-induced secretion of PDI and vWF from endothelial cells after silencing of HPS6.[31] A recent study also found that endothelial secretion of vWF in response to administration of the vasopressin analog 1-deamino-8-D-arginine vasopressin (DDAVP) was delayed and/or decreased in pallid, ruby eye and pale ear mice, murine models of HPS-9, HPS-6 and HPS-1, respectively.[33] This provides an explanation for earlier observations that long bleeding times in ruby eye and pale ear mice were not corrected by DDAVP,[34] but possibly also for the variable response of HPS patients to DDAVP.[35-37] Taken together, this suggests that defects in maturation of WPB decrease their ability to undergo exocytosis.

In this study, we show that BOEC from an HPS-2 patient have a moderate (but not complete) defect in stimulated vWF secretion, a phenotype that we found to be closely correlated with the absence of VAMP8 on mature WPB. We propose that, during maturation, LRO also acquire components of their fusion machinery, thereby increasing their ability to undergo exocytosis. In some LRO, such as dense granules, defects in LRO maturation result in the absence of the secretory granule at issue, which obscures a secretory defect by the lack of the fusion machinery recruitment. This becomes apparent in LRO, such as WPB, which have already been formed before their failure to interact with the endo/lysosomal system, preventing them from acquiring additional content (CD63) or fusion machinery components (VAMP8) (Figure 5).

Funding

This study was supported by grants from the Landsteiner Stichting voor Bloedtransfusie Research (LSBR-1244, LSBR-1517 and LSBR-1707), Sanquin (PPOC-2015-24P and PPOC-2018-21) and the Dutch Thrombosis Foundation (TSN 56-2015 and 2017-01). RB is supported by a European Hematology Association Research Fellowship.

References

1. Schillemans M, Karampini E, Kat M, Bierings R. Exocytosis of Weibel-Palade bodies: how to unpack a vascular emergency kit. J Thromb Haemost. 2019;17(1):6-18.
2. Metcalf DJ, Nightingale TD, Zenner HL, Lui-Roberts WW, Cutler DF. Formation and function of Weibel-Palade bodies. J Cell Sci. 2008;31(9):882–888.
3. Rondaij MG, Bierings R, Kragt A, van Mourik JA, Voorberg J. Dynamics and plasticity of Weibel-Palade bodies in endothelial cells. Arterioscler Thromb Vasc Biol 2006;26(5):1002–1007.
4. Marks MS, Heijnen HFG, Raposo G. Lysosome-related organelles: Unusual compartments become mainstream. Curr Opin

Cell Biol. 2013;25(4):495–505.
5. Kobayashi T, Vischer UM, Rosnoblet C, et al. The tetraspanin CD63/lamp3 cycles between endocytic and secretory compartments in human endothelial cells. Mol Biol Cell. 2000;11(5):1829–1843.
6. Arribas M, Cutler DF. Weibel-Palade body membrane proteins exhibit differential trafficking after exocytosis in endothelial cells. Traffic. 2000;1(10):783–793.
7. Harrison-Lavoie KJ, Michaux G, Hewlett L, et al. P-selectin and CD63 use different mechanisms for delivery to Weibel-Palade bodies. Traffic. 2006;7(6):647–662.
8. Robinson MS, Bonifacino JS. Adaptor-related proteins. Curr Opin Cell Biol. 2001;13(4):444–453.
9. Bonifacino JS, Traub LM. Signals for sorting of transmembrane proteins to endosomes and lysosomes. Annu Rev Biochem. 2003;72:395–72447.
10. Newell-Litwa K, Seong E, Burmeister M, Faundez V. Neuronal and non-neuronal functions of the AP-3 sorting machinery. J Cell Sci. 2007;120(Pt 4):531–541.
11. Rous BA, Reaves BJ, Ihrke G, et al. Role of adaptor complex AP-3 in targeting wild-type and mutated CD63 to lysosomes. Mol Biol Cell. 2002;13(3):1071–1082.
12. Wei ML. Hermansky-Pudlak syndrome: a disease of protein trafficking and organelle function. Pigment Cell Res. 2006;19(1):19–42.
13. Dell'Angelica EC, Shotelersuk V, Aguilar RC, Gahl WA, Bonifacino JS. Altered trafficking of lysosomal proteins in Hermansky-Pudlak syndrome due to mutations in the beta 3A subunit of the AP-3 adaptor. Mol Cell. 1999;3(1):11–21.
14. Clark RH, Stinchcombe JC, Day A, et al. Adaptor protein 3-dependent microtubule-mediated movement of lytic granules to the immunological synapse. Nat Immunol. 2003;4(11):1111–1120.
15. Wenham M, Grieve S, Cummins M, et al. Two patients with Hermansky Pudlak syndrome type 2 and novel mutations in AP3B1. Haematologica. 2010;95(2):333–337.
16. de Boer M, van Leeuwen K, Geissler J, et al. Hermansky-Pudlak syndrome type 2: Aberrant pre-mRNA splicing and mislocalization of granule proteins in neutrophils. Hum Mutat. 2017;38(10):1402–1411.
17. Martin-Ramirez J, Kok MGM, Hofman M, et al. Individual with subclinical atherosclerosis have impaired proliferation of blood outgrowth endothelial cells, which can be restored by statin therapy. PLoS One. 2014;9(6):e99890.
18. Bierings R, Hellen N, Kiskin N, et al. The interplay between the Rab27A effectors Slp4-a and MyRIP controls hormone-evoked Weibel-Palade body exocytosis. Blood. 2012;120(13):2757–2767.
19. van Breevoort D, Snijders AP, Hellen N, et al. STXBP1 promotes Weibel-Palade body exocytosis through its interaction with the Rab27A effector Slp4-a. Blood. 2014;123(20):3185–3194.
20. Azevedo C, Burton A, Ruiz-Mateos E, Marsh M, Saiardi A. Inositol pyrophosphate mediated pyrophosphorylation of AP3B1 regulates HIV-1 Gag release. Proc Natl Acad Sci U S A. 2009;106(50):21161–21166.
21. Schillemans M, Karampini E, van den Eshof BL, et al. Weibel-Palade Body Localized Syntaxin-3 Modulates Von Willebrand Factor Secretion From Endothelial Cells. Arterioscler Thromb Vasc Biol. 2018;38(7):1549–1561.
22. Poeter M, Brandherm I, Rossaint J, et al. Annexin A8 controls leukocyte recruitment to activated endothelial cells via cell surface delivery of CD63. Nat Commun. 2014;5(3738):3738.
23. Liu L, Sutton J, Woodruff E, Villalta F, Spearman P, Dong X. Defective HIV-1 particle assembly in AP-3-deficient cells derived from patients with Hermansky-Pudlak syndrome type 2. J Virol. 2012;86(20):11242–11253.
24. Peden AA, Rudge RE, Lui WWY, Robinson MS. Assembly and function of AP-3 complexes in cells expressing mutant subunits. J Cell Biol. 2002;156(2):327–336.
25. Pulido IR, Jahn R, Gerke V. VAMP3 is associated with endothelial Weibel-Palade bodies and participates in their Ca(2+)-dependent exocytosis. Biochim Biophys Acta. 2011;1813(5):1038–1044.
26. Martinez-Arca S, Rudge R, Vacca M, et al. A dual mechanism controlling the localization and function of exocytic v-SNAREs. Proc Natl Acad Sci U S A. 2003;100(15):9011–9006.
27. Kent HM, Evans PR, Schäfer IB, et al. Structural basis of the intracellular sorting of the SNARE VAMP7 by the AP3 adaptor complex. Dev Cell. 2012;22(5):979–988.
28. Jani RA, Purushothaman LK, Rani S, Bergam P, Setty SRG. STX13 regulates cargo delivery from recycling endosomes during melanosome biogenesis. J Cell Sci. 2015;128(17):3263–3276.
29. Fu J, Naren AP, Gao X, Ahmmed GU, Malik AB. Protease-activated receptor-1 activation of endothelial cells induces protein kinase Calpha-dependent phosphorylation of syntaxin 4 and Munc18c: role in signaling p-selectin expression. J Biol Chem. 2005;280(5):3178–3184.
30. Graham GJ, Ren Q, Dilks JR, Blair P, Whiteheart SW, Flaumenhaft R. Endobrevin/VAMP-8-dependent dense granule release mediates thrombus formation in vivo. Blood. 2009;114(5):1083–1090.
31. Sharda A, Kim SH, Jasuja R, et al. Defective PDI release from platelets and endothelial cells impairs thrombus formation in Hermansky-Pudlak syndrome. Blood. 2015;125(10):1633–1642.
32. Thon JN, Peters CG, Machlus KR, et al. T granules in human platelets function in TLR9 organization and signaling. J Cell Biol. 2012;198(4):561–574.
33. Ma J, Zhang Z, Yang L, Kriston-Vizi J, Cutler DF, Li W. BLOC-2 subunit HPS6 deficiency affects the tubulation and secretion of von Willebrand factor from mouse endothelial cells. J Genet Genomics. 2016;43(12):686–693.
34. Sweeney JD, Novak EK, Reddington M, Takeuchi KH, Swank RT. The RIIIS/J inbred mouse strain as a model for von Willebrand disease. Blood. 1990;76(11):2258–2265.
35. Van Dorp DB, Wijermans PW, Meire F, Vrensen G. The Hermansky-Pudlak syndrome. Variable reaction to 1-desamino-8D-arginine vasopressin for correction of the bleeding time. Ophthalmic Paediatr Genet. 1990;11(3):237–244.
36. Zatik J, Póka R, Borsos A, Pfliegler G. Variable response of Hermansky-Pudlak syndrome to prophylactic administration of 1-desamino 8D-arginine in subsequent pregnancies. Eur J Obstet Gynecol Reprod Biol. 2002;104(2):165–166.
37. Cordova A, Barrios NJ, Ortiz I, Rivera E, Cadilla C, Santiago-Borrero PJ. Poor response to desmopressin acetate (DDAVP) in children with Hermansky-Pudlak syndrome. Pediatr Blood Cancer. 2005;44(1):51–54.

Ferrata Storti Foundation

Haematologica 2019
Volume 104(10):2100-2106

Mode of delivery in hemophilia: vaginal delivery and Cesarean section carry similar risks for intracranial hemorrhages and other major bleeds

Nadine G. Andersson,[1,2] Elizabeth A. Chalmers,[3] Gili Kenet,[4] Rolf Ljung,[2] Anne Mäkipernaa,[5] Hervé Chambost;[6] on behalf of the PedNet Haemophilia Research Foundation

[1]Centre for Thrombosis and Hemostasis, Skåne University Hospital, Malmö, Sweden; [2]Lund University, Department of Clinical Sciences, Lund, Sweden; [3]Department of Haematology, Royal Hospital for Children, Glasgow, UK; [4]National Hemophilia Center, Sheba Medical Center, Tel Hashomer and Sackler School of Medicine, Tel Aviv University, Israel; [5]Children's Hospital and Hematology, Comprehensive Cancer Center, Helsinki University Hospital, University of Helsinki, Helsinki, Finland and [6]Pediatric Haematology Oncology Department, Children Hospital La Timone, AP-HM, and Aix Marseille Université, INSERM, INRA, C2VN, Faculté de Médecine, Marseille, France

ABSTRACT

The optimal mode of delivery for a pregnant hemophilia carrier is still a matter of debate. The aim of the study was to determine the incidence of intracranial hemorrhage and other major bleeds in neonates with moderate and severe hemophilia in relationship to mode of delivery and known family history. A total of 926 neonates, 786 with severe and 140 with moderate hemophilia were included in this PedNet multicenter study. Vaginal delivery was performed in 68.3% (n=633) and Cesarean section in 31.6% (n=293). Twenty intracranial hemorrhages (2.2%) and 44 other major bleeds (4.8%) occurred. Intracranial hemorrhages occurred in 2.4% of neonates following vaginal delivery compared to 1.7% after Cesarean section (*P*=not significant); other major bleeds occurred in 4.2% born by vaginal delivery and in 5.8% after Cesarean section (*P*=not significant). Further analysis of subgroups (n=813) identified vaginal delivery with instruments being a significant risk factor for both intracranial hemorrhages and major bleeds (Relative Risk: 4.78-7.39; *P*<0.01); no other significant differences were found between vaginal delivery without instruments, Cesarean section prior to and during labor. There was no significant difference in frequency for intracranial hemorrhages and major bleeds between a planned Cesarean section and a planned vaginal delivery. Children with a family history of hemophilia (n=466) were more likely to be born by Cesarean section (35.8% *vs.* 27.6%), but no difference in the rate of intracranial hemorrhages or major bleeds was found. In summary, vaginal delivery and Cesarean section carry similar risks of intracranial hemorrhages and major bleeds. The 'PedNet Registry' is registered at *clinicaltrials.gov identifier: 02979119*.

Correspondence:

NADINE G. ANDERSSON
nadine.gretenkort_andersson@med.lu.se

Received: October 18, 2018.

Accepted: February 14, 2019.

Pre-published: February 21, 2019.

doi:10.3324/haematol.2018.209619

Check the online version for the most updated information on this article, online supplements, and information on authorship & disclosures: www.haematologica.org/content/104/10/2100

Introduction

The optimal mode of delivery for a known hemophilia carrier, i.e. either vaginal delivery (VD) or Cesarean section (CS), is still a matter of debate. A carrier may have an increased bleeding risk herself that might need to be taken into account in the obstetric planning but, from the fetal point of view, the key question is how the mode of delivery may impact on the risk of major bleeds, and in particular intracranial hemorrhages (ICH). These life threatening bleeds can also impair the outcome in survivors due to serious neurological sequelae.[1,2] Moreover, the require-

ment for intensive replacement therapy has been identified as a risk factor for inhibitor development in patients with hemophilia A.[3]

Several studies have been published with quite a uniform consensus that around 3-4% of boys with hemophilia born in countries with a good standard of obstetric care have had ICH diagnosed during the neonatal period.[2,4-6] It has also been shown that instrumental delivery using forceps or vacuum extraction (VE) is a major risk factor for intra- and extracranial bleeds in neonates with hemophilia.[5,7,8] However, figures for bleeds associated with uncomplicated VD and CS and, consequently, recommendations on mode of delivery vary between publications and guidelines.[7,9-11] It is undisputed that the risk of a neonatal bleed in a child with hemophilia is considerably higher than that expected in a non-hemophilia population, although few figures are available. The largest series, among the few studies published on mode of delivery in the normal population, suggests an incidence of ICH of 1 per 1,900 in spontaneous VD, 1 per 2,750 in CS with no labor, 1 per 907 delivered by CS during labor, 1 per 860 deliveries with VE, and 1 per 664 delivered with the use of forceps.[12] Using these numbers as a reference, the risk for ICH in hemophilia boys is 60 times higher compared to healthy neonates born by VD.

Knowledge of carrier status in a pregnant woman, or the knowledge of confirmed hemophilia in the fetus following prenatal diagnosis (PND), may impact on obstetric care, especially when planning the mode of delivery. In recent cohorts, around 50% of all cases of hemophilia are sporadic, i.e. newly diagnosed boys without family history of hemophilia or without any knowledge of carrier status in the mother at birth.[13] Many published studies on the delivery of a hemophilia child have not been able to distinguish between sporadic cases and cases with a known family history of hemophilia. Some studies include neonates with mild hemophilia and, furthermore, it is not always possible to distinguish between CS performed as a result of the baby having hemophilia or for other reasons, and this complicates comparisons between studies.

The PedNet Registry is a prospective, multicenter database that includes all children born since 1st January 2000 diagnosed with hemophilia A (HA) or B (HB) of all severities and treated in the 31 participating hemophilia centers in Europe, Canada and Israel.[14] Baseline data regarding the neonatal period are collected on mode of delivery, neonatal events, family history of hemophilia, and gestational age. This longitudinal prospectively collected cohort study makes it possible to address questions of interest on obstetric and neonatal issues.

The aim of this paper was to study the frequency of ICH and other major bleeds in neonates with hemophilia and the association with mode of delivery to improve counseling of pregnant carriers in the future. Furthermore, the results will be stratified according to the presence or absence of a prior knowledge of hemophilia in the family.

Methods

Study group

Data were retrieved from the 'PedNet Registry' which is owned and administered by the 'PedNet Haemophilia Research Foundation', consisting of 31 international hemophilia treatment centers and registered at *clinicaltrials.gov identifier: 02979119*. The purpose of the registry is to promote and facilitate research and healthcare development in children with hemophilia. The PedNet Registry includes all consecutive patients diagnosed and treated in each center born after 1st January 2000. The aim of the PedNet registry is to establish large well-documented birth cohorts of patients with hemophilia enabling studies on side effects and outcome of treatment. Patient data are collected from birth onwards prospectively and consist of all data concerning treatment, side effects and outcome of treatment. Information is collected on mode of delivery and during the first 75 exposure days of treatment with factor concentrate; all major bleeds including ICH are registered with detailed information. Approval for data collection was obtained from the institutional review boards of each of the 31 centers taking part in the study, and written informed consent was obtained from the parents or guardians of all participants in accordance with the Declaration of Helsinki. The data quality in the PedNet Registry is monitored regularly and independent audits are carried out in all participating centers.[14]

Study population

All children included in the Registry by 1st January 2015 with severe (factor VIII/IX activity, < 0.01 IU/mL) or moderate (factor VIII/IX activity, 0.01-0.05 IU/mL) HA and HB and with at least one follow up covering the neonatal period after the initial baseline report were enrolled. This resulted in 926 children born between 1st January 2000 and 1st January 2015 with data on mode of delivery and the neonatal period, defined as 28 days after birth. Prematurity was defined as up to 36 weeks of gestational age.

Data collection

We uniformly collected data on the mode of delivery (including vaginal, vaginal instrumental, CS), and major bleeds including ICH in the neonatal period. Data were also recorded on whether an affected newborn belonged to a family with a known history of hemophilia or was a sporadic case.

Statistical analysis

The primary outcome was ICH and major bleeds, the latter defined as a bleed requiring treatment with factor concentrate and not resolving within 24 hours during the neonatal period. The determinants of outcome were mode of delivery and family history of hemophilia, either known or unknown. Statistical comparisons between different groups were made using χ^2 test or Fisher´s exact test at a significance level of 0.05. In the comparison of four subgroups on mode of delivery, an overall test was performed to compare the frequencies between all groups simultaneously. If an overall test was significant, it was followed by pairwise comparisons between the groups. The results of the pairwise comparisons were corrected for multiple testing by Bonferroni correction. Statistical power was shown by the width and magnitude of the 95% Confidence Interval (95%CI) according to the CONSORT guidelines. All analyses were performed using IBM SPSS Statistics for Windows, Version 24.0. Armonk, NY: IBM Corp., NY, USA, or R: A language and environment for statistical Computing, version 3.4.2. Vienna, Austria, R Foundation for Statistical Computing.

Results

Cohort demography

A total of 926 patients were included, 140 with moderate and 786 with severe hemophilia comprising those with HA [n = 803 (86.7%)], and HB [n=123 (13.3%)]. MOD in the 926 patients was vaginal in 633 (68.4%) and

CS in 293 (31.6%). Sixty-two (6.7%) of the included patients were preterm. For more detailed information on cohort demographics see Table 1.

Intracranial hemorrhages and major bleeds

Twenty ICH (2.2%) and 44 other major bleeds (4.8%) were recorded in the 926 children. The majority of major bleeds were soft tissue bleeds (n=14), followed by muscle bleeds (n=7) and mucous membrane bleeds (n=3). One patient each suffered from a shoulder bleed, subgaleal bleed, scalp bleed, cephalohematoma, hematemesis, and a hepatic bleed; in 14 patients the bleeds were not further defined. No significant difference was observed in the frequency of bleeds when comparing HA to HB or moderate to severe hemophilia.

In the whole cohort, major bleeds occurred at a frequency of 4.3% (27 of 633) after all vaginal deliveries and 5.8% (17 of 293) after CS (P=0.32). The frequencies of ICH after all vaginal deliveries was 2.4% (15 of 633), compared to 1.7% after CS (5 of 293), with no significance (P=0.631).

Term and preterm neonates

Data on gestational age was available in 849 of 926 neonates. When comparing major bleeds in term and preterm deliveries, major bleeds occurred in 5.2% (41 of 787) of term and in 6.4% (3 of 62) of preterm babies with no significant statistical difference between the groups (P=1.0). The frequency of ICH in the term delivery group was 2.5% (20 of 787) and no cases of ICH was reported in the preterm delivery group (n=62). In the preterm group, neonates were born at a median of 35 gestational weeks (range 26-36 weeks) and only 11 of 62 (17.7%) neonates were very or extremely preterm (born before the 33rd gestational week). Unfortunately, in 77 cases, gestation at delivery was not recorded, but no major bleeds were reported in this group (Table 2). Because there was no difference between the groups based on gestational age, all further analysis was carried out on the whole cohort.

Mode of delivery

In 813 of 926 patients, more information about the mode of delivery was available and further subgroups could be defined: non-instrumental vaginal delivery (n=541), vaginal with instruments, e.g. forceps or vacuum extraction (n=68), CS prior to labor (n=125), and CS during labor (n=79). The frequencies for ICH were 1.5% (8 of 541) for non-instrumental vaginal delivery, 10.2% (7 of 68) for instrumental vaginal delivery, 1.6% (2 of 125) CS prior labor, and 2.5% (2 of 79) during labor. Regarding major bleeds, the frequencies showed 2.6% (14 of 541) for non-instrumental vaginal delivery, 19.1% (13 of 68) for instrumental vaginal delivery, 4.0% (5 of 125) CS prior to labor, and 8.9% (7 of 79) for CS during labor. The results identify vaginal instrumental delivery as a significant risk factor in comparison to vaginal delivery without instruments and CS prior to labor for both major bleeds and ICH: the Relative Risk (RR) for ICH was 6.96 (95%CI: 2.61-18.6; P=0.0005) and the RR for major bleeds was 7.39 (95%CI: 3.63-15.05; P<0.0001) for comparison with vaginal delivery without instruments; compared to CS prior to labor the RR was 6.43 (95%CI: 1.37-30.12; P=0.010) for ICH and 4.78 (95%CI: 1.78-12.84; P=0.0012) for major bleeds. Regarding major bleeds only at a significance level of P<0.05, vaginal delivery without instruments was significantly safer than CS during labor (P=0.011; RR 3.42, 95%CI: 1.43, 8.22) but no difference for ICH could be seen (P=0.37). All other groups showed no significances in comparison; there was no significant difference in the rate of ICH or major bleeds when comparing instrumental vaginal delivery with CS during labor. For more details see Tables 3 and 4.

A subanalysis of moderate *versus* severe hemophilia was made showing similar results regarding ICH: 2.14% (3 of 140) ICH for moderate and 2.16% (17 of 786) for severe hemophilia without statistical significance. However, major bleeds were significantly more often reported in severe hemophilia 5.5% (43 of 786) than in moderate

Table 1. Basic characteristics of study group.

	n (%)
Type and severity of hemophilia	
Moderate hemophilia A	110 (11.9)
Severe hemophilia A	693 (74.8)
Moderate hemophilia B	30 (3.2)
Severe hemophilia B	93 (10.0)
Family history of hemophilia	
No known family history	445 (48.1)
Known family history	466 (50.3)
No data on family history	15 (1.6)
Mode of delivery	
Vaginal delivery	633 (68.4)
Cesarean section	293 (31.6)
Gestational age	
Born term	787 (85.0)
Born preterm	62 (6.7)
No data term/preterm	77 (8.3)
Total	926

Table 2. Major bleed and intracranial hemorrhage (ICH) in term or preterm delivery in the first 28 days.

	All	Major bleed n (%)	ICH n (%)
Term	787	41 (5.2)	20(2.5)
Preterm	62	3 (6.4)	0 (0)
Missing data term/preterm	77	0 (0)	0 (0)
Total	926	44	20

Table 3. Intracranial hemorrhage (ICH) and major bleeds and mode of delivery.

	All n	ICH n (%)	Major bleeds n (%)
Vaginal delivery without instruments	541	8 (1.5)	14 (2.6)
Vaginal instrumental	68	7 (10.2)	13 (19.1)
Cesarean prior to labor	125	2 (1.6)	5 (4.0)
Cesarean during labor	79	2 (2.5)	7 (8.9)
No detailed information on MOD	113	1 (0.8)	5 (4.4)
Total	926	20	44

MOD: mode of delivery.

hemophilia 0.7% (1 of 140) (P=0.009) where only one major bleed in the neonatal period was reported.

The analysis of major bleeds in severe hemophilia only showed the same significant results regarding vaginal instrumental delivery as a risk factor compared to vaginal delivery without instruments (P<0.0001; RR 7.28) and CS prior to labor (P=0.0004; RR 6.05) (Table 3); therefore, these groups were kept together in the further analysis.

Family history of hemophilia

In 466 neonates there was a known family history of hemophilia. In 445 cases, no family history of hemophilia was known; these patients represent sporadic cases where no influence on mode of delivery could be made. The rate of CS differed significantly between the groups (P=0.009): 35.8% (167 of 466) in the group with known family history were born by CS and 27.6% (123 of 445) of the sporadic cases (Table 5). The reason for planned CS in the group of known family history was hemophilia carrier status and/or known hemophilia status of the child in 45.2% (38 of 84 cases), in 14.3% (12 of 84 cases) due to a combination of hemophilia status and maternal/fetal issues, and in 29.8% not related to hemophilia (n=16 cases, maternal; n=9 cases, fetal). The reasons recorded for a planned CS in the group with no known family history of hemophilia (n=49) were maternal reasons in 65.3% (n=32), fetal reasons in 24.5% (n=12), combined reasons in 4.1% (n=2), and Other in 6.1% (n=3). Vaginal instrumental deliveries occurred less often when a family history was known (18 of 466) than in the group with no known family history (48 of 445) (P=0.00038).

However, there was no significant difference in the frequency of major bleeds and ICH between the group with known family history (KFH) and the group with no known family history (NFH) (P=0.87 and P=0.37, respectively). In the KFH group, we found an overall frequency of 4.7% (22 of 466) for major bleeds and 1.7% (8 of 466) for ICH. In comparison, in NFH the frequency was of 4.5% (20 of 445) for major bleeds and 2.7% (12 of 445) for ICH. For more detailed information see Table 5.

Prenatal diagnosis

Prenatal diagnosis was performed in 13.7% (62 of 466) of the children with a known family history of hemophilia. In this group, the rate of CS was significantly higher (32 of 62; 51.6% *vs.* 135 of 404, 33.4%) than in the group with known family history and no PND (P=0.0068).

Mortality

One child with no known family history died after CS in labor due to ICH in the neonatal period. The patient was diagnosed with ICH at six days of age and the diagnosis of hemophilia A was made on the same day; this child was included in the analysis.

No other deaths related to major bleeds or ICH were reported.

Counseling of a pregnant carrier of hemophilia

In counseling a pregnant carrier, the decision to be taken is between a planned CS (in most cases prior to labor) compared to planned vaginal delivery which can result in vaginal delivery with or without instruments or CS during labor. Patients with planned vaginal delivery (n=703) had a non-instrumental vaginal delivery in 77% (541 of 703), an instrumental delivery in 9.7% (68 of 703), and a CS during labor in 9.9% (70 of 703); in 24 patients it was unknown if the vaginal delivery was with or without instruments (3.4%). Patients with planned CS (n=134) had a CS prior to labor in 93.2% (125 of 134) and in 9 patients the CS was performed in labor (6.8%) (Table 6). We compared planned CS (n=134) to planned vaginal delivery (n=703) for the whole cohort, and no significant difference could be seen for both ICH (P=0.75) and major bleeds (P=0.82). The frequencies for ICH were 1.5% (2 of 134) for planned CS and 2.4% (17 of 703) for planned vaginal delivery. Frequencies for major bleeds were 3.7% (5 of 134) for planned CS and 4.8% (34 of 703) for planned vaginal delivery. (See Table 6 for an overview.) We also compared the subgroup of patients with known family history of hemophilia and compared the number of major bleeds and ICH in planned CS (n=84) and planned vaginal delivery (n=327); even here, there was no significant difference (P=0.777 for major bleeds, P=1 for ICH).

Discussion

In this multicenter study, no statistical difference was

Table 4. Pairwise comparisons between groups on mode of delivery.

Reference group	Comparison group	ICH *P*-value; RR (95%CI)	Major bleeding *P*-value; RR (95%CI)/severe hemophilia only
Vaginal delivery without instruments	Vaginal instrumental	§*0.0005; 6.96 (2.61,18.60)	§*<0.0001; 7.39 (3.63,15.05)/ §*<0.0001; 7.28 (3.60,14.72)
Vaginal delivery without instruments	Cesarian prior to labor	1.0000; 1.08 (0.23,5.03)	0.3758; 1.55 (0.57,4.21)/ 0.3408; 1.20 (0.4.;3.58)
Vaginal delivery without instruments	Cesarian during labor	0.3709; 1.71 (0.37,7.92)	*0.0110; 3.42 (1.43,8.22)/ *0.0209; 3.20 (1.34; 7.66)
Cesarian prior to labor	Vaginal instrumental	*0.0100; 6.43 (1.37,30.12)	§*0.0012; 4.78(1.78,12.84)/ §*0.0004; 6.05 (2.07, 17.72)
Cesarian during labor	Vaginal instrumental	0.0814; 4.07 (0.87,18.92)	0.0918; 2.16 (0.91,5.10)/ 0.1263; 2.27 (0.97, 5.32)
Cesarian prior to labor	Cesarian during labor	0.6417; 1.58 (0.23,11.01)	0.2207; 2.22 (0.73,6.74)/ 0.09396; 2.66 (0.81, 8.76)

ICH: intracranial hemorrhage; RR. relative risk; CI: Confidence Interval. *Significant at significance level P<0.05; §significant after Bonferroni correction P<0.0083.

Table 5. Known and unknown family history of hemophilia.

	All	Known family history of hemophilia	Unknown family history of hemophilia	Family history not known
	n	n (%)	n (%)	n
ICH	20	8 (1.7)	12 (2.7)	0
Major bleeds	44	22 (4.7)	20 (4.5)	2
Vaginal delivery	633	299 (64.2)	322 (72.4)	12
VD without instruments	541	285	274	5
VD instrumental	68	14	48	6
Not known with/without instruments	24	13	10	1
Cesarean section	293	167 (35.8)*	123 (27.6)	3
Planned CS	134	84	49	1
Reason:				
Hemophilia		37	–	0
Combined hemophilia and maternal or fetal status		12	–	0
Maternal		16	32	1
Fetal		9	12	0
Combined maternal/fetal		0	2	0
Other/unknown		9/1	3/0	0
Total number	926	466	445	15

*Significant at $P<0.05$ in comparison to unknown family history of hemophilia. n: number; ICH: intracranial hemorrhage; VD: vaginal delivery; CS: Cesarean section.

found in the rate of major bleeds and intracranial hemorrhage in neonates with moderate and severe hemophilia between vaginal delivery and Cesarean section: major bleeds occurred in 4.3% neonates born by VD and in 5.8% after CS (P=not significant, ns); ICH in 2.4% following VD and 1.7% after CS (P=not significat, ns). Further analysis of subgroups by MOD (VD with and without instruments, CS prior to and during labor) revealed instrumental VD as a risk factor for major bleeds and intracranial hemorrhage compared to non-instrumental VD (RR 7.39 major bleed; 6.96 ICH) and CS prior to labor. Neonates with moderate hemophilia had a similar risk regarding ICH compared to severe hemophilia, but a lower risk for other major bleeds. No other significant differences were found between the subgroups of vaginal delivery without instruments, CS prior and CS during labor. The CS rate was higher in neonates with a known family history and reason was hemophilia in more than half of the cases. However, no significant difference was found between the group with and without a known family history of hemophilia regarding major bleeds and ICH. The comparison of planned CS (including CS prior to labor in 93.2% but also including some cases during labor) to planned VD (including VD without instruments in 77% and also instrumental VD and CS during labor) also showed no significant difference in the group with known family history

To our knowledge, this study represents the largest prospective, monitored series recording comprehensive data on mode of delivery and neonatal bleeds in patients with moderate and severe hemophilia. The data come from countries with a good and quite uniform standard of health care which should make the results relevant and applicable for these countries, although the results may also be applicable to countries with different health care standards. Due to the inclusion of all consecutive cases in the participating centers, selection bias should be low but cannot be totally excluded. Missing data is a problem for most registries. Earlier publications of the PedNet registry show high quality data regarding baseline data and first 75 exposure days including bleeds, with only 4% missing data.[14] The subanalysis on detailed information on mode of delivery (vaginal with instruments, CS prior to or during labor, reason for CS) was available in 813 of 926 (87.8%) patients, which means that in 12.2% of included patients these data are missing, which is still acceptable for analysis. However, the frequencies for both major bleeds and ICH are low, and small differences between the groups analyzed cannot be detected due to the limited number of included patients. For example, to show a difference between ICH in vaginal delivery of 2.4% to CS of 1.7%, over 12,000 patients would have to be included, which is not feasible. We excluded mild hemophilia from our analysis since the diagnosis in these patients is often made at an older age and undiagnosed cases born during the study period have not yet been included in the PedNet Registry.[15]

Both term and preterm neonates were included in the calculations and one could question if data should have been presented separately since ICH is a well-known complication of, in particular, delivery of an extremely premature neonate.[16] Our series included 849 children with data on gestational week of birth, of whom 62 (7.3%) were born prematurely, but only 11 children (1.3%) were born before the 33rd gestational week, i.e. very or extremely premature. There were three major bleeds in the premature group (5.2%) and no cases of ICH. In term births, 41 major bleeds in 787 neonates (6.4%) occurred, and 20 ICH (20 of 787; 2.5%). Since there was no significant difference in the frequency of bleeds between the term and preterm groups we considered it justified to merge them together in the calculations. The premature group was still a rather small group, and a much larger group would be needed in order to draw any conclusions between the more extremely premature and less premature on this issue. In another neonatal series,

Richards *et al*.,[8] with an overall head bleed rate of 3.5% and some data on prematurity (29 premature children; 6.0% in the series), had the same issue. It is, however, possible that extreme prematurity is under-represented in the registry due to mortality before diagnosis.

The frequency of major bleeds and ICH for all neonates was similar to previous studies.[9,17,18] When splitting the group into instrumental VD and non-instrumental VD, and CS prior to and during labor, only instrumental VD was identified as a risk factor. A recent study from the UK on ICH in bleeding disorders had similar findings and identified instrumental delivery as a clear risk factor with a RR of 10.6.[19] This is also known from the normal population, but in lower frequencies: Towner *et al*. reported ICH frequencies of 1 of 860 for VE and 1 of 664 for forceps and VE, which means that the risk for ICH in hemophilic neonates born by instrumental delivery is roughly 80-fold higher in our series.[12] In a recent published meta-analysis from Davies and Kadir, CS was proposed as a safer option for children born with hemophilia, but the comparison was made with historical cohorts.[7] In our prospective cohort, there was no difference in incidence of major bleeds and ICH in neonates born by vaginal delivery (both instrumental and non-instrumental) compared to CS (prior to and during labor): 5.2% *versus* 6.4% in major bleeds, and 2.3% *versus* 1.7% for ICH. A planned CS with the intention to perform CS prior to labor did not prevent neonates from experiencing ICH or major bleeds in comparison to planned VD. This information is important when counseling a pregnant carrier. It has also been shown in other studies that CS does not prevent neonatal bleeds.[4,8,9] Studies from the normal population with 583,340 births included show that vaginal delivery without instruments and CS prior to labor were the safest option but ICH still occurred (1 of 2,750 CS prior to labor, and 1 of 1,900 delivered spontaneously).[12]

A known family history of hemophilia (KFH) had some influence on the mode of delivery: 36% (167 of 466) were delivered by CS in the KFH group compared to 28% (123 of 445) in the no known family history group (NFH) (P=0.00038). The group of neonates in the NFH group present the 'true risk' of neonatal bleeds in a child with hemophilia, since no precautionary measures had been taken with respect to hemophilia on the obstetric procedures. However, there was no significant difference in the rate of major bleeds and ICH between KFH and NFH. Regarding vaginal delivery, 4.5% of the children in the NFH group compared to 4.7% in the KFH had a major bleed and 2.7% had ICH in the NFH-group compared to 1.7% in the KFH-group. This may be explained by our findings, that the mode of delivery (CS *vs.* vaginal delivery) did not impact the rate of major bleeds and ICH. Similar findings were shown in a recent study of Kulkarni *et al*. in which 547 neonates with all severities of hemophilia were included.[20] The reason to choose a planned CS was hemophilia in 45%; but in 55%, other maternal and fetal reasons played a role illustrating that the planning of a delivery is a complicated and multifactorial task.

Prenatal diagnosis was performed in 14% (62 of 466) of known carriers, and in these cases it was definitely known that they were carrying a child with hemophilia. In this subgroup, 51.6% were delivered by CS, demonstrating a statistically significant impact on the decision to choose a CS delivery. We do not have data on how many carriers terminated pregnancy after PND with an affected fetus, so the numbers on PND might be underestimated. However, recent figures from Sweden indicate that carriers today often choose PND in order to prepare for having a hemophilia child and not for termination of the pregnancy; but this may not be the case in all participating centers.[21]

Table 6. Planned vaginal delivery *versus* planned Cesarean section – major bleeds and intracranial hemorrhage (ICH).

	n	ICH n (%)	Major bleeds n (%)
Planned VD	703	17 (2.4)	34 (4.8)
VD without instruments	541	10	18
VD instrumental	68	7	13
CS during labor	70	0	3
VD not known with or without instruments	24	0	0
Planned CS	134	2 (1.5)	5 (3.7)
CS prior to labor	125	2	5
CS during labor	9	0	0
Planning not known	89	1	5
P-value; RR (CI)		0.753; 1.62 (0.38,6.93)	0.822; 1.30 (0.52,3.25)

VD: vaginal delivery; CS: Cesarean section; RR: relative risk.

One child died from ICH, representing 1 of 786 boys with severe hemophilia (0.13%), and 1 of 20 of all ICH (5%). These numbers are low compared to historical data, but they are in line with a recent CDC report that included all ICH with a mortality rate of around 2.5%.[22] These numbers may be underestimated due to undiagnosed or unreported cases.

It would have been of interest to analyze the risks and outcomes for the carrier mothers who gave birth to a child with hemophilia according to delivery mode, but our registry is limited to pediatric data.

In summary, vaginal delivery and Cesarean section carry similar risks of ICH and major bleeds in neonates with severe and moderate hemophilia, and pregnant carriers of hemophilia should be informed about different options for mode of delivery and their potential risks.

Acknowledgments

The authors thank study coordinator Ella van Hardeveld and statistician Susann Ullén for their help with this study. We would like to acknowledge unrestricted funding from Bayer AG, Baxter/Baxalta/ Shire, CSL Behring, Pfizer, Novonordisk, Sobi and Grifols to the PedNet group that were partly used for this study.

Appendix

PedNet Haemophilia Research Foundation contributors to this study.

Europe

C Altisent Roca, Unitat Hemofilia, Hospital Vall d'Hebron, Barcelona, Spain; MT Alvarez Romàn, Unidad de Coagulopatías, Hospital Universitario La Paz, Madrid, Spain

M Bührlen, Gesundheit Nord, Klinikum Bremen Mitte, Prof.-Hess-Kinderklinik, Bremen, Germany; HM van den Berg, PedNet Haemophilia Research Foundation, Baarn, The Netherlands; E Chalmers, Department of Haematology, Royal Hospital for Children, Glasgow, UK; H Chambost, Pediatric Haematology Oncology Department, Children Hospital La

Timone, AP-HM, and INSERM, INRA, C2VN, Faculté de Médecine, Aix-Marseille University, Marseille, France; A Rosa Cid, Unidad de Hemostasia y Trombosis, Hospital Universitario y Politécnico La Fe, Valencia, Spain; S Claeyssens, Centre Regional d'Hemophilie, Centre Hospitalo Universitaire, Toulouse, France; C Escuriola, HZRM Hämophilie Zentrum Rhein Main GmbH, Mörfelden-Walldorf, Germany; K Fischer, Van Creveld Kliniek, University Medical Center Utrecht, Utrecht, The Netherlands; C Van Geet, Catholic University of Leuven, Campus Gasthuisberg, Service of Pediatric Haematology, Leuven, Belgium; R Kobelt, Hämophiliezentrum, Wabern and Children's Hospital of the University of Berne, Switzerland; C Königs, J .W. Goethe University Hospital, Department of Pediatrics, Frankfurt, Germany; K Kurnik, Dr. V. Haunersches Kinderspital, University of Munich, Munich, Germany; R Liesner, Hemophilia Center, Department of Haematology, Great Ormond Street Hospital for Children, London, UK; R Ljung, Department of Clinical Sciences, Lund University, Lund; Department of Pediatrics and Malmö Centre for Thrombosis and Haemostasis, Skåne University Hospital, Malmö, Sweden; A Mäkipernaa, Children's Hospital , Helsinki University Central Hospital and University of Helsinki, Helsinki, Finland; A Molinari, Dipartimento di Ematologia ed Oncologia, Unità Trombosi ed Emostasi, Ospedale Pediatrico Giannina Gaslini, Genova, Italy; W Muntean, Universitäts-Klinik für Kinder- und Jugendheilkunde, Graz, Austria; B Nolan, Department of Paediatric Haematology, Our Lady's Children's Hospital for Sick Children, Crumlin, Dublin, Ireland; J Oldenburg, Institut für Experimentelle Hämatologie und Transfusionsmedizin, Universitätsklinikum Bonn, Germany; R Pérez Garrido, Hospital General Unidad de Hemofilia, Hospitales Universitarios Virgen del Rocio, Sevilla, Spain; H Platokouki, Haemophilia-Haemostasis Unit, St. Sophia Children's Hospital, Athens, Greece; A Rafowicz, Centre de Référence pour le Traitement des Maladies Hémorragiques (CRTH), Hôpital Bicêtre, Kremlin Bicêtre AP-HP , France; S Ranta, Department of Pediatrics, Clinic of Coagulation Disorders, Karolinska Hospital, Stockholm,Sweden; E Santagostino, ME Mancuso, Angelo Bianchi Bonomi Hemophilia and Thrombosis Center, Fondazione, IRCCS Ca' Granda, Ospedale Maggiore Policlinico, Milan, Italy; T Stamm Mikkelsen, Department of Pediatrics, University Hospital of Aarhus at Skejby, Aarhus, Denmark; A Thomas, Royal Hospital for Sick Children, Edinburgh, UK; M Williams, Department of Haematology, The Children's Hospital, Birmingham, UK.

Israel

G Kenet, National Hemophilia Center, Ministry of Health, Sheba Medical Center, Tel Hashomer, Israel

Canada

M Carcao, Division of Haematology/Oncology, Hospital for Sick Children, Toronto, Canada; G Rivard, Division of Hematology/Oncology, Hôpital St Justine, Montréal, Canada.

References

1. Stieltjes N, Calvez T, Demiguel V, et al. Intracranial haemorrhages in French haemophilia patients (1991-2001): clinical presentation, management and prognosis factors for death. Haemophilia. 2005;11 (5):452-458.
2. Klinge J, Auberger K, Auerswald G, Brackmann HH, Mauz-Korholz C, Kreuz W. Prevalence and outcome of intracranial haemorrhage in haemophiliacs--a survey of the paediatric group of the German Society of Thrombosis and Haemostasis (GTH). Eur J Pediatr. 1999;158 Suppl 3:S162-165.
3. Gouw SC, van der Bom JG, Marijke van den Berg H. Treatment-related risk factors of inhibitor development in previously untreated patients with hemophilia A: the CANAL cohort study. Blood. 2007;109 (11):4648-4654.
4. Kulkarni R, Lusher JM. Intracranial and extracranial hemorrhages in newborns with hemophilia: a review of the literature. J Pediatr Hematol Oncol. 1999;21(4):289-295.
5. Ljung R, Lindgren AC, Petrini P, Tengborn L. Normal vaginal delivery is to be recommended for haemophilia carrier gravidae. Acta Paediatr. 1994;83(6):609-611.
6. Revel-Vilk S, Golomb MR, Achonu C, et al. Effect of intracranial bleeds on the health and quality of life of boys with hemophilia. J Pediatr. 2004;144(4):490-495.
7. Davies J, Kadir RA. Mode of delivery and cranial bleeding in newborns with haemophilia: a systematic review and meta-analysis of the literature. Haemophilia. 2016;22(1):32-38.
8. Richards M, Lavigne Lissalde G, Combescure C, et al. Neonatal bleeding in haemophilia: a European cohort study. Br J Haematol. 2012;156(3):374-382.
9. Nazir HF, Al Lawati T, Beshlawi I, et al. Mode of delivery and risk of intracranial haemorrhage in newborns with severe haemophilia A: a multicentre study in Gulf region. Haemophilia. 2016;22(3):e134-138.
10. Ljung R. The optimal mode of delivery for the haemophilia carrier expecting an affected infant is vaginal delivery. Haemophilia. 2010;16(3):415-419.
11. James AH, Hoots K. The optimal mode of delivery for the haemophilia carrier expecting an affected infant is caesarean delivery. Haemophilia. 2010;16(3):420-424.
12. Towner D, Castro MA, Eby-Wilkens E, Gilbert WM. Effect of mode of delivery in nulliparous women on neonatal intracranial injury. N Engl J Med. 1999;341 (23):1709-1714.
13. Kasper CK, Lin JC. Prevalence of sporadic and familial haemophilia. Haemophilia. 2007;13(1):90-92.
14. Fischer K, Ljung R, Platokouki H, et al. Prospective observational cohort studies for studying rare diseases: the European PedNet Haemophilia Registry. Haemophilia. 2014;20(4):e280-286.
15. Chambost H, Gaboulaud V, Coatmelec B, Rafowicz A, Schneider P, Calvez T. What factors influence the age at diagnosis of hemophilia? Results of the French hemophilia cohort. J Pediatr. 2002;141(4):548-552.
16. Stoll BJ, Hansen NI, Bell EF, et al. Trends in Care Practices, Morbidity, and Mortality of Extremely Preterm Neonates, 1993-2012. Jama. 2015;314(10):1039-1051.
17. Ljung RC. Intracranial haemorrhage in haemophilia A and B. Br J Haematol. 2008;140(4):378-384.
18. Palomo Bravo A, Nunez R, Gutierrez Pimentel MJ, Nieto MD, Cos C, Perez R. Haemophilia neonates: mode of delivery and perinatal complications. Haemophilia. 2016;22(3):e225-228.
19. Chalmers EA, Alamelu J, Collins PW, et al. Intracranial haemorrhage in children with inherited bleeding disorders in the UK 2003-2015: A national cohort study. Haemophilia. 2018;24(4):641-647.
20. Kulkarni R, Presley RJ, Lusher JM, et al. Complications of haemophilia in babies (first two years of life): a report from the Centers for Disease Control and Prevention Universal Data Collection System. Haemophilia. 2017;23(2):207-214.
21. Martensson A, Tedgard U, Ljung R. Prenatal diagnosis of haemophilia in Sweden now more commonly used for psychological preparation than termination of pregnancy. Haemophilia. 2014;20 (6):854-858.
22. Witmer CM. Low mortality from intracranial haemorrhage in paediatric patients with haemophilia. Haemophilia. 2015;21 (5):e359-363.

ARTICLE

The International Hereditary Thrombotic Thrombocytopenic Purpura Registry: key findings at enrollment until 2017

Hendrika A. van Dorland,[1,2] Magnus Mansouri Taleghani,[1] Kazuya Sakai,[3] Kenneth D. Friedman,[4] James N. George,[5] Ingrid Hrachovinova,[6] Paul N. Knöbl,[7] Anne Sophie von Krogh,[8] Reinhard Schneppenheim,[9] Isabella Aebi-Huber,[1,2] Lukas Bütikofer,[10] Carlo R. Largiadèr,[11] Zuzana Cermakova,[12] Koichi Kokame,[13] Toshiyuki Miyata,[13,14] Hideo Yagi,[3,15] Deirdra R. Terrell,[5] Sara K. Vesely,[5] Masanori Matsumoto,[3] Bernhard Lämmle,[1,16] Yoshihiro Fujimura[3,17] and Johanna A. Kremer Hovinga;[1,2] Hereditary TTP Registry

[1]Department of Hematology and Central Hematology Laboratory, Inselspital, Bern University Hospital, Bern, Switzerland; [2]Department for BioMedical Research, University of Bern, Bern, Switzerland; [3]Department of Blood Transfusion Medicine, Nara Medical University, Kashihara, Japan; [4]Division of Hematology and Oncology, Medical College of Wisconsin, Milwaukee, WI, USA; [5]Department of Biostatistics Epidemiology, University of Oklahoma Health Sciences Center, Oklahoma City, OK, USA; [6]NRL for Hemostasis, Institute of Hematology and Blood Transfusion, Prague, Czech Republic; [7]Division of Hematology and Hemostasis, Department of Medicine 1, Medical University of Vienna, Austria; [8]Department of Hematology, St Olavs Hospital, Trondheim University Hospital, Trondheim, Norway; [9]Department of Paediatric Haematology and Oncology, University Medical Centre Hamburg-Eppendorf, Hamburg, Germany; [10]CTU Bern, University of Bern, Bern, Switzerland; [11]University Institute of Clinical Chemistry, Inselspital, Bern University Hospital, Bern, Switzerland; [12]Blood Center, University Hospital Ostrava, Ostrava, Czech Republic; [13]Department of Molecular Pathogenesis, National Cerebral and Cardiovascular Center, Suita, Japan; [14]Department of Cerebrovascular Medicine, National Cerebral and Cardiovascular Center, Suita, Japan; [15]Department of Hematology, Nara Prefecture General Medical Center, Nara, Japan; [16]Center for Thrombosis and Hemostasis, University Medical Center Mainz, Mainz, Germany and [17]Japanese Red Cross Kinki Block Blood Center, Ibaraki, Osaka, Japan

Haematologica 2019
Volume 104(10):2107-2115

ABSTRACT

Congenital thrombotic thrombocytopenic purpura is an autosomal recessive inherited disease with a clinically heterogeneous course and an incompletely understood genotype-phenotype correlation. In 2006, the Hereditary TTP Registry started recruitment for a study which aimed to improve the understanding of this ultra-rare disease. The objective of this study is to present characteristics of the cohort until the end of 2017 and to explore the relationship between overt disease onset and ADAMTS13 activity with emphasis on the recurring *ADAMTS13* c.4143_4144dupA mutation. Diagnosis of congenital thrombotic thrombocytopenic purpura was confirmed by severely deficient ADAMTS13 activity (≤10% of normal) in the absence of a functional inhibitor and the presence of *ADAMTS13* mutations on both alleles. By the end of 2017, 123 confirmed patients had been enrolled from Europe (n=55), Asia (n=52, 90% from Japan), the Americas (n=14), and Africa (n=2). First recognized disease manifestation occurred from around birth up to the age of 70 years. Of the 98 different *ADAMTS13* mutations detected, c.4143_4144dupA (exon 29; p.Glu1382Argfs*6) was the most frequent mutation, present on 60 of 246 alleles. We found a larger proportion of compound heterozygous than homozygous carriers of *ADAMTS13* c.4143_4144dupA with overt disease onset at < 3 months of age (50% *vs.* 37%), despite the fact that ADAMTS13 activity was <1% in 18 of 20 homozygous, but in only 8 of 14 compound heterozygous carriers. An evaluation of overt disease onset in all patients with an available sensitive ADAMTS13 activity assay (n=97) shows that residual ADAMTS13 activity is not the only determinant of age at first disease manifestation. Registered at *clinicaltrials.gov identifier NCT01257269.*

Correspondence:

JOHANNA A. KREMER HOVINGA
johanna.kremer@insel.ch

Received: January 16, 2019.

Accepted: February 20, 2019.

Pre-published: February 21, 2019.

doi:10.3324/haematol.2019.216796

Check the online version for the most updated information on this article, online supplements, and information on authorship & disclosures: www.haematologica.org/content/104/10/2107

Introduction

Hereditary or congenital thrombotic thrombocytopenic purpura (cTTP; also known as Upshaw-Schulman syndrome; OMIM: 274150) is an autosomal recessive inherited thrombotic microangiopathy (TMA), which can manifest with acute life-threatening disease episodes and frequent relapses.[1-5] The underlying pathophysiology is an absent or severely reduced activity of ADAMTS13 (a disintegrin and metalloproteinase with thrombospondin type 1 repeats, member 13) caused by bi-allelic mutations in the *ADAMTS13* gene.[6-9] In the absence of functional ADAMTS13, large von Willebrand factor multimeric strings are not cleaved into normal-sized ones. As a result, platelets adhere to these unusually large, extremely adhesive multimers leading to occlusive microvascular thrombosis. The clinical manifestations of acute TTP include the concomitant occurrence of often severe thrombocytopenia, microangiopathic hemolytic anemia, and a variable degree of ischemic organ damage, particularly affecting the brain, heart and kidneys. If left untreated, mortality exceeds 90%.[10]

Congenital TTP (cTTP) is an ultra-rare disease, affecting about one per 1,000,000 persons.[5,11] Its rarity makes it difficult to unravel what contributes to its complex and varied clinical presentation and course of disease. Adding to this challenge is the large variety of *ADAMTS13* gene mutations (> 200)[11-14] that have been identified (missense, nonsense, splice site mutations, and frameshift mutations caused by small deletions and insertions), and new mutations are being continuously revealed. *ADAMTS13* gene variants may abolish or impair ADAMTS13 synthesis, secretion or activity.[12,14,15] Some data suggest that the severity of disease in cTTP is related to residual ADAMTS13 activity.[13,16] In a cohort of 29 cTTP patients, Lotta *et al.*[17] found residual ADAMTS13 activity of < 3% to be associated with an early disease onset (< 18 years of age), an annual event rate of >1, and a need for prophylactic plasma therapy. Age at overt onset and diagnosis of cTTP shows, in general, a seemingly dichotomous distribution, with approximately half of patients presenting within their first five years of life, and the other half experiencing disease onset in early adulthood, often during a first pregnancy.[11,18-21] Childhood-onset cTTP often starts in the neonatal period with hematologic features and severe jaundice.[11,22] Moreover, Schneppenheim *et al.*[23] and von Krogh *et al.*[24] reported on variable disease courses in cTTP patients homozygous for the *ADAMTS13* c.4143_4144dupA mutation, typically having an ADAMTS13 activity <1% of normal. Consequently, the question was asked as to whether residual ADAMTS13 activity is really the major determinant of clinical heterogeneity in cTTP.[25]

The Hereditary TTP Registry (*clinicaltrials.gov identifier: NCT01257269*) started in 2006 as an international open and ambidirectional cohort study for patients with confirmed and suspected cTTP and their family members.[26] The Registry's overall aim is to document individual clinical courses, treatment requirements, and to identify possible triggers of acute TTP episodes and disease modifiers in relation to the disease-causing *ADAMTS13* mutations. The primary aim of this report is to provide the demographic and clinical characterization of the cTTP cohort at enrollment from when the study started until the end of 2017. A second objective was to evaluate residual ADAMTS13 activity and its relation to apparent disease onset in the whole cohort, with emphasis on carriers of *ADAMTS13* c.4143_4144dupA (p.Glu1382Argfs*6) mutation.

Methods

Eligibility

The Hereditary TTP Registry enrolls patients from all over the globe. Those eligible for participation are patients with confirmed or suspected cTTP and their family members (for diagnostic criteria see the *Online Supplementary Appendix*). In the current study, enrollment data from patients with confirmed cTTP were used for evaluation.

Patient recruitment

Initially, eligible patients were identified through the Bern TTP Registry and the Nara Medical University Registry on thrombotic microangiopathies (TMA), and enrolled through their treating physicians. Later, patients or their physicians approached the Registry directly through the website (*www.ttpregistry.net*), based on its related publications[24,26] and contributions at national and international congresses. The Hereditary TTP Registry includes patients from published reports, and patients who have been newly identified. By the end of 2017, around two-thirds of the 123 confirmed cTTP patients had been reported in case reports and case series between 1981 and 2018 (*Online Supplementary Appendix B*), prior to their enrollment in the Registry.

The Hereditary TTP Registry was approved by the Lead Cantonal Ethics Committee (CEC) in Bern in 2006 (CEC n. 031/06). The protocol was approved by the Institutional Review Boards or Ethics Committees and Institutional Boards responsible, as applicable, at each site. All Registry participants or their legal representatives provided written informed consent before enrollment.

Data collection at enrollment

Data collection at enrollment is described in the *Online Supplementary Appendix*.

ADAMTS13 parameters

In the majority of patients (n=96), ADAMTS13 activity assays, functional inhibitors, anti-ADAMTS13 antibodies, as well as molecular analysis of the *ADAMTS13* gene, were performed in the Central Hematology Laboratory, Bern University Hospital, University of Bern, Switzerland (50 patients), and in the Department of Blood Transfusion Medicine, Nara Medical University, Japan (46 patients). In the remaining 27 confirmed patients, analyses were performed in other laboratories employing various assays. For two patients, ADAMTS13 activity values were not reported.

ADAMTS13 activity was determined in Bern by the modified FRETS-VWF73 assay [lower limit of quantification (LLQ) 1%][27,28] and in Nara by the chromogenic ADAMTS13-act-ELISA (LLQ 0.5%).[29]

Before combining ADAMTS13 activity data for descriptive analysis, we carried out an assay comparison on 41 plasma samples of cTTP patients (*Online Supplementary Table S1*).

Functional ADAMTS13 inhibitors were assessed by a Bethesda-like assay and reported in Bethesda units (BU)/mL, a value ≤0.4 BU/mL is considered negative.[27,30] Anti-ADAMTS13 IgG antibodies were assessed by an in-house ELISA,[11] or a commercially available ELISA (Technoclone®) according to the manufacturer's instructions. A patient's sample was defined negative for anti-

ADAMTS13 IgG antibodies if the titer value was < 25 for the former method,[11] and < 15 arbitrary units/mL for the commercially available ELISA (Technoclone®) method.

DNA extraction from leukocytes, amplification of all 29 *ADAMTS13* exons with flanking intron–exon boundaries and sequencing were performed using standard methods. Amino acids and nucleotides are numbered according to the recommendation of the Human Genome Variation Society.[31]

Overt disease onset and acute episode definitions

Definition of overt disease onset and acute episode can be found in the *Online Supplementary Appendix*.

Statistical analysis

The statistical analysis is described in the *Online Supplementary Appendix*.

Results

Demographics, clinical and biochemical characteristics

During the period from the beginning of the project in 2006 (*clinicaltrials.gov identifier NCT01257269*) until the end of 2017, 149 patients were assessed for enrollment in the Hereditary TTP Registry; seven patients were excluded as they did not have cTTP. Of the 142 enrolled patients, 19 patients from 19 families were categorized at the end of 2017 as suspected cTTP patients and did not undergo further analysis in this study; the remaining 123 patients from 117 families had confirmed cTTP (Table 1 and *Online Supplementary Figure S1*). The female to male ratio was 1:1. Fifty-five and 52 patients were enrolled from Europe and Asia, respectively, 14 from the Americas, and 2 from one site on the African continent (*Online Supplementary Figure S2*). Accordingly, 65 participants were Caucasian, 52 Asian, and 3 Hispanic. Median age at enrollment was 26.1 years (range: 0.1-75.0 years), median age at clinical diagnosis was 16.7 years (range: 0-69.8 years), and median age at reported overt disease onset was 4.5 years (range: 0-69.8 years). Figure 1 shows the relationship between overt disease onset, clinical diagnosis, and confirmation of the diagnosis for each patient over time.

ADAMTS13 activity values were reported for 121 of 123 patients and ≤10% in 121/121 (Table 1). Despite missing ADAMTS13 activity values, two patients were diagnosed with cTTP based on the molecular analysis of the *ADAMTS13* gene showing two disease-causing mutations.

ADAMTS13 functional inhibitors were negative in all reported cases, but 12 of 103 patients analyzed had a positive anti-ADAMTS13 antibody result by ELISA (Table 1). Consanguinity of the parents was acknowledged in 14 out of 104 cTTP patients for whom this information was provided. Forty-seven patients were homozygous and 76 compound heterozygous mutation carriers. In total, 98 different *ADAMTS13* mutations were identified in 123 confirmed cTTP patients.

Occurrence of diseases and disorders up until enrollment

Information on the occurrence of concomitant diseases and disorders up until enrollment was available for 120 cTTP patients (Table 2). Jaundice (due to hemolysis or liver disease, 49%) and arterial thromboembolic events (28%) were frequently reported. Stroke had occurred in 21%, and transient ischemic attack in 10%. Arterial thromboembolic events had occurred in all age groups. In the groups >40-50 years and >50 years, 50% or more of the cTTP patients had suffered from at least one arterial thromboembolic event (Figure 2). Other neurological disorders included epileptic seizures (6 patients), headache (5 patients), and psychiatric conditions (depression, behavioral and mental disorders; 20 patients).

Renal insufficiency occurred in 25% of the cohort. Twelve patients needed hemodialysis and 3 underwent a kidney transplantation. Autoimmune disorders (hypothyroidism, IgA nephritis, hyperthyroidism) were rare. Finally, transfusion-transmitted viral diseases were reported in 13 of 120 patients (11%).

Table 1. Demographic and clinical features and ADAMTS13-related laboratory findings in congenital thrombotic thrombocytopenic purpura patients at enrollment.

Characteristic	All patients (N=123)
Median age at enrollment (n=118)†	26.1 [0.1, 15.1, 37.2, 75.0]
Median age at overt disease onset (n=111)	4.52 [0.00, 0.01, 20.1, 69.8]
Median age at clinical diagnosis (n=122)	16.7 [0.00, 4.00, 28.6, 69.8]
Gender (F/M)	62/61
Ethnicity (self-reported)	
Caucasian	65 (53%)
Hispanic	3 (2.4%)
Asian	52 (42%)
Other	3 (2.4%)
ADAMTS13 activity (≤10%)	121/121
ADAMTS13 functional inhibitor (+)	0/114
Anti-ADAMTS13 antibodies (+)§	12/103
Consanguinity of parents	14/104
Homozygous genotypes	47/123
Compound heterozygous genotypes	76/123

N: total number of patients; n: number of patients with available values; F: female; M: male. Continuous variables are presented as median (minimum, 25th percentile, 75th percentile, maximum). Categorical variables are presented as number and percentage of all patients, or as number of n patients. †Five patients from five families were enrolled postmortem by consent of their family members. §A patient's sample was defined positive for Anti-ADAMTS13 IgG antibodies if the titer value was >25 for the in-house ELISA method,[11] and >15 arbitrary units/mL for the commercially available ELISA (Technoclone®) method.

Reported acute episodes and their context

A total of 291 distinct acute TTP episodes were recorded in 81 patients (*Online Supplementary Table S2*), while there was no detailed information on acute episodes in 42 patients. Patients had experienced a median of 2 episodes (range: 1-22) prior to enrollment, corresponding to a median of 0.10 (range: 0.02-8.91) acute episodes per year. Median duration of an episode was seven days (range: < 1-128 days).

For 287 of the 291 episodes, information on possible triggers of the acute episode was available; in 190 of 287 episodes one or more trigger(s) was/were presumed by the treating physicians (Figure 3). Infection was the most frequent trigger reported (41% of episodes). Alcohol excess was the trigger for 30 episodes and was observed only in male patients, while 28 episodes occurred during

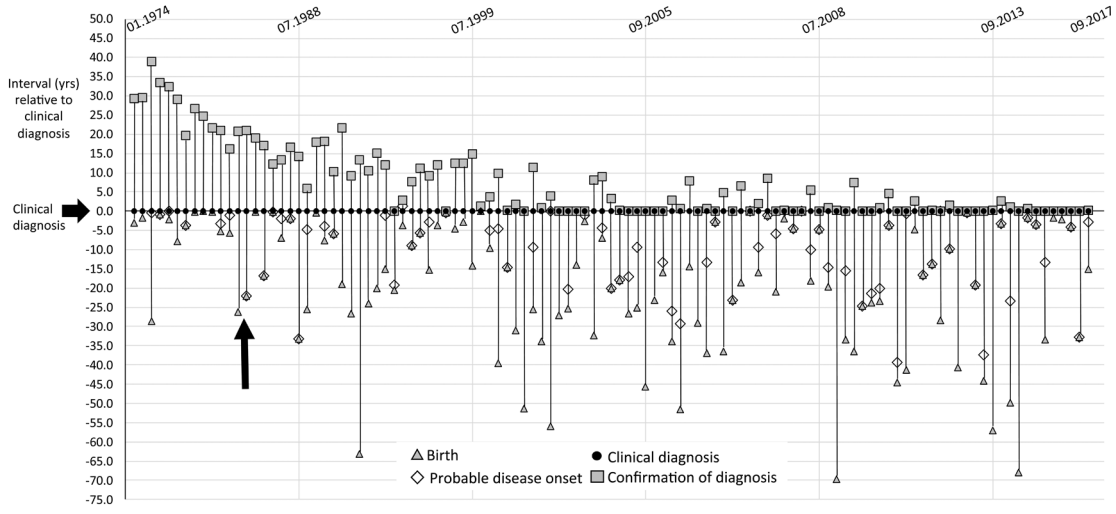

Figure 1. Clinical diagnosis and confirmation of diagnosis in relation to overt disease onset: information available for 111 confirmed congenital thrombotic thrombocytopenic purpura (cTTP) patients. x-axis: each patient's individual time point of clinical diagnosis is shown. Below the x-axis, the interval (in years, yrs) between birth, (probable) disease onset, and clinical diagnosis is shown. Above the x-axis, the interval (in yrs) between clinical diagnosis and confirmation of diagnosis is shown. Disease onset varied from as early as the new-born period up to 70 years of age. The earliest clinical diagnosis of TTP in a Registry patient was put forward in January 1974. The patient highlighted by a vertical arrow was born 22 years before the clinical diagnosis of cTTP was established although disease onset was documented in the neonatal period. Confirmation of the cTTP diagnosis was achieved by means of ADAMTS13 testing 21 years after the clinical diagnosis. NB: ADAMTS13 was first described in 1996, ADAMTS13 assays became more widely available around the turn of the millennium.

pregnancy. In addition, drug/medication use was assumed as trigger for 13 episodes, and 18 episodes seemed to be triggered by the patient's birth, injury, food poisoning, and various others.

Prophylactic treatment

Seventy-one percent of the 117 cTTP patients with available information received regular treatment, predominantly with plasma products (99%) (Table 3). Plasma products used included fresh frozen plasma in 68 patients, two received fresh frozen plasma and cryo-poor plasma, and 12 patients received solvent/detergent plasma. One patient received a plasma-derived FVIII product (Koate®). The median interval of the regular treatments was 14.0 days (range: 2-75 days). Thirty-four patients were treated on demand. These data represent a snap-shot at the time of enrollment, whereby regular treatment was intensified or reduced depending on the patient's individual requirements.

ADAMTS13 mutations

In the 123 confirmed cTTP patients, 98 different *ADAMTS13* mutations were identified in 245 alleles (*Online Supplementary Table S3*). There were 57 missense, 12 nonsense, 21 frameshift due to deletions or insertions, and 8 splice site mutations. In one patient, only one mutation was detected and diagnosis of cTTP was confirmed through a plasma infusion trial. The most frequent mutation observed was *ADAMTS13* c.4143_4144dupA (present on 60 of 246 alleles) followed by c.3178C>T (13 of 246 alleles) and c.577C>T (11 of 246 alleles) (*Online Supplementary Figure S4*). In addition, there were three mutations found in six of 246 alleles (2.4%), one mutation in 5 of 246 alleles (2.0%), 4 mutations in four of 246 alleles (1.6%), six mutations in 3 of 246 alleles (1.2%), and 81 mutations were found only once (n=58) or twice (n=23). The mutation c.3650T>C was the only mutation found on three different continents: the Americas, Asia, and Europe, involving 4, 1, and 1 alleles, respectively. Mutation c.4143_4144dupA was found on one and 59 alleles, and c.3178C>T on 3 and 10 alleles in the Americas and Europe, respectively. Mutation c.3616C>T was found with one allele in Europe and two alleles in Asia, and mutation c.4006C>T was found in both Europe and Asia with two alleles each. All other mutations were restricted to one single continent each. In Asia, c.577C>T is the most frequent mutation, found exclusively in Japan (11 alleles) (*Online Supplementary Table S3*).

Nineteen of the 98 mutations have not been reported before. Mutations were found across the *ADAMTS13* gene and in all protein domains without indication for a genetic hot-spot.

Characteristics, overt disease onset and ADAMTS13 activity in homozygous and compound heterozygous carriers of *ADAMTS13* 4143_4144dupA mutation

Carriers of the *ADAMTS13* c.4143_4144dupA (p.Glu1382Argfs*6) mutation in exon 29 were enrolled from sites in Austria, Czech Republic, Hungary, Norway, Poland, and the USA. The number of homozygous and compound heterozygous carriers was about equal (P=0.51). Age at first diagnosis and at enrollment tended to be lower in compound heterozygous compared to homozygous carriers (P=0.06 and P=0.08, respectively) (Table 4). Information on recognized overt disease onset was available for 14 compound heterozygotes and 19 homozygotes. Homozygotes had a numerically higher age at overt onset (5.0 years; range 0-22.3 years) than com-

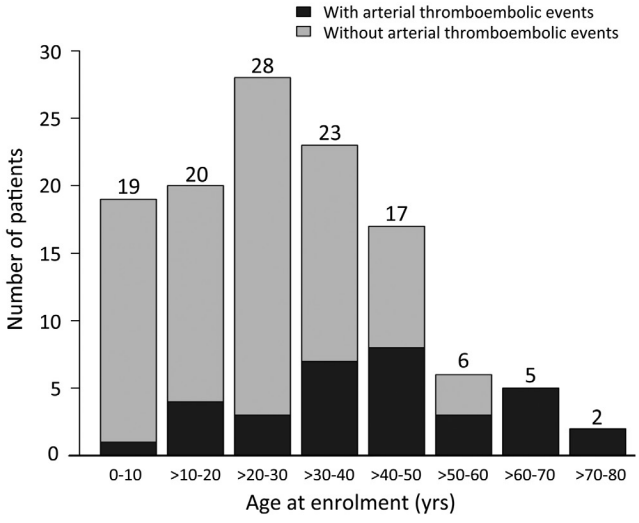

Figure 2. Number of congenital thrombotic thrombocytopenic purpura (cTTP) patients with or without a history of arterial thromboembolic events by age category at enrollment. Data are available for 120 of 123 confirmed cTTP patients. For five deceased patients, age at death was used. Yrs: years.

pound heterozygotes (1.1 years; 0-35.0 years), however, the difference was not significant (P=0.6), nor were the differences of all the other clinical characteristics (Table 4). Reported onset in homozygous *ADAMTS13* c.4143_4144dupA carriers has a bimodal pattern with peaks in the neonatal period and between six years and <18 years of age, whereas in compound heterozygotes the proportion of patients with later overt onset steadily declines (*Online Supplementary Figure S3A*).

In 34 of 38 *ADAMTS13* c.4143_4144dupA carriers, ADAMTS13 activity was assessed by the modified FRETS-VWF73 assay at the Central Hematology Laboratory, Bern University Hospital, Bern, Switzerland. ADAMTS13 activity was <1% in 18 of 20 (90%) homozygous and in 8 of 14 (57%) compound heterozygous carriers (*Online Supplementary Figure S3B*). The second *ADAMTS13* mutation in these eight patients was: c.1520G>A (p.Arg507Glu) in 5 alleles; c.1313G>T (p.Cys438Phe), c.2455delG (p.Ala819Leufs*24), and c.4091_4092insA (p.His1364Glnfs*) each in one allele. In the five compound heterozygotes with an ADAMTS13 activity of 1% to < 5%, we found the following five mutations: c.1313G>T (p.Cys438Phe), c.2410T>C (p.Cys804Arg), c.2836T>C (p.Cys946Arg), c.3178C>T (p.Arg1060Trp) and c.3650T>C (p.Ile1217Thr). c.3178C>T (p.Arg1060Trp) was also present in the compound heterozygous carrier with an ADAMTS13 activity of 6.3%. In c.4143_4144dupA carriers having an ADAMTS13 activity <1%, information on disease onset was available in 15 homozygotes and seven compound heterozygotes, with a trend for later disease onset in homozygotes (*Online Supplementary Figure S3C*).

Overt disease onset and ADAMTS13 activity in all congenital thrombotic thrombocytopenic purpura patients

Reported overt disease onset in 97 cTTP patients whose ADAMTS13 activity was measured either in Bern, Switzerland, or Nara, Japan, is shown in relation to the measured ADAMTS13 activity (Figure 4). Twenty-eight of 70 patients with ADAMTS13 activity <1% had overt disease onset in the neonatal period, but there were also 20 patients with overt disease onset at age >15-57 years. Most patients with measurable ADAMTS13 activity (≥ 1%) had a reported disease onset at >5 years of age. Overall, we found a weak but significant correlation between age at overt onset and ADAMTS13 activity (r_s=0.25, P<0.01).

Table 2. Reported concomitant diseases and disorders in congenital thrombotic thrombocytopenic purpura patients up to enrollment.

Type of disease/disorder	All patients (N=120)
Arterial thromboembolic diseases†	33 (28%)
Myocardial infarction	5 (4.2%)
Transient ischemic attack	12 (10%)
Stroke	25 (21%)
Other	6 (5.0%)
Other neurological disorders†	27 (22%)
Epileptic seizure	6 (5.0%)
Headache	5 (4.2%)
Various other	20 (17%)
Renal insufficiency†	30 (25%)
Hemodialysis	12 (10%)
Kidney transplant	3 (2.5%)
Jaundice (hemolysis or liver disease)	59 (49%)
Hyperbilirubinemia in neonatal period††	30 (25%)
Anemia	
Iron deficiency	8 (6.7%)
Renal anemia	8 (6.7%)
Other diseases	
Cancer	2 (1.7%)
Autoimmune disorders	4 (3.3%)
Transfusion-transmitted viral infection†	13 (11%)
HBV	3 (2.5%)
HCV	10 (8.3%)
HIV	1 (0.83%)

N: total number of patients with information available; HBV: hepatitis B viral infection; HCV: hepatitis C viral infection; HIV: human immunodeficiency virus infection. Categorical variables are presented as numbers and percentage of all patients. †For different disease categories the total number of affected patients is given (as a patient may have incurred more than one disorder per category, the sum of all conditions per category may be larger than that of the number of affected patients). ††No information reported for seven patients on hyperbilirubinemia in the neonatal period.

Discussion

We report the successful implementation of an International Registry for the ultra-rare disease cTTP. After many years of preparation, patient recruitment and enrollment, by the end of 2017, a total of 123 confirmed cTTP patients from 117 families were included in the study by centers from all over the world with the help of numerous primary care physicians (see the complete list in *Online Supplementary Appendix A*).

Congenital TTP is often not recognized at the first occurrence of disease manifestation, e.g. in the newborn

period or during childhood.[8,11,32,33] As demonstrated for the 111 patients with available information, a substantial number of affected subjects showed thrombocytopenia, hemolysis, jaundice, petechiae and/or anemia during the neonatal period, often leading to therapeutic interventions such as exchange blood transfusion, sometimes many years before clinical diagnosis of TTP (Figure 1). Other patients, however, seemed to present the first signs of TTP only in adulthood. Before the late 1990s cTTP was purely a clinical diagnosis. Today, clarification of its pathophysiology,[3,34-36] the advent of ADAMTS13 assays, and the possibility of sequencing the *ADAMTS13* gene emerging over the past two decades[6,7,9,11,12,35-38] allows the diagnosis of both autoimmune and congenital TTP to be quickly and efficiently confirmed (for consensus definitions of diagnosis see Scully *et al.*[4,22] and Kremer Hovinga *et al.*[5]). During recent years, we have been able to confirm the clinical diagnosis of many of our patients within days or weeks through the use of appropriate assays (Figure 1).

The systematic collection of clinical data in individual patients revealed substantial comorbidities in cTTP patients (Table 2 and Figure 2). Most notable is the high proportion of patients who had suffered from premature arterial thromboembolic events, mainly transient ischemic attacks, ischemic strokes and, to a lesser extent, myocardial infarctions. At 40-50 years of age and over, more than 50% of cTTP patients had suffered from at least one arterial thromboembolic event. In addition, several patients seem to suffer from headache, mental or depressive disorders, which is similar to the situation in acquired TTP.[39,40] Of note, 25% of cTTP patients had renal insufficiency at the time of enrollment and 12.5% had required hemodialysis or underwent kidney transplantation (Table 2). Severe and, sometimes transient, renal failure has been described in case reports or series of cTTP patients,[41-43] which is distinct from acquired TTP where a creatinine ≥2mg/dL (≥180 μmol/L) is a clear exception.[5,22,44]

Detailed information on 291 acute episodes in 81 cTTP patients was available at the time of enrollment. The frequency of acute manifestations varied considerably in individual patients with a median of approximately 0.1 acute episode per patient-year and a range of 0.02-9 yearly acute episodes per patient (*Online Supplementary Table S2*). In two-thirds of episodes, the responsible physicians assumed a triggering factor, mainly mild to moderately severe infections, alcohol excess in men, pregnancy in women, and various other potential triggers (Figure 3). Pregnancy is a well-known trigger for acute disease episodes in cTTP[13,18-20,45] and it is conceivable that pregnancy and other conditions leading to an increased endothelial von Willebrand factor secretion may bring about acute disease in the face of absent or severely reduced ADAMTS13 activity. It is generally thought that an acute episode in cTTP is rapidly controlled by simple plasma

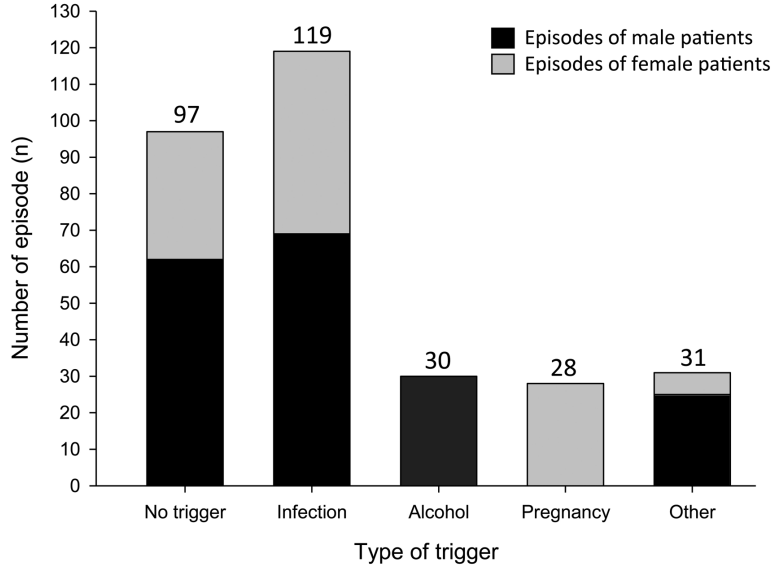

Figure 3. Triggers of acute thrombotic thrombocytopenic purpura (TTP) episodes until enrollment in male and female congenital thrombotic thrombocytopenic purpura patients. For 287 of 291 acute TTP episodes documented in the Hereditary TTP Registry information on triggers of the acute bout was known. Seventy-nine patients had episodes with or without presumed triggers: for 97 episodes in 46 patients no trigger was reported; for 190 episodes in 58 patients triggers were reported. Triggers do not sum up as a patient may have had more than one trigger of an acute episode, nor do patients as they may have had episodes with or without triggers.

Table 3. Reported treatment in congenital thrombotic thrombocytopenic purpura patients at enrollment.

Variables	All patients (N = 117)*
Mode of treatment	
Patients with regular prophylactic treatment	83 (71%)
Patients with on demand treatment	34 (29%)
Plasma and Factor products applied among regularly treated patients	
Plasma products†	82 (99%)
Plasma derived FVIII product	1 (1.2%)
Median interval of most recent treatment (days) (n=78)††	14.0 [2.0, 14.0, 21.0, 75.0]

N: total number of patients; n: number of patients with available values. Continuous variables are presented as median [(minimum, 25th percentile, 75th percentile, maximum)]. Categorical variables are presented as number and percentage of all patients, or as number (n) of patients. *Information on current treatment missing for two male and four female patients. †Fresh frozen plasma (n=68); fresh frozen plasma and cryo-poor plasma (n=2), solvent/detergent plasma (n=12). ††Interval missing for five patients.

infusion;[2,18] however, data from our Registry show that the median duration of over 200 well-documented episodes was seven days, probably because of delayed plasma therapy or illness from the triggering event.

Information on prophylactic treatment was available for 117 of 123 cTTP patients (Table 3). Twenty-nine percent of the patients had no regular prophylaxis and received plasma only on demand. Seventy-one percent were on prophylactic treatment, usually with fresh frozen plasma or solvent/detergent plasma infusions, while only one patient was treated with a commercial Factor VIII concentrate (Koate®). Dosing intervals mostly varied between two and three weeks, as had been proposed earlier on the basis of platelet count measurements.[18] Whether such a dosing interval sufficiently controls minor TTP-related symptoms is questionable given the frequently reported

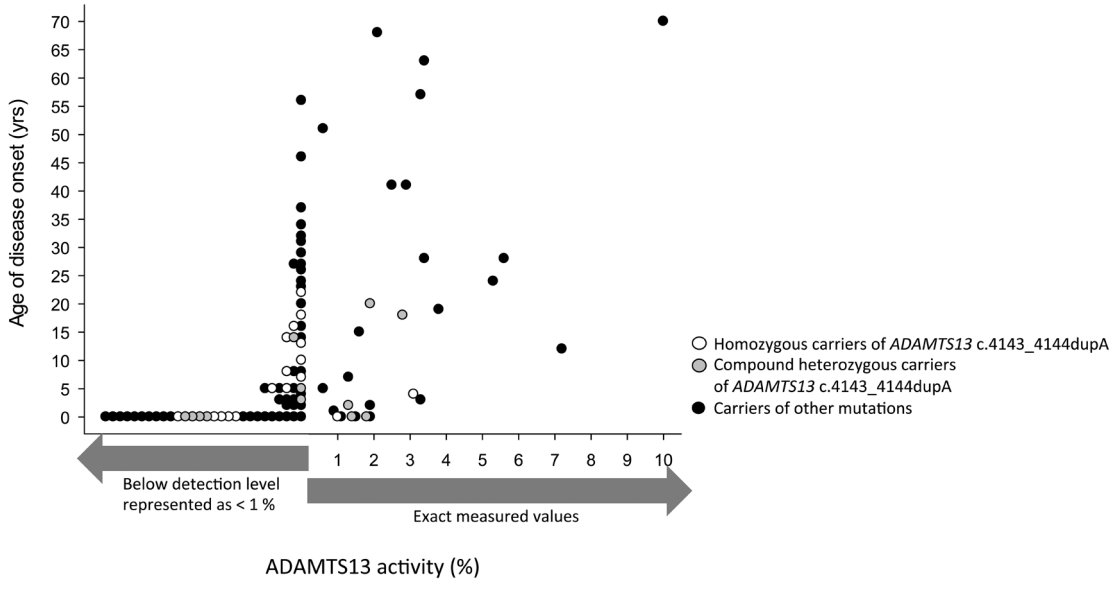

Figure 4. Age at disease onset in relation to ADAMTS13 activity in 97 congenital thrombotic thrombocytopenic purpura (cTTP) patients. Ninety-seven confirmed cTTP patients had information on disease onset and an ADAMTS13 activity determination performed either at the Central Hematology Laboratory, Bern University Hospital, Switzerland, or at the Department of Blood Transfusion Medicine, Nara Medical University, Japan. Patients are labeled according to their *ADAMTS13* mutations: 17 homozygous carriers and 12 compound heterozygous carriers of *ADAMTS13* c.4143_4144dupA are shown with white and gray circles, respectively. Black circles represent carriers of other mutations. Spearman's rank correlation coefficient for age at overt disease onset *versus* ADAMTS13 activity: r_s=0.25, *P*<0.01. yrs: years.

Table 4. Characteristics of congenital thrombotic thrombocytopenic purpura patients carrying one or two *ADAMTS13* c.4143_4144dupA alleles.

Variables	Genotype		
	Homozygous (N = 22)	Compound heterozygous (N = 16)	*P*
Median age of patient at enrollment (yrs)	31.2 [17.0, 60.1]	23.2 [4.0, 60.1]	0.08
Median age of patient at clinical diagnosis (yrs)	20.4 [1.8, 51.5]	4.35 [0.2, 39.6]	0.06
Female sex	8 (36%)	9 (56%)	0.32
Occurrence of major diseases/disorders			
Transient ischemic attack	4 (18%)	4 (25%)	0.70
Stroke	5 (23%)	4 (25%)	1.00
(Chronic) renal insufficiency	7 (32%)	6 (38%)	0.72
Jaundice (hemolysis or liver disease)	5 (23%)	2 (13%)	0.68
Diagnosis of a transfusion transmitted viral disease	1 (4.5%)	0 (0%)	1.00
Mode of treatment			
Number of patients with regular prophylactic treatment	17 (77%)	11 (69%)	0.71
Median interval of most recent treatment (days)*	21.0 [7.00, 75.0]	14.0 [14.0, 56.0]	0.19
Reported episodes			
Number of patients with reported episodes prior to enrollment	15 (68%)	11 (69%)	1.00
Median number of episodes per patient	6.00 [1.00, 11.0]	1.00 [1.00, 12.0]	0.13
Number of retrospective episodes per year	0.15 [0.03, 0.35]	0.12 [0.03, 0.80]	0.62

N: total number of patients. Continuous variables are presented as median (minimum, maximum). Categorical variables are presented as number and percentage of all patients. *Interval missing for two homozygous patients. yrs: years

symptoms like headache or mental disorders. Even though ADAMTS13 half-life in plasma is about 2-4 days[46,47] almost all patients will have unmeasurable ADAMTS13 levels within 7-10 days after infusion of 2-4 units of fresh frozen plasma. Evidently, a prospective follow up of cTTP patients will be needed to optimize replacement therapy. In the near future, the availability of rhADAMTS13, successfully tested in a pharmacokinetics and safety study in 15 cTTP patients,[48] will greatly facilitate regular prophylactic treatment, and will probably allow treatment to be carried forward at home. In addition, given the high risk of acute episodes, ischemic strokes and other sequelae, a general prophylactic ADAMTS13 replacement in cTTP may be indicated.

ADAMTS13 mutations were found in all except one cTTP Bi-allelic patient (*Online Supplementary Table S3 and Online Supplementary Figure S4*); a total of 98 different mutations spread throughout the *ADAMTS13* gene were identified, including several mutations that have not so far been described. Eighty-one mutations occurred only once (58 alleles) or twice, 14 different mutations were identified on 3-6 alleles, whereas three variants were present on 11 (c.577C>T), 13 (c.3178C>T), and 60 (c.4143_4144dupA) alleles, respectively. The latter three recurring mutations have been repeatedly found in Japanese (c.577C>T)[11,37] and Caucasian (c.3178C>T and c.4143_4144dupA) patients.[15,20,23,24,45,49] It has been postulated that mutations leading to a completely absent ADAMTS13 activity show a more severe phenotype than those associated with some residual ADAMTS13 activity.[13,16,17,49] We compared disease characteristics of 22 homozygous and 16 compound heterozygous carriers of the c.4143_4144dupA mutation (Table 4 and *Online Supplementary Figure S3A-C*). Median age at diagnosis tended to be higher in homozygous carriers, even though there was a wide range of age at diagnosis from 0.2-51.5 years in both groups. There was no difference in any other of the disease characteristics. Despite a severely deficient ADAMTS13 activity (< 0.5-1% of normal) in homozygous c.4143_4144dupA carriers, almost half of affected patients had an overt disease onset at an age of > 6 years that seemed to be higher than in compound heterozygotes with equally severe ADAMTS13 deficiency (*Online Supplementary Figure S3C*). Shang *et al.*[50] suggested that the c.4143_4144dupA mutation might be associated with defective apical, but preserved basolateral, secretion by endothelial cells. Whether some ADAMTS13 activity at the endothelial cell layer in the absence of plasmatic ADAMTS13 activity is present that may explain a delayed TTP onset in a proportion of homozygous carriers needs further study.

We then tested whether overt disease onset was related with residual plasma ADAMTS13 activity in all patients whose ADAMTS13 activity was measured in Nara or Bern after a comparative evaluation had shown a good agreement of activity levels in the very low range below 5-10% (*Online Supplementary Table S1*). For 97 patients with available information, it was evident that overt disease onset was not strictly related to residual ADAMTS13 activity. Whereas about 40% of cTTP patients with an ADAMTS13 activity <1% had a neonatal disease onset, 20% seemed to have a first TTP manifestation at age >20 years. On the other hand, most cTTP patients with an ADAMTS13 activity >1-2% had a delayed apparent disease manifestation (Figure 4). Thus, residual ADAMTS13 activity is clearly not the only determinant of disease severity, as reflected by age at overt onset.

In conclusion, the Hereditary TTP Registry has provided substantial information, but it will be of utmost importance for the development of an optimized management strategy to enlarge the cohort by directly enrolling more patients from around the globe, and through embarking on collaborations with other established registries on cTTP. It would be highly desirable to prospectively follow all cTTP patients at regular intervals and evaluate the best prophylactic strategy to avoid unnecessary deaths and late sequelae in this treatable condition.

A complete list of the collaborators of the Hereditary TTP Registry appears in the *Online Supplementary Appendix A.*

Acknowledgments

Acknowledgments to the late professor Miha Furlan for his pioneering work on discovery of von Willebrand factor-cleaving protease ADAMTS13 and its deficiency in TTP more than 20 years ago. The authors thank the teams of the laboratories in Bern, Switzerland and Nara, Japan for work on ADAMTS13-related assays and molecular analyses of the ADAMTS13 gene. Corinne Eschler is thanked for her assistance in data collection and entry.

Funding

The hereditary TTP registry has received support through grants from the Swiss National Science Foundation (Grant 32003B-124892), the Mach-Gaensslen Foundation Switzerland, the ISTH 2007 Presidential Fund, the NFG Foundation, as well as research grants from Baxalta US Inc., member of the Takeda group of companies, Bannockburn, IL, USA (IIR Grant no H10-000600 and H16-36165). Furthermore, this work was supported in part by grants-in-aid from the Ministry of Health, Labor, and Welfare of Japan, and Takeda Science Foundation (to YF and MM), and National Heart, Lung, and Blood Institute of the National Institutes of Health under Award Number 1K01HL135466 (to DRT).

References

1. Upshaw JD Jr. Congenital deficiency of a factor in normal plasma that reverses microangiopathic hemolysis and thrombocytopenia. N Engl J Med. 1978;298(24):1350-1352.
2. Kinoshita S, Yoshioka A, Park YD, et al. Upshaw-Schulman syndrome revisited: a concept of congenital thrombotic thrombocytopenic purpura. Int J Hematol. 2001;74(1):101-108.
3. Moake JL. Thrombotic microangiopathies. N Engl J Med. 2002;347(8):589-600.
4. Scully M, Cataland S, Coppo P, et al. Consensus on the standardization of terminology in thrombotic thrombocytopenic purpura and related thrombotic microangiopathies. J Thromb Haemost. 2017; 15(2):312-322.
5. Kremer Hovinga JA, Coppo P, Lämmle B, Moake JL, Miyata T, Vanhoorelbeke K. Thrombotic thrombocytopenic purpura. Nat Rev Dis Primers. 2017;3:17020.
6. Levy GG, Nichols WC, Lian EC, et al. Mutations in a member of the ADAMTS gene family cause thrombotic thrombocytopenic purpura. Nature. 2001; 413(6855): 488-494.
7. Kokame K, Matsumoto M, Soejima K, et al. Mutations and common polymorphisms in ADAMTS13 gene responsible for von Willebrand factor-cleaving protease activity. Proc Natl Acad Sci U S A. 2002;99(18):11902-11907.
8. Schneppenheim R, Budde U, Oyen F, et al. von Willebrand factor cleaving protease and ADAMTS13 mutations in childhood TTP. Blood. 2003;101(5):1845-1850.
9. Veyradier A, Lavergne JM, Ribba AS, et al.

Ten candidate ADAMTS13 mutations in six French families with congenital thrombotic thrombocytopenic purpura (Upshaw-Schulman syndrome). J Thromb Haemost. 2004;2(3):424-429.
10. Amorosi EL, Ultmann JE. Thrombotic thrombocytopenia purpura: Report of 16 cases and review of the literature. Medicine. 1966;45 (2):139-160.
11. Fujimura Y, Matsumoto M, Isonishi A, et al. Natural history of Upshaw-Schulman syndrome based on ADAMTS13 gene analysis in Japan. J Thromb Haemost. 2011;9 Suppl 1:283-301.
12. Lotta LA, Garagiola I, Palla R, Cairo A, Peyvandi F. ADAMTS13 mutations and polymorphisms in congenital thrombotic thrombocytopenic purpura. Hum Mutat. 2010;31(1):11-19.
13. Camilleri RS, Scully M, Thomas M, et al. A phenotype-genotype correlation of ADAMTS13 mutations in congenital thrombotic thrombocytopenic purpura patients treated in the United Kingdom. J Thromb Haemost. 2012;10(9):1792-1801.
14. Joly BS, Boisseau P, Roose E, et al. ADAMTS13 Gene Mutations Influence ADAMTS13 Conformation and Disease Age-Onset in the French Cohort of Upshaw-Schulman Syndrome. Thromb Haemost. 2018;118(11):1902-1917.
15. Pimanda JE, Maekawa A, Wind T, Paxton J, Chesterman CN, Hogg PJ. Congenital thrombotic thrombocytopenic purpura in association with a mutation in the second CUB domain of ADAMTS13. Blood. 2004;103(2): 627-629.
16. Lotta LA, Wu HM, Musallam KM, Peyvandi F. The emerging concept of residual ADAMTS13 activity in ADAMTS13-deficient thrombotic thrombocytopenic purpura. Blood Rev. 2013;27(2):71-76.
17. Lotta LA, Wu HM, Mackie IJ, et al. Residual plasmatic activity of ADAMTS13 is correlated with phenotype severity in congenital thrombotic thrombocytopenic purpura. Blood. 2012;120(2):440-448.
18. Furlan M, Lämmle B. Aetiology and pathogenesis of thrombotic thrombocytopenic purpura and haemolytic uraemic syndrome: the role of von Willebrand factor-cleaving protease. Best Pract Res Clin Haematol. 2001;14(2):437-454.
19. Fujimura Y, Matsumoto M, Kokame K, et al. Pregnancy-induced thrombocytopenia and TTP, and the risk of fetal death, in Upshaw-Schulman syndrome: a series of 15 pregnancies in 9 genotyped patients. Br J Haematol. 2009;144(5):742-754.
20. Moatti-Cohen M, Garrec C, Wolf M, et al. Unexpected frequency of Upshaw-Schulman syndrome in pregnancy-onset thrombotic thrombocytopenic purpura. Blood. 2012;119(24):5888-5897.
21. Scully M, Thomas M, Underwood M, et al. Thrombotic thrombocytopenic purpura and pregnancy: presentation, management, and subsequent pregnancy outcomes. Blood. 2014;124(2):211-219.
22. Scully M, Hunt BJ, Benjamin S, et al. Guidelines on the diagnosis and management of thrombotic thrombocytopenic purpura and other thrombotic microangiopathies. Br J Haematol. 2012;158(3):323-335.
23. Schneppenheim R, Kremer Hovinga JA, Becker T, et al. A common origin of the 4143insA ADAMTS13 mutation. Thromb Haemost. 2006;96(1):3-6.
24. von Krogh AS, Quist-Paulsen P, Waage A, et al. High prevalence of hereditary thrombotic thrombocytopenic purpura in central Norway: from clinical observation to evidence. J Thromb Haemost. 2016;14(1):73-82.
25. Kremer Hovinga JA, Heeb SR, Skowronska M, Schaller M. Pathophysiology of thrombotic thrombocytopenic purpura and hemolytic uremic syndrome. J Thromb Haemost. 2018;16(4):618-629.
26. Mansouri Taleghani M, von Krogh AS, Fujimura Y, et al. Hereditary thrombotic thrombocytopenic purpura and the hereditary TTP registry. Hamostaseologie. 2013; 33(2):138-143.
27. Kremer Hovinga JA, Vesely SK, Terrell DR, Lämmle B, George JN. Survival and relapse in patients with thrombotic thrombocytopenic purpura. Blood. 2010;115(8):1500-1511.
28. Froehlich-Zahnd R, George JN, Vesely SK, et al. Evidence for a role of anti-ADAMTS13 autoantibodies despite normal ADAMTS13 activity in recurrent thrombotic thrombocytopenic purpura. Haematologica. 2012; 97(2):297-303.
29. Kato S, Matsumoto M, Matsuyama T, Isonishi A, Hiura H, Fujimura Y. Novel monoclonal antibody-based enzyme immunoassay for determining plasma levels of ADAMTS13 activity. Transfusion. 2006; 46(8):1444-1452.
30. Page EE, Kremer Hovinga JA, Terrell DR, Vesely SK, George JN. Thrombotic thrombocytopenic purpura: diagnostic criteria, clinical features, and long-term outcomes from 1995 through 2015. Blood Adv. 2017; 1(10):590-600.
31. Dunnen JT, Dalgleish R, Maglott DR, et al. HGVS Recommendations for the Description of Sequence Variants: 2016 Update. Hum Mutat. 2016;37(6):564-569.
32. Häberle J, Kehrel B, Ritter J, Jürgens H, Lämmle B, Furlan M. New strategies in diagnosis and treatment of thrombotic thrombocytopenic purpura: case report and review. Eur J Pediatr. 1999;158(11):883-887.
33. Scully M, Starke R, Lee R, Mackie I, Machin S, Cohen H. Successful management of pregnancy in women with a history of thrombotic thrombocytopaenic purpura. Blood Coagul Fibrinolysis. 2006;17(6):459-463.
34. Furlan M, Robles R, Galbusera M, et al. von Willebrand factor-cleaving protease in thrombotic thrombocytopenic purpura and the hemolytic-uremic syndrome. N Engl J Med. 1998;339(22):1578-1584.
35. Saha M, McDaniel JK, Zheng XL. Thrombotic thrombocytopenic purpura: pathogenesis, diagnosis and potential novel therapeutics. J Thromb Haemost. 2017; 15(10):1889-1900.
36. Joly BS, Coppo P, Veyradier A. Thrombotic thrombocytopenic purpura. Blood. 2017; 129(21):2836-2846.
37. Matsumoto M, Kokame K, Soejima K, et al. Molecular characterization of ADAMTS13 gene mutations in Japanese patients with Upshaw-Schulman syndrome. Blood. 2004;103(4):1305-1310.
38. Kokame K, Nobe Y, Kokubo Y, Okayama A, Miyata T. FRETS-VWF73, a first fluorogenic substrate for ADAMTS13 assay. Br J Haematol. 2005;129(1):93-100.
39. Deford CC, Reese JA, Schwartz LH, et al. Multiple major morbidities and increased mortality during long-term follow-up after recovery from thrombotic thrombocytopenic purpura. Blood. 2013;122(12):2023-2029.
40. Falter T, Schmitt V, Herold S, et al. Depression and cognitive deficits as long-term consequences of thrombotic thrombocytopenic purpura. Transfusion. 2017; 57(5):1152-1162.
41. Furlan M, Robles R, Solenthaler M, Wassmer M, Sandoz P, Lämmle B. Deficient activity of von Willebrand factor-cleaving protease in chronic relapsing thrombotic thrombocytopenic purpura. Blood. 1997;89(9):3097-3103.
42. Remuzzi G, Galbusera M, Noris M, et al. von Willebrand factor cleaving protease (ADAMTS13) is deficient in recurrent and familial thrombotic thrombocytopenic purpura and hemolytic uremic syndrome. Blood. 2002;100(3):778-785.
43. Fan X, Kremer Hovinga JA, Shirotani-Ikejima H, et al. Genetic variations in complement factors in patients with congenital thrombotic thrombocytopenic purpura with renal insufficiency. Int J Hematol. 2016;103(3):283-291.
44. Bendapudi PK, Hurwitz S, Fry A, et al. Derivation and external validation of the PLASMIC score for rapid assessment of adults with thrombotic microangiopathies: a cohort study. Lancet Haematol. 2017;4(4): e157-e164.
45. Camilleri RS, Cohen H, Mackie IJ, et al. Prevalence of the ADAMTS-13 missense mutation R1060W in late onset adult thrombotic thrombocytopenic purpura. J Thromb Haemost. 2008;6(2):331-338.
46. Furlan M, Robles R, Morselli B, Sandoz P, Lämmle B. Recovery and half-life of von Willebrand factor-cleaving protease after plasma therapy in patients with thrombotic thrombocytopenic purpura. Thromb Haemost. 1999;81(1):8-13.
47. Fujimura Y, Kokame K, Yagi H, Isonishi A, Matsumoto M, Miyata T. Hereditary Deficiency of ADAMTS13 Activity: Upshaw–Schulman Syndrome. In: Rodgers GM, ed. ADAMTS13: Biology and Disease. Cham: Springer International Publishing, 2015:73-90.
48. Scully M, Knöbl P, Kentouche K, et al. Recombinant ADAMTS-13: first-in-human pharmacokinetics and safety in congenital thrombotic thrombocytopenic purpura. Blood. 2017;130(19):2055-2063.
49. Rurali E, Banterla F, Donadelli R, et al. ADAMTS13 Secretion and Residual Activity among Patients with Congenital Thrombotic Thrombocytopenic Purpura with and without Renal Impairment. Clin J Am Soc Nephrol. 2015;10(11):2002-2012.
50. Shang D, Zheng XW, Niiya M, Zheng XL. Apical sorting of ADAMTS13 in vascular endothelial cells and Madin-Darby canine kidney cells depends on the CUB domains and their association with lipid rafts. Blood. 2006;108(7):2207-2215.

Recurrent stroke: the role of thrombophilia in a large international pediatric stroke population

Gabrielle deVeber,[1]* Fenella Kirkham,[2,3]* Kelsey Shannon,[1] Leonardo Brandão,[1] Ronald Sträter,[4] Gili Kenet,[5] Hartmut Clausnizer,[6] Mahendranath Moharir,[1] Martina Kausch,[6] Rand Askalan,[1] Daune MacGregor,[1] Monika Stoll,[7] Antje Torge,[6] Nomazulu Dlamini,[1] Vijeja Ganesan,[2] Mara Prengler,[2] Jaspal Singh[3] and Ulrike Nowak-Göttl[4/6]

[1]The Hospital for Sick Children, Toronto, Canada; [2]Developmental Neurosciences Programme, UCL Great Ormond Street Institute of Child Health, London, UK; [3]University Hospital Southampton, UK; [4]Department of Paediatric Haematology/Oncology, University of Münster, Münster, Germany; [5]Pediatric Coagulation Service, National Hemophilia Centre and Institute of Thrombosis and Hemostasis Sheba Medical Center, Tel-Hashomer, Israel; [6]Institute of Clinical Chemistry, University Hospital Kiel-Lübeck, Kiel, Germany and [7]Department of Genetic Epidemiology, University of Münster, Münster, Germany

*GdeV and FK contributed equally to this work.

doi:10.3324/haematol.2019.234666

In the article pre-published online on January 24, 2019 and published in the paper version of Haematologica [volume 104(8):1676-1681; doi:10.3324/haematol2018.211433] we have to correct:

➢ that recurrent stroke occurred in **160/872** (instead of 160 / 880) children [page 1678, second column, line 6].

➢ the incidence rates of recurrent AIS with respect to the individual exposure time in years given in the abstract (page 1676, lines 16-18) and in the results section (page 1679, paragraph "prothrombotic risk factors", lines 38-40). As explained in the methods section, we calculated the absolute risk of AIS recurrence as incidence rates per 100 patient-years (%). According to the individual exposure times (years) to antithrombin, lipoprotein (a) and the presence of more than one prothrombotic risk factor the **incidence rates calculated per 100 patient-years** are presented in the table below.

Type of thrombophilia	Exposure time (years)	Event (n)	Incidence per 100 patient-years % (95% CI)
Antithrombin deficiency	2437	7	0.3 (0.1-0.6)
Elevated lipoprotein(a)	1938	23	1.2 (0.7-1.7)
More than one prothrombotic risk factor	2887	23	0.8 (0.5-1.1)

CI: Confidence interval; n: number.

RESEARCH, READ & CONNECT

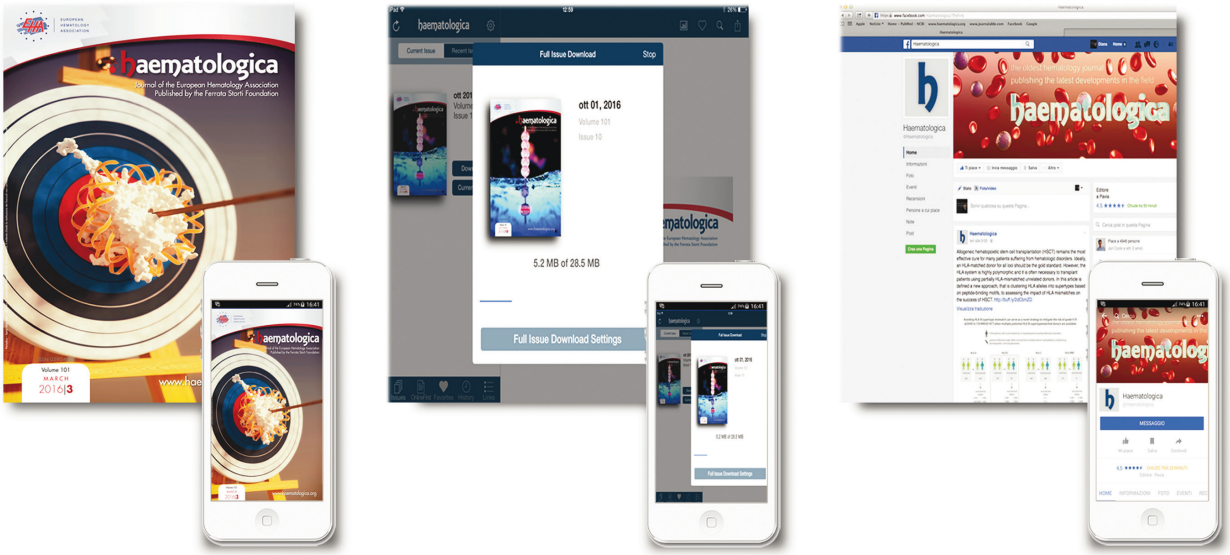

We reach more than
6 hundred thousand readers each year

The first Hematology Journal in Europe

Impressions YTD

9,621,645

Digital Readers

4,431

Total Audience

554,484

Worldwide rank	Impact factor	Total citations
7 th	7.570	16,255

haematologica

Journal of the Ferrata Storti Foundation

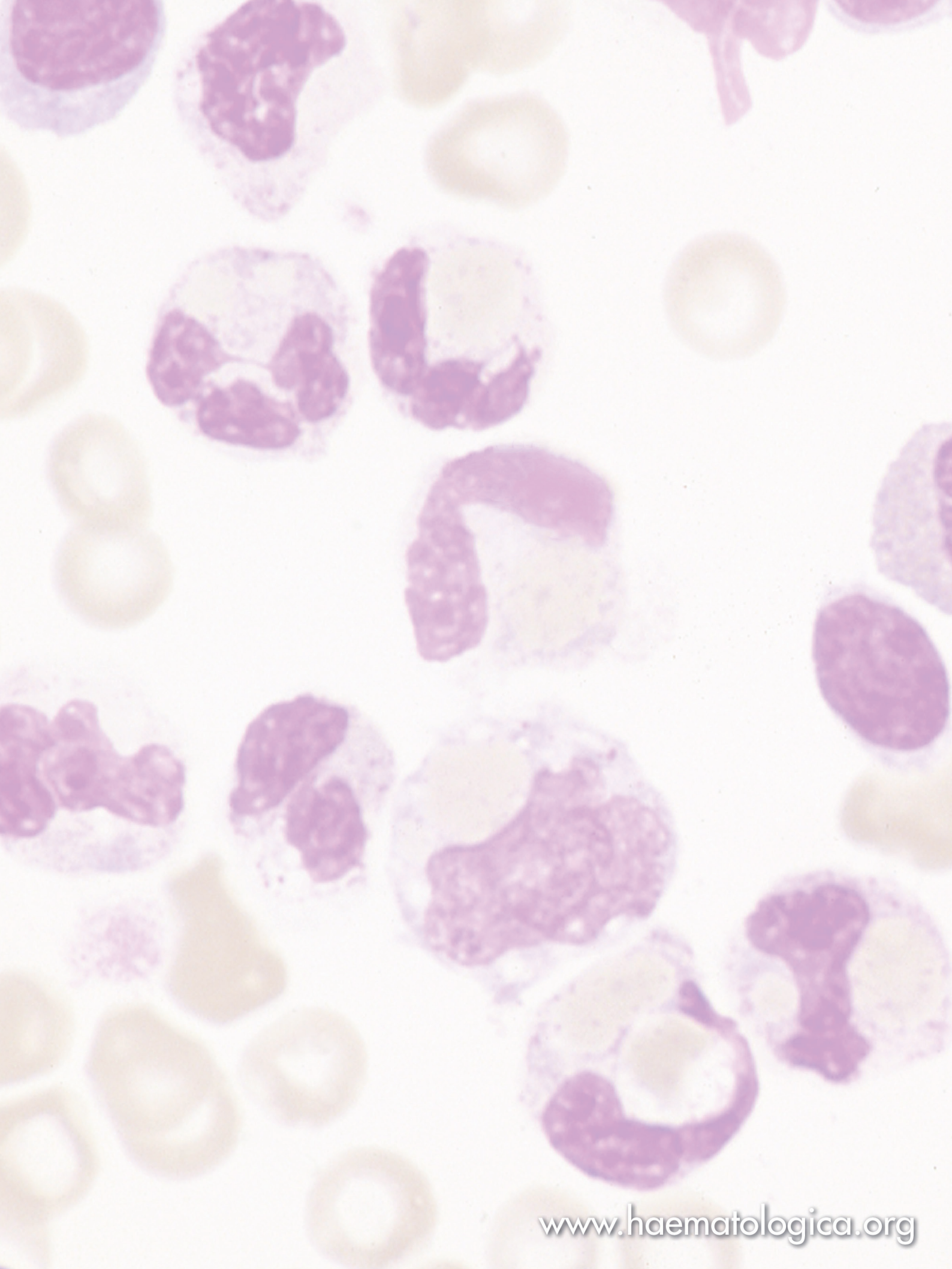

haematologica — Vol. 104 n. 10 — October 2019 — 1907-2116